Engineering & Development Proceedings of Technical Groups Vol. 29

Proceedings

IPENZ

Engineering & Development in HAZARDOUS TERRAIN

ENGINEERING & DEVELOPMENT IN HAZARDOUS TERRAIN

NEW ZEALAND GEOTECHNICAL SOCIETY 2001 SYMPOSIUM

Engineering and Development in Hazardous Terrain

New Zealand Geotechnical Society 2001 Symposium

Christchurch, August 2001

Organising Committee:

Kevin McManus, University of Canterbury
Guy Grocott, Golder Associates (NZ) Ltd
Marton Sinclair, Eliot Sinclair and Partners Ltd
Peter Kingsbury, Environment Canterbury
Bruce Riddolls, Golder Associates (NZ) Ltd

Conference Organisers:
Conference Office, University of Canterbury

Published by:
The Institution of Professional Engineers
New Zealand
PO Box 12241
Wellington
New Zealand

Proceedings of Technical Groups Vol 29
Issue 2 (GM) 2001
ISSN 0111-9532

Symposium Sponsors

Beca Carter Hollings & Ferner Ltd
Earthquake Commission
Environment Canterbury
Solid Energy
Tonkin and Taylor Ltd
Transit New Zealand
Transpower NZ Ltd

The printing of the Symposium Proceedings is sponsored by:

Beca

SOLID ENERGY

Dedicated to Brian Paterson 1937 – 1999

The symposium theme, "Engineering and Development in Hazardous Terrain", was first conceived by Brian during his early involvement on the organising committee. Brian was an engineering geologist whose professional life was extensively involved with development in difficult terrain. He was very active, particularly during his early career with the New Zealand Geological Survey in establishing engineering geological logging and mapping procedures that are fundamental to current practice.
One of Brian's last major projects, the Otira Viaduct project on SH73 near Arthur's Pass, is a tribute to his considerable technical skills and expertise.
An obituary to Brian appeared in issue No. 57 (June 1999) of Geomechanics News.

NZ Geotechnical Symposium 2001
Table of Contents

Poster Presentations

Slope Failures II

Volcanic Hazards/Other Issues

Geomechanics Lecture 2001

Hazardous Terrain – An Engineering Geological Perspective

Warwick M. Prebble
Dept. of Geology, The University of Auckland

Abstract

New Zealand is well endowed with hazardous terrain. Examples discussed here are from the Taupo Volcanic Zone, East Coast Deformed Belt, Southern Alps and North Island weak rock.

Placing each site in a geological context and focusing in from the regional view leads to appropriate geotechnical models. Many faults, landslides, volcanoes and areas of geothermal activity are not obvious at the site but are identifiable at the regional scale.

Debris avalanches from weakened andesite volcanoes are large, infrequent, extremely hazardous events. Conditions promoting failure persist and smaller, frequent avalanches and flows are known. Sensitive rhyolitic silts are widespread in northern regions and fail as slide-flows. Greywacke and schist rock masses of the Southern Alps are subject to large, deep-seated topples, which lead to rock slide avalanches. Debris aprons are found below deep ravines in toppled slopes of the Alps and also in toppled limestone dip slopes of the East Coast Deformed Belt. Overtoppling of dip slopes is probably underestimated. Block sliding on tectonic clay seams is now well known from many areas of weak rock.

Comparative geomorphology, remote sensing and mapping have assisted identification of block slides on clay seams in deeply weathered weak rock throughout the Auckland region. At Tokaanu and Tongariro, the same approach, including outcrop mapping at considerable distances from the "site" has led to recognition of faults, explosion craters, grabens, geothermally weakened ground, landslides and run-out areas for collapsing volcanoes.

Introduction

This paper offers a personal view of the contribution that engineering geology has made to our understanding of hazardous terrain, drawing upon 35 years of experience in field-based research on engineering projects and in areas selected for their hazardous and challenging nature. The examples are from a collection of case histories with which I have been closely involved. To some extent this may deliver a single point of view, however this is balanced and reinforced by the contributions of many co-investigators over the years;- colleagues, associates, clients and graduate students.

Recognition and assessment of geologic hazards is a basic platform of engineering geological practice and a prerequisite for successful geotechnical engineering. Without earth surface processes and deeper crustal tectonics this land of ours could not exist and we would be deprived of the immense challenge and professional satisfaction that is offered by practising on an obliquely convergent, complex plate margin. New Zealand is a highly varied landmass with many different terrains (Fig. 1) displaying defective and difficult rock masses and soil masses, crafted by a collection of hazardous geologic processes.

I intend to take this opportunity to reflect upon the value of a comprehensive approach to geotechnical mapping as a critical first step for field investigations and developing tentative site models. An essential part of this process is to start with a regional picture and then focus down to the actual site. "Total"mapping as it is sometimes called involves many factors, which make up our analysis of hazardous "terrain". Geomorphology, defects, materials, groundwater, geologic history, structure, tectonics and volcanism all play a part. Recognition and understanding of geotechnical hazards demands investigation across a huge range of scales – from the microscopic fabric of rock and soils to the morphology of mega-landslides.

A comprehensive approach can provide a reasonably complete picture of the site or region . The coordinated use of remote sensing, geomorphology and field mapping over a significant region is a way of identifying hazards and difficult ground conditions, which are present at the site but concealed from view by weathering and overlying deposits.

This paper presents information from a wide range of hazardous terrain. Included are: Hydrothermally weakened andesite stratovolcanoes, altered and faulted massifs in an active volcanic rift, ignimbritic plateaus and terrace remnants, elevated and defective sedimentary rock of the East Coast Deformed Belt, areas of greywacke and schist mountain range collapse and block slides in weak rock. Both the science and art of engineering geology will be alluded to – the science of gathering data and information and the art of observation which makes this process possible in the first place.

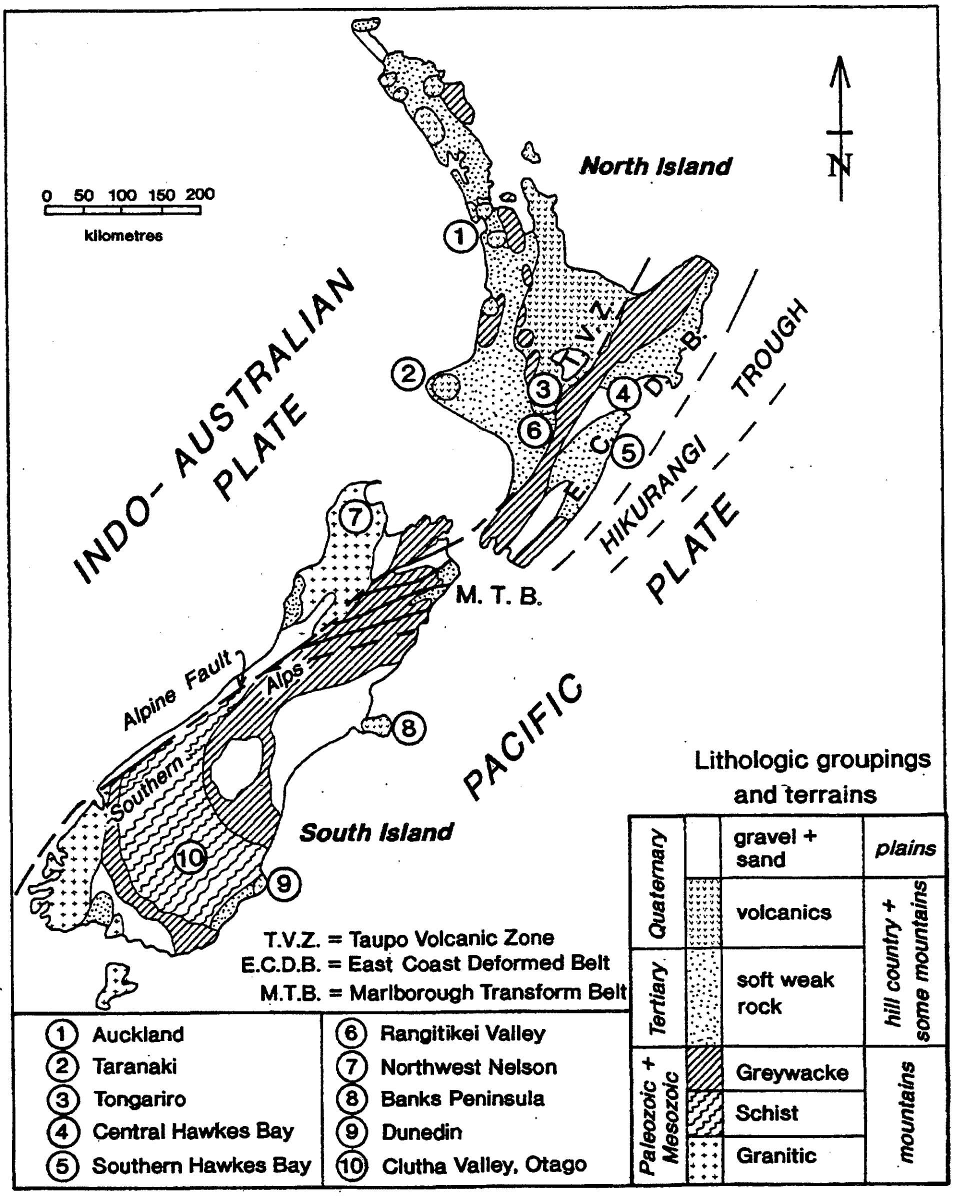

Figure 1. Major tectonic features, main lithologic groupings and engineering geological terrains of New Zealand

Active Volcanic Terrain

My first experience with engineering geological endeavour of any kind was to grapple with the challenges facing the Tongariro Power Development in the mid-1960s. I soon grew accustomed to the extreme variety of andesitic and rhyolitic deposits and the complex geometric relationships between them. A period of secondment to the relatively stable and predictable granitic terrain of the Snowy Mountains Scheme quickly disavowed me of any complacency about Tongariro and served to impress upon me just how very active, unstable and unpredictable the whole of the TPD area is. I rapidly discovered that the challenge was twofold. Firstly there was the threat from renewed volcanic activity and other hazards such as landslides, hydrothermal eruptions, faulting and earthquake. Secondly there was the legacy of past volcanic activity – the collection of rock masses, soils, groundwater systems and topography in which the scheme had to be sited and built.

The area around the Tokaanu Power Project and the Otamangakau and Te Whaiau dams (Fig.2) was particularly enigmatic. A successful resolution came only with the help of the regional approach and photo-geology. The complex Tongariro Volcano with its collection of craters, thermal areas and lava flows became a type area for elucidating the obscure and altered formations at Tokaanu and also provided clues as to the source of unusual deposits at Te Whaiau and Otamangakau.

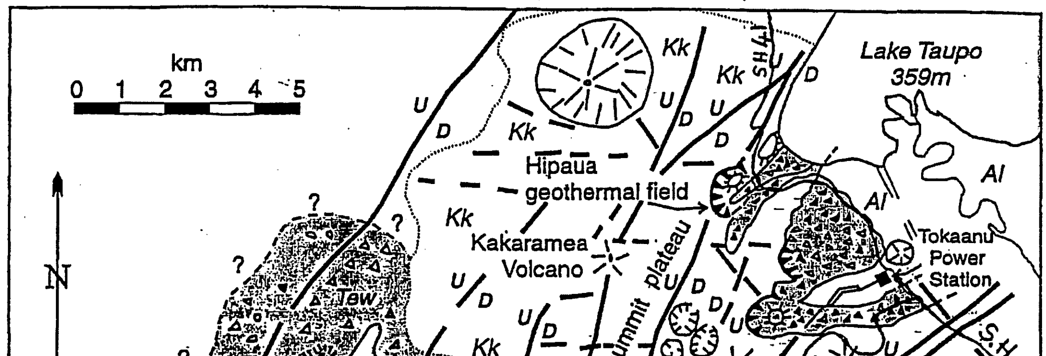

Figure 2. Tongariro Volcano, north-west ring plain and the Tokaanu area. Taupo Volcanic Zone. Cover beds of volcanic ash and tephra have been omitted.

Legend

A : Slope movement features and deposits

headscarp to landslide / debris flow

slide block

debris mound

debris field, debris fan, tongue

trench, pull-away zone (E.N.E. only, on Tongariro North Crater)

Tew — Te Whalau Formation (avalanche debris)

Al — alluvium of Rotoaira and Taupo basin

B : Faults and Volcanic Craters

Fault, (U) Upthrown (D) Downthrown (N.E. set)

Faults, inferred (NE, SW + E-W sets)

Summit crater

Large basin-shaped crater (? explosion crater or lava filled crater)

rhyolitic dome

C : Lava flow and scoria fields, originating from the following volcanoes:-

tm — Te Mari Crater } Tongariro volcano
nc — North Crater } Tongariro volcano

to — Tongariro volcano, older massif

Pi — Pihanga volcano

Kk — Kakaramea volcano

Legend for Figure 2: Tongariro Volcano, north-west ring plain and the Tokaanu area.

My day to day professional involvement was, of necessity, at the distinctly practical level. Whenever time allowed I pursued background research in the form of field mapping on Tongariro Volcano. This work gave rise to the site models for places like Tokaanu and Te Whaiau – Otamangakau. It also began to reveal the greater extent and nature of hazards from the volcanoes but it was to be several more years before the sector collapse and eruption of Mt St Helens provided us with a classic example of a major cone slope failure and debris avalanche.

Debris avalanches and debris flows from andesite cones

Active andesite cones in the Taupo and Taranaki Volcanic Zones have a history of generating lahars and ash frequently and, less often, pyroclastic flows and lava. They are also subject to much larger, less frequent but catastrophic cone collapse, giving rise to large debris avalanches, debris flows and mud flows.(Palmer, Alloway and Neall 1991). Sector collapse, similar to that seen at Mt St Helens in 1980 (Schuster, 1983) is inferred to have happened numerous times at Taranaki and Ruapehu. Some original field work (Prebble, 1967) and current research (LeCointre, Neall, Wallace and Prebble in press) indicate that similar events are also characteristic of the Tongariro volcano, affecting in particular the north-western summit, cone and ring plain. Some debris avalanche and debris flow deposits from the region are shown in Fig. 3 and the geomorphology of the volcano in Figs 4a and 4b. Modern, smaller debris avalanches and flows caused by the collapse of hydrothermally weakened ground along fault scarps in the Hipaua geothermal field (Fig. 2) high above Lake Taupo, have happened twice in the last 150 years. These clay rich flows overwhelmed local villages. Prehistoric debris flow deposits are also found in the Tokaanu area (Figs 2 and 3).

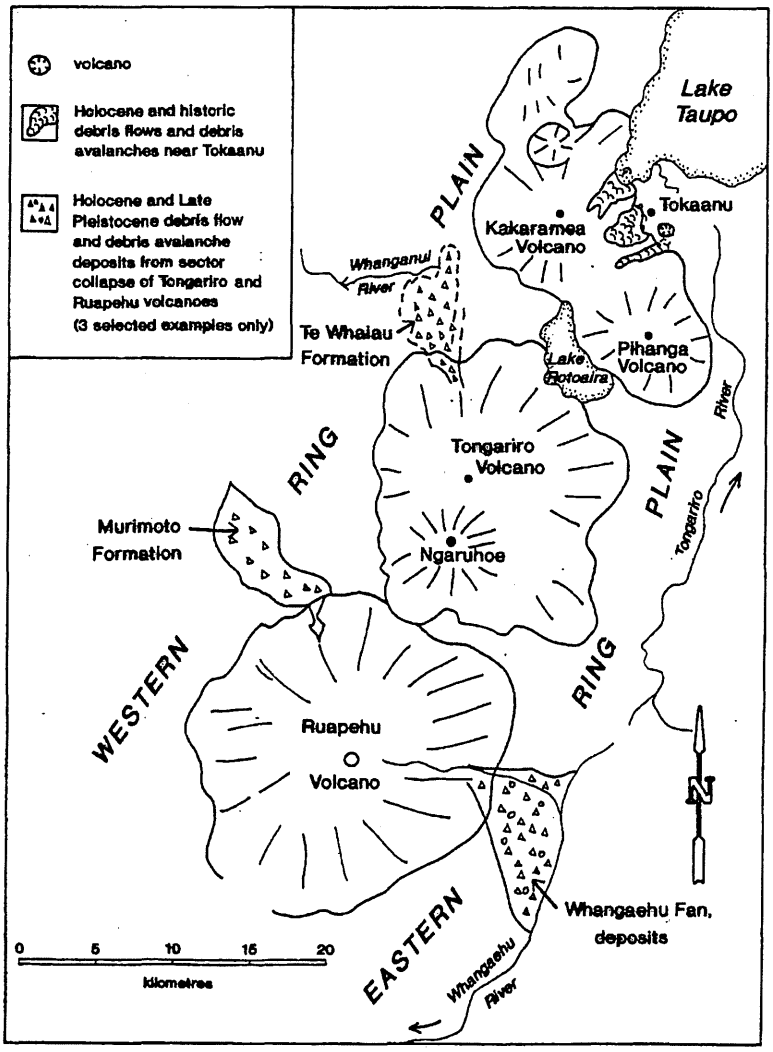

Figure 3. Selected debris avalanche and debris flow deposits in the Tongariro Volcanic District, southern Taupo Volcanic Zone. The Te Whaiau Formation and 2 other large, more recent (Holocene) debris avalanche deposits are shown. The Holocene and historic debris flow deposits from the Kakaramea Volcano behind Tokaanu are also shown.

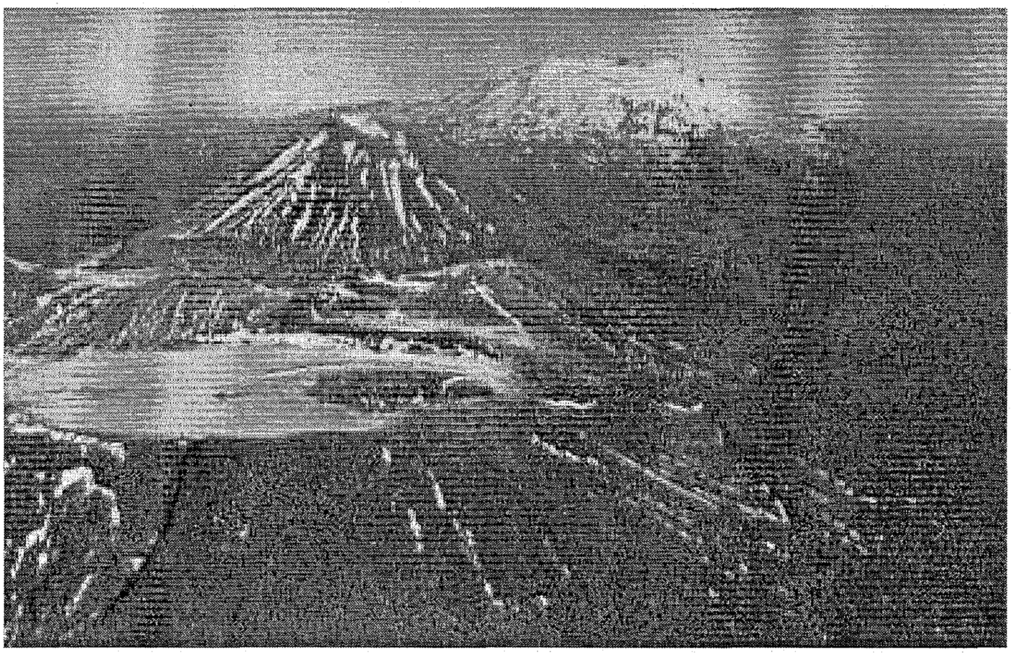

Figure 4a. Aerial view of Tongariro Volcano from the North. The flat-topped North Crater in the foreground lies in front of the old altered massif of the summit of Mt Tongariro, considered to be the remnants of the source area for the Te Whaiau Formation. A model derived from this view is shown below in Fig. 4b.

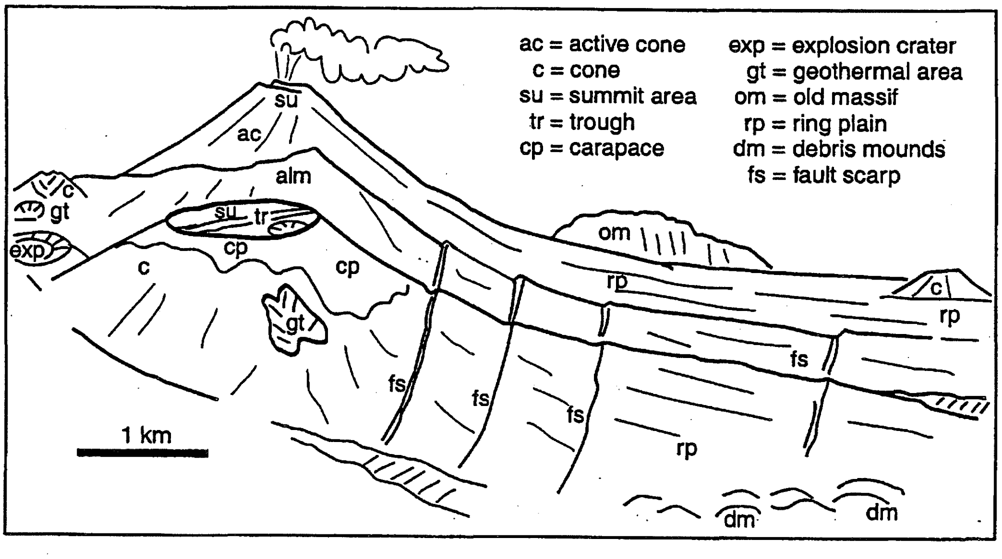

Figure 4b. Geomorphic elements of a complex andesite volcano. This model is based upon the Tongariro volcano, illustrated above in the photograph, Fig.4a. Note that "alm" in the figure represents the altered massif of the old Tongariro volcano.

The Te Whaiau Formation (Figs 2 and 3) is a cohesive debris flow deposit, which originated from a massive debris avalanche on Tongariro volcano. This example shows the value of a regional approach in which field mapping and geomorphology were combined in order to clarify of the origin, nature and distribution of the formation. This was critical to the Power Development in two ways. Firstly the formation provided a foundation for 2 dams displaced for geological reasons from their original sites during excavation. Secondly it marks a major debris avalanche and debris flow event which could happen again.

The Te Whaiau formation was first recognised at Otamangakau and Te Whaiau (Fig. 2) and informally named the blue-grey clayey silt formation (Prebble, 1967). At the time it was seen as being strangely out of character with the alluvial soils and tephra deposits with which it is interbedded in the ring plain. Of particular note were the angular fragments of hydrothermally altered andesite, the blue-grey clayey matrix, the breccia like texture and the low mounds of debris, which the deposit formed. These contrasted with the outwash fans, terraces and swamps which surround them and led to the conclusion that the formation was a debris flow deposit from a violent phreatic eruption of Tongariro volcano (Prebble, 1967 and 1969a). Other volcanoes in the area are not hydrothermally altered and were discounted as a possible source. Moreover, fieldwork at the time on Tongariro revealed several exposures of altered material within the old massif of the volcano. Geothermal activity at Ketetahi and Red Crater supported the notion of a hydrothermal origin and an eruption involving water, giving rise to the debris flow. From the point of view of the geological model at the dam sites this theory reinforced the picture of an irregular, thick layer of the impermeable blue-grey clay overlying deeper alluvial deposits of the ring plain. This was important to the determination of founding levels for the dams and the containment of the reservoirs.

A problem at the time of investigation was the presence of "gravel lenses" encountered by the drillholes within the clayey silt. Unlike the permeable artesian gravels beneath the clayey silt, these "lenses"were fairly impermeable and did not appear to have any hydraulic connection outside the clayey silt as determined by the testing programme. However they remained a concern, from a possible leakage point of view. An explanation was eventually provided by the logging of the foundation and core trench (Prebble and Dow, 1969). Large blocks of bedded, compact, andesitic clayey gravel and fragile very weak conglomerate, up to 10m across, were exposed by the excavation. These are megaclasts, rafted along in the debris flow from a source higher up on the volcano. Easily disaggregated, they probably gave rise to the gravel lenses encountered during the drilling.

I hold the conviction that this example highlights the merits of regional engineering geological mapping, in this case up to 15 km from the dam sites but driven specifically by the need to understand the geotechnical setting of andesite volcanoes and their ring plains. Moreover, a comprehensive approach to data collection, including geomorphic data, was vital to success. Further, investigation never stops and the logging of excavations during construction was part of the feedback necessary to answer questions posed at an earlier stage – in this case the mysterious gravel lenses.

This deposit was renamed the Te Whaiau formation (Prebble, 1995a) and has been reviewed in the light of volcanological knowledge gained since the power development investigations of the 1960s. This current study (LeCointre, Neall, Wallace and Prebble, in press) confirms that the Te Whaiau Formation is a single, massive volcaniclastic deposit interbedded within gravelly and sandy sediments of the north-west ring plain of Tongariro volcano. The approximately 0.5 km^3 clay-rich, matrix-supported gravel has lithologic and physical properties that are typical of a cohesive debris flow. Clays in the matrix are derived from hydrothermally altered andesite lava, breccia and tuff. Distribution of the deposit and the clay assemblage suggest a source area in the vicinity of the present Tongariro summit. Most of the proximal part of the deposit is buried under a carapace of late Pleistocene lavas forming the north-western summit (North Crater) and flank of the mountain. Further out on the ring plain the medial and distal lithofacies are exposed, especially in new roads cuts of SH 47, and include large volcaniclastic megaclasts (Fig.5) like those seen over 30 years ago in the dam excavations. Other very large clasts include blocks of fractured andesite. These megaclasts show that the matrix was very supportive of large fragile blocks and is very thick, filling in stream channels and shallow gullies. Small hummocks are present only at the distal end of the deposit. These features suggest that the Te Whaiau Formation has been emplaced by a fluid-saturated debris avalanche that changed into a clay-rich debris flow which was stopped at 15 km from source by elevated terrain across large boundary faults of the Taupo Volcanic Zone.

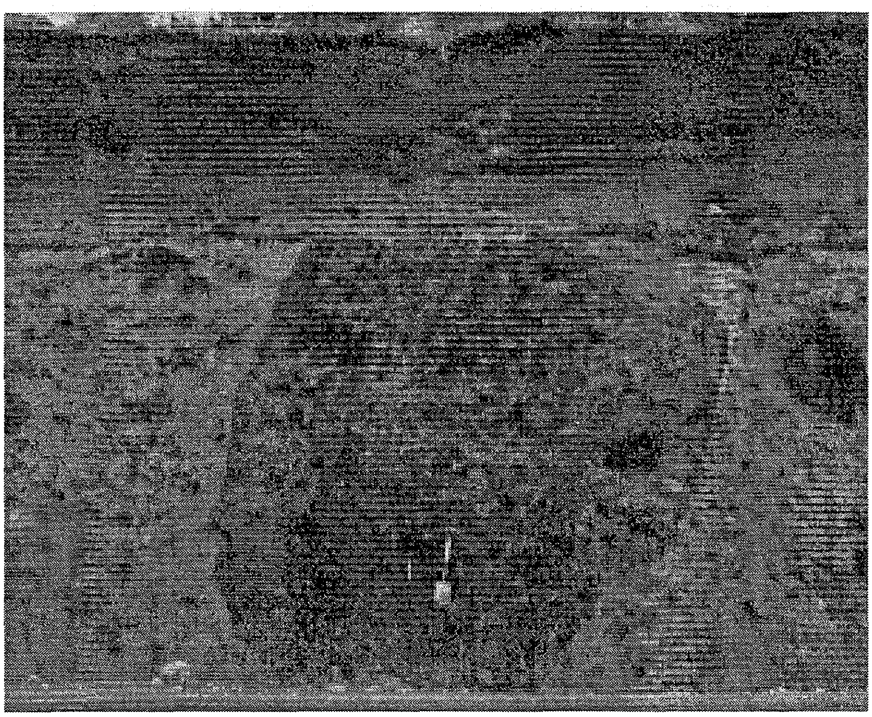

Figure 5. Te Whaiau Formation cohesive debris flow deposit exposed at the side of State highway 47. The large dark block in the centre with the spade for scale is a megaclast of compact andesitic gravel, with the bedding now tipped up almost to the vertical. The megaclast is supported in the clayey matrix gravel, which makes up most of the formation. The covering beds of volcanic ash lie on top of an erosion surface cut across the Te Whaiau Formation.

Stratigraphy of the cover beds and dates on an underlying lava flow indicate that the Te Whaiau Formation was emplaced between 55 and 60 ka. Jigsaw- fit fractured volcanic bombs suggest that an explosive eruption through hydrothermally altered rock and pyroclastics of the summit geothermal field triggered a deep-seated slope failure of a massive sector of the proto-Tongariro volcano to form the initial avalanche. Since then the new carapace of North Crater has been built up over the geothermal field and part of the deeply altered old massif, thus perpetuating the conditions for instability. A sequence of tephras, loess, paleosols and debris deposits in the ring plain overly the Te Whaiau Formation and indicate continuing activity and cone building since the collapse, which created the deposit. The lack of a distinctive head scarp in the source area indicates that the initial scar and pull away have been either eroded away or buried by younger lavas or destroyed by subsequent eruptions. It appears that younger lavas now conceal the head of the old slope failure. A well-developed trench across the surface of the North Crater of Tongariro may be an incipient pull away zone for the next sector collapse.

By international standards the Te Whaiau Formation is relatively small volcanic mass flow deposit. The lithology and geometry of the formation reflect high mobility of the initial saturated avalanche, rapid transformation of the avalanche into a clay-rich debris flow and preservation of the carrying capacity of the slug-like flow to at least 15 km from source.

Devastating avalanche –induced debris flows must be considered a potential volcanic hazard for the north-west ring plain of Tongariro.

Altered and faulted andesitic massifs

The andesitic massifs of Kakaramea and Tihia volcanoes lie in the centre of the Taupo Volcanic Zone rift, south of Lake Taupo (Figs 2 and 6). The form of these volcanoes has been much modified by erosion, faulting and graben development into a series of step-like scarps and benches.

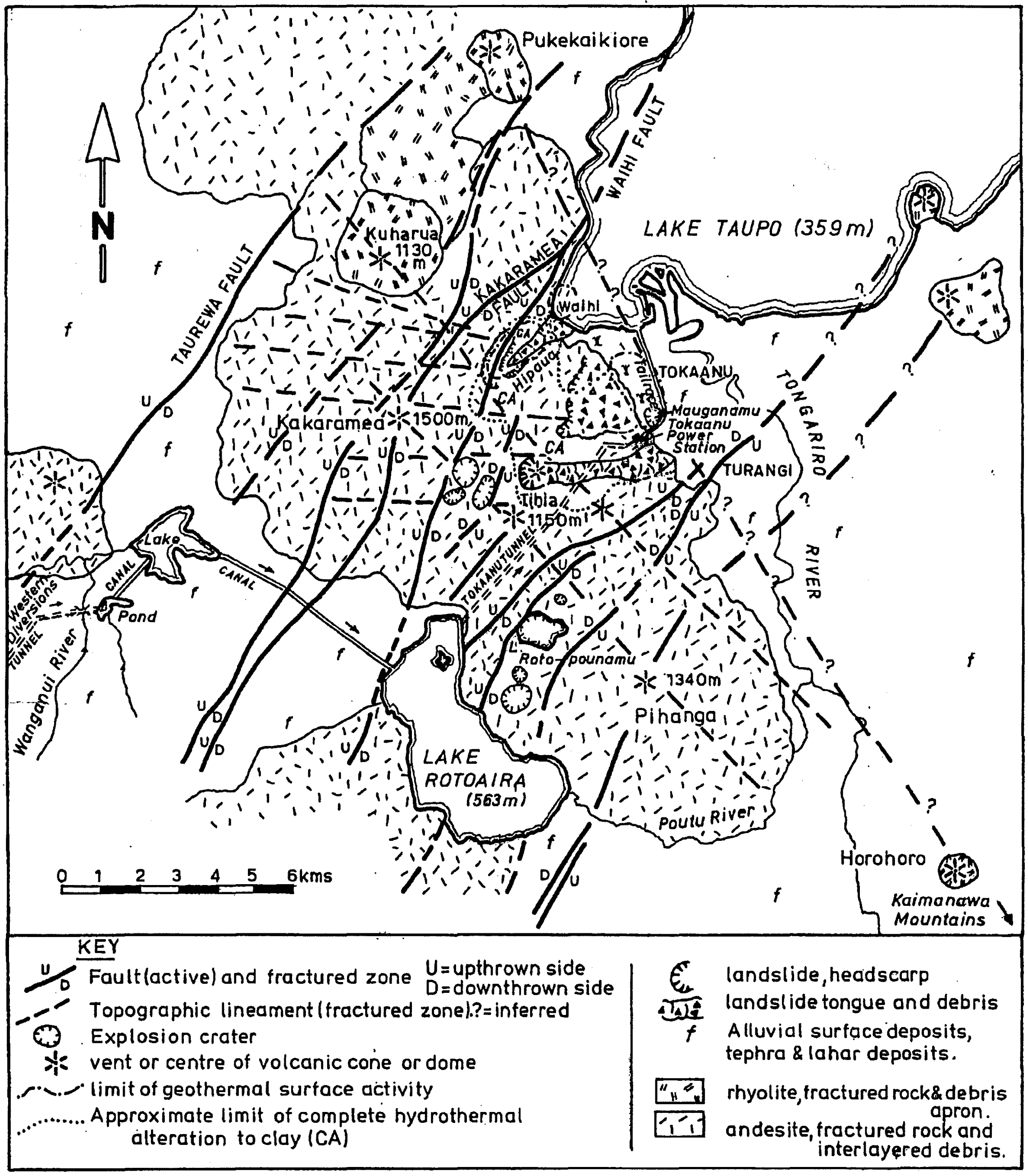

Figure 6. Geology of the faulted andesitic massifs of Kakaramea and Tihia volcanoes, in the centre of the Taupo Volcanic Zone, south of Lake Taupo.

In addition to the youngest NNE striking faults of the Taupo rift, several other sets of faults and fractured zones are inferred from the geomorphology and were confirmed by ground conditions in the Tokaanu Tunnel. The northern part of Tihia is extensively hydrothermally altered. A thick ash cover, weathering, alteration and dense mature forest cover meant that considerable reliance had to be placed upon geomorphic interpretation of aerial photographs and comparison with other volcanoes in the region.

The Hipaua geothermal field is situated along the zone of the Waihi Fault (Fig 6), in steep unstable ground 500m above lake Taupo. Thermal activity is concentrated along 1 km of the fault scarp where it is intersected by E-W and NW-SE trending topographic lineaments. The latter lineament is defined by breaks in slope, saddles, small andesitic cones, a rhyolite dome and stream directions. It can be followed into the Kaimanawa Mountains as a series of co-linear streams, saddles and valleys, which probably follow a large fractured zone. Similar evidence for the fracture control of geothermal fields north of Taupo is presented by Wan Tianfeng and Hedenquist(1981) and also by Hamlin and Prebble(1998). Where the major NW-SE lineament was intersected in Tokaanu Tunnel, a 1 km wide zone of soft extremely weak smectite clay was encountered with some very closely fractured and altered rock, crushed zones, gouge, water inflows and temperatures of 27 to 40°C (Prebble, 1977 and 1986). The smectite clay made up 50 to 80 % of the ground and caused severe swelling in the 1km long section of weak material.

The lineaments were interpreted as fractured zones and possible faults. The NW-SE lineament along the foot of the volcanoes coincides with the Tokaanu and Waihi geothermal fields and crosses the Tokaanu Power Station and tailrace canal. High groundwater temperatures were found beneath the tailrace excavation where it is crossed by the lineament. Investigation drillholes met water at 100°C at 30m depth and "played"as geysers to about 30m above the ground. Situations such as that raised the possibility of hydrothermal eruptions as a consequence of removal of lithostatic or hydrostatic load.

The tailrace design was considerably modified, with a raised invert, reduced lining and increased width.

Most of the north-east slopes of Tihia behind Tokaanu and Waihi show signs of slope failure (Figs 2 and 6). Long sinuous tongues and shorter lobes of hummocky slope are more or less ubiquitous, except for the penstocks ridge which is considered to be in place. The penstocks are founded on ribs of fractured andesite. In the case of the bottom rib beneath anchor block 1 and the rear wall of the power house the rock is also very seamy with a network of soft clay seams and gouge. The ribs are surrounded by firm to stiff clay, a fairly uniform residual andesitic soil mass derived from alteration of lava, breccia and rubbly scoria. Reference to the exposures on the Tongariro volcano (Fig. 7, for instance) clarified the origin of the formations at Tokaanu through a careful textural and stratigraphic comparison at a range of scales.

Large curved landslide scarps and slide blocks are found along the Waihi Fault scarp (Fig.6) where alteration has weakened the ground. The landslide area covers up to 12 km^2 and extends up to 500m above Lake Taupo. Historic landslides in 1846 and 1910 originated as massive failures of the fault scarp in the geothermal field and culminated in debris avalanches and debris flows which engulfed the lower slopes south of the present Waihi village. The debris forms a huge fan, which protrudes out into the south-west corner of the lake. Very soft, extremely weak clayey deposits are found in a broad zone for 2 km along the Waihi Fault scarp where it coincides with the Hipaua geothermal field. Above this zone, tension cracks several m deep and some up to many m wide were recorded in the andesite flow rock mass and breccia along and parallel to the top of the fault scarp (Prebble, 1986). The soft clay and thermal activity are directly below. Continuing retrogressive failure of the scarp is to be expected. Elevated topography and permeable ground above the continuing thermal activity will presumably maintain a groundwater supply and significant pore pressures in the extremely weak clayey materials.

Complex rotational-translational slope failures and debris flows are postulated for this area and seem to be compatible with the eye witness descriptions of the 1846 and 1910 landslides (Prebble, 1986).

Similar but older landslide masses make up most of the slopes behind Tokaanu and on either side of the penstocks and power station. The head of this broad landslide zone is the edge of the Mt Tihia summit plateau and graben in which there are at least 4 shallow explosion craters. One of these is breached by a slope failure, which sent a clay-rich debris flow of very soft altered material down the slope a few hundred metres south of the power station. This deposit is very similar in content to the Te Whaiau Formation but is a smaller event and much younger. It possibly flowed down the slope in the last 1000 to 2000 years. During power project construction of roads and spoil dumps small slope failures were initiated on either side of the penstock slope.

The selection of a tunnel route and power station site in the Kakaramea-Tihia altered and faulted massif poses several challenges for hazard identification and assessment. Lying right in the centre of the TaupoVolcanic Zone active rift, it is in particularly hazardous terrain. The tunnel route avoids active faults, grabens , explosion craters, landslides and geothermal fields. Even so it encountered hot swelling ground (Prebble, 1977). The power station faced a very restricted choice of possible sites and narrowly avoided the hazards referred to except for geothermal activity, which forced a change of design for the tailrace (Prebble, 1969b).

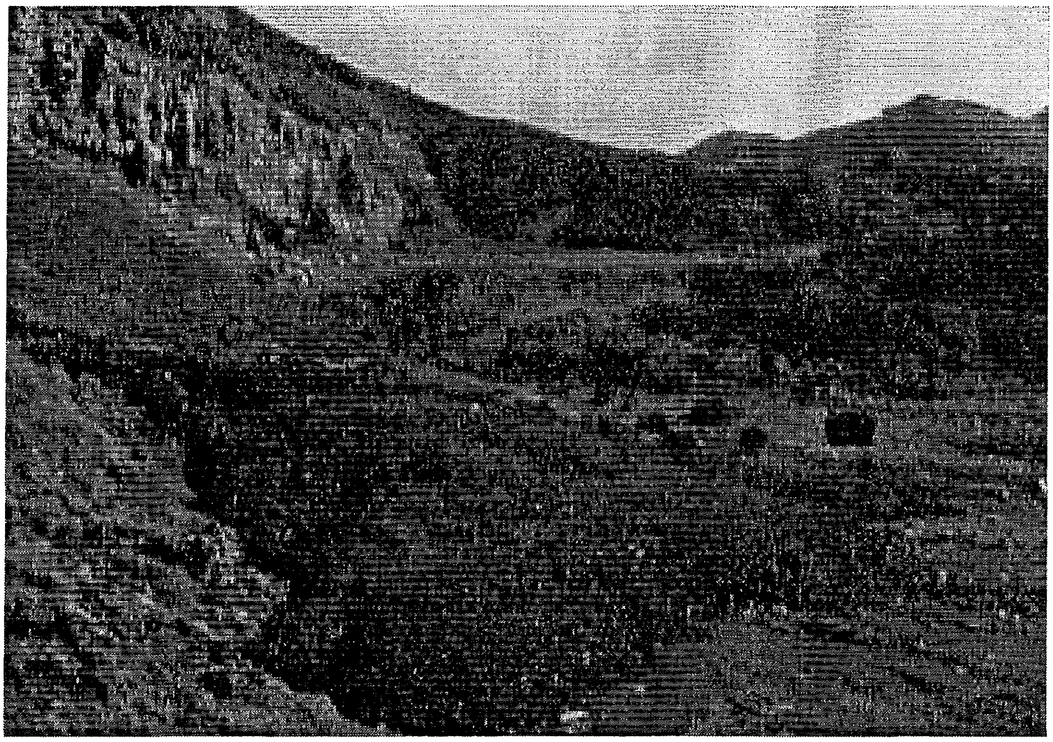

Figure 7. A reference locality for an engineering geological model of andesitic deposits, at the base of Ngauruhoe volcano in the head of the Mangatepopo valley. A fractured rock tongue (lava flow) is exposed at top left. Scoria rubble covers lava flows to the right. Avalanche debris and reworked alluvial deposits are seen in the foreground.

In the Tokaanu area, accurate geomorphic interpretation was essential to hazard identification and assessment Recognition of volcanic facies through a mask of intense alteration was an important step towards distinguishing landslide deposits from in-situ ground. Regional geological information and a detailed knowledge of the range of facies that could be met came only with experience of the volcanoes to the south, in particular Tongariro. Figures 4 and 7 are examples of reference localities, which were used for information on andesite volcanoes.

Landslides are present in other geothermal areas and altered ground further north in the Taupo Volcanic Zone. There are some similarities to Tokaanu, for instance at Te Kopia where the Paeroa Fault scarp has generated large debris avalanche deposits from thermally altered ground and active thermal areas, including the current geothermal field. At Orakei Korako (Figs 8 and 9), thermal activity and alteration have generated earth slides, slumps and earth flows at the head of a slope which steps up progressively across several fault scarps. Facing similar constraints to the Tokaanu area because of lack of exposure, the interpretation of the geomorphology and geology, especially of faulting, landslides and geothermal features was achieved here by remote sensing (Hamlin and Prebble, 1998).

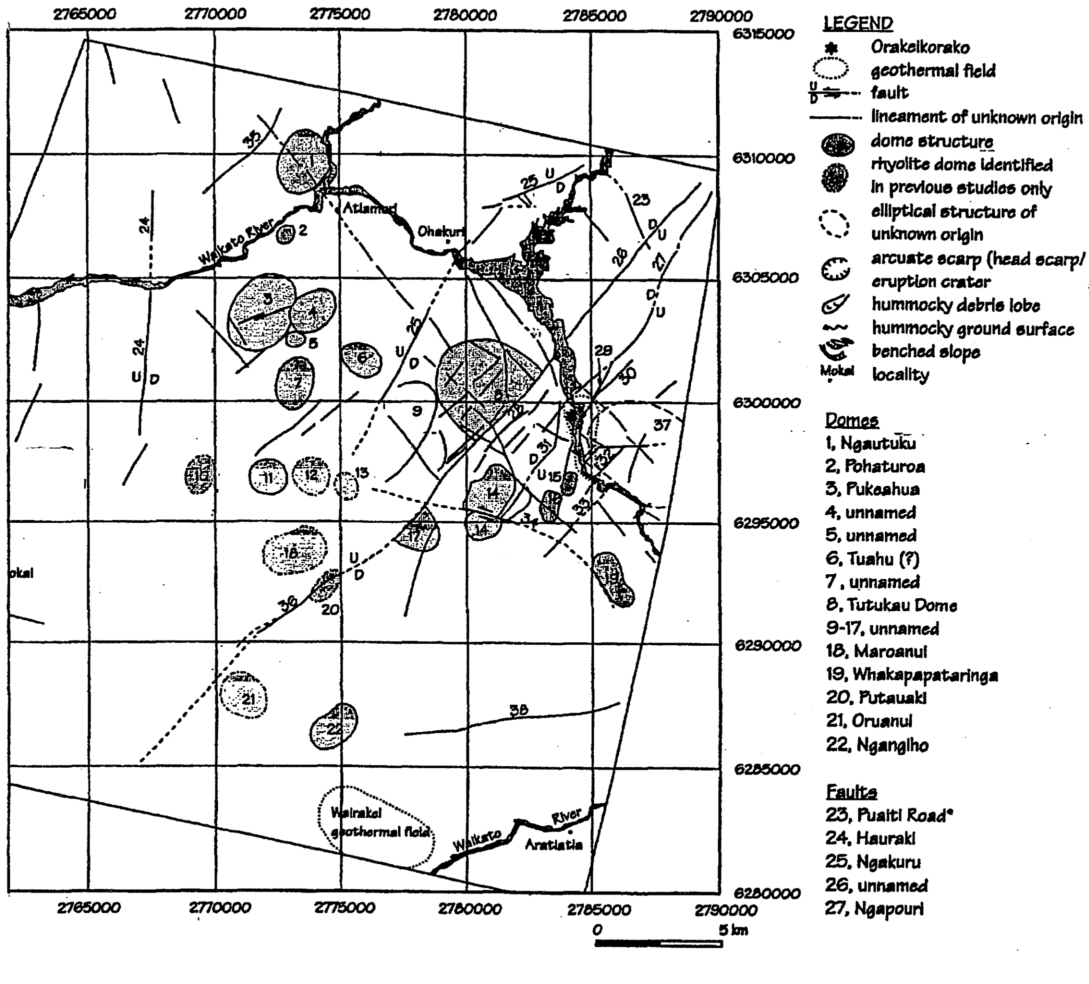

Figure 8. An example of an interpretative map of regional geomorphic features produced from remote sensing. This is the main part of a map for the Orakei Korako – Atiamuri area, Taupo Volcanic Zone, by K. A. Hamlin, from Hamlin and Prebble (1998). Legend continues alongside Figure 9, on the next page.

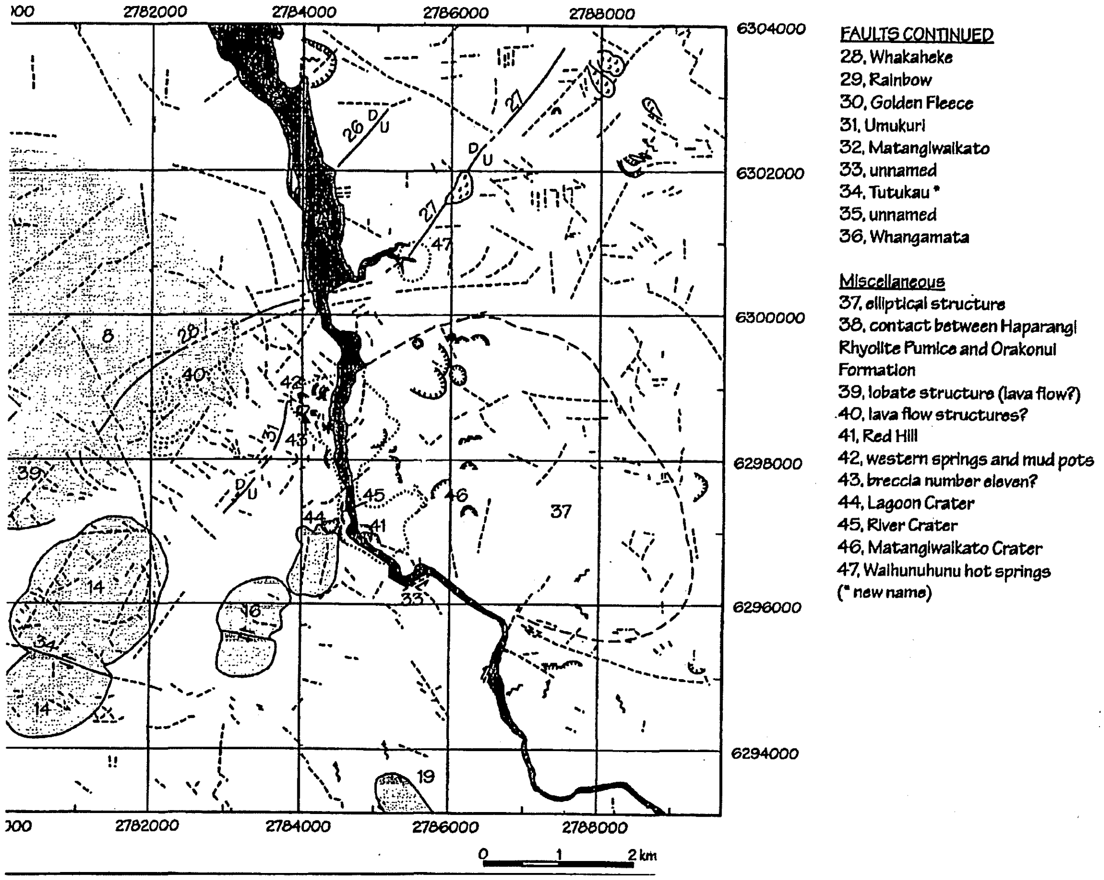

Figure 9. An example of an interpretative map of local geomorphic features for the Orakei Korako area. This is the main part of a map produced from remote sensing by K. A. Hamlin, from Hamlin and Prebble (1998). Note that the Legend is a continuation from alongside Figure 8, back on the previous page.

Earth slides and flows from ignimbritic plateaus and terrace remnants.

Events in the Bay of Plenty twenty years ago demonstrated the potential for instability in ignimbritic soil masses of rhyolitic composition in certain situations, such as elevated terrace remnants. Topography at the edge of the volcanic plateau, in the Bay of Plenty, is characterised by numerous slender, steep-sided, finger-like terrace remnants. Similar features are found also in the Auckland region, adjacent to the main estuaries and harbours. Each remnant belongs to a formerly more extensive terrace constructed from a series of either pyroclastic flow deposits or tephra and pyroclastic material which has been eroded and then redeposited. The deposits are of 2 main types, interlayered with each other: thick, irregular, undulating layers of rhyolitic sand, pumice and breccia and thinner intervening layers of very soft to stiff clay. Plaeosols are often found at the top of the clay layers. Considerable physical variation exists: lateral changes in strength, abrupt vertical changes in grain size and soil type and a wide variation in water content. Figures 10a and 10b illustrate soil mass conditions typical of the Ruahihi area and are broadly applicable to other places with irregular, undulating and interbedded layers of coarse and fine soil masses. These are consistent with a series of buried topographies or paleo-topography, each of which is marked by discontinuous faint paleosols at the top of the fine clayey layers.

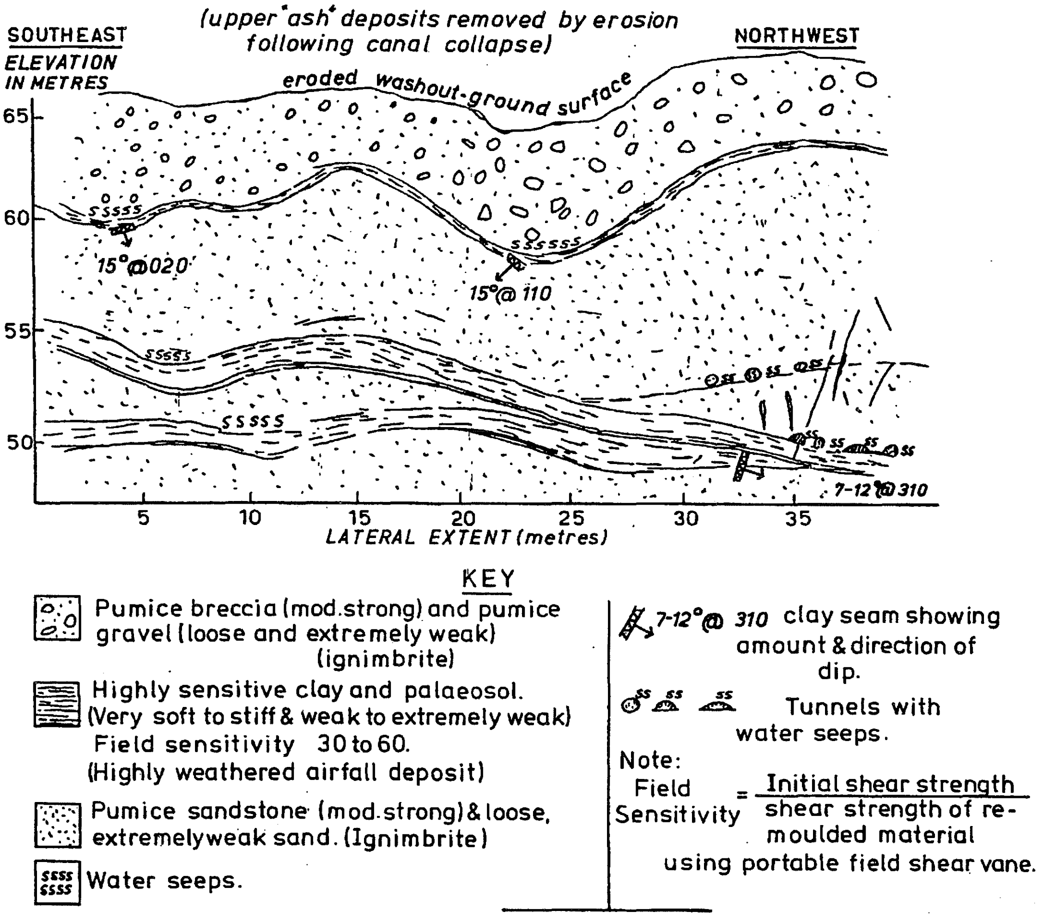

Figure 10a. Elevation sketch of a portion of in-situ ground beneath the Ruahihi Canal washout. The exposure is a vertical face located in the deepest part of the centre of the main gully, which formed immediately after the collapse of the canal. Undulating, irregular layers of sensitive clay overly rhyolitic pumice sand to sandstone. A photograph of this exposure appears below in Fig. 10b.

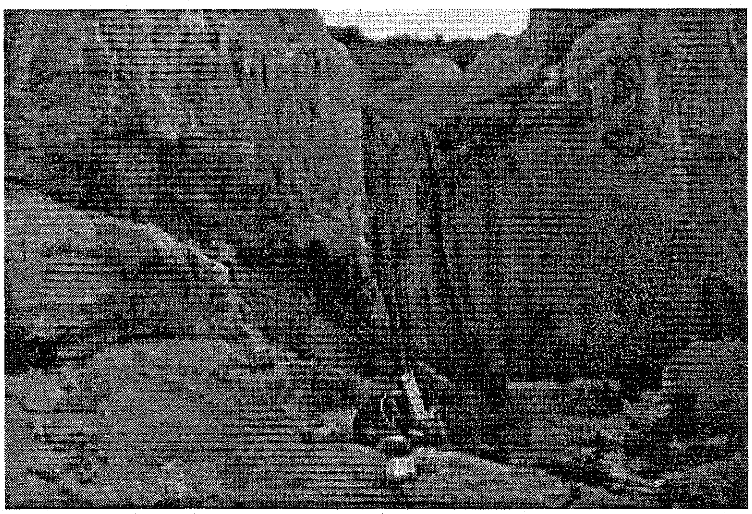

Figure 10b. Moderately strong rhyolitic pumice sandstone, sand and extremely weak, highly sensitive clay layers exposed beneath the Ruahihi Canal collapse. A laminated sensitive clay layer dips down to the right in the middle distance. This exposure is also illustrated above in line drawing Fig. 10b.

Successive periods of eruption and deposition followed by erosion and weathering are envisaged to have produced this valley-in-valley form and the sensitive clays. In these non-welded deposits the open porous fabric of rhyolitic pumice and the soils derived from it have a potential for holding water and for some collapse. Weathering would produce clays and a delicate very porous microfabric similar to that found in some thermally altered deposits. Delicate and open fabrics have a high potential for collapse, water release and flow.

At Ruahihi for instance, many soils have low density, high porosity, high sensitivity and a potential for collapse and flow. Ranges of water contents exceeded liquid limits and field shear vane sensitivities of 30 to 60 were common. Even after several months of drainage water was still flowing out of natural pipes at low points in the sands above the clays. This situation led to the notion of a series of perched, confined, superposed ribbon aquifers. This is a consequence of the paleotopography, which involved superposition, deposition, erosion and weathering – repeated several times over to make up the deposits of each terrace.

Springs are found issuing from the base of blind gully head-walls and side-walls at the low points in the paleosols. Hummocky ground and mounds are often found some distance downslope. These features are indicative of very mobile fluid slide-flows in the sensitive layers and have been identified in the area around Ruahihi, elsewhere in the Bay of Plenty, and at a number of places in Auckland such as the upper Waitemata Harbour, Manukau lowlands and Beachlands. Similarly sensitive rhyolitic materials of a residual hydrothermal alteration origin at Orakei Korako are thought to have encouraged large block slides.

The key to understanding these slope failures at Ruahihi and Auckland was provided by detailed mapping of exposures, which revealed the succession of paleotopographic surfaces, ribbon aquifers and sensitive clay layers. Combined with the subtle geomorphology of the terrace remnants, this suggested a slide-flow model for failure of the soil masses. At Orakei Korako, detailed geomorphology, outcrop logging and alteration mineralogy are providing a deeper understanding and a useful model as part of a current study.

Deep seated topples in the southern East Coast Deformed Belt

Toppling has been known for some time in scarp slopes (anaclinal slopes or "back slopes"). However it also happens in dip slopes, in particular cataclinal underdip slopes in which the dominant, pervasive defects dip in the same direction as the slope but a steeper angle. Traditional wisdom would suggest that these slopes are inherently stable and more or less self- buttressed against failure. Such is not the case. This came as a surprise and was only discovered by a very comprehensive programme of regional and detailed engineering geological mapping over a very large area, coupled with a study of stereo-pair aerial photographs.

Thirty-six dip slopes in Marlborough were studied, initially for their apparent stability compared to other areas of the East Coast Deformed Belt. Only 4 rock slides were found, in areas of more gently dipping limestone. There are also many relatively surficial earth and debris flows across all rock types, including shales.

The strong limestones are non-porous materials with an interlocking mosaic of microscopic grains of calcite and quartz whereas the very weak shales are slightly porous with a continuous "turbulent"network of clay microaggregrates wrapped around microscopic grains of calcite.

The relationship between rock type and defects to slope failure was described by Prebble (1995b and 1996) and is summarised in Table 1. Rock type, defects and geomorphology were mapped over an area of 120 km ^{2}. Some of the 36 slopes showed scarps, benches, screes, mounds and a few ravines with lodes extending downslope from them. (Table 1.).

Table 1. Relationship of rock type and defects to slope failure in Marlborough

Rock type Rock mass	Dominant Defects	Slope Failure	Subsequent Slope Movement	Topography
Strong limestone, tabular rock mass	Crush zones. Extremely closely spaced fractures. Dips 30° to 80°. Slope angle less at 15° to 42°	Overtopples (flexural and block flexural, complex, leading to rock mass bulging)	Stony debris flows. Rock fall and screes Debris avalanche	Convex slope, uphill facing scarps. Bulges, screes. Ravines with stony debris flow lobes. Debris aprons below
Strong limestone, tabular rock mass	Crush zones. Extremely closely spaced fractures. Dips 15° to 25°, parallel to slope.	Rock slides	Debris flows from toe	Head scarps Block fields Pull away zones, ponds and swamps
Very weak shale. Fissile rock mass to clay gouge soil	Wide clayey crush zones	Debris flows	Debris flow	Stream-like and glacier –like lobes.

Close examination revealed that the scarps were reverse (facing uphill). Other important differences from the usual forms of slope failure then emerged such as a head bench instead of a steep head scarp, a convex and slightly bulging main body instead of a concave and depleted one, and the absence of an override zone or bulging toe. It was clear that some form of mass movement had taken place in these slopes. Detailed mapping showed that the bedrock was very disturbed and dilated and had been bent over towards the valley in the middle of the convex and bulging part of the slope. Deep and very unstable ravines down the middle of a few slopes gave critical data on the detail and depth of the bending over of the tabular limestone rock mass. From that information the model of toppling and over-turning of the rock mass was developed. Toppling has also been reported in cataclinal underdip slopes by Cruden and Hu (1994).

Using geomorphology to compare slopes without ravines or sufficient exposures, it was concluded that 32 cataclinal underdip slopes showed evidence of deep seated toppling. The term "overtoppling" was put forward (Prebble, 1996) as a way of distinguishing this variety of toppling from the commonly observed modes in scarp slopes (anaclinal slopes). The toppled masses extend to 50m deep and are in the order of 1 km^2 in area. Rock above the bending surfaces varies from coherent masses to chaotic debris. Considerable dilation and loosening has reduced mass strength to that of coarse gravel. As a result the toppled masses are subject to debris flow and to collapse as catastrophic rock and debris avalanches.

An example of overtoppling is given in Fig.11. Age and recurrence of toppling and collapse are not well constrained. Stratigraphy in the run out area for debris avalanches indicates that a large collapse took place in the last 3500 to 5000 years. Successive aerial photos show that the ravine discharges significant debris flows every 50 years. These are sufficiently large to carry through to the river 1 km below. Comparative geomorphology indicates that the scarps on the bulge may be 100 to 500 years old.

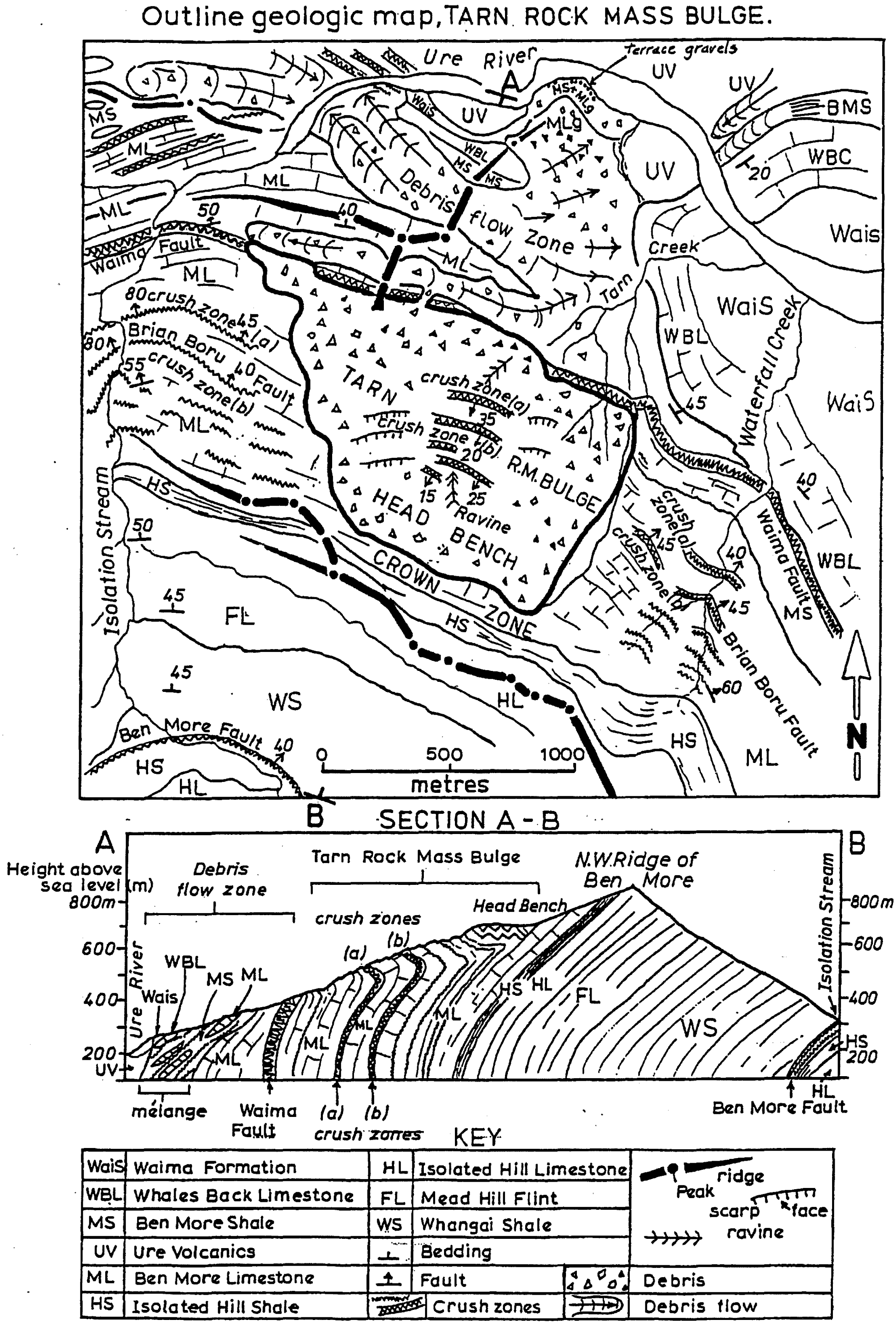

Figure 11. An example of an overtopple. The Tarn slope failure – a rock mass bulge in Marlborough.

Recognition of overtoppling in Marlborough testifies to the value of comprehensive geotechnical field mapping and remote sensing, at a range of scales, over a large area of common tectonic and lithologic character.

Mountain Range collapse in the greywackes of the SouthernAlps

Recognition of toppling in Marlborough led to a search for similar features in the Southern Alps and in particular an examination of scarps described as ridge rents and gravity faults (Beck, 1968). Two areas have been visited, Arthur's Pass and Mt Cook. Each is complex, with major active faults. Possible splays of these faults could also be present. Although the rock at each area is referred to as greywacke, some of it is low-grade schist.

Large uphill facing scarps are seen around Arthur's Pass and are particularly well developed on the Kelly Range, 15 km north of the Pass and near the acute intersection of the Alpine and Hope Faults. Uphill facing scarps in this area may be attributable to faulting and subsequently to toppling. Some are probably the direct result of toppling. A considerable amount of fracture dilation on the Kelly Range, up to 1m in places, indicates significant ridge top cracking and therefore ridge crest spreading. Toppling is seen on both sides of the range and is associated with deep ravines, screes and highly unstable edges to the ridge crest. A major difference from Marlborough is the well-developed glacial topography which has left deep, steep sided valleys and high level benches, now unsupported that the ice has gone.

Spectacular uphill facing scarps can be seen on the Sealy Range above the Hooker Valley and near Mt Cook village. Some of these have trapped bogs and ponds behind them such as the famous Sealy Tarns. Toppling on this scarp slope (anaclinal slope) has produced a series of scarps on the side of the ridge, which is a sloping bench and was previously referred to as the Sealy Tarns rock mass bulge (topple complex) by Prebble (1995a) and is shown in the map on Fig.12. This bench terminates along the side of the ridge, in a deep ravine with a large fan below it. Several bending surfaces and progressive block toppling are exposed in the ravine (Fig. 13). The other side of the range is, at least in part, a cataclinal slope and is occupied by a large, chaotic, slide-topple complex (Fig. 14). This was referred to in the 1995 account as the Mt Ollivier rock mass bulge. One scenario for geomorphic development suggests that the ravines are the sites of previous collapses and that the Sealy Tarns bench will be the next bulge to fail. Failure can also be take the form of combined sliding and toppling as seen on the Mueller Glacier side of the range. The two styles of failure combine to produce mountain range collapse.

The uphill facing scarps are compatible with a flexural toppling mode, but the multiple bending surfaces seen in most of the topples suggest that complex toppling modes are involved. Multiple block toppling, block-flexural toppling and collapse mixed in with toppling should all be considered.

Firm conclusions cannot be drawn at this stage but it appears that the role of toppling in mountain range collapse in the Alps may be very significant. It could also be that deep-seated toppling is a realistic alternative to the gravity faulting mechanism proposed by Beck. Toppling does not require either the double-sided, symmetrical aspect of his model or the very deep gravity faults, which Beck proposed through the base of the mountain ranges.

Most of the toppling is asymmetric and very messy. One particularly large toppled mass of 20 km^2 with a very intricate and wavy pattern of uphill facing scarps and some very large chaotic block fields has been identified in greywacke and schist west of Arthur's Pass. Large ruptures and a collapse in the centre of the toppled mass have left a deep broad ravine. This enables an estimate to be made of the volume of the topple, which is around 1 to 2 km^3.

In all these examples, remote sensing with stereopair vertical photos and field mapping at a range of scales were used to identify tectonic features and slope movement. Mapping included lithologic, structural, geomorphic and geotechnical criteria.

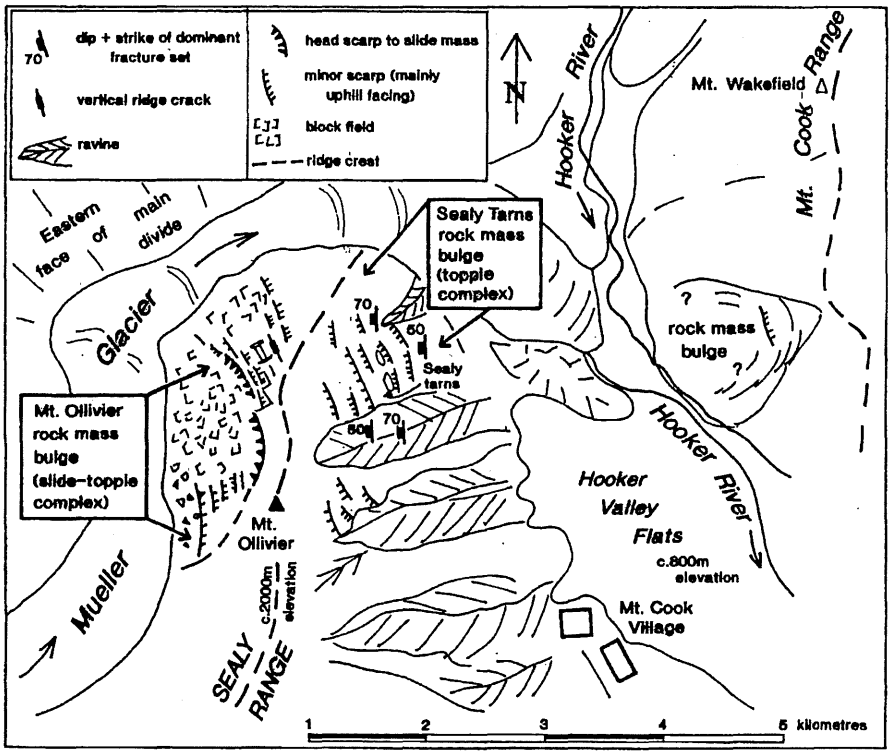

Figure 12. Map of the Sealy Range, showing large complex topples at the Sealy Tarns and below Mt Ollivier. Referred to as rockmass bulges by Prebble (1995a).

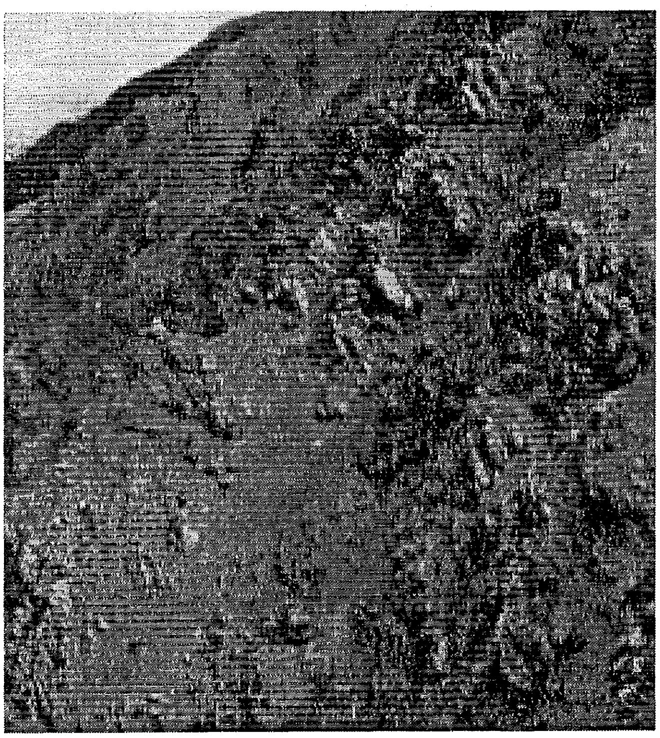

Figure 13. Toppling in closely fractured and crushed greywacke, adjacent to the Sealy Tarns, Mt Cook National Park. Exposed face is a few hundred m high. Deep gullying cuts through the dilated and toppled rock mass, 700 m above the Hooker Valley.

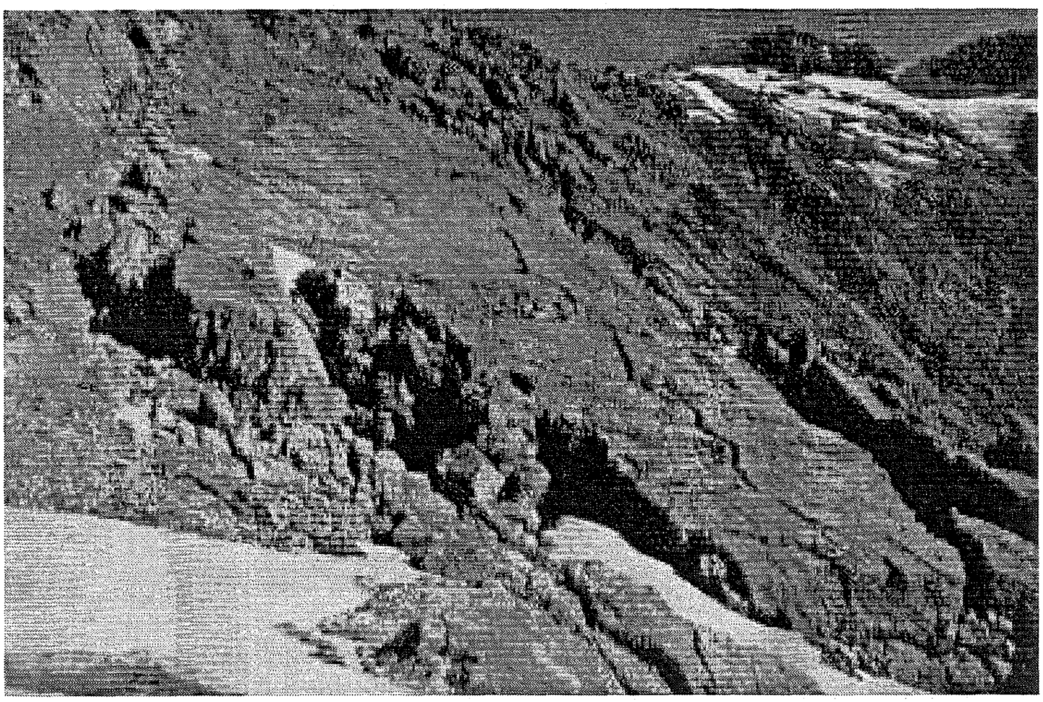

Figure 14. A topple – rock slide complex on the Sealy Range, above the Mueller Glacier, Mt Cook NationalPark. Open ridge cracks, fracture dilation, uphill facing scarps (these are dark and in the shade in the photograph) and secondary block sliding are found in this complex slope failure. Further downslope to the right is a block field of chaotic rock fall debris.

Block slides in weak rock terrain

During the last 25 years it has been recognised that in weak sedimentary rock, generally of late Tertiary age, bedding parallel clay seams and crush zones give rise to block and debris slides. Originally known mainly from events such as the Abbotsford Slide in Dunedin (Coombs and Norris, 1981) these seams were once considered to be "unique" in terms of New Zealand experience (Gallen, Beca, McCraw and Roberts, 1980). However these clay seams have been identified as basal rupture surfaces to landslides in many other localities of geotechnically similar rock masses such as the Rangitikei Valley (Stout 1997, Thompson 1981, Prebble 1995a), Hawkes Bay (Pettinga, 1987) and Auckland (Prebble, 1995a). Refer to Fig.1 for these localities.

Research has shown that far from being "unique", as originally suggested for Abbotsford, clay seams acting as basal ruptures and others, which potentially could do so, are found throughout weak sedimentary rock terrain in New Zealand. Stout (1977), Thompson (1981), Pettinga (1987) and Prebble(1995a and b) document the presence of clay seams as basal rupture surfaces and describe aspects of the complexity and multi-stage development of these landslides over the last approximately 10,000 years. Areas of several km^2 and volumes ranging up to 0.1 km^3 are involved. These studies depended upon regional and comprehensive mapping over large areas in order to recognise the presence and importance of the pervasive clay seams and put together appropriate engineering geological models. They were all carried out in areas of relatively well-exposed rocks, rapid uplift and erosion and less intense chemical weathering than further north in New Zealand.

Block slides and clay seams in Auckland

It was some time before clay seams and block slides were confirmed in the Auckland region, leading to the recognition of the southern landslide zone (Prebble, 1995a). This is an area of around 100 km^2 (Fig. 15) in which most of the slopes have deep-seated failures on bedding-parallel clay seam rupture surfaces. Wedge and complex failures are also found. Slope instability was known to be widespread in the area (Kermode, 1991).

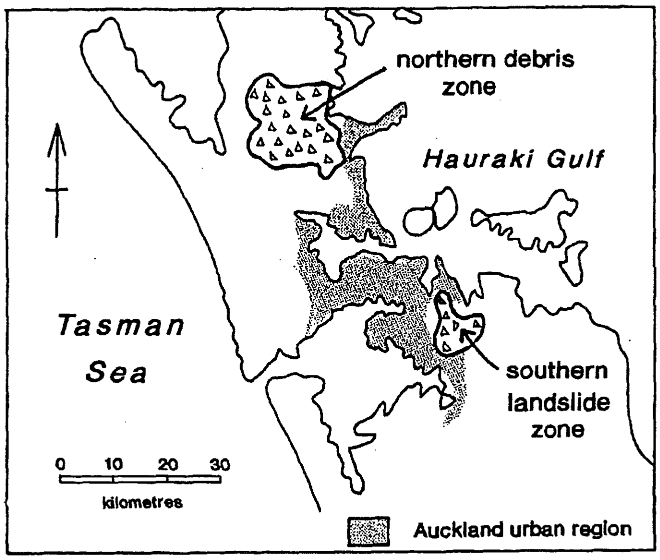

Figure 15. Map of the Auckland region showing location of the southern landslide zone. The northern debris zone is Miocene but has Holocene reactivation. (After Kermode, 1991).

Clay seams of significant continuity were confirmed by Wylie (1989) in a water supply tunnel and reservoir platform (Fig. 16). Residual soils up to 20m thick, close fracturing and faulting of the bedrock and the relatively slow rate of uplift and erosion all reduce the opportunity for inland exposures. The landslide topography is subtle. Geomorphic mapping as in Fig.17 for instance (Prebble, 1990 and 1999) and regional studies (Table 2) for seismic hazards and for earthquake-induced slope instability (Williams and Prebble, 1998) indicate that clay seams are likely to be present throughout the southern landslide zone and elsewhere in weak rock terrain in Auckland. The seams are found throughout all weathering grades and deep within unweathered rock. They vary from coatings on fractures to seams of gouge and show crushed wall rock and splays, typical of a tectonic origin, probably that of flexural slip at depth during macroscopic open folding. A flexural slip origin for bedding plane shears in gently dipping claystone and siltstone was proposed by Fell, Sullivan and Macgregor (1988). The shears provided rupture surfaces for slope failures. Hutchinson (1988 and 1995) contends that the potential for flexural slip has been underestimated as an origin for shears, which can develop into basal ruptures of landslides.

A major problem in developing a rigorous engineering geological model is determining the variability, continuity and strength of the clay seams. These are all critical to stability. Continuity of a seam over 50 m, with continuous exposure, was provided in a tunnel excavation in South Auckland. However, correlation of seams between drillholes during investigation is usually very difficult unless there are distinctive marker beds. Careful and detailed logging of cores, inspection shafts, trenches and natural exposures has achieved such correlation at sites in the southern landslide zone. Earthworks have subsequently confirmed the continuity of the seams and all aspects of the model in general (Fig. 18).

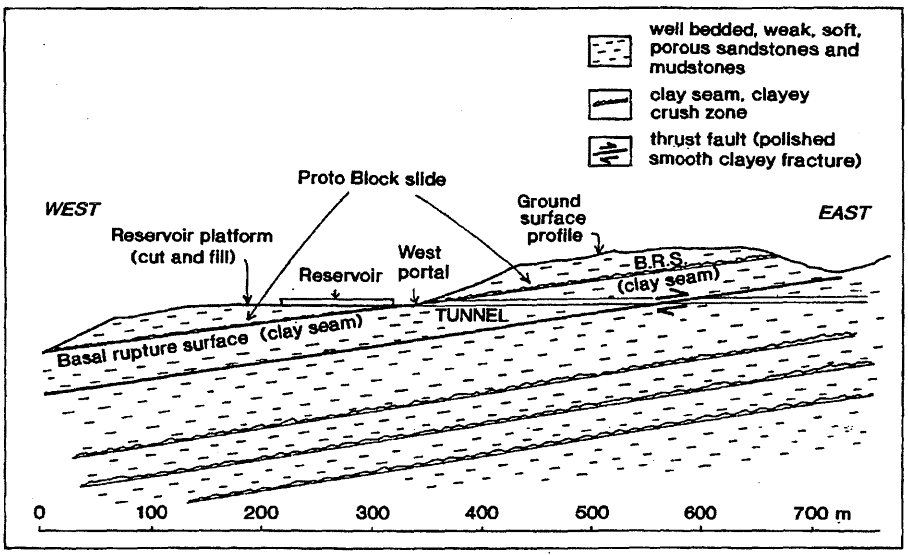

Figure 16. Section through a proto block slide, clay seams and crush zones in weak rock in a water supply tunnel, southern landslide zone, Auckland. (After Wylie, 1989).

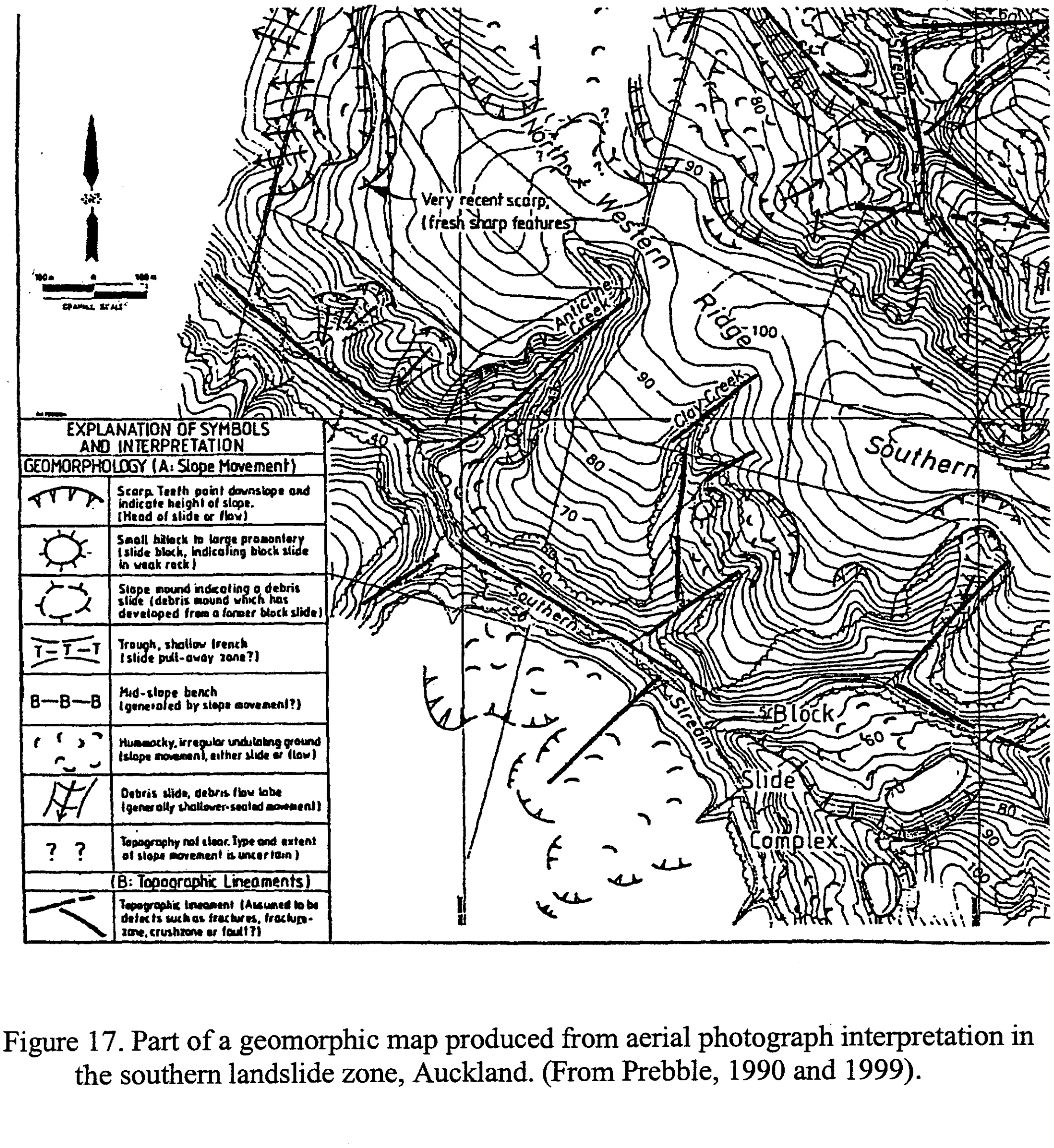

Figure 17. Part of a geomorphic map produced from aerial photograph interpretation in the southern landslide zone, Auckland. (From Prebble, 1990 and 1999).

Landslide hazard mapping in Auckland

Information on block sliding in the southern landslide zone in particular has contributed to the overall understanding of landsliding in the region. This was integrated into the analysis of landslide hazard during earthquake and heavy rainfall for the Auckland region as part of the recent lifelines study. Using the GIS-based Arc-Info system, areas susceptible to ground shaking, slope instability and liquefaction were identified and presented as a series of maps. A 2000 year return period earthquake was used, both a distributed hazard model based on the existing seismic records and a specific epicentre model based on the Kerepehi Fault to the East of Auckland. Table 2 from Williams and Prebble (1998) shows the properties of the soil and rock mass groups that were used. Criteria in this table are critical to the integrity of the whole analysis and were the result of accumulated engineering geological mapping and logging experience. A series of scoring (rating) tables for soil and rock mass category, slope grade and ground acceleration during earthquake were devised and gave scores which were summed to provide a hazard score. An interpretation was made of that score in terms of a relative hazard class, approximate factor of safety and percentage of slopes expected to fail. These classes were shown on final maps produced for the Auckland Engineering Lifelines Project and have also been presented and described by Williams and Prebble (1998).

Table 2: Soil and rock groups: Physical properties and response to earthquakes

Soil / rock mass group	Soil foundation condition	Soil category	Engineering description of soils/rock	SPT blows/ 300mm (N)	Shear wave velocity (m/s)*	Typical ground failures resulting from earthquakes
1	Residual Soil Overlying Rock	Residual and colluvial soils, ash and weathered tuff:- up to 30m, overlying greywacke; up to 20m overlying interbedded sandstone and mudstone; conglomerate and basalt	CW:-** sand/silt/clay; HW:- gravel in a silty sand/clay matrix; MW:- very weak rock; SW-UW:- weak to moderately strong rock	5 - 25+ 15 - 50+ 30 - 100+ 50 - 200+	100 - 300 200 - 500 300 - 1000 500 - 2000	Generally minor to nil damage to gentle slopes; Movements on critically steep slopes, and on gentle slopes in sandstone and mudstone with clay seams, undercut by streams and coastal erosion.
2	Firm to Stiff Sediment of Pleistocene age	Alluvium; and basalt, ash and tuff overlying alluvium	Soft to very stiff alluvium; Sensitive pumiceous silt; silt, peat and clay; Loose to dense sand and breccia; Ash, tuff and basalt overlying these deposits	5 - 25***	100 - 300	Widespread failure of coastal cliffs and river banks; Movement on moderate to steep slopes; Localised liquefaction of saturated loose sand lenses in severe**** shaking
3	Coastal Deposits	Beach and dune sands; Man-made fills overlying zone 1 or 2 deposits	Medium dense fine sand and shell, saturated; Loose fine sand, unsaturated	5 - 40	100 - 500	Localised liquefaction of saturated loose sand pockets
4	Estuarine Deposits of Holocene age	Stream alluvium and swamp deposits; Man-made fills overlying zone 3 or 4 deposits	Very soft to stiff mud, silt, peat, pumiceous clay; typically saturated	0 - 10	50 - 200	Widespread sliding failures of moderate slopes; Widespread liquefaction of saturated sand deposits in moderate shaking

* Values of shear wave velocity are assessed

** Rock Weathering Grades: - CW completely weathered; HW highly weathered (soil); MW moderately weathered (very weak rock); SW slightly weathered; UW unweathered (rock)

*** Where basalt rock overlies deep alluvium, the rock stiffness does not significantly influence site behaviour

**** Shaking levels: - Severe ≥ 0.40g ≥ Strong 0.20g ≥ Moderate 0.15g ≥ Moderate to Low 0.1g ≥ Low 0.05g

Table 2. Classification of soil and rock groups and their physical properties and response to earthquakes, in the Auckland region. Produced for the Auckland Engineering Lifelines Project. From Williams and Prebble (1998).

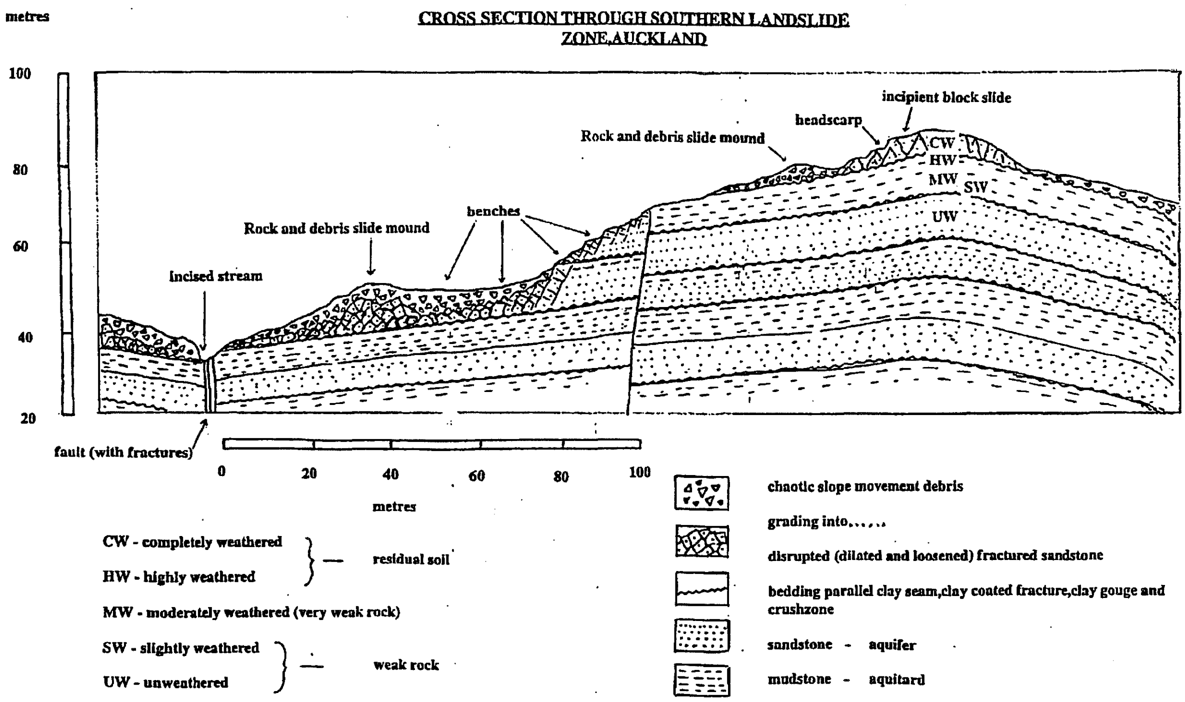

Figure 18. Cross section view of a general model for block sliding in the southern landslide zone, Auckland

Incipient sliding and proto block slides

A clay seam in a tunnel in the southern landslide zone penetrates narrow fractures above the seam, but not the fractures below it, which are tightly closed. This may be evidence for a very small displacement or incipient block sliding on the seam and is referred to as a proto block slide (Figs. 16 and 18). Trenches adjacent to the tunnel confirmed the presence of pull away zones and sliding which could be related to the seam in the tunnel. Proto block slides in which the movement has been several cm were recognised in the gorge walls of the Rangitikei River (Fig. 19). Geomorphology of the gorge and terrace surfaces indicated that short displacement block sliding and slabbing, on clay seams was an important process of gorge widening. It was observed that the proto block slide shown in Fig. 19 is at the narrowest part of the gorge for that section of the river. The argument was put forward that it is the narrowest part because it will be the next portion of the wall to fail. The age of the terraces are known so that a rate of gorge widening and of river downcutting can be established.

Age and rate of block sliding

This seems an appropriate note on which to finish presenting information and discussion on examples from my collection of case histories. Age and rate of movement are somewhat complex concepts in this context. Age can be the onset of a first time slide or reactivation of an existing one. It may refer either to the time of pull away or to the time of arrival of debris at the bottom of the slope or further down the channel. In a slide that has moved many times, age may refer to any one or more of many separate movements, Slides will also evolve and change over time. Rate of movement may be merely an average and not the appropriate velocity for any one particular movement.

Thompson (1981) established the age of numerous slides in the Rangitikei valley from a distinctive sequence of tephra, which enabled him to assess their development over the last approximately 10,000 years and identify some as old as perhaps 20,000 years. Le Cointre, Neall, Wallace and Prebble (in Press) have used a sequence of tephra, dated lava flows and radiocarbon to determine the age of debris avalanches at Tongariro. In the Auckland region tephra sequences are well preserved in the sediments which fill in basaltic explosion craters, such as Onepoto Basin on the North Shore. Recently completed stratigraphic drilling programmes will provide dated sequences which may be used by correlation to determine the age of pull away zones, overrides and toe dams for block slides in the southern landslide zone, for instance.

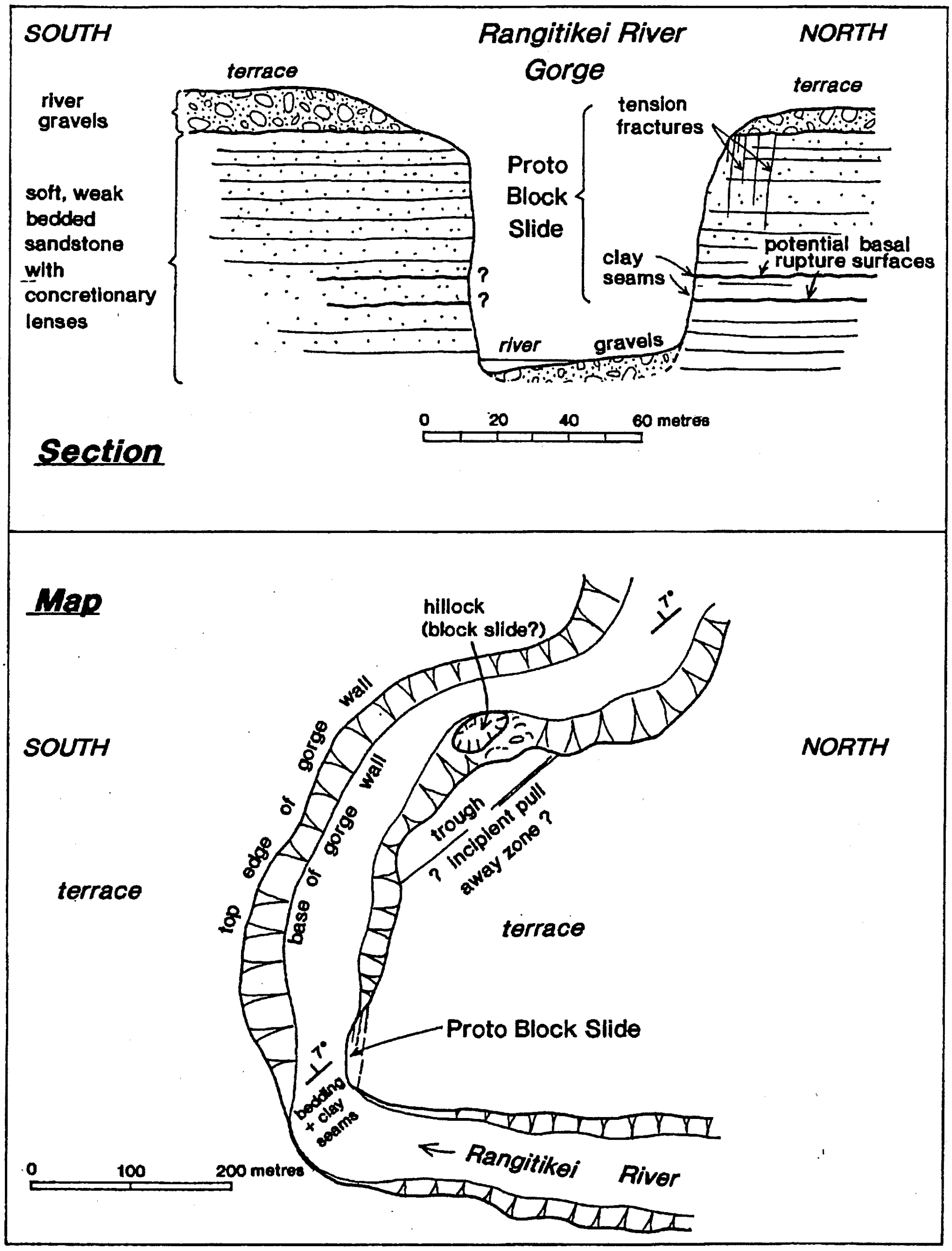

Figure 19. Map and section through a proto block slide in the gorge of the Rangitikei valley, central North Island. (From Prebble, 1995a).

Conclusions

The tectonic framework of New Zealand is one of rapid oblique convergence, shear and uplift. Volcanism in the North gives way to mainly compressional shear in the South.

Coupled with an axial core of fractured greywacke and schist terrain, the alpine regions of the South Island are failing by toppling and sliding. In this active tectonic and geomorphic setting rock mass bulging is considered to be widespread and is caused mainly by deep seated toppling.

In its severest form, overturning of tabular rock masses (overtoppling) is caused by dilational flexural-block toppling in cataclinal underdip slopes. Widespread toppling of this type in limestones of the East Coast Deformed Belt in Marlborough was only identified when comprehensive geotechnical mapping was done over a large area, in combination with a geomorphic and aerial photograph study.

Andesitic cones are subject to collapse. Alteration created by high level geothermal activity on cones can give rise to large, mobile, clay-rich debris avalanches and cohesive debris flows. The conditions which create these devastating flows continue today and include northern Tongariro, Kakaramea and Tihia volcanoes. Identification of the Te Whaiau formation as a large cohesive debris flow deposit was facilitated by regional engineering geological mapping, geomorphlogy, outrop logging over several years and foundation logging in combinatoin with review of the drillhole data.

Altered and faulted massifs in the centre of the volcanic rift are subject to a diverse assemblage of hazards: faulting, geothermal, explosion craters, landslides, swelling ground, residual hot ground and highly unpredictable ground conditions. Accurate geomorphic interpretation, recognition of volcanic facies through comparative studies and regional engineering geological mapping were essential to the recognition of these hazards.

Ignimbritic plateaus and terrace remnants contain highly sensitive rhyolitic soils and ribbon aquifers which combine to give rise to a series of superposed potential basal ruptures for rapid slide-flow failure. These conditions are as widespread as the deposits, which extend into the Auckland region. Similarly sensitive rhyolitic deposits of a residual hydrothermal origin have probably assisted slope failures in the Orakei Korako geothermal field. Key elements in the identification and understanding of these slope failures came from very detailed engineering geological mapping of exposures, geomorphology and the recognition of paleotopography, ribbon aquifers and sensitive clay layers.

Block slides on clay seams of tectonic origin in weak rock are known throughout the North Island and also in the South Island. The southern landslide zone in Auckland is a concentration of such failures, adjacent to a rapidly growing urban region.

Total mapping – comprehensive geotechnical mapping at a range of scales and including geomorphology and remote sensing continues to be an effective investigation method.

The regional picture, often of a large area up to considerable distance from the site is essential in order to obtain the relevant setting when the site is focused on in detail.

Informative, well exposed or geomorphically well preserved "type"geotechnical localities can provide the critical model for understanding enigmatic engineering sites.

Stratigraphy, structure, tectonics, geologic history and geomorphic development, the petrographic and mineralogic properties of materials and defects and a consideration of a range of earth surface processes have all contributed to the examples discussed in this paper. They are all part of the "total mapping" process and are all essential factors in the recognition and assessment of hazardous terrain and in the development of site models for geotechnical purposes.

Acknowledgements

It is a privilege and an honour to give the Geomechanics Lecture. I am very grateful to the New Zealand Geotechnical Society for the opportunity and recognition, which this provides. It is also a pleasure to share some of my engineering geological experiences with the membership at large throughout the country. I must point out that any contribution to the profession and to engineering geological knowledge, which I have made over the years has received input from many others. I would like to thank those people who have directly helped me build up my experience and develop my view of engineering geology and I would also like to acknowledge the organisations, which have made it possible.

First the organisations. The Geology Department of Victoria University of Wellington provided a learning environment and academic mentors second to none, complete with the enrichment that comes from fieldwork in exciting places and the unique experience of expeditions to Antarctica. Employment with the former Geological Survey and Ministry of Works (Tongariro Power Development) provided invaluable work experience and amazing challenges. Secondment to the Snowy Mountains Authority at an early stage gave me training and experience in engineering geology not available anywhere in New Zealand at that time. Later on, Beca, Carter, Hollings and Ferner added significantly to that and introduced me to the world of consulting practice. This connection has continued and expanded with the help of many other consultants who have also included me in their work. The former National Water and Soil Conservation Authority, the Foundation for Research Science and Technology, The Auckland Regional Council, Environment Bay of Plenty, Environment Waikato, University of Auckland Research Committee and IGNS Ltd have given funding for many of the research projects and graduate students over many years. Finally, The University of Auckland gave me the opportunity to develop new courses in engineering geology and to carry out research-informed teaching with very talented young people and with valued colleagues.

Next the many people. It is difficult to know where to stop. I thank all my present and former colleagues at the University of Auckland. In particular those who have directly helped form my view of engineering geology: Mick Pender, Laurie Wesley, Tam Larkin, John St George, Graham Duske, Peter Taylor, Murray Gregory, Bernhard Sporli, Basil Beamish, Kerry Rodgers, Philippa Black, Ian Smith, Terry Sameshima, Pat Browne and Manfred Hochstein. Present and former graduate students who have worked with me on geologic hazards: Jarg Pettinga, Roger Thompson, Ann Williams, Maurice Fraser, Cam Wylie, Janak Patel, Bevan Hill, Justin Franklin, Monique Daalman, Alanna Simpson, Dennis McManus, David Whyte, Peter Manning, Brian Shakes, Darryn Wise, Mazin Al Salim, Tony Cowbourne, Anthony Gladding, Greg Cocks, Matthew Brown, Stephen Blackmore, Steven Tyson, Susan Tilsley, Aaron George, Paul Salter, Ian Jenkins, Keith Simpson, Matthew Free, Iwan Tejakusuma, Shao-chun Cong and Steven Price. Former teachers at Victoria University of Wellington: Bob Clark, Harold Wellman, John Bradley, Paul Vella and Ed Ghent. Those with whom I worked at Geological Survey and the Ministry of Works: Les Oborn, Graham Mansergh, David Kear, Les Kermode, Graham Hancox, Bernhard Hegan, John Dow, Brian Paterson, John Buckeridge, Warren Gibson, Bert Dekker, Barry Campbell, Bill Espie, Peter Swan, Kerry Scott, Tony Hinkley, John Gardenier, Peter Armstrong, Gary Gay, Gilbert Natusch, Ian MacKellar and John Hawley. Those with whom I worked in Beca Carter Hollings and Ferner ltd: John Blakeley, Sir Ron Carter, Ian Billings, Peter Riley, John Hollings and with whom that work continued over the years since: Do Van Toan. Other consultants: Raj Jairaj, Grant Knocker, Debbie Fellows, Wayne Russell, Simon Woodward, Alan Barrowclough, Bruce Riddolls, Guy Grocott. My constructive critics in other Universities: David Bell, Vicki Moon, Michael Selby, Martin Stout, Jim Cole, Steve Weaver and others whom I have already referred to. My research associates at Massey University: Vince Neall, Jerome Lecointre and Clell Wallace. Many colleagues overseas in the IAEG, but especially Paul Marinos, John Gartner, Kobus Venter and Brian Hawkins. Former mentors on the Snowy Mountains Scheme: Kees Silverschoon, David Stapledon, Peter Burgess and David Jordan.

I am grateful to Bothwell Wong for help in formatting this paper and to Louise Cotterall for assistance with drafting.

References

Beck, A. C., (1968). "Gravity Faulting as a mechanism of topographic adjustment". *New Zealand Journal of Geology and Geophysics.* 11(1), pp. 191-199.

Coombs, D.S. and Norris, R.J., (1981). "The East Abbotsford, Dunedin, New Zealand Landslide of August 8, 1979. An interim report". *Bulletin de Liaison de Laboratoire des Ponts at Chaussees.Special X.* pp 27-34. (Proceedings of the 26th International Geological Congress, Paris, 1980).

Cruden, D. M. and Hu, Xian-Qin, (1994). "Topples on underdip slopes in the Highwood Pass, Alberta, Canada.". *The Quarterly Journal of Engineering Geology".* 27, pp. 57-68.

Fell, R., Sullivan, T. D. and MacGregor, J. P. (1988). "The influence of bedding plane shears on slope instability in sedimentary rocks". Proceedings of the Fifth International Symposium on Landslides. In: *Landslides: Glissements de Terrain,* Balkema, Vol. 2, pp 129-134.

Gallen, R.G., Beca, G.S., McGraw, J.D. and Roberts T.A. (1980). "Report of the Commission of Inquiry into the Abbotsford Landslip Disaster". *Governemnt Printer, Wellington, N.Z.* 196pp.

Hamlin, K.A. and Prebble, W.M. (1998). "Structural setting and geomorphic features of the Orakeikorako geothermal Field, TaupoVolcanic Zone: A remote sensing approach". *Proceedings of the 20th New Zealand Geothermal Workshop,* Ed: Simmons, S.F., Morgan O.E and Dunstall M.G., Geothermal Institute, The University of Auckland, pp. 277-284

Hutchinson, J.N. (1988). "Morphological and geotechnical parameters of landslides in relation to geology and hydrogeology". Proceedings of the Fifth International Symposium on Landslides. In: *Landslides: Glissements de Terrain,* Balkema, Vol. 1, pp 3-35.

Hutchinson, J.N. (1995). "Landslide Hazard Assessment". Keynote Paper. Proceedings of the Sixth International Symposium on Landslides. In: *Landslides: Glissements de Terrain,* Ed: Bell, D.H., Balkema, Rotterdam, Vol 3, pp 1805-1841.

Kermode, L.O. (1991). "Whangaparaoa-Auckalnd". Infomap 290 Sheet R10/11, 1:100,000. New Zealand land Inventory, Rock Types. *Department of Survey and Land information, Wellington, New Zealand.* Map sheet.

Lecointre, J.A., Neall, V.E., Wallace,R.C. and Prebble, W.M. (2001). "The 55-60 ka Te Whaiau Formation: A catastrophic, avalanche-induced, clay-rich debris flow deposit from Proto-Tongariro Volcano, New Zealand". (*Bulletin of Volcanology*, in press).

Palmer, B.A., Alloway, B.V. and Neall, V.E. (1991). "Volcanic debris avalanche deposits in New Zealand – Lithofacies organisation in unconfined, wet-avalanche flows". In "Sedimentation in Volcanic Settings*", SEPM Special Publication* 45: 98-109".

Pettinga, J.R. (1987). "Ponui Landslide: a deep-seated wedge failure in Tertiary weak-rock flysch, Southern Hawkes Bay, New Zealand". *New Zealand Journal of Geology and Geophysics,* Vol. 30, pp 415-430.

Prebble, W. M. (1967). "Tongariro Power Development. Western Diversions. Report on the Geology of Otamangakau upper dam site". *NZ geological Survey,* Wellington. 8p.

Prebble, W.M. (1969a). "Tongariro Power Development. Engineering Geology of the Te Whaiau dam site. A report on the geological investigations". *NZ Geological Survey,* Wellington. 10pp + annex.

Prebble, W.M. (1969b). "Foundation and geothermal problems at Tokaanu power station, Tongariro power development". *Abstracts. Geological Society of New Zealand Conference, Dunedin, 1969.*

Prebble, W.M. and Dow, J.A.S. (1969). "Tongariro Power Development. Otamangakau Dam Foundation Excavations Geological Log". *NZ Geological Survey, TPD.* Plan.

Prebble, W.M. (1977). "Engineering geological investigations for tunnel location and design". *Proceedings of the Symposium on Tunnelling in New Zealand.* NZ Geomechanics Society. NZ Institution of Engineers. Proceedings of Technical Groups, Vol. 3, Issue 3(G), pp 2.1-2.11.

Prebble, W.M. (1986). "Geotechnical Problems in the Taupo Volcanic Zone". In: *"Volcanic Hazards Assessment in New Zealand".*Ed: Gregory, J.G. and Watters, W A.. New Zealand Geological Survey Record 10, pp. 65-80.

Prebble, W.M. (1990). "Manukau Sanitary Landfill. Report on the Geology of the site north of Caldwells and Sandstone Roads, near Whitford". *Auckland UniServices Limited.* Map to accompany report.

Prebble, W.M. (1995a). "Landslides in New Zealand". Keynote paper. Proceedings of the Sixth International Symposium on Landslides. In: *Landslides: Glissements de Terrain,* Ed: Bell, D.H., Balkema, Rotterdam, Vol.3, pp. 2101-2123.

Prebble, W.M. (1995b) "Landslides in tabular rock masses of an active convergent margin". Proceedings of the Sixth International Symposium on Landslides. In: *Landslides: Glissements de Terrain,* Ed: Bell, D.H., Balkema, Rotterdam, Vol. 3, pp. 2145-2151.

Prebble, W.M. (1996) "Identification and analysis of landslides in an area of steep land and complex geology". The New Zealand Geomechanics Society. Proceedings of the Symposium on "Geotechnical Issues in Land development". *IPENZ Proceedings of Technical Groups,* Vol. 22, Issue 1(G), pp.74-86.

Prebble, W.M. (1999). "Geomorphology and Photogeology". Manukau Sanitary landfill. Site north of Caldwells and Sandstone Roads, near Whitford, Auckland. Updated version of Map originally produced for 1990 report and again in 1993. *Auckland UniServices Ltd and Beca Carter Hollings and Ferner Ltd.* Map sheet.

Schuster, R.L., (1983). "Engineering Aspects of the 1980 Mt St Helens eruption". *Bulletin of the Association of Engineering Geologists.* 20(2), pp125-143.

Stout, M.L. (1977). "Utiku Landslide, North Island, New Zealand". *Geological Society of America Reviews in Engineering Geology,* III, pp 171-184.

Thompson, R.C. (1981). "Landsliding in Cenozoic soft rocks of the Taihape-Mangaweka area, North Island, New Zealand". *Bulletin de Liaison de laboratoire des Ponts et Chaussees.* Special X, pp 93-100. Proceedings of the 26th International geological Congress, Paris, 1980.

Wan Tienfeng and Hedenquist, J.W., (1981). "The structural characteristics of the Taupo Volcanic Zone and the Broadlands geothermal field, New Zealand". *Geothermal Institute, University of Auckland.* Report 80.023.

Williams, A.L. and Prebble, W.M. (1998). "Auckland Engineering Lifelines Project: Seismic hazard assessment". Proceedings of the Eighth International Congress of the International Association for Engineering Geology and the Environment. In: *Engineering Geology. A GlobalView from the Pacific Rim,* Eds; Moore, D.P. and Hungr, O., Balkema, Rotterdam, Vol. 2, pp 809-815.

Wylie, C.A. (1989). "Engineering Geology of a Soft, Weak Rock Tunnel: ARA Redoubt Road No. 2 Inlet Tunnel. *MSc thesis in Geology, The University of Auckland.*

Slope Failures 1

Opencast Highwall Slope Design, Rotowaro Coalfield

D. Fergusson
Technical Manager, Solid Energy North

M. Paris
Senior Mining Engineer, Solid Energy North

C. K. Anderson
Principal Geotechnical Engineer, URS New Zealand Ltd

T. McMorran
Senior Engineering Geologist, URS New Zealand Ltd

D. Johnson
Senior Engineering Geologist, Tonkin and Taylor Ltd

Abstract

This paper describes the development for the final highwalls for Township Opencast coal mine in the Rotowaro Coalfield, in the Waikato, New Zealand. The highwalls are up to 100 m high and are being constructed within a sequence consisting of weak Mesozoic greywackes (Newcastle Group), weak to extremely weak, early to mid Tertiary mudrocks (Te Kuiti Group) and fine-grained Quaternary soils (Tauranga Group).

Highwall design is complicated by residual strength bedding shears, geological structures at pit limits, such as into-pit dipping normal faults and basement paleorelief surfaces, as well as the deleterious effects of historic underground coal extraction in the target seams. The mine limits are also situated close to civil and mining infrastructure such as roading, streams and drains, therefore reliable slope performance is essential.

Probabilistic stability methods and have been extensively applied to develop highwall designs which maximise economic benefits within tolerable risk criteria. This paper discusses the design process, starting with scoping of the initial site investigations, followed by development of preliminary designs and concluding with the optimisation process to determine the final highwall configuration. Also described are the site engineering geology, geotechnical characteristics of the materials, aspects of the probabilistic stability methodology used, and the risk assessment and design optimisation processes.

A fundamental realisation from this project is that the optimisation of highwall designs is a highly iterative process that requires effective communication and information sharing between the owner, designer(s) and the construction contractor.

Introduction

Solid Energy North (SEN) is extending the Township Opencast Mine into the South and West Pits at Rotowaro, near Huntly (Figure 1). These pits contain a recoverable coal reserve of 4M tonnes, however, in developing this mine, SEN has identified a number of geotechnical risks, most of which are related to the unfavourable engineering geology for stability of the proposed highwalls.

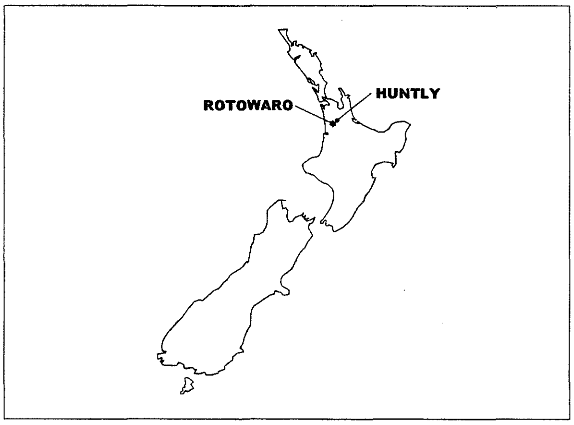

Figure 1: Locality Plan - Rotowaro is 8 km Southwest of Huntly

This paper presents an overview of geotechnical aspects of the mine design project with emphasis on the application of probabilistic methods to the design of the Southern and Western Highwalls (Figure 2). On completion, these highwalls will be up to 100 m high. The paper addresses aspects of the site investigation, laboratory testing, assessment of groundwater and groundwater conditions and key elements of the stability models. It demonstrates how the application of probabilistic-based risk analysis can be used to make informed risk management decisions with respect to design selection and optimisation.

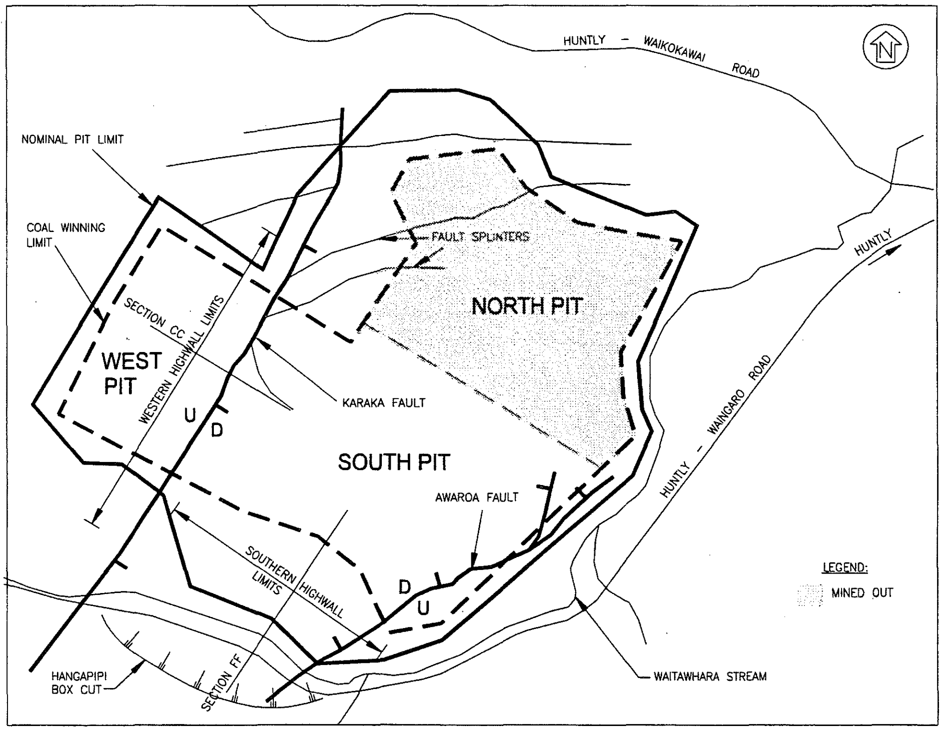

Figure 2: Plan View of Township Opencast Mine

Project Description

The purpose of this project was to design the optimal development and mining plan for Township Opencast. Emphasis has been placed on geotechnical risk management, mine economics, and long-term performance. Complete design covers the mining sequence, the highwall cuts, disposal of the backfill and the mine's end-use, after site rehabilitation.

The project objective has been to maximise economic returns from the Township Opencast mine by optimising the designs of the final highwalls against the adverse operational and environmental impacts that result from slope failures. An inherent requirement is the protection of civil engineering structures, such as the Rotowaro Road, and the associated Waitawhara Stream diversion (Figure 2), situated close to the southern economic limit of the opencast mine. Other factors that introduce uncertainty for mine design have been incorporated into the development models, including the presence of the historic Alison underground mine workings, in which the main economic seams were mined between 1939 and 1974.

The resultant highwall designs have to strike an acceptable balance between the risk of slope failure, the stripping ratio, and maximising coal recovery. The designs also need to be consistent with the mining operation i.e., the machinery being used, high excavation rates, the high rate of backfill placement, and constructability. Concurrently, design work has been undertaken to optimise the backfill dump development as the Township Opencast is opened up. The approach to the investigation, design and the risk management of fill slope construction and performance was similar to that for the highwall design, however, the backfill component of the project will not be elaborated on in this paper.

Site Investigation and Design Process

Multi-phase Programme

The highwall design project was managed in three phases (Figure 3). Phase I comprised a review of the available geotechnical and geological data, construction of the initial engineering geological and geotechnical models, followed by preliminary stability and risk analysis to identify key uncertainties and sensitivities. The key outcomes from Phase I were the identification of areas where additional geotechnical data would be required for stability and risk assessment and design, and development of an investigation programme to obtain that data.

The main conclusions of the Phase I study were:

- There was significant uncertainty regarding orientation of weak failure surfaces within the basement rocks underlying the coal bearing strata.
- There was significant uncertainty regarding the presence and orientation of weak discontinuities close to major geological structures (e.g. Karaka and Awaroa Faults). See Figure 2.
- There was uncertainty regarding the groundwater systems and short to long-term groundwater pressure response to mining, dewatering and rainfall within the strata sequence.
- There was a basic lack of shear strength data for the rock discontinuities and presheared bedding surfaces.
- There was uncertainty regarding the distribution and thickness of historic backfill soils and the nature of the contact between these soils and the underlying ground.

An investigation programme was developed and undertaken to address these uncertainties (Table 1).

Phase II of the design process (Figure 3) involved revision of the engineering geology and geotechnical models using the new investigation data. Focus was put on establishing the acceptable risk criteria for highwall designs. The process of defining risk criteria is discussed in more detail in the following sections. The Phase II highwall designs enabled an initial assessment of the available reserves and mining economics, and highlighted the main design and construction issues to be resolved during optimisation.

Phase III (Figure 3) involved optimisation of the highwall designs with respect to geotechnical risk and operational efficiency, including addressing sequencing of cuts and assessment of construction tolerances.

The following discussion focuses on the final models developed with supplementary data presented only where additional clarification is either critical to understanding the design assumptions or are of particular interest.

Table 1: Summary of Investigation Programme

Investigation Method	Summary of Investigations
Review of old underground workings data	Plans of the old workings were scrutinised to establish the distribution of first and pillared workings and geological structures in the vicinity of the new highwalls.
Engineering geological mapping (including scanlines)	Exposures in the vicinity of the proposed highwalls and nearby pit exposures were mapped to collect discontinuity data and to take samples for material strength testing. Hangapipi Boxcut behind the Southern Highwall provided an excellent exposure.
Investigation trenching	Five trenches were excavated across the Karaka Fault to better locate the subcropping fault and associated discontinuities, and to ascertain the distribution of near surface materials.
Investigation drilling	New drilling comprised eight cored drillholes (totalling 477 m) along the Western Highwall and three cored drillholes (totalling 308 m) along the Southern Highwall. Eight of these eleven holes were declined 45-70° to allow core orientation for orienting bedding and discontinuities. A further 13 vertical partly cored holes were drilled to refine the location of the Awaroa Fault (5 holes) and Karaka Fault (8 holes).
Instrumentation	All cored drillholes were instrumented with piezometers. A total 12 vibrating wire, four pneumatic and two Casagrande type piezometers were constructed. An additional two casagrande piezometers were installed in the West Pit.
Material property testing	Material property testing included: Ring shear tests (5) XRD analyses (6) Clay fractions (29) Plasticity Index tests (29)

Engineering Geology Model

The geological setting for the Rotowaro Coalfield has been reviewed by Edbrooke *et al.* (1994), Kear and Waterhouse (1978) and Kear and Schofield (1966), and numerous mining studies over the past 20 years.

Site specific engineering geological models have been developed for the Township Opencast based on a collation of all available data including an extensive drillhole database of the mine (~450 holes) and additional investigations undertaken as part of this design project. An overview of the strata sequence is given on Table 2. A summary of the engineering geological models developed is given on Figure 4 for two sections from the Western (Section CC) and Southern (Section FF) highwalls respectively. The location of these sections is illustrated on Figure 2.

Key engineering geological features controlling highwall stability include:

- Bedding-parallel sheared zones ("bedding shears") in the Marine Tertiary (MT) and Waikato Coal Measures (WCM). These had previously been recognised as contributing to failures within the pits, especially adjacent to faults and basement highs. Bedding shears are extensively developed along the Western Highwall on the down-thrown (east) side of Karaka Fault (Figure 2). Some evidence for low strength shear surfaces in the basement was noted in cored investigations holes. Pre-shearing is inferred to result from flexural slip along unit contacts during induration, folding and faulting of the strata.

- The Karaka and Awaroa Fault zones associated with the proposed Western and Southern highwalls, respectively (Figure 2). Adjacent to these faults is a wide disturbance zone of highly fractured/shattered basement and sheared, drag-folded MT and WCM. Drag folding accentuates the dip of bedding on the down-thrown side dipping toward the proposed pit (Figure 2).

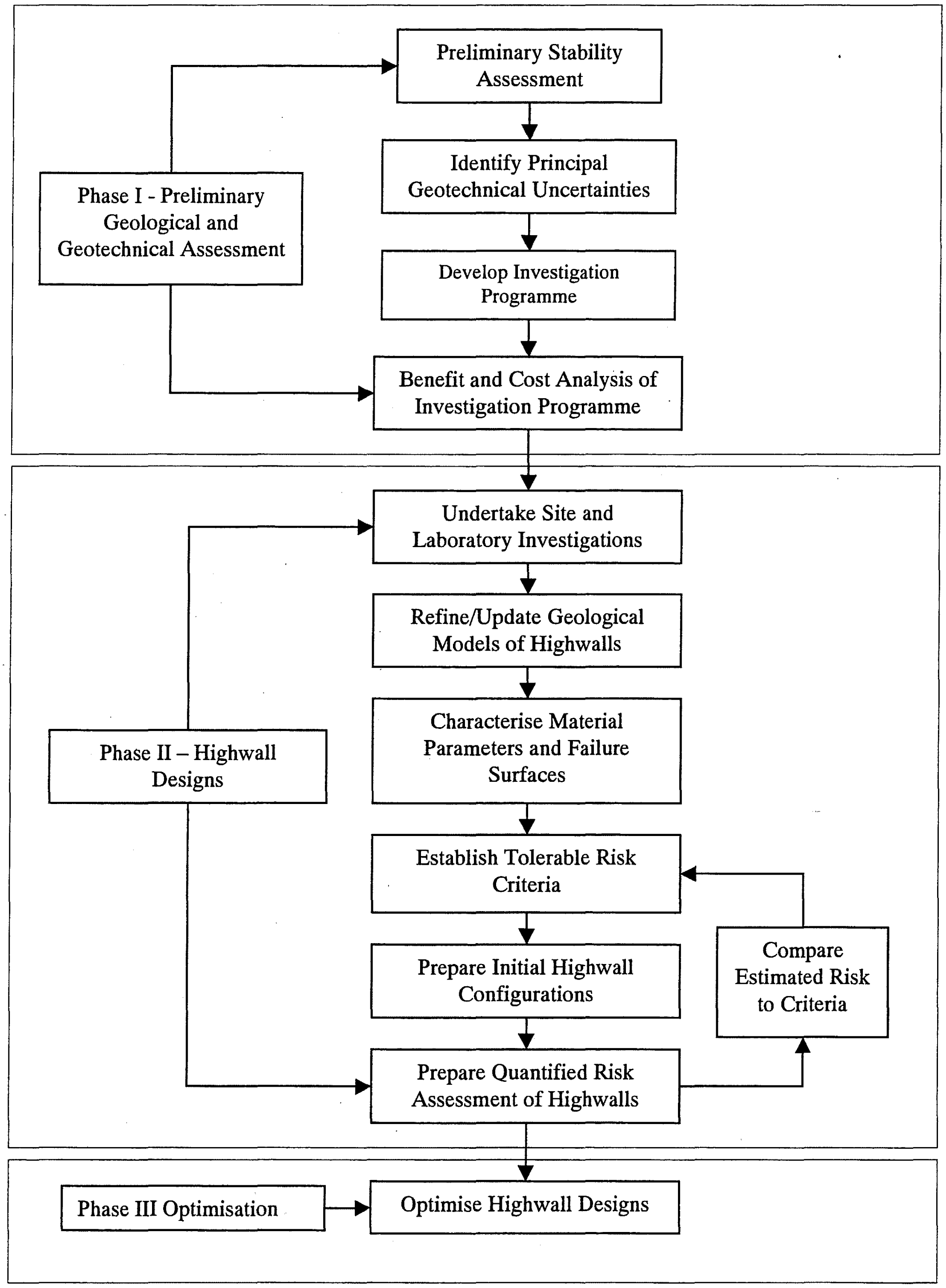

Figure 3: Phases of Project

Table 2: Overview of Stratigraphic Column and Unit Characteristics

Simplified Lithostratigraphy	Geological Characteristics	General Term
Tauranga Group (Quaternary) • Swamp alluvium • Recent alluvium • Hamilton Ash Formation	Fine-grained soils composed of swamp deposits and alluvium derived from underlying mudrocks; volcanic ashes (colluvial deposits at foot of slopes). Groundwater systems perched, med. permeability.	Quaternary soils
	Unconformity	
Te Kuiti Group (Tertiary)		
Rotowaro Formation (Oligocene)	Non-calcareous siltstones and claystones sometimes separated by glauconitic sandy mudstone beds. Highly weathered in upper 15 m. Presheared bedding-parallel surfaces, at unit boundaries. Perched groundwater system, low permeability.	Marine Tertiary (MT)
Waikato Coal Measures (Eocene)	Mainly carbonaceous siltstone, claystone ("fireclay"), with occasional fine sandstone or coarser beds, shales, and coal seams. Highly weathered in upper 10-15m where underlying Tauranga Group. Presheared bedding-parallel surfaces, especially at coal and basement contacts. Fireclay poor draining. Coal seams free draining.	Waikato Coal Measures (WCM)
	Unconformity	
Newcastle Group (Mesozoic)	"Greywacke' and argillite usually highly weathered in upper 10 to 20 m. Subartesian groundwater system wrt WCM base, poor drainage.	Basement "greywacke"

- The upper 10-20 m of Greywacke basement immediately underlying the WCM is highly weathered. This weathered material forms a potential failure zone.
- An oblique down-dip component toward the pit was identified in the western side of the proposed Southern Highwall with basement rising to the southwest. Smaller scale paleorelief on the basement surface has been mapped from drillholes and underground workings along the Western Highwall.
- Four major high-angle joint sets are present, sub-perpendicular and conjugated to the main faults. A number of minor joint sets are locally developed around minor faults and basement highs.
- Zones of disturbed ground above Alison underground mine workings west of the Karaka Fault, which typically extend about six metres above bord and pillar ("first") workings and 20 m above the seam roof in areas where the pillars have been extracted ("pillared" workings).

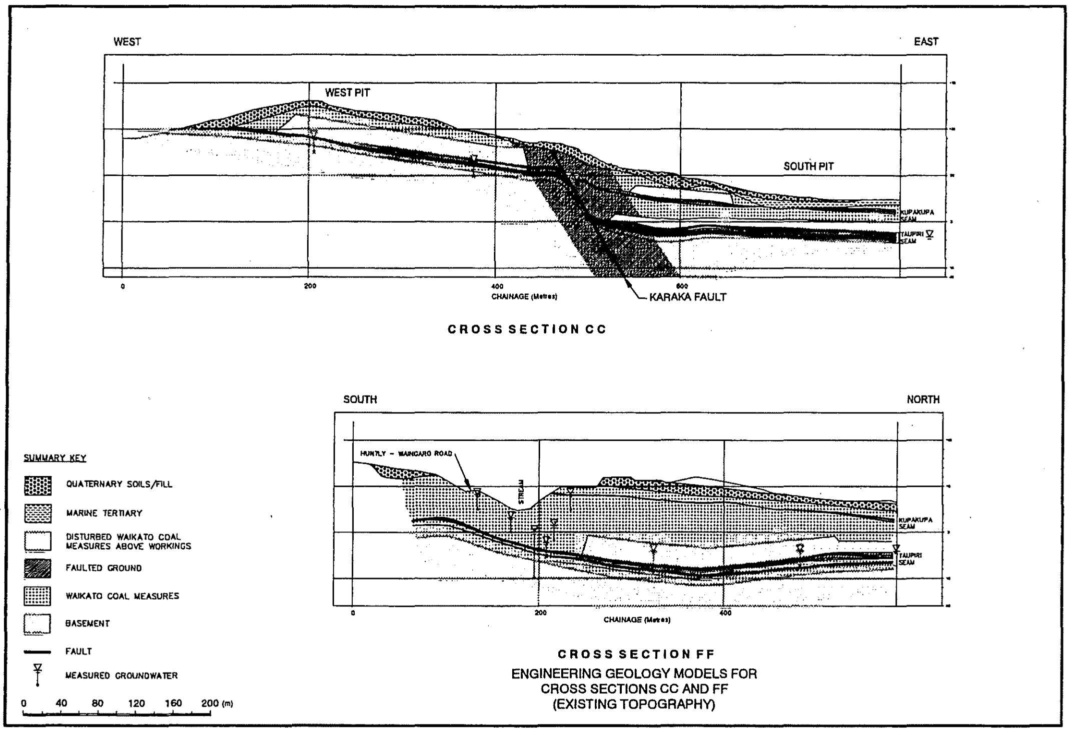

Figure 4: Engineering Geological Models of Western and Southern Highwalls

Piezometric data collected from a network of piezometers installed over the site coupled with an understanding of the engineering geology have enabled a groundwater model of the site to be developed as summarised on Figure 5.

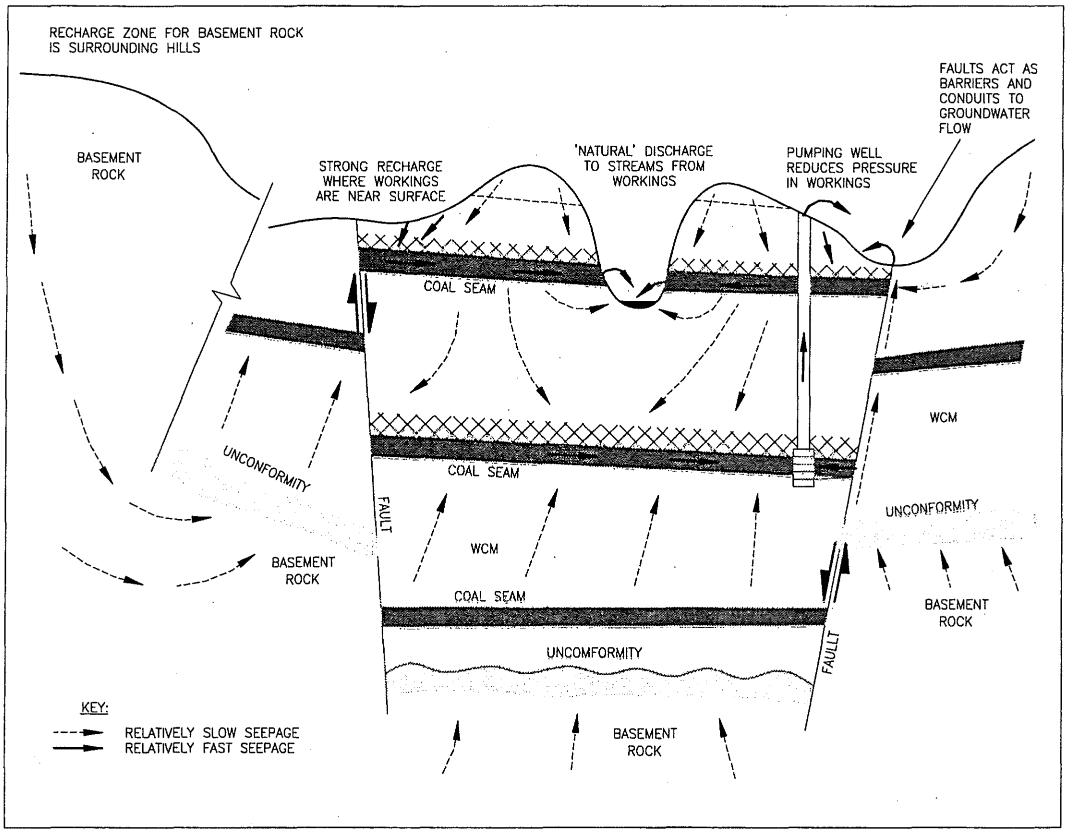

Figure 5: Conceptual Groundwater Model (Pre-Mining)

The main observations and features of the groundwater system are:

- Following development of the mine void and the attendant dewatering, the basement rocks act as a source of upward flow toward the free-draining coal seams, while groundwater in the fireclay units of the WCM flows up or down toward the nearest coal seam under the influence of the local seepage and pumping gradients.
- Perched groundwater systems are present in the Marine Tertiary, Quaternary and backfill.
- The Marine Tertiary sequence is nearly fully saturated with groundwater perched on a persistent, one to two metre thick sheared zone at the MT-WCM contact. Groundwater levels in the Marine Tertiary sequence tend to respond only slowly to the dewatering influence of the mine, but are responsive to rainfall events.
- Variable groundwater conditions exist in the WCM's with extensive drainage due to the Alison underground mine workings and the relatively permeable coal seams. The water levels in the old mine workings are largely controlled by dewatering bore pumping. Where the WCM's are not drained by either old mine workings or opencast mine developments, high groundwater conditions prevail.
- Water levels in the basement are also variable. In general, the basement has high groundwater levels controlled by regional recharge and stream levels about the area, however, the basement groundwater levels are locally depressed owing to leakage paths to the WCM and old mine workings or opencast void. In the vicinity of the Southern Highwall a sub-artesian piezometric head exists due to the direct hydraulic recharge into the basement high at the western end of the Hangapipi Boxcut by the Waitawhara stream (Figure 2), and limited dewatering from the comparatively distant Alison workings (Section FF, Figure 4).
- The Karaka and Awaroa Faults have been found to be aquicludes to groundwater across the faults, with high water levels confined on the up-thrown sides, behind the faults (Section CC, Figure 4).Recent pumping of the old workings has shown that leakage paths from basement to coal seams exist on the down-thrown side of the Awaroa Fault. Consequently, the piezometric profile in basement is controlled (stepped) by the major faults.

Geotechnical Model

Characterisation of Materials

The characterisation of materials was developed from the data of previous studies and the site specific testing undertaken for this project. A data base was developed from which to assess the statistical properties of the material for the quantitative risk assessment.

A key parameter in controlling stability was identified to be the residual strength of the presheared surfaces present at several levels though the stratigraphic sequence, especially associated with the coal seams. The importance of understanding the effective residual shear strength of these surfaces lead to extensive investigation and testing of these features. The following discussion focuses on how the statistical parameters of effective residual shear strength were assessed. The derivation of other material parameters is not dealt with here for reasons of brevity.

Available Data for Residual Shear Strength of Presheared Surfaces

A summary of the statistical data derived for the presheared surfaces is presented in Table 3. It incorporates an assessment of the strength data available from existing reports reviewed for Phase I with the laboratory testing performed during Phase II.

The Phase I reports of previous tests for the WCM bedding plane shear materials yielded mean effective residual strength parameters of $c'=0$ kPa and $\varnothing' = 11°$. However, back analysis of a large failure in WCM on presheared surfaces at the nearby Waipuna Opencast provided an mean shear strength estimate of $c' = 0$ kPa, $\varnothing' = 17°$ indicating a mean shape factor contribution of about 6°. The standard deviation was estimated to be 3° by combining the separate standard deviations of the material and shape contributions to shear strength.

Correlations for Presheared Surface Residual Strength

Determination of the shear strength parameters for the various bedding parallel shears was based on the tests summarised in Tables 3 and 4. Established correlations between the clay fraction (CF), liquid limit (LL) and ring shear tests (Stark and Eid, 1994) were used to extend the ring shear testing values into a data set large enough to provide statistical parameters for the quantitative risk analysis. The XRD testing of clay mineralogy and percentages of other minerals helped to corroborate the likely shear strength values.

Table 3: Summary of Data for the Probabilistic Residual Strength Parameters

Shear Zone	**Ring Shear Test Results**		**Probabilistic Parameters Derived for Phase II Risk Analysis**					
	# of tests	Residual angle @ 850 kPa	Material Strength Parameters		Shape Factor Parameters		Combined Parameters	
			μ	σ	μ	σ	μ	σ
MT/WCM	Not tested		Insufficient data for statistical analysis				11°	1°
WCM bedding	3	14.4–17.8°	15°	2.2°	3°	0.5°	18°[1]	2.2°[1]
Basement	3	7-9°	Insufficient data for statistical analysis				17°	2°

Note: 1. Phase I parameters of Ø'= 17°, retained for Phase II analysis with σ = 2.2°.

Table 4: Summary of Residual Strength Classification Testing

Shear Zone Location	**LL %**	**CF %**	**XRD Mineralogy**	**Implications for Shear Strength Derivation**
MT/WCM interface	42-46 Med 44	53-57 Med 55	Kaol 20% Qtz 80%	High CF indicates clay fraction will dictate shear strength (Mesri and Cepeda-Diaz, 1986). Kaolinite has basic residual friction angle of 12° setting lower strength bound (Mitchell, 1976).
WCM bedding	26-45 Med 37	34-66 Med 45	Kaol 10-30% Qtz 70-90%	
Basement	33-65 Med 45	31-75 Med 47	Mont 20-70% Kaol 10-45% Qtz 30-80%	Presence of montmorillonite clay raised potential for very weak shear strength surfaces.

Twenty-nine shear zone samples were tested for their liquid limit (LL) and clay fraction (CF) percentages to estimate their likely effective residual strengths using the correlations developed by Stark and Eid (1994). For three out of the six WCM and basement ring shear tests, close agreement (≤3 ° variation) was obtained between the residual friction angles obtained by the ring shear test and those predicted from the correlations of the ratio LL/CF (Stark and Eid, 1994). For the remaining three tests the correlation predicted higher residual friction angles (+8-11°) than that obtained by ring shear. The correlations between LL/CF and $\varnothing'_r$ are well established in the literature for materials compositionally similar to those Rotowaro (Mesri and Cepeda-Diaz, 1986). The reason for these anomalous results is considered to be related to the difficulty of releasing the entire clay fraction from the soft rock adjacent to the shear zones during test sample preparation. The thinness of the presheared soil material in these zones sometimes required grinding up some of the adjacent soft rock to obtain sufficient defect infill sample to fill the testing ring. The ring shear test results are summarised in Table 3. Six XRD tests were also carried out, the results of which are summarise in Table 4.

Selection of WCM Bedding Residual Shear Strength

The basic material strength values were combined with the assessed contribution of bedding shear surface roughness (shape factor) supported by field mapping (scanlines) of exposures in the Township Pit and nearby Awaroa Pits and analysed using the method described in ISRM (1981).

The combined mean residual shear strength of the specific testing for this study (c' = 0, ∅' = 18°) compares closely with the Phase I values of c' = 0, ∅' = 17°. The mean residual shear strength values selected for the ongoing Phase II analyses were ∅' = 17° and σ = 2.2° because of the support given to the mean value (17°) by back analysis of the Waipuna failure which should provide for spatial averaging across this large slide. The use of σ = 2.2° to model the variation in WCM bedding residual strength is based on the natural variations indicated by the Phase II testing program.

The following material characteristics were also considered in assessing the reasonableness of the final selection of WCM bedding shear zone strength values for highwall design:

- The influence of kaolinite on shear strength of the WCM bedding shears is evident from the number of ring shear results between 13° and 18°. Kaolinite's characteristic frictional strength in its pure form is about 12° (Mitchell, 1976).
- The existence of residual strengths as low as 8° in the Phase I database can be assumed to not dictate the WCM bedding strength, given the absence of significant pit wall stability problems in WCM materials.
- Similarly, if the combined standard deviation for the mean WCM shear strength was higher than 2.2° then mean bedding shear strengths as low 11° (i.e. 18° - 3 std deviations) would be expected. Consequently, there should be a higher incidence of highwall failures in WCM than is actually observed. The lack of gross instability problems supports the selection of a low standard deviation.
- The selection of a low shear strength standard deviation in conditions of "uniform" geology also reflects, in part, the phenomenon of spatial averaging observed by other investigators (Christian, 1996).

Development of Piezometric Surfaces

The expected piezometric surfaces were derived from the piezometer data, an understanding of the regional groundwater system and the transmissivity characteristics of the various geological units within each highwall cross-section. Contributing factors that may influence long-term piezometric pressures include:

- Cessation of dewatering bore pumping from underground workings.
- Development of a lake to RL 25 m assuming the void will not be used for future backfill capacity.

A key uncertainty in developing the groundwater models for the proposed cut slopes is the response of the groundwater profiles in each of the major geological units. This is especially so for the basement groundwater condition along the Southern Highwall, where the effects of changes in leakage characteristics are presently uncertain.

To account for the uncertainty in the probabilistic analysis, normal statistical distributions of piezometric levels about a mean level were assumed. These are shown in Table 5. In general there is a high level of uncertainty in the selection of a best estimate of the piezometric surface and where these values have been assumed, a large standard deviation has been adopted.

Where drainage measures are used the standard deviation was set to zero, reflecting the assumption that effective drainage removes the risk of adverse piezometric rises and therefore decreases failure probability. It is, however, noted that the measured variances in the natural groundwater systems unaffected by mine operations and pumping were about 1 m. Therefore, where greater confidence could be placed on expected groundwater conditions or where more conservative groundwater profiles were adopted, the variance for some selected groundwater profiles was reduced to reflect the response of the natural groundwater systems.

Table 5: Standard Deviations Adopted for Variations in Piezometric Head

Groundwater System Characteristics	Standard Deviation (m)
Undrained, high uncertainty of upper piezometric level	5
Undrained, high confidence of upper piezometric level	1.2
Drainage installed, piezometric levels prevented from uncontrolled rise.	0

Characterisation of Failure Modes and Surfaces

Historical slope performance for cuts in the various materials about the Rotowaro area indicated that the most significant failure mechanisms for highwall design were large block slides (>100,000 m^3) on presheared surfaces, and circular failures close to the pit wall in the order of 10,000 to 100,000 m^3. Wedge failures controlled by joints and bedding generally result in small failure volumes (up to 30,000 m^3).

Risk Assessment Methodology

Risk is the combined measurement of both probability of failure (P_f) and its consequence. Quantitative risk assessment differs from the deterministic approach in that it incorporates the explicit assessment of the numerical risk of highwall instability into the stability analysis and design. It can also include the vulnerability of assets and life to slope failure as part of the consequences assessment (UNSW, 1999). For highwall design in the South Pit the most likely consequences are economic losses in the form of coal reserves, damage to the road in the Hangapipi Boxcut (behind the Southern Highwall) and possibly adverse environmental effects, such as the Waitawhara Stream discharging into the pit.

Quantitative risk assessment methods were selected for this project as it was considered to be the most rigorous means of developing designs that have levels of stability directly linked to risk of failure.

Quantification of Probability

As part of the risk assessment methodology, an estimate of probability of highwall failure by a range of failure modes was required along with a statistical distribution of the values for the key stability input parameters. The key variable inputs for highwall design were bedding shear strengths, piezometric head acting on the failure surfaces and the attitude of bedding and structural discontinuities.

Various algorithms are available to estimate the probability of failure within the conventional framework of stability limit equilibrium analysis. Two, which are readily applicable to the highwall design, are the Monte Carlo and First Order Second Moment (FOSM) methods.

For the Phase I preliminary stability and risk assessments the Monte Carlo method was used principally because of its speed and ready application from within the slope analysis software being used (SLOPE/W). We found that this method does not easily lend itself to the interrogation and identification of the key risk components in design. For this reason as part of the Phase II risk assessment, the FOSM method (Christian, 1996) was used, enabling a more discrete assessment of the risk components within a particular section of highwall. The FOSM procedure is rigorous and allows the relative importance of input parameters and their uncertainty to be understood via the sensitivity process.

Having confirmed the key components influencing the risk models and confirming the models using FOSM methods, at the optimisation stage of design Monte Carlo methods were again adopted to enable a large number of analyses to be undertaken in relatively short time frame.

Consequences of Failure

At an early stage in the project, it was apparent that the scale design process would be highly iterative and that a simple and easy to use measure of consequence was required. Options to develop a detailed cost:benefit analysis of designs were initially considered. Finally, an estimate of failure volume was adopted as a value-index to assess the consequences of failure. This approach recognises that consequences are heavily dependent on the scale of failure.

Some judgement is required in the assessment of failure volume. There is no direct method of predicting failure volume from a 2-D analysis for block and circular modes of failure. Hence, the expected failure width for each section was estimated by considering the mid-point of a distribution between the minimum and maximum likely failure widths, taking into account any obvious geological or geometric constraints. The "expected failure volume" then simply became the expected failure width multiplied by the critical failure cross-sectional area determined by conventional stability analysis. To calibrate this assessment of failure volume to site experience, the methods were found to provide good agreement with observed relationships between failure length and widths for historic large-scale failures at the Waipuna Opencast.

As part of a final check of the design optimisation, three-dimensional wedge analyses have been carried out to address possible small volume (up to 30,000 m^3), discontinuity-controlled failures.

Defining an Acceptable Risk Criteria for Design

An assessment the tolerable risk criteria was developed setting an upper bound on levels of acceptable risk as shown in Figure 6. Choosing a separate and lower tolerable risk volume (i.e. $P_f \times$ failure volume = constant) for the Southern Highwall reflects the need to ensure that the road and stream diversions through the Hangapipi Boxcut behind this area are unaffected in the long-term by mining and the subsequent pit end use (a lake). The risk-volume criteria make an allowance for small, but high probability failures to be acceptable within the design. However, larger scale failures require high levels of stability (low probabilities of failure) to achieve the design criteria.

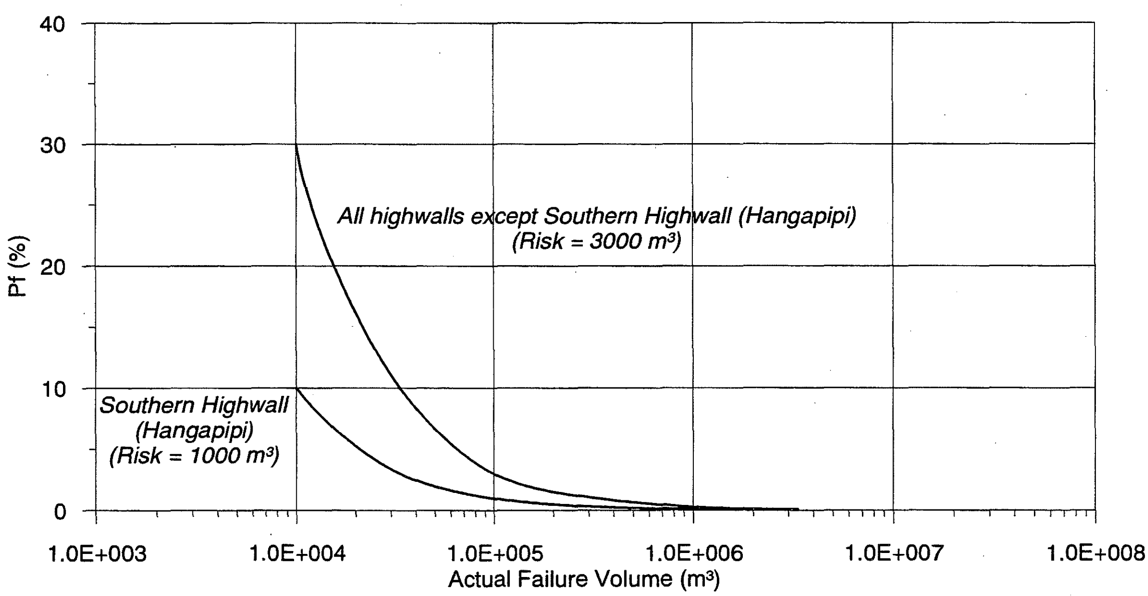

Figure 6: Tolerable Risk Criteria

The adoption of the risk volume criteria is consistent with the mining industries greater tolerance of small failures and intolerance of large failures. For example, a risk volume criteria of 1,000 m³ would equate to a 10,000 m³ failure having a 10% probability. While small failures of this size represent an inconvenience to the mining operation, possibly adding to operational cost, they do not result in a major loss, disruption or cessation of mining. Conversely, a large failure, say 400,000 m³ in volume, would have a major adverse consequence. To meet a risk volume criterion of 1,000 m³, the probability of failure would need to be 0.25% or lower.

Risk Assessment Results for Phase II

Numerous analyses were performed as part of the Phase II risk assessment and subsequent Phase III design optimisation process. For the Phase II slope designs the key objectives were to maximise the coal won while attaining the tolerable risk criteria. Table 7 illustrates typical outputs for Sections CC and FF as part of the Phase II design.

Table 7: Phase II - Typical Risk Assessment Results

Highwall	Load Case	Failure Surface Location	Expected FOS	P_f (%)		Expected Vol. (m^3)	Expected Risk Volume (P_f*Exp.Vol.)	
				Without Drainage	With Drainage		Without Drainage	With Drainage
Western (Section CC')	Long Term/ Pre Lake with buttress	Taupri	1.4	0.01	0.01	396,000	40	40
		WCM/ Basement	1.34	0.01	0.01	871,200	87	87
		Basement	1.38	0.01	0.01	922,350	92	92
						Total Risk	219	219
Southern (Section FF')	Construction	Taupri	1.3	0.01	0.01	102,450	10	10
		WCM/ Basement	1.23	4	0.01	1,956,600	78,264	196
		Front Face	1.41	0.5	0.01	142,900	715	14
						Total Risk	78,989	220

Note: Results are for expected piezometric conditions with block failures.

From these analyses, a first-pass pit shell was developed which complied with the design criteria, and enabled an initial assessment of pit reserves and economics for the remaining life of Township Opencast. Key points to note from the risk assessment were:

- Total risk is taken to be the sum of risk from failures on known failure surface locations.
- As the factors of safety (FOS) decrease there is a corresponding increase in failure probability. Above a FOS of about 1.5, which is commonly used in the civil engineering design of infrastructure, the failure probability is generally low, corresponding with past experience.
- For large potential failures, even with relatively high FOS and low probability of failure, the assessed risk volumes on many sections of the Southern Highwall were higher than the expected smaller-volume, high probability face failures. This is primarily due to the influence of an extensive area of adversely dipping strata close to the expected mean assessed friction angle for bedding shears and the high levels of uncertainty in assessing post-excavation groundwater levels in basement.

- This is illustrated on Section FF (Figure 7) where adversely dipping bedding shears and sub-artesian groundwater pressures exist in the basement. The resulting FOS for failures affecting the stream and road are of the order of 1.6 to 1.7, but the steep inclination and uncertainty in groundwater level results in calculated risk volumes of between 500 m^3 and the tolerable risk volume of 1000 m^3 on many sections of the Southern Highwall. Conversely, small volume face failures with FOS of 1.2 and P_f values of the order of 1-3% can have less risk volume (<100 m^3).
- Where applicable, installation of effective drainage can have a dramatic effect on reducing failure probability and total risk. This is especially so in the case of the Southern Highwall (Table 7).
- Where the risk assessment indicated very low P_f levels (<0.01%), a default value of 0.01% was used to reflect the inherent uncertainties in the P_f estimates.

Optimisation (Phase III Design)

Using the pit shell from Phase II as a reference point, a series of additional analyses were developed. The optimisation process included a series of analyses to assess not only the coal-winning limit in more detail and to look at construction issues, such as highwall transitions and benching/battering configurations. A key component in the assessment of sequence options was the identification of mining limits that required head unloading of the design cut before the final highwall could be developed. This design element is critical for highwall construction along the Karaka Fault and formation of the final Southern Highwall. Figure 7 illustrates the design developed for Sections CC and FF.

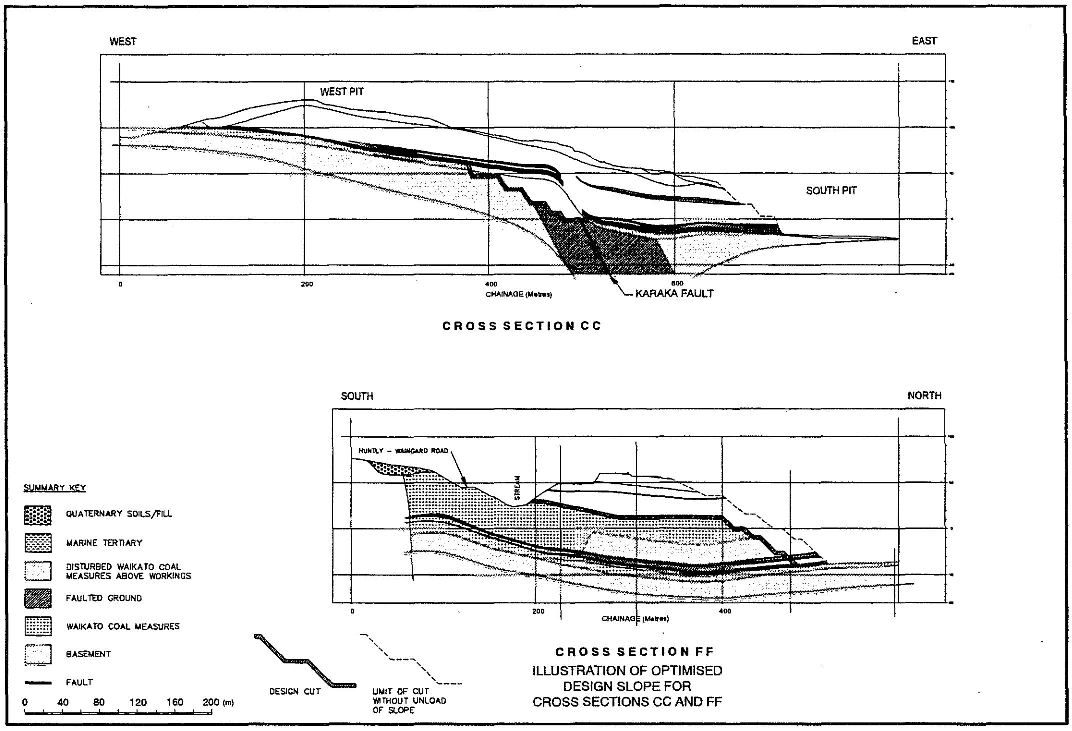

Figure 7: Optimised Highwall Profiles

It is noted that while the overall design concepts developed from the Phase II design remained essentially the same, some adjustments to the design evolved out of the additional analyses. Key points that arose out of the optimisation programme are summarised below.

On one section of slope along the Western Highwall, further drilling was undertaken to refine the position of the Karaka Fault, and the dip of the footwall sequence. Two additional piezometers were installed in the West Pit to reduce the uncertainty in the groundwater model

(Table 1). The additional drilling resulted in a better-constrained geometry model and a more reliable design for this section of slope.

As part of the final design check, additional analyses were made to address possible wedge failures in the 10,000 - 30,000 m^3 volume range that may affect the design, in particular where coal winning would be undertaken below the basement cut into the Karaka Fault. These potential failures have been addressed for safety reasons and to highlight considerations for slope performance monitoring and construction supervision.

On the Southern Highwall the risks, and potential benefits, associated with reducing the sub-artesian groundwater pressures in the basement through drainage have been explored. The expected groundwater model was refined based on a pump test in the old mine workings to assess the basement groundwater to dewatering. There remains a risk that the drainage works will not be effective and that assumed post-drainage groundwater levels may not be achieved. A programme of additional groundwater monitoring has been developed to enable the risk of "worse than expected" groundwater conditions developing and the effectiveness of possible drainage options to be better quantified.

The optimisation process has identified several configurations for the highwalls. All options have similar risk volumes in terms of the 2-D stability analysis, but have different implications for mine design and planning, *vis*:

- *Mining economics* - For each option the quantity of recoverable coal needs to be assessed along with the estimated cost of recovering the coal. The most economic option is the one that returns the maximum Net Present Value (NPV). An initial simplistic approach currently being undertaken is to compare the marginal economic cost and benefit between the various options.
- *Short-term construction risk* - One option for the Western Highwall involves buttressing of the upper section of highwall above the Karaka Fault in order to achieve the long-term design criteria. While this option may potentially offer operational benefits by allowing more flexibility in terms of the mine development and mining sequence, it is not favoured due to the short-term construction risk.
- *Reliability* - One of the options identified for the Southern Highwall involves well drainage in order to improve slope stability, allowing recovery of more coal. There are large potential cost savings with this option compared to other options that involve unloading the highwall to achieve stability. The reliability of this option will require careful evaluation in respect to the required spacing of the drains, and the installation and performance risks.
- *3-D mine design verification* - In order to determine recoverable reserves and overburden quantities for assessment of mining economics, preliminary 3-D designs ("pit shells") have been developed using Vulcan mine planning software. The pit shells are based on the 2-D cross-sectional designs, but do not honour the 2-D designs exactly due to practical benching and battering constraints. Following selection of the most economic option, the 3-D design will be verified and, if necessary, adjusted, to ensure (geotechnical) risk criteria have not been exceeded.
- *Slope performance monitoring* - During excavation of the highwalls, performance monitoring and inspections will be required to confirm some model assumptions and, where possible, to further optimise the designs. The Western Highwall may be able to be optimised further if the extent of the sheared and disturbed ground on the up-thrown side of the fault is less than adopted in the models. Inspection and mapping of the basement exposures will be required, with timely feedback to the designer.
- *Groundwater monitoring* - The Southern Highwall design is the most sensitive to the basement groundwater condition. Monitoring of basement groundwater to ascertain its response during excavation and leakage to the mine workings will be necessary. Depending on this response, the design may need to be changed to reduce the risk of failure or, alternatively, optimised to recover more coal for acceptable extra cost.

Regular exchange of piezometric data between the mine and the designer will be required to capture these risks and opportunities.

Conclusions

This project has highlighted the benefits that probabilistic slope stability analysis and quantitative risk assessment bring to mine design in an area where (engineering) geological uncertainty, and low tolerance to non-performance of slopes dictate the terms of operational success. The approach adopted for the Township Opencast, though in need of some refinement, allowed the complex relationship between engineering geology, geotechnical parameters, geotechnical risk and mining economics to be more fully understood and incorporated in to the mine design processes. The cut slope designs resulting from this approach incorporate the following benefits:

- Account for the uncertainty in ground conditions;
- Provide a consistent measure of stability and risk between analyses;
- Enable design options to be compared using a rigorous approach;
- Allow design selection to be made based on a set of geotechnical criteria that reflect levels of economic and operational risk; and
- Result in more informative communication of risk between the owner, designers and the construction contractor.

Key geotechnical engineering understandings developed through this project include:

- The potential failure geometry with the lowest factor of safety (FOS) does not always reflect the highest risk condition, as FOS does not provide a direct measure of consequence of failure.
- The value of the quantitative risk approach is in the economic balance that can be brought to the decision making process in design selection and optimisation.
- An iterative approach to site investigations, engineering geological data analysis and geotechnical risk assessment ensures geological uncertainties can be minimised to acceptable levels for design.
- Risk criteria which incorporate the probability of failure with the immediate consequences (failure volume) are very practical and make for more immediate and consistent comparisons between different designs.

Acknowledgments

The authors thank Solid Energy New Zealand Ltd for permission to publish this paper.

References

Edbrooke, S. W., Sykes, R. and Pocknall, D. T. (1994): “Geology of the Waikato Coal Measures, Waikato Coal Region, New Zealand.” Institute of Geological and Nuclear Sciences Monograph 6

ISRM Suggested Methods (1981): “Rock Characterisation, Testing and Monitoring,” Ed. Brown E.T. Pergamon Press

Kear, D. and Schofield, J. C. (1966): “Geology of the Ngaruawahia Subdivision” New Zealand Geological Survey Bulletin 88.

Kear, D and Waterhouse, B. C. (1978): “Waikato Coalfields: Rotowaro Coalfield 1:15 840.” New Zealand Geological Survey Miscellaneous Series Maps 9 (Geology) and 10A (Mining); maps (3) and notes.

Mitchell J. K. (1976). “Fundamentals of Soil Behaviour,” John Wiley and Sons Inc.

Mesri G. and Cepeda-Diaz A.F. (1986). "Residual shear Strength of Clays and Shales" *Geotechnique* Vol. 36, N°2, pp 269-274

Christian J. (1996) "Reliability Methods for Stability of Existing Slopes", Conference Proceedings *Uncertainty in the Geologic Environment from Theory to Practice- Proceedings of Uncertainty 96,* Eds Shackelford C.D., Nelson P.P., Wroth M.J.S., ASCE pp 409-418

Stark and Eid (1994): "Drained Residual Strength of Cohesive Soils"*Journal of Geotechnical Engineering* Vol. 120 No 5. May 1994, pp 856 to 871

University of New South Wales (1999). "*Quantitative Risk Assessment of Soil and Rock Slopes.*"

AGS hillside development project

F J Baynes
Consulting Engineering Geologist, Western Australia

(paper not available at time of printing)

Managing a Landslide Hazard in the Roxburgh Gorge

Don Macfarlane
URS New Zealand Ltd, P O Box 4479, Christchurch

Ken Roberts
Contact Energy Ltd, P O Box 25, Clyde

Abstract

International case history data shows that most slope instability problems or failures affecting reservoirs occur during lake filling or within the first few years of operations. Pre-existing landslides along the Roxburgh Gorge were partially inundated when the Roxburgh dam reservoir was filled in 1956. There have been no major shoreline instability problems along the Roxburgh reservoir in over 40 years.

To manage the landslide hazards, the reservoir operator (Contact Energy) has carried out a systematic, staged investigations programme to determine the extent and age of the landslides, and their activity prior to and after filling of the reservoir. Survey monitoring is providing on-going information that will allow changes in behaviour of major landslides to be detected at an early stage. The monitoring to date has indicated creep rates varying between 0 and 80mm/yr. From this, the relative hazard potential of the landslides has been assessed. The overall annual probability of a failure large enough to cause partial or complete blockage of the reservoir is judged to be in the order of 1 in 50,000 under present conditions.

The reservoir operator has developed a management strategy for these pre-existing landslides based on the observational approach with its three components of monitoring, evaluation and action planning. A formalised data evaluation and review process has been developed, and emergency response plans are being developed.

Introduction

Landslides are a common natural hazard throughout the world and are widespread in the schist rocks of Central Otago. Landsliding is a natural phenomenon that occurs on steep slopes as part of the erosion and valley-forming processes. Rapid slope failure is usually caused by some 'trigger' event such as intense rainfall, earthquake shaking or erosional undercutting, but may also occur as a result of the gradual loss of strength of the slope-forming materials.

Since the 1970's, the schist landslides in the Kawarau, Cromwell and Roxburgh Gorges have been mapped and monitored in varying detail. Both the Cromwell and Roxburgh Gorges are occupied by reservoirs created for hydro power generation purposes. As described by Gillon & Hancox (1992), extensive remedial works were implemented on some of the Cromwell Gorge landslides adjacent to the Clyde dam reservoir prior to lake filling to ensure their long term stability.

In contrast, the Roxburgh dam reservoir was filled very rapidly (within a period of a few days) more than 40 years ago, apparently with no consideration of potential landsliding other than small scale shoreline slumping. While it is not known to have experienced problems due to slope instability either during or since that lake filling, the Roxburgh Gorge landslides had been relatively little studied until Contact Energy implemented a staged investigation programme to identify, map, classify and monitor the landslides.

Hazard and Risk Issues

Pre-existing landslides along valleys that become reservoirs can be affected both by reservoir formation and subsequently by reservoir operations. Two key issues are the effect of the reservoir on the stability of the slope, and the potential effect of the landslide on the reservoir. Both risks must be actively managed by responsible reservoir operators.

The possible effects of a large scale slope failure into a narrow reservoir include valley blockage, partial blockage and the formation of impulse waves as the reservoir is displaced.

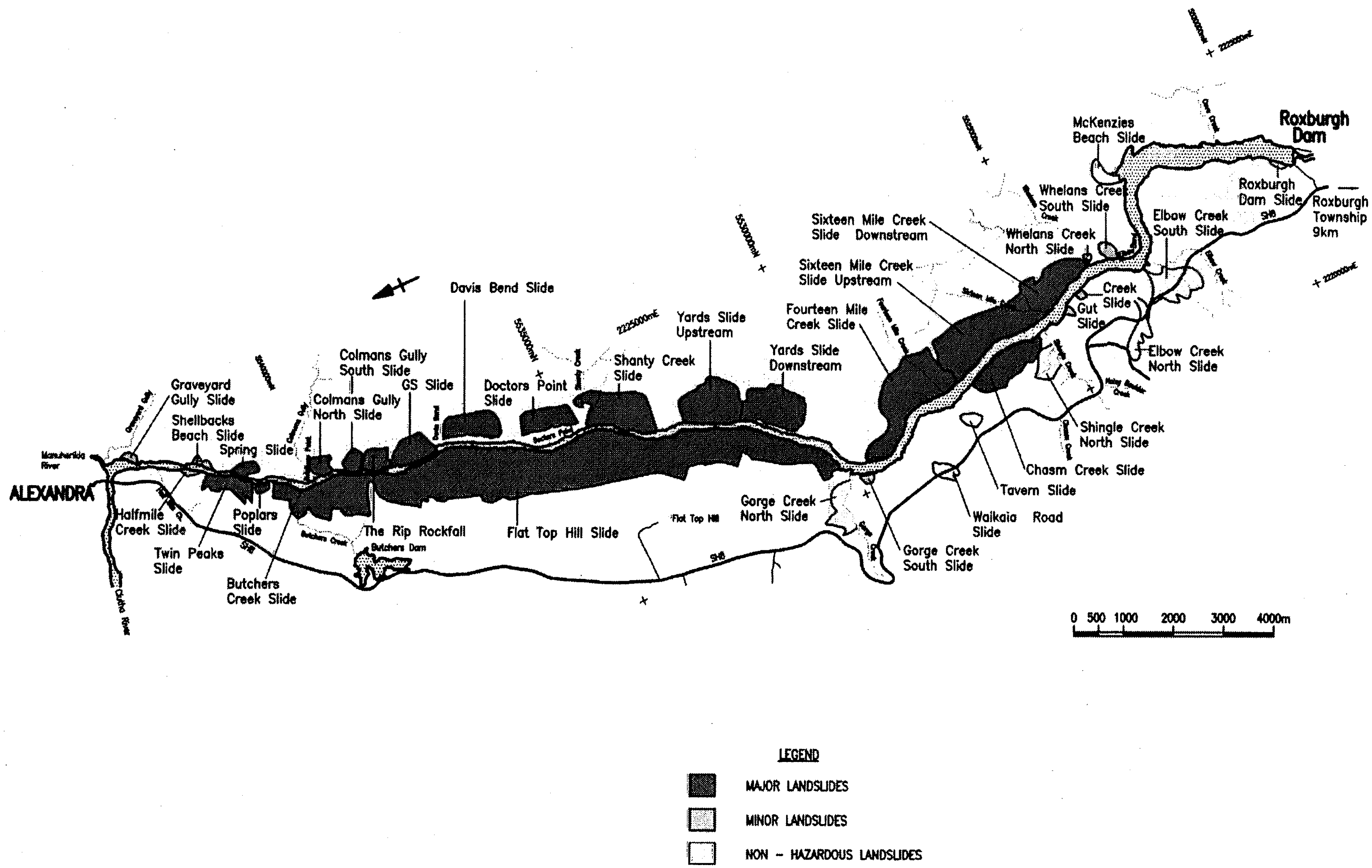

Figure 1. Location and classification of Roxburgh Gorge landslides

The consequences of valley blockage may include upstream flooding, or catastrophic failure of the landslide dam leading to extensive downstream damage and loss of life. The Vaiont landslide in the Italian Alps, one of the most documented reservoir landslide failures, occurred during lake filling (eg. Hendron & Patton 1986) and caused both valley blockage and the formation of an impulse wave that overtopped the dam and caused massive downstream damage and loss of life. Vaiont became the precedent catastrophic landslide. It is largely responsible for a marked change in the emphasis placed on understanding and managing the stability of reservoir slopes in recent decades.

International case history data shows that most slope instability problems or failures affecting reservoirs occur during lake filling or the first few years of operations. Literature searches have identified reservoir-slope interaction reports at 176 reservoirs in over 40 countries. A study of 60 case histories (Riemer, 1992) concluded that the most critical period is first filling of the reservoir, and reported that 85% of the documented slide events started during construction and filling or within two years after completion of the project. Other studies have shown similar pronounced risk recession with the passage of time (eg. Jones *et al* 1961, Nakamura 1985). As at Vaiont, the problems experienced commonly relate to changes to the groundwater system within or beneath the landslide.

The 30 km long Roxburgh dam reservoir extends upstream to the town of Alexandra, sited at the head of the lake, mainly within a narrow gorge. A large scale slope failure into the reservoir could cause valley blockage (ie. a landslide dam) with consequent flooding of Alexandra, or a partial blockage constricting flows and increasing the risk of flooding at Alexandra. Failure of such a landslide dam could result in damage to or even loss of the Roxburgh dam, with serious downstream effects, possibly including loss of life. Any of these scenarios has huge economic consequences and is totally unacceptable to the owner and the community. Damage resulting from a landslide-induced wave is unlikely due to the small volume and narrow nature of the reservoir.

Studies undertaken

Since 1995, Contact Energy has undertaken a systematic staged investigation of the extent, nature and activity of the Roxburgh gorge landslides. The work completed to date has been:

Stage 1 air photo interpretation and preliminary engineering geological mapping to identify all landslides along the reservoir and assess their relative activity before and since lake filling

Stage 2 a preliminary evaluation of the probability of landslide failure under normal operational conditions, extreme flood conditions or earthquake

Stage 3 a review of the information collected to classify the landslides and to determine and prioritise appropriate subsequent investigations

Stage 4 more detailed mapping of selected landslides within the narrowest part of the gorge to better define their nature and activity, and to identify sites for the installation of survey monitoring

Stage 5 additional engineering geological and geomorphological mapping of the remaining large landslides to better define their nature and activity, and to identify sites for the installation of further survey monitoring

Stage 6 installation of a survey monitoring network on those landslides considered to have sufficient volume to block the reservoir if they failed rapidly.

Stage 7 implementation of a management strategy that includes regular monitoring surveys and interpreting the monitoring data.

This systematic approach has ensured that the assessment of each package of new information is reviewed and used as the basis for deciding the most appropriate activity to be next undertaken.

Results of Studies

Extent of Landsliding

The initial air photo interpretation and mapping identified 34 landslides along the Roxburgh Gorge (Figure 1), many of them large in relation to the width of the reservoir (see also Figure 2). All of the landslides were present before lake filling. Figure 3 is a photo that helps to illustrate the extent and nature of landslides in the narrowest part of the gorge.

Subsequent work has classified 18 of the landslides as 'major', 8 as 'minor' on the basis of their size and location. It has also been determined that the eight other landslides show movement or past movement towards tributary streams or gullies rather than towards the lake, and are thus of no potential hazard to the reservoir.

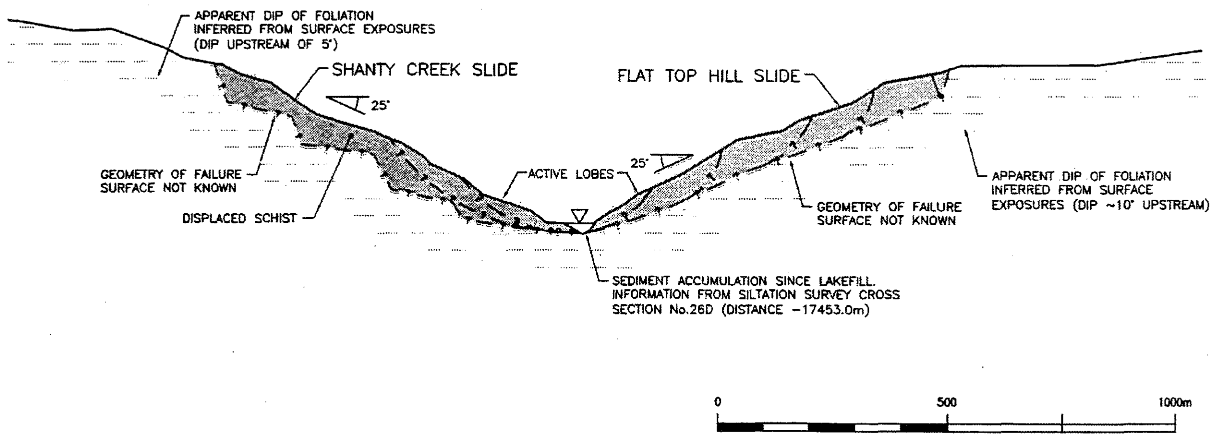

Figure 2. Typical cross section of Roxbugh Gorge.

Nature of the Landslides

Field evidence indicates that the landslides are large, dormant or creeping features. Some are deep seated and extend down to below lake level; these were present along the river prior to lake filling. Other landslides are perched high on the valley walls above rock bluffs (eg. Doctors Point Slide in Figure 2). Several left bank slides, including the Shanty Creek Slide (Figure 2), appear to be partly perched and partly deep seated, possibly indicating that they originally failed onto an eroded rock bench with a later failure of the rock bluffs causing deepening of the slide base.

The Rip Rockslide (Figure 4), the only obvious geomorphic evidence suggesting a past landslide blockage of the Roxburgh Gorge, appears to be an example of a later failure of part of an original slide perched above rock bluffs. While it seems likely that this conspicuous feature formed a landslide dam in the Roxburgh Gorge at some stage in the past, specific investigations found no conclusive evidence to confirm this. Geological and pedological studies have indicated that the Rip Rockslide is probably more than 80,000 years old and could be older than 110,000 years. There is no other clear evidence that any pre-existing landslide within the Roxburgh Gorge has ever undergone large scale rapid movement.

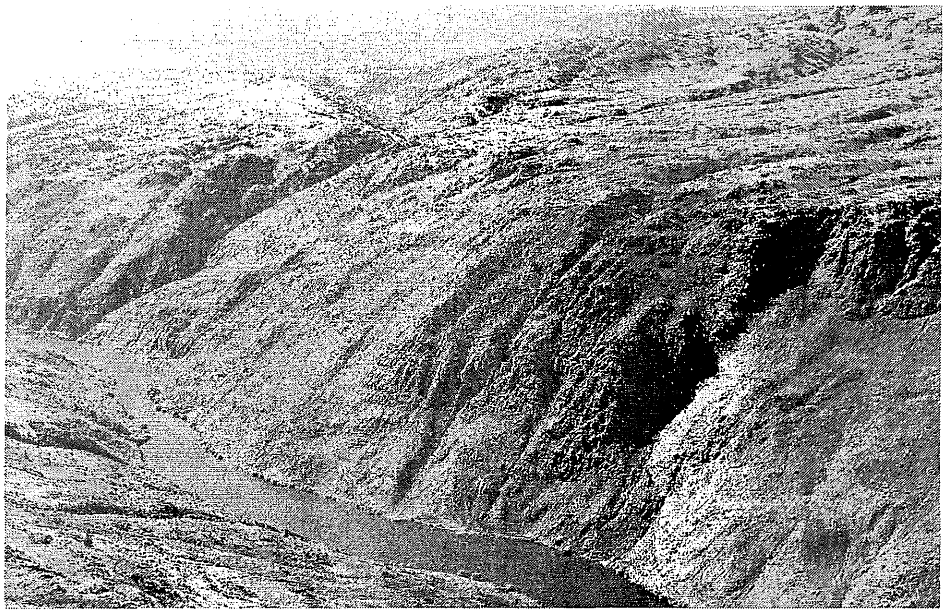

Figure 3. View upstream from Flat Top Hill Slide showing Shanty Creek Slide between the incised creek and the bluffs extending down to the lake. Yards Upstream Slide is to the right of the bluffs, and Doctors Point Slide is perched above the low bluffs upstream from the deeply incised Shanty Creek. The low relief surface above the slides is the Otago peneplain.

Figure 4. Aerial oblique view of the Rip Rockslide, a probable breached landslide dam about 7 km downstream from Alexandra. The slopes above the low bluffs to the right of the debris tongue are also slide debris and are inferred to have been part of the original slide mass.

Field Evidence for Landslide Activity

Air photos show that the geomorphology of the Roxburgh Gorge has not changed significantly since 1949, indicating that lake filling in 1956 did not cause large displacements of the landslides or other parts of the shoreline.

The air photo interpretation and mapping show that at least 8 of the 'major' landslides were active immediately prior to lake filling although movement rates at that time are unknown. It has not been possible to determine the activity of 6 other 'major' landslides immediately prior to lake filling because the data are unavailable or inconclusive.

Changes to scarps, tension cracks and other surface features identified by interpretation of air photos taken at different times suggests that 13 of the 'major' slides were active in the period between lake filling and 1968. Air photo interpretation also suggests that movement rates between 1968 and 1996 have in many cases halved compared with the period immediately following lake filling (1958 to 1968).

Comparison of the length of sedimentation survey cross section lines has also been used to help estimate slide movement rates. Only 14 of the 47 sediment survey lines show shortening, mostly in a few localised areas, since their installation in 1962.

Probability of Failure

A preliminary evaluation of the probability of landslide failure completed in 1996, although of a general nature, considered a number of factors that could affect slope stability and concluded that complete or partial lake blockage could occur if a relatively small part of a 'major' landslide was to fail. It was judged that the overall annual probability of a critical sized failure was about 1 in 12,000 under present conditions, and that some severe external event (such as earthquake or extreme rainfall) is probably necessary to initiate a large scale rapid failure. A review of the probability of failure was undertaken in 2000 with improved appreciation of the geology and the age of the Rip Rockslide. This review concluded that the overall annual probability of failure was in the order of 1 in 50,000 and noted that each of the likely trigger events could occur regardless of the presence of the lake.

Comparison between Roxburgh and Clyde landslides

There are a number of differences between the geology and landsliding of the Roxburgh and Cromwell gorges that have allowed different approaches to hazard management.

Geology

Most of the Clyde (Cromwell Gorge) landslides, and also many in the Kawarau Gorge, are controlled by the foliation (layering) within the schist bedrock. Failure occurs on shears parallel to foliation where the foliation is sloping at more than about 20-25 degrees towards the gorge, or on low angle faults sloping towards the gorge. The landslides therefore tend to be on one side of the valley as on the other side of the valley the foliation slopes away from the gorge. In addition, many of the landslides controlled by foliation have (or had) very high uplift pressures acting on them because groundwater recharge from further upslope had entered the rock and was trapped in sloping aquifers between shear zones within the rockmass.

In the Roxburgh Gorge foliation is relatively flat lying, with some local exceptions, and does not generally appear to be controlling slide development to the same extent. Because the foliation is flat lying there is no preferential side of the valley for the landslides. The slopes are generally dry, with few springs or perennial streams, and it is inferred that there is little chance that high groundwater pressures have developed within them. It is believed that the flat-lying foliation (and foliation shears) will act to reduce or prevent the development of large confined aquifers acting on the landslides.

As more detailed geological mapping has been carried out in the Roxburgh Gorge, it has been found that there is more rock outcrop in some of the slopes mapped as landslides than was previously thought. Several landslides appear to consist partly or entirely of debris that is spilling over rock bluffs that are located above lake level. Where the landslide base is above the lake, the lake does not affect the stability of the landslide.

History

The toes of many of the landslides in the Cromwell Gorge were to be inundated by the formation of Lake Dunstan behind the Clyde Dam. Analyses showed that there would be significant reductions in stability for those landslides with confined groundwater systems, and that other landslides would undergo large changes in groundwater levels. Consequently, stabilisation measures were carried out on many of the landslides and a controlled lake filling strategy was adopted. Of those landslides that were stabilised, many are now creeping at rates less than was observed prior to construction of the stabilisation works. Some that were not stabilised are now creeping slowly.

There are good monitoring records extending back to the period prior to lake filling. From these, it is known that movement rates vary between dormant (no detectable movement) and 80-100mm/yr. Some slides show a short term rate increase in response to abnormal rainfall events (eg. Macfarlane & Gillon, 1996).

In contrast, Lake Roxburgh was filled over a period of a few days, apparently without any realisation that large landslides were present. Fortunately, the geological (and by inference groundwater) conditions were favourable and although comparisons of air photos indicate some increased activity, no major slope movement occurred due to lake filling.

During the geological mapping work undertaken since 1995 several landslides were identified as having unvegetated scarps suggesting recent activity (within the last 50-100 years). Few of these scarps have been shown to relate to lake filling. Comparisons between 1958 and 1968 air photos indicate localised movement at rates of up to 230 mm/yr over that period. The section of slope that was moving at 230 mm/yr between 1958 and 1968 is indicated to have moved at 60 mm/yr between 1968 and 1996 from air photo interpretation. Current survey monitoring indicates that the manyy of landslides are dormant or creeping at less than 10 mm/yr. A few slides are moving at rates ranging from 10mm/yr to 35mm/yr.

Management strategies

Factors influencing the management strategy

The key objective of reservoir slope management is to ensure that the slopes adjacent to a reservoir are sufficiently safe to enable it to be operated. Sufficiently safe means that the slopes do not pose an unacceptable risk to people or property. Risk management processes are an important aid to achieving this objective.

A fundamental consideration for Roxburgh is that the lake has been filled and operated for over 40 years with no adverse effects on slope stability. A second important consideration is that because the reservoir is narrow and much of it is quite shallow, the upstream flooding effects of a slope failure (in terms of time) are little changed from the pre-lake situation. Thirdly, the most probable triggers for a slope failure (extreme rainfall, flood, earthquake) are all natural events that could occur regardless of the presence of the lake.

Adopted management strategy

Risk analysis has indicated that a landslide dam in the Roxburgh Gorge has an extremely low probability of occurrence. Risk reduction and management principles that are appropriate for the Roxburgh Gorge landslides include visual inspections and monitoring, development of appropriate action plans, and regular safety reviews.

Contact Energy is following a management approach like that recommended by the International Commission on Large Dams (ICOLD, in prep). The basic philosophy is that it is not possible to provide an absolute guarantee of the stability of all slopes around a reservoir. Uncertainty inevitably remains, regardless of the degree of investigation, analysis and remedial works undertaken. This uncertainty can be realistically managed only by using the observational approach (Peck, 1969).

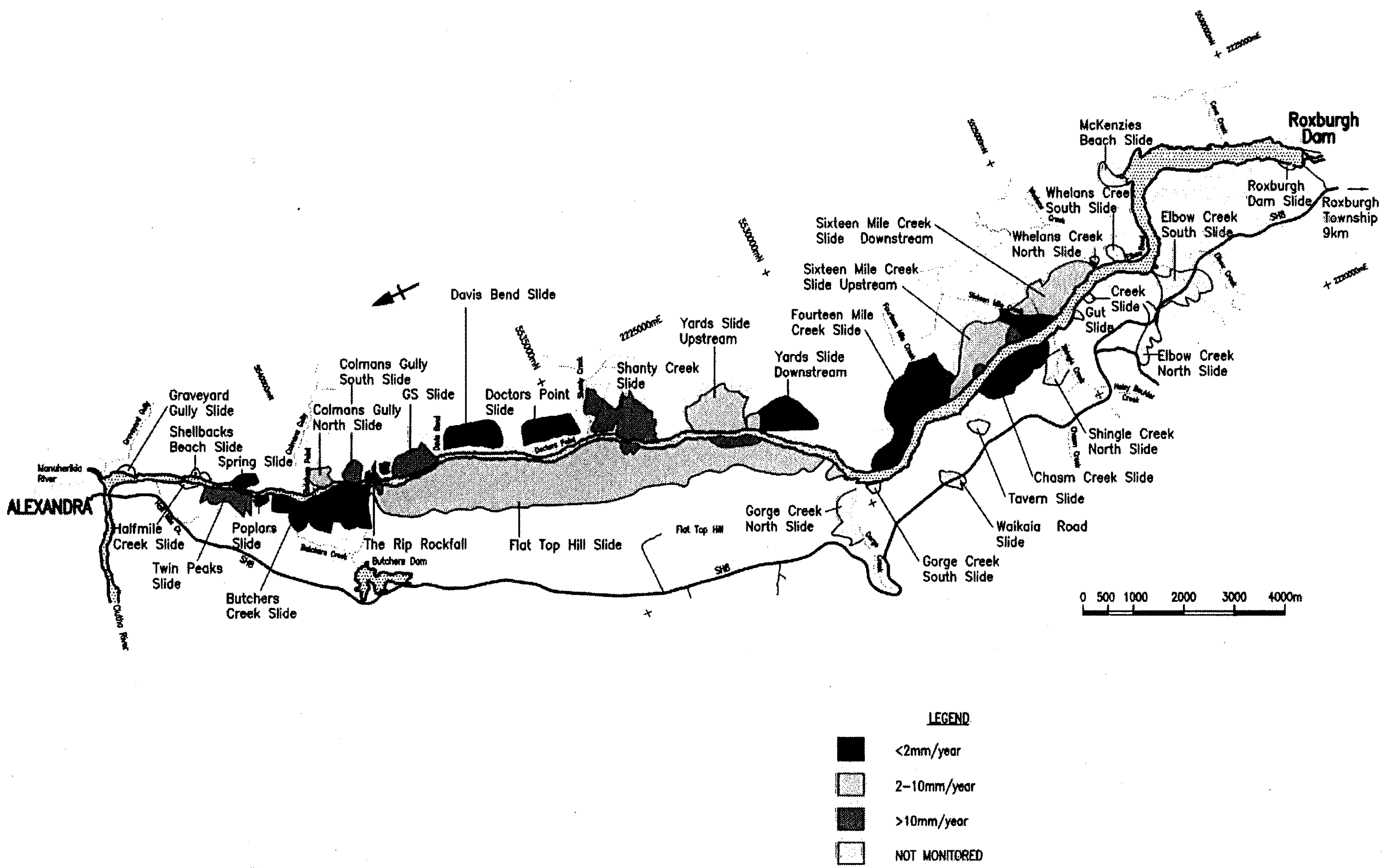

Figure 5. Current movement rates for Roxburgh Gorge landslides

The observational approach is based on the concept, supported by case histories, that most landslide events other than those caused by extreme events (eg. earthquake-induced failures) do not occur without warning (Riemer, 1992). The method comprises three elements:

- a monitoring system that is capable of detecting warning signs reliably and accurately
- a strategy of actions to be taken in the event of unacceptable slope movements
- an efficient organisational approach that reduces (processes) incoming data, evaluates the observations and decides which action to take, and when.

Contact Energy has had a system like that described above in place for many years to manage the Cromwell Gorge landslides and has installed survey monitoring on the 'major' Roxburgh landslides. The survey method used is considered accurate to 5 mm (approx.) and is sufficiently precise for landslide monitoring. Difficulties with establishing stable control points were recognised and addressed in the design of the surveys. Both survey and inclinometer monitoring is carried out on the small 'Roxburgh Dam Slide' adjacent to the right abutment of the dam.

The data is regularly collected, currently every 3 months, and is reduced and evaluated as it is received. Except for the 'Roxburgh Dam Slide', which has been monitored since lake filling, the survey monitoring instrumentation was installed in 1998 and 1999. Instruments installed in 1998 are beginning to show trends but there has generally been too short a data record from instruments installed in 1999 from which to draw meaningful conclusions about the rate and distribution of activity.

This system will be reviewed and upgraded as investigations and findings dictate. Contact Energy has procedures in place for regular quarterly and annual review of the monitoring data by specialist engineers and engineering geologists, and also has procedures for regular, independent comprehensive safety reviews.

Contact Energy has systems in place that ensure the detection of unacceptable slope movements and is working to develop action plans (including notification plans) that can be implemented should unacceptable movements, partial blockage or complete blockage occur. As part of this process, consideration is being given to monitoring options that would allow more frequent data to be obtained from critical locations.

Conclusions

The Roxburgh reservoir was filled rapidly over 40 years ago and has since experienced no problems with landslide instability.

A large scale failure of any slope in the Roxburgh Gorge would almost certainly block the valley and result in upstream flooding. Resultant flooding would occur regardless of whether or not a reservoir was present.

The main triggers for a slope failure are natural events. Formation of the reservoir has not significantly altered the probability of failure of the landslides.

So long as the landslides continue to creep at the slow rates indicated from existing information, they will not pose a particular risk. An observational (monitoring) approach based on surveys and visual inspections, with regular review, has been adopted.

The monitoring carried out by Contact Energy will provide a warning of landslide movement that would not otherwise have been available to the adjacent communities.

References

Gillon, M.D.; Hancox, G.T. (1992) Cromwell Gorge landslides - a general overview. *Proceedings 6th International Symposium on Landslides, Christchurch* p83-102

ICOLD (in prep) Reservoir Landslides: Guidelines for Investigation and Management

Hendron, A.J.; Patton, F.D. (1986) A geotechnical analysis of the behaviour of the Vaiont slide. *Civil Engineering Practice 1:* p65-130

Jones, F.O.; Embody, D.R.; Peterson, W.L. (1961) Landslides along the Columbia River Valley, Northeastern Washington. *US Geological Survey Professional Paper 367.* p98

Nakamura, H. (1985) Mechanism of reservoir-induced landslides. *Proceedings 4th International Field Workshop Landslides.* p219-226

Macfarlane, D.F.; Gillon, M.D. (1996) The performance of landslide stabilisation measures, Clyde Power Project, New Zealand. *Proceedings 7th International Symposium on Landslides, Trondheim* p1747-1757

Peck, R.B. (1969) Advantages and limitations of the observational method in applied soil mechanics. *Geotechnique 19:* p171-187

Riemer, W. (1992) Landslides and reservoirs. Keynote Paper. *Proceedings 6th International Symposium on Landslides, Christchurch.* p1973-2004

Engineering Geology of the Golden Cross Landslide

G.E. Winkler
Tonkin & Taylor Ltd, Auckland

Abstract

The Golden Cross Landslide is a large scale deep seated translational reactivated earth-rock slide underlying the Golden Cross Gold mine site, Waihi. It is some 2100m long, 500 to 1000m wide, up to 145m deep, and occupies approximately 135 hectares of land. It has essentially involved one geological formation displacing over two older formations. The tailings dam for the mine was constructed across what was subsequently interpreted to be the upper part of the landslide, and underwent extensional and shear deformation as a result of slide displacement. Due to concerns with the effect of the landslide on the dam, a significant investigation, monitoring and stabilisation programme took place immediately following discovery of deep-seated movement near the dam foundation in August 1995. More than 11km of borehole was drilled, 52 inclinometers were installed, and 105 survey monuments were monitored as part of the investigation to define the extent of the landslide, as the lateral margins and toe of the slide could not be easily identified in the geomorphology. More than 35km of horizontal drains were installed as part of the stabilisation works, along with a number of pumping wells, and the construction of a deep-level drainage drive beneath the landslide. Slope unloading was also carried out. Current monitoring data confirms that the landslide stabilisation works have proven to be successful.

Introduction

The Golden Cross Landslide is located at the Golden Cross gold mine, Waihi, New Zealand (Figure 1). It underlies moderate sloping farmland at the head of the Waitekauri Valley (Figure 2) at elevations between 250 and 500m above sea level. Surrounding the mine site are steep-sided bush covered ranges with summit elevations between 580m and 750m. Average annual rainfall is between 2500 and 3000mm.

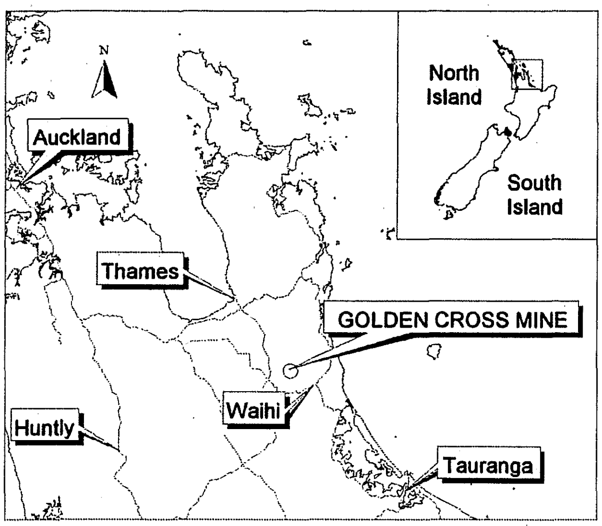

Figure 1: Location of the Golden Cross Mine

Recent mining at the site began in the early 1990's, comprising both open pit and underground mining of gold and silver. Tailings slurry, produced from the extraction of the metals, was pumped to a 700m long and up to 65m high engineered earthfill dam. While the significant extent of instability and characteristics of the landslide are now well understood, there was little evidence in the geomorphology or the geological model at the time of mine development to suggest that such a landslide existed or could exist. In August 1995 however, a 80m long, 100mm wide crack was identified in natural ground near the left abutment of the tailings dam signaling the possibility of instability beneath the dam. Unresolvable discrepancies had also appeared in the benchmark survey data. Initial investigations showed that shear movement was occurring some 60m beneath the surface.

Due to the significant consequences of dam failure, an extensive investigation was undertaken to determine the landslide extent, its characteristics, and likely requirements for stabilisation measures. Subsurface drainage using horizontal drains also began immediately. A number of consulting firms were engaged by the gold mining company to address the issue, with internationally recognised specialist engineering geologists and engineers engaged for review. However, due to the size of the landslide and complexity of its failure surface, it still took

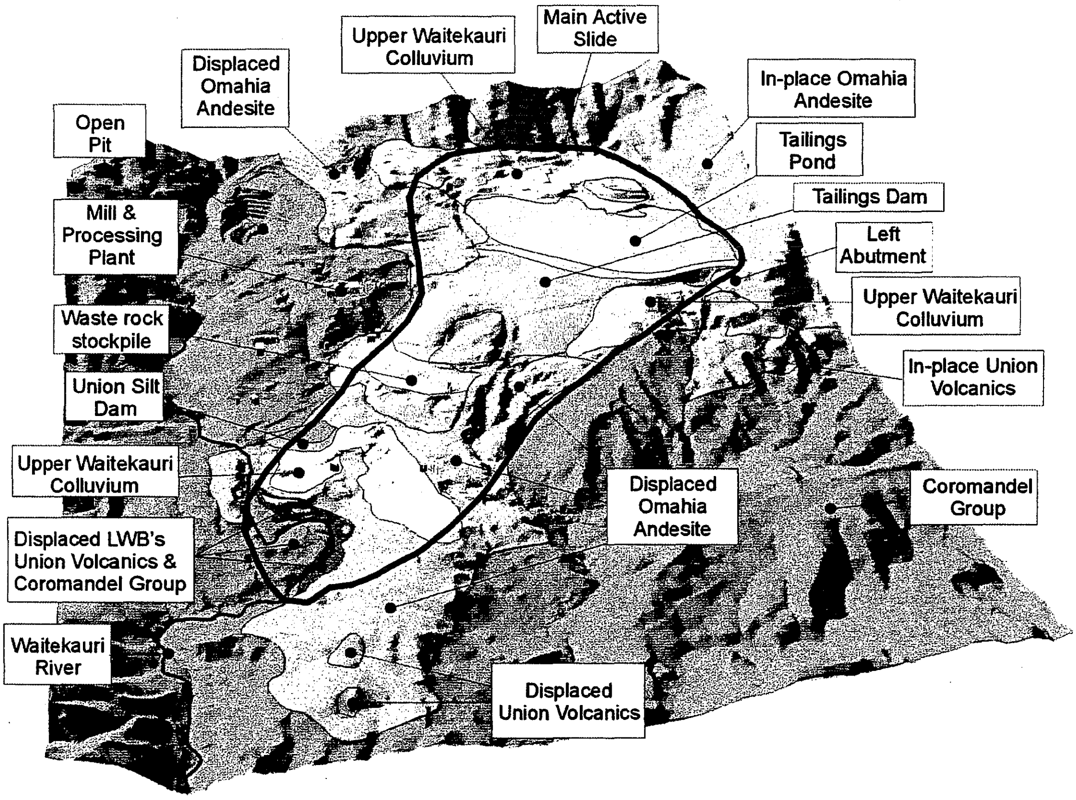

Figure 2: General site surface geology and the location of the Golden Cross Landslide

approximately 2 years of investigation and monitoring to obtain a satisfactory understanding of its geometry and movement characteristics, and approximately 2.5 years of remedial works to significantly reduce movement rates to an acceptable level. As a whole, the Golden Cross Landslide presented numerous geological, investigation, monitoring, and stabilisation challenges. The objective of this paper is to present a summary of the landslide, its characteristics, and a summary of the investigation, monitoring and stabilisation programme which was carried out.

Landslide Investigation

Following the discovery of deep-seated movement beneath the tailings dam in August 1995, an intensive and extensive investigation was carried out in an attempt to classify the nature and cause of landsliding. The major focus was to accurately determine the location of the landslide toe, and to determine whether continued movement would result in rapid failure of the landslide and, by implication, the tailings dam. Although a large proportion of the hillside upon which the mine was developed is now recognised as being upon the Golden Cross Landslide, the extent of the landslide was not and still is not easily identified in the slope geomorphology. In fact, most of the lateral margins and the slide's toe were first identified by monitoring data and geological modelling rather than visually, despite numerous walkovers and aerial photograph analysis. This lack of clear geomorphological definition is considered

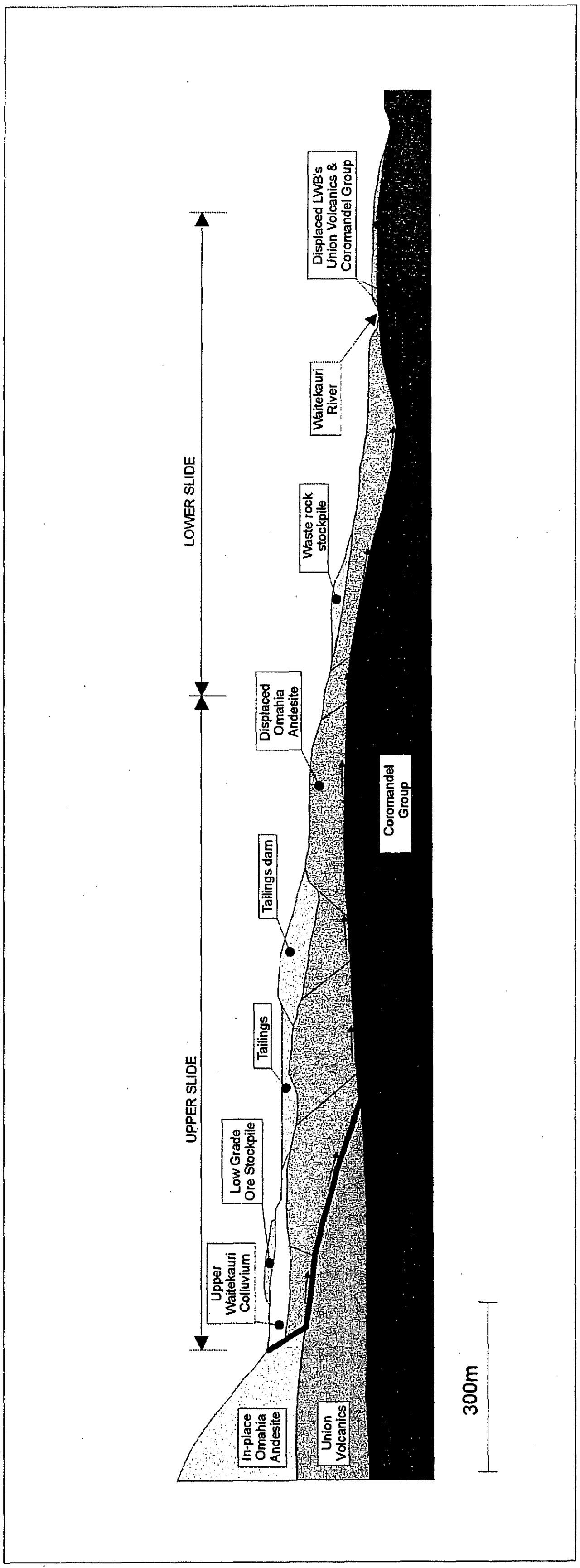

Figure 3: Geological cross-section of the Golden Cross Landslide

to be primarily due to the age of the landslide, which may date back to immediately following the emplacement of the Omahia Andesite over the Coromandel Group terrain, and the extremely slow to static slide movement rates prior to mine development. In other words, the landslide essentially exhibits the morphology of a *dormant* to *relict* landslide. It took approximately two years to clearly define the location of the slides toe and lateral margins.

Drilling

One hundred and sixty boreholes with a total length exceeding 11km were drilled for the investigation. Borehole depths generally ranged between 60m and 140m, with some extending up to over 250m in length. The average depth of hole drilled was approximately 100m. Up to five drill rigs from several different companies were on site, generally working 24 hours per day to meet the investigation schedule. Drilling at the site was classified by all drillers as being extremely difficult, mainly due to the wide range of material types and strengths within each hole (e.g. from very strong andesitic boulders to stiff plastic swelling clays) and the significant depth of the holes. PQ sized core was obtained in preference to HQ or smaller to enable better core recovery in the difficult ground at the site. The average metre rate was around 10m per 12hr shift for PQ-sized core, down to as little as 2m per shift. Literally hundreds of thousands of dollars worth of drilling equipment in total was lost down the holes. In addition to the investigation drilling, numerous mine development investigation drillholes, exploration boreholes, and pumping well boreholes contributed to the landslide investigation information database. Drill hole data from the horizontal drains also proved to be useful.

Instrumentation

A large number of inclinometers, standpipes and pneumatic piezometers were installed for the investigation (Table 1), as well as a number of borehole extensometers (shear monitors). Time Domain Reflectometry (TDR) was also tested as a means of monitoring displacement at the failure surface of the landslide, although this proved to be unsuitable.

The surface survey network comprised up to 105 survey monuments over the investigation period. Furthermore, 15 surface extensometers were installed during the investigation period to monitor surface cracking. Real Time Kinematic (RTK) GPS survey monitoring equipment was initially used to monitor the survey monuments, in preference to theodolite, due to the extent of the area being investigated, the faster rate of point measurement, and the hilly terrain (which would require numerous "set-ups" using traditional methods). Static GPS monitoring began in late 1997, when slide displacement rates reduced to within the error circle for RTK GPS.

Monitoring Instrument	Number of installations
Inclinometers	52
GPS Monuments	105
Shear Monitors	5
TDR	4
Standpipe Piezometers	99
Pneumatic Piezometers	68

Table 1: Summary of monitoring installations

Three people were permanently employed to monitor the network of instruments and to process the data. Monitoring of the flows from horizontal drains and pumping wells was also carried out, including measurements of pH and conductivity. Monitoring was carried out at a frequency of two readings per instrument per week during the investigation. Monitoring data was then compiled and issued on a weekly basis.

Geology

The site is located within a NNW trending belt of predominantly Miocene to Pliocene age andesitic and rhyolitic/dacitic volcanics erupted 4 to 11 million years ago forming much of the Coromandel Ranges. At Golden Cross, three main geologically and hydrogeologically distinctive geological formations form the Golden Cross Landslide (see Figure 3). These are the Coromandel Group and Union Volcanics (Whitianga Group), which are in turn are unconformably overlain by Omahia Andesite lava and breccias which form the landslide mass (Figure 3). Thin variably carbonaceous terrestrial sediments deposited between volcanic eruptive episodes (referred to as Lower Waitekauri Beds) generally separate the main geological units. More detailed engineering geological and hydrogeological descriptions of these units are presented in the following sections.

Coromandel Group

The Coromandel Group is effectively "basement" and generally consists of moderately to intensely hydrothermally altered andesitic volcaniclastic breccias, tuffs, and lava flows. It is the host rock for mineralisation, and outcrops in the western and southeastern part of the mine site. The upper 25 to 50m of the Coromandel Group is generally strongly to intensely hydrothermally altered to light bluish /greenish clay-rich low strength materials ranging from extremely weak rock to very stiff soil which is generally highly plastic and contains a high percentage of smectite clays (swelling clays). Where these materials are overlain by Omahia Andesite the top 5 to 10 m is highly to extremely sheared and crushed, of which the top 1-5m is typically pervasively sheared. At depth, the rocks have generally undergone lesser degrees of hydrothermal alteration and are stronger overall. The shearing near the unconformable contact with the Omahia Andesite may have initially occurred during the emplacement of the Omahia Andesite lavas.

Union Volcanics (informal)

The Union Volcanics comprise predominantly unaltered fresh to slightly weathered rhyolitic ignimbrite, volcaniclastic breccias, and dacitic lava flows belonging to the Whitianga Group. They are distinctly different in nature to the Coromandel Group. The unit appears to be up to 80m thick beneath the eastern part of the tailings basin, thinning markedly to the west (see Figure 3). Localised "blocks" of the unit up to 100m wide also exist within the landslide mass in the lower slide area which are generally incorporated within a mixture (i.e. melange) of predominantly Union Volcanics and Lower Waitekauri Beds. These blocks are believed to be remnants of aspirates in the pre Omahia Andesite paleotopography that were sheared off during long term landslide displacement. Material strengths range from very weak to weak (ignimbrites) to strong (dacitic lavas), and joints are typically moderately to widely spaced (200mm to 2m).

Lower Waitekauri Beds

The Lower Waitekauri Beds refer to a relatively thin variable unit of mainly lake and fluvial terrestrial deposits including sandstones to mudstones, lignite and volcaniclastic grits/conglomerates up to 10m thick. The beds are found between the Coromandel Group and Union Volcanics and also overlying the Union Volcanics. The unit is closely associated with the failure surface of the landslide, and as a result, is typically highly sheared and crushed comprising variable mixtures of stiff to very stiff clays, silts, sands and gravels sized fragments of parent material. The unit has a low to moderate vertical permeability.

Omahia Andesite

The Omahia Andesite comprises variably weathered autoclastic breccias, pyroclastic breccias, and lava flows which show little sign of hydrothermal alteration. Within the slide mass the Omahia Andesite generally consists of a moderately to highly weathered highly variable chaotic mixture of boulder-gravel-sand-silt incorporating 1 metre to 100 metre sized blocks of strong to very strong unweathered andesite lava. Soils within the unit are non-plastic. The materials.

Upper Waitekauri Colluvium (informal)

The name Upper Waitekauri Colluvium is assigned to a relatively thick (up to at least 48m) mantle of weathered generally very stiff to hard colluvium, fluvial, lake, and airfall deposits identified immediately below the main escarpment. Older and deeply weathered colluviual deposits also occur over parts of the lower slide areas. The unit is probably of Pleistocene age as it is mantled by Late Pleistocene tephra.

Late Pleistocene Tephra

A thin (<3m) veneer of Late Pleistocene tephra covers much of the site. Lower tephra layers are derived from the Taupo Volcanic Zone, including the Rotoehu Ash and Hamilton Ashes. The upper part of the tephra sequence contains the circa 6340 year old yellowish brown Tuhua Tephra erupted from Major Island. Most of the tephras are highly allophanic.

Structure

The upper Waitekauri Valley is largely dominated by NNE/SSW trending normal faults that dip steeply to the east and west. Major faults pass through the site, with numerous minor normal faults generally spaced at 10-20m intervals identified within the underground workings trending sub parallel to these faults in which the ore body has formed. While structural defects may have had some influence on the pre Omahia Andesite SW to SSW trending paleotopography, sliding is paleotopographically controlled, rather that structurally controlled.

Groundwater

The three main geological units have distinctive aquifer characteristics. Typically the top 10m of the Coromandel Group is impermeable, with permeability increasing with depth. Zones of any significant permeability were generally confined to quartz veining (i.e. ore body) located approximately 200m to the northwest of the landslide. The Omahia Andesite is relatively permeable overall, although there are high permeability contrasts between the low permeability weathered soil strength generally sandy-silty matrix materials and the more competent open jointed andesite boulders and larger blocks of lava. Wedged between these two formations is the structurally massive Union Volcanics, which are typified by a high fracture permeability but low storativity.

Groundwater within the relatively permeable Omahia Andesite is perched above the clay-rich Coromandel Group. Although the geometry of the Omahia Andesite was such that groundwater was trapped within the rockmass forming a reservoir, groundwater levels were typically greater than 20m below the surface.

Landslide Characteristics

The landslide mass comprises sliding of the relatively permeable Omahia Andesite over the underlying clay-rich, generally impermeable altered Coromandel Group and structurally massive unaltered Union Volcanics.

Extent of Sliding

The total area of land affected by deep-seated mass movement at the site over the period of mining is approximately 170 hectares (plan area). This area not only includes the landslide upon which the tailings dam is located (135 hectares), but also includes 35 hectares of land forming the highwall of the open pit area that also failed on the same weak interface (see Figure 2). The overall length of this slide is some 2100m in length, and is between 500m and 1000m wide.

Depth of Sliding

In-slide inclinometers have shown that the landslide's failure surface is strongly geologically controlled involving largely Omahia Andesite materials sliding over Coromandel Group and over Union Volcanics at the rear of the slide. The depth to the failure surface is therefore large and ranges from 60 to 80 m between the toe of the slide to the mid slide area and around the periphery of the tailings pond areas. It increases to a maximum known depth of 146 m beneath the tailings dam and pond. The approximate volume of the main active slide is 100 million m^3.

Figure 4: Slide failure surface contours (10m intervals), and movement vectors. Elevations shown in mRL.

Slide failure surface and failure zone characteristics

The slide failure surface topography is shown on Figure 4, which also generally represents the pre-Omahia paleotopography formed in the Coromandel Group and Union Volcanics. Beneath the upper slide area the surface is bowl shaped narrowing down to and rising up to a saddle, before it drops in elevation down to the base of the paleovalley below the present day valley floor. The dam was located above this saddle, where the interface dips back to the east and is isolated from the westerly dipping interface downslope. In the toe of the landslide the failure surface passes through a relatively thick mixture ("melange") of mainly highly sheared and disrupted

Coromandel Group, Lower Waitekauri Beds and Union Volcanics, before breaking out on the western side of the Waitekauri River.

Core recovered from boreholes drilled through the slide failure surface and inclinometer data indicate that shearing throughout much of the slide generally occurs within the top one to two metres of soil-strength clays at the upper surface of the Coromandel Group. Shearing does not occur exactly at the Omahia Andesite / Coromandel Group contact, although it is typically very close to this. The smectite-rich clays forming the failure zone typically exhibit a sub-horizontal pervasive shear fabric. It appears, however, that recent displacement occurred across a single highly polished surface in most places. Laboratory testing has indicated residual friction angles on these surfaces of between 6° and 11°.Failure of the Upper Slide over the Union Volcanics behind the tailings pond appears to have occurred within or on top of a very thin veneer of Lower Waitekauri Beds which overly the unit. The zone of deformation identified in drillhole core from within this unit is only thin (<10mm), although this may be thicker elsewhere.

Movement rates, distribution, and styles

During the landslide's most active monitored period (winter 1996), recorded movement rates averaged 2.8 to 4mm/day for the Lower Slide areas, although daily movement rates at times were up to 10mm/day at times in that area. Movement rates progressively reduced for areas further upslope from 1 to 1.5mm/day in the mid slide area down to 0.1 to 0.3mm/day for the area behind the tailings pond below the headscarp of the slide. The landslide was therefore undergoing significant extension, including the left abutment area of the tailings dam which was being stretched at an average of up to 0.85mm/day. During that period displacement was occurring continuously in the lower and mid slide areas, becoming stick-slip towards the back of the slide. Based on GPS and inclinometer data, slide movement rates during that period were classified as being *"very slow to slow"* (after Cruden and Varnes, 1996), equal to movement rates between 16mm and 1.6m/year.

During the investigation movement rates were the slowest around the periphery at the back of the slide, with movement vectors trending inwards towards the mid slide area where the paleotopography-controlled failure surface of the landslide narrows. Subsequently rates of movement in this narrower area were greater. Below this paleo-saddle area, the failure surface plunges beneath the lower slide, where movement rates were the most rapid. Also, movement rates were greatest down through the central direction of "flow", with lesser rates of movement being observed towards the slide margins (including the lower slide).

Total horizontal movement

Since monitoring of the landslide began in August 1995, survey data show that the lower landslide displaced between 800mm and 1400mm until it stabilised in August 1997. The mid slide (below the tailings dam) moved SW by some 500mm, and the upper slide areas by 250mm to 300mm.

When pre-August 1995 benchmark survey data for these areas is included, the total horizontal movement for the mid and upper slide areas increases to approximately 1000mm and 500mm for those slide areas respectively. Based on this, the lower slide is estimated to have displaced between 1500mm and 3000mm over the period of mining. The reduction of total horizontal movement from the lower slide back through to the headscarp clearly indicates that the slide mass has undergone relatively significant extension since construction of the tailings dam began in 1990.

Landslide Stabilisation

Subsurface drainage

Lowering of piezometric levels within and around the head of the slide mass was a major objective of the remedial works. The methods of achieving this objective were the installation of horizontal drainhole fans, pumping wells, and deep-subslide drainage. Overall, significant drainage has been achieved by targeting the larger andesite blocks within the Omahia Andesite. This has typically resulted in moderate to high yields and rapid, sustained drawdown (i.e. high transmissivity and low storativity). In zones of the slide mass which were predominantly soil-rich (e.g. gravel-silt units) effective lowering of piezometric levels required a much greater density of drainholes and wells. The response of the Coromandel Group aquifer to drainage was very "sluggish" in comparison to the Omahia and Union Volcanics aquifers, mainly due to its low permeability. Prior to drainage works, piezometric levels within the Coromandel Group were at about the same level as those at the base of the Omahia Andesite landslide mass. This reflected the equilibrium reached between the two aquifers over the long term. Following subsurface drainage, pressures within the Omahia Andesite reduced leaving the Coromandel Group pressures elevated as a result of the low hydraulic conductivity and resultant slow dissipation of pore pressures. The response to the subsurface drainage on slide movement rates was therefore not immediate, but took time as pressures re-equilibrated.

Horizontal drains

25 horizontal drain fans and over 220 individual horizontal drainholes with lengths up to 348m were installed around the site (Figure 5). The total length drilled is more than 35,000m (35km). Up to four drill rigs were used simultaneously to install the drain fans, which were typically set out in an array of holes from a centralised location. Approximately 70% of the drain holes were 120mm in diameter, with 25% being 200 mm in diameter. Slotted Class E uPVC pipe or 70mm galvanised steel pipe was installed within the drainholes to minimise potential clogging from hole collapse. All holes were collared with a minimum of 6m long steel casing. Flows from many of the holes were spectacular, with initial flows of 400 to 600 litres per minute being relatively common and some holes initially producing flows in excess of 2000 litres per minute. The effect of the drainhole fans was very favourable overall, with piezometric drawdown of more than 10m being common. The maximum drawdown achieved from any of the drains was 29m.

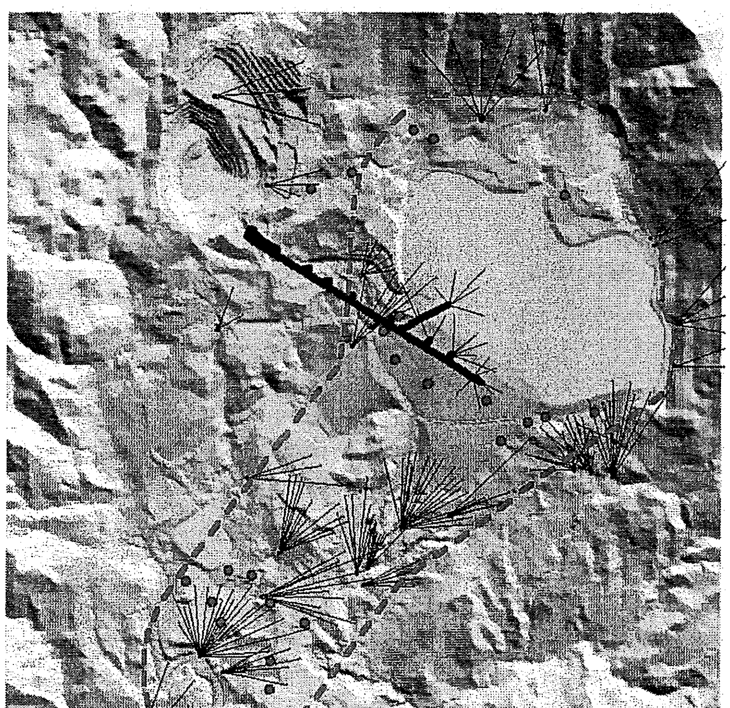

Figure 5: Drainage plan showing locations of horizontal drains, pumping wells, and drainage drive

Pumping Wells

Twenty five pumping wells were installed to assist in the deep level drainage of the slide. The wells were mainly installed in areas where it was difficult to achieve deep-level drainage from the horizontal drains. The objective of the wells was to lower piezometric levels above and below the slide base and therefore were relatively deep (between 60 and 120m depth). Well drillholes were generally between 200mm and 360mm diameter, were fully cased with 150mm diameter steel tube, and six inch submerged pumps were installed. While the local effect of the pumping wells varied, the overall effect of the pumps was favourable. Very wide cones of influence (e.g. up to 400m diameter) were achieved from some of the pumping wells, lowering piezometric levels in places by 60m or more over a wide area. Some of the wells which produced only minor flows were converted into standpipe piezometers to improve the groundwater monitoring coverage.

Drainage Drive

A 5 x 5m drainage drive was driven beneath the tailings dam from the underground mine workings to provide underground drainage drilling access beneath the landslide. The main drive was 763m in length, and a "cross cut" was driven 150m upslope from the main drive beneath the tailings pond. Drill and blast methods were used to advance the drive, with support comprising mesh and rock bolts at 2m centres. It was initially intended to advance the main drive a total of 1060m to the left abutment area of the tailings dam, but the initial design was modified due to unexpected very difficult tunneling conditions encountered from 710m. A gravity drainage network consisting of 20 drainholes totaling more than 2200m of drilling was installed from the tunnel network. Water collected from the drainholes was then pumped to the surface. Like the horizontal drains, many of the drainholes produced spectacular initial flows ranging between 200 and 2000 litres per minute, although these flow rates abated as piezometric levels were lowered within the landslide. The drainage drive drainholes rapidly reduced piezometric levels in the vicinity of the tailings dam by up to 73m, with a cone of influence extending beneath the tailings pond by more than 400m from the hole.

Slope Regrading

In the later stages of the stabilisation programme relocation of waste-rock and ore stockpiles located in two main areas on the landslide was carried out to improve its stability. Some 500,000m^3 of waste rock was removed from the top half of the lower slide, and some 350,000m^3 of low grade ore was removed from the area behind the tailings pond at the rear of the slide. The effect of the fill relocation was very positive as slide-wide movement rates slowed significantly during and following their removal.

Crack sealing

Crack sealing earthworks were carried out in two main areas of deformation, generally located within the transition zone between the lower and upper slide areas. Large cracks up to 300mm wide developed in this area. The aim of the sealing was to limit the ingress of surface runoff into the slide mass, thereby reducing the impact of rainstorm events on pressurisation of tension cracks within the slide. The sealing at these two areas was considered to be particularly important as they formed part of the headscarp of the Lower Slide.

Effect of Stabilisation

As a result of the significant subsurface drainage stabilisation works and unloading of material located over unfavourable parts of the landslide, the slide movement rates were gradually reduced (see Figure 6). By August 1997 the lower slide was stabilised and upper slide areas reduced to minor stick-slip movement (generally less than 0.02mm/day) following major rainstorm events. The upper slide may now generally be described as *"very slow to extremely slow moving"* (<16mm/yr), while the lower slide is *static*. Movement rates in the upper slide areas are expected to slow further, as internal blocks progressively lock up against the static lower slide.

During the initial stages of the landslide stabilisation project the landslide was very responsive to rainfall with movement rates increasing with as little as 40mm per day of rain. The sensitivity of the slide to rainfall has been significantly reduced following the installation of the drainage network, with only minor displacements being recorded for the peripheral areas in response to rainfall events of 250mm or more.

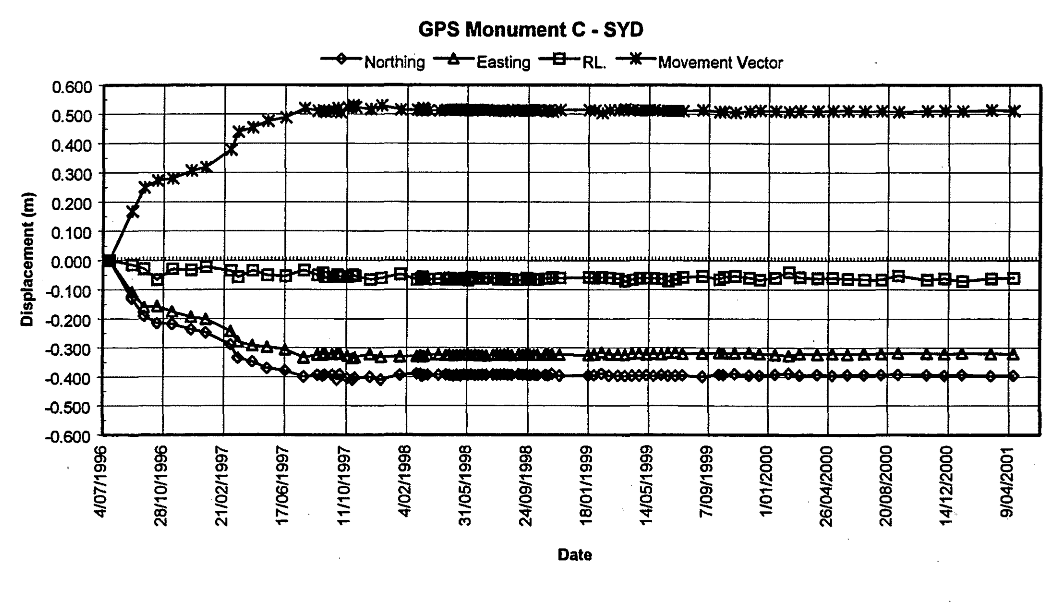

Figure 6: Central lower slide GPS monument C-SYD, showing change from continuous movement to stability in August 1997

Age and Causes of Landsliding

The age of the Golden Cross landslide has not yet been accurately defined, although it is likely to be very ancient and may have even been initiated soon after the emplacement of the Omahia Andesite (~6.6 million years ago). The indistinctive geomorphology of the landslide also gives some indication of the age of the feature. Furthermore, the blocks of Union Volcanics found in the toe of the lower slide are more than 1400m from their parent insitu location beneath the tailings dam at the back of the landslide. Assuming a constant slide-wide movement rate of 4mm/day (i.e. the most rapid overall movement rate recorded) the landslide would need to be at least 1000 years old for the separation to develop at that rate. It is likely that movement rates were far less than that prior to mining and the subsequent significant changes to the landslides surface.

Given the age of the landslide and its indistinctive geomorphology, it is likely that the landslide was close to equilibrium prior to mining. Minor displacements may have occurred following very significant rainfall events (e.g. large cyclones) and also the erosion of material from the toe of the slide by the Waitekauri River, until equilibrium was again reached. Reactivation of the Golden Cross Landslide, however, is considered to have occurred as a result of the many modifications to the surface of the slide that took place since mining began at Golden Cross in the 1890's and recent mine development and operations. Reactivation is believed to have been initiated by the construction and widening of the Golden Cross Road across the toe of the landslide early this century and later further widening of by up to 10m.

This effectively would have had the same effect as massive toe erosion by the Waitekauri River.

Summary of Conclusions

The Golden Cross Landslide is classified as a reactivated ancient, large-scale, deep-seated ancient translational earth-rock slide. The kinematics of the slide are closely related to the contrasting underlying geology, and essentially involve relatively permeable and deeply weathered unaltered andesitic lava and volcaniclastic materials (Omahia Andesite) moving over a paleo-surface of hydrothermally altered, clay-rich Coromandel Group and unaltered rhyolitic/dacitic volcaniclastics (Union Volcanics) near the back of the slide. The landslide is considered to be at least 6340 years old (the age of the youngest tephra cover), but is very likely to be considerably older. The slide mass comprises many smaller blocks, that become smaller towards the rear of the Upper Slide. The body of the slide essentially moved in a manner very similar to a glacier. During the investigation total recorded horizontal displacement of the slide ranged from less than 250mm to 500mm in the Upper Slide and from 800mm to 1400mm in the Lower Slide over a 2.5 year period. While average movement rates of up to 4mm/day were recorded for the lower slide at the height of slide activity, the slide was still classified as slow to very slow moving. Since the stabilisation works the lower slide has stabilised, while very minor displacements of the upper slide occur following significant rainfall as individual blocks take up extensional slack. Removal of material from the toe of the slide for the construction and widening of the Golden Cross Road and placement of fill in the upper half of the lower slide are considered to have triggered slide reactivation. Significant lowering of piezometric levels across the site, in conjunction with fill relocation from unfavourable slide locations has effectively caused the Golden Cross Landslide to stabilise.

Acknowledgements

The current mine owner is Coeur Gold NZ Ltd. Mine manager, Mr Randy MacGillivray, is gratefully acknowledged for reviewing this paper. Woodward Clyde NZ and a number of other consultants were involved with the project and their contribution to the understanding of the Golden Cross Landslide is also acknowledged.

References

Loney. G. A (2001) " Golden Cross Landslide - Dam Protection Measures" (in prep.)

Tonkin & Taylor Ltd (1997). "Golden Cross Project – Interpretive Report for October 1997: Report reference 12520

Turner, K.A. and Schuster, R.L (editors) (1996) "Landslides: Investigation and Mitigation" Special Report 247, Transportation Research Board, National Research Council, U.S.

Golden Cross Landslide – Dam Protection Works

G. A. Loney
Senior Geotechnical Engineer
Tonkin & Taylor Ltd, Auckland

Abstract

The Golden Cross Landslide is a large scale, deep-seated landslide located at the Golden Cross gold mine, Waihi, New Zealand.The mine tailings dam was constructed on what was later established to be the upper part of the landslide while the site silt collection and detention dam was intersected by the landslide margin. Both dams sustained significant deformations as a result of landslide movement. As part of the stabilisation and protection works carried out at the site, downstream filter buttresses were constructed on each dam to provide a high degree of protection against piping at critical locations. This paper describes the design rationale and aspects of the construction. Observation of the deformation of the silt dam indicated that large movement had been sustained without damage to the dam, probably due to the highly plastic material within the dam core.

Introduction

The Golden Cross gold mine is located on the Coromandel Peninsula, approximately 8 km northwest of Waihi township (Figure 1). It was first mined in the last part of the nineteenth century and, as a result of significant subsequent improvements in the gold extraction techniques, mining re-commenced at the site in 1991. The recent mining comprised both open pit and underground mining of gold and silver bearing ore. The processing of the ore results in a tailings slurry which was pumped to a tailings pond in a nearby valley drained by the Union Stream. The tailings are retained by a "main" dam across the valley and a "saddle" dam across an adjacent smaller valley (Figure 2). The entire structure is known as the Union Embankment. Surface water runoff from the catchment is mainly diverted away from the tailings storage area and under-drainage is provided for the streams within the area. The Union Embankment is constructed of overburden and mine waste materials, particularly from the open pit. It is a complex multi-zoned structure with a low permeability facing, internal chimney drainage system and high strength zones in the downstream shoulder. It's foundation is intersected by a number of faults and the dam is designed to accommodate lateral and vertical movement on the faults. It has in fact been designed as though it is a water retention structure even though the tailings have significant shear strength which continuing

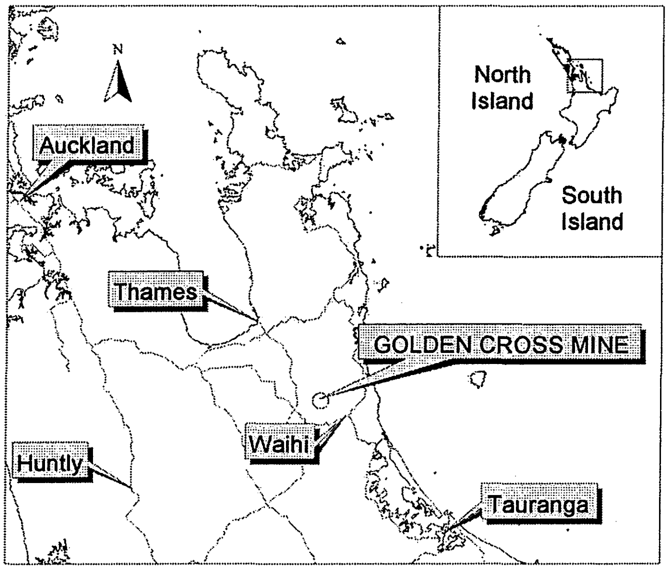

Figure 1: Location of the Golden Cross Mine

consolidation increases with time. In this regard the dam differs greatly from many overseas tailings dams which are actually built of tailings.

During routine investigation and surveillance in August 1995, some cracks were observed adjacent to the tailings dam in natural ground, known as Trig J Hill. On further investigation, other signs of widespread ground movement were discovered and a major site investigation, monitoring and landslide stabilisation programme was initiated. The investigation programme continued on a "fast track" until late 1997, by which time the geological model had been determined to a high degree of confidence. The site-wide monitoring programme continues to be operative even though mining ceased in 1998. The successful landslide stabilisation programme mainly focused on subsurface drainage using horizontal drains, vertical pumping wells and a deep-level drainage drive beneath the landslide.

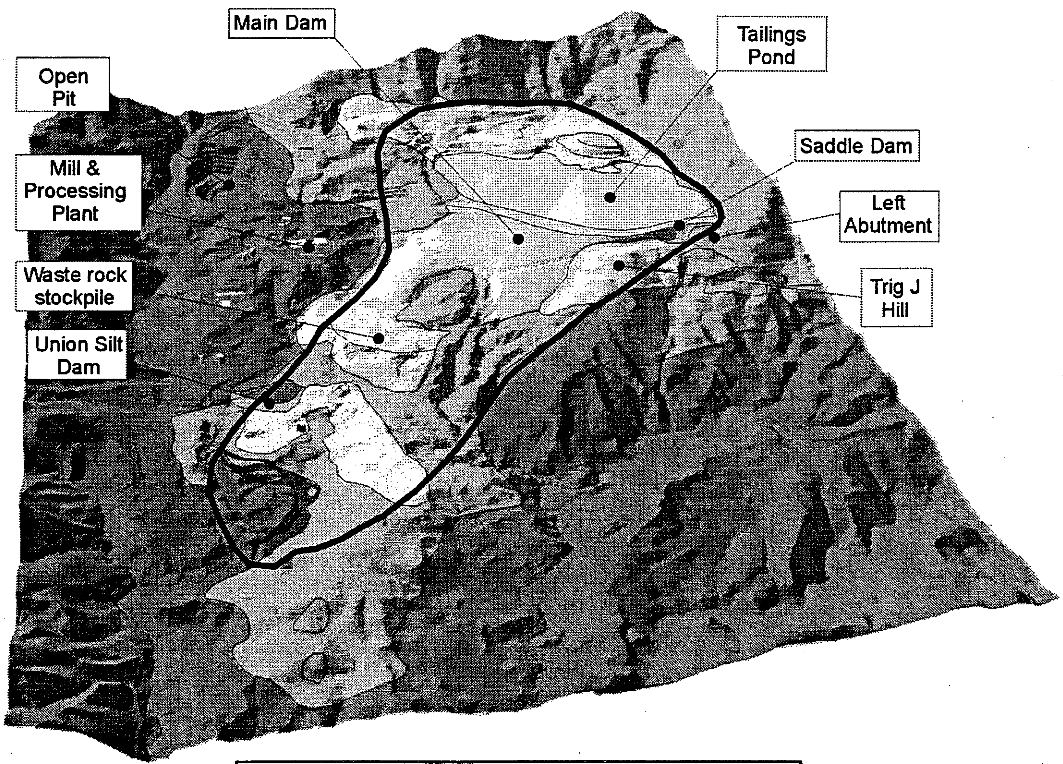

Figure 2: General Site Layout

This paper is a companion paper to "Golden Cross Landslide – Engineering Geology" by G.E. Winkler, presented at this symposium. That paper presents the investigations carried out and describes the geology, geomorphology and hydrology of the Golden Cross Landslide, while also presenting details of the dewatering stabilisation works carried out.

The following sections present details of observed damage to the Union Embankment and the silt collection and detention pond at the bottom of the site, the Union Silt Dam.They describe the design philosophy and construction details for the downstream filter buttresses installed on both dams as protection against piping of the dam embankments.

Dam Protection Works

Surface Manifestation of Ground Movement

A significant number of surface indicators of ground movement (following the Trig J cracking) were found in 1995 and 1996 with the most important being:

- cracking of the shotcrete lining within the Southern Diversion Drain (SDD) adjacent to the left abutment
- development of a tomo at the left abutment possibly associated with the above cracking
- zones of minor seepage on the downstream shoulder of the Saddle dam within 100 m of the left abutment
- cracking and plastic deformation of the Union Silt Dam at the bottom of the site.

These details are shown on Figure 3.

In addition, the inclinometers and GPS data indicated that the slide was moving at speeds up to 3 mm/day near Trig J and up to 10 mm/day at the toe of the landslide. (Refer to Figure 4). These were the movement rates pertaining at the time of design of the buttresses.

Saddle Dam Protection

The Saddle Dam part of the Union Embankment was always the area of greatest concern for dam integrity due to its construction across the rear slide margin. The damage observations and GPS data indicated that it was located between a relatively slow moving zone adjacent to the left abutment and the more rapidly moving "Trig J" part of the the slide. Accordingly, the embankment was in tension i.e. underlain by a zone of extension within the landslide. This prompted concerns about the possibility of tension cracks forming and being eroded leading to potential piping of the dam. In addition, the unfavourable orientation of the landslide failure surface posed stability concerns as did the relatively steep 2.5(H):1(V) downstream shoulder and its proximity to the Trig J Hill and left abutment cracking. Accordingly, a decision was made to construct a substantial downstream graded filter comprising 1 m horizontal thickness of sand (Type G drainage material) covered by of 4 m horizontal thickness of filter compatible gravel (Type A drainage and selected GAP 65). The details of this construction, known as the Saddle Filter Buttress, are shown on Figure 5.

The design criteria for the graded filter were:

A. Seal tension induced cracks and pipes that might occur through the dam embankment by retaining fine material on the sand interface
B. Prevent tailings (average particle size 0.05 mm) from finding their way through any such cracks and pipes
C. Provide sufficient thickness of filter material to retain protection of the embankment even with a maximum movement rate of 75 mm/year. This was achieved in accordance with the following rationale:
   - the Saddle Dam was being stretched
   - design requirement to provide 3 m lateral displacement tolerance

   This gives:
   - 100 years of protection at a movement rate of 30 mm/year – the expected annual movement rate when the SFB was designed
   - 40 years of protection at a movement rate of 75 mm/year – an upper bound but acceptable movement rate that provides sufficient time for the tailings to become immobile

     (During the last 12 months the range of total movement for the landslide was between zero in the toe and 8 mm in the central part of the slide, i.e. significantly less than assumed in design.)

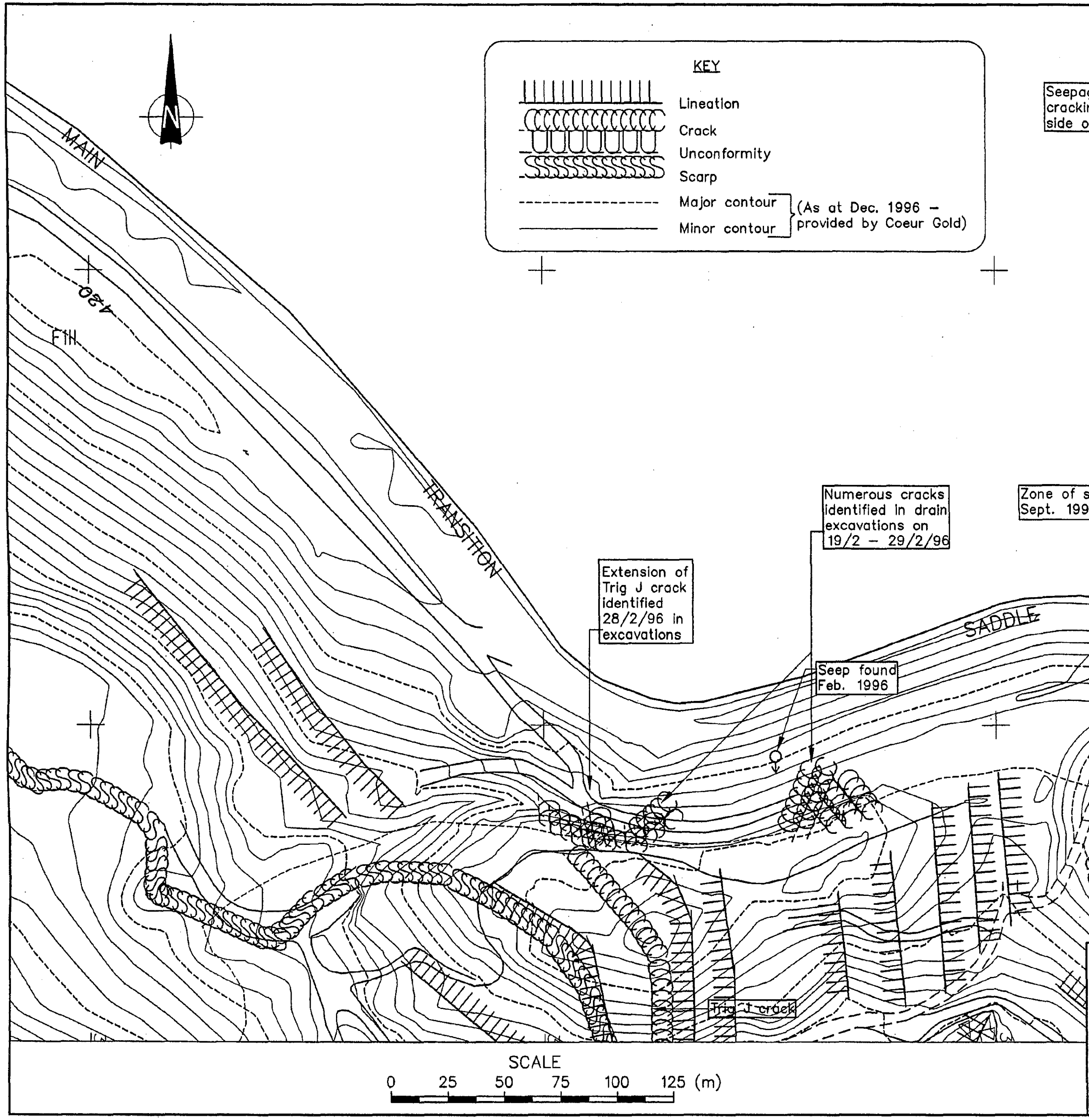

Figure 3

LEFT ABUTMENT
TRIG J AREAS
OBSERVED DAMAGE

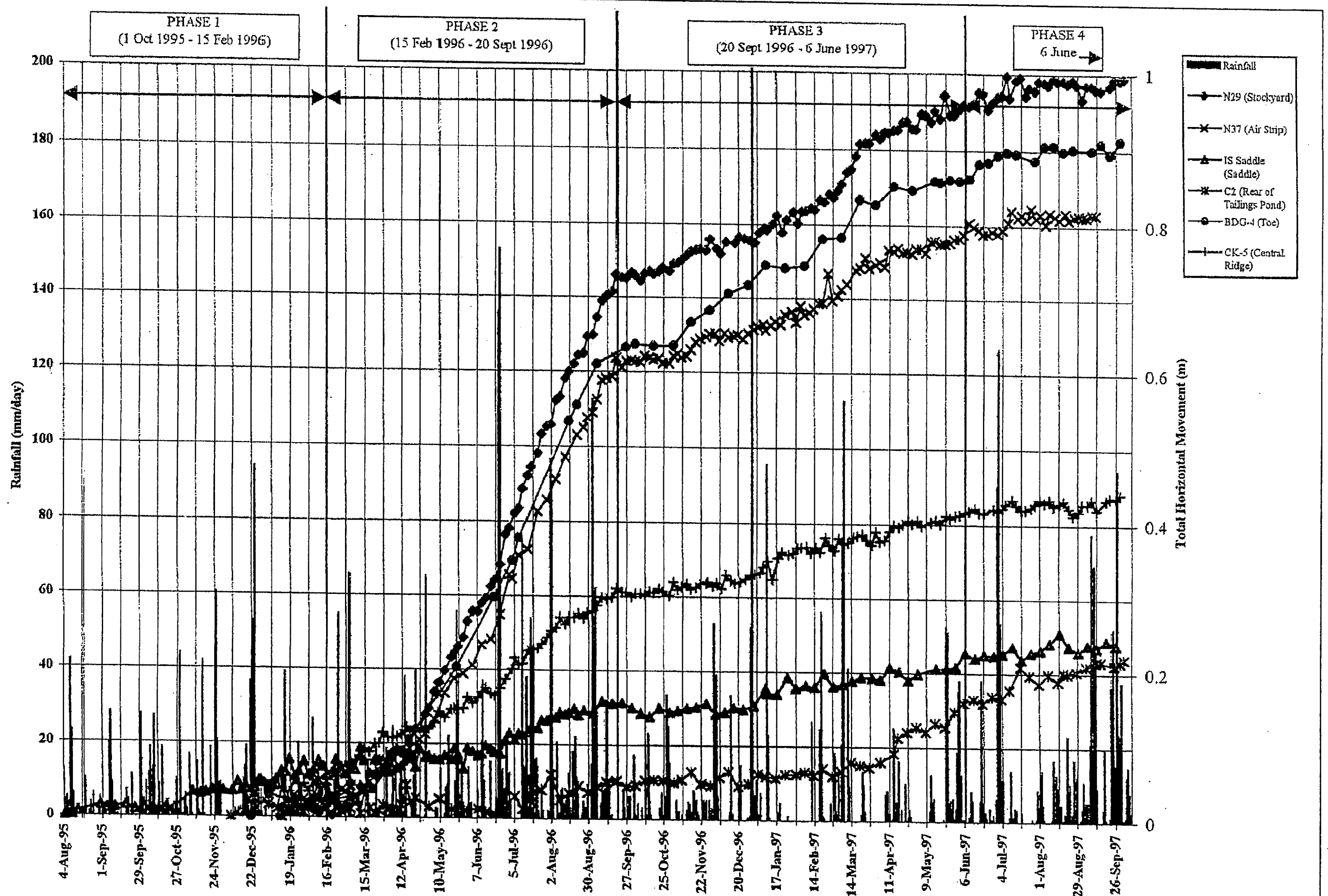

Figure 4.1 : GPS Total horizontal movement of the slide surface showing four main phases of movement activity.

JPW
30/10/97

Figure 4

SURFACE MOVEMENT
OF LANDSLIDE

N.T.S

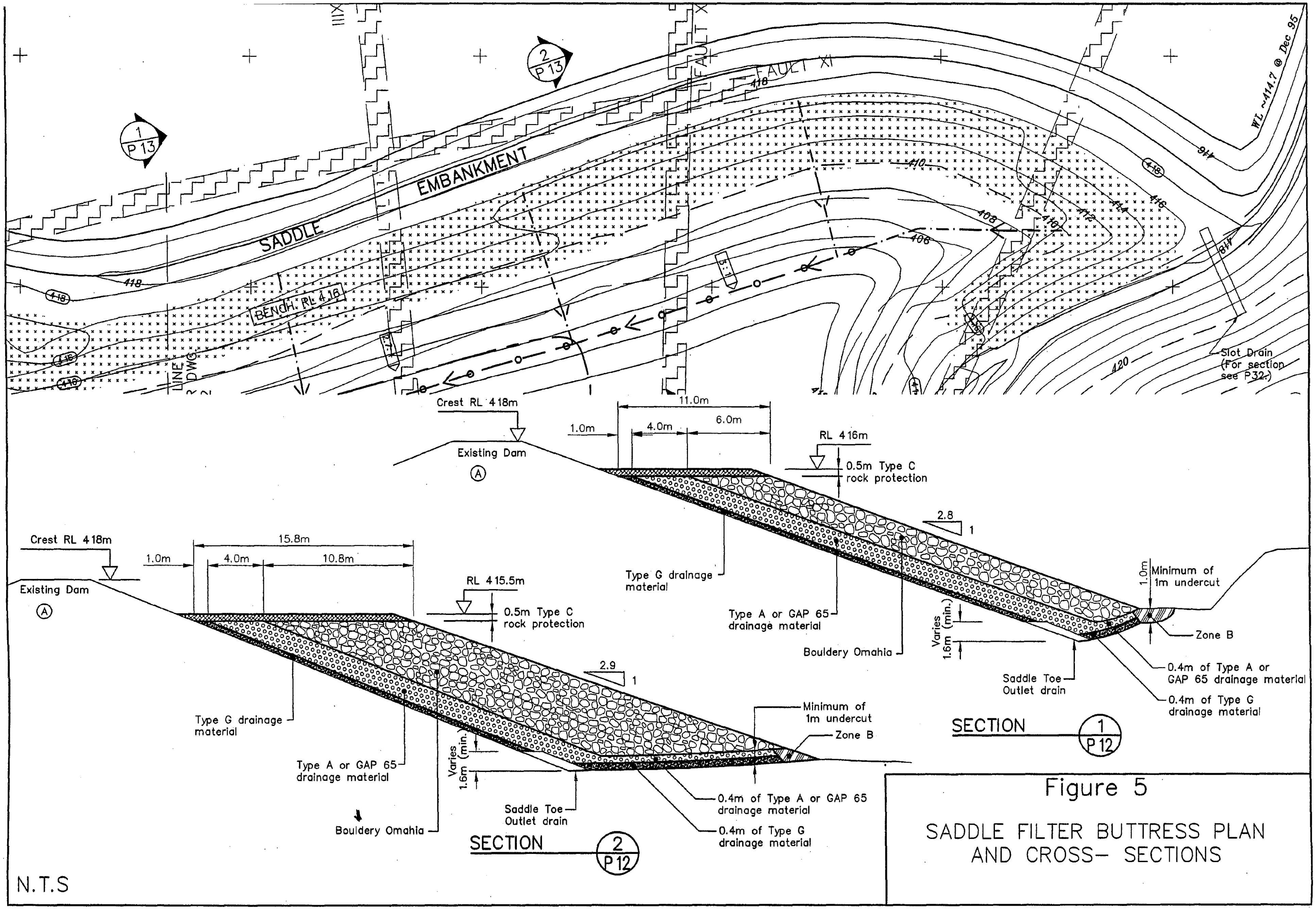

Figure 5

SADDLE FILTER BUTTRESS PLAN AND CROSS- SECTIONS

Within the 300 m distance from the left abutment to Trig J, there were at least three zones of observed cracking where deformation had been occurring (e.g. left abutment, buttress foundation, Trig J). Therefore it was considered reasonable to assume three movement zones each with 1 m of displacement. Accordingly, it was decided to provide 1 m minimum horizontal thickness of sand thickness and for extra protection include 4.0 m minimum horizontal thickness of filter gravel.

Filter design was carried out following the recommendations of J.L. Sherard (see references) as follows:

$$(1) \quad \frac{D_{15\,filter}}{D_{85\,base}} \leq 5 \quad \frac{D_{15\,sand}}{D_{85\,core\ or\ tailings}} = \frac{0.25}{0.05} = 5$$

$$(2) \quad C_u\,(D_{60}\,/\,D_{10})\ \text{for primary filter in range 2 to 5} \quad \frac{D_{60\,sand}}{D_{10\,sand}} = \frac{0.65}{0.25} = 2.6$$

$$\text{For sand/gravel compatibility}\ \frac{D_{15\,GAP65}}{D_{85\,sand}} = \frac{0.8}{0.4} = 2 < 5$$

Note:

$D_{15filter}$: For the filter material the size such that 15% (by weight) of particles have a smaller nominal diameter

$D_{85\,base}$: For the base (or protected) material the size such that 85% (by weight) of particles have a smaller nominal diameter

C_u : The Uniformity Coefficient

Concerns with the observed cracking and tomo near the left abutment indicated that a significant "wrap around" at the left abutment would be a prudent measure to provide added security at a critical location. Accordingly, a 50 m return from the abutment contact was incorporated in the design. Requirements for using the filter buttress as a haul road necessitated the construction of a significant rock fill zone on the outside of the embankment.

Other features of note in the design and construction included:

- installation of a large size filter cloth-wrapped gravel drain at the inside toe (the Saddle Toe Outlet Drain) which conveys seepage to the main embankment underdrainage system
- installation of an approximately 6 m deep x 2 m wide filter cloth-wrapped gravel drain (a "slot" drain) through the crack zone near the left abutment to provide extra protection
- installation of chimney drain collector drains at 60 m longitudinal spacing and connection to the Saddle Toe Outlet drain to facilitate future crest raising
- the presence of a zone of "en echelon" cracks within the foundation of the Saddle Filter Buttress (refer to Figure 3). These were excavated, treated with pleated filter cloth and backfilled with impermeable material in accordance with standard dam foundation practice
- the approximate fill volume was 500,000 m³ (solid) with some 50,000 m³ (solid) of excavation at the toe.

The above measures appear to have been successful with no signs of cracking, seepage or damage of any kind apparent on the dam embankment following construction which was completed in mid-1997.

Union Silt Dam Protection

During the mining and rehabilitation phases of the project, stormwater runoff, often heavily silt laden, was collected by the Union Silt Dam located near the bottom of the approximately 60 ha catchment (Figure 6). This is an approximately 12 m high zoned earth dam with an impermeable central core and a seepage control chimney drain downstream of the core (Figure 7).

Ground movements in this area of the slide were the fastest in the landslide. A GPS surface survey monument located approximately 100m northeast of the dam showed nearly 1400 mm of movement towards the southwest from October 1995 to August 1997 (an average rate of about 2.1 mm/day). As a result, cracking and distortion of the dam crest occurred (refer to Figure 8). In the case of the Union Silt Dam, a localised part of the embankment was in direct shear as opposed to the more complex extension situation of the saddle dam. Accordingly, a sophisticated monitoring system comprising six GPS points and an inclinometer, N55, were established (refer to Figure 6). These helped to accurately define the landslide margin in this area with movement only occurring east of the inferred slide boundary indicated. Plots of GPS Station USP 8 and inclinometer N55 are included as Figure 9. They show N55 shearing after about 28 mm of deformation and approximately 550 mm of movement at UPS 8 up till March 1997. Clearly the magnitude of movement was cause for concern and it was therefore decided to install a downstream graded filter buttress as shown on Figure 7. The design criteria for the Union Silt Dam filter buttress were similar to the Saddle Filter Buttress although design was simpler because the movement was a localised shear zone rather than a large zone of tension.

The design philosophy was to:

- seal landslide-induced cracks and pipes that might occur through the dam embankment on the landslide margin by retaining fine material on the sand interface
- provide extra mass on the downstream shoulder to improve overall embankment stability
- provide significant new underdrainage in the form of filtered gravel buttress drains to lower the piezometric surface within the downstream shoulder
- provide sufficient thickness of filter material to retain protection to the embankment even with a movement rate of up to 2 mm/day. The 1 m horizontal thickness of sand would have provided approximately 1.4 years of full filter protection and this was considered adequate given the relatively short required life of the dam. The additional 4 m of filter gravel containing up to 10% sand-sized particles provides useful extra filter protection. (The landslide stabilisation works have now reduced long-term movement rates in the toe area of the slide to near zero.)

The materials used in the filter buttress were the same as for the Saddle Filter Buttress viz. sand, medium gravel (MAP65) and rockfill. An extra redundancy was incorporated with the placement of a 1 m thick zone of GAP65 on the upstream shoulder. The design intent was for fines in the GAP65 to be washed into any cracks forming on the upstream shoulder in an attempt to seal them to minimise the potential for crack development downstream.

Monitoring of underdrainage flows had been carried out prior to installation of the Saddle Filter Buttress and interestingly, there was no noticeable increase in flows despite the distortion of the dam. The photo in Figure 6, taken in February 1997, clearly shows the large

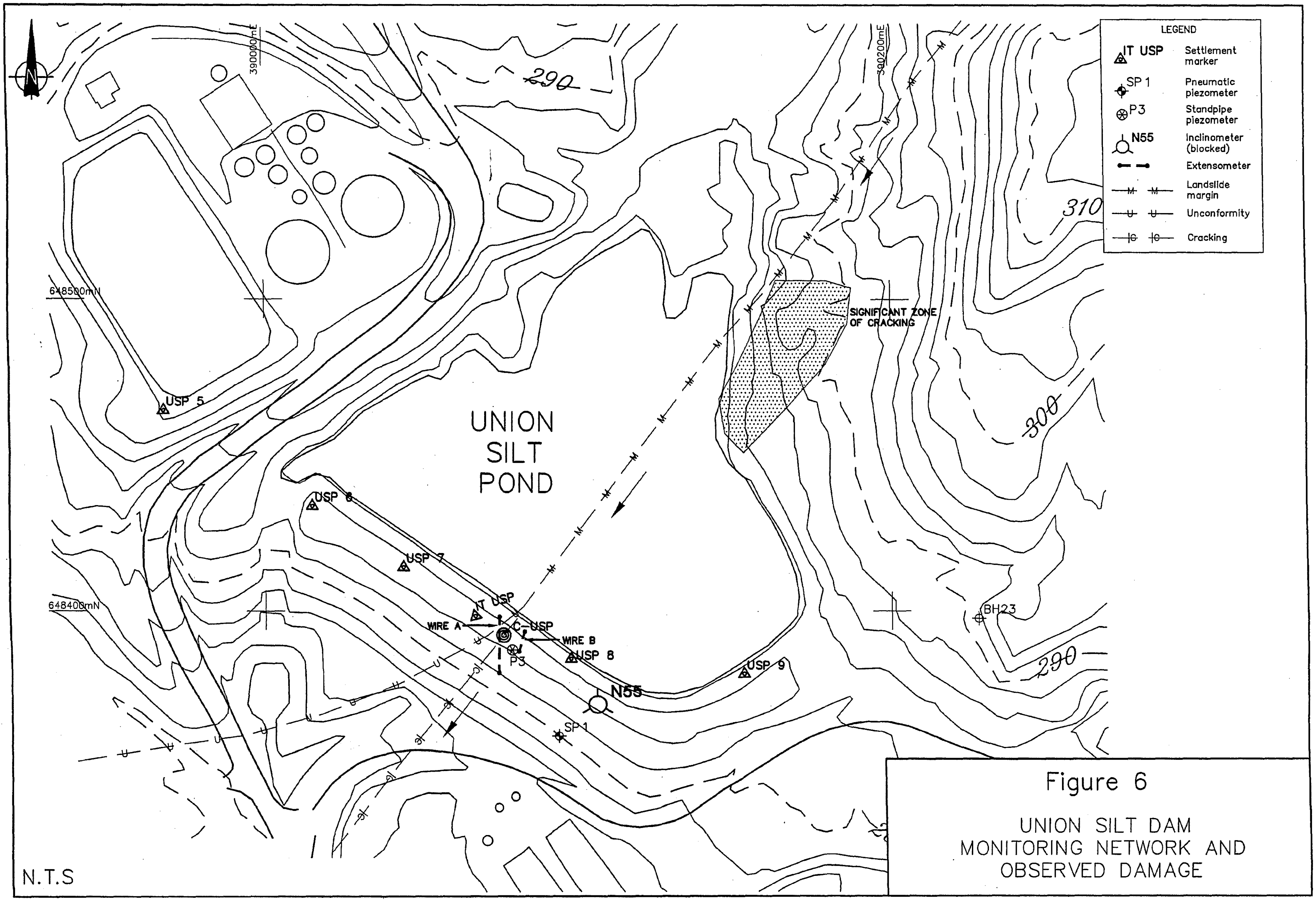

Figure 6

UNION SILT DAM
MONITORING NETWORK AND
OBSERVED DAMAGE

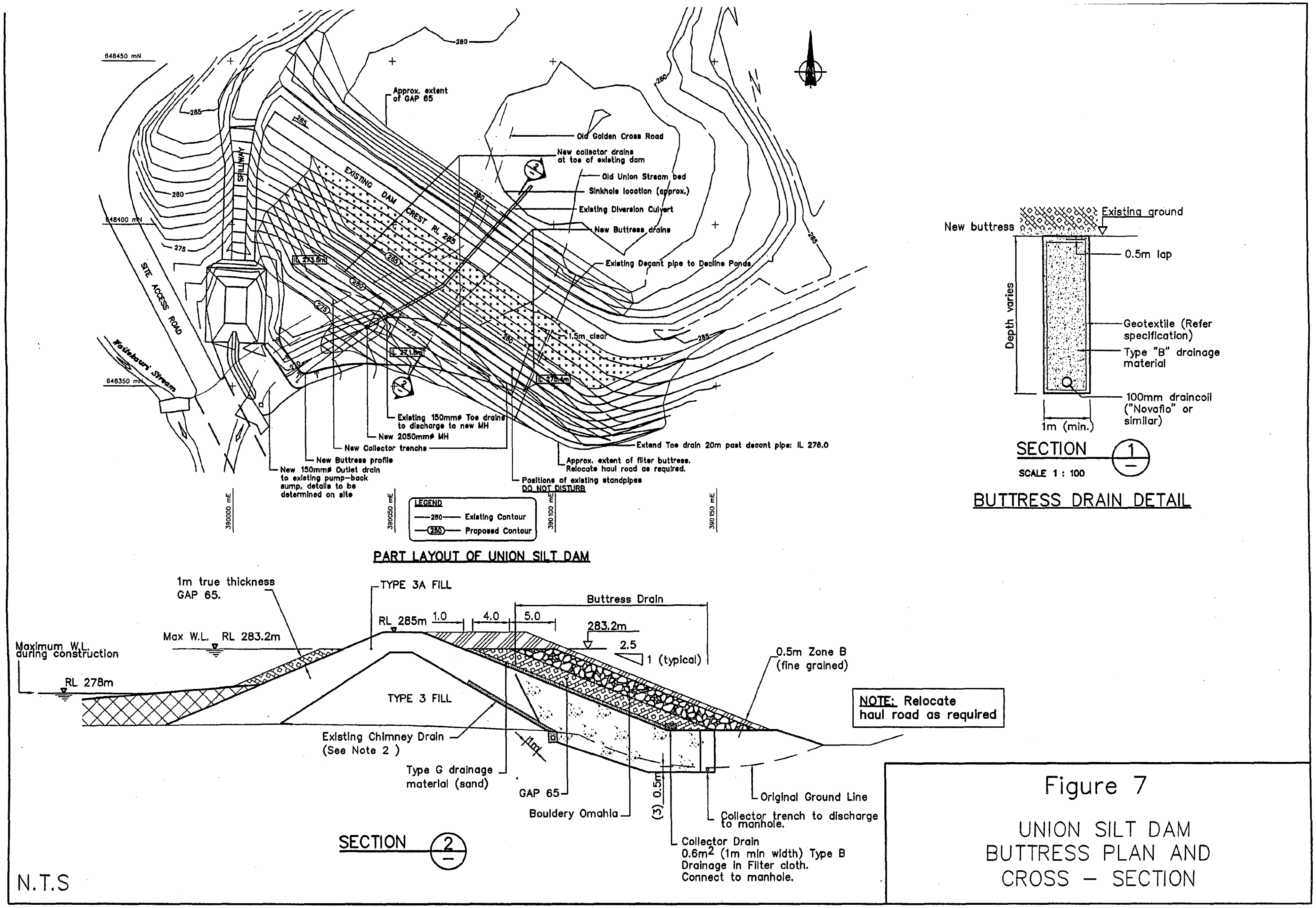

Figure 7

UNION SILT DAM BUTTRESS PLAN AND CROSS – SECTION

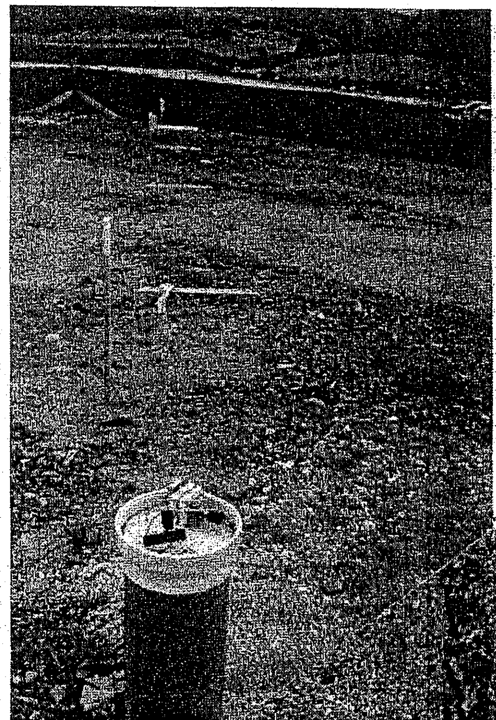

EXTENSOMETER ARRAY

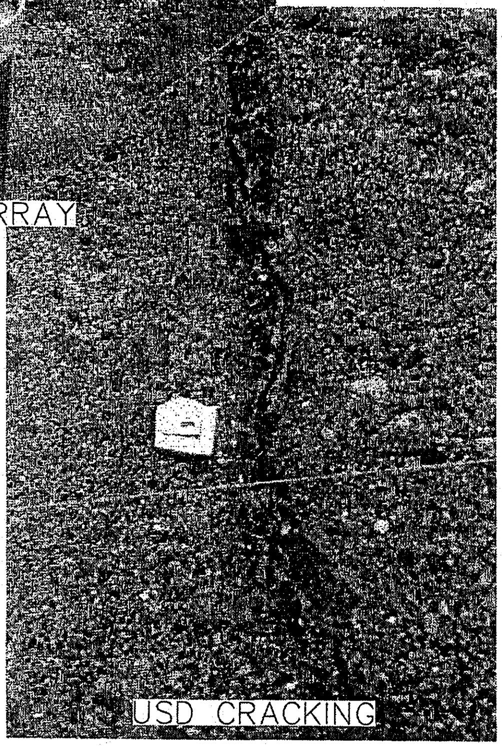

USD CRACKING

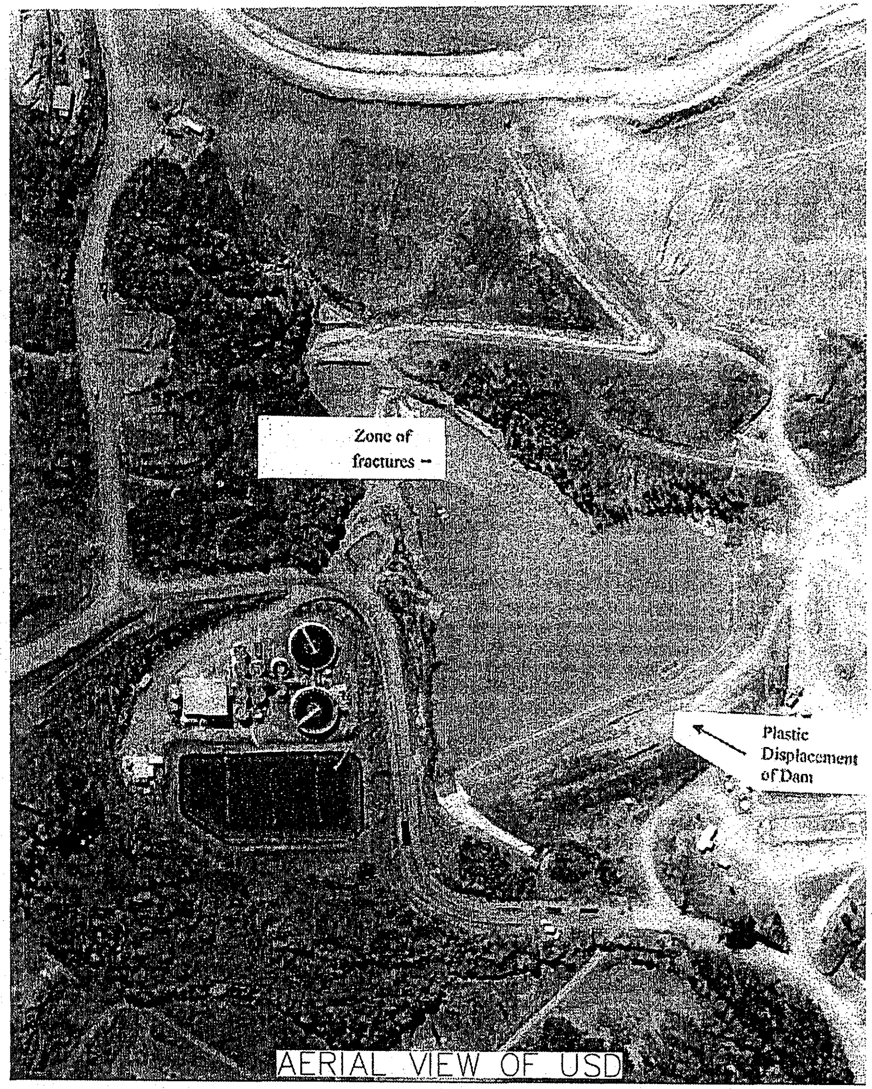

AERIAL VIEW OF USD

Figure 8

PHOTOS

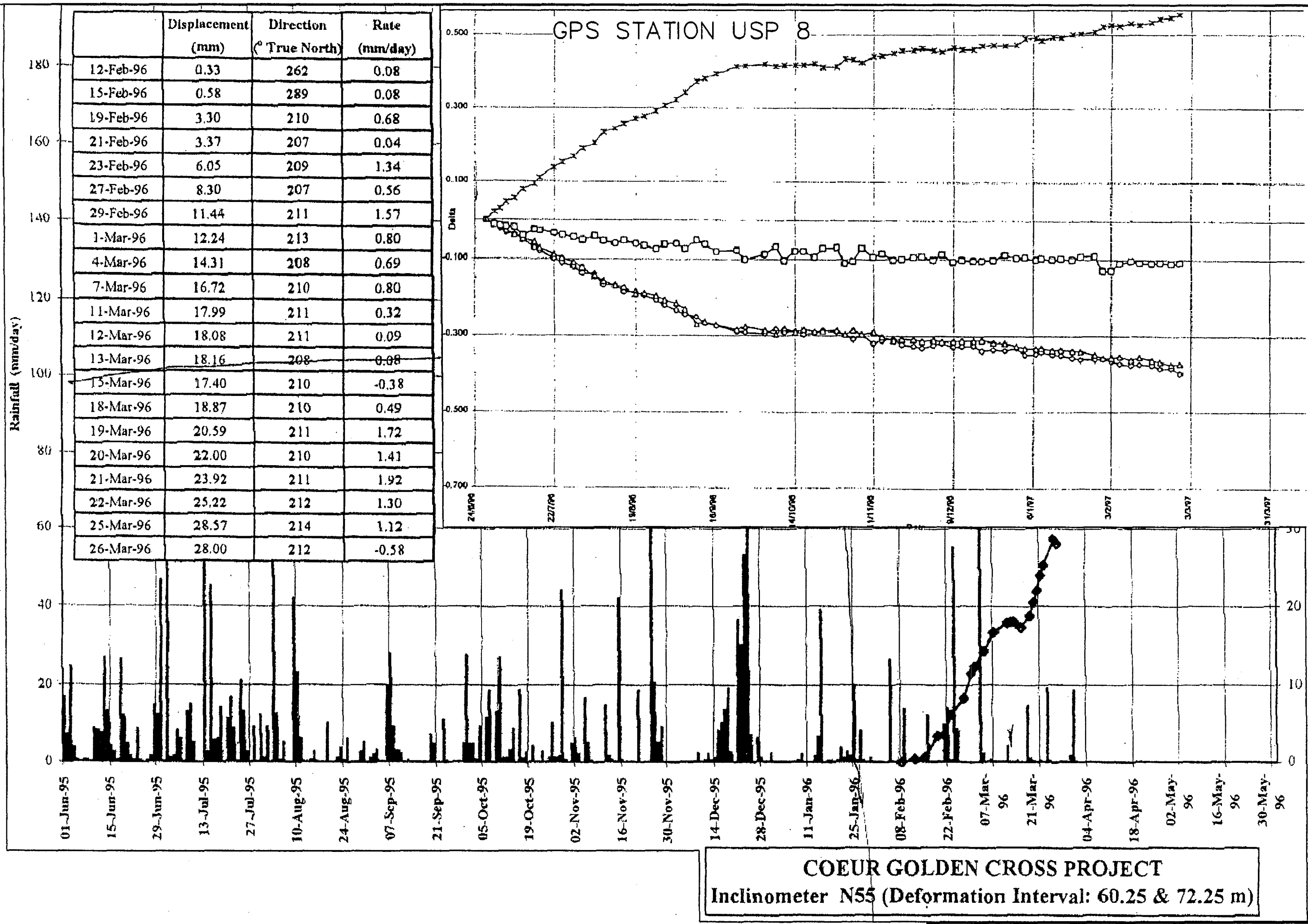

	Displacement (mm)	Direction (° True North)	Rate (mm/day)
12-Feb-96	0.33	262	0.08
15-Feb-96	0.58	289	0.08
19-Feb-96	3.30	210	0.68
21-Feb-96	3.37	207	0.04
23-Feb-96	6.05	209	1.34
27-Feb-96	8.30	207	0.56
29-Feb-96	11.44	211	1.57
1-Mar-96	12.24	213	0.80
4-Mar-96	14.31	208	0.69
7-Mar-96	16.72	210	0.80
11-Mar-96	17.99	211	0.32
12-Mar-96	18.08	211	0.09
13-Mar-96	18.16	208	0.08
15-Mar-96	17.40	210	-0.38
18-Mar-96	18.87	210	0.49
19-Mar-96	20.59	211	1.72
20-Mar-96	22.00	210	1.41
21-Mar-96	23.92	211	1.92
22-Mar-96	25.22	212	1.30
25-Mar-96	28.57	214	1.12
26-Mar-96	28.00	212	-0.58

Figure 9

INCLINOMETER AND GPS DATA

N.T.S

amount of distortion at the dam crest (up to about 1.5 m). The observation that the dam has deformed up to 1.5m plastically without any indicators of functional damage having occurred is a strong indicator of the relative flexibility of earth dams. For the Union Silt Dam, this ability to sustain large strains without distress is likely to be enhanced by the high plasticity of the argillic material which comprises the central core This material is an unusual hydrothermally altered, highly weathered clay rich Coromandel Group Andesite with a high smectite content. It was selected as dam core material because of its high plasticity and this appears to have been a sound choice.

Conclusions

Downstream graded filter buttresses have been used successfully at Golden Cross to protect critical areas of dam embankments affected by landsliding and to minimise the likelihood of piping within landslide movement- induced cracks. The Saddle Filter Buttress was constructed on a zone of embankment under tension while the Union Silt Dam Filter Buttress was constructed across a rapidly moving shear zone. Design of the filters was based on the recommendations of J.L. Sherard et al. There has been no sign of leakage observed from either dam either prior to or following the filter installation.

The ability of earthfill dams to absorb movement without damage has been demonstrated by the performance of both dams. In particular, the highly plastic clay-rich material forming the core of the Union Silt Dam has been shown to be successful in absorbing very large deformations without practical distress. The use of such materials in dam embankments that may be subject to large strains is recommended.

Acknowledgements

Cyprus Gold was the original mine owner and developer and the current owner is Coeur Gold NZ Ltd. The assistance of the mine manager, Mr Randy MaGillivray,in reviewing this paper is gratefully acknowledged. Woodward Clyde NZ assisted in the design of other stabilising works on the site.

References

Sherard, J.L. and Dunnigan (1989). "Critical Filters for Impervious Soils."

Sherard, J.L. and Dunnigan (1984). "Filters for Silts and Clays."

Sherard, J.L. and Dunnigan (ca 1988). "Basic Properties for Sand and Gravel Filters."

Sinclair, T.J.E. and Freer, C.J. (1994). "Aspects of Tailings Dam Design for the Golden Cross Mine."

Tonkin & Taylor Ltd (1996). "Golden Cross Joint Venture – Union Embankment Tailings Storage – Designer Report for May 1995 to December 1996."

Tonkin & Taylor Ltd (1997). "Golden Cross Project – Interpretive Report for October 1997."

Tonkin & Taylor Ltd (1998). "Golden Cross Joint Venture – Union Embankment Tailings Storage – Designer Report for January to December 1997."

Winkler, G.E.(2001). "Engineering Geology of the Golden Cross Landslide."

Woodward Clyde (February 1996). "Coeur Golden Cross – Independent Review of Tailings Dam Stability, Coeur Golden Cross Mine, Waihi, New Zealand."

Risk Assessment

Geological hazards and the road network

Dr Robin Dunlop
Chief Executive, Transit New Zealand

Ian Cox
Regional Asset Manager, Transit New Zealand

Abstract

With New Zealand's geological youth and tectonic nature, all roads are subject to geological hazard. The network was established without serious consideration of risks relevant to the safety of roadworkers and users, as well as the high level of reliability expected today.

In recent times, seismic screening and detailed evaluation of the country's major structures have supported a targeted seismic retrofit programme. In particular, the analysis of the Auckland Harbour Bridge and the Thorndon Overbridge in Wellington have lead to innovative solutions to deal with active faulting, earthquake shaking and soil liquefaction.

Construction of the Otira Viaduct to combat active erosion of an alpine rock face in an area of current seismic activity is described. Construction of an overhead debris chute and waterfall over the highway on structures to protect the travelling public below on the same highway, are also covered.

Other mitigation techniques, including New Zealand's largest mechanically stabilised earth wall, a tension hoop beam on mini piles and cemented soil columns will be described in the paper, along with Transit New Zealand's overall risk management strategy.

General Risk Management Process

Background

Transit New Zealand (Transit) is responsible for the stewardship of New Zealand's State highways, comprising approximately 10,775 km of roads with an asset value of over $10 billion. In developing, maintaining and operating the asset Transit has the responsibility for the expenditure of more than $0.5 billion of road sector funds each year. Transits' State highway maintenance, operation, improvement and replacement activities impact both road users and communities and success or failure is critically judged not only against economic criteria but also against social and environmental imperatives (i.e. Triple Bottom Line).

The relevant expectations that stakeholders have placed on Transit, and the expectations for excellence that Transit has in turn placed both upon itself and its suppliers, are demanding. Any potential for non-achievement of these expectations defines areas of risk requiring effective management.

Existing Processes

It is critical therefore that, as an organisation Transit is confident that sufficient (cost-effective) effort is input to identify, consider and manage the significant and broad range of risks facing it. In this regard key operational processes have evolved with an implicit focus on identifying and managing risk. Examples including Transit's State Highway Safety Management System, Asset (including Bridges) Management Plan and Seismic Assessment/Screening Programmes.

In order to complement existing initiatives and provide further levels of assurance with respect to the effective management of risks a high level and systematic Risk Management Process has also been developed.

Risk Management Process Overview

The purpose of the Risk Management Process is to act as a central reference point for, and to define and encourage the use of best risk management practices for general aspects of Transit's business. The principle objective is to identify and eliminate any gaps in risk management application and to provide further input to, and added confidence as to the appropriateness of critical decisions, and the priorities accorded to existing programmes plans and actions.

In achieving the above Transit has adopted the practice and discipline of the Australasian Risk Management standard AS/NS 4360. This includes the definition of "risk" in terms of the assessed consequence and likelihood of a postulated event and "risk management" as the process of risk:

- identification,
- analysis (scoring of consequence and likelihood per risk),
- evaluation (ranking of scored risks),
- treatment (mitigation of risk consequence and/or likelihood),
- monitoring, and
- communication.

In regards to Transit's business the Process places particular emphasis on actions and activities associated with higher-level objectives and performance expectations in the areas of:

- Project development and delivery,
- Asset management and operation, and
- Corporate and business strategies and plans.

Workshops have been adopted as a standard methodology for facilitating this type of systematic risk management and have been established in an alignment with the above activities. Key workshop considerations are that the context for the assessment is well defined and that the representation and competence on the team correlates with that context.

The menu of significant risks to be considered by a given workshop depends on the subject area under consideration but typically encompasses risks of excessive cost, delays, loss of asset value, image damage, social (e.g. health, safety, community coherence etc) and/or environmental impacts caused through [typically] poor or inadequate:

- planning,
- consultation,
- design,
- maintenance,
- security,
- contract management,
- knowledge of environmental or social effects,
- knowledge of geo-technical conditions, and
- anticipation of natural events etc.

Where practicable and effective this type of risk management approach is or will be built directly into operational process. To date this has been achieved with project development and delivery where it has been tailored to specific project attributes (e.g. project cost, phase etc) and incorporated into practice via management procedures and contracts. It is likely that asset management and operation practices will follow suit.

Geo-technical Risk Management

Geo-technical risk is a critical engineering and economic item in the menu of risks facing the maintenance, operation and, in particular improvement of the asset. Its practical management is consistent with that applied to other risk areas with the proviso that the science of the subject dictates the use of appropriate expertise and inevitably the use of more specific and sophisticated risk management tools (e.g. sensitivity and probability analyses) with the objective of providing more detailed and specific input to technical decision making, where possible.

For large works that can be specifically identified, this is a practical approach and the scientific method with the use of sophisticated tools can be applied. Time is often the governing factor since it will separate the cases where there is an ability to apply the tools from those where response times are too short for other than a best engineering approach because the risk is already manifest. Size is also a restraint as the number of risk points on New Zealand's highways is beyond the practical resource limits for every identified site to be studied individually. Therefore risk assessment needs to be applied by priority, with the highest priority going to those sites or structures that demonstrably would have considerable social consequences if the availability of the highway was affected for an extended period. The case studies that follow will demonstrate the approaches taken in a variety of cases, and the innovation that is being achieved in this field.

Case Study One: Auckland Harbour Bridge

Introduction

The Auckland Harbour Bridge was constructed in the late 1950's and was widened ten years later. The original bridge comprised four spans of deck trusses for the southern approach, and a three-span truss over the navigation opening. The main span is 244m and the main piers are massive cellular reinforced concrete structures supported on bedrock.

The widening employed haunched steel box girders, one on each side of the original bridge, with steel piers supported on steel extensions anchored to each side of the existing concrete piers. There are now effectively three separate bridge superstructures, on common piers, spanning the harbour.

The bridge is an essential element in the State Highway 1 system linking the Auckland with the North Shore. Loss of use of the crossing due to earthquakes would have serious social and economic consequences for the Auckland region and beyond. There is potential for the three structures to "hammer" in a seismic event and to address this problem Transit commissioned an assessment and retrofit study.

Auckland is in a region of moderate seismicity and a site-specific seismic hazard study indicated that the seismic loads at the site would be expected to be less than half those given in the current New Zealand loadings code.

Assessment Methodology

The process contained three main parts:

- Characterisation of the events, their periodicity and their consequences in terms of damage to the bridge, injuries to users and effects on traffic operation;
- An analysis of the traffic effects of closures of part or all of the bridge; and
- A cost/benefit analysis.

There were three independent sets of uncertain natural events in the analysis: earthquakes, high wind velocities and extreme traffic loading. The primary task was to characterise each of these by magnitude and periodicity. The characterisation of events was influenced by the anticipated response of structural elements of the bridge, so a feedback process was necessary.

Disruptions to bridge operation, arising from operations closures for safety reasons or as a result of structural damage from wind or earthquake were linked to wind traffic and earthquake event levels and corresponding return periods. In some cases the damage outcome from a given event level was itself uncertain and a number of possible structural damage outcomes associated with that event level were each assigned a probability.

As a result of the immediate damages from an event, some traffic lanes were expected to be unusable for a period of time because of damage sustained or the need for precautionary closures while they were inspected.

After the initial "clean-up" period following an extreme event, there would be continuing traffic lane closures while damage was repaired. The effect of long period closures on traffic delay and diversion costs would influence the methods employed in reinstating the bridge and the time of day during which work is carried out, so the consequences of lane closures would affect the time of day at which repairs are scheduled and inspections are carried out for the lesser damaging events.

Seismic Hazard Assessment

There are several identifiable, active geological features reasonably close to the site, which make the threat of seismic shaking to the bridge a real one. The results of the seismic hazard assessment comprise estimates of ground motion and seismic loading which were required for the structural assessment. The seismic ground motions had a major impact on the assessment and retrofitting concepts. The consultant carried out the seismic hazard assessment using probabilistic methods. This combined a seismicity model of the area with appropriate attenuation relationships.

A three stage seismic assessment of the bridge was completed:

- Stage 1 comprised the development of performance criteria, the preliminary assessment of the truss and extension bridges and the Shelley Beach flyover and a detailed assessment of the approaches;
- Stage 2 completed the assessment of the truss and extension bridges, approaches and approach viaducts; and
- Stage 3 consisted of the concept design of retrofits to vulnerable components, the preparation of cost estimates and the economic analysis.

As a result of the Stage 2 final seismic assessment, the steel pier brackets that support the box girder extension bridges were found to be deficient not only for seismic loads, but also for wind loads and combined wind and traffic loads. Strengthening of the bracket components with the most serious wind and traffic vulnerabilities was carried out over the period June to October 1997 and restrictions on traffic in high wind conditions have been implemented.

As well as retrofit concept design for seismic vulnerabilities, Stage 3 incorporated the concept design of retrofits for wind and traffic vulnerabilities identified in the extension bridge supports.

Performance Criteria

For a facility with the importance and complexity of the Auckland Harbour Bridge it is necessary to formulate the seismic performance standard considered appropriate at the onset of the project. A general standard does not yet exist for important bridges in New Zealand.

For the first stage of the study the following earthquake ground motions were adopted for each objective.

- **Objective 1** – 200 year return period. *High development of occurrence in bridge life, damage and disruption to traffic minimal.*
- **Objective 2** – 2,000 year return period. *Low risk of occurrence in bridge life, loss of life risk low, at least from lanes open and reparable in a few days.*
- **Objective 3** – Maximum credible earthquake. *No structural collapse and major loss of life prevented. Bridge may be closed for some time and some permanent loss of function.*

Geotechnical and Liquefaction Assessment

Geotechnical analyses were undertaken as part of the project. The primary purpose of the geotechnical analyses was to predict the response of the foundation materials to earthquake shaking, such that the overall performance of the bridge and its approaches could be assessed against the performance standard.

The underlying geology at the site comprises Waitemata Group sandstones. In the Auckland harbour area the sandstones are overlain with varying depths of intertidal mud and marine deposits. The depth of these sediments varies from approximately 15 metres on the south side of the harbour to only a very shallow depth on the north side. As well, both the south and north approaches are constructed on reclaimed land.

Details obtained from technical papers, drawings, and specifications described the reclamations as being constructed with pumped sandy hydraulic fill for the south approach, and rolled clay fill for the north side. The approximately 4m-thick reclamations are contained within rock faced scoria sea wall bunds.
The stability of the approach embankment slopes and the likely magnitude of vertical and lateral displacements following liquefaction were also assessed. The performance of the south embankments may prove to be critical to the overall seismic performance of the crossing.

Derived Effects

The seismic assessment of the bridge and the wind and traffic load assessment of the extension bridge supports identified a number of at-risk components in the existing structural detailing, resulting in a structure not meeting required performance standards. Potential consequences of this were:

- Probable collapse of a span of the northern approach viaducts under earthquake shaking for a return period less than 2,000 years, resulting in loss of service of four lanes for a month;
- Possible damage to or collapse of the extension bridges for wind loads with a return period of less than 100 years, resulting in loss of service of four lanes for approximately two years;
- Possible collapse of the extension bridges for earthquake shaking at less than the maximum credible earthquake level, also resulting in the loss of service of four lanes for approximately two years;
- Possible collapse of both extension bridges and several spans of the truss bridge for maximum credible earthquake level shaking, resulting in complete loss of service of the eight traffic lanes, water and gas mains for a period of the order of two years; and
- Possible major loss of life should collapse due to earthquake shaking coincide with heavy traffic flows.

Retrofit Outcomes

A total retrofit concept to address the at-risk components and bring the bridge up to the required performance standards were developed and costed. The retrofit comprised:

- Installation of seat extension frames and strengthening of brace components in the approach viaducts to prevent collapse of spans under earthquake shaking;
- Strengthening of extension bridge pier trestle columns to prevent extension bridge damage or collapse under seismic and wind loads;
- Strengthening of truss deck bracing to avoid deck panel collapse under maximum credible earthquake level shaking;
- Installation of 'wind braces' to provide alternative lateral load path from the extension bridges to the piers to avoid possible damage or collapse of the extension bridge under wind loading due to trestle and bracket vulnerabilities;
- Strengthening of various bridge pier bracket components to achieve the desired seismic, wind and traffic load performance standards;
- Strengthening of concrete pier upper walls to achieve the desired wind and traffic load performance standard; and
- Strengthening of various other items including truss members to reduce seismic pounding damage.

The total cost to complete this retrofit was of the order of $2.5 million and the economic analysis gave a significant economic outcome at this level of funding because of the significance of the likely effects of the various event scenarios. In this case the risk based assessment proved to be a very good tool to demonstrate the need for the work to be done, including risk elements based on more than geotechnical assessment alone.

Residual Risk

The structural retrofit of the bridge has been carried out successfully and the bridge is capable of acting in accordance with the performance criteria for various earthquake intensities. However these still remains the risk that liquefaction of the southern approaches will disrupt traffic flows on the bridge.

Case Study Two: Thorndon Overbridge

Introduction

The Thorndon Overbridge is a 1.3 kilometre-long, elevated concrete structure, which carries the Wellington motorway north out of the city above the rail yards and the Inter-island Ferry terminal. The bridge was designed and constructed in the late 1960's. On- and off-ramps provide access to Aotea Quay about midway along the bridge and are tied to the main structure. The bridge and associated motorway is built along the shores of the Wellington Harbour on reclaimed land. At the north end of the bridge, the reclaimed land is retained by a gravity seawall that is close to the bridge foundations the performance of which affects the seismic performance of the bridge structure. In addition, there were other structures adjacent to the bridge such as the Golden Bay cement silos, which could have effects on the structure by clashing or toppling during ground motion.

The Wellington Fault runs alongside and passes under the bridge. Part of the geotechnical testing was aimed at specifically locating the point where the fault line passed under the structure. There had been concern for some time that a reasonable sized earthquake had high probability within a short enough timeframe to be a serious risk to the structure, and that the bridge was old technology when considered against modern design codes. Initial work was done in the late 1980's to consider strengthening the bridge, which culminated in the installation of horizontal tie rods to tie the spans together. Further impetus was given by the introduction of the country's first integrated lifelines project to consider the consequences to the city of the loss of particular, significant lifeline features and the affect this would have on restoring the city after a serious earthquake.

The Wellington Lifelines project provided the first significant information on the characterisation and probabilities of earthquake events likely to occur along the Wellington Fault. It also identified the Thorndon Overbridge as a critical structure required for the restoration of the city following an earthquake. In parallel Transit began a process to carry out full risk assessment of the structure with the aim of retrofitting the bridge as necessary, as was happening in California following the seismic events that had occurred there.

Seismic Risk Assessment

This study had an advantage in that it followed on from a significant amount of work done by others to characterise the likely events with significant probabilities that might arise due to a rupture of the Wellington Fault. Past studies have included defining the past rupture history of the fault, measuring stress and strain on the fault itself, determining the likelihood and magnitude of ground displacement in any future event and quantifying the social consequences of each event magnitude. This provided the base information of the event return periods, likely effects and possible consequences.

The assessment was developed through a number of stages.

- Detailed geotechnical investigation of the site to characterise the ground response;
- Applying each of the event levels to the site to determine the effects on the structure. This was particularly important at the threshold where toppling of the seawall reduced the lateral support at several of the northern piers;
- Analysing the structure in detail to evaluate the response to the ground movements produced by each event;
- Determining the thresholds that were the maximum for each level of response to determine those events which were critical in terms of the structure response;

- Considering the event probabilities to evaluate the likelihood x consequence for the likely remaining life of the upgraded structure, which would help determine the maximum credible event level;
- Developing a set of acceptance criteria based on providing public safety, having considered the likely structure response, and developing a set of retrofit concepts to match the acceptance criteria;
- Carrying out a risk study based on local and international data to assess appropriate risk levels applicable to each of the retrofit proposals; and
- Completing an economic analysis to ensure that the level of retrofit targeted is appropriate.

It should be noted that the return periods for the threshold events and maximum credible earthquake are considerably greater than might be expected and do not relate to the probabilities of exceedance in the normal way. The reason for this is very simple. Due to the fact that the Wellington Fault has not ruptured for approximately 415 years, its probability of rupture is greater than the return periods imply. Therefore the scale of the likely events and their accompanying likelihood x consequence is much greater in these circumstances. The events characterised below in Table 1 are the threshold events for which the retrofit schemes were developed.

Retrofit Scheme	Return Period (Years)	Design Earthquake Level			Assessment Report Event Level
		Spectral Acceleration (T=1 sec.)	Peak Ground Acceleration	Peak Ground Displacement (1)	
I	500	0.84 g	0.45 g	400 mm	3B
II	300	0.50 g	0.28 g	300 mm	3A
III	200	0.34 g	0.22 g	200 mm	2
Note: (1) Estimated peak elastic ground displacement caused by seismic ground wave.					

Table 1: Design Earthquake levels for the retrofit schemes.

The seismic assessment indicated that the structure was vulnerable to major damage and/or collapse at relatively low levels of seismic ground shaking. Vulnerable items included collapse of the off-ramp due to liquefaction of an underlying sand layer, collapse of spans due to either insufficient seating length or due to failure of the bridge pilecaps, and collapse of spans onto the ferry terminal due to failure of the seawall and retained ground in this area. In an earthquake caused by the Wellington Fault, which run under the bridge, collapse of the main bridge and the off-ramp, where they cross the fault line, can be expected.

The acceptance criteria were based on prevention of catastrophic failure thereby providing security to any persons either on or under the structure in a major event. Individual elements of the structure could yield provided that the structure was still erect after the event. In the event of major ground displacement along the fault line, it would be impossible to provide certainty of integrity to the structure over three affected spans, but it was unacceptable to have the deck fall to any degree as there was a high probability of having the area under the bridge at this point occupied during an event. Therefore the acceptance criteria were summarised as follows:

1. Under the action of moderate earthquakes of such a magnitude that they are unlikely to cause significant ground movements, the bridge structures were to be capable of remaining fully serviceable with only minor repairs being necessary (full service);
2. Under the action of larger earthquakes of such a magnitude that localised ground movements may occur, the bridge structures were to be capable of being brought back into service (albeit at a reduced level) a short time after the event, and capable of being repaired to a full level of

service. The risk to human life, both on or adjacent to the bridge, in an event of this magnitude, to be reduced to a low level (limited service–temporary/emergency); and

3. Under the action of a very large earthquake the response of the bridge structures was to be investigated and measures that would significantly improve their performance and reduce the risk to human life on and adjacent to the bridge were to be identified (safety-no collapse).

Retrofit Concepts

The possible levels of retrofitting for the Thorndon Overbridge ranged from extensive schemes to retrofit against severe ground shaking to a minimal scheme that addressed only the worst seismic deficiencies. Three basic retrofit schemes were developed.

- **Retrofit Scheme I:** An *extensive* retrofit scheme, designed for a ground shaking level corresponding to the 500-year return period, and designed to mitigate against the collapse of the bridge due to movement of the Wellington Fault;
- **Retrofit Scheme II:** An *intermediate* retrofit scheme designed for a ground shaking level corresponding to the 300-year return period; and
- **Retrofit Scheme III:** A *minimal* retrofit scheme designed for a ground shaking level corresponding to the 200-year return period.

The minimal scheme only includes the higher risk components. This would have left the structure vulnerable to major damage and/or collapse when subjected to higher-level events and consequently was unlikely to meet the acceptance criteria. It could have been considered as an interim securing level only.

The extensive retrofit scheme addressed most of the vulnerable areas of the structure that had been identified. The scheme was expected to meet the acceptance criteria and to represent the highest retrofit level realistically achievable at the site. This was because at higher levels of ground shaking, large widespread ground displacements occur which would cause significant and irreparable damage to the piles. These displacements could only be retrofitted against by an extensive programme of ground improvement, similar to that done for the Te Papa site, at very high cost and with major disruption of the site to the detriment of the rail yards, the ferry terminal and adjacent buildings and roads.

The intermediate scheme was targeted at a level of ground shaking between the other two, set at a level that would have included retrofitting of many of the vulnerable areas of the structure.

Retrofit for movements on the Wellington Fault were included in Scheme I only. There were two reasons for this. Firstly the Wellington Fault movement retrofit required the restrainers through the piercaps to yield and to achieve this the pier pilecaps in the area also had to be retrofitted. This was true even with a number of the existing restrainers removed. Those pilecaps were retrofitted in Scheme I only. If their retrofit were then included in Scheme II, then Scheme II would no longer be significantly different from Scheme I and could essentially be discarded. The second reason for including the retrofit for movements of the Wellington Fault only in Scheme I is because of the dominance of this fault in generating the higher levels of ground shaking. The Wellington Fault has a significantly higher probability of being the cause of the earthquake (over the Ohariu or Wairarapa Faults) at the higher level of ground shaking.

Table 2 summarises the elements of each of the retrofit schemes for comparison.

For each of the retrofit schemes consideration was given to those elements whose failure, at ground shaking levels slightly greater than the design retrofit level, would cause collapse by such means as unseating of spans. The design return periods for such items were taken as 1000, 500 and 300 years foe Schemes I, II and III respectively.

Area of Structure		Retrofit Scheme I	Retrofit Scheme II	Retrofit Scheme III
Superstructure Linkages		Test linkage and hold-down bolts. Retrofit linkage bolts at all piers. Add seat extensions at ramps and abutments.	Retrofit linkage bolts at 20 piers, add seat extensions at ramps.	No retrofit.
Wellington Fault		Support frames at main structure. Sliding braced frames at off-ramp.	No retrofit.	No retrofit.
Foundations and Columns at Main Structure	Pier Group A (4 column-bents at far north end – 9 piers total)	Steel column jackets. Infill concrete walls. Pilecap overlays.	Steel column jackets and pilecap overlays.	Steel column jackets and pilecap overlays.
	Pier Groups B-I (Area north of Aotea Quay – 35 columns and 31 pilecaps, total)	Steel Jackets on all columns. Overlays on all pilecaps. Post-tension 27 pilecaps. New piles at pier 19.	Test existing pilecap and pilecap plus overlay. Steel jackets on 23 columns. Overlays on 28 pilecaps. Post-tension 10 pilecaps.	Steel jacket 3 columns. Overlay 10 pilecaps. Post-tension 7 pilecaps.
	Pier Groups J-M (Area south of Aotea Quay – 32 columns and pilecaps, total)	Test pilecap plus overlay. Steel jackets on 2 columns. Overlays on 14 pilecaps. Post-tension 18 pilecaps.	Test existing pilecap. Steel jackets on 2 columns. Overlays on 4 pilecaps. No post-tensioning.	Overlay on 4 pilecaps.
Off-ramp	Piers	Overlay on 7 pilecaps.	No retrofit.	No retrofit.
	Ground Improvement	Stone columns in soil.	Stone columns in soil.	Stone columns in soil.
On-ramp		Overlay on 4 pilecaps.	No retrofit.	No retrofit.

Table 2: Summary of Retrofit Measures

In addition to the three basic schemes above, a further scheme was developed for a ground shaking design level of 1,000 years and included retrofitting for major seawards movement of the site. This scheme, designated Scheme I + Ground Improvement, comprised the components of Scheme I plus ground improvement in a limited area to mitigate against block sliding of the site under the bridge.

Retrofit Performance

The retrofit schemes were each characterised with respect to the three acceptance criteria levels above. Each of them was defined by the probability of exceedance in 50 years in accordance with the defined acceptance criteria performance levels. The 50-year period approximates the estimated remaining service life of the bridge. The outcome can be demonstrated by considering the example of retrofit Scheme I. Once the retrofitting has been carried out the following seismic performance over the remaining 50-year service life can be expected to be:

- There is a 15% chance that an earthquake will occur that exceeds the full service criterion level, that is after the earthquake, at least some of the traffic-carrying capacity of the bridge must be shut down;

- There is a 10% chance that an earthquake will exceed the limited service criterion level, that is after the earthquake, no traffic can pass over the bridge, not even temporary or emergency traffic; and
- There is a 5% chance that some portion of the bridge may collapse.

The last figure for each of the retrofit schemes has been transferred into Table 3 for comparison. Note that the performance for the off-ramp has been presented separately because there was an option to retrofit the off-ramp to a different level than the main structure.

	Retrofit Level				
	Unretrofitted	Scheme III	Scheme II	Scheme I	Scheme I plus Ground Improvements
1. Safety Performance (Probability of collapse in 50 years)					
1.1 Main Bridge Structure and On-ramp	20%	20%	15%	5%	1%
1.2 Off-ramp	24%	11%	11%	1%	1%
2. Earthquake Fatalities (Expected value in 50 years)	4.3	4.1	3.8	0.3	0
3. Retrofit Costs ($millions)	-	7	9	19	59
4. Benefit/Cost Ratios (25year analysis)					
4.1 Ratio of expected benefit to expected cost	-	0.8	0.7	0.9	0.6
4.2 Expected value of ratio of benefit to cost*	-	1.0	0.6	1.3	0.6
* Negative cost outcomes excluded.					

Table 3: Summary of Performance Data for Retrofit Schemes

By comparison, it can be seen that retrofit Scheme III provided little benefit over the option of not retrofitting the bridge.

The differences that can be seen between the probabilities of collapse between Schemes III and II for item 1.1 is due to the better performance of the on-ramp structure in Scheme II, not the main structure.

The Scheme I and Scheme I + Ground Improvement retrofits show significantly improved performance over the others with reduced risk to human life and reduced economic losses. The latter has a larger effect on reducing economic losses, but a much greater cost as demonstrated by the economic analysis. The Scheme I retrofit gives the highest economic return.

In consideration of the above, Scheme I was the preferred level of retrofit for the Thorndon Overbridge.

Comparative Seismic Risk Study

This study investigated accepted risks and design levels for: bridges in other jurisdictions (namely North America), new structures, new and existing facilities in Wellington, and by society generally for a variety of hazards. The purpose was to provide a conceptual framework for the decision-makers to compare various accepted levels of risk in order to consider whether the retrofitting of the Thorndon Overbridge was targeted at the correct level. It concluded that:

- Criteria adopted in North America, in particular those adopted by California were appropriate for application to this structure;

- Retrofit Scheme I + Ground Improvement (1,000 year return period retrofit level) comes closest to satisfying California's retrofit criteria. Retrofit Scheme I (500 year return period retrofit level) comes closest to satisfying British Columbia's retrofit criteria;
- A retrofit scheme addressing at least the 500 year return period retrofit level would produce a level of performance compatible with the expected performance of the roading system dependent on the bridge;
- A retrofit scheme addressing the 500 year return period retrofit level would produce an appropriate level of performance of the bridge relative to the performance of other lifelines and important buildings in Wellington; and
- The residual risk inherent in Scheme I is similar to that from other engineered structures, while that from Scheme I + Ground Improvement is less than that from other engineered structures.

While higher levels of performance might apply in California, other matters must be taken into account in arriving at the appropriate decision for the Thorndon Overbridge upgrade. In particular, the very large increase in relative costs to achieve that level, the amount of disruption to achieve it, the reduced level of benefit to achieve it and the fact that it is out of keeping with the risks and damage likely to occur to the surrounding infrastructure and buildings.

Taking into account the findings of the performance and economic evaluations and the seismic risk study, the recommendation was that the Scheme I retrofit be applied to the Thorndon Overbridge. That recommendation was accepted and the retrofit is now complete to Scheme I level.

Case Study Three: Otira Viaduct

Introduction

Prior to 1999, State Highway 73 descended down the Otira Gorge over a large active rock avalanche debris slope, a section of road known as the Zigzag. This section of road was opened in 1866, and had been realigned on a number of occasions. The 1929 Arthur's Pass earthquake caused a large section of the road to fall into the river and in 1943 further erosion at the toe of the slope caused a further realignment.

Since the 1940's minor realignments had been made to keep the route open, however by the mid 1990's the point was reached where this could not continue, and another major slip would cut off the highway.

Death's Corner is a remnant of a 2000-year-old rock avalanche that originated at the ridge, 600 m above the riverbed and dammed the valley. The river has subsequently cut a notch into the dam and is actively eroding the base of the scree slope that supported the Zigzag.

The old highway over the Zigzag was also subjected to rock fall from the slope and peaks above. Perhaps the most recent and publicised occurrences of this were in 1994 and 1995 resulting form the Avoca River earthquake and Arthur's pass earthquakes respectively, where blocks of up to 1.5 metres in diameter either landed on or bounced off the State Highway.

Risk Assessment

The evaluation of the possible occurrences focussed on three possible outcomes:

- Loss of the road due to undermining of the supporting slope by river erosion;
- Failure of the road due to a seismic event; and
- The risks to the safety of the travelling public from rock falls.

As can be seen from the photograph in figure 1, the supporting slope below the road was already heavily eroded and oversteepened due to river erosion. The Zigzag had been created by cycles of erosion as progressive slope failure has caused the road to be carried away and reformed at a point higher up the slope, the last of which was in the 1960's. The road has progressively been raised 100 metres vertically further up the hill. The ongoing progressive failure at the time construction started had reached the edge of the seal and was undermining the existing roadway. The configuration of the slope had reached a point where no further retreat of the road could be achieved. The risk assessment indicated that there was a 90% probability that catastrophic failure of the road would occur before 1999. The consequence of this occurrence was assessed as being critical and therefore the risk was extreme, requiring action to avoid or eliminate the risk.

Secondly, consideration was given to risks as a result of a seismic event. The site is located within 20 kilometres of the active Alpine Fault, New Zealand's most dominant seismic feature and a number of smaller faults, such as the Kakapo fault exist close by. As such it is the most seismically active area in New Zealand. Analysis was done to establish the scale and likelihood of seismic events that could produce significant effects at the site and a site-specific seismic hazard study showed expected response levels 30 to 40% higher than normal bridge code values. Then consideration was given to the consequences of the possible events. In the first instance it was assessed that no fault rupture was likely to occur in the immediate vicinity of the zigzag (or viaduct) and fault ruptures of magnitudes of significance in proximity of the site were unlikely to occur within the construction timeframe or to have greater consequences elsewhere in the future. The likeliest occurrences were expected to be the triggering of slope movements, either above or below the road, which could result in either a section of road being buried or carried away. In the final analysis these were considered to be less significant than the erosion risk, but were further developed to consider the selection of the preferred option.

The third issue was that of the safety of the travelling public as a result of rock falls onto the road. Current traffic volume is of the order of 1,000 vehicles per day and the probability of a significant effect due to a vehicle being struck by a falling rock were assessed as being very low due to very low exposure. However, there was a reasonable risk of an effect due to a vehicle striking a rock, or rocks, which had fallen onto the road, even given the inspection regime in place due to established needs. There were then benefits that accrued to options that eliminated those risks. To give an idea of the probabilities of such impacts, there were a couple of small earthquakes that impacted on the site during construction, although the effects were very minor.

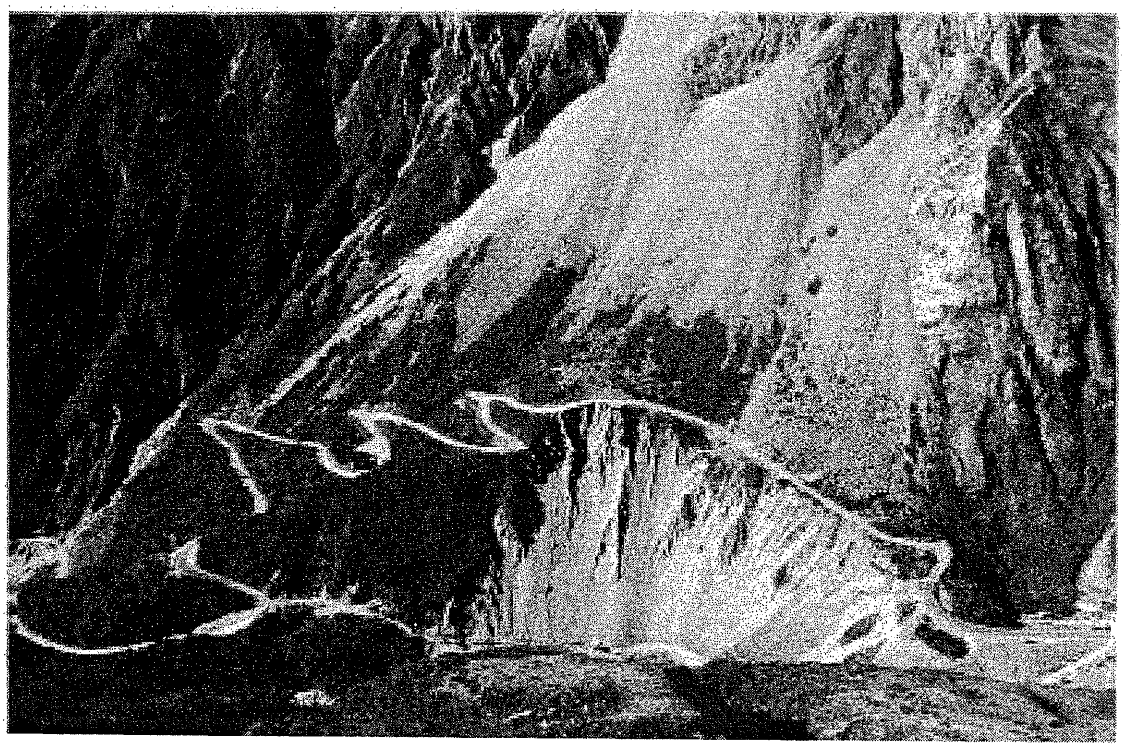

Figure 1: The Zigzag and overhanging scree slopes

Options

A number of options were considered for securing the highway, ranging from "permanent" retaining walls in the rock avalanche scree slope, tunnels on the western side of the valley in combination with bridges, an embankment at the base of the scree slope and steel and concrete viaduct options down the Otira riverbed. All of the options had to be developed in consideration of the principle that the road was situated in a National Park and that the environmental effects of the preferred option had to be mitigated to an acceptable level. Economic outcomes could be derived for each option based on travel time, vehicle operating and crash costs, plus the costs from the risk analysis in accordance with the degree of risk elimination achieved.

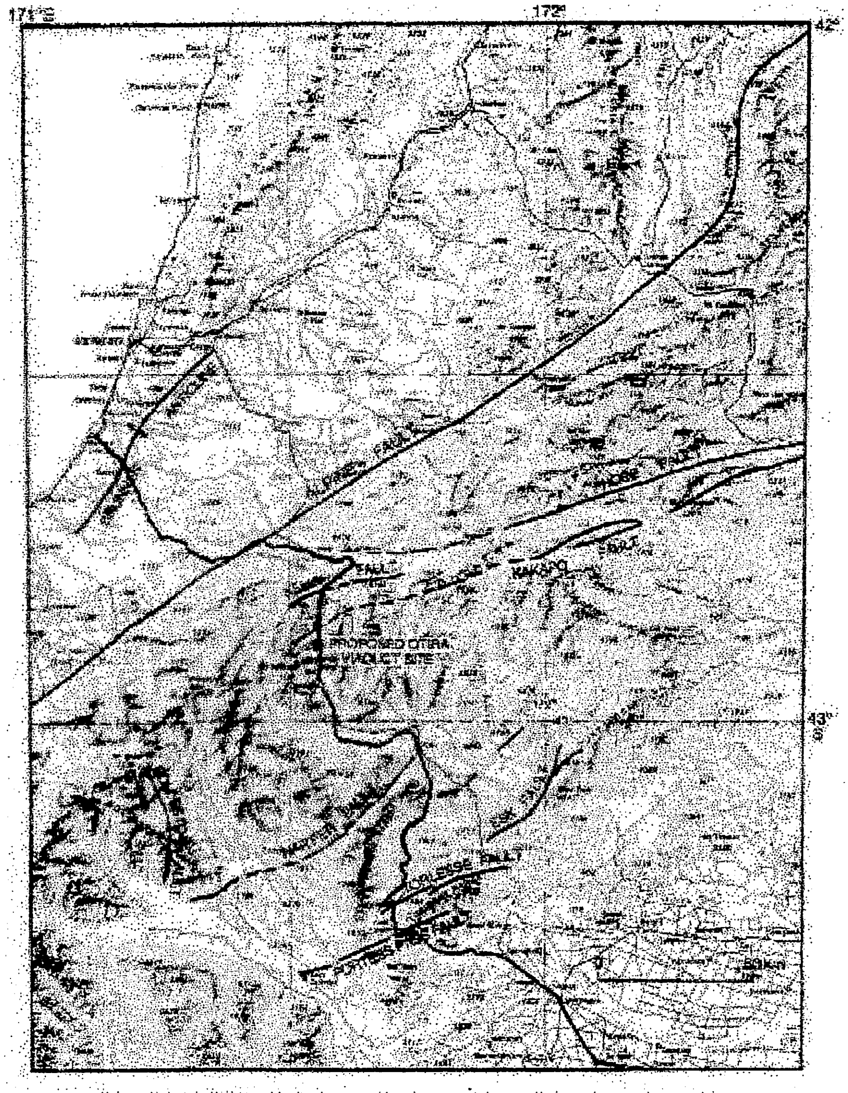

Figure 2: Major active faults within 50 km of proposed Otira Viaduct site and discussed in text.

As a result of economic and environmental considerations, a curved viaduct down the valley was chosen to proceed to detailed design. The options of an embankment at the base of the scree slope or improved road across the scree slope on the true right of the river would still be subject to rock falls, and the instability of the scree slope. Combined tunnelling and bridging options on the true left side of the valley were ruled out as they would be very expensive, and a combination bridging and embankment on true left option was discounted as it would require significant cutting on the left side of the valley destabilising the slope above. Aside from the environmental issues associated with the location within the Arthur's Pass National Park, the geological, geotechnical, hydraulics and seismic issues were significantly improved by the viaduct option beyond the capability of the other options. This was demonstrable and on the basis of the analysis, the viaduct was chosen as the preferred option. The viaduct has been designed accordingly with plastic hinges detailed on the top and bottom of each pier, and special detailing in piers 1 and 3 to prevent ratchetting of the piers during seismic shaking.

Residual Risk

The Otira River is slowly degrading at the site and historically maintenance has been undertaken to construct a Knick Point, to control the river grade, and limit degradation. As part of the viaduct project maintenance was carried out on the Knick Point, reinforcing it with more large rocks, with the intention of prolonging the period before significant degradation occurs beneath the southern approach and south abutment of the viaduct. Further maintenance will be required in the future.

The Otira River rises rapidly during flood conditions and has caused significant erosion in the past. Loss of control of the river could seriously affect the viaduct and scour protection (rip rap) has been placed at critical locations such as the southern abutment, Pier 1 and Pier 3 to mitigate this risk. Scour allowances have also been made when designing the depth of the pile foundations.

The foundations of the viaduct are located within rock avalanche material. This material ranges in size from silt matrix to very large boulders and comprises greywacke boulders with compressive strengths of up to 250 megapascals. In addition, as the debris mass is porous the ground water conditions are extremely variable and complex with artesian conditions present at the base of Death's Corner.

Selection of foundation types included consideration of potential solutions including deep cylinders, piled pads, and circular pad foundations. The potential methods were evaluated from the point of view of capacity, and construction feasibility, noting that whatever type was chosen, construction would be challenging. Pads and piled pads were not considered practical, as the caps would potentially be very large and have to be buried deep in a steep slope (requiring very high temporary slopes) or below scour level when adjacent to the river. If embedment was inadequate or scour provisions were underestimated there was the risk of the pad being uncovered and governing the size of the scour hole leading to a risk of undermining of the foundation. Deep cylinders were considered a practical foundation option for the structure, as a number of methodologies appeared to be available.

The actual methodology for construction of the foundations was left open to the tenderers, and the method adopted by the contractor is illustrated in the figure below. The design required the installation of 4m diameter steel cased piles, and the contractor elected to achieve this by installing a ring of secant piles, creating a concrete tube in the ground inside which excavation could occur. The secant piles were drilled with a NUMA percussion drill of 762mm diameter. The overlapping drill holes were then tremie concreted full to form the concrete "casing".

The expected extra difficulties and expense of foundations for the construction had a significant influence on the bridge type and spans, the number of foundations was minimised, maximising the span of the superstructure. Options investigated during the preliminary design stages included bridges of up to 7 spans (requiring 6 piers), however a 4 span option with three piers was chosen. The high seismic loads and requirement to allow for river scour necessitated cantilever foundations of approximately 25 metres depth for each pier.

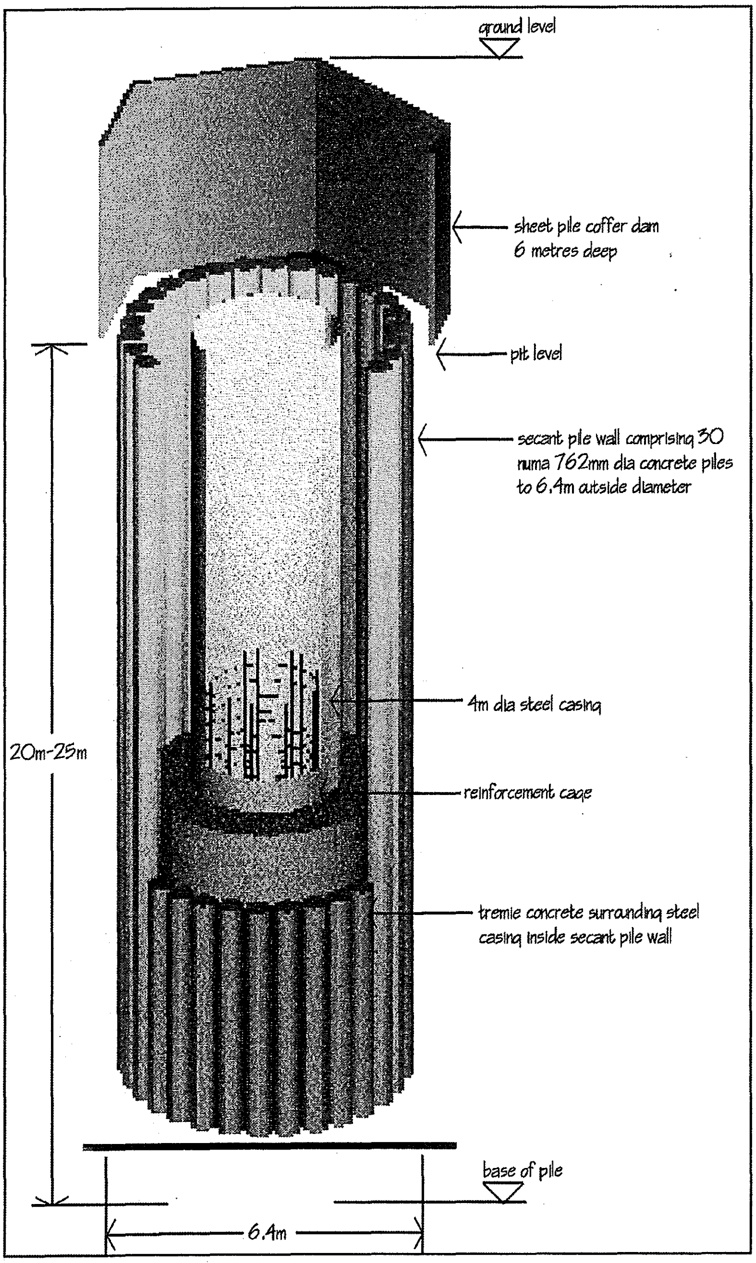

Figure 3: Foundation construction method employed to build the bridge.

Rock fall remains a risk, even now that the road does not traverse the scree slope. A review of the probable source of rock fall, indicated that rocks from the ridges above would be focussed towards the central pier location, however the other piers 1 and 3 could still be affected by large blocks being released from the lower slopes by freeze thaw action and water erosion. It is anticipated that these blocks would slide or roll rather than bounce.

Specific analyses were undertaken in an effort to model the effect of blocks descending from the Hills peak ridge above the site. These analyses indicated that although they may be travelling as fast as 20 m/s, they would follow a low trajectory.

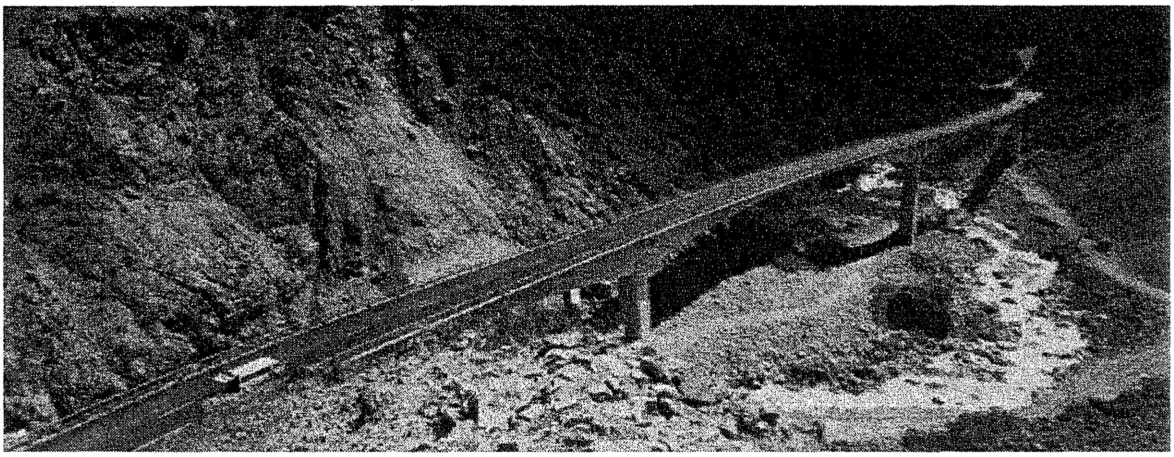

Figure 4: The completed viaduct as seen from the Zigzag

To mitigate against rock fall damage to the bridge piers a 'vee' shaped rock fall protection or deflection structure has been provided above piers 1 and 3, and a deflection bund provided at pier 2. Construction of an intermediate structure such as a rock fall deflection structure was considered the lowest risk option with regard to the serviceability of the viaduct. In the event of a rock fall, the "expendable" protection structure would dissipate energy and suffer any damage, rather than the piers of the more expensive superstructure.

Case Study Four: Candy's Bend Road Widening, Arthur's Pass

Introduction

The Candy's Bend to Starvation Point project is an 850metre length of State Highway (SH) 73 in the Arthur's Pass National Park in the Southern Alps of New Zealand. The site has long been prone to rock fall and was single lane for much of its length. It has steep grades (around 16%) tight curves and limited visibility. It was also governed by a bylaw restricting vehicles to 13 metres in length. These factors meant that, as traffic volumes grew, delays and conflicts on the route were occurring with increasing frequency.

Furthermore, the site is immediately downhill of the new Otira viaduct and other improvements were being made to SH 73 that would make this section the pinch point. The site would be of a considerably lower standard than the adjacent sections and accident migration could be expected if improvements were not made.

The site passes through an alpine pass with steep slopes extending several hundred metres above the road and near vertical drops of between 20 and 70 metres to the river below the road. Realigning and widening the existing road is therefore sensitive to comparatively small lateral movements. For example widening of less than one metre out of the hillside can require building new structures while moving into the hillside can require large cut volumes and impose adverse environmental effects associated with large, and possibly unstable, cut faces. Therefore capacity improvements would need to be balanced with assessment of induced geological risks and also aim to militate the highest likelihood events with the most serious consequences of the identifiable, existing risks.

The steep topography and limited width of the existing, single lane, road bench also meant that any construction or widening on the existing alignment would inevitably interfere with traffic flow and require a strong focus on constructability. Potential loss of access introduced wider social risks.

Existing Geological Risks

The site is located in one of the most seismically active areas of New Zealand: within five kilometres of the active Kakapo fault and within 20 kilometres of the main alpine fault. An earthquake in 1994 dislodged a significant block of material (approximately 7000m3) from above the "Passing Bay".
Its alpine location means that this site experiences extreme weather conditions. These include frequent heavy rainfall events as well as snow and ice during winter. The average annual rainfall is in the range of 4 to 5 metres.
The steep slopes and fractured rock above the road, combined with freeze/thaw action, extreme rainfall, and seismic events mean that the road is subject to frequent rock fall. This poses a significant safety hazard to traffic and also leads to periodic road closures and ongoing maintenance requirements.
The spacing and orientation of rock bedding defects is quite variable throughout the site and there is potential for unfavourable orientation of defects to combine locally to produce unstable zones in new rock cuttings.
There are also a number of shear zones in the rock. Intersection of several of these formed the basal failure planes of a rockslide initiated at the "Passing Bay" in the 1994 earthquake.
Additionally there are two steeply dipping fault zones 1-2m thick in the rock mass at Starvation Point. This sheared rock is highly weathered which significantly reduces the strength of the rock mass in this area.
Candy's Bend comprises a narrow ridge of greywacke. However, from Candy's Bend to just past the northern end of Candy's bridge the road crosses an open bush covered slope. This is a continuous debris slope extending from the river below to the top of extensive scree deposits at the foot of Hills Peak ridge. Candy's creek follows a very steep slope down the bedrock/slope deposit interface.
Debris flows occur in Candy's creek at 5 to 10 year intervals and have damaged the existing bridge many times. In 1988 a debris flow destroyed the bridge deck and covered the bridge in debris up to 5 metres deep.

Options Considered

Earlier studies identified 5 broad options to improve this section of road. These included:

- Option 1, following the existing road with a short bridge at Candy's Creek
- Option 2, following the existing road with a long bridge at Candy's Creek.
- Option 3, two bridges and a sidling cut on the true left bank of the river opposite the existing road.
- Option 4, two bridges and a tunnel on the true left bank of the river.
- Option 5, a viaduct along the true left bank of the river.

Following extensive investigation and consultation, option 1 was identified as the preferred option to meet the project objectives and give an acceptable balance between risk and cost. This was because, by staying as close as possible to the existing alignment, environmental impact and construction cost were minimised allowing a fundable project to be developed while including project features to directly militate identified risks to an acceptable degree.

The Solution

The developed solution is shown in plan on figure 5. Key features include:

- Widening of the existing Candy's Creek Bridge downstream.
- An overhead chute to carry the waterfall and rock debris over the road at Reid's Falls.
- A cantilever half bridge structure between Reid's Falls and the Passing Bay.
- An overhead rock fall protection structure at the Passing Bay.
- A propped half bridge structure between the Passing Bay and Starvation Point.

It should be appreciated that this highway is a low speed environment with curve design speeds of between 50 and 65 km/hr. By comparison, the typically recommended speed environment for

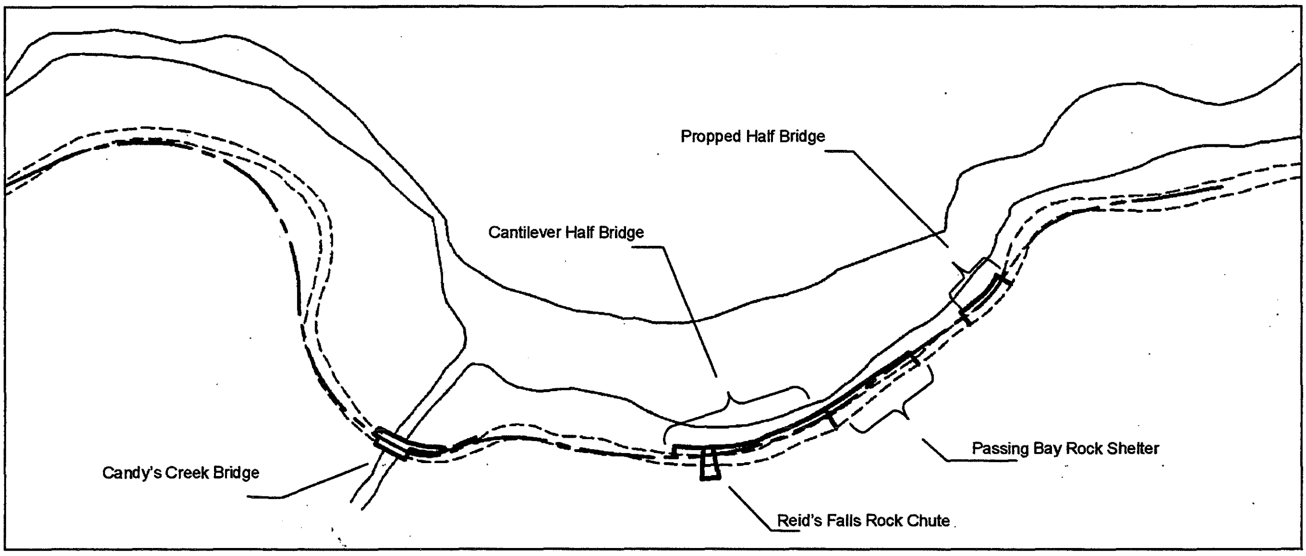

Figure 5: Layout plan of Candy's Bend widening.

mountainous terrain is 70km/hr with design speeds for individual curves of 60 to 65 km/hr. The lower than typical design speed environment is appropriate due to the nature of this site. In particular the topography "closes in" the site. This will be reinforced by the continuous guardrail and the two overhead rock shelters. The combination of these effects will lead to a lower expectation of the speed environment by drivers.

Iterative Design Process

Having determined that option 1 was preferred it was then subjected to an intensive iterative design process to optimise the selection of the alignment. This was essential to fully integrate potentially conflicting requirements while recognising the extreme constraints of the topography. For example a geometric design which resolved an issue at one area by a small movement in or out of the hill could create a more significant problem by requiring a similar or larger magnitude movement elsewhere.

In simple terms, a trade-off was required between the cost of structural widening and the risk, cost and environmental impact of significant cuts into the hillside.

The key to understanding the various issues and integrating them fully into the final design concept was to understand the site in three dimensions. This understanding was achieved by using detailed 3-Delectronic modelling and geometric design in MOSS combined with conceptual structural design and a continuously updated cost plan. The iterative cycle was repeated about a dozen times to refine option 1. Further understanding of the site was also gained by plotting important features onto topographical plans. All plotting was to the same scale and on the same base topographical plans. In this way quite different facets of the problem could be integrated into the design solution. Examples include:

- Mapping of geological defects;
- Mapping of sources and paths of rock fall; and
- Development of a risk plan for the site which defined 12 separate areas giving a visual representation of original and residual risk. This was important, as it was not economic to militate against all risks, such as rock fall, at all areas of this site.

The iterative process defined the preferred solution in considerable detail and largely fixed the road geometry. Subsequent detailed design efforts largely concentrated on design of the structures and slope stabilisation measures.

The Structures

Site-specific seismic studies were undertaken as part of the design of the Otira viaduct immediately uphill of Candy's Bend. Interpretation and application of those studies to the Candy's Bend to Starvation Point Project led to an equivalent static force for design of 0.7g. This is 40% higher than the maximum value normally used as a result of the seismic risk assessment. Concrete and steel were both considered for all structures but concrete was preferred because concrete sections offered more robust solutions less susceptible to damage from rock fall and debris flow impact

The Candy's Creek Bridge crosses a moderately steep slope (30°) comprised of alluvial materials deposited by old landslide events. However the existing abutments have performed satisfactorily during two recent earthquakes and many debris flows. It was resolved to re-use these and widen the bridge downstream to avoid constricting the channel further as would occur with widening upstream.

Bored piles were selected and extend 12 metres into the bouldery gravels. These are deep enough to found below scour depths and provide some measure of resistance to deformation in a large earthquake. However, the proximity of the piles to the steep slope below the road and gravelly nature of the slope material meant that ground anchors are also required to resist seismic loads on the structure.

This was one of the easier structures from a constructability perspective as work could proceed off the line of the existing road.

Analysis of the defects in rock below the road bench indicated the potential for defects to combine giving stepped planar or wedge failure if excessive loads were applied to the outer edge of the rock bench. Accordingly piled support was required with pile penetration of 15 metres. The selected final design was four 190mm diameter micro piles per transverse beam. While larger piles were considered, this part of the site has very restricted access and thus piling rig size became a limiting factor. The top 3 metres of these piles were cased to ensure load transfer to the rock at a lower level.

Assessment of rock fall risk in the zone of this half bridge indicated the risk of damage to the bridge deck was comparatively small as most rock was small in diameter and also would most likely first impact on the road bench rather than on the structure. While damage due to rock fall is possible it was considered appropriate to accept the risk and repair the bridge should damage occur.

Stressed rock anchors feature in two aspects of this design. Firstly the rock slopes below the prop locations were reinforced to ensure stability. Secondly, lateral seismic restraint was provided at deck level by 12-metre long anchors fixed to the transverse beams.

Design investigations discovered an old debris flow gully above this bridge. This gully has not been active for a number of years and is currently stable. While there is a high probability that this gully will become active again in the next 10 years a probability based economic assessment indicated that additional protection measures (such as overhead structures) could not be justified.

Passing Bay Rock Shelter

The section of hillside adjacent to the existing passing bay is an open expanse of rock left exposed after a significant block of material (about 7000m^3) was dislodged during the 1994 earthquake event. This slope is quite extensive and the countryside above provides little natural confinement of rock fall that can be initiated considerable distances up the slope above the highway. Thus this section of road suffers the highest frequency of rock fall. The main source of rock fall at this site is debris flows of colluvium (comprising sandy gravel with some boulders) from a debris chute approximately 70 metres above the road. This material has a maximum boulder size of about 1 metre although the predominant size is much less.

The solution to the rock fall safety issue was to provide a 60-metre overhead protection structure along the base of this slope. Rock fall impact design loading is not codified and was derived from a combination of analysis and judgement. The outcome was an impact load based on a 2.5 tonne boulder bouncing down the slope. Load combinations also had to be derived. The design combinations allowed for the as built roof cushion with a further 2 metre thick layer (assumed built up over time) combined with the rock impact loads and Earthquake loads. The other important load combination was a build up of loose gravel to an angle of 37° above the as built roof cushion. No dynamic rock fall load or earthquake load was combined with this maximum gravity load, as the likelihood was not considered

sufficiently high. However, the implication of the load combination assumptions is that maintenance will be required to limit the gradual build up of rock on the roof to 2 metres above the as built level to limit the acceptable risk, and that rock will be removed immediately following a major rock fall event. The vertical loads to be resisted by the structure are very significant. Hence it was essential that the geometric design moved the road back into the hillside at this location to ensure ability to transfer the loads to the rock bench. Also a 1.2 metre layer of polystyrene was placed above the structure roof. This was to provide load spread capacity to the structure below while minimising the weight supported by the structure. A 1.0 metre energy absorbing gravel cushion is placed above the polystyrene.
End walls were required to contain rock build up and prevent overspill from the chute ends.
Seismic restraint is supplied at roof level by three 15-metre long rock anchors at each frame.

Reid's Falls Rock Chute

The topography of the hills above the road at Reid's Falls provides natural confinement of the rock debris originating in this area. There is a basin approximately 20m above the existing road, which collects debris until an extreme rainfall event flushes the basin and deposits as much as 500 m^3 of material on the road below. This poses both a safety hazard and an ongoing maintenance problem. The solution selected at this site was to provide a chute to carry the waterfall and any rock fall debris over the road and into the river below. The general arrangement is shown on figure 6.

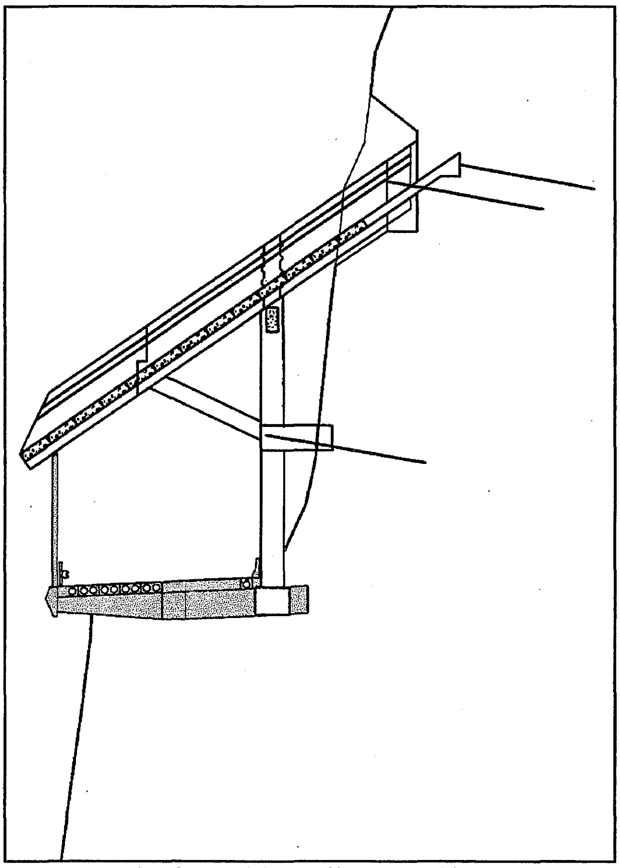

Fig 6 – Reid's Falls Rock Chute

This is a very constrained part of the site and this structure overlaps the cantilever half bridge. It was not feasible to move the road into the hillside at this location due to the near vertical faces above the road. However it was essential to carry design loads to the inside face of the rock bench. This dictated

the design solution shown which effectively cantilevers the chute over the vertical column and carries the load down to the rock bench via spread footings.
Seismic restraint and static load stability is provided by rock anchors at the upper end of the rock chute.
Railway irons were cast into the chute floor to protect the concrete against abrasion from the continuous passage of rock.

Conclusion

The Candy's Bend to Starvation Point project traverses an extremely complex and difficult alpine site. The challenge of this project has been met by a design process that fully integrated environmental, cost, constructability, and engineering issues from conceptual through detailed design phases. The solution incorporates a number of unique concrete structures that are outlined in some detail in this paper. Design assumptions have been consistently validated as the works progressed.
The sheer complexity and diversity of this site have necessitated providing only a brief overview of the design. The design incorporates considerable additional risk assessment, geotechnical investigation and rock slope design, structural analysis, and environmental assessment than can be described in the space available here.

Case Study Five: Arthur's Pass Rock Fall Maintenance Strategy

Introduction

On the West Coast side of the Candy's Bend work on SH73, there are 10 rock fall sites characterised by long debris slides which were mobilised by significant earthquakes in the 1980's. These slides are now more easily mobilised by storms and smaller earthquakes causing debris movement, which has become a road maintenance problem. Using the available maintenance cost data, it is possible to get a picture of the frequency of the problem.

Risk Assessment

Much of the data came from the adjacent Candy's Bend project, as the same risk assessment is appropriate. In addition, the frequency of occurrence and evaluation of the consequences could be further estimated from anecdotal evidence from suppliers, stakeholders and neighbours, contractor's response records and from records related to affected people such as insurance, crash and hospital records. From this data an estimate could be made of the likelihood and consequences of events under current management regimes for each of the sites.
As with the adjacent projects, acceptable risk criteria were adopted from nuclear industry standards to provide target achievement levels. At these achievement levels, the likeliest consequences were of crashes due to debris on the road rather than of crashes as a result of falling debris. The overall level of exposure is very low because of the size of rock required to be mobilised to be a serious risk and the infrequency of vehicles passing.

Risk Mitigation

As the achievable target was to reduce the risk of vehicles striking debris on the road, the methodologies to be applied were targeted at techniques to reduce the exposure of the travelling public to such risks. Techniques fell into three separate areas:

- Changes to maintenance techniques to reduce the amount of time the debris was allowed to remain on the road. This included mobilisation of plant during storm events, increased inspection during and after storm events and rapid response to seismic events;
- Debris restraint methods such as catch fences or gabion walls to limit the material able to reach the road; and
- Introducing better protection methods such as debris chutes to ensure that debris had alternative paths.

Conclusion

Each of the sites was evaluated for the best technique or combination of techniques to give the most acceptable method to reach the achievement level required. From the evaluation, a credible maintenance strategy for SH73 giving acceptable level of service was developed and documented.

Case Study Six: Stockman's Hill Slips

The Geology

At Stockman's Hill, State Highway (SH) 3 climbs up and follows along a natural ridge before dropping down the far end into the Awakino River valley at Mahoenui. The ridge consists of a silty clay soil mass, from two to twelve metres thick, sitting on impermeable bedrock made up of a mixture of siltstone and mudstone. All the hillsides in the immediate area show evidence of instability and areas along Stockman's Hill have previously been planted where earth movements have occurred.

The Events

Two separate and consecutive major events were the causes of the two major failures in 1998. In July of that year, two weeks of intense rainfall triggered a 100-year flood event across the Waikato catchments. The northernmost of the two major slips occurred catastrophically in this period. In October, rain every day of the month was measured as the wettest October on record and one of the wettest months ever recorded. The southern slip was triggered progressively through the month and into early November and progressed towards the State highway in increments.

The Failures

The failures were all characterised by the amount of water in the soil mass. The impermeability of the bedrock meant heightened pore pressures at the soil/rock interface and the degree of saturation lead to increased weight on a lubricated slope. Some of the smaller failures were stabilised by draining the interface at a number of points, and then reinstating the top of the slope adjacent to the road.

The northern major failure occurred in a minor, upper catchment separated from the rest of the main ridge by spur ridges on either side. The base of the slope, after the failure, was a vertical scarp face and the remainder of the toe material was deposited in the downstream channel for some distance. It would appear that the water flowing out of the base of the slope scoured out the toe buttressing, allowing the whole slope to slide as a single mass. A section of SH3 was carried six metres down the slope as it gave way. Only the narrowing of the catchment at the toe compressing the sliding material prevented it sliding any further.

The southern major failure started as a single, massive, circular slope failure. Initially the top scarp was some distance from SH3, but the top scarp continued to retreat towards the road as the over-steepened upper slope continued to slip as it tried to reach an equilibrium. By the time that the weather improved and the slope started to reach that equilibrium, SH3 had been reduced to an insecure, single lane, especially as the slope on the other side of the road also had signs of long-term stability problems.

Alternatives

Alternative routes to realign SH3 around the problem area were considered. There was no clear alternative route that would be an improvement over the existing one because they would be longer, expensive, poorer in alignment, rugged and through country with similar risks. They would also require an unacceptably long lead-in time to resolve a final alignment.

Risk Assessment

Only the northern failure closed the highway, but in both cases of the major failures, and to a degree with each of the others, the immediate reinstatement to re-establish the route could only be considered to have marginal stability. The material that these sections were either sitting on or against would be of uncertain stability in a wet condition, so that it was assessed that a solution needed to be in place before the next winter to minimise future risk. There was real concern about the continued stability of the northern failure through the October event. Additional drainage was established and the highway was given additional monitoring to ensure swift response to any indication of further movement.

Time was the governing factor. The contractor could not be expected to work around the traffic and have the work completed by the next winter. There was a local authority road that bypassed the area, although significantly longer and of poor alignment and width, that the road users were prepared to use for an agreed period. This road was upgraded by Transit and sealed by the local authority to act as the diversion route. It should be noted that this route had been flooded and therefore closed at times during the major events; hence while it had been used as a detour it had not been reliable.

In considering the long-term stability, for each of the major slips, and for one of the smaller failures, structures keyed into the underlying bedrock would be required for acceptable residual risk levels at the key points.

Final Strategy

Once the decision had been made that SH3 was to remain on its current alignment and that the traffic would be diverted to give certainty of timing, work focussed on finalising the design and getting the detour route up to a suitable standard. The second failure then ended up piggybacking on the work already done and the contract was being tendered as the final design was proceeding for the second wall.

The Consultant chose a mechanically stabilised earth wall as the means of providing the structural support at the two main failures. While such a design has been successfully used before in New Zealand, no previous structure has been to the height and overall scale of the walls proposed on this project. In addition, at the southern of the two, the instabilities on both sides of the road required that for half the length of the work the walls were formed on both sides of the road, with the mesh reinforcing overlapped and tied under the centre of the road. Lowering the vertical crest to the north, giving an improved vertical profile, reduced the height of the northern wall. The wall was retreated from the failure surface by amending the horizontal alignment and building a buttressed, engineered fill on its southern side using all the excavated material.

The smaller failures were re-established by installing proper drainage and proper backfilling using toe support methods such as gabions and planting. The remaining wall was a simple tieback arrangement, founded using steel H-piles.

Residual Risk

Between the works was over a kilometre of SH3 on the ridge in its original condition. This section of the highway over Stockman's Hill is considered to be the site for the greatest area of residual risk following completion of the works.

The residual risk was lowered as much as possible by an appropriate level of tree planting along both sides of the ridge in conjunction with the reinstatement work. However, the entire scheme could not guarantee total stability long-term, and even at the end of the project there were signs of other instabilities adjacent to the road. In addition to ongoing planting, a monitoring programme is in place to ensure that problems are identified as early as possible and actioned before there is significant risk to SH3. Changes to funding policies allow more focus to be given to prevention rather than cure.

For any further failures, the options have been explored and methods of reinstatement are understood so that response times in future should be reduced.

Case Study Seven: Innovative Reinstatement Techniques

Waiwera Hill Slip

This site is 47 kilometres north of Auckland, where SH 1 passes through a coastal mountainous area. This narrow winding carriageway sits on a sidling cut into a moderate to highly weathered, thinly interbedded sandstone and mudstone of the Waitemata group. At the site the radius of the SH is approximately 60 metres, with a "W" section guard rail on the outside and above a five metre localised, near vertical face which then lessens into a debris slope with a slope ratio of 1.5 horizontal/one vertical, terminating at a house. Fretting of the near vertical face had removed the support to the guardrail and unchecked would have reduced the SH, which has a daily traffic volume of 13,500 vehicles per day, to one lane.

The solution therefore needed to restore the support of the guard railing, to prevent errant vehicles from breaking through it, remove the threat to loosing the southbound lane and be constructed in such a way so as to accommodate peak traffic flows. There is no practical alternative to this route until the ALPURT bypass project is completed.

The solution was a 38-metre tension hoop beam, supported on raked minipiles, wrapped around the out side of the curve, to support the guardrail. This hoop beam, which was constructed in very tight space constraints had the following advantages:

1 Traffic delays were minimised, allowing restoration of both lanes of traffic for peak flows, plus eliminating the need for placing of tie back anchors in the northbound lane.
2 The threat to losing the lane was removed by the ring beam supporting the granular portion of the upper formation.
3 The ring beam supplied the necessary lateral support to enable the W section guardrail to perform as designed if stuck by an errant vehicle.

The installation went smoothly and has proved to be a cost effective solution.

Woodhill Slip

State Highway 16 passes through Woodhill, which is 40 kilometres northwest of Auckland and has a daily traffic volume of 5,000 vehicles per day at this location. The site is on the edge of the flood plain of the Kaipara River, which is in a drowned valley. The 1.5 metres of fill, which forms the road formation, sits on alluvial material, consisting of loose sand, soft clay and peat to a depth of 15 metres. The site has a relatively high environmental speed, at the end of a moderate southbound curve. There is little warning of any uneven pavement surface and sudden downward movements of 100 millimetres have occurred. The prime reasons for repairing the slip is safety, in that eliminating the pavement irregularities, removes the threat that vehicles may loose control. Approximately $35,000 per year of asphaltic concrete top up repairs have been necessary to maintain safety, however the extra weight appears to have been accelerating the instability.

Drainage solutions were not feasible due high ground water levels and the frequency of flooding. Toe loading and conventional retaining systems were considered and discarded. The chosen option to use the soil cement columns, which will increase the shear resistance of the insitu material, allow the stabilisation work to be carried out clear of traffic lanes and a high-pressure gas line. This stabilisation will also enable SH16 to be widened and is clear of the nearby railway embankment.

Conclusion

Risk assessment is a growing area of expertise. While a large proportion of the emphasis is targeted to applying risk assessment techniques to new construction, because of the geological nature of New Zealand it is also very necessary to consider the technique in optimising decision-making both in anticipation and in responses to events. There are a number of research projects underway to develop approaches that the general practitioner can apply in various risk situations.

In the case studies above, the overriding theme is that there is a similarity in the approaches that are applied to retrofitting or managing the road. These can be summarised as:

1. Set out the objectives that it is intended to satisfy;
2. Consider each of the risk events that apply to the situation under evaluation;
3. Evaluate the likelihood of each of the risk events identified;
4. Consider the consequences of each of the events identified;
5. Consider the likelihood and consequences of the events together to develop a set of risk acceptance criteria to evaluate and optimise the outcomes;
6. Develop a set of treatment options and consider the extent to which they mitigate the events; and
7. Select the optimum solution based on the acceptance, cost and benefit factors appropriate to the decision, and leaving acceptable residual risk.

Acknowledgements

I wish to acknowledge the following people and organisations for assistance in producing this paper:

- Garry Butler of Transit for the information provided on the Risk Management Process;
- Terry Brown of Transit and Ian Billings of Beca Carter Hollings and Ferner Ltd (BCHF) for information provided relating to the Auckland Harbour Bridge retrofit;
- Ian Billings of BCHF for information provided relating to the Thorndon Overbridge retrofit;
- Richard Holyoake of BCHF and David Bates of Transit for information provided relating to the Otira Viaduct;
- Melvyn Maylin of Opus International Consultants Ltd and David Bates of Transit for information provided relating to the Candy's Bend upgrading;
- David Bates of Transit for information provided relating to the Arthur's Pass rock fall maintenance strategy;
- Ian Cox of Transit for information provided relating to the Stockman's Hill reinstatement; and
- Philip Sutton and Terry Boyle of Transit for information provided relating to the innovative retrofit techniques used in Auckland.

Quantitative Risk Assessment Methods for Determining Slope Instability Risk

PJ Horrey

Golder Associates (NZ) Ltd., Christchurch, New Zealand

GG Grocott

Golder Associates (NZ) Ltd., Christchurch, New Zealand

Abstract

Estimation of the risk posed by slope instability is a common requirement for projects located in hazardous terrain. Typically geotechnical practitioners rely heavily on experience-based judgement and provide qualitative assessments of risk.

The use of quantitative risk assessment (QRA) for evaluating slope instability risk provides a systematic methodology to understanding slope processes and the consequences of failure. One of the main benefits of QRA methods is that the practitioner is required to consider all cause and effect relationships, which is not always the case when qualitative approaches are used which focus more on the probability of failure rather than the consequences should failure occur. QRA provides decision-makers with a relatively simple but powerful tool for numerically expressing risk, which may then be compared with risk acceptability guidelines.

By way of example, QRA techniques have been used to assess the risk posed by rockfall to road users on SH73 between Springfield to Arthur's Pass at the locality known as Paddy's Slip. From a consideration of the site geology, maintenance records, accident history, road geometry and traffic volume, it has been possible to evaluate the potential risk to motorists, and to compare this to risk acceptability guidelines suggested in the literature. A range of physical works remedial options that could be implemented to both lower the rockfall risk and reduce road maintenance costs has been considered.

A simple economic analysis has been performed by comparing the cost of each remedial option and its likely effectiveness in reducing rockfall activity against the cost of maintaining the present road maintenance programme. The benefit cost ratio has been determined for each remedial option, in order to identify the cost optimal maintenance programme. At Paddy's Slip it was found that remedial works are likely to result in an overall cost saving over the present maintenance programme.

QRA provides an additional analytical tool to assist decision makers on geotechnical projects. Like all quantitative techniques applied in geotechnical engineering, its application must be tempered by precedent and experienced judgement. It recognised that some sites are not amenable to the use of QRA techniques.

Background to Quantitative Risk Assessment

Traditionally geotechnical practitioners have relied on experience to judge the adequacy of the stability of a slope to allow development, complemented by the use of numerical techniques such as the factor of safety concept to provide reassurance. New techniques have arisen out of areas such as the nuclear and hazardous waste industries and dam safety evaluation that can be applied in quantifying the uncertainty associated with the stability of slopes. These techniques use subjective judgement and/or numerical methods to assist in quantifying the risks inherent in any system such as a slope, and are collectively referred to as Quantitative Risk Assessment (QRA). QRA consists of two components, namely the assessment of the probability of slope failure and identification of the consequences of failure.

The use of QRA is not intended to replace those established and accepted procedures. Rather, it offers the possibility of expressing numerically the risk attached to any particular slope. It can be used to compare the numerical value of the assessed risk against risk acceptance criteria, and therefore has the potential to be used within the framework of international standards such as the recently published AS/NZS 4360: 1999 "Risk Management".

Although QRA concepts are well established, its use to evaluate slope stability risk is very much an emerging concept overseas and still in its infancy in New Zealand.

Definitions

Risk assessment in general and landslide risk assessment in particular has resulted in many different definitions by a range of different authors, resulting in confusion, misinterpretation and misuse of terminology. "Risk" means different things to different people.

The definitions below come from a recent publication (Fell & Hartford, 1997) and have been promulgated for use with landslide QRA and appear to be gaining wider acceptance.

Hazard: a condition with the potential for causing an undesirable consequence. Descriptions of landslide hazard, particularly for zoning purposes, should include the volume or area of the landslide, and the probability of its occurrence. There may also be value in describing the velocity, and the differential velocity of the landslide (Varnes, 1984; Fell, 1994; United Nations, 1991).

Probability: the likelihood of a specific outcome, measured by the ratio of specific outcomes to the total number of possible outcomes. Probability is expressed as a number between 0 and 1, with 0 indicating an impossible outcome and 1 indicating an outcome is certain (Standards Australia and Standards New Zealand, 1995).

Risk: a measure of the probability and severity of an adverse effect to health, property or the environment (Canadian Standards Association 1991).

Vulnerability: the degree of loss to a given element or set of elements within the area of influence affected by the landslide(s). It is expressed on a scale of 0 (no damage) to 1 (total loss) (Varnes, 1984; Fell, 1994).

For a property, the loss will be the value of the property; for persons, it will be the probability that a particular life (the element at risk) will be lost, given the person(s) affected by the landslide.

The Quantitative Risk Assessment Process

The QRA process includes risk analysis, risk assessment and risk management, as illustrated by the flow chart in Figure 1, which is based on work presented by Fell & Hartford (1997) and the IUGS Working Group on Landslides (1997).

Risk Analysis

Risk analysis involves identification of the landslide hazard and assessment of probability of failure P(F), as well as consideration of the consequences of landsliding if persons and/or property are impacted by failure. An assessment of the types, characteristics and probability or frequency of landslides in a given study area is carried out. If the frequency cannot be determined directly from field evidence, or where engineered slopes are involved, analytical techniques such as first order second moment extrapolation (Christian, 1996) the point estimate method (Harr, 1987, Mostyn and Li, 1993) or Monte Carlo simulation are required to evaluate the probability of failure.

Figure 1: Quantitative Risk Assessment (based on Fell & Hartford 1997; IUGS, 1997)

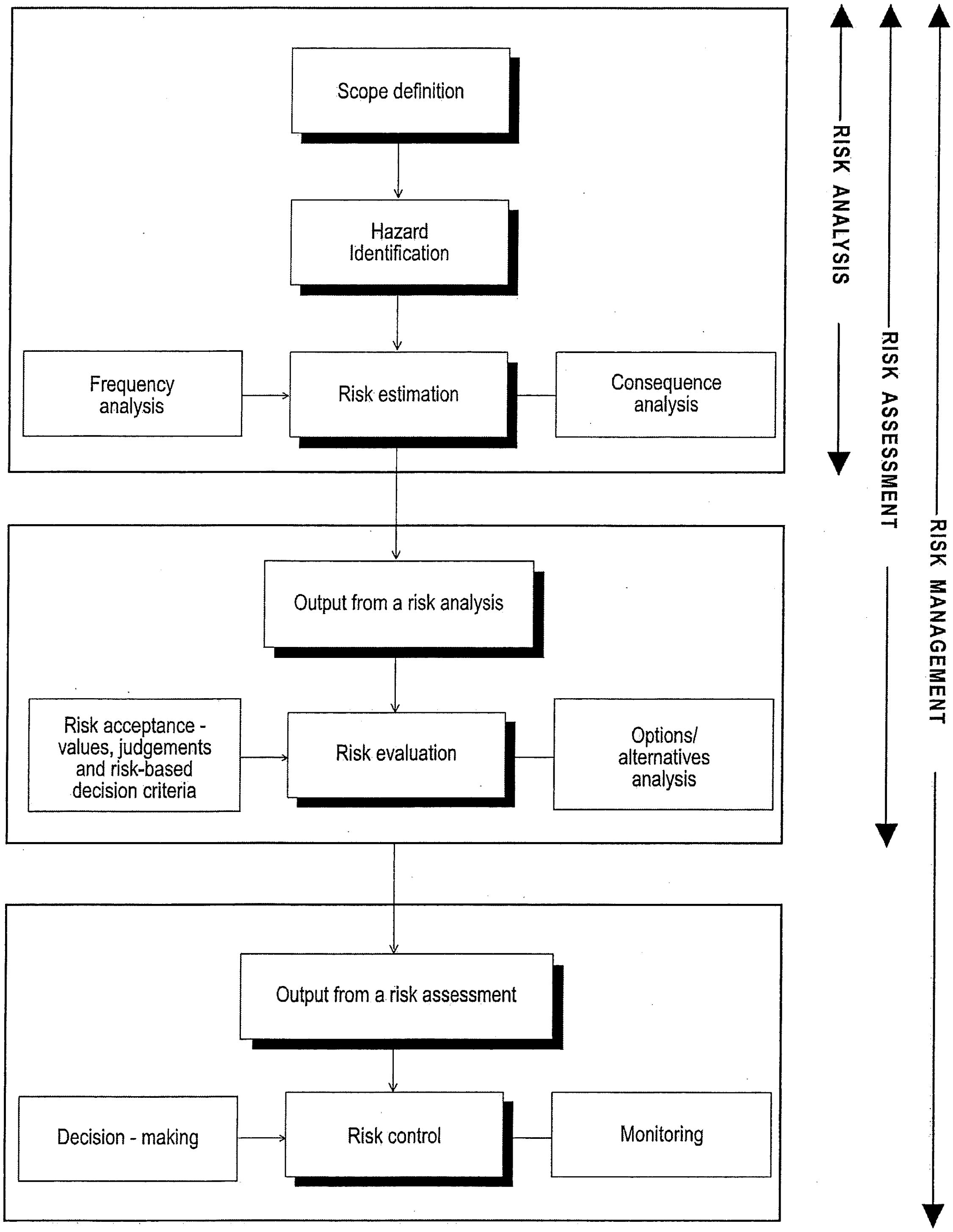

If analytical techniques are used, the expected variation in input parameters, both spatially and over time must be known or estimated.

Consequence analysis is then carried out to establish the elements at risk from failure and to determine their vulnerability. The elements at risk are relatively easy to identify in terms of people and property potentially exposed to the landslide hazard.

Assessment of the probability of a consequence occurring to the elements at risk is much more difficult to quantify and requires consideration of:

- where will the landslide occur and what will be the probability of the element at risk being impacted by the failure, termed the spatial probability, P(S)
- what is the probability of the element at risk being present at the time of impact, termed the temporal impact, P(T). Normally this conditional probability would not apply to property due to it being fixed in space, other than to moving vehicles on transportation routes, where the proportion of time the vehicle is exposed to the hazard needs to be considered.
- what is the probability of loss of life, or what proportion of the property value will be damaged, given impact by the failure. This is termed Vulnerability, V.

Each of the above components of risk P(S), P(T), and V are conditional probabilities expressed as values from 0 to 1. Once these are quantified, allowance can be made for the location of an element at risk in relation to the landslide and the length of time of exposure to the hazard. The risk of a particular consequence occurring to a specific element at risk due to slope instability may be expressed numerically as:

$$\text{Risk} = P(F) \times P(S) \times P(T) \times V.$$

Risk Assessment

Risk assessment is risk analysis considered together with risk evaluation (Figure 1). Risk evaluation requires the calculated risk value to be compared against risk acceptance criteria for the slope to determine the importance of the numerical value. This could include comparison with levels of acceptable risk for other activities, or the economic, social and environmental consequences were failure to occur. Typically, the decision as to whether to accept the calculated risk is made by the client, owner or regulators, rather than their technical advisers, whose role is primarily to determine the risk.

Risk Management

Risk management, is risk analysis and risk assessment considered together with risk control. Risk control involves the evaluation of options for risk treatment including risk mitigation, risk acceptance, and risk avoidance.

Uncertainty

One of the main limitations of QRA analysis is that almost inevitably there is some uncertainty attached to the various input parameters, particularly in the assessment of the probability or frequency of landsliding.

Parameter uncertainty can be accounted for in a risk analysis using Monte Carlo simulation. Monte Carlo simulation involves repeating the risk estimation many times, each time using input values selected from their respective probability distributions. As the analysis is repeated the outcomes themselves build up probability distributions. This technique allows the uncertainty in the calculated risk to be considered during the risk estimation stage of the QRA. Monte Carlo simulation can be readily carried out using commercially available software.

Case Study – SH73, Paddy's Bend

Introduction

The following case study was carried out during 1998-99 as part of a Transfund New Zealand funded study (Riddolls & Grocott Ltd, 1998,1999) to evaluate the usefulness of a QRA approach to the management of rockfall hazard.

The Problem

In 1982, construction commenced on upgrading a 2.2 km long section of SH73 immediately west of TranzRail's Midland Railway bridge across the Waimakariri River (see Figures 2, 3, and 4). The work involved easing the sharpest corners and widening sections of road located on failed retaining walls, by excavating a minimal distance into the slope. Soon after construction commenced at the western end, reactivation of an existing rock slide known locally as "Paddy's Slip" occurred, temporarily closing the highway (Paterson 1982a). Further widening was postponed indefinitely, although local widening was later carried out near the eastern (Midland bridge) end of the highway.

Figure 2: Site location plan

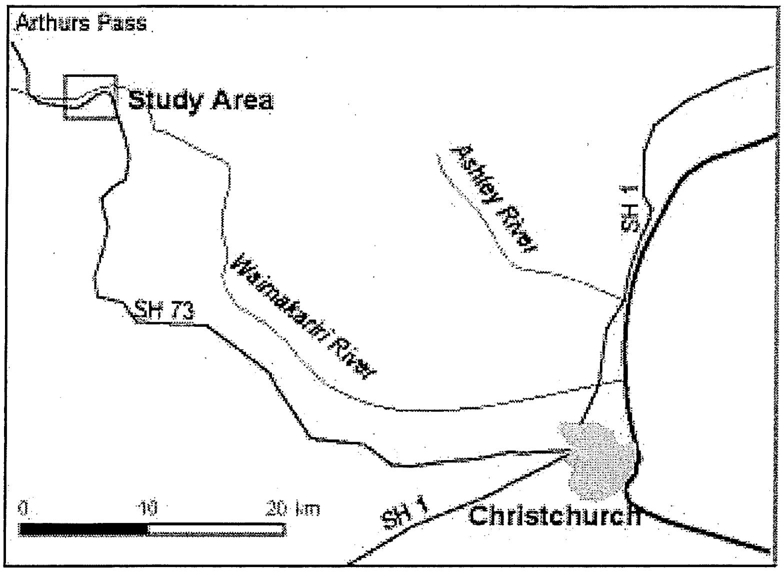

Figure 3. Air photograph of SH 73, showing Paddy's Slip

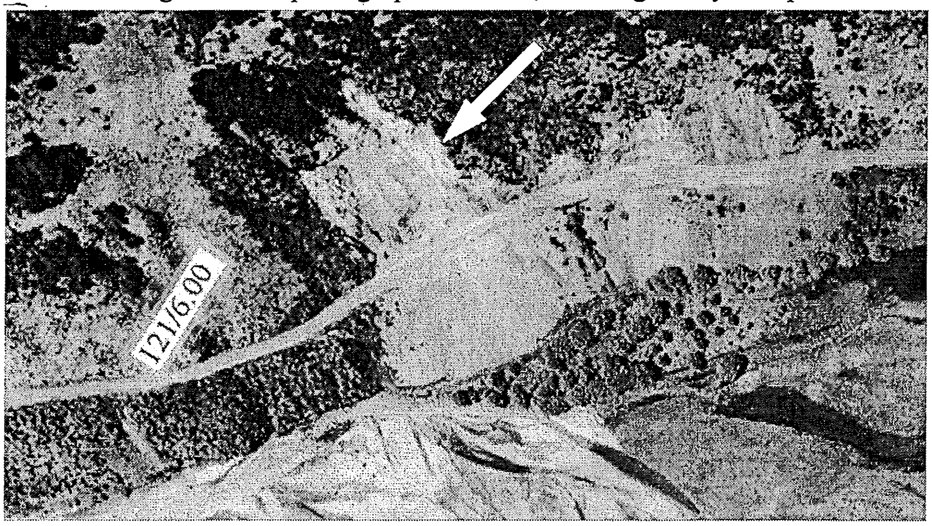

Figure 4: View of instability at Paddy's Slip from SH 73

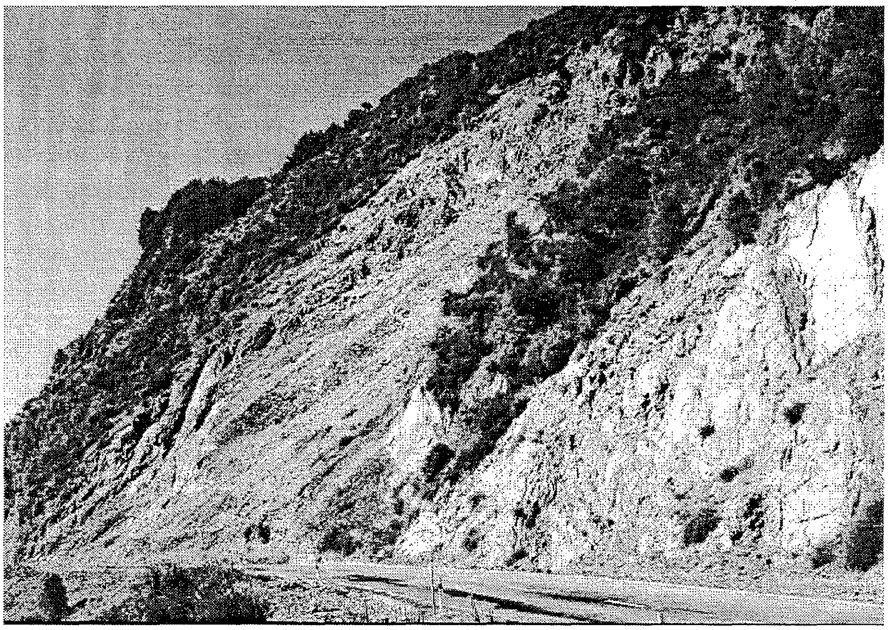

Prior to 1982, slope instability consisted of minor rockfalls, particularly during winter, from steep cut batters mainly near the eastern end of this section of highway, while at the western end, subsidence of the retained outer edge of the highway and rockfalls from slopes above the highway occurred. In 1982 and 1983, several significant rock debris slides closed this stretch of highway, one of which occurred at Paddy's Slip (Paterson 1982a and b).

Subsequent to 1982, rockfalls have been a continuing problem at Paddy's Slip where a large area of exposed bedrock is now contributing a significant number of rockfalls on to the road. Small rockfalls occur almost on a daily basis, and much of this material ultimately ends up on the road in the form of detritus. Large falls of discrete blocks also occur infrequently, one such being in 1997 when "several blocks up to 0.6 m in size" failed (Montgomery Watson 1997b). Rockfall activity increases during severe north west rainfall activity, and during the winter freeze-thaw.

The site was affected by the 18 June 1994 Arthur's Pass and 29 May 1995 Mount White earthquakes (Paterson & Coates Associates 1995) resulting in the loosening and dilation of rock blocks in cut batters, and the dislodgment of blocks onto the road. Also, rockfalls occurred from high rock bluffs above the site and open cracks were noted, indicating a possible long term hazard. The frequency and size of rockfalls have increased since the 1994 and 1995 earthquakes.

In addition to rockfall, rock slides have also occurred in response to high rainfall events. These comprise moderate to large volumes of debris up to 100 m^3, though their occurrence is infrequent.

The following measures have been carried out by Transit New Zealand in order to mitigate adverse effects on road users:

- the introduction of a "no stopping" zone
- scaling (using hand, wire rope technology and helicopter water sluicing techniques) of cut batters
- construction of a low (500 mm high) rock fill bund on the inside of the road
- regular mechanical sweeping of the road surface to remove detritus and rock blocks
- on demand call outs for the clearance of large rockfalls and slips

Remedial measures have also included consideration of the construction of a rockfall protection fence (Paterson & Coates Associates 1997), but this has not been implemented at this time.

Risk Analysis

In order to determine the risk currently faced by road users driving through the site it was first necessary to estimate the frequency of rockfall. This was done through interviews with maintenance staff, vehicle recovery operators, police, and mapping of rockfall impact marks on the carriageway seal. The results indicate over 2000 individual rockfall events impinge upon the carriageway each year, although many of these are very minor in nature. Four modes of rockfall were considered based solely on the size of the falling rocks. Estimates of the relative frequency of occurrence of each failure mode were made on the basis of maintenance records and visual estimates of rock sizes in the stockpiles of detritus adjacent to the site.

The following consequences of rockfall were considered:

- Detritus clearance
- Service disruption (ie temporary road closure)
- Fatal accident
- Serious accident
- Minor accident
- Non-injury accident

The annual risks for detritus clearance and service disruption were back calculated from maintenance records.

Formal accident records for the site do not indicate any fatal, serious or minor accidents directly attributable to rockfall. Several deaths have however occurred in the immediate vicinity, and rockfall may have been a contributing factor. Non-injury accidents are common, and include broken headlights, windscreens, sumps and damaged tyres. For each of the four accident classes the risk has been estimated as follows:

Risk of accident = P(F) x P(S) x P(T) x V

where:

P(F) is the expected frequency of rockfall as determined above

P(S) is spatial probability that debris encroaches onto carriageway. The failure frequency has been determined from records of rockfall onto the carriageway, and as such rocks which miss the carriageway are not counted. In this case, therefore, P(S) is 1.0.

P(T) is the temporal probability of impact, which has two components. Firstly, a vehicle has a certain probability of being on a section of road where it cannot stop in time to avoid fallen debris. This is a function of traffic volume, vehicle speed and site distances approaching Paddy's Slip. Secondly, a vehicle has a certain probability of being hit by a falling rock. This is a function of the proportion of time vehicles are present directly below the slip, which requires a consideration of traffic volume, average vehicle length and vehicle speed. These probabilities were calculated using an average annual daily traffic (AADT) value factored up to account for the projected increase in traffic over 25 years.

V is the vulnerability of the vehicle occupant in the event of collision. This varies with the severity of accident, and has been assessed subjectively, with the vulnerability in the case of a non-injury accident being several orders of magnitude more than fatal accidents.

The average expected risks for each accident class over the next 25 years , incorporating projected traffic increases, and assuming continuation of the present programme of detritus clearance, are presented in Table 1.

Table 1. Summary of Theoretical Vehicle Accident Risks (projected average over the next 25 years)

Accident class	Annual Risk
C3 Fatal	0.027 (2.7 per 100 years)
C4 Serious	0.048 (4.8 per 100 years)
C5 Minor	0.48 (48 per 100 years)
C6 Non-injury	52 (5200 per 100 years)

Alternative Maintenance Options

A range of alternative maintenance activities for mitigation of slope failure risk have been identified. One or more activities have been combined to form individual maintenance programmes (Table 2).

Table 2. Summary of alternative slope failure maintenance activities and programmes.

Maintenance Programme	Maintenance Activities									
	Detritus and Rockfall clearance	Monitoring	Scaling	Rock bolting	Gabion Wall Rockfall catch fence	Wire mesh rock fall catch fence	Wire mesh netting protection	Road realignment	Earthworks	Concrete rock fall shed
M0	●									
M1		●								
M2						●				
M3			●	●	●					
M4			●	●			●			
M5										●

A brief description of each maintenance activity is provided below:

i) Rockfall detritus clearance.

This activity represents the existing detritus clearing and rockfall and slip call outs, and incorporates the existing 500 mm high rock fill bund on the inside of the road . This activity represents the unmitigated (ie "do minimum") maintenance programme.

ii) Monitoring

This is a reactive management approach, and has been included to allow additional comparison of the various range of maintenance strategies. This involves the monitoring of slope instability by means of video and image sensing techniques. Such a scheme would entail mounting of a video camera on a pole to cover the site distance with image sensing to detect items greater than 150 mm diameter that are stationary on the road, as a warning to road users. The system would also be linked to Transit New Zealand's network maintenance contractor's base as a signal to clear the road.

iii) Scaling

This involves the removal of loose masses of rock from the cut road batter by either hand or mechanical means. Scaling is generally carried out in combination with other activities (Table 2).

iv) Rock bolting

This involves the mechanical reinforcement of rock by means of drilled and fastened rock bolts into a rock face.

v) Gabion wall rockfall catch fence

This involves the construction of a 2 m high by 1 m wide gabion rock wall catch fence for protection against rockfall. Rockfall computer simulations suggest that it will be successful in blocking most possible rockfall events. Such a structure would have only limited capacity to reduce the effects of a rock slide. The gabion wall would be required to be constructed a short distance out from the existing toe of the slope, requiring reconstruction of the carriageway as part of this option.

vi) Wire mesh (netting) protection

This option involves the fastening and placement of double twist hexagonal wire mesh over a rock face to prevent rocks becoming dislodged from the face.

vii) Wire mesh rockfall catch fence

This involves the construction of a vertical rockfall wire mesh catch fence incorporating horizontal steel cables for reinforcement, as a defence against rockfall and rock roll. This structure is sited at the toe of the cut slope, and is limited in the size of rockfall which it is capable of impeding, generally considered to be of the order of 2500 kilojoules impact force. The results of rockfall computer simulations have been used to select a fence height of 3 m as being necessary for the successful blocking of most rockfalls. Such a structure would have only limited capacity to reduce the effects of a rock slide.

viii) Concrete rockfall shed

A reinforced concrete rockfall shed has been considered, similar to those regularly constructed in Europe and North America, and further west on SH 73 at Candy's Bend. This would be designed to mitigate the effects of all slope instability, including rockfall and rock slides.

Costs and effectiveness

The implementation and maintenance costs of each alternative maintenance programme were estimated, using Monte Carlo simulation to accommodate cost uncertainty. Ongoing maintenance costs have been discounted to net present value (NPV) over 25 years to allow comparison. The effectiveness (E) of each maintenance programme has been estimated and is expressed quantitatively in terms of the fractional reduction in each of the conditional probabilities that make up risk, i.e. P(F), P(S), P(T) and V from the unmitigated (baseline) case. The effectiveness of each maintenance activity is uncertain, and best expressed in terms of a probability distribution.

Cost-Optimal Solution

Continuation of the current programme of detritus clearance for the next 25 years has an associated overall cost which is made up of both maintenance costs and expected accident costs. Each alternative maintenance option has an implementation cost, and an associated benefit in terms of reduction of risk, and therefore the likely accident costs. The cost optimal maintenance programme is that which has the greatest benefit/cost (B/C) ratio compared to the existing programme of detritus clearance.

A spreadsheet numerical simulation was set up , and benefit/cost ratios were determined for each maintenance programme. A simple economic analysis was carried out, discounting benefits and costs of each alternative maintenance option to net present value over 25 years, and incorporating uncertainty in the various inputs by Monte Carlo simulation. The results were expressed as probability distributions of benefit/cost (see Figure 5). The results indicate maintenance programme M2 (wire mesh catch fence) to be cost optimal (B/C ratio around 13) when considered over 25 years.

Figure 5: B/C Ratios for each maintenance programme approximated to normal distributions

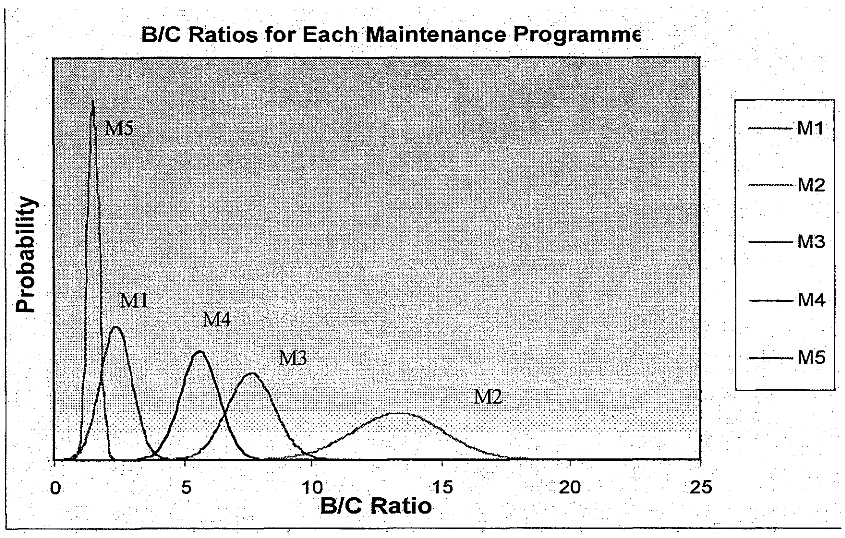

Risk acceptability

Levels of acceptable and tolerable risk are contentious, and require consultation and consensus within the wider community. However, the expected risk of a fatal accident at Paddy's Slip over the next 25 years (Table 1) is generally higher than most proposed guidelines on societal risk acceptability. Implementation of maintenance programme M2 is expected to reduce the annual risk of a fatal accident to around 4×10^{-3} . Whilst this is still higher than some authors advocate (Australian Geotechnical Society, 2000), it does falls within the "accepted" level proposed by Whitman, (1984). Implementation of M2 will result in a demonstrable reduction in the risk of a fatal accident at the site due to rockfall.

Conclusion

Quantitative risk assessment of rockfall risk at Paddy's Slip suggests that construction of a fully engineered rockfall catch fence at the toe of the slope will prove more cost effective in the long run compared to the existing programme of reactive detritus clearance. The works can also be justified on the grounds of risk reduction.

As with any analytical procedure, there are limitations associated with quantifying the various input parameters to the risk assessment. These can be recognised and accommodated to some extent through Monte Carlo simulation or similar techniques. QRA does however provide a systematic approach to an improved site specific understanding of slope stability risk. In this way it compliments rather than replaces engineering judgement and precedence in managing slope instability risk at this and other sites.

Acknowledgment

The authors are grateful to Transit New Zealand and Transfund New Zealand for permission to publish this paper.

References

Bunce, C.M., Cruden, D.M. & Morgenstern, N.R., 1997: Assessment of the hazard from rockfall on a highway. Canadian Geotechnical Journal. 34: pp. 344 © 356.

Canadian Standards Association, 1991: Risk analysis requirements and guidelines, Toronto, Canada, CAN/CSA-Q634-91, Canadian Standards Association, 42p.

Christian, J.T., 1996. Reliability methods for stability of existing slopes. In: Uncertainty in the geologic environment: From theory to Practice. Shackelford, C.D, Nelson, P.P, and Roth, M.S.J Eds., ASCE

Finlay, P.J., Mostyn, G.R., Fell, R.; 1999: Landslides: Prediction of travel distance and guidelines for vulnerability of persons. Proceedings, 8th Australia New Zealand Conference on Geomechanics, Hobart, Vol 1 pp 105-113.

Fell, Robin, 1994: Landslide risk assessment and acceptable risk. Canadian Geotechnical Journal 31, pp. 261 - 272.

Fell, Robin & Hartford, Des., 1997: Landslide risk management. In Landslide Risk Assessment. Eds. David M. Cruden and Robin Fell, Proceedings International Workshop on Landslide Risk Assessment, Honolulu, Hawaii, USA, 19 - 21 February 1997, pp. 51 -108.

Harr, M E, 1987. Reliability based design in civil engineering. McGraw Hill

International Union of Geological Sciences Working Group on Landslides, Committee on Risk Assessment, 1997: Quantitative risk assessment for slopes and landslides - The state of the art. In Landslide Risk Assessment. Proceedings International Workshop on Landslide Risk Assessment, Honolulu, Hawaii, USA, 19 - 21 February 1997, pp. 3 - 12.

Montgomery Watson, 1997: Paddy's bend - Rockfall. Internal consultants Memorandum detailing the results of a large rockfall at site 2, together with possible mitigation measures, dated 3 April 1997.

Mostyn, G.R, and Li, V. S, 1993. Probabilistic Slope Analysis – state of play. In Proceedings Conference on Probabilistic Methods in Geotechnical Engineering, Canberra, Australia. Eds Li, K.S, and Lo, S.C.R. Balkema

Paterson & Coates Associates, 1995: SH73 Paddys Bend , 29 May 1995 Earthquake Damage. Engineering geological assessment of slope stability hazards. Unpublished consultants report for Transit New Zealand.

Paterson & Coates Associates, 1997: SH73 Paddys bend – Site Assessment for Design & Installation of a Geobrugg Rockfall Protection Fence. Unpublished consultants report prepared for Transit New Zealand, 28 May 1997.

Paterson, B.R., 1982a: Geological appraisal or road widening proposals SH73. NZ Geological Survey EG Immediate report 82/008, May 1982.

Paterson, B.R., 1982b: Slope failure at Paddys Bend near Cass. NZ Geological Survey EG Immediate report 82/043, November 1982.

Riddolls & Grocott Ltd, 1999 "Risk assessment procedure for selection of optimum highway slope maintenance programmes" *Transfund New Zealand Research Report No: 135.* 1999

Riddolls & Grocott Ltd "Risk assessment techniques for selection of optimum highway slope maintenance programmes" *Transfund New Zealand Research Report No: 134.* 1998

Standards Australia and Standards New Zealand, 1995: Risk management. Standards Australia, Sydney, Australia, 32p.

United Nations, 1991: Mitigating natural disasters: Phenomena, effects and options. A Manual for Policy Makers and Planners, New York, USA, United Nations, 164p.

Varnes, D.J. 1984: Landslide Hazard Zonation: A Review of Principles and Practice. UNESCO, Paris, pp 11 - 33. *Edition*, Ed: Fang, H., Chapman & Hall, New York.

Capability and risk approach to assessing geotechnical design issues in hazardous terrain: Splendido Taal project, Philippines

M.J. Eggers
Pells Sullivan Meynink Pty Ltd, Sydney Australia

Abstract

Splendido Taal is a large residential and recreational development situated on the upper slopes of the Taal caldera, an active volcanic centre 80km south of Manila in the Philippines.

A preliminary engineering geological assessment of the site highlighted areas of slope instability which could impact on the development as initially proposed. To assist the designers, capability plans were developed based on an assessment of the interaction between geology, landforms, soils and hydrologic features. These plans were used to define suitable forms of land use consistent with the physical limitations of the site and the amount of disturbance the slopes could sustain.

Reconsideration of the development mix on the basis of the capability plans resulted in reduced levels of risk. Geotechnical design guidelines and constraints were also formulated on the basis of the capability plans for the bulk earthworks, road pavements, fill batters and retaining walls, cuttings and soil nail walls, and foundation design.

This case study is presented as an example of how the application of capability and qualitative risk techniques can be used to plan and manage developments in difficult and complex physical settings. These methods also serve as an excellent communications tool, efficiently presenting detailed technical information in a form easily comprehended by planners and designers. Fundamental to this approach is a good understanding of the regional setting of the proposed site and development of a thorough engineering geological model.

Introduction

Splendido Taal is a major development comprising a residential subdivision, an 18-hole golf course, a resort-style country club and a hotel. Located on the rim of the Taal caldera about 80km south of metro Manila, the project represented a major geotechnical challenge with steep slopes and low strength materials within an active volcanic centre.

The site is some 236 hectares in size and a large earthworks program was used to engineer a landform suitable for development. A total of about 10 million cubic metres of material were moved. The works involved cutting the top 40m from the two main ridge crests for filling a central valley to depths up to 50m.

A capability and risk approach was adopted to assist planners and designers to optimise the most appropriate development plan taking into account the severe physical limitations of the site. The methodology required a good understanding of the regional setting and a thorough engineering geological model as a basis for developing the capability plans and undertaking the risk assessment.

Assessment of hazards during this study was restricted to slope instability. Volcanic and seismic hazards were considered by separate studies.

Taal volcanic centre

Caldera geological setting

Splendido Taal is located on Tagaytay Ridge situated on the upper northwestern slopes of the Taal caldera (Figure 1). The caldera is occupied by a lake which is a composite of at least two coalesced collapse centres set inside a graben (Torres etal, 1995). The linear nature of

Tagaytay Ridge suggests caldera collapse was controlled by regional structures including the Macolod Corridor, Marikina Fault and Sibuyan Sea Fault, an active splay of the Philippine Fault (Listanco, 1994).

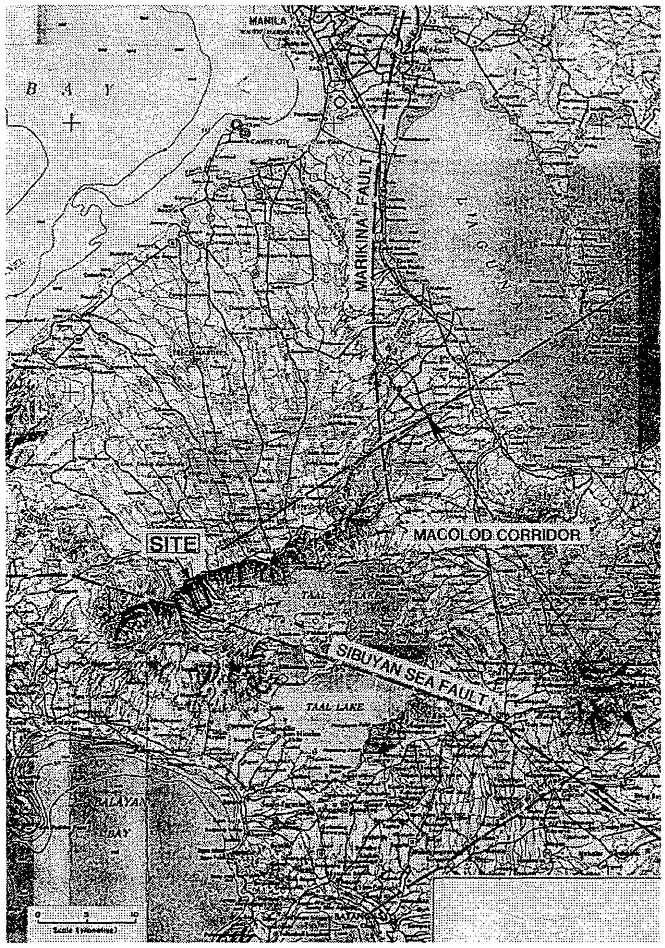

Figure 1. Site location and regional structures.

At least four major ignimbrite-generating eruptions have been inferred. The older ignimbrites are in the range 100,000 to 500,000 years old (Torres etal, 1995) while the youngest dated example of an extensive caldera related unit returned a radiocarbon age of 5380±170 years old (Listanco, 1994). These units were deposited by pyroclastic flows which were able to surmount Tagaytay Ridge providing evidence of violent emplacement. In fact Taal volcano is widely considered to be the Philippine's most important active volcano due to it's low elevation, past eruptive history and high density of people living in the immediate region.

Regional seismicity

The Philippines is located in an active seismic zone situated on the boundary of the Philippine Sea and Eurasian tectonic plates. The Philippine Fault is described as one of the major strike-slip faults of the world extending for over 1200km in length.

The Sibuyan Sea Fault is a significant branch of the Philippine Fault which extends for 350km striking west-northwest through the Taal caldera and possibly near the southwest corner of the Splendido site. The fault zone has not been mapped on the Splendido side of Lake Taal and appears to be covered by Quaternary and Recent volcanic deposits. Preliminary assessments suggest a 200 to 300km offset along the fault qualifying the Sibuyan Sea branch as a world class fault which is understood to be still active (Bischke, 1990 & Forster, 1990).

Volcanic deposits

The most common activities from Taal volcano have been phreatic and phreatomagmatic eruptions (Torres etal, 1995). As such it is expected deposits in the vicinity of the Splendido site will be products of base surges (pyroclastic flows), pyroclastic airfalls and lava flows.

Overall facets of Taal volcano are poorly understood particularly the local stratigraphy. An old geological map of slopes to the north of the caldera rim suggest the site is probably underlain by the Tagaytay Pyroclastics described as, "*Thick, extensive intermediate to basic pyroclastics consisting of heterogeneous, unsorted assemblage of ashes, lapilli, cinder and other volcanic ejecta.*" (Province of Cavite, date unknown).

Splendido Taal engineering geological model

Topography and drainage

The site comprises a series of sharp ridgelines and narrow valleys which trend approximately perpendicular to the caldera rim (Figure 2). Ridge slopes are steep and average around 30° but range to over 40° in some areas. In long section the ridge crests are characterised by a mound and saddle topography interpreted to be eroded remnants of a series of normal faults inferred to underlie the site (Figure 3). These faults are considered to be related to caldera formation where crater collapse occurred along this family of structures.

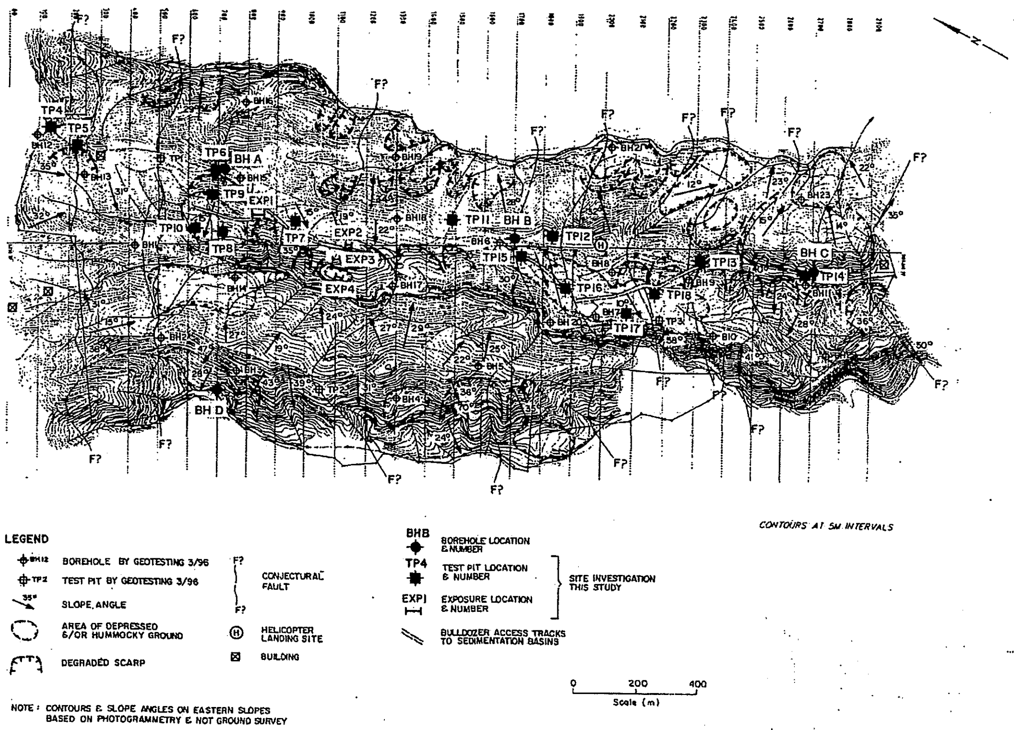

Figure 2. Engineering geology plan.

Drainage generally forms a dendritic pattern with irregular branching streams often entrenched in narrow and very steep sided gullies or gorges. This pattern is indicative of soft rocks such as pyroclastic deposits.

Sub-surface conditions

Composite stratigraphic sections were compiled from the results of cored boreholes, test pits and mapping of natural outcrops and access road cuttings. An example is shown in Figure 4 which represents sub-surface conditions under the central slopes and main stream.

The younger lithic tuff is the upper most unit with a maximum thickness of about 177m and a typical strength ranging from a hard soil to an extremely low strength rock (unconfined compressive strength, UCS, of about 0.7MPa). Three separate horizons were recognised in the younger lithic tuff representing different stages in the eruptive sequence. These horizons allowed stratigraphic position to be determined in the field when exposed.

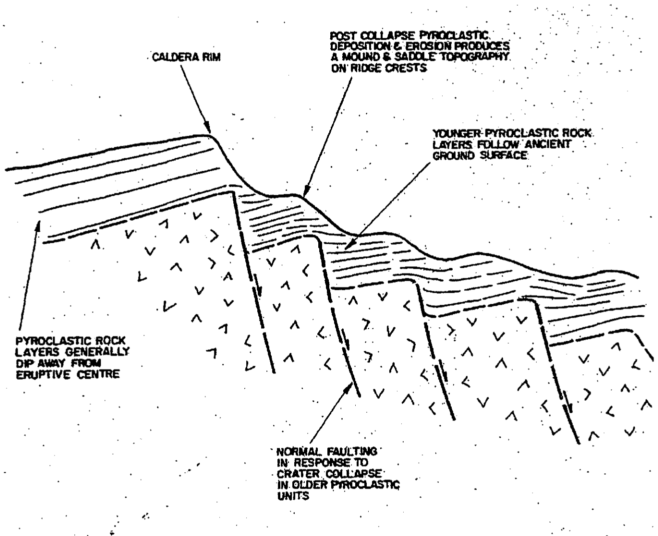

Figure 3. Schematic section showing normal faulting resulting in mound and saddle topography.

The older lithic tuff was distinguished from the younger unit by a coarser grain size and more consolidated nature with an average estimated UCS of 1.5 to 3MPa and an upper bound of 25MPa. The contact between the two units comprises cinder and banded pumice gravel layers which follow the shape of the contact surface and are probably products of a pyroclastic flow event which marked the end of the older lithic tuff/start of the younger lithic tuff deposition.

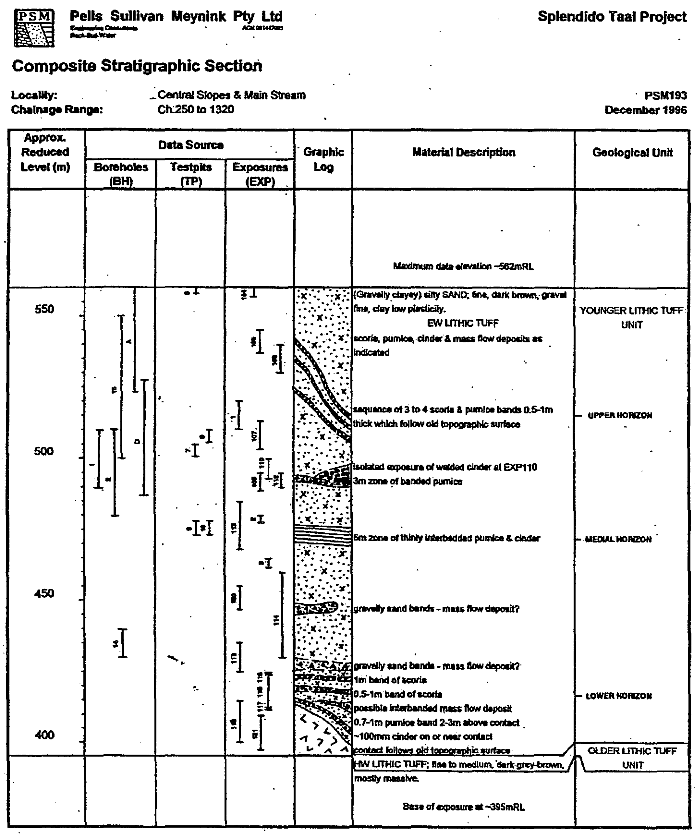

Figure 4. Example of a composite stratigraphic section.

Colluvium was exposed in some areas mostly comprising an unsorted mixture of different grain sized materials in a loose to medium dense/stiff consistency. Cinder fragments were a common component and it is possible at least some of the ancient slope instability may be related to failure in the younger tuff on or close to cinder bands in the lower horizon. These bands may control local groundwater levels particularly during large rainstorm events.

Slope instability features

The results of aerial photography interpretation and mapping showed a number of degraded scarps and areas of depressed and/or hummocky ground (Figure 2). Three types of slope failures were recognised:

- Numerous debris slide-avalanches less than 50m wide and up to 100m long originating from drainage depressions on steep slopes often adjacent to stream courses,
- Rotational slides up to 200m wide typically located toward the upper reaches of the ridge slopes, and
- One example of a possible rock slide-avalanche up to 400m wide.

Geomorphic history

A geomorphological history was compiled for the site as summarised in Table 1. The history highlights the possibility of ancient medium to large-scale slope failures underlying the current slopes which have been buried by subsequent pyroclastic deposits. The possibility also exists for old, buried ground surfaces to occur which could potentially form slide surfaces.

Table 1. Geomorphic history.

Event	Description
1	Ancient eruptions build a volcanic cone of lava and pyroclastic deposits in layers dipping away from the eruptive centre.
2	Formation of the caldera by crater collapse controlled by regional structures. The caldera possibly forms in a piecemeal manner following a series of large eruption and/or seismic events.
3	Extensive and rapid erosion into the weak pyroclastic materials form narrow valleys, sharp ridges and oversteepened slopes.
4	Medium and large scale landslides involving deep-seated rotational slides and planar slide-avalanches within a high rainfall environment.
5	Pyroclastic deposits from subsequent eruptions smooth out the eroded topography with a new phase of erosion and slope movement rapidly overprinting the ancient landform.
6	Possible stream base level change inducing a current phase of rapid downcutting producing stream gorges in older volcanic deposits.

Capability assessment

Approach

The primary objective of the capability and risk assessment was to consider limitations to development due to past, present and potential slope instability. The approach adopted was to:

- Develop a capability plan based on an assessment of the interaction between geology, landforms, soils and hydrologic features,
- Define suitable forms of land use consistent with the physical limitations and the amount of disturbance that could be sustained, and
- Use the capability plan to assess the qualitative risk of slope instability and the implications to development.

Classification system

The system developed was based on the framework used by the Soil Conservation Service of New South Wales for urban capability assessment (Hannam and Hicks, 1976). The site is divided into a number of units assessed on their potential effect on land use and management. Five primary classes are defined (Table 2) on the basis of the most intensive land use recommended.

Table 2. Urban capability classes.

Class	Description
A	Areas with little or no physical limitations to urban development.
B	Areas with minor to moderate physical limitations to urban development. These limitations may influence design and impose certain management requirements on development to ensure a stable land surface is maintained both during and after development.
C	Areas with moderate physical limitations to urban development. These limitations can be overcome by careful design and by adoption of site management techniques to ensure the maintenance of a stable land surface.
D	Areas with severe physical limitations to urban development which will be difficult to overcome, requiring detailed site investigation and engineering design.
E	Areas where no form of urban development is recommended because of very severe physical limitations to development that are very difficult to overcome.

These classes are further divided based on the dominant physical limitation that will restrict development. In this case the slope type represents the potential limitation and the sub-division adopted is listed in Table 3.

Table 3. Slope types.

Code	Description
n	natural slope
c	cut slope
v	valley fill: inclination of fill surface
l	slope fill: inclination of fill base
d	area containing degraded scarps, depressed and/or hummocky ground

Each slope type was further classified based on the slope gradient intervals given in Table 4. For natural and cut slopes the gradient was based on the ground surface angle. For valley fill areas where the fill material was constrained between two ridge slopes the gradient was based on the slope angle of the fill surface. For slope fill areas the overall stability of the fill will be controlled by the gradient of the underlying foundation surface and this angle was used in the classification.

Table 4. Slope gradient intervals.

Code	Description	Gradient interval	
		Degrees	Approx. percentage
t	very gentle	0 to 6°	0 to 10%
g	gentle	6 to 12°	10 to 20%
m	moderate	12 to 24°	20 to 45%
s	steep	24 to 42°	45 to 90%
p	very steep	>42°	> 90%

Capability plans

Capability plans were prepared for pre- and post-bulk earthwork landforms to investigate the change in capacity of the site to sustain development with respect to slope stability.

A majority of the pre-development, natural slopes were zoned Class D based on steep slope gradients and/or the presence of slope instability features (Figure 5). Areas of the central valley contained slightly shallower, Class C slopes while very steep gradients adjacent to the main stream and on the western area of the site were zoned Class E. Overall the natural slopes held severe physical limitations to development that would be difficult to overcome even with extensive and detailed investigation and design.

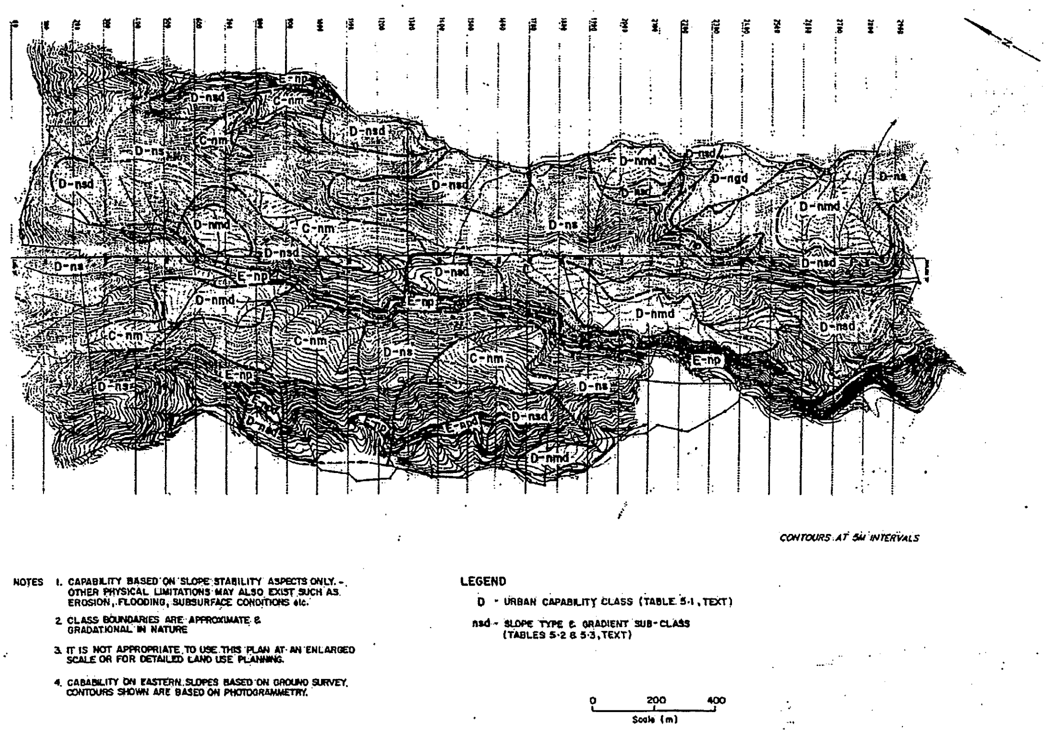

Figure 5. Capability plan of natural (pre-development) slopes.

The initial development proposal comprised extensive bulk earthworks including cutting away the top half of the main ridge, filling the central valley and placing fill in gullies on the eastern slopes. The capability plan formulated for this proposal demonstrated little to no improvement in the capacity of the eastern slopes to sustain development due to steep foundation gradients under the slope fills.

As a result of this preliminary work the earthworks program was reconsidered including the removal of the slope fills. In essence about a third of the eastern facing slopes would be cut leaving natural slopes in the lower two thirds and extensive filling in the central valley. The result was an increase in development capacity (Figure 6) with most of the cut slopes zoned Class B or C and the very gentle to gentle valley fill surface gradients zoned Class A or B.

Substantial investigations were carried out to design the earthworks including specification, compaction control and stability of major fill and cut slopes including seismic loading. The end result would be an engineered landform able to sustain the levels of development called for by the design.

Risk assessment

Categories of development

Once the capability of the post-earthworks slopes had been established the risk posed by the development mix was assessed. This requires the value or type of land use to be defined. The system adopted in this case followed Hannam and Hicks, 1976 as summarised in Table 5.

The Splendido Taal development mix was categorised as shown in Table 6 for the purposes of the risk assessment.

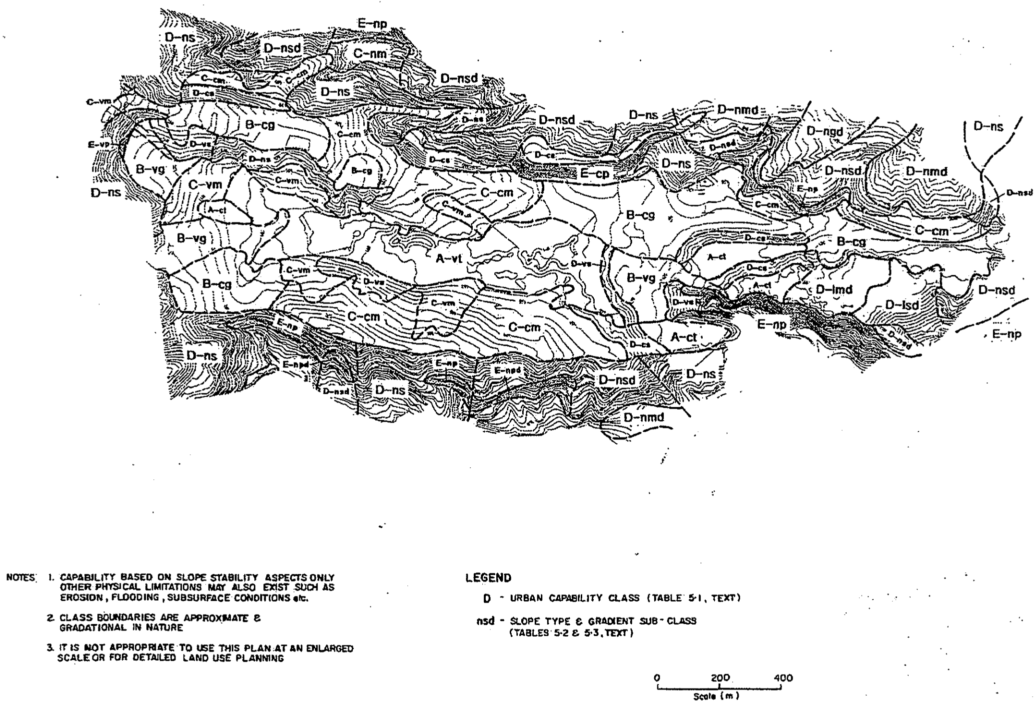

Figure 6. Capability plan of post-earthworks slopes.

Table 5. Categories of urban development

Category	Description
Extensive Building Complex (EBC)	Refers to the development of centres such as offices, shopping malls, hotels, which require large scale clearing and levelling for broad areas of floor space and parking bays.
Residential (RES)	Refers to detached residential developments including buildings, roads, drainage and services to cater for housing allotments of about 500 to $2000m^2$.
Low Density Residential (LD RES)	Blocks of 0.5 hectares or larger.
Strategic Residential	This implies areas unsuitable for widespread development, but where more detailed investigation may permit isolated pockets of land for individual house site, or definition of engineering measures required to maintain stability of what would otherwise be unsuitable land for development.
Active Recreation (ACT REC)	Ovals, campsites and other activities requiring extensive clearing or levelling for facilities.
Passive Recreation (PAS REC)	This implies walking tracks, parkland, drainage reserves and the like, where minor shaping, clearing, and possible revegetation may be desirable to provide for a particular use, but no extensive disturbance is permitted.

Explanation of risk

For the purposes of this study risk was defined as the expected consequence of a future event. In other words, risk is equal to the expected occurrence of an event (hazard) multiplied by the vulnerability and value of the development at risk (Speden and Crozier, 1984).

For the same capability sub-class it can be expected that a higher category of development, such as extensive building complexes, would have a higher risk compared with a lower category of development like an active recreation area. This is a function of the increased vulnerability and value of higher categories of development.

Table 6. Categorisation of proposed development.

Proposed development	Category
resort village	extensive building complex
hotel/spa	extensive building complex
country club	extensive building complex
golf clubhouse	extensive building complex
enclaves 1 to 12	residential
estate administration	equivalent to residential
golf maintenance facility	equivalent to residential
golf course	active recreation
outdoor sports facilities	active recreation
nature park	passive recreation
open spaces	passive recreation

Slope instability risk was divided into four levels based on the old Australian Geomechanics Society system (AGS, 1985):

- Low (L),
- Medium (M),
- High (H), and
- Very high (VH).

Risk of slope instability

The risk of slope instability was qualitatively assessed for each capability sub-class and development type as shown in Table 7.

Table 7. Assessment of slope instability risk.

Capability sub-class	Risk of slope instability				
	EBC	RES	LD RES	ACT REC	PAS REC
A-vt, A-ct	L	L	L	L	L
B-cg, B-vg	M	M	M	L	L
C-nm, C-cm, C-vm, C-lm	H	M	M	L	L
D-ns, D-cs, D-vs, D-ls	VH	H	M	M	L
D-nmd, D-nsd, D-csd, D-lmd,D-ngd, D-lsd	VH	VH	H	M	L
E-np, E-npd, E-vp	VH	VH	VH	VH	H

This risk matrix was used to assess the development mix as originally proposed by the planners prior to this study. High and very high levels of slope instability risk were highlighted for important components such as the village centre, hotel, country club, golf clubhouse and some residential areas. These significant levels of risk were associated with steep valley fill surface gradients, moderate to steep natural and cut slopes and inappropriate development in areas of past and present slope instability.

To assist the planners, development categories suitable for each major capability sub-class were recommended. The development layout was revised using the capability plan of the post-earthworks slopes as a framework. The resulting development plan was sub-divided into zones indicating the different levels of qualitative risk as shown in Figure 7. A majority of the development was classified as low and medium risk. However, there remained areas of high and very high risk.

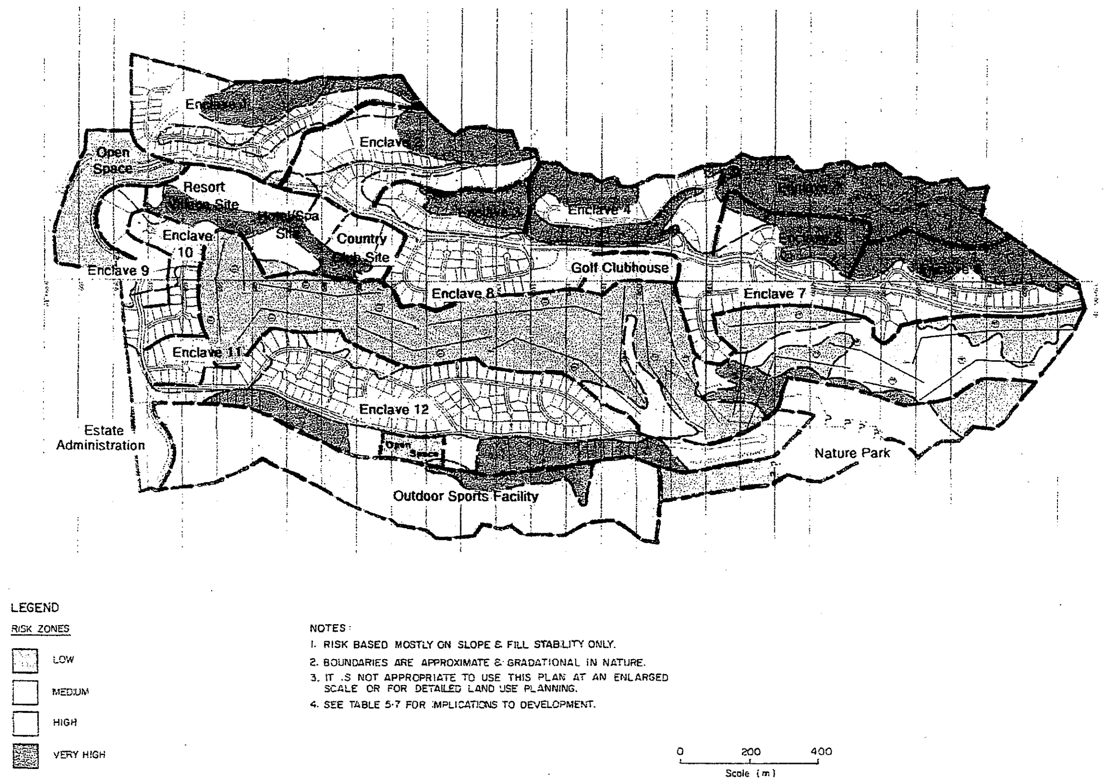

Figure 7. Qualitative risk plan.

Implications to development

Due to the difficult site location and hazardous terrain, successful completion of the project would be controlled to a large extent by the geological and geotechnical. Recommended levels of geotechnical investigation and engineering design work were made for each degree of risk as summarised in Table 8. These recommendations were based on AGS 1985.

Table 8. Recommended level of geotechnical investigations.

Risk level	Recommended investigation and design work
Very high	Unsuitable for development unless major geotechnical work can satisfactorily improve stability. Extensive geotechnical investigations necessary.
High	Development restrictions required and/or major geotechnical works necessary to satisfactorily improve stability. Extensive geotechnical site investigations required.
Medium	Development restrictions may be required. Engineering practices suitable to hillside construction necessary. Geotechnical investigation required.
Low	Good engineering practices suitable for hillside construction required. Geotechnical site investigation may be necessary in selected areas.

In the high and very high risk zones the degree of risk after development may still be higher than what is normally accepted. Recommendations were provided to the planners to remove these significant risk areas. Examples of such recommendations are:

- Relocation of the resort village, hotel and country club sites a distance at least 30m back from the crest of steep natural slopes, and
- Rezoning of enclaves 1 to 6 to low density/strategic residential and recreational use to lower the consequence compared with higher density residential.

Following the capability and risk assessment process, detailed site investigations and engineering design studies were carried out following the guidelines presented in Table 8. In addition to the bulk earthworks design guidelines, site development recommendations were provided for:

- Fill batters and retaining walls,
- Cuttings and soil nail walls,
- Foundation design,
- Road pavement design, and
- Erosion, site drainage and stormwater management.

Conclusions

Capability plans of the natural slopes illustrated severe physical limitations to development if the landform was used without modification. A number of feedback loops were required in the planning process before an engineered landform was designed capable of sustaining the level of development proposed.

Formulation of a qualitative risk matrix specific to the project conditions allowed the proposed development mix to be assessed. Recommended categories of development for each capability sub-class were used to revise the development plan to limit the physical constraints (in this case, slope instability), establish more suitable forms of land use and thereby reduce the level of risk. Recommended levels of investigations and design work for each risk level were used to guide studies on aspects such as road pavements, fill batters and retaining walls, cuttings and soil nail walls, and foundation design.

Capability and risk techniques are effective tools for planning and managing developments in difficult and complex physical settings. These methods also serve as an excellent communications medium, efficiently presenting detailed technical information in a form easily comprehended by planners and designers. Fundamental to this approach is a good understanding of the regional setting of the proposed site and development of a thorough engineering geological model.

References

Australian Geomechanics Society (1985). “Geotechnical risks associated with hillside development”, *Australian Geomechanics News*, Number 10.

Bischke, R.E., Suppe, J. and del Pilar, R. (1990). “A new branch of the Philippine fault system as observed from aeromagnetic and seismic data”, *Tectonophysics*, 183, pp. 243-264.

Hannam, I.D. and Hicks, R.W. (1976). “Soil conservation and urban land use planning”, *Soil Conservation Service of New South Wales*, Sydney NSW.

Listanco, E. (1994). “Space-time patterns in the geologic and magmatic evolution of calderas: a case study at Taal Volcano, Philippines”, *Unpublished PhD thesis*, Tokyo University, Japan.

Province of Cavity Geological Map (date unknown). Publisher unknown.

Speden, I. and Crozier, M.J. (1984). “Natural hazards in New Zealand”, *New Zealand National Commission for UNESCO.*

Torres, R.C., Self, S. and Punongbayan, R.S. (1995). “Attention focuses on Taal: decade volcano of the Philippines”, Eo*s, Transactions*, *American Geophysical Union*, Vol. 76, No. 24, pp. 241, 246-247.

Acknowledgements

Permission from Maunsell Pty Ltd to use the information presented in this paper is gratefully acknowledged.

Aspects of Risk Management for Rainfall -Triggered Landsliding

P. Flentje and R. Chowdhury
Faculty of Engineering, University of Wollongong

Abstract

The assessment and management of the risk of slope movement and landsliding requires careful consideration of hazard, elements at risk and their vulnerability within an interdisciplinary framework embracing geotechnical engineering, geology and geomorphology. This paper gives two examples of Australian practice at Local Government Level that is now undergoing review and change in the light of keen awareness of the need for more effective and systematic approaches. Four examples of systematic assessment approaches are also provided, emphasizing a hazard-consequence matrix framework and, in one case, a quantitative approach for mapping hazard and risk over a whole city. The paper highlights two aspects of the research work carried out at the University of Wollongong, in New South Wales, Australia. The spatial and temporal variability of a major rainstorm event and rainfall thresholds for landsliding are discussed in detail.

Introduction

The International Decade for Natural Disaster Reduction (IDNDR), 1990 – 1999 has highlighted the enormous economic damage and loss of life associated with natural disasters including landslides. The annual economic losses from slope movements and landslides in the United States, Japan, Italy and India have been estimated respectively at US $billion 2, 4.5, 2.6 and 1.5 (Schuster 1996). It is estimated that the total Australian cost of landslide related damage for the period 1803-1999 is $500 million (IDNDR, 1999). Climate change and rising sea levels would cause a significant increase in hazard and to the losses associated with landslide problems. With increased awareness of the vast scale, extent and impact of problems posed by natural hazards including landslides, efforts to develop better methods of risk assessment and management have gained considerable momentum at local, national and international levels. This has been accompanied by social and political responses in both developing and developed countries.

This paper is concerned with current landslide risk management practice in Australia as well as aspects of research being carried out at the University of Wollongong (UoW) in New South Wales, Australia. For the last few years, a landslide research project at the University of Wollongong funded under the Australian Research Council (ARC) Strategic Partnership Industry Research and Training (SPIRT) has been in progress. Another SPIRT project concerning landslide risk management has now been started for the three-year period, mid 2001 to mid 2004. The industry partners are the Wollongong City Council (WCC) and the Rail Infrastructure Corporation (RIC), and the partner Investigator is the Australian Geological Survey Organisation (AGSO).

In this paper, two important aspects of risk management will be highlighted. One concerns a systematic approach for the assessment of risk using a hazard-consequence matrix approach. This is of key importance as a basis for decision-making. With reliable assessments of hazard and risk, realistic options for preventative or remedial options can be identified and developed. Moreover, sites and areas can be prioritised according to the degree of hazard or risk so that resources, which are always limited, can be used most efficiently.

The second aspect concerns the detailed study of rainfall as a triggering agent or factor. It is necessary to gain an improved understanding of the link between the intensity and duration of rainfall on the one hand and the occurrence of landslides on the other. In this connection, it is also important to note that different types of landslides will occur under different conditions. In addition to improved understanding, this research will lead to the development of better systems for early warning and for real-time or near real-time warnings.

Before discussing these two key aspects of recent research, the past practice concerning risk assessment and management in Australia is reviewed briefly. This practice is already under review and is expected to be updated in time with modern developments such as (a) the use of GIS based maps which are flexible, and updateable and (b) the use of systematic approaches such as the hazard-consequence matrix approach. Moreover, there will be a trend towards progression from qualitative to quantitative approaches.

Examples of Australian Local Government Practice

Example 1 – Wollongong City Council in the State of New South Wales

In recognition of landslide hazard and risk within the local government area, the Wollongong City Council (WCC) has a policy regarding the development of land that may be subject to land instability. This policy was most recently updated in 1996, although it is known to have been in existence from at least the mid 1970's. The policy provides a procedure for a) assessment of proposed development of land that may be subject to instability, b) professional requirements of engineering geologists and geotechnical/civil engineers who submit reports to the council and c) ensuring that the documents supplied to WCC provide sufficient information for decisions to be made.

In summary, this policy document requires that landslide risk be classified according to the Australian Geomechanics Society (AGS) publication entitled "Geotechnical Risk Associated with Hillside Development" (Walker et al, 1985). If the land is classified as Low risk or Very Low risk, the application for development can be processed without the requirement of a geotechnical stability assessment. Medium Risk sites require a geotechnical stability assessment from a qualified and approved geotechnical engineer or engineering geologist. The WCC will not accept development on lands classified as High or Very High risk and may refer disputed assessments to an internal geotechnical group or to a third party geotechnical consultant. Structural and associated Civil engineering reports are also required from developers and must confirm that the submitted plans conform to the geotechnical report and to engineering design practice.

Professional requirements of engineering geologists and geotechnical engineers preparing reports to be submitted to the WCC include membership of professional organisations and a base level of local experience.

WCC has also developed in-house GIS-based hazard maps showing areas with two categories of landslide hazard, (a) all active landslides which have been identified and (b) other areas considered to be potentially having a high risk of landsliding. Development is unlikely to be approved within known landslide sites unless detailed geotechnical advice by an expert is provided supporting the request for development and/or documenting the remedial works and post construction monitoring required and/or confirming the good performance of the site during months or years immediately preceding the application for development.

Example 2 – Colac Otway Shire in the State of Victoria

The Colac – Otway Shire (COS) is located in the southwestern coastal area of Victoria. This shire has been established several years ago following the amalgamation of several smaller shires including Otway and Colac shires. This new shire encompass a large portion of the Otway Ranges and a section of the Great Ocean Road and has inherited the landslide management practices of these smaller shires.

The COS currently uses an "Erosion Management Overlay" (EMO) which brings areas under its footprint into a council assessment system whereby 'a visual assessment of the slope stability of the site and surrounding areas' is required by geotechnical consultants acting for the developer. Currently, this system does not specify what information is required in the geotechnical assessment or what method of assessment is to be used. Furthermore, the EMO covers only a portion of the former Otway Shire, and not the amalgamated COS.

Having realised that this is not the current best practice, the shire officers have appointed expert geotechnical consultants to review and recommend future directions to better manage landslide risk. Preliminary findings of this work include a GIS –based constraints map which identifies areas in need of geotechnical consideration or assessment. If geotechnical consideration is required as a result of this GIS-based constraints map, it is being recommended that consultants should follow the Hazard-Consequence matrix approach outlined recently by the Australian Geomechanics Society (AGS, 2000). Furthermore, a formalised process for assessment of consultants reports will be provided in the form of a flow chart.

Examples of Systematic Assessment approaches

Management of landslide hazard and risk requires a formalised and systematic approach for assessment which recognises different requirements for individual projects and the availability of resources. A systematic approach requires three components: (1) an assessment methodology (2) a management process that identifies which areas or sites require assessment, and (3) a process to incorporate the assessments into management priorities and actions. Four examples are given below which illustrate systematic approaches.

The assessment of landslide hazard and risk has reached a useful level of rigour and the capture of this information into a management and planning framework is essential for future sustainable development and to promote future development of landslide assessment and management techniques.

A Matrix based Hazard - Consequence risk assessment approach covering a wide range of applications is highlighted in an Australia/New Zealand Standard for Risk Management (AS/NZS 4360:1999). A matrix approach includes the assessment of hazard independent of the identification and assessment of elements at risk and the assessment of associated consequences/vulnerability of those elements. This standard does not refer to landslides or even to natural hazards. However, some organisations such as the Roads and Traffic Authority and the Rail Services Authority in New South Wales have developed in-house procedures for geotechnical risk that follow an informal matrix approach. These procedures remain largely unreported in the published literature. However, recent developments and applications are set to change this situation and several examples of systematic assessment will be appearing in learned journals and proceedings of conferences in the near future.

Example A – Australian Geological Survey Organisation (AGSO) Quantitative Landslide Risk Assessment of Cairns

In 1999 AGSO completed a Quantitative Landslide Risk Assessment of Cairns (Leiba et al 1999). The study objective was to provide to the Cairns City Council, for planning and emergency management purposes, in a GIS based environment, information on landslide types, community vulnerability and risks. A map of landslides was prepared and two main slope processes identified. These slope processes are, firstly, landslides that occur on the slopes and include falls, slides, and small debris flows, and secondly, large debris flows which extend from the major gully systems on to the coastal plains as debris fans. Magnitude-recurrence relationships were tentatively established for these two main slope processes.

Three main polygon categories have been identified as a) escarpment b) areas which could be affected by proximal portions of debris flows and c) areas which could be affected by distal portions of debris flows. Numerical hazard values have been produced for each polygon type and each polygon has been assessed for the nature and number of elements at risk.

Using the assumed or inferred recurrence relationships, landslide hazard was estimated as the probability of a point being impacted by a landslide. Elements at risk (residents, buildings and roads) was determined from a comprehensive GIS database and their vulnerability to destruction by landsliding were assessed on the basis of information provided by the Cairns City Council and some information already compiled by the Australian Geological Survey

Organisation (AGSO) as part of their Australian Landslide Database. The range of vulnerability values was tabulated. Consequently specific risk and total risk values could be calculated.

It is of note that this Quantitative Landslide Risk Assessment of Cairns represents only one facet of a Multi Hazard Risk Assessment of Cairns, which included other Natural Hazards such as (1) Tropical Cyclone and associated storm surge and flooding and (2) Earthquake hazard and risk.

Example B - Geotechnical Team - August 1998 Wollongong rain storm event

A three man team, including the first author, an engineering geologist, and two geotechnical engineers were brought together by the police, local council and the State Emergency Services following an unprecedented rainfall event from 15th to the 17th August 1998. The aim was to assess known and other reported geotechnical problem sites associated with this rainstorm event. The rainfall event recorded 750mm of rainfall over 5 days and 450mm in 24 hours during the 17th August. A total of 192 problem sites were identified, of which 145 were landslide related sites.

The 3-man team used a Hazard - Consequence matrix approach to assess each site in terms of risk to Human life and separately to the risk to Property. Assessments were made on site and confirmed during de-briefings at the end of each day. The risk was assessed separately for Human Life and Property as one of five risk categories, Very High, High, Medium, Low and Very Low. Actions for all Very High and High Risk sites were referred to the necessary public authority or private party as soon as practical following the assessment. A comprehensive report was produced and actions to be taken were outlined for each site.

Example C - University of Wollongong Multi-level Approach

A three level approach to risk assessment has been proposed at the University of Wollongong (Ko Ko et al 1999). Three levels or types of assessment are envisaged and one, two or all levels of assessment may be carried out (Flentje et al 2000). Type I is a reconnaissance or walkover level of assessment and a series of field sheets are provided to assist the user to make a semi-quantitative hazard - consequence risk assessments based on the scoring of answers to a range of questions concerning the factors which influence or control slope stability. Individual field sheets are provided for different types of slopes, namely, natural slopes, embankments and cuttings in soil or rock. A five-level numeric scale of risk is used in the Hazard - Consequence matrix.

Type II approach is used for the assessment of large areas considering key causal factors such as rainfall, earthquakes, geology and topography. This type of assessment is greatly facilitated by;

- the use of GIS based information and analyses
- the use of comprehensive geology, geotechnical and landslide databases
- temporal and spatial analyses of rainfall,
- an observational approach whereby the monitoring of landslide surface and subsurface movements and pore water pressures is carried out and the results analysed

Type II assessments will highlight important regional factors and relationships in quantitative terms which may, in turn, be used for more reliable risk assessment of individual sites.

Type III assessments involve the use of proven geotechnical modelling and sophisticated methods of deterministic and/or probabilistic analysis based on comprehensive subsurface investigations. Such assessments would follow initial Type I and/or Type II assessments that have enabled prioritisation of sites requiring detailed investigation and assessment. Whilst dependent on the level of the investigation, major uncertainties relate to the spatial and temporal variability of geotechnical parameters, mechanisms of failure and the analytical models (Chowdhury and Flentje, 2002).

Example D - Australian Geomechanics Society (AGS) 2000

A paper entitled 'Landslide Management Concepts and Guidelines' (AGS, 2000) includes a Hazard - Consequence matrix approach with a table of Qualitative Measure of Likelihood having six categories of likelihood and a table of Qualitative Measures of Consequence to Property with 5 categories of consequences (Table 1). These categories of likelihood and consequences are combined to enable definition of five levels of risk as reproduced in Table 2.

At the time of writing, the AGS 2000 methodology has been available for 12 months. The first author is aware that at least one local government in Victoria requires its use for stability assessment reports whilst another in New South Wales is awaiting industry response to the document.

Table 1. AGS 2000 Risk Matrix

LIKELIHOOD	**CONSEQUENCE**				
	1 *Catastrophic*	**2** *Major*	**3** *Medium*	**4** *Minor*	**5** *Insignificant*
A *Almost Certain*	Very High	Very High	High	High	Moderate
B *Likely*	Very High	High	High	Moderate	Low-Moderate
C *Possible*	High	High	Moderate	Low-Moderate	Very Low-Low
D *Unlikely*	Moderate - High	Moderate	Low-Moderate	Very Low-Low	Very Low
E *Rare*	Moderate-Low	Low-Moderate	Very Low-Low	Very Low	Very Low
F *Not Credible*	Very Low	Very Low	Very Low	Very Low	Very Low

Table 2. AGS 2000 Risk Categories with example Implications

Risk Level		**Example Implications ***
VH	*Very High Risk*	Extensive detailed investigation and research, planning and implementation of treatment options essential to reduce risk to acceptable levels: may be too expensive and not practical
H	*High Risk*	Detailed investigation, planning and implementation of treatment options required to reduce risk to acceptable levels
M	*Moderate Risk*	Tolerable provided treatment plan is implemented to maintain or reduce risks. May be accepted. May require investigation and planning of treatment options.
L	*Low Risk*	Usually accepted. Treatment requirements and responsibility to be defined to maintain or reduce risk.
VL	*Very Low Risk*	Acceptable. Manage by normal slope maintennance procedures.

* Impilcations should be determined by all parties to the risk assessment, those given above are only a guide

Rainfall as triggering factor (threshold and variability)

Rainfall is recognised nationally and internationally as a major triggering factor for the initiation of slope instability and the initiation of landslide movement that may range from minor to catastrophic in terms of velocity and travel distance. Extensive global research efforts have focused on the development of rainfall thresholds for the initiation of slope movements. However, an important source of uncertainty in hazard and risk assessment comes from both the spatial and temporal variation of rainfall (Chowdhury and Flentje, 2002).

At the University of Wollongong significant research has been directed to the analyses of rainfall and slope movements enabling estimation of such thresholds and the associated uncertainties. The Antecedent Rainfall Percentage Exceedance Time (ARPET) methodology has been presented in recent papers (Flentje and Chowdhury 1999, Chowdhury and Flentje, 2002) and will not be discussed further here.

It is important to recognise and assess the spatial and temporal variation of rainfall. As stated earlier, Wollongong experienced a major rainstorm event during the period 15th – 20th August 1998. The intensity-frequency-duration curves derived from pluviometer rainfall monitoring stations around the city show that for intervals between 3 hours and 12 hours, some stations exceeded a 1 in 100 year event, and rainfall totals at one station for an 8 hour interval exceeded a 1 in 200 year event. However, many parts of the city experienced significantly less falls over a wide range of durations equating to say a 1 in 20 year event for a 24 hour period. Figure 1 shows rainfall totals for the 6 hour duration prior to 7pm on the 17th August 1998 and known landslides that occurred during the event. The rainfall isohyets have been prepared recently by AGSO (Murray 2001) for the ARC SPIRT team. This figure clearly shows the spatial variability of the rainfall over this 6 hour period. Similar spatial variation exists for the 4 and 12 hour period preceding 7pm and some preliminary results of a spatial analysis of this data is given in Figure 2. This figure shows a Landslide-Rainfall distribution curve for 4 hr, 6 hr and 12 hr pluviometer periods, upon which is superimposed a threshold line for the triggering of debris flows in August 1998 in Wollongong. This threshold line is drawn through points at which each curve starts to ascend steeply.

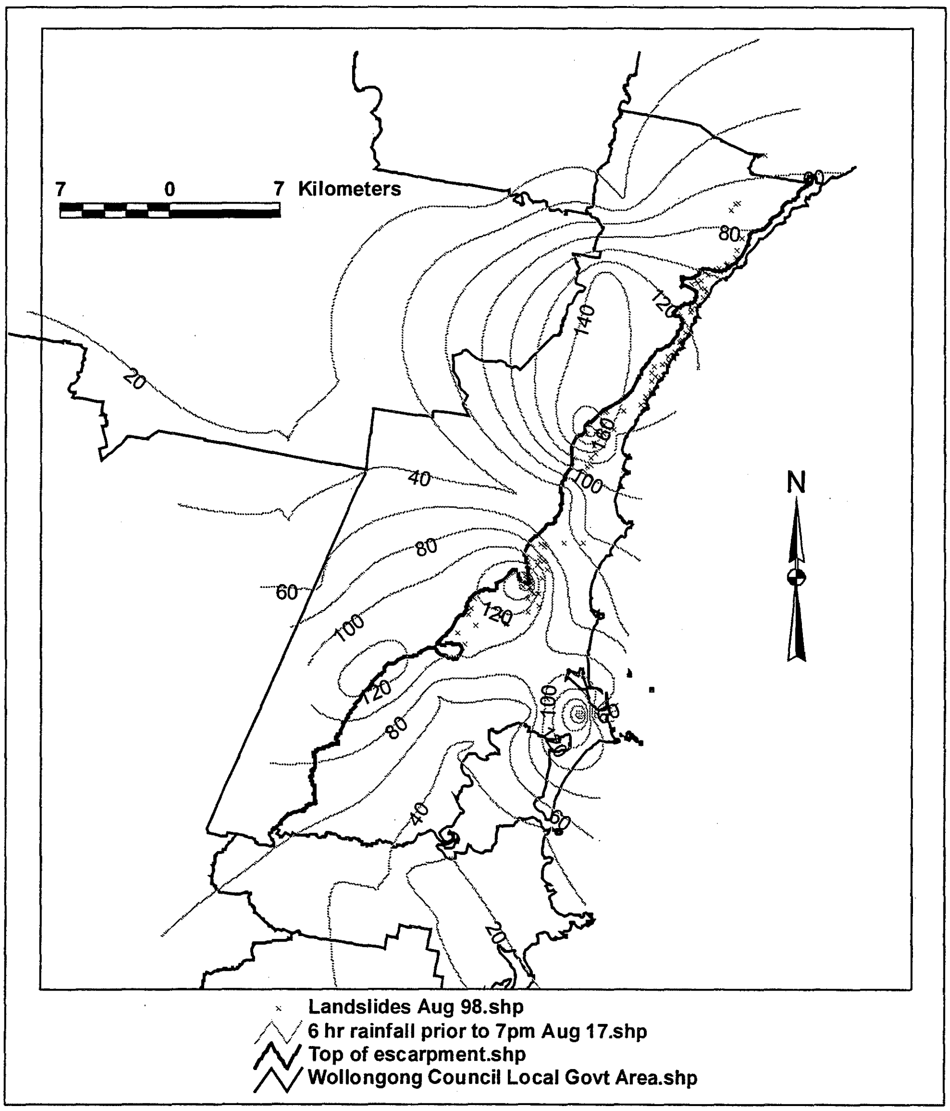

Figure 1. GIS based 6 hr rainfall distribution prior to 7pm on August 17th 1998, with documented landslides. Local Government Area boundary and top of Escarpment are shown.

A rainfall intensity/duration graph of all landslide types (including debris flows) in the Illawarra during the August 1998 rain storm is shown in Figure 3. A threshold relationship developed by Caine (1980) for internationally published rainfall intensity/duration and debris flow occurrence data on undisturbed slopes has been superimposed on the Wollongong data. An excellent correlation is found with the Wollongong data for debris flows associated with rainfall over a short duration. The Wollongong August 1998 series falls below the Caine threshold line for rainfall of longer durations. This would have been expected since the longer durations are clearly more relevant to deep seated landsliding. For this range of durations (240 hrs or 10 days up to 2280 hrs or 120 days), ARPET thresholds (Flentje 1998) for deep seated slow moving landslides have been developed during previous research and are also shown on Figure 3.

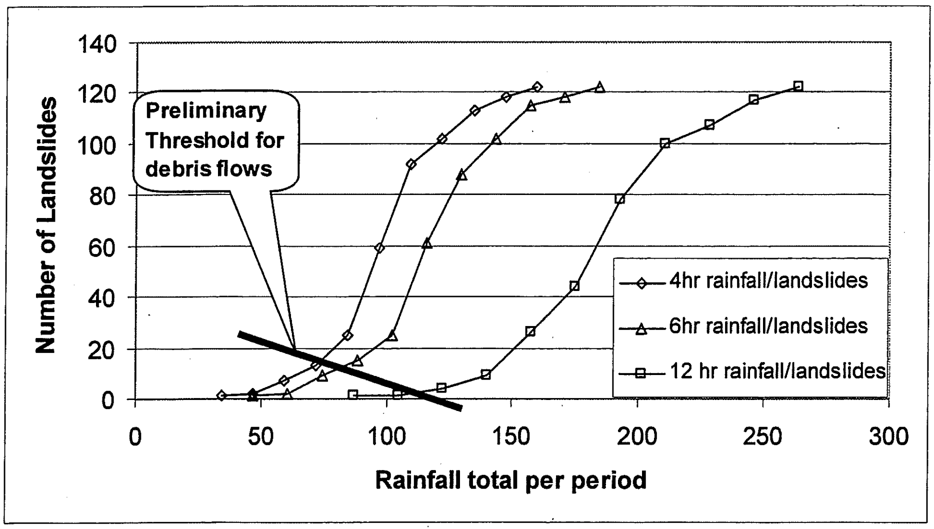

Figure 2. Number of landslides outside of given rainfall contour (20mm rainfall contours) with preliminary debris flow threshold for the Illawarra (after Murray 2001).

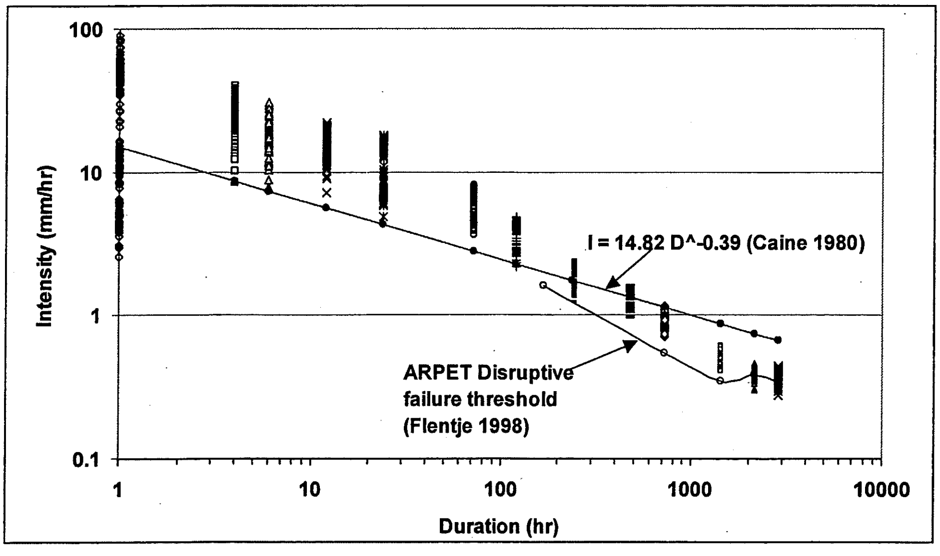

Figure 3. Rainfall intensity/duration thresholds for initiation of all landslide types (including debris flows) in the Illawarra during the August 1998 rainstorm event (vertical data series at various cumulative periods). Included is the Caine (1980) threshold line for internationally published rainfall intensity/duration and associated debris flow data on undisturbed slopes (Murray 2001). ARPET threshold line for disruptive failure involving deep-seated, slow-moving landslides (Flentje 1998) is also included.

Conclusion

Increasing awareness of the limitations of current practice concerning landslide hazard and risk assessment is leading to the development of more systematic approaches. These range from qualitative to increasingly quantitative methods. The use of a hazard-consequence matrix approach facilitates improved and reliable assessments and is a powerful strategy for coping with different situations and considering the limited extent of resources. The matrix approach may be used within an integrated framework that incorporates different types or levels of assessment. To improve the understanding of rainfall as a trigger and its spatial and temporal variability, detailed GIS-based study of recorded rainfall distributions and intensities is highlighted. This has led to the assessment of threshold magnitudes for different rainfall periods. Such research also enables the development of improved early warning systems and real-time or near real-time warning systems.

References

AGS, (2000). "Landslide Risk Management Concepts and Guidelines," In *Journal and News of the Australian Geomechanics Society* (AGS) Volume 35, Number 1, March 2000, pp 49-92

AS/NZS 4360:(1999). "Risk Management," *Australian Standard/New Zealand Standard 4360*. Standards Association of Australia/New Zealand.

Caine, N. (1980). "The Rainfall Intensity – Duration Control of Shallow landslides and Debris Flows," *Geografiska Annaler*, Vol 62, A 1-2, pp 23 – 27.

Chowdhury and Flentje. (2002). "Uncertainties in Rainfall Induced Landslide Hazard," *Quarterly Journal of Engineering Geology*, Symposium in Print, (under review).

Flentje, P.N. (1998). "Computer Based Landslides Hazard and Risk Assessment-Northern Illawarra Region of New South Wales, Australia," *Doctor of Philosophy Thesis*, University of Wollongong, New South Wales, Australia. Unpublished, 525p.

Flentje, P., Chowdhury, R. N. and Chit Ko Ko. (2000). "A Matrix Approach for Landslide Risk Assessment," *Proceedings of GeoEng2000*, an International Conference on Geotechnical and Geological Engineering. Melbourne, November 19 – 24. Technomic, Pennsylvania, on CD ROM paper number SNES0252.Pdf.

Flentje, P. and Chowdhury, R. N., (1999). 'Quantitative Landslide Hazard Assessment in an Urban Area', 8th Australia-New Zealand Conf on Geomechanics, Hobart, Tasmania Feb., 1999, Vol.1, 115-120

IDNDR (1999). *Final Report of Australia's Coordination Committee for the International Decade for Natural Disaster Reduction* (IDNDR) 1990-2000. IDNDR Programme Forum, Geneva Switzerland, July 5-9, 134 pages.

KoKo, C., Flentje, P. and Chowdhury, R.N., (1999). 'Landslide Risk Assessment - Development of a Hazard - Consequence Approach', *Proc. International Symposium On Slope Stability Engineering.* Geotechnical and Geoenvironmental Aspects, Matsuyama, Shikoku, Japan, Nov 8-11, 1309-1315.

Leiba, M.M., Baynes, F. Scott, G. (1999). "Quantitative Landslide Risk Assessment of Cairns," *Australian Geological Survey Organisation Record* 1999/36, Department of Industry, Science and Resources, 51 pages plus Appendices.

Murray, E, (2001). "Rainfall Thresholds for Landslide Initiation in the Wollongong Region," Internal report to Australian Geological Survey Organisation and SPIRT Project Team at the University of Wollongong.

Schuster, R.L. (1996) "Socioeconomic Significance of Landslides", in Turner, A. K. and Schuster, R. L., editors (1996). *Landslides, Investigation and Mitigation* Special Report 247. Transportation Research Board, National Research Council. National Academy Press Washington DC, 673 pages.

Walker, B., Dale, M., Fell, R., Jeffrey, A., Leventhal, A., McMahon, M., Mostyn, G., and Phillips, A. (1985). "Geotechnical Risk Associated with Hillside Development," In *Australian Geomechanics News*, No. 10, December 1985.

Seismic Hazards

Waimakariri District Liquefaction Hazard

S A Christensen
Beca Carter Hollings & Ferner Ltd, Christchurch

Abstract

A study has been undertaken to enhance the knowledge of the liquefaction hazard of the eastern side of the Waimakariri District in Canterbury, an area of historical liquefaction. Field investigations, including 26 boreholes, were used to supplement existing regional data and provide the basis for analysis. Two earthquake scenarios were used in three liquefaction prediction models to assess the earthquake hazard for the Study Region and consequently produce a liquefaction hazard map. It was found that the eastern side of the Study Region, which contains deep coastal sand deposits, has a high susceptibility to liquefaction. This high susceptibility extends out to the western boundary of the Study Region in three locations and into the heart of the largest town in the Study Region, Kaiapoi. Level ground liquefaction settlements were also predicted for both earthquake scenarios.

Introduction

Summarised herein are the results of a liquefaction investigation undertaken for the eastern side of the Waimakariri District (refer to Figure 1 for the extent of the Study Region). The investigation included a desktop study of existing information, review of historical evidence, physical field investigations, analysis, and the creation of a liquefaction hazard map. The study is based on a relatively limited level of investigation aimed at providing a regional view of liquefaction hazard.

Study Objectives

An objective of this investigation is to assist the Waimakariri District Council and Environment Canterbury (formerly Canterbury Regional Council, CRC) to fulfil statutory functions and duties. The two Councils have respective functions under the Resource Management Act 1991 (RMA) s31(b) and s30(1)(c) to collect information on natural hazards and to develop objectives and policies for hazard avoidance and mitigation. The District Council also has duties under RMA s106 when considering applications for subdivision consent, not to grant consent if it considers that the land is likely to be subject to damage by land movement. Furthermore, it has the responsibility in terms of the Building Act 1991 s31(2) to provide any information it knows about potential land movement or inundation that may affect any building work. Finally, the Local Government Official Information and Meetings Act 1987, s44(a) also requires the District Council to provide information it knows that identifies land subject to movement or inundation.

From these requirements, the study objective was defined as providing a better definition of areas susceptible to liquefaction allowing the district and regional councils to discharge their statutory obligations. Information is now available for ratepayers through Resource and Building Consents (PIMs and LIMs), and the council's have information for planning, emergency management, environmental and education/advice.

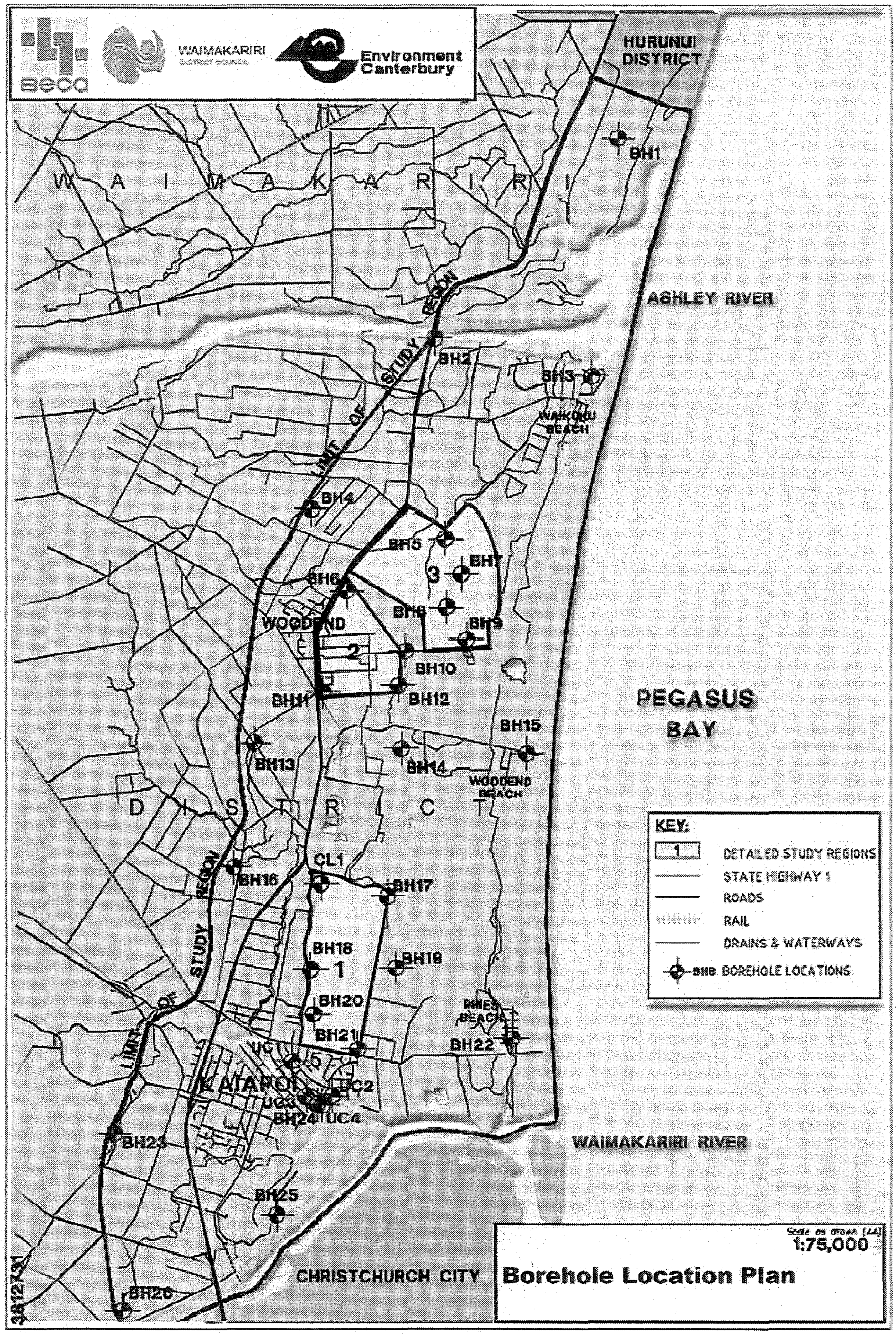

Figure 1 Study Region and location of study boreholes.

Historical Evidence of Liquefaction

The University of Canterbury has investigated liquefaction that occurred in the 1901 Cheviot Earthquake and especially its effects in Kaiapoi (Berrill et. al., March and September 1994). In summary, the 1901 Cheviot Earthquake, which had a Richter Magnitude 6.9 ± 0.2, caused sand boils and other liquefaction effects at Kaiapoi at a distance of at least 90km from the epicentre of the earthquake. Liquefaction occurred over an area of about two or three town blocks on the north bank of the Kaiapoi River. In addition to these occurrences, minor occurrences of liquefaction at Waikuku and Leithfield beaches in the 1922 Motunau Earthquake are reported by Sterling et. al. (1999).

Definition of the Study Region

The northern and southern edges of the Study Region are bounded by the limits of Waimakariri District and the eastern extent by the coastline of Pegasus Bay. The western boundary is defined by the maximum inland extent of post-glacial marine transgression, some 6,500 to 6,000 years before present (refer to Figure 1 for the Study Region boundaries).

Soils are susceptible to liquefaction when they are recently deposited (less than 10,000 years old). A 15m investigation depth was adopted as radiocarbon tests indicate that 7,000 year old deposits are located at depths of 9 to 15 m below ground level (Brown, 1973). It is probable that the Study Region will not cover all liquefaction possibilities within the Waimakariri District, as the western boundary does not include recent inland deposits from the Waimakariri or Ashley Rivers.

Existing Soil Information

The eastern extent of the Canterbury Plains in the vicinity of the Waimakariri District consists of outwash alluvial deposits of gravel, sand, silt, clay and peat. More specifically, the coastal margin of the district is bounded with sand dune and inter-dune deposits. Brown and Weeber (1992) state: "Coastal outbuilding or progradation began after the present sea level became established about 6,500 – 6,000 years ago".

Environment Canterbury operates a well database for the Canterbury Region, from which a total of 355 well logs were examined within the Study Region. Generally the borelogs contained simple descriptions of the strata encountered (e.g. clay, silt, sand or gravel), but the database does not store soil strength/density information such as Standard Penetration Tests. These logs show that gravel was scarce along the coastline and became more prevalent inland, along the western boundary of the Study Region.

A further 22 Cone Penetration Test (CPT's) and three rotary borehole logs were reviewed from liquefaction investigations within the district (Berrill et. al., March 1994 and Connell Wagner, 1999).

The 355 Environment Canterbury bore logs used in this study give a general indication of soils in parts of the Study Region. However, the description of soils is basic and there are no soil densities recorded with the bore logs. Consequently, the bore logs are of limited use by themselves in this liquefaction study. The in situ testing undertaken by the University of Canterbury and Canterbury Lakes is restricted to depths of up to 10 m.

Investigation Methods

Based on existing information, the investigation envelope was expected to encounter thick seams of gravel, gravelly soils, and very dense sands. Therefore, CPT probes would probably not have been able to penetrate to 15m depth in dense gravel and sand deposits. While the gravels are predominately located at the bottom of the investigation envelope, they are also widespread at higher elevations and overlay fine-grained soils that could be susceptible to liquefaction. Therefore, rotary boring with Standard Penetration Tests (SPT's) was recommended for this investigation.

The field investigations provided a general idea of the distribution of deposits within the investigation envelope. As soil types are likely to vary greatly within short distances, especially within the Springston Formation deposits, a closely spaced mesh of boreholes would be required to delineate changes in strata; this was not considered economic for a regional study. Furthermore, complex laboratory testing of soil samples was not considered warranted given the large distances between boreholes and hence discrete nature of the study. Laboratory testing was restricted to particle size distribution tests.

Soil Encountered

Gravel was encountered in the majority of the boreholes (21 of 26) undertaken, with the exceptions being those located along the coastline. The level and/or elevation where gravel was first encountered within the boreholes was variable and trends were not apparent, except that the likelihood of encountering gravels increases with distance from the coastline. In half of the boreholes gravel was encountered within 5m of the ground surface.

Sands dominated in the soil samples recovered in this investigation. Sands were encountered in all but one borehole, and accounted for 61 per cent of the samples recovered. The sands were more prevalent along the coastline of Pegasus Bay and conversely were less apparent along the western boundary of the Study Region. The sands encountered were typically described as uniformly graded fine sands.

Silt sized soils were relatively uncommon across the Study Region and accounted for only 6 per cent of the soil samples recovered. When the silts were encountered they were typically within 5m of the ground surface (Springston Formation soils). Silts and other finer-grained soils were more prevalent on the western side of the Study Region.

Clays and peats were encountered in 11 of the 26 boreholes drilled. Often the clay seams were relatively thick at around 4m to 5m. These fine-grained soils did not appear to be restricted to any particular depth or elevation. However, they were not widely encountered in the Christchurch Formation soils along the coastline of Pegasus Bay.

Soil densities were indirectly assessed based on SPT's. The weaker soils with N-values less than 10 blows/300mm were typically comprised of sand or smaller sized particles and were located within 10m of the ground surface. These low strength soils comprised approximately one quarter of the soils encountered and of this approximately half were sandy soils. Dense to very dense (N>30 blows/300mm) soils were regularly encountered throughout the Study Region and more especially below a depth of around 8m to 9m. SPT N-values were consistently highest along the northern side of Kaiapoi.

Liquefaction Assessment

Earthquake Scenarios

The project brief stated "It is considered that the latest publication from CRC is the most definitive summary of the frequency and characteristics of earthquakes in the Canterbury Region." The report being referenced is the Probabilistic Seismic Assessment and Earthquake Scenarios for the Canterbury Region, and Historic Earthquakes in Christchurch (Stirling et. al., 1999). The two chosen earthquake scenarios chosen for this study are summarised in Table 1.

Table 1. Earthquake Parameters Used in Analysis (Stirling et. al., 1999)

Parameter	Foothills Earthquake	Alpine Earthquake
Return Period	150 years	475 years
Peak Ground Acceleration	0.28g	0.44g
Modified Mercalli Intensity (MMI)	8.2	8.7
Richter Magnitude (M)	7.2	8.0
Epicentral Distance	50km	150km

The Foothills Earthquake scenario originates on the faults located in foothills of the Southern Alps, and will produce shaking of up to MMI 8 for around 30 seconds. This earthquake will be likely to originate at depths of less than 15 km on the Ashley, Springbank and Porters Pass – Amberley Faults. Disruption to services and utilities closest to the fault rupture is likely. Many aftershocks of M5 to 6 are expected in the vicinity of the main shock, but these are unlikely to cause damage at the towns. The closest historical analogues to this scenario earthquake are the 1888 North Canterbury earthquake and the 1901 Cheviot earthquake (Stirling et. al., 1999).

MMI 7-8 shaking and accelerations for the Alpine Earthquake may be less than for the Foothills Earthquake scenario, but the duration of shaking will be much longer (60 seconds or more). Liquefaction will be extensive with lateral spreading along many river and estuary margins. It is possible that there will be major disruption to utilities and services, and this could continue for days or weeks. The many M 6-7 aftershocks that will accompany the earthquake will not produce significant shaking in any of the towns (Stirling et. al., 1999).

Prediction Models

Three well-known liquefaction prediction models; Law et. al. (1990); Taiping et. al. (1984); and Youd and Idriss, 1997 (Modified Seed Method) were used to predict liquefaction for the design earthquake based on SPT results. A full explanation of these liquefaction prediction methods can be found in their respective references and are briefly described below.

Taiping, Chenchun, Lunian and Huishan Method

The Taiping et. al. (1984) method is a modified form of the Liquefaction Potential Index suggested by Iwasaki et. al. (1982). Taiping et. al.'s equation takes the following form:

$$N' = N_1[1 + 0.125(d_s - 3) - 0.05(d_w - 2) - 0.07d_c] \qquad \textbf{(1)}$$

Where: N' = standard penetration (SPT) value;

N_1 = critical SPT value in the case of d_w=2 and d_s=3. With earthquake intensities of 7, 8, & 9, N_1 is taken to be 6, 10 & 16 respectively;

d_s = depth of soil, (m);

d_w = depth of ground water, (m);

d_c = content of clay grains (d<0.005 mm) in the soil, (%). Maximum 10%.

Law, Cao and He Method

Law et. al. propose an energy method that is based on laboratory and in situ tests from 15 major earthquakes (magnitudes ranging from 5.5 to 8.4). Cyclic triaxial and cyclic simple shear tests showed that a relationship exists between the dissipated energy during cyclic loading and the excess pore pressure. This relationship was then combined with an energy attenuation relation. Equation 2 indicates that liquefaction will take place when the seismic energy intensity function, T(M,R), exceeds the liquefaction resistance function, $\eta_L(N_1)$:

$$\frac{T(M,R)}{\eta_L(N_1)} \geq 1.0 \qquad \textbf{(2)}$$

where: $T(M,R) = 10^{1.5M} / R^{4.3}$ **(3)**

and: $\eta_L(N_1) = 2.28 x N_1^{11.5} x 10^{-10}$ *for sand* **(4)**

$\eta_L(N_1) = 1.14 x N_1^{11.5} x 10^{-9}$ *for silty sand* **(5)**

where: N_1 = corrected SPT value;

M = earthquake magnitude;

R = hypocentral distance.

Modified Seed Simplified Procedure

The Seed Simplified Procedure has been used over the past 30 years to evaluate the liquefaction resistance of soils. Since its first inception it has undergone many refinements. Predominantly the refinements have accounted for additional earthquake reconnaissance data. In this study, the 1997 NCEER Workshop on the Evaluation of Liquefaction Resistance of Soils (Youd and Idriss) is used as the basis for the Simplified Procedure. In this method, the onset of liquefaction occurs when the Cyclic Stress Ratio (CSR) exceeds the Cyclic Resistance Ratio (CRR) as follows:

$$CSR = 0.65\left(\frac{a_{max}}{g}\right)\left(\frac{\sigma_{vo}}{\sigma_{vo}'}\right) r_d \qquad \textbf{(6)}$$

where a_{max} = maximum horizontal acceleration at the ground surface.
g = 9.81 m/s^2 acceleration due to gravity.
σ_{vo} = total vertical overburden stress.
σ_{vo}' = effective vertical overburden stress.

and r_d = $1.0 - 0.00765z$ if $z < 9.15m$ **(7)**
= $1.174 - 0.0267z$ if $z = 9.15$ to $23m$

where z = depth in metres

The simplified procedure uses the SPT N-value that is standardised according to equation 8.

$$(N_1)_{60} = NC_NC_EC_BC_RC_S \qquad \textbf{(8)}$$

where $(N_1)_{60}$ = Corrected SPT N-value (blows/300mm)
N = raw SPT N-value (blows/300mm)
C = correction factors set out in Table 2 below

Table 2. Corrections to the SPT

Factor	Equipment Variable	Correction
Overburden Pressure C_N		$(100kPa/\sigma_{vo}')^{0.5}$ but ≤ 2
Energy Ratio C_E	Donut Hammer	0.5 to 1.0
	Safety Hammer	0.7 to 1.2
	Automatic Hammer	0.8 to 1.5
Borehole diameter C_B	65 to 115 mm	1.0
	150mm	1.05
	200mm	1.15
Rod length C_R	3 to 4m	0.75
	4 to 6m	0.85
	6 to 10m	0.95
	10 to 30m	1.0
Sampling method C_S	Standard sampler	1.0
	Sampler without liner	1.1 to 1.3

The corrected SPT N-value is further corrected to allow for variations in fines content. The fines correction used has the following format:

$$(N_1)_{60cs} = \alpha + \beta\,(N_1)_{60} \qquad \textbf{(9)}$$

Where α and β are coefficients determined from the following equations:

$\alpha = 0$ for $FC \leq 5\%$ **(10a)**

$\alpha = \exp\,[1.76 - (190/FC^2)]$ for $5\% < FC < 35\%$ **(10b)**

$\alpha = 5.0$ for $FC \geq 35\%$ **(10c)**

$\beta = 1.0$ for $FC \leq 5\%$ **(11a)**

$$\beta = [0.99 + FC^{1.5}/1000)] \qquad \text{for } 5\% < FC < 35\% \qquad \textbf{(11b)}$$

$$\beta = 1.2 \qquad \text{for } FC \geq 35\% \qquad \textbf{(11c)}$$

Where FC is the fines content measured from laboratory gradation tests on retrieved soil samples. Finally, $CRR_{7.5}$ is modified to account for variations in earthquake magnitudes (original relationship was developed for only magnitude 7.5 earthquakes) using equation 12 (Youd & Idriss).

$$MSF = 173\ (M)^{-2.56} \qquad \textbf{(12)}$$

where MSF = Magnitude scaling factor
M = Earthquake magnitude

Liquefaction Prediction

Laboratory soil gradings were available for around 8 per cent of the soils recovered during this investigation, the remaining soil particle size distributions were estimated based on these results and their field descriptions. The liquefaction prediction methods of Law et. al. (1990), Taiping et. al. (1984) and the Simplified Seed Method (Youd and Idriss, 1997) were used to evaluate liquefaction susceptibility using these soil parameters and field testing results. Following evaluation of all of the soils potential to liquefy, the results were then filtered to eliminate soils not noted as being liquefiable. For example: soils above the water table; peats, clays and clayey soils with moderate to high plasticity; and those that lay outside the criteria set by the prediction models, were considered unlikely to liquefy. This analysis was repeated for both the Foothills and Alpine Earthquake scenarios.

The results for each borehole were then compiled together and plotted on a single graph, the Alpine Earthquake scenario graph is shown in Figure 2. Susceptibility trends from one borehole to adjacent ones were not clear in this format, nor were trends in a cross section format. Consequently, regional liquefaction susceptibility trends are not easily defined.

Figure 2 is interpreted in the following manner. Where a pyramid is absent then the soil at this depth and for that borehole is not considered liquefiable, by any of the three prediction methods. Furthermore, where pyramids exist, their heights depict the level of susceptibility. A full height pyramid indicates a soil that is predicted to be liquefiable by all three models ("High Susceptibility"). Whereas, a pyramid that is truncated to a low level depicts a soil that was classified by only one prediction model ("Low Susceptibility").

Both the Alpine and Foothills Earthquake scenarios predicted a similar range of soils to liquefy. Although, the severity and number of soils predicted to liquefy is higher in the Alpine Earthquake scenario, albeit marginally (20 per cent). Notwithstanding this, their maps of liquefaction hazard are exactly the same.

Some regional observations are made as follows:

- A large number, 60 per cent, of the soils predicted to liquefy are located near to the ground surface (i.e. within 5m). The reason for this is that they are the youngest soils and therefore more prone to liquefaction. Furthermore, their confining stresses are low.
- Conversely the soils between 10m to 15m depth are the least prone to liquefaction with only 10 to 15 per cent of the soils predicted to liquefy. On average the tendency to liquefy decreases with depth. Notwithstanding this, the exception to this rule is evident in some of the boreholes.
- Another spatial observation that could be developed is that the severity of liquefaction appears to decrease with distance back from Pegasus Bay. This trend could be expected as the thickness of sand deposits (primarily Christchurch Formation sands) decreases with distance inland from the coastline and also the average age of the soil increases. In general 17 per cent of the soils examined for the Foothills Earthquake were found to be liquefiable and 21 per cent for the Alpine Earthquake. Furthermore, around one third of

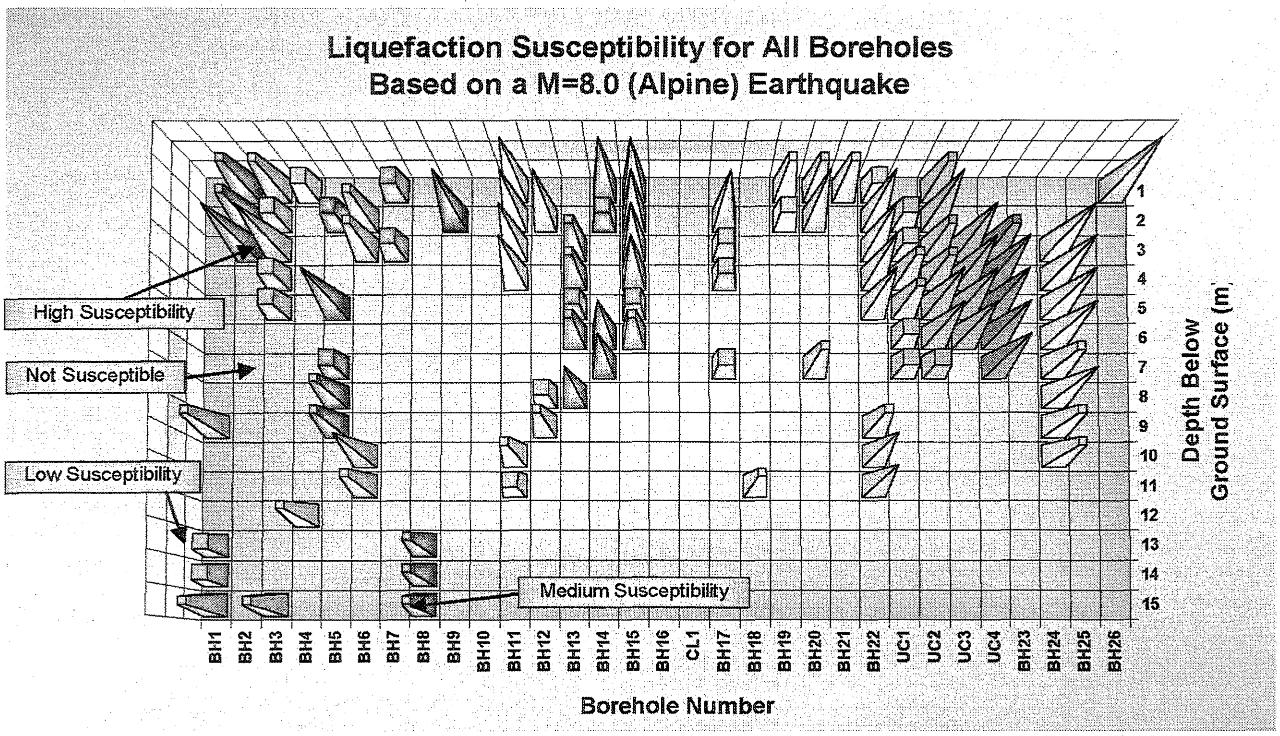

Figure 2. Liquefaction susceptibility for all boreholes based on a M=8.0 Alpine Earthquake

the silts and sands encountered during this investigation were found to be liquefiable to some degree.

Liquefaction Hazard Map

For ease of reference, the three-dimensional results generated have been plotted on a Liquefaction Hazard Map (Figure 3). The Liquefaction Hazard Map was generated by the method outlined in Table 3 to reduce the 3-D data to a 2-D map. This procedure in Table 3 helps to quantify that many metres depth of soil predicted to have medium susceptibility may cause greater ground damage than only a single metre thickness of soil predicted to have high susceptibility.

Table 3. Logic for Defining Levels of Liquefaction Hazard

Soil Susceptibility	Liquefaction Hazard
Any soil with high susceptibility	HIGH
Greater than one metre of soil with medium susceptibility	HIGH
Less than one metre of soil with medium susceptibility	MEDIUM
Greater than one metre of soil with low susceptibility	MEDIUM
Less than one metre of soil with low susceptibility	LOW

Three sets of data were used to generate the map as follows:

- The results of this current borehole investigation were used to define regions of high, medium and low hazard of liquefaction. These results were given a high rating in terms of accuracy.
- The CPT results (Berrill et. al., March 1994 and Connell Wagner, 1999) were treated in a similar manner to results from this study and were given a high accuracy rating.
- Lastly the Environment Canterbury well logs (January 2000) were used, albeit cautiously, to in-fill areas between the above two sets of data. This set of data was given a low rating in terms of accuracy and therefore when a conflict arose, the more highly rated data above was given priority. Environment Canterbury well data was mapped as follows:
  - 0 – 1m of sand recorded within 15m of ground surface – low susceptibility

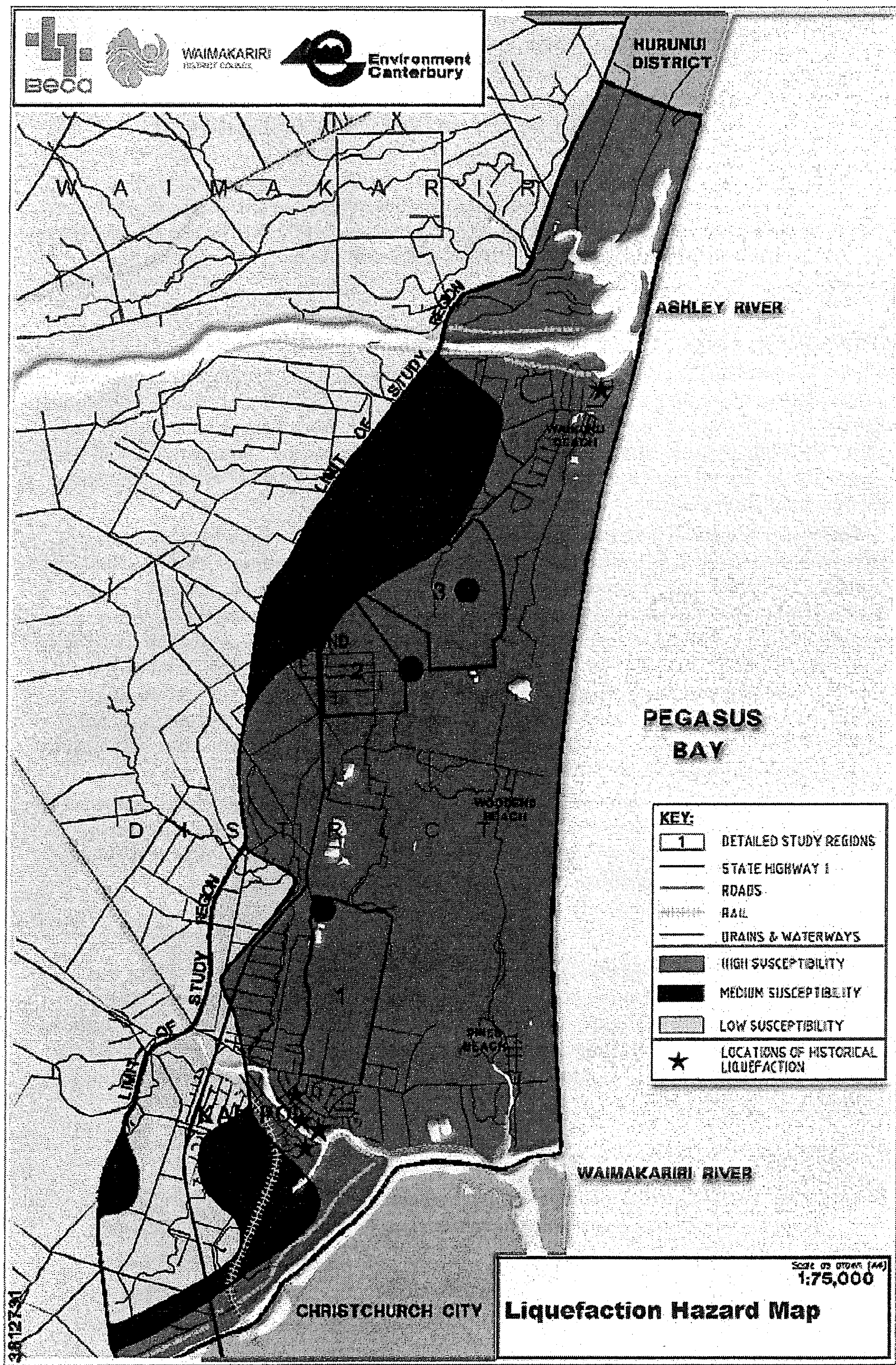

Figure 3 Liquefaction Hazard Map for the Study Region, showing locations of historical liquefaction.

- 2 – 5m of sand recorded within 15m of ground surface – medium susceptibility
- 5 – 15m of sand recorded within 15m of the ground surface – high susceptibility

Liquefaction settlements were calculated for both the Foothills and Alpine Earthquake scenarios based on the method of Bartlett & Youd (1992). Historically, there has been a lack of detailed investigations into observed liquefaction settlement and hence empirical prediction formulae should be considered indicative only. Level ground settlements ranged up to an average of 300mm for both the Foothills and Alpine Earthquake scenarios. By far the largest predicted settlements are predicted to occur adjacent to the coastline and beside Kaiapoi River (i.e. at the location of the youngest soils). Large settlements are also predicted for the south/south-western end of Woodend.

Conclusions

A study has been undertaken to provide a better understanding of the liquefaction potential that may affect the eastern side of the Waimakariri District in Canterbury, an area of historical liquefaction. Twenty-six new boreholes were used to supplement existing geotechnical data within the Study Region. Using two earthquake scenarios (a nearby Foothills Earthquake and a more distant Alpine Fault Earthquake), liquefaction susceptibility was defined using three different prediction models.

The results generated indicated that the eastern side of the Study Region, which contains deep dune sand deposits (Christchurch Formation), has a high susceptibility to liquefaction. Furthermore, 21 per cent of the soils encountered within 15m of the ground surface were found to be liquefiable in an Alpine Earthquake scenario. The high susceptibility zone extends out to the western boundary of the Study Region in three locations and into the heart of the largest town, Kaiapoi. Average level ground liquefaction settlements of up to 300mm were predicted for both earthquake scenarios (peak settlements are likely to exceed this valve). The extent of areas classified as having a high susceptibility to liquefaction is not significantly different to those in the eastern side of Christchurch and some other geologically young coastal areas around New Zealand.

A major benefit of this regional liquefaction study is that the need for detailed site investigations has been defined. Furthermore, information is now available for ratepayers through Resource and Building Consents (PIMs and LIMs), and information is available for planning, emergency management, environmental and education/advice.

Acknowledgements

I would like to thank Waimakariri District Council and Environment Canterbury for the assistance during, and the funding of, this project. We wish to thank the landowners for permission to undertake the fieldwork and Environment Canterbury, University of Canterbury and Canterbury Lakes Development Ltd for making their investigation records available for inspection and use. Finally, I would like to thank Dr Toan for his assistance with the study project.

References

Bartlett, S. F. and T. L. Youd 1992. Empirical Prediction of Lateral Spread Displacement. *Proc. 4th Japan-US Workshop on Earthquake Resistant Design of Lifeline Facilities, Honolulu.* pp 351-366.

Beca Carter Hollings & Ferner Ltd, 2000. Liquefaction Study. *Beca Carter Hollings & Ferner Ltd Job No. 3812731,* Prepared for Waimakariri District Council (Contract #99/17) and Environment Canterbury (EC Pub No. U00/12).

Berrill JB, PC Mulqueen, ETC Ooi and J-L Pautre, March 1994. Liquefaction at Kaiapoi in the 1901 Cheviot, New Zealand Earthquake. *Research Report, Dept. of Civil Eng., University of Canterbury*, Report 94/3.

Berrill, JB, PC Mulqueen and ETC Ooi, September 1994. Liquefaction at Kaiapoi in the 1901 Cheviot, New Zealand, Earthquake. *Bull. NZ Nat. Soc. of Earthquake Eng.*, Vol. 27, N° 3.

Brown LJ, 1973. Geological Map of New Zealand, Sheet 76, Kaiapoi, 1:63,360. *NZGS.*

Brown LJ and JH Weeber, 1992. Geology of the Christchurch Urban Area, 1:25,000. *IGNS*,.

Connell Wagner Ltd, 1999. Canterbury Lakes Development Sub-division Consent Application Liquefaction Study Report, Alabaster, D and B Fairburn, for Canterbury Lakes Development Ltd.

Environment Canterbury, 2000. Wells With Strata Data. Unpublished data.

Law, K., Y. Cao and G. He, 1990. An Energy Approach for Assessing Seismic Liquefaction Potential. *Can. Geotech. J.* Vol. 27, No. 3, pp 320-329.

Stirling, M, M Yetton, J Pettinga, K Berryman and G Downes, 1999. Probabilistic Seismic Hazard Assessment and Earthquake Scenarios for the Canterbury Region, and Historic Earthquakes in Christchurch: Stage 1 (Part B) of Canterbury Regional Council's Earthquake Hazard and Risk Assessment Study. *IGNS.* Canterbury Regional Council Report N° U99/18.

Taiping, Q., W. Chenchun, W. Lunian and L. Huishan, 1984. Liquefaction Risk Evaluation During Earthquakes. *Int. Conf. on Case Histories in Eng.- Proc.*, St Louis, Vol. 1, pp 445-454.

Waimakariri District Council and Canterbury Regional Council, 1999. Professional Services Contract 99/17 Liquefaction Study. Tender Documents.

Youd, T. L. and I. M. Idriss, 1997. Proceedings of the NCEER Workshop on Evaluation of Liquefaction Resistance of Soils. *Technical Report NCEER-97-0022.* Salt Lake City, Utah.

Soil liquefaction hazard in Christchurch

K. J. McManus

Dept. of Civil Engineering, University of Canterbury

J. B. Berrill

Dept. of Civil Engineering, University of Canterbury

Abstract

The risk of soil liquefaction occurring at four sites in Christchurch is studied. Cone penetrometer data from each of the sites is examined and three commonly used procedures are used to predict whether or not liquefaction is likely to occur during a scenario earthquake of M_w 7.5 at an epicentral distance of 50 km.

Two of the sites are located in the dune sand deposits of the eastern coastal margin and were found to be of low risk because the sands were generally very dense. By contrast, the two sites in the highly variable soils of western Christchurch were found to be of high risk with loose sand and silty sand horizons in a profile of interbedded silts, sands, peats, and clays.

Analysis of cone penetrometer data from Adapazari, which suffered substantial damage from soil liquefaction during the Marmara Sea earthquake in 1999, showed strong similarities to the soil profiles of the test sites from western Christchurch, providing a warning of the extent of damage that might be expected for the scenario earthquake in Christchurch

Results of this study suggest that existing liquefaction hazard maps for Christchurch may be overly conservative in mapping the eastern dune sands as all medium or high risk, and unconservative in mapping much of the western city as low risk. The benefit of mapping is questionable given that pockets of liquefiable soils probably exist in most areas of the city and may only be discovered with site-by-site investigations.

Introduction

Christchurch is located at the confluence of three main geomorphic regions: the Banks Peninsula volcanic complex, a river floodplain, and the coastal margin. At the time of the post-glacial climatic maximum of 6500 years before present, the coastal margin had moved inland approximately 10 km from its present location (Brown & Weeber, 1992) to be situated close to present day Riccarton. Since then, the beachfront and associated ridges and sand dunes have moved steadily seaward, leaving behind a confusion of swamps, estuarine deposits, sand dunes, spring-fed meandering streams, and river flood deposits.

The near surface depositional environment, with the exception of the sand dunes and gravels of the river flood deposits, has generally been of extreme low-energy with pockets of loose fine sands, silts, and peats distributed across much of the City. This environment is likely to contain deposits of liquefiable soils.

The potential significance of the soil liquefaction hazard for Christchurch has been increasingly recognised since the publicity surrounding the enormous damage caused by soil liquefaction during the Niigata earthquake of 1961 (e.g. Eiby 1968, Fairless & Berrill 1984, Elder et. al. 1991, Guilhem and Berrill 1993, Berrill 1997, Cassassuce and Berrill 2000.)

Recently, the city of Adapazari, Turkey, was badly damaged by soil liquefaction during the 1999 Mw 7.4 Marmara Sea earthquake, centred some 30 km distant. There are significant similarities in subsoil conditions between Adapazari and Christchurch and a scenario earthquake for Christchurch proposed by the Christchurch Lifelines Study (Lamb 1997) is of similar magnitude and distance (Mw 7.5 at 50 km). As may happen in Christchurch, ground deformations were generally "patchy" throughout the area with some areas having no damage or only minor damage while other areas were affected by ground fractures and lateral movements and heaving associated with settlement of adjacent buildings. In the worst affected areas building settlements of one metre were typical, as shown in Figure 1, with some buildings becoming unstable and tipping over, as in Figure 2. Pipeline damage in Adapazari was extensive. Sand boils were not widely observed but close inspection of many settled buildings showed small amounts of ejected, stratified, fine sand.

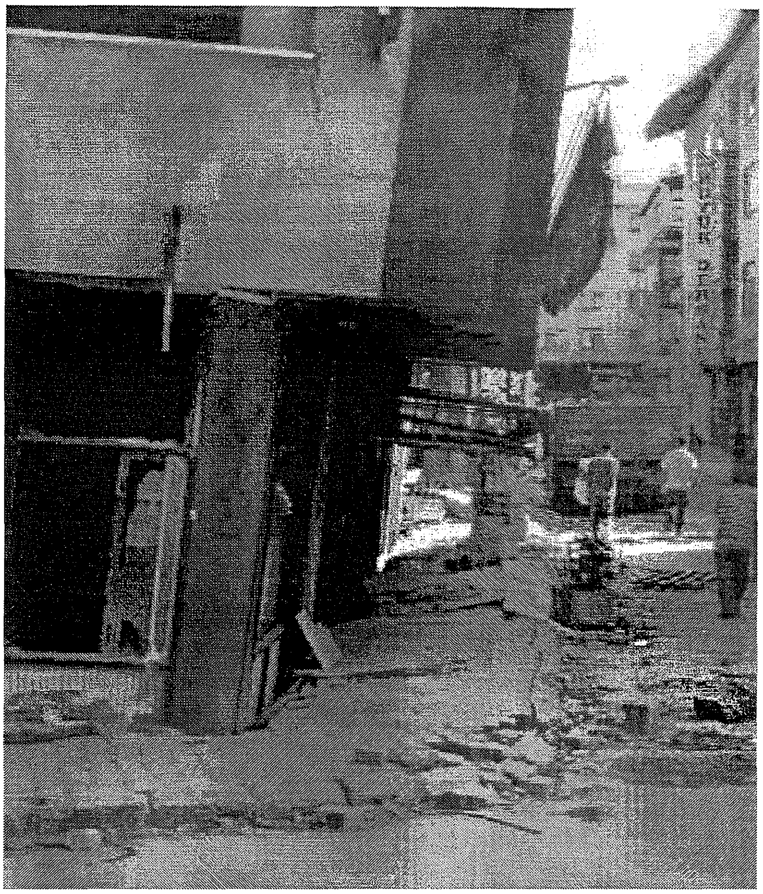

Figure 1. Settlement of building on raft foundation in Adapazari, Marmara Sea earthquake, 1999.

A liquefaction susceptibility map for Christchurch, shown in Figure 3, has been proposed by Brown and Weeber (1992) and is based on near surface geology. This map conforms to the traditional view that the majority of soil liquefaction hazard in Christchurch lies east of Cathedral Square where there are obvious and extensive sand deposits and a high water table.

This paper will challenge that traditional view and propose a more or less opposite one: that the extensive dune sands of eastern Christchurch are unlikely to liquefy while the highly variable and finely interbedded sediments distributed throughout much of the rest of the city do contain highly susceptible deposits. High quality data from recent cone-penetrometer (CPT) soundings at two sites in the dune sand areas will be used to show that these sand deposits can be very dense and unlikely to liquefy. Data from two CPT soundings west of Hagley Park, generally mapped as "Low" in Figure 3, will be used to illustrate the high risk that exists in these highly variable deposits. Comparisons will be drawn to similar high risk deposits in Adapazari also by using CPT data from tests performed after the earthquake there.

Sand boils were observed in Kaiapoi during the Mw 6 – 7.5 Cheviot earthquake of 1901 (Eiby 1968, Berrill et al., 1994) but there were no recorded observations in Christchurch. However, there were few sand boils observed in Adpazari despite the enormous damage that occurred and the large number of highly qualified observers who visited soon afterwards.

Sand ejection was probably suppressed by the surface crust of silty clay with minor ejecta being evident around building foundations and utility poles.

Scenario Earthquake

The scenario earthquake of the recent Christchurch Engineering Lifelines Study (Lamb, 1997) was adopted for this study: An M_w 7.5 earthquake originating in the foothills of the Southern Alps, some 50 km distant, with an estimated return period of 150 years. Such an earthquake is expected to cause peak ground accelerations of 0.45 g at strong soil sites in Christchurch.

Figure 2. Overturning of building in Adapazari during Maramara Sea earthquake, 1999.

Methodology

Liquefaction hazard at each of the sites was evaluated from high-quality cone penetrometer (CPT) sounding data. Three commonly used procedures were applied to the data from each site to identify strata that are likely to liquefy during the scenario earthquake: Davis and Berrill (1982), Law (1990), and Shibata and Teparaksa(1988). Davis and Berrill and Law are both energy dissipation based procedures while the procedure of Shibata and Teparaksa is a stress based approach.

An automated algorithm was used to analyse the CPT data and predict soil liquefaction with the following key steps:

1. The CPT data was smoothed over 50 mm increments and the sleeve friction measurements moved forwards by 100 mm to overlay the cone tip measurements.
2. Soil type was interpreted from the smoothed tip and sleeve measurements using the method of Robertson and Campanella (1983).
3. The two coarsest soil types (sands and silt-sand) were considered potentially liquefiable while the remaining soil types were not considered as being liquefiable.
4. Total and effective overburden stresses were calculated by using average soil unit weights obtained from Hough (1969).

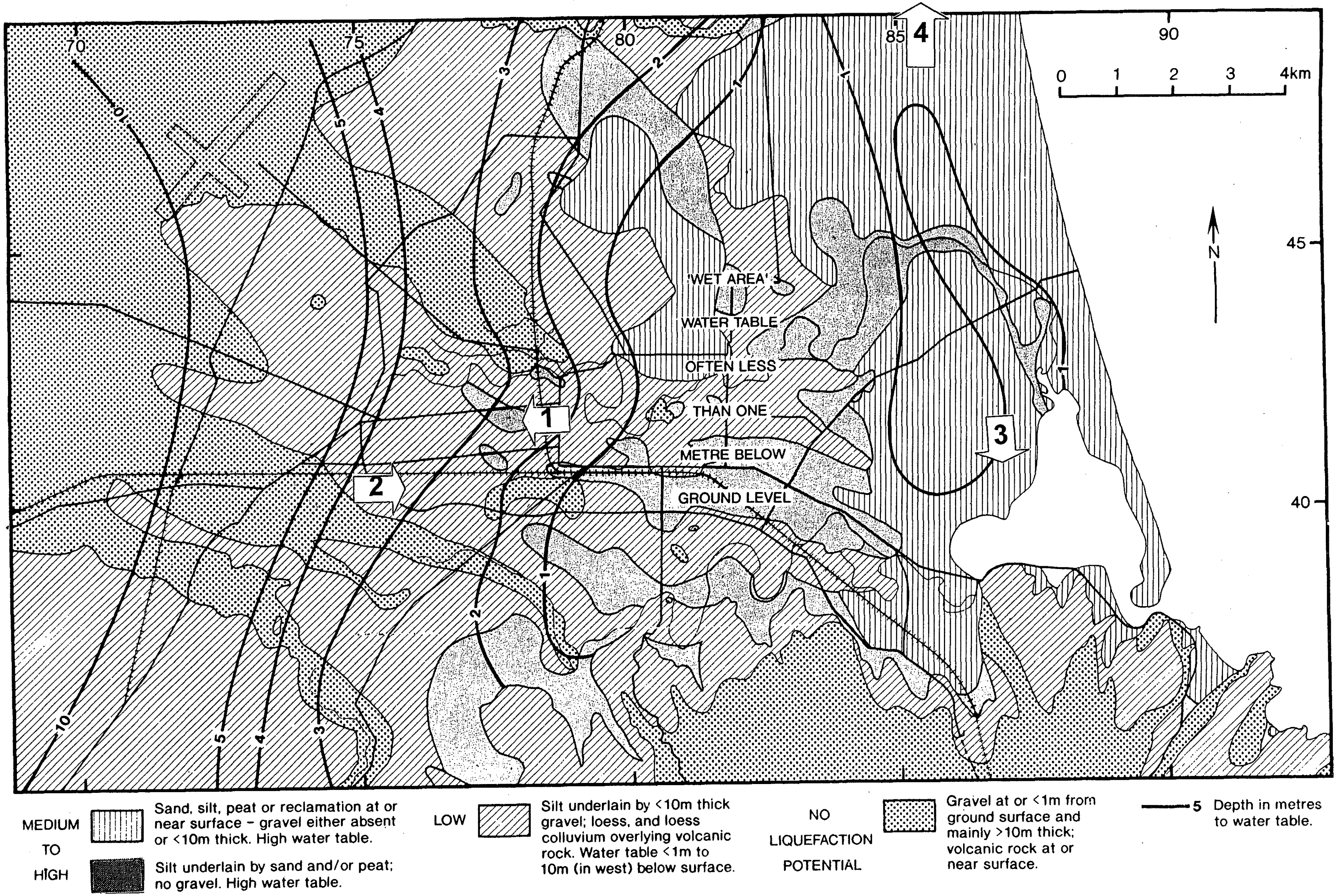

Figure 3. Liquefaction hazard map for Christchurch. Location of study sites indicated by arrows. (Source: Brown and Weeber, 1992)

5. For each 50 mm increment of smoothed data each of the three liquefaction assessment procedures were applied and the results assessed as indicating high or low risk of liquefaction.

The results of the analyses are presented graphically in Figures 5 through 9. In each of these figures the smoothed CPT data is shown plotted versus depth and there are four shaded bands indicating susceptible soil types and high risk strata predicted by each of the three procedures.

The procedures of Davis and Berrill and Law both require SPT blow count (N) data as input and so the CPT tip resistance (q_c) was used to predict corresponding N values using the following commonly used relationship:

$$N = \frac{q_c}{0.4} \tag{1}$$

The procedure of Shibata and Teparaksa requires values of soil cyclic stress ratio as input and these were estimated using the procedure of Tokimatsu and Yoshimi (1983).

The procedures of Davis and Berrill and Law both provide predictions of increase in pore pressure caused by the design earthquake (Δu). For this study, high risk of liquefaction was assumed for a ratio $\Delta u/\sigma'_v > 1$ and low risk otherwise.

The procedure of Shibata and Teparaksa predicts a critical value of cyclic stress ratio required to cause liquefaction based directly on the CPT measurements. For this study, the ratio of the cyclic stress ratio applied by the design earthquake to this critical cyclic stress ratio:

$$\frac{applied\ CSR\ from\ design\ EQ}{critical\ CSR\ from\ CPT} \tag{2}$$

was used to rank the risk of soil liquefaction: a value > 1 was taken as being high risk and low risk otherwise.

Adapazari

The part of Adapazari which was badly affected by soil liquefaction during the 1999 Marmara Sea earthquake was situated on level ground on a river flood plain. Adapazari was located approximately 30 km from the fault trace of earthquake, as shown in Figure 4. At the time of the earthquake the only information available concerning the sub-surface soil conditions was from some borehole logs with some SPT blow count data. Since the earthquake, a major international effort has been made to study the damage and underlying soils including a large number of CPT soundings with the as yet unpublished results available on the internet (Youd et. al.). The result from one of these CPT soundings from central Adapazari is shown in Figure 5 and indicates 8 metres of weak and thinly interbedded silts, sands, and clays.

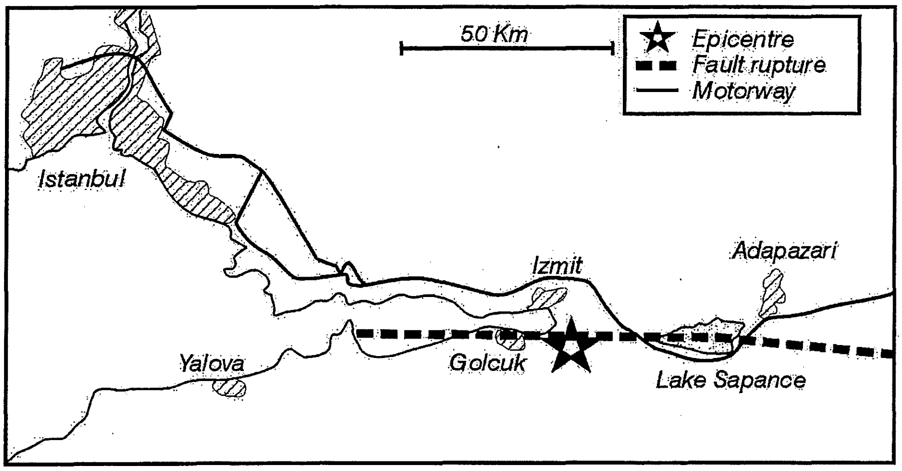

Figure 4. Surface trace of the Maramara Sea earthquake, 1999.

Typical foundation conditions are illustrated in Figure 2 with a heavy raft foundation (often hollow and ribbed) founded in the upper silty-clay material. Failure has presumably occurred because of liquefaction in shallow underlying sand strata (as seen in Figure 5) allowing a punching failure under one side of the foundation.

The data from the CPT sounding of Figure 5 has been analysed for this study using the methodology described herein and the measured parameters of the Marmara Sea earthquake: Richter magnitude of M_w 7.4, epicentral distance of 30 km. A ground acceleration of 0.41 g was adopted being the largest of the reported near field strong motion measurements (Sharpe et. al. 2000). The resulting predictions of soil liquefaction are shown graphically as the shaded bands in Figure 5.

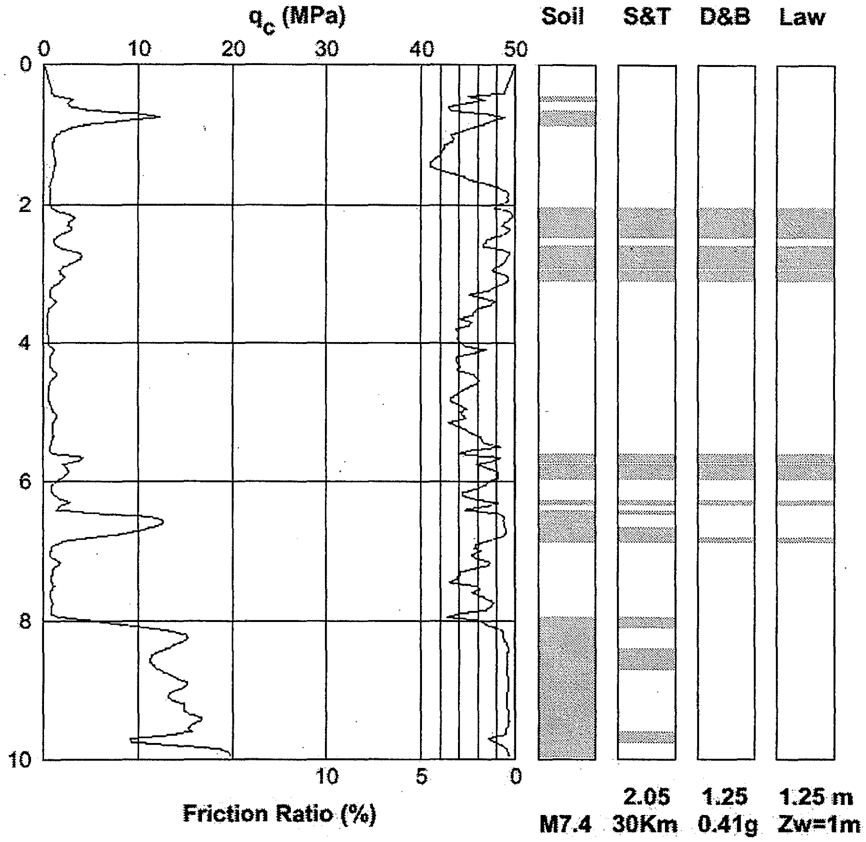

Figure 5. CPT profile and liquefaction assessment for site in Adapazari.

All three procedures used in this study predict a high risk of liquefaction in shallow, thinly interbedded sands (classified as silty sands by the analysis procedure used herein) between 2 and 3 metres below the surface. The modest thickness of liquefiable materials identified in this CPT sounding (less than 1 m in the first interval), together with the 2 m thick capping of cohesive materials, probably explains the lack of sand boil activity reported.

The soil profile of Figure 5 is remarkably similar to Figure 6 for a site in Riccarton which also shows a 2 m thick capping of cohesive materials then thin bands of silty sands interbedded with more silts.

Site 1: Riccarton

The profile for the Riccarton site is shown in Figure 6, and consists of thinly interbedded silts, sands, and clays, over dense gravel and with a 2 m thick crust of silty clay at the ground surface. A striking similarity with the profile for Adapazari in Figure 5 is evident.

All three procedures predict that soil liquefaction will occur in the susceptible strata under the scenario earthquake. The total thickness of soil liquefaction (1.55 to 2.35 m) is not very large but is greater than the thickness predicted for Adapazari and is likely to lead to similar failures for heavy structures on shallow foundations and extensive damage to in-ground services.

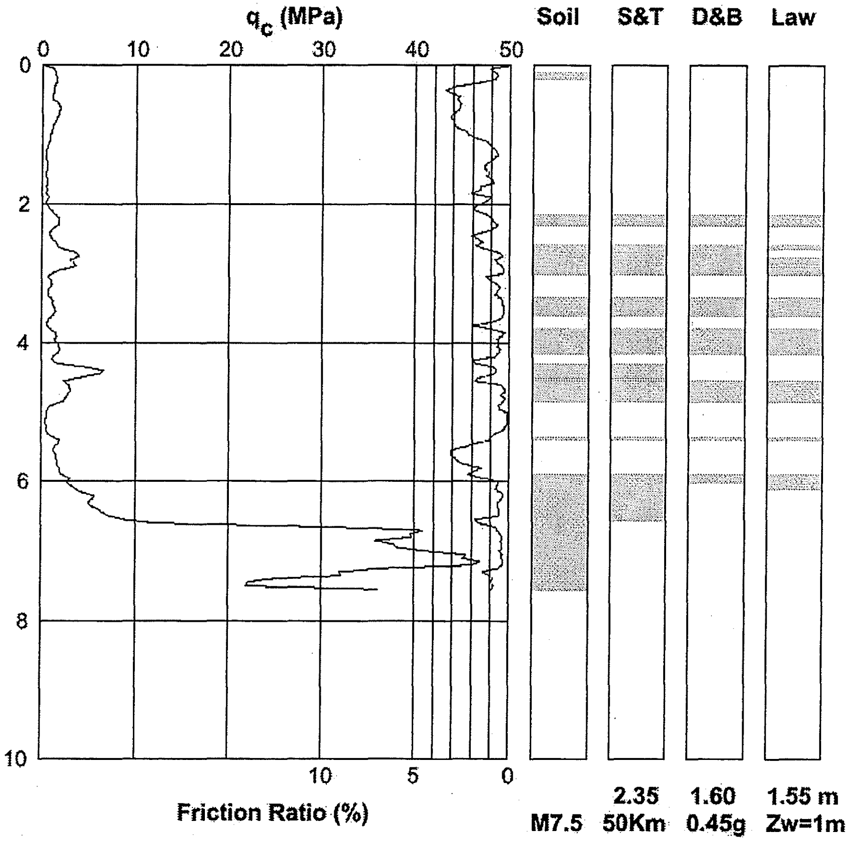

Figure 6. CPT profile and liquefaction assessment for Site 1, Riccarton.

The surface crust of silty clay may suppress the development of sand boils but is unlikely to prevent lateral spreading, as observed in Adapazari.

This site is considered to represent a *high* hazard from soil liquefaction and is probably typical of soil conditions that exist in many parts of Christchurch albeit in isolated pockets that are difficult to locate and map accurately. In this instance, the site is mapped correctly as being *high* hazard by the map of Brown and Weeber shown in Figure 3.

Site 2: Annex Road

The Annex Road site contains relatively thicker sand bearing strata of more than 1 m thick interbedded with silts, clays, and peats, as shown in Figure 7. All three procedures predict that the upper most sand strata (2 to 4 m) is likely to liquefy in the scenario earthquake, more than twice the thickness that liquefied at Adapazari. Additional liquefiable zones are identified at greater depths.

This site also represents a *high* hazard to structures on shallow foundations and to in-ground services, but is mapped incorrectly as a *low* risk area on the liquefaction hazard map of Figure 3.

Site 3: Bromley

This site lies in the dune sand belt of the coastal margin and Figure 8 shows a typical CPT profile of dense sands overlain by a shallow peat bed.

The three procedures predict that there is little risk of liquefaction occurring at this site apart from a narrow (0.25 to 0.5 m) band of loose sand immediately under the peat bed. The stress based procedure of Shibata and Teparaksa predicts additional thin bands of liquefaction lower in the profile but the energy based procedures of Davis and Berrill and Law do not.

This site represents a *low* hazard but is mapped as *medium* on the liquefaction hazard map of Figure 3.

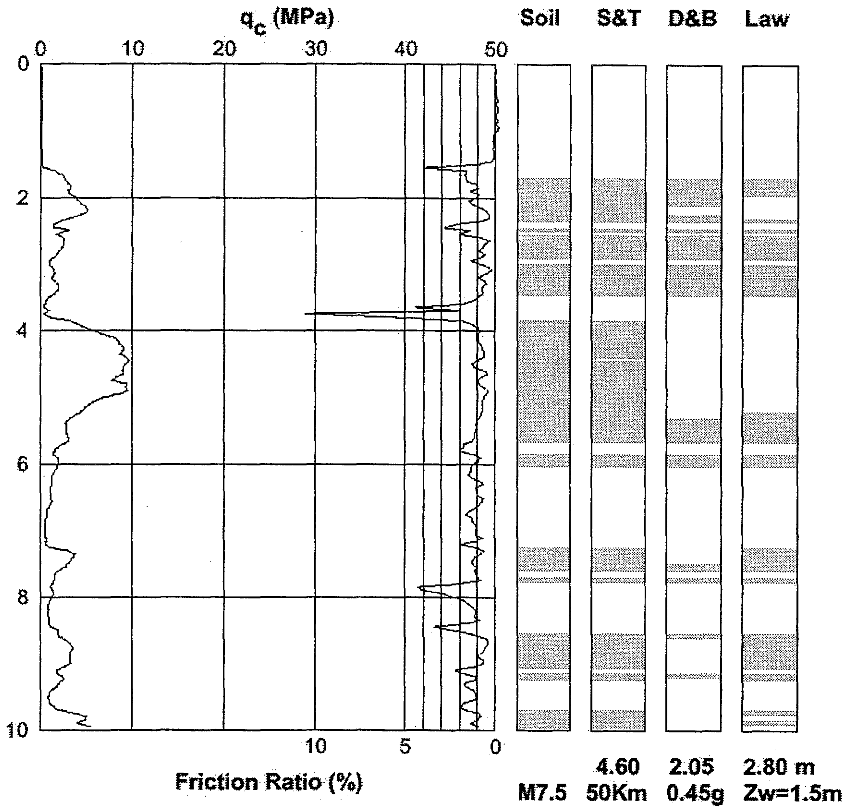

Figure 7. CPT profile and liquefaction assessment for Site 2, Annex Road.

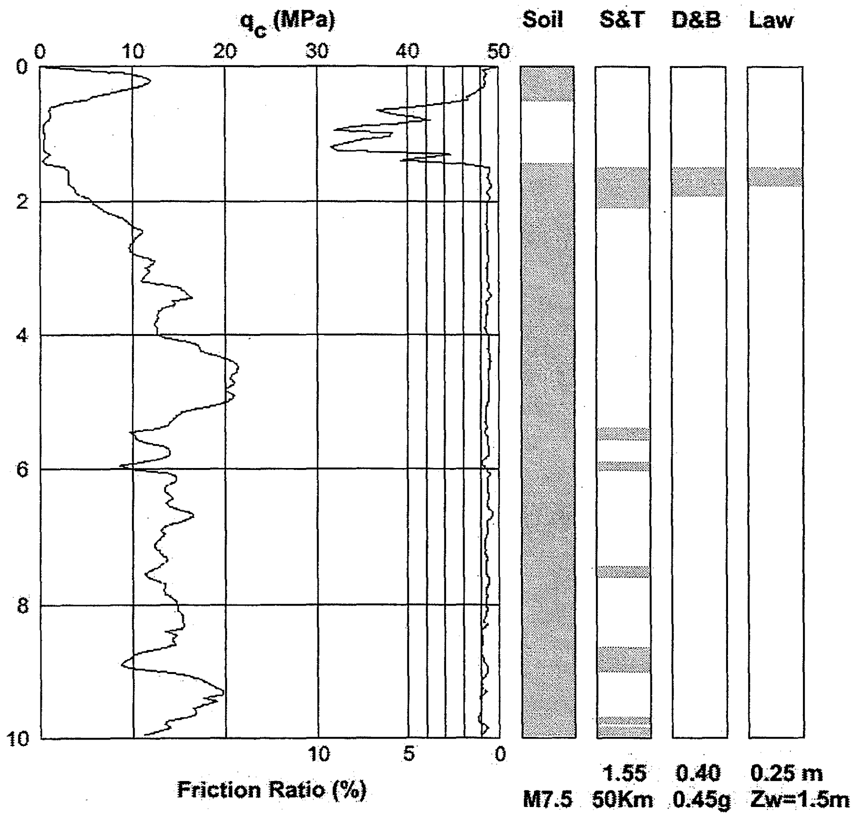

Figure 8. CPT profile and liquefaction assessment for Site 3, Bromley.

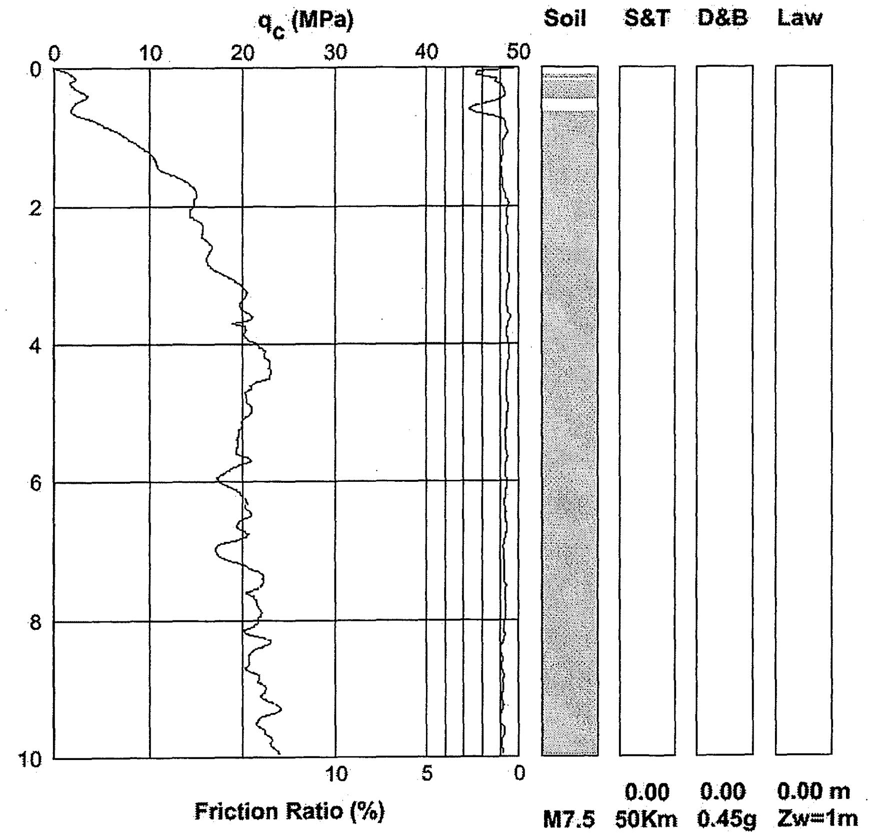

Figure 9. CPT profile and liquefaction assessment for Site 4, Stewarts Gully.

Site 4: Stewarts Gully

This site is outside the Christchurch City limit but is included in this study as a further example of the generally high density and consequent low liquefaction hazard of the dune sand deposits of the coastal margin.

The CPT profile is shown in Figure 9 and indicates 10 m of very dense sand. All three procedures agree that there is little risk of soil liquefaction at this site under the scenario earthquake.

Conclusions

Cone penetrometer data from four sites in Christchurch was analysed using three commonly used procedures to determine the risk of soil liquefaction occurring under a scenario earthquake of M_w 7.5 at 50 km distance. Two sites were located in the eastern dune sands of the coastal margin and were found to have a low risk of liquefying. Two sites in the western part of Christchurch, with complex profiles of interbedded silts, sands, and peats, were found to have a high risk of liquefying.

Comparisons were drawn between the two sites in western Christchurch and a site in Adapazari which was badly damaged by soil liquefaction during the recent Maramara Sea earthquake of 1999. Although there was little reported sand boil activity, probably because of a 2 m thick crust of silty clay, there was extensive damage to buildings on shallow foundations and to in-ground services. The extensive damage at Adapazari demonstrates that thinly interbedded pockets of liquefiable materials do represent a serious hazard, contrary to popular contemporary wisdom.

The results of this study suggest that existing liquefaction hazard maps for Christchurch may be overly conservative in mapping the eastern dune sands as all medium or high risk, and unconservative in mapping much of the western city as low risk. The benefit of mapping is questionable given that pockets of liquefiable soils probably exist in most areas of the city and may only be discovered with site-by-site investigations.

References

Berrill, J.B. (1997) "Seismic Liquefaction and Lifelines", Chapter X in A.J.W. Lamb (ed) *Risk & Realities*, Centre for Advanced Engineering, Univ. of Canterbury, Christchurch, NZ, pp. 47-70.

Berrill, J.B., Mulqueen P.C., and Ooi, E.T.C. (1994) "Liquefaction at Kaiapoi in the 1901 Cheviot, N. Zealand Earthquake", *Bull. NZ Nat. Soc. Earthq. Eng.*, Vol. 27, pp. 178-189.

Brown, L.J. and Weeber, J.H. (1992) *Geology of the Christchurch Urban Area*, Inst. Of Geological and Nuclear Sciences, Lower Hutt, New Zealand, 104 p.

Cassassuce, F. and Berrill, J.B. (2000) "CPT and Seismic Cone Site Investigation," *Research Report 2000-8*, Dept. of Civil Engineering, University of Canterbury, Christchurch.

Davis, R.O. and Berrill, J.B. (1982) "Energy Dissipation and Seismic Liquefaction in Sands," *Intl. Jnl. Earthq. Eng. and Struct. Dyn.*, Vol. 10, pp. 59-68.

Eiby, G A. (1989) *Earthquakes*, Heinemann Reed, Auckland, 166p.

Elder, D.McG., Yetton, M.D., and McCahon, I.T. (1991) "Christchurch: The Earthquake Hazard". Unpublished report by Soils and Foundations Ltd. for the Earthquake Commission, 290 p.

Guilhem, O and Berrill, J B. (1993) "Cone penetrometer results and estimates of Liquefaction Potential at some key Christchurch Lifeline Sites", *Canterprise Report CP/2245*, Univ of Canterbury, 53p.

Lamb, A.J.W. (Ed.) (1997) *Risks and Realities*, Centre for Advanced Engg., University of Canterbury, Christchurch.

Law, K., Cao, Y., and He, G. (1990) "An Energy Approach for Assessing Seismic Liquefaction Potential," *Canadian Geotechnical Jnl.*, Vol. 27, No. 3, pp. 320-329.

Robertson, P. K. and Campanella, R. G. (1983) "Interpretation of Cone Penetration Tests. Part I: Sand," *Canadian Geotechnical Journal,* Vol. 20, No. 4, pp. 718-733.

Sharpe, R.D., Bradshaw, D., Brown, N., Van Dissen, R., Kirkcaldie, D., McManus, K.J., Pham, T., and Stevenson, C., "Marmara Sea Earthquake Reconnaissance Report," *Bulletin of the N.Z. Soc. for Earthquake Engg.,* Vol. 33, No. 2, June 2000.

Shibata, T. and Teparaksa, W. (1988) "Evaluation of Liquefaction Potential of Soils Using Cone Penetration Tests," *Soils and Foundations*, Vol. 28, No. 2, pp. 49-60.

Tokimatsu, K. and Yoshimi, Y. (1983) "Empirical Correlation of Soil Liquefaction Based on SPT and Fines Content," *Soils and Foundations,* Vol. 23, No 4, pp. 56-74.

Hough, B. K. (1969) *Basic Soils Engineering*, 2nd. Ed., Ronald Press, New York, 634 p.

Youd, T.L., Bray, J.D., Onalp, A., Durgonuglu, H.T., and Stewart, J. (2001) "Documenting Incidents of Ground Failure Resulting from the August 17, 1999 Kocaeli, Turkey Earthquake," Internet Site http://nisee.berkeley.edu/turkey/adapazari/.

Liquefaction Hazard Assessment in Marine and Volcanic Flow Deposits, New Ireland Province, Papua New Guinea

N. A. Ridgley
Beca Carter Hollings & Ferner Ltd

A. L. Williams
Beca Carter Hollings & Ferner Ltd

D. V. Toan
Beca Carter Hollings & Ferner Ltd

A. L. Creighton
Lihir Management Company Ltd

Abstract

Lihir is one of four volcanic island groups which lie in a seismically and hydrothermally active area, north-east of the New Ireland coastline, some 600km north-east of the Papua New Guinea mainland. The island comprises a series of 5 stratovolcanoes of less than 3 million years old. One of these, the Luise volcano, located on the eastern coast of Lihir, is host to the Ladolam epithermal gold deposit, presently mined by Lihir Gold Ltd. The offshore area is dominated by a major debris flow associated with collapse of the volcano some 350,000 to 150,000 years ago, overlain by loose to medium dense interlayered marine sediment and tephra, and volcanic-rich sand. The site is expected to experience accelerations of 0.3g and 0.4g (Richter magnitude 7) at return periods of 80 and 500 years respectively.

At the mine site, the island comprises volcanic hillslopes rising steeply above a fringing terrace, leaving little land area onshore for stockpiling low grade ore (LGO) for later processing. For this reason, LGO is being stockpiled on a reclamation constructed into the Harbour. Previous studies based on cone penetration test (CPT) results have indicated that sediments underlying the reclamation are susceptible to liquefaction, indicating a risk to the reclamation and potential loss of the stockpiled LGO in a significant earthquake.

Additional field investigations comprising machine-drilled boreholes with standard penetrometer testing (SPT's) and laboratory testing including dynamic triaxial tests and accelerator mass spectrometry dating have been used to assess liquefaction hazard based on recently developed correlations and analysis techniques. The recent investigations highlight the importance of "Good Practise" for in-situ testing, and indicate that the sediments are likely to be less susceptible to liquefaction than indicated from previous analyses based on CPT's.

Introduction

Liquefaction can induce failure by a number of mechanisms including almost total loss of soil strength, lateral spreading (flow failure) of slopes, large settlements, loss of bearing capacity and buoyant rise of buried structures. Assessment of liquefaction risk and its potential affect on structures is therefore an important part of determining performance and likelihood of damage to structures due to earthquake shaking.

While the performance of clean sand during and following earthquake shaking is relatively well understood, the performance of silty sands, sandy silts and silts is more variable and criteria for evaluating liquefaction risk are less conclusive.

This paper provides a short review of liquefaction risk assessment techniques as applied to silty sands and sandy silts underlying a coastal reclamation. An accurate assessment of liquefaction potential is important because the reclamation is to be used for stockpiling low-grade ore (LGO) for future gold extraction. Also of interest is the difference between results of in-situ strength testing obtained in investigations carried out at similar locations in 1999 and 2000.

Geological and Site Setting

Geological Setting

Lihir is one of four volcanic island groups (Tabar-Lihir-Tanga-Feni (TLTF)) which lie north-east of, and parallel to the New Ireland coastline, some 600km north-east of Papua New Guinea (Figure 1). Volcanism is believed to have commenced about 3.5 million years ago at Tabar, and migrated south-east. The youngest sub-aerial eruptions have been dated at about 2300 years before present on Feni Island (Licence et al 1987).

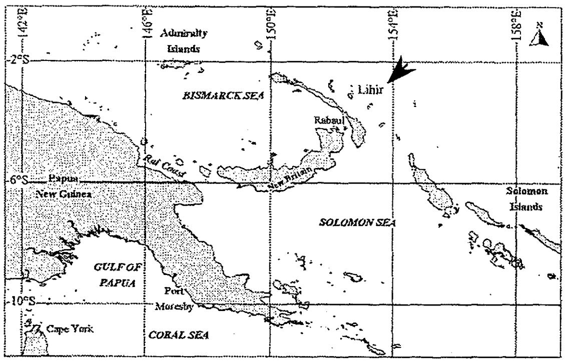

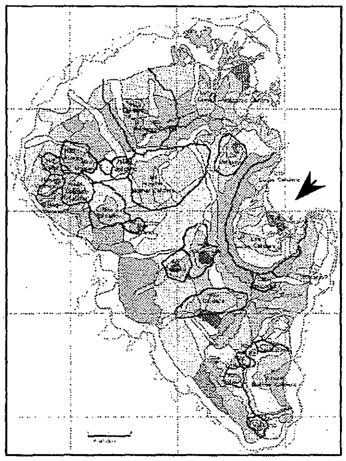

Figure 1. Lihir Island, Papua New Guinea

Four recently active submarine volcanoes (World, TUBAF, Conical and Edison seamounts) have been identified on the flanks of Lihir Island (Herzig et al 1994, Herzig et al 1998). Present day volcanism and hydrothermal activity are believed to be associated with active extension of the New Ireland Basin along a conjugate set of north-east/north-west trending faults in the vicinity of Lihir.

Lihir Island itself comprises a series of five stratovolcanoes of Pliocene to Pleistocene age (between 3.5 million to less than 1 million years old). One of these, the Luise volcano, located on the east coast of Lihir, is host to the Ladolam epithermal gold deposit. Ladolam has a gold resource of over 40 million ounces, representing the largest epithermal gold deposit discovered to date. The mining operation consists of an open pit gold mine and processing facilities and has an anticipated life of greater than 30 years.

Major debris flows associated with collapse of the Luise volcano dominate the seafloor topography east of the island. These materials are overlain by a significant thickness of sediments derived from both marine and volcanic sources of less than 5000 years old.

Offshore Geology, Lihir Minesite

The LGO stockpile and reclamation are located adjacent to the modern shoreline within the breached "crater" of the Luise volcano. Surveys of the seafloor topography in the area of the reclamation indicate that the seafloor beneath the reclamation is sloping north-east at a gradient of around 3-5%. The gradient of the seafloor steepens at a water depth of around 30m, to between 10 and 15%.

The reclamation has been created by progressive back-dumping from trucks and spreading of the deposited materials by bulldozer. Reclamation currently extends some 180m to 300m from the natural shoreline to a maximum water depth of between 18m and 20m. The existing stockpile on the reclamation is around 20m high.

Sediments encountered below the reclamation comprise a relatively uniform volcanic-rich sand overlying a variable interlayered flow deposit of marine and "lacustrine" sediment and tephra, inferred to have developed as sea-levels altered and tephra was deposited from this and other neighbouring surface and subsurface volcanoes.

Andesitic to basaltic breccia was encountered beneath the sediments. The breccia exhibits significant variability in nature and strength.

Seismicity

Lihir lies in a seismically and hydrothermally active area. Several site-specific seismic hazard studies have been carried out, the latest of which was completed in 2000 using updated attenuation relationships and earthquake data (Beca, 2000a,b). This study identified that Richter Magnitude 7 earthquakes with peak ground accelerations (PGAs) of 0.3g and 0.4g have return periods of around 80 and 500 years respectively and that the "maximum credible shaking or acceleration" for this site is around 0.45g which has an assessed return period of 1000 years.

Geotechnical Investigations

A number of geotechnical field investigations have been undertaken to determine the nature and strength of the soils underlying the proposed reclamation at the mine site. These have included Cone Penetrometer Testing (CPT), and machine boreholes at around 26 locations prior to construction of the reclamation in 1991/92 and eight machine boreholes with standard penetrometer testing (SPT) drilled through the reclamation and into the underlying soils, four in 1999 and a further four in 2000. The four holes drilled in 2000 were located near to those drilled in 1999 for the purpose of confirming in-situ strength measurements and obtaining samples for laboratory testing.

The machine boreholes drilled in 1999 and 2000 were undertaken by a drilling company accustomed to investigating mine geology for progressing mine development. The crew and equipment were therefore experienced in hard rock coring techniques, but unfamiliar with drilling and recovery of poorly consolidated soils and in-situ strength testing.

The SPT measurements recorded in the 1999 and 2000 investigations are plotted against depth in Figure 2.

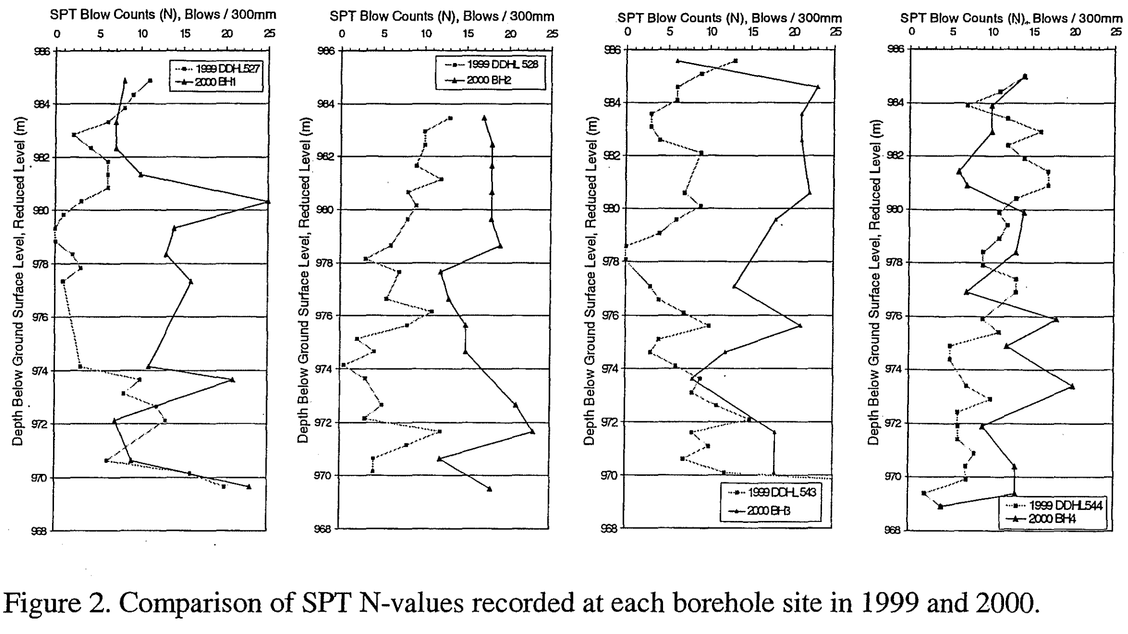

Figure 2. Comparison of SPT N-values recorded at each borehole site in 1999 and 2000.

Reliability and accuracy of SPT testing is dependent on the skills and experience of the driller, the equipment used and the materials investigated.

Particular care was needed in undertaking the SPT tests because hard andesite cobbles from the overlying reclamation could be readily pushed ahead of the drill bit and the drilling equipment available did not allow lost soil and rock to be effectively washed out of the hole. The sandy materials could also become disturbed beyond the drilled depth, in particular during casing installation. Key differences in drilling technique between the 1999 and 2000 investigations include advancing casing a small depth at a time, regular washing out of the hole, and effective recovery of samples by piston tube sampling and large diameter push tubes.

Soil Profile

The soil profile derived from borehole logs comprises:

Unit 1 – Reclamation Fill

Some 16m to 20m of loose to medium dense gravel to cobble sized andesitic breccia (with rare blocks of coral and monzodiorite) in a matrix of clay, silt and sand principally derived from the breakdown of hydrothermally altered andesite.

Unit 2 – Volcanic Rich Sand

Between 3m and 7m thick, medium dense and typically non-plastic, with a fines content (silt/clay component) varying between 10% and 33%, (average 20%). Triaxial tests indicate an effective angle of friction of 36.5° to 38°.

In Boreholes BH1 and BH4, located at either end of the reclamation (2000 investigation), SPT blowcounts were less (typically less than 10 blows/300mm) than recorded in BH2 and BH3 (18-22 blows/300mm). This difference was consistent with CPT data (1991/1992) which identified loose sand with end resistances of 0.5 to 0.9 MPa close to BH1, and of 1.7 to 2.5MPa close to BH3. These results suggest that the volcanogenic sand is more dense beneath the central part of the reclamation than at either end.

Unit 3 –Mixed Marine, "Lacustrine" and Tephra Deposit

Medium dense sand and firm to stiff sandy silt to silt of 10m to 15m thickness. Atterberg Limit testing indicates a moderately plastic material (average PL of 25%, LL of 43% and PI of 14%). Grading tests identify a fines content varying between 5% and 65% with an average of around 40%. Triaxial testing indicate an effective angle of friction of between 36° and 38.5°. SPT tests indicate that the strength of this layer is consistent across the site.

Liquefaction Assessment Techniques

There are a number of factors that affect the susceptibility of a site to liquefaction or that can be used to assess the risk of liquefaction. A range of these techniques have been applied to data obtained from the 2000 investigations.

Historical Criteria

Evidence of past liquefaction (such as sand boils) at or near to a site suggests that the site may be susceptible to liquefaction. We are not aware of the observation of such phenomena at or near this site.

Geologic Age and Origin

Studies suggest that susceptibility of older soil deposits to liquefaction is generally lower than that of younger deposits, and that liquefaction of Pleistocene age deposits (ie. >10,000 years) is uncommon.

Samples of partly decomposed wood were obtained from both the volcanogenic sands and underlying interlayered marine and tephra deposits and dated using AMS dating techniques. The dates are presented in Table 1.

Table 1. AMS Carbon Dates

Sample	δC^{13} (‰)	C^{14} Radiocarbon Age (years before present)
Volcanic – rich sand (19-22m depth BH4)	-27.9 ± 0.2	1398 ± 58
Mixed marine/tephra deposit (23-24m depth BH1)	-28.2 ± 0.2	4000 ± 70

Note: The seawater reservoir correction is not known for Lihir, however the local value for the Huon Peninsula, Papua New Guinea is 400 ± 70 years and this is the order of correction that should be subtracted from the conventional C^{14} value (Chappell & Polach 1991). This level of accuracy was not required for this study.

Both dates are significantly less than the 10,000 year criteria indicating that the sediments underlying the reclamation may be susceptible to liquefaction. The volcanogenic sand (Unit 2) is about 1000 years old (assuming a seawater reservoir correction of 400 years) indicating that this material is younger than the marine/tephra soils (Unit 3) and potentially more susceptible to liquefaction than the Unit 3 soils.

Particle Size and Soil Classification

The potential for a soil to liquefy decreases with increasing fines content, plasticity index, liquid limit and clay content.

Fines Content and Plasticity Index

Chinese Criteria (1979) state that a soil comprising more than 15% by weight of "fines" (silts and clays finer than 0.005mm), a liquid limit greater than 35% and in-situ water content less than 0.9 times the liquid limit, does not generally liquefy (Seed 1983, Wang 1979 in NCEER 1997).

Unit 2 is typically non-plastic with a clay content less than 10%. This unit does not meet the Chinese criteria for non-liquefiable soils, and may therefore be liquefiable.

Based on liquid limit and water content data, *Unit 3* lies within the "safe" zone, and is unlikely to liquefy. However, the fines content is 10% to 12% which is below the 15% criterion identified. Based on these criteria, the liquefaction potential of Unit 3 is inconclusive, but more likely to be non-liquefiable.

Particle Size Distribution

Tsuchida and Hayashi (1971) collected case records for sites where liquefaction has occurred and from this data determined ranges of particle size distribution for liquefiable soils;

The particle size grading curve for *Unit 2* lies within the "very easily liquefy" zone for both a uniform and well graded soil and would therefore be considered susceptible to liquefaction.

Unit 3 is better graded than Unit 2 (more variable grain size) and although a significant portion of the particle size grading curves lie within the "Very Easily Liquefy" zone, the lower end of the grading curves (fines content) lie above this area.

On this basis, Unit 3 is considered less susceptible to liquefaction than Unit 2.

Clay Content and Liquid Limit

Andrews and Martin (2000) determined that soils with a liquid limit greater than 32% and "clay" (particles finer than 0.002mm) content greater than 10% are not generally susceptible to liquefaction. These criteria are a refinement of the 1970's Chinese Criteria and are likely to provide a more accurate assessment.

Unit 2 has a low fines content and is not suitable for consideration under this criterion.

Unit 3 data for these criteria showed that around half the data points lie within the "Not Susceptible" zone, and half lie within the zones of "Further Study Required". Only one point lies within the zone "Susceptible" (Figure 3).

Based on these criteria, the liquefaction potential of Unit 3 is inconclusive, but more likely to be non-liquefiable.

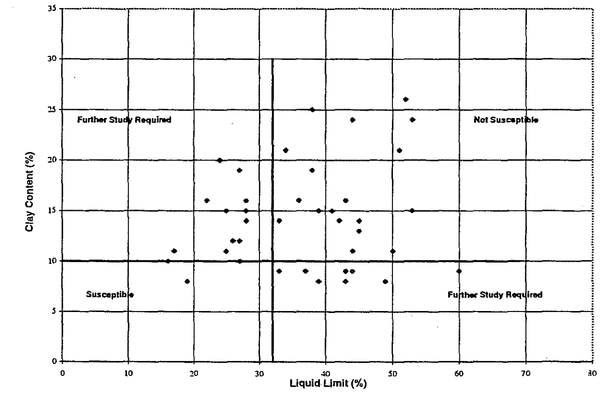

Figure 3. Andrews & Martin (2000) criteria, Unit 3

Saturation

Unsaturated soils have been reported to liquefy, however it is generally considered that at least 80 to 85 percent saturation is necessary for liquefaction to occur. The soils under consideration at this site lie well below mean sea level.

Soil Relative Density

The potential for liquefaction decreases with increased relative density and greater penetration resistance. Methods of assessing liquefaction potential based on the SPT and the CPT are (NCEER 1997) were applied.

Soil Penetration Resistance

The susceptibility of Units 2 and 3 to liquefaction was undertaken using the results of the 2000 investigation and the Modified Seed Procedure (in NCEER 1997). In this method, the onset of liquefaction is considered to occur when the Cyclic Stress Ratio (CSR) exceeds the Cyclic Resistance Ratio (CRR). The SPT results were corrected for overburden pressure, energy ratio, borehole diameter, rod length, sampling method and fines content.

The CRR (base curve) was calculated using the equation formulated by Youd & Idriss (NCEER 1997). The base curve was corrected to account for variations in earthquake magnitude using the appropriate magnitude scaling factor for an earthquake of Richter Magnitude 7.

The CSR was calculated in accordance with the simplified approach (NCEER 1997) using peak ground accelerations of 0.3g, 0.4g and 0.45g and was corrected for overburden pressure where the effective overburden pressure was greater than 100kPa.

The analyses indicate that *Unit 2* may liquefy, in particular where looser sand occurs beneath each end of the reclamation (Figure 4a). *Unit 3* is unlikely to liquefy in earthquakes with PGA up to 0.4g, but localised liquefaction may occur in earthquakes of 0.45g (Figure 4b).

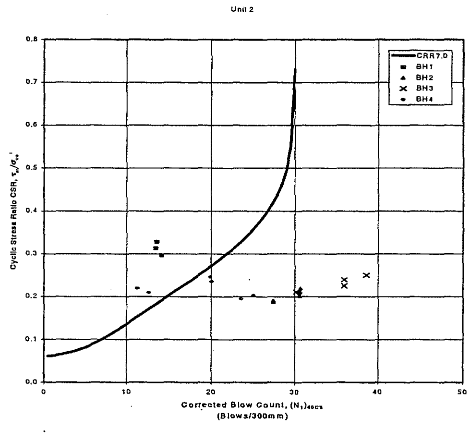

4a

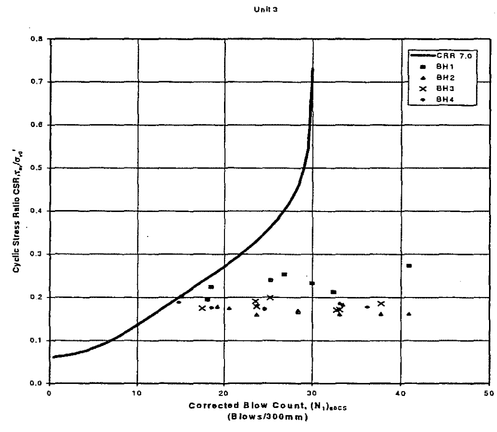

4b

Figure 4. Liquefaction prediction Modified Seed Procedure. 4a Unit 2; 4b Unit 3

Cone Penetrometer Testing

CPT data can also be used to assess the liquefaction resistance of soils. The primary advantage of the CPT is that a nearly continuous profile of penetration resistance is obtained for stratigraphic interpretation. However studies by Martin (NCEER 1997) suggest that liquefaction resistance estimated from the CPT procedure is lower than liquefaction resistance determined from parallel SPT tests. CPT testing undertaken at Lihir was completed prior to construction of the 16m to 20m thick reclamation. As the soils are likely to have consolidated and gained in strength beneath the weight of the reclamation, the CPT results are not applicable to assessment of liquefaction potential beneath the reclamation.

Laboratory Testing - Dynamic Triaxial Test Results

Dynamic triaxial testing was carried out at cyclic stress ratios representative of earthquakes with PGA's of 0.3g and 0.4g (ie. Cyclic stress ratios of 0.16 to 0.25 based on reclamation and proposed stockpile elevations). A summary of the results is presented in Table 2.

Table 2. Summary of Dynamic Triaxial Tests

Borehole	Depth	Silt/Clay Content (%)	$(N_1)_{60cs}$	PGA	Cycles to Liquefaction
4	21 (Unit 2)	32	20	0.3	> 150
2	24 (Unit 2)	16	27	0.4	40
2	30 (Unit 3)	65	28,37	0.4	20
3	30 (Unit 3)	43	17	0.3	> 150
				0.4	~ 30
2	33 (Unit 3)	41	23	0.3	> 150
				0.4	20 – 30

Dynamic triaxial tests indicate that at around 0.3g, liquefaction of both *Unit 2* and *Unit 3* is unlikely to occur. However, at a PGA of around 0.4g, liquefaction could occur, however the number of cycles to generate liquefaction (or zero effective stress) was greater than 20 (15 cycles is generally considered the equivalent effect of a Richter Magnitude 7.5 earthquake).

Immediately following cyclic testing, a monotonic load test was carried out. In this case the soil sample is loaded vertically to determine its strength at failure (after liquefaction). Three of the five samples could not be failed at the maximum load available. Two tests reached failure. These tests indicate that there was no strength loss following liquefaction with angles of friction remaining at around 38° to 39°.

All Methods

A summary of the findings of each test method is presented in Table 3. The results indicate that Unit 2, the volcanogenic sand, is likely to be susceptible to liquefaction, in particular beneath each end of the reclamation, and when PGAs exceed 0.3g. Unit 3 is less susceptible to liquefaction, and is unlikely to liquefy in a Richter Magnitude 7 earthquake with PGA of 0.4g or less. However, localised liquefaction of looser sandy zones could occur at a PGA of about 0.45g.

For the soils tested, analyses based on in-situ (SPT) testing and dynamic triaxial tests proved the most conclusive, however the accuracy of these methods is reliant on well controlled field testing and sampling techniques.

Table 3. Evaluation of Liquefaction Assessment Criteria

Criteria	Liquefiable		Non-liquefiable		Inconclusive	
	Unit 2	Unit 3	Unit 2	Unit 3	Unit 2	Unit 3
Historical					✔	✔
Geologic age	✔	✔				
% fines, LL, Wc (Wang 1979, Seed 1983)	✔			Probably		✔
Particle size (Tsuchida & Hayashi 1971)	✔	Possibly				✔
% clay, LL (Andrews & Martin 2000)	✔			Probably		✔
SPT (modified Seed in NCEER 1997)	✔ PGA > 0.3g	✔ PGA > 0.4g		✔ PGA < 0.4g		
Dynamic triaxial test	Possibly PGA > 0.4g	Possibly PGA > 0.4g	✔ PGA < 0.4g	✔ PGA < 0.4g		

Conclusion

The assessment of liquefaction hazard and risk to structures is an important part of evaluating performance and likelihood of damage to structures due to earthquake shaking.

The liquefaction risk at Lihir was assessed using a range of techniques including age, depositional environment, soil composition and plasticity, in-situ strength testing and dynamic laboratory testing. All methods provided some insight into the potential behaviour of the soils due to earthquake shaking, however analysis of the liquefaction potential of more silty soils proved less conclusive.

Geotechnical investigations at Lihir to determine in-situ strength using SPT have shown that SPT results are dependent on the skills and experience of the driller, the equipment used and the materials investigated. Highly variable results will occur if field testing and sampling is not well controlled.

For the soils considered, analysis based on carefully controlled in-situ (SPT) testing coupled with dynamic triaxial testing proved the most conclusive. The results indicated that the younger volcanogenic sand is likely to be susceptible to liquefaction, particularly looser zones encountered beneath either end of the reclamation and at PGAs in excess of 0.3g. The more silty interlayered marine and tephra deposit is less susceptible to liquefaction, with the potential for localised liquefaction of more sandy zones at a PGA of around 0.45g.

References

Andrews and Martin, 2000: "Criteria for Liquefaction of Silty Soils", *12th World Conference on Earthquake Engineering.*

Beca International Consultants Ltd, 2000a: Lihir Seismic Hazard Review.

Beca International Consultant Ltd, 2000b: Lihir Seismic Hazard Review, Addendum.

CIRIA 1995: Report 143 "The Standard Penetration Test (SPT): Methods and Use".

Herzig, P et al 1994: Submarine Volcanism and Hydrothermal Venting Studied in papua New Guinea. *EOS, Transactions American Geophysical Union* 75: 513-516.

Herzig, P et al 1998: Volcanism, Hydrothermal Processes and Biological Communities at Shallow SubmarineVolcanoes of the New Ireland Fore-Arc (Papua New Guinea). *Cruise Report Sonne – 133* (BMBF FK 03G0133A) July 10 – August 10, 1998. Freiberg University of Mining and Technology.

Licence, P.S., Terril, J.E., Fergusson, L.J., 1987: Epithermal Gold Mineralisation, Ambittle Island, Papua New Guinea. In: *Proceedings Pacific Rim Conference 1987: Australian Institute of Mining and Metallurgy*, Melbourne: 273-278.

National Centre for Earthquake Engineering and Research (NCEER) 1997: "Proceeding of the NCEER Workshop on Evaluation of Liquefaction Resistance of Soils".

Skempton, A. W. 1986: "Standard Penetration Test Procedures and the Effects in Sands of Overburden Pressure, Relative Density, Particle Size, Ageing and Overconsolidation". *Geotechnique* 36, No3, 425-447.

Tsuchida and Hayashi 1971: "Estimation of Liquefaction Potential of Sandy Soils" *US Japan Panel on Wind and Seismic Effects.*

US Department of Commerce 1998: *National Technical Information Service*, December 1998 "Training Course".

Late Quaternary Faulting beneath Matahina Dam

Tim McMorran

URS New Zealand Limited (previously Woodward-Clyde), 287 Durham Street, Christchurch

Kelvin Berryman

Institute of Geological and Nuclear Sciences Limited, 69 Gracefield Road, Lower Hutt

Abstract

Matahina Dam is an earth and rockfill embankment 82 m high and approximately 400 m long, located on the Rangitaiki River in the Bay of Plenty region of the North Island of New Zealand. A detailed Seismic Safety Evaluation completed in 1997 concluded that faults within the dam foundations are part of the active Waiohau Fault system. On the basis of that study, modifications were designed to enable the dam to withstand the Safety Evaluation Earthquake, a Mw 7.2 event on the Waiohau Fault.

During construction of the remedial works in 1997-98, six faults striking approximately normal to the dam (parallel to the Waiohau Fault System) were recognised in the foundation, all cutting Matahina Ignimbrite. Three of these also displace the overlying Rangitaiki Alluvium which has an estimated maximum age of 20 000 years. None of the faults reached the preconstruction ground surface that has been interpreted as an 1800 yr BP outwash terrace. One faulting event has been bracketed, between radiocarbon dated layers within the alluvium in the core trench, at between 10600 and 3690 years before present. This date is consistent with the last rupture event on the Waiohau Fault (between 4800 years and 1800 years before present) based on paleoseismic studies carried out during the Seismic Safety Evaluation.

Introduction

Matahina Dam is located on the Rangitaiki River in the Bay of Plenty region of the North Island. The dam has been owned and operated by TrustPower Ltd since 1999, and was previously owned and operated by the Electricity Corporation of New Zealand (ECNZ). It is an 80 m high, 400 m long earth and rockfill dam built during the 1960's.

Seismic hazard evaluation studies by Woodward-Clyde (now URS) and the Institute of Geological & Nuclear Sciences Ltd (Woodward-Clyde 1997a) indicated that part of the Waiohau Fault Zone is located beneath the foundation of Matahina Dam. These faults have a high probability for accommodating movement during surface rupture of the fault zone. The derivation of the safety evaluation earthquake is described in Freeman et al. (2000). The Waiohau Fault zone has a maximum earthquake of Mw 7.2 with an average recurrence interval of 3000 years. A displacement of 3 m of oblique slip (2 horizontal:1 vertical) on the fault has an estimated exceedence probability of between 1/6000 and 1/11000 annually.

The Matahina Dam Strengthening Project was a $60M seismic retrofit designed by Woodward-Clyde (1997b) to prevent piping failure of the dam should the core be ruptured by fault movement. The design is described in detail by Mejia et al. (1999). The project involved excavation of the downstream shoulder of the original dam, construction of a leakage resistant filter and transition zone within the dam, and replacement of the shoulder buttress material with enhanced drainage downstream of the new leakage resistant zone. Excavations for the leakage resistant zone extended to below the original foundation level, effectively forming a cut-off trench beneath the downstream shoulder of the dam.

Matahina is one of the few examples of a dam that have been remediated to withstand the potential effects of active foundation faults (Allen and Cluff, 2000). The objective of this paper is to describe the evidence for Late Quaternary fault activity that was found within the foundation excavation during the Matahina Dam Strengthening Project and discuss how these observations conform with the design expectations of the project.

Regional geology

Matahina Dam is located near the boundary between two tectonic provinces in the North Island; the Taupo Volcanic Zone (TVZ) and the North Island Shear Belt (NISB) (Figure 1). A sequence of Late Tertiary and Quaternary volcanics and sediments overlies greywacke basement in the northern part of the central North Island (Healy et al. 1964). Mesozoic age Urewera greywacke basement outcrops about 3 km to the east of the site.

The Rangitaiki River flows north from the Waiohau Basin into Lake Matahina, which is a 5 km long, relatively straight, narrow and steep sided reservoir. Downstream of the dam, the valley widens into the Rangitaiki Plains. At the damsite the valley floor is approximately 200 to 300 m below the adjacent hillcrests.

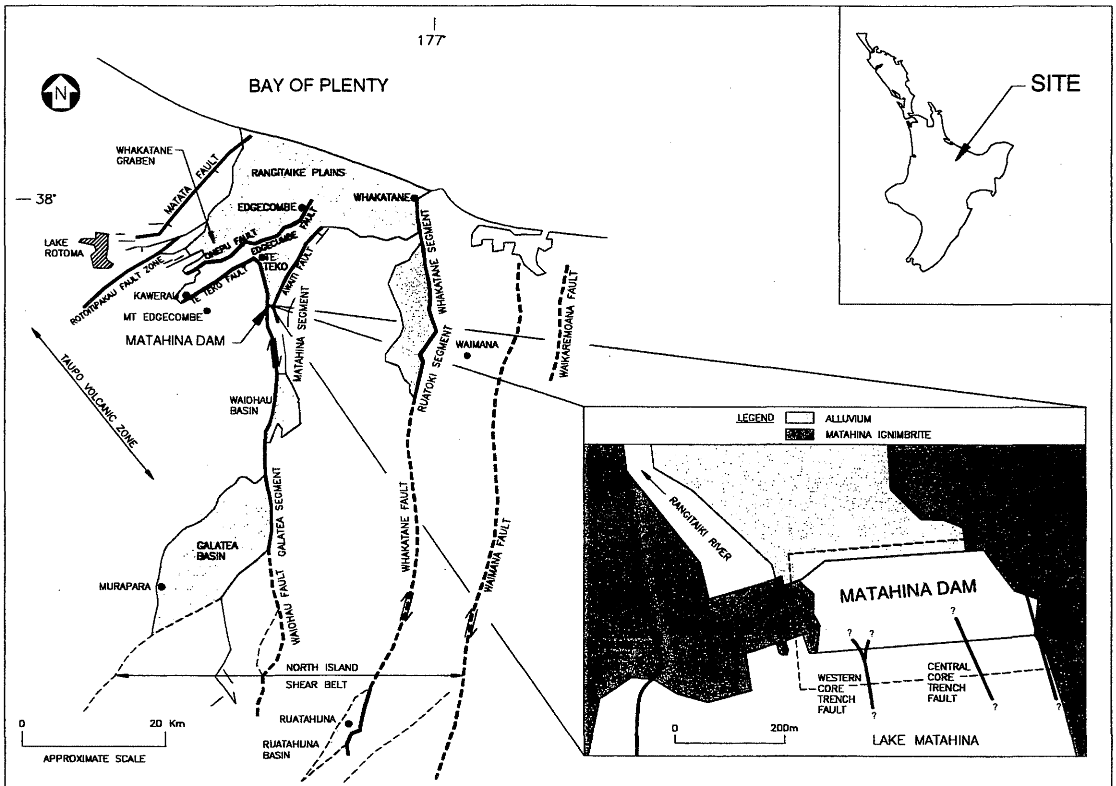

MATAHINA DAM REGIONAL GEOLOGICAL SETTING

FIGURE 1

The Rangitaiki River has eroded the valley occupied by the Matahina dam and reservoir along the Waiohau Fault Zone, which is dominantly a dextral-normal oblique strike slip fault and is the western-most fault in the NISB. Previous studies (Woodward-Clyde, 1997a) indicate that the Waiohau Fault Zone consists of 10 or more subparallel traces occupying a zone 2 km wide in the vicinity of the dam. At the dam site, displacement has been accommodated on the "Western Abutment Ridge Fault" which passes approximately 150 m west of the dam spillway, and a series of faults which cross beneath the dam embankment (Figure 1). In addition, the "Eastern Heights Faults" are a series of parallel, north-trending faults located to the east of the dam.

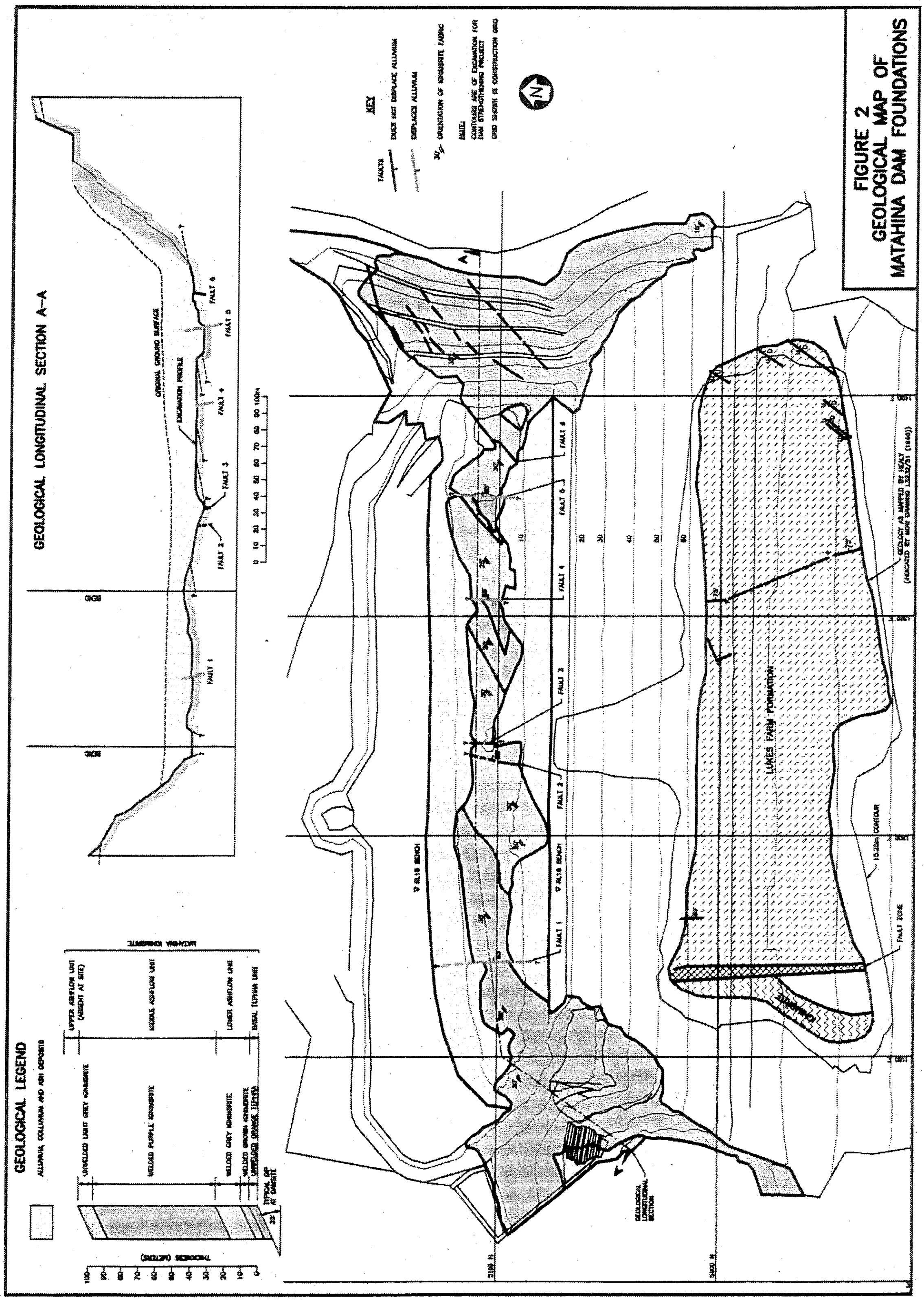

FIGURE 2
GEOLOGICAL MAP OF
MATAHINA DAM FOUNDATIONS

During initial dam construction, many faults were documented during geological mapping of the core trench, including the three 'core trench faults' (Figure 1) that were subsequently recognised (Woodward-Clyde, 1997a) to represent the most significant seismic hazard. No offset of Rangitaiki River alluvium was reported on these faults in the dam construction records. It was concluded by Healy (1964) that none of the faults passing under the dam had ruptured in the time since deposition of the alluvium, which was estimated at 20 000 years.

The recent seismic hazard evaluation (Woodward-Clyde 1997a) included a paleoseismic study of the Waiohau Fault Zone, largely carried out by the Institute of Geological and Nuclear Sciences. The study concluded that the Waiohau Fault Zone ruptures with an average return period of 3000 years, based on evidence (recorded in exploratory trenches) of four surface faulting events during the last 11 800 years. The maximum earthquake for the fault zone was judged to be a magnitude Mw 7.2 event resulting from an 80 km long fault rupture. The estimated ground surface displacement associated with this event is 3 m total oblique displacement with a horizontal to vertical ratio of 2:1.

Dam Site Geology

A 20 m thick layer of Rangitaiki River alluvium, comprising predominantly bouldery gravels and sands, occupies the valley floor at the damsite. Healy referred this material as "Valley Fill Alluvium". Radiocarbon dates of wood and paleosol material that were obtained from within the alluvium ranged in age from 3,700 to 10,600 years B.P. The surface of the valley fill is interpreted to be a Taupo pumice alluvium surface of <1800 years B.P.

Local filling of the old river channels was carried out during initial dam construction. According to the construction records this fill is up to 7 m in thickness, but it is difficult to distinguish the fill from the native alluvium because the fill is typically a product of the alluvium and/or colluvium, and commonly has similar appearance to equivalent in situ materials.

The dam and reservoir are underlain by the Matahina Ignimbrite, a c. 280 000 year old rhyolitic ignimbrite. The ignimbrite sheet thickens to the east away from the Haroharo Caldera, which was the eruptive centre, towards the fault angle depression of the Waiohau Fault where it attains a maximum thickness of 200 m. At the dam site it has a thickness of about 100 m.

Alluvium

In the cut-off trench for the new filter zone, alluvium typically comprised massive or crudely bedded coarse bouldery gravels. Rare lenses of sandy fine gravel and silty sand also occurred. The coarse boulder fraction comprised subrounded boulders of ignimbrite typically in the size range 0.2 to 1.0 m, but rarely up to 2.0 m across. The finer fraction of the bouldery alluvium typically comprised greywacke pebbles (<30 mm) and sand, with some of the sand fraction being of pumiceous origin.

A discontinuous layer of light grey pumiceous sand outcropped at each end of the cut-off trench between RL 12 and RL 18. Light grey massive silty sand containing abundant charred wood was exposed at the east end of the cut-off trench. Other samples of wood and organic-rich soils were collected from alluvium in the cut-off trench for radiocarbon dating. The results of these are presented in Table 1.

Table 1

Results of radiocarbon dating of wood samples from alluvium

Sample	^{14}C Age	Location	Comments
Wk6255	3700+/-60 BP	Downstream batter of the cut-off at RL15 m, Sta. 13+30 m.	Tree branch, lying horizontally in a fine pebbly ironstained gravel bed
Wk6254	3690+/-60 BP	Near to a temporary north-south batter at RL15 m, Sta. 13+60 m	Small charred tree branch lying in a matrix of massive light grey silty sand
Wk6252	5230+/-110 BP	Upstream batter of the cut-off trench at RL14 m, Sta. 11+35 m	Paleosol underlying a layer of light grey pumiceous sand
Wk6253	10,600+/-80 BP	Sample located at RL8, Sta. 13+65 on the upstream batter of the cut-off trench.	Tree branch, lying horizontally in a 0.5 m thick grey silt layer, truncated by Fault 5.

Note: Samples radiocarbon dated by University of Waikato.

While the results in Table 1 indicate ages of up to 10,600 years B.P. for the alluvium, this may not represent the maximum age of the alluvium as sample Wk6253 was taken several metres above the ignimbrite contact.

Matahina Ignimbrite

As described by Bailey and Carr (1994), the Matahina Ignimbrite comprises four distinct members: a basal tephra and three ashflow deposits. The lower ashflow unit is welded, as is most of the middle ashflow unit, but the upper part of the middle ashflow unit is unwelded. The contact between the lower and middle ashflow units is also welded, but is recognisable by a distinct colour change. The upper ashflow unit is a thin, discontinuous, unwelded unit.

While Matahina Ignimbrite is generally a flat lying formation, the formation dips approximately 25° towards north or north-east in the Left Abutment Ridge on which the spillway, penstocks and powerhouse sit, and beneath the dam.

In the cut-off trench a conformable sequence comprising a tephra or unwelded ignimbrite unit, and two mostly welded ignimbrite units was recognised. These are interpreted to be the basal tephra and the lower and middle ashflow members described by Bailey and Carr. The variation in Matahina Ignimbrite lithology provides marker horizons which indicate the magnitude of fault displacement since 280 000 years B.P. The sequence is summarised in Figure 2. The upper part of the middle ashflow member is unwelded at the damsite.

As illustrated in Figure 2, Matahina Ignimbrite strikes obliquely to the cut-off trench (with a dip of 25-30° and a dip direction of approximately 330°). Towards the right abutment side of the trench, the basal tephra materials were recognised; the lower ashflow unit was exposed in the trench floor between Sta.12+00 m and Sta. 14+00 m; and the middle ashflow unit was exposed in both abutments and in the trench floor west of Sta. 12+00 m.

Basal unwelded ignimbrite or tephra

A pinkish orange unwelded unit was exposed in the cut-off trench between Sta. 12+90 m and Sta. 13+08 m and between Sta. 13+40 m and Sta. 13+58 m. This material comprises a 10 metre thick sequence of slightly welded (or cemented) light pinkish orange, silty sand sized ash materials, with the lower part containing fragments of light grey pumice up to 20 mm. At Sta. 13+50 to Sta. 13+58 a massive, unwelded light pinkish grey, medium grained sand was exposed. There was no indication that this material was deposited in water. This material appeared to be the stratigrahically lowest member of the materials exposed in the cut-off trench.

Lower Ashflow Unit

Conformably overlying the unwelded basal unit was a welded ignimbrite member of approximately 10-20 metres thickness. The base of this unit was a massive moderately strong brown fine-grained ignimbrite containing yellow brown pumice fragments. This material graded upwards through a strong grey-brown fine grained ignimbrite to a coarse grey crudely laminated ignimbrite, containing abundant black glass in elongate clasts up to 20 mm long. The ignimbrite contained white or grey quartz phenocrysts up to 2 mm across. The rock matrix was very fine grained with no apparent structure.

Middle Ashflow Unit

A purple-grey or purple-brown welded ignimbrite about 50 metres thick conformably overlies the lower ashflow unit. The ignimbrite contained quartz phenocrysts up to 2 mm across in a very fine-grained matrix. Clasts of dark grey pumice and other rock fragments were found throughout the ignimbrite. Many pumice fragments were flattened into dark grey streaks up to 20 mm long. In the upper part of the unit, fragments of weak pumice up to 50 mm across were evident. A contact zone comprising a brown very strong layer of ignimbrite a few metres thick was exposed at approximately Sta. 12+00 m. This material was absent at the contact between the lower and middle flow units at Sta. 14+00 m. The upper 20 m of the middle ashflow unit grades vertically into a light grey weak unwelded ignimbrite material, which is exposed above RL 50 on the left abutment.

Upper Ashflow Unit

The upper ashflow unit described by Bailey & Carr consists of a thin (<20 m thick) discontinuous deposit of unwelded ignimbrite. This unit was not recognised in the cut-off trench or in the abutments.

Faulting

As described below, six faults that cut the Matahina Ignimbrite were recognised in the floor of the cut-off trench. Three of these displaced the valley fill alluvium.

Fault 1

Fault 1 is oriented approximately 090/85 and was visible for the full width of the trench. The fault had a 1.0 m thick crushed zone of highly crushed and sheared ignimbrite, with an adjacent relatively fractured rock mass approximately 10 m wide on the east side, containing several smaller splaying crush zones. The rock mass quality improved quickly to the west of the fault (the footwall side). No striations were found to indicate a relative movement vector for Fault 1.

In the batters, a sharp contact was evident between the highly sheared ignimbrite and the adjacent bouldery alluvium, suggesting that approximately 1.5 m of apparent vertical displacement (east side up) has occurred since deposition of the alluvium. Truncated sand lenses and rotated pebbles (with vertically aligned long axes) in the alluvium above the fault plane confirm that the displaced alluvium/ignimbrite contact is the result of faulting and not fluvial downcutting of the weak fault zone.

An earlier exposure of the fault, in an exploratory trench excavated in the cut-off floor, showed two parallel fault planes about 0.3 m apart, each with ~1 m of apparent vertical movement (east side up). Only a single fault plane was evident in the final trench excavation.

A continuous exposure in the cut-off trench, with no identified faults, was observed from the base of the middle flow unit at Sta. 12+00 m to Fault 1 at Sta. 11+45 m. The rock in this interval contained no well-defined joint patterns. In contrast, ignimbrite to the west of Fault 1 generally had well defined joint patterns, suggesting that the footwall (west side of the fault) comprises rock from higher in the middle flow unit than the hanging wall. This is consistent with the apparent displacement sense of the alluvium/ ignimbrite contact (east side up).

Offset sand lenses were found as high as ~RL12 in the alluvium, but these were not clearly correlable across the fault. These sand lenses suggest that lateral as well as vertical displacement may have occurred on this fault. No displaced marker horizon was found, which would allow this displacement to be measured.

Fault 2

On the upstream face of the cut-off trench Fault 2 was exposed cutting through ignimbrite from the trench floor (RL 3) to the ignimbrite/alluvium contact (RL12). The fault consisted of a steeply dipping, 0.5 m thick zone of crushed rock, with a 20 mm thick brown clay seam on the western side. The dip direction was measured at 094°. The ignimbrite/alluvium contact indicated that erosion of a narrow V-shaped channel approximately 1 m wide and 1 m deep had occurred at the fault, but there was no indication of offset of the ignimbrite/alluvium contact.

A lithological change from brown welded ignimbrite on the east to coarse grey welded ignimbrite to the west was evident across this fault. The brown ignimbrite is similar to the lowest five metres of the lower ash flow unit, and the coarse grey ignimbrite is similar to that which has been mapped 5 to 10 m higher in that unit.

The lithological change across the fault represents an apparent vertical offset of 5 to 10 m with the east side upthrown. No striations were evident in the crush zone to indicate a relative motion vector.

A change in dip direction of the rock fabric, from 310° at 12+40 m to 330° at 12+30 m was also evident across this fault.

Fault 3

A trough in the ignimbrite/alluvium contact, oriented NW-SE, extended down to RL-2 at approximately Sta. 12+40 m. The western margin of the trough was steep sided and the eastern margin had a flatter slope.

On the downstream side of the cut-off trench, highly crushed ignimbrite was exposed over a zone 1 to 2 m wide. On the upstream side of the trench highly crushed ignimbrite was also exposed. A defined fault plane with a measurable orientation was not found.

To the west of the trough the rock was hard, brown welded ignimbrite as described on the eastern side of the fault at Sta. 12+32 m. The rock on the east of the trough was grey, coarse textured ignimbrite. No faults were evident in the rock sequence between the trough and the bottom of the lower ash flow unit at about Sta. 12+85.

The presence of an eroded trough, an abrupt lithological change and the crushed ignimbrite at Sta. 12+42, all suggest a fault striking across the trench at this location. The orientation of the fault could not be measured, however the trough was oriented obliquely to the trench axis (trending slightly west of north) and this may reflect the fault strike. The lithological change suggests an apparent vertical offset of 5 to 10 m, upthrown to the west. A dextral strike slip movement sense could also explain this apparent vertical offset. No striations were found to confirm a relative motion vector.

No evidence was found for offset of the alluvium or of the ignimbrite/alluvium contact.

Fault 4

A planar contact, oriented 090/85, between unwelded orange ignimbrite on the west and welded coarse grey ignimbrite on the east was exposed at 13+08 m. A 0.5 to 1.0 m wide zone of crushed dark grey ignimbrite was exposed at the contact. No clay gouge or striations were found within the crush zone.

Within the unwelded ignimbrite, a series of thin shears (<5 mm thickness of light grey silt) were evident. These shears were generally steeply dipping and had dip directions of 120° or 300°. Weakly developed corrugations on these features plunge 10° to 25° to the south.

The inferred movement sense for this fault is west side up with an apparent throw of 10 to 15 m based on the change in lithology. Alternatively a dextral displacement of 20 to 30 m could juxtapose the lithologies. The weak corrugations exposed on the shears suggest a dominant dextral component in the relative motion vector for Fault 4.

A pocket of olive grey sandy alluvium containing ignimbrite cobbles was present overlying the unwelded orange ignimbrite to the west of the fault on the upstream side of the cut-off trench. This alluvium has a fault contact with the coarse grey ignimbrite indicating that Fault 4 has moved since deposition of the overlying alluvium. The pocket of alluvium also appeared to be displaced by about 0.3 m on the west side by one of the shears described above.

The post-alluvium movement of Fault 4 is approximately 1 m in an apparent vertical sense, with the east side upthrown. Fault displacement could not be followed upwards into the overlying bouldery alluvium, but at this location there were no fine-grained layers evident in the alluvium to highlight any offset. The timing of this movement on Fault 4 and the associated shears is uncertain, as the maximum age of the alluvium is unknown.

Fault 5

A sharply defined channel edge 4 to 5 m high, trending 035°, was uncovered at ~Sta. 13+40 m. The channel edge was developed along a joint set oriented 125/70. The channel floor exposed unwelded orange ignimbrite at RL 1 m. At Sta. 13+52 m a fault contact was exposed with an orientation of 095/85, which faulted welded grey ignimbrite (to the east) against unwelded orange ignimbrite.

A 0.5 to 1 m wide contact zone comprising subangular pebble and cobble sized fragments of grey ignimbrite in a moderately dense sandy silt matrix, was traced across the floor of the cut-off trench. No greywacke pebbles were found within this material, which is inferred to be a fault breccia. A 30 mm wide seam of brown, high plasticity clay was present on the western margin of the fault breccia.

Further east at Sta. 13+55 m a channel edge trending 035° was exposed (this channel edge is oriented similarly to that at Sta. 13+40 m, and appears to be offset by the fault at Sta. 13+52 m). The channel floor is at RL 1 m on the west of the fault and RL 3 m on the east.

In the upstream batter of the cut-off trench, a 5 m high fault contact between alluvium and unwelded ignimbrite confirms that fault movement has occurred since the alluvium was deposited.

An apparent vertical offset of about 10 metres is indicated by the change in lithology across the fault with the east side downthrown. The offset channel in the alluvium/ignimbrite contact indicates dextral strike slip, with a magnitude of 20 to 25 m, and with the East Side upthrown by 2 m. The age of the offset channel is not known. However, it is at least 10,600years old, as indicated by radiocarbon sample Wk6253.

Fault offset in the alluvium on the upstream batter of the cut-off trench was evident as high as RL 10 m. Pumiceous sand materials at RL 12 m were strongly folded, but this was not unequivocally fault deformation. A wood-bearing silty sand layer at RL 8 to 9 m was faulted out against bouldery alluvium. Wood from this horizon (Wk6253) had a radiocarbon age of 10,600 years B.P. A layer of massive silty sand overlying Fault 5 at RL 15 to 18 had a radiocarbon age of 3690 years B.P. This layer showed no evidence of fault displacement, suggesting that the last movement of Fault 5 occurred between 3690 and 10,600 years B.P.

Right Abutment Faults

A series of steeply dipping discontinuous, splayed faults were mapped crossing the right abutment cut slope. These faults consisted of narrow (0.1-0.3 m wide) zones of crushed rock that were evident following several weeks of weathering of the cut slope. The faults did not appear to displace any reference horizons, though the right abutment consists only of middle flow unit, welded ignimbrite, which has no distinct marker horizons. One of these faults crosses the floor of the cutoff trench. A 0.5 m thick crushed zone with a steep dip towards 140° was encountered in ignimbrite near the upstream side of the cut-off trench at Sta. 13+73 m. To the west of the fault grey welded ignimbrite from the lower ash flow member was exposed and to the east purple welded ignimbrite from the middle flow member was exposed. This juxtaposition implies a minimum apparent vertical offset of about 5 m. No striations were found in the crush zone and no offset of the ignimbrite/alluvium contact was evident

Correlation between faults in the cut-off trench and faults mapped during construction

As shown in Figure 2, Healy (1964) mapped several faults in the core trench excavation for the original dam, located approximately 100 m upstream from the cut-off trench of the current project. The Western Core Trench Fault projects along strike to Fault 1 at Sta.11+45. Healy mapped several faults in "early Pleistocene sediments" between Sta. 12+80 and Sta. 13+20 m, with strikes ranging from north-south to about 340°. Some of these project along strike to Faults 3 and 4. Healy found no fault along strike from Fault 5 (at Sta. 13+60 m).

Healy mapped several faults that had north-easterly strike in the right abutment area of the original core trench excavation. During the current project several faults that had north-easterly strikes were also mapped at the right abutment end of the cut-off trench.

Implications of new data

Though several faults extend up into the alluvium, none have been found to extend to the pre-construction ground surface that is interpreted as an 1800 years B.P. Taupo alluvium terrace.

The only dated faulting event in the cut-off trench is the silt layer at RL 8 m (that has a radiocarbon age of 10,600+/-80 BP) which is truncated by Fault 5. This age represents a maximum age for the last rupture event on this fault. The apparently unfaulted sandy silt layer at RL 15 which overlies the trace of Fault 5 has a radiocarbon age of 3690+/-60 BP making this a minimum age for the last event on Fault 5. This is consistent with a last fault rupture event for the Waiohau Fault Zone of older than 1800 yr. and younger than 4800 yr. as indicated by trenching across a strand of the fault at the south end of the reservoir, reported from the 1996 seismic hazard assessment (Woodward-Clyde 1997a).

There are a few indications of dextral motion on faults exposed in the cut-off trench. However, none of the exposures give a clear relative fault motion vector for the fault zone. Offset of a channel cut in rock suggests a relative fault motion of 10:1 horizontal to vertical for Fault 5, but this is not certain.

Displacements of the base of the alluvium are probably in the range of 10 to 25 m which suggests a slip rate of 0.5 to 1 mm/yr for the faults underlying the dam. This represents a considerable proportion of the total slip rate for the Waiohau Fault Zone of 1mm/yr.

No observations made in the cut-off trench can usefully evaluate the 3 m single event displacement for the Waiohau Fault Zone that was a conclusion of the 1996 study.

Conclusions

Three faults that displaced Rangitaiki River alluvium were observed crossing the dam foundation. This observation confirms the design assumption that active strands of the Waiohao Fault zone were present beneath the dam. The observations were consistent with the Safety Evaluation Earthquake of 3 m of oblique slip (2 horizontal:1 vertical), but could not usefully evaluate single event displacements on any of the faults. Whether the fault system ruptures on one fault plane at a time or in a distributed manner over the faults beneath and outside the dam footprint, could not be evaluated.

References

Allen, C. R. and Cluff, L. S., 2000: "Active Faults in Dam Foundations: An Update". Proceedings of 12th World Congress on Earthquake Engineering.

Bailey, R. A. and Carr, R. G., 1994: "Physical geology and eruptive history of the Matahina Ignimbrite, Taupo Volcanic Zone, North Island, New Zealand." New Zealand Journal of Geology and Geophysics, Vol. 37, No. 3

Freeman, S. T., Gillon, M. D., Berryman, K.R., Moriwaki, Y., Somerville, P. and Mėjia, L., 2000: "Matahina Dam Fault Surface Displacement Design Criteria". Proceedings of 12th World Congress on Earthquake Engineering.

Gillon, M.D. and Newton, C., 1991: "Abutment repairs at the Matahina Dam." Proceedings of the 17th ICOLD Congress

Healy, J. 1964: "Geology of the core trench excavation, Matahina Dam." New Zealand Geological Survey unpublished report (11 October 1964)

Healy, J., Schofield, J. C. and Thompson, B. N., 1964: Sheet 5 Rotorua, Geological Map of New Zealand 1:250 000. Department of Scientific and Industrial Research, Wellington, NZ

Mejia, L., Forrest, M., Bishoff, J., Gillon, M., and Everitt, S, 1999: "Upgrading of Matahina Dam for Foundation Fault Displacement" Proceedings of Waterpower '99, ASCE, Las Vegas.

Woodward-Clyde 1997a: Matahina Power Station Seismic Hazard Assessment. Unpublished report to ECNZ

Woodward-Clyde 1997b: Matahina Dam Strengthening Project Final Design Report. Unpublished report to ECNZ

Woodward-Clyde 1998: Matahina Dam Strengthening Project Geological Completion Report. Unpublished report to ECNZ

Poster Presentations

Seismic Wave Amplification at the Edge of a Soft Layer

Brian M. Adams

URS New Zealand Limited, PO Box 4479, Christchurch, NZ (brian_adams@urscorp.com)

Rob O. Davis

Dept of Civil Engineering, University of Canterbury, Private Bag 4800, Christchurch, NZ (r.davis@civil.canterbury.ac.nz)

Abstract

Seismic waves are often amplified by the geometry and material properties of soft sediments at the edge of basins and valleys. This paper investigates the behaviour of plane horizontally-polarised shear (SH) waves as they impinge on the edge of a semi-infinite soft layer at the surface of a stiff half-space. In this simple two-dimensional problem both the layer and the half-space are assigned uniform elastic material properties. A geometrical ray path analysis is first used to investigate the initial occurrences of reflection and refraction at the layer edge, and a finite-element analysis is then used to show the effect of diffraction, total reflection and the development of inhomogeneous waveforms. For input frequencies greater than the fundamental of the layer, amplification of peak ground motion occurs within a discrete zone some distance out from the edge due to constructive interference involving various edge-generated wave fields. An example of edge amplification in the Lower Hut Valley, New Zealand, is used to illustrate these ideas.

Introduction

The importance of seismic amplification near the edge of sedimentary deposits is apparent in the aftermath of recent major earthquakes such as Northridge (1994) and Kobe (1995) where anomalously severe damage occurred on deep soft sediments adjacent to a basin edge. Subsequent numerical studies of wave propagation within 2-D and 3-D models of the local geology at Santa Monica (Graves et al., 1998; Alex and Olsen, 1998) and in Osaka Bay (Kawase, 1996; Motosaka and Nagano, 1997; Pitaka et al., 1998, Higashi, 2000) have indicated that the most likely cause of this damage is constructive interference between near-vertically propagating body waves and edge-generated surface waves. This mechanism of seismic amplification has been termed the *basin-edge effect* (Kawase, 1996).

Observations of amplification or intense damage near the edge of sedimentary basins are not only limited to recent earthquakes. Moczo and Bard (1993) mention bands of intense damage adjacent to geologic lateral discontinuities from the 1909 France, 1979 Montenegro (Italy) and 1980 Irpinia (Italy) earthquakes. Other occurrences basin-edge damage have been reported following the 1963 Skopje (Yugoslavia) earthquake (Poceski, 1969), the 1978 Miyagiken-Oki (Japan) earthquake (Kubo and Isoyama, 1980), the 1976 Longlin (China) earthquake (Yuan et al., 1992). In New Zealand there is evidence of anomalously strong shaking adjacent to the edge of the Lower Hutt Valley during the 1934 Paihiatua earthquake (Downes et al., 1999).

The nature of seismic shaking experienced at any location is fundamentally dependent on at least three different processes. Firstly the earthquake will generate a wave field that is a function of the magnitude, orientation, and various other rupture characteristics of the source event; secondly propagation of the wave field from the source to the site will result in attenuation and scattering of seismic energy; and thirdly the nature of the local geology and topography at the site may drastically alter the nature of shaking. Soft sedimentary deposits in particular have the effect of both amplifying and trapping seismic energy by internal reflection. When such sediments are laterally confined by a more rigid basement rock as in an alluvial basin or valley, the seismic behaviour becomes significantly more complex.

Interaction of the incoming wave field with a basin edge generates horizontally-propagating surface waves which are the primary contributors to spatially varying amplification adjacent to the edge.

Basin edge effects have been studied is several different ways. Analytical solutions to anti-plane particle motion within simple wedge-shaped elastic solids (Hudson, 1963; Hong and Helmberger, 1977; Wojcik, 1977; Sanchez-Sesma and Velázquez, 1987) have clearly identified wave fields generated at a normally-dipping edge, yet fail to account for interaction from base-generated wave fields. Numerical solutions to various hypothetical (Dezfulian and Seed, 1970; Moczo and Bard, 1993) and real (eg. Kawase, 1996; Graves et al.,1998) basin configurations have given insights into surface response yet provide little understanding of the causative wave field interactions.

In this paper we investigate the basic physical mechanisms that alter the velocity, form and magnitude of seismic SH waves that hit the edge of a sedimentary basin. Of principal interest is the geometry and material properties of the local geology that act to change the incoming wave field by reflection, refraction and diffraction at each of the various material boundaries within the stratigraphy. In the case of a two-dimensional basin edge (ie. an infinitely long edge), horizontally polarised shear (SH) waves are represented by particle motion in the anti-plane (edge parallel) orientation.

First we describe the results of a ray path analysis of plane wave propagation at the edge of a generic sedimentary basin. We then make a numerical analysis using a finite element method (FEM) to simulate elastic wave propagation through the same model, and finally use these concepts to investigate basin-edge effects in the Lower Hutt Valley, New Zealand. It is hoped that a basic physical understanding of such effects will lead to a wiser choice of design earthquake parameters for use in civil and structural design near the edge of sedimentary basins.

Ray Path Analysis

The model shown in Figure 1 represents the edge of a basin where soft sediments exist to a given depth, H (typically between 10m ad 2km deep), and are bounded below and to one side by a much stiffer basement rock. Both the sediments and rock are modelled as homogeneous elastic solids with a shear wave velocity, β, a shear modulus, μ, and a bulk density, ρ. The shear wave velocity of the sediments typically ranges between 50 and 1000m/s, whereas in the rock the shear waves travel much faster at around 1000-3000m/s.

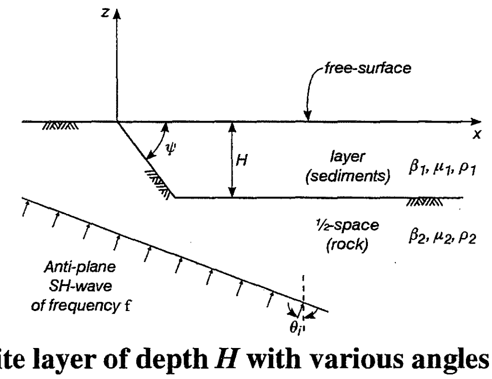

Figure 1. A semi-infinite layer of depth H with various angles of edge-slope overlies a uniform half-space.

The edge of the basin dips at an angle, ψ, which commonly ranges between 15° and 120° depending on the geological processes that have formed the basin. As examples; for simple dipping geology ψ may be quite small, for a normal fault structure ψ may be in the order of 60°, for an oblique fault the edge will be vertical ($\psi = 90°$), and for an overhanging edge formed by thrust action ψ will be greater than 90°. The incident wave field is assumed to be coherent and arriving as a plane homogeneous wave at an angle, θ_i, to the vertical.

When a wave refracts into a soft basin from a stiff bedrock it's velocity decreases from β_2 to β_1, it's angle of propagation decreases from θ_i to θ_1 (the direction of travel tends normal to the material interface) as governed by Snell's law,

$$\frac{\sin\theta_1}{\beta_1} = \frac{\sin\theta_i}{\beta_2} \tag{1}$$

and it's amplitude increases from A_i to A_1

$$A_1 = A_i \frac{2\rho_2\beta_2\cos\theta_i}{\rho_2\beta_2\cos\theta_i + \rho_1\beta_1\cos\theta_1} \tag{2}$$

It is well known that sub-critical reflection and refraction of anti-plane motion within a flat layer of sediments over a uniform half space will resonate at n^{th}-mode frequencies, f_n, given by (Haskell, 1960)

$$f_n = \frac{\beta_1}{4H}(2n+1) \qquad n = 0,1,2,\ldots\infty \tag{3}$$

If conditions for total internal (post-critical) reflection are satisfied within the layer then antiplane energy will propagate horizontally as Love waves (Love, 1911) with a phase velocity, c_n, given by the solution of

$$\tan\left(\omega H\sqrt{\frac{1}{\beta_1^2} - \frac{1}{c_n^2}} - n\pi\right) = \frac{\mu_2}{\mu_1}\frac{\sqrt{\frac{1}{c_n^2} - \frac{1}{\beta_2^2}}}{\sqrt{\frac{1}{\beta_1^2} - \frac{1}{c_n^2}}} \qquad n = 0,1,2,\ldots\infty \tag{4}$$

and a group velocity, U, given by

$$U = c + k\frac{dc}{dk} \tag{5}$$

where the circular frequency, $\omega = 2\pi f$, and the wave number, $k = \omega/c$.

What is not so well understood is how the layer responds to seismic input when it is bounded by bedrock on one side. Figure 2 shows a geometrical ray path analysis of refraction and reflection within our model. The processes of diffraction and total reflection are not able to be modelled accurately as they involve frequency-dependent phase changes, yet we can gain a qualitative understanding of their effect.

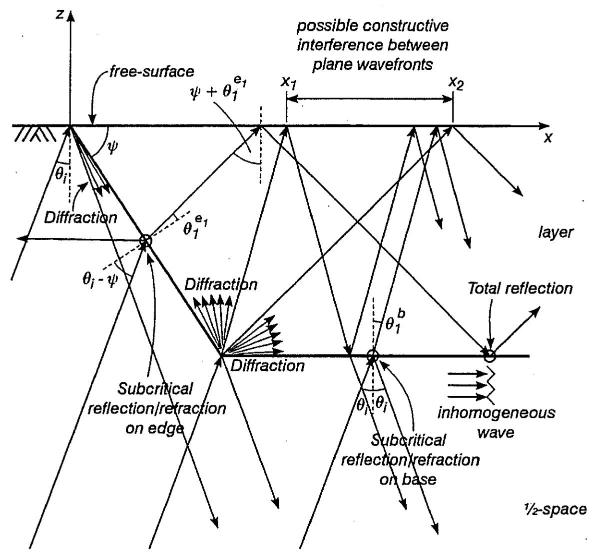

Figure 2. Ray path diagram of wave propagation within the generic model for one possible combination of θ_i, ψ and β_2/β_1.

The incident wave initially sets up three different wavefields within the layer. The first is a near-vertically travelling wavefront that is refracted upward from the base of the layer and which becomes partially trapped within the layer by repeated sub-critical reflection between the surface and the base of the sediments. A second wavefront is refracted or reflected near-horizontally by the edge. This wave front becomes trapped within the layer by total reflection at the base of the soft sediments. Frequency dispersion by total reflection eventually leads to the development of a Love wave propagating away from the edge. A third wave field is generated by diffraction of a small amount of incident energy at the vertices of the edge and enhances the frequency-dependant nature of the response.

Constructive Interference within the Sediments

The first two wave fields mentioned above are generally expected to be much stronger than the latter. In the example shown in Figure 2 the base refracted and edge refracted wave fields converge and will produce both constructive and destructive interference within the sediments. The interference pattern will obviously be highly dependent on the incident waveform. For a single pulse we can easily calculate the time dependant position, $[x(t), z(t)]$, of constructive interference as it moves from the lower vertex diagonally up toward the surface

$$x(t) = \left[H\left(\frac{\tan\theta_1^b}{\tan\theta_i} - 1\right) + \beta_1 t\left(\frac{1}{\cos\theta_1^b} - \frac{1}{\cos(\psi + \theta_1^{e1})}\right)\right]\left(\frac{1}{\tan\theta_1^b - \tan(\psi + \theta_1^{e1})}\right) \quad (6)$$

$$z(t) = \frac{\beta_1 t - x(t)\sin(\psi + \theta_1^{e1})}{\cos(\psi + \theta_1^{e1})} \quad (7)$$

where θ_i^{e1} and θ_i^b are the angles of refraction from the edge and base respectively

$$\sin\theta_1^{e1} = \frac{\beta_1}{\beta_2}\sin(\theta_i - \psi) \quad (8)$$

$$\sin\theta_1^b = \frac{\beta_1}{\beta_2}\sin\theta_i \quad (9)$$

Equations 6 and 7 represent the location of a high amplitude pulse within the sediments. The pulse reaches the ground surface a distance x^c out from the basin edge.

$$x^c = \left(\frac{\beta_1}{\sin(\psi + \theta_1^{e1})}\right)\frac{\left(\frac{H}{\tan\theta_i} - \frac{H}{\tan\theta_1^b}\right)}{\left(\frac{\beta_1}{\sin(\psi + \theta_1^{e1})} - \frac{\beta_1}{\sin\theta_1^b}\right)} \quad (10)$$

which is in fact the solution to Equations 6 and 7 when $z = 0$, and is the product of the apparent velocity of the edge-refracted wave front and the time difference between the surface arrivals of the base-refracted and direct waves.

The derivation of Equations 6 to 10 are shown in Adams (2000). Figure 3 shows a graphical representation of Equation 10 for various combinations of angle of incidence, θ_i, and edge-slope angle, ψ. It is apparent that the angle of the edge has significantly more effect on the position of the high-amplitude pulse than does the angle of incidence. In addition, we note that x^c is undefined over a significant portion of the graph where the two undispersed wave fields do not interact.

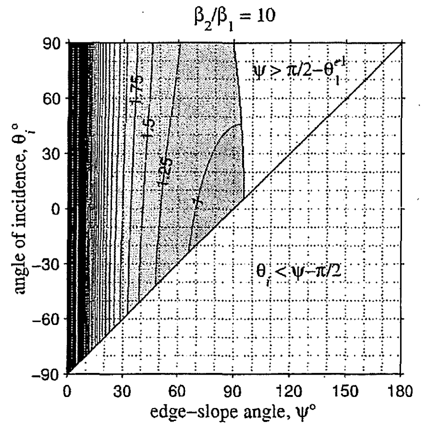

Figure 3. A graphical interpretation of Equation 10 in which contour height represents the distance out from the edge, x^c, of constructive interference between undispersed base and edge refracted waves.

For an incident wave field containing a whole suite of pulses, a corresponding suite of edge refracted pulses is generated within the layer, each of which may interact with each of the pulses in the corresponding base-refracted wave field. In this way there could feasibly be a large number of positions across the basin where successive constructive interferences could take place, with the net effect being a broad zone of amplification.

A ray path analysis thus allows us to predict the transient positions of plane homogeneous wave fronts within and outside the sedimentary layer. It is apparent that for many combinations of velocity contrast, angle of incidence and edge-slope angle there will be a high amplitude pulse of energy caused by constructive interference between each undispersed edge-and base-refracted wave front. While we can predict the timing and position of such interference with neat geometrical expressions, it is important to understand that constructive edge-amplification is also likely to be highly dependent on dispersive effects associated with the diffraction and total reflection.

Finite Element Analysis

Figure 4 shows transient displacement results of a 2-D numerical analysis with the FEM software package, Archimedes (Bao et al., 1998), used to model the propagation of a vertically incident ($\theta_i = 0°$) Ricker wavelet interacting with the normal edge of a soft basin ($\psi = 60°$). The Ricker wavelet (Ricker, 1940) is a triple peaked function containing a range of frequencies up to approximately three times its characteristic (strongest) frequency, f_c. In this example we use a velocity contrast, $\beta_2/\beta_1 = 10$ and a dimensionless characteristic frequency, $f_c/f_0 = 2$, where f_0 is the fundamental vertical frequency of the layer ($n = 0$ in Equation 3).

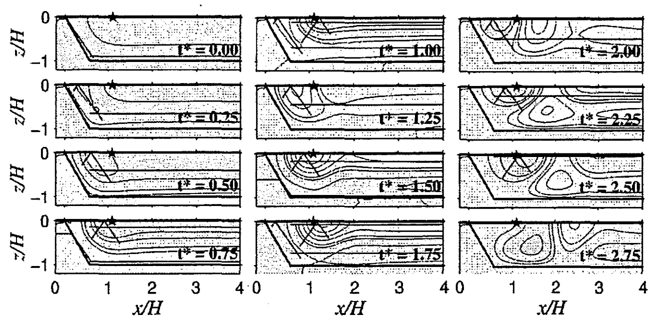

Figure 4. FEM results shown as consecutive frames of contoured anti-plane displacement in the *x*-*z* plane. The time variable, $t^* = \beta_1 t/H$, is dimensionless.

Overlain on the contoured FEM results is a series of lines showing the position of each of the three peaks in the undispersed Ricker wave field. The position of these lines has been calculated using the ray path analysis described in the previous section. In addition a small pentagram indicates the expected position, x^c (from Equation 10), of constructive interference between undistorted wave fronts on the surface. Since we are most interested in the displacement response on the surface of the model, we can look specifically at this as it changes with time in Figure 5.

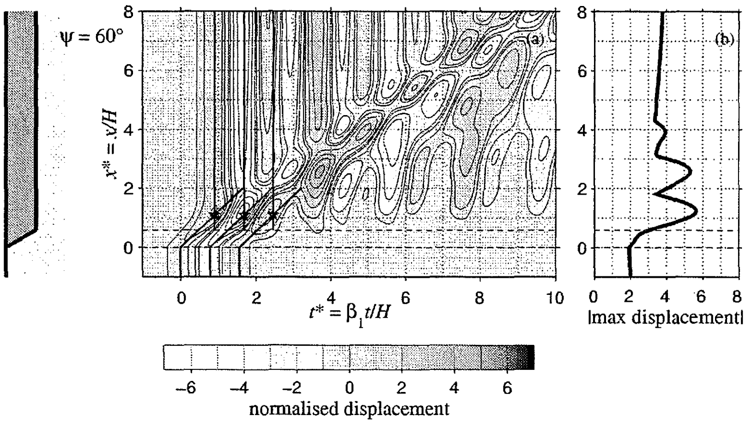

Figure 5. Contours of transient anti-plane displacement on the surface of the FEM model. Peak displacement is shown on the right-hand plot.

FEM contours show clearly the higher amplitude pulses associated with constructive interference some distance out from the edge. In this example, the position of peak displacement calculated by the finite element analysis almost matches that calculated by the ray path analysis of a plane undispersed wave field (Equation 10). While the first peak is undoubtedly the strongest, constructive interference between the horizontally propagating Love wave and vertically propagating SH wave can be seen to occur consecutively across the layer (diagonally across the contour plot in Figure 5). This is a result of repeated vertical reflections of the base-refracted wavefronts, and of the multi-peaked nature of the Ricker wavelet. The position of constructive interference is better related to the velocity of the dispersed wave field and resultant Love wave than the initial edge-refracted pulse.

In further modelling not presented here (Adams, 2000) with Ricker wavelets of various central frequencies, it was found that when the frequency of the input wave is very high compared to the fundamental frequency of the sediments, f_0, the basin-edge effect creates a discrete point of amplification by constructive interference. When the input frequency is close to f_0 a wide zone of amplification develops by coupling between vertical resonance in the layer and the Airy phase of the Love wave. For low velocity contrasts, however, the Airy phase effect becomes much less important. For input frequencies less than f_0, little amplification occurs as most of the Love wave energy travels as a inhomogeneous wave in the basement.

Edge Response in the Lower Hutt Valley

The north-western edge of the Lower Hutt valley is lineated by the active Wellington Fault which has formed a vertical edge to a 300-metre deep layer of Quaternary sediments (β = 175-880m/s) bounded below and to the side by a much older and stiffer basement rock (Torlesse greywacke and argillite, $\beta \approx$ 1500m/s). The surface trace of the fault visible in Figure 6 defines the location of the vertical basin-edge structure some 160 metres out from the base of the hills.

A finite element analysis of Ricker pulse propagation through a 2-D geological model of the Lower Hutt Valley (Adams, 2000) has generated the displacement results shown in Figure 7. The bedrock boundary is shown with the thickest line and the soft sediments have been modelled as six horizontally layered units.

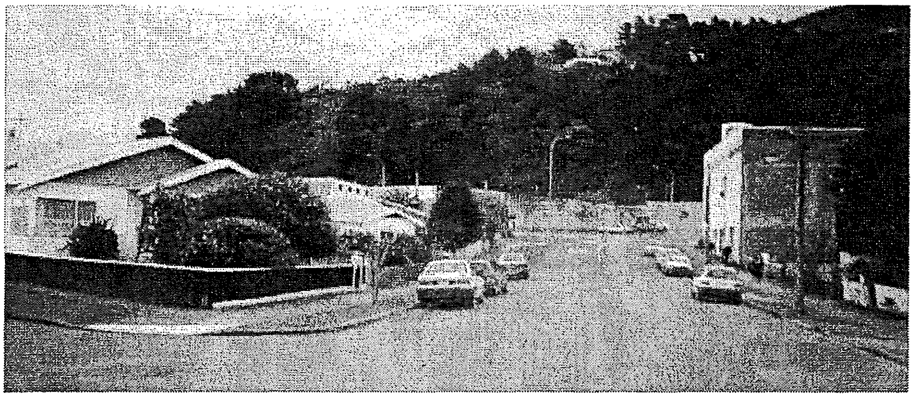

Figure 6. The surface trace of the Wellington Fault in Lower Hutt is indicated by the small rise at the far end of Te Mome Street.

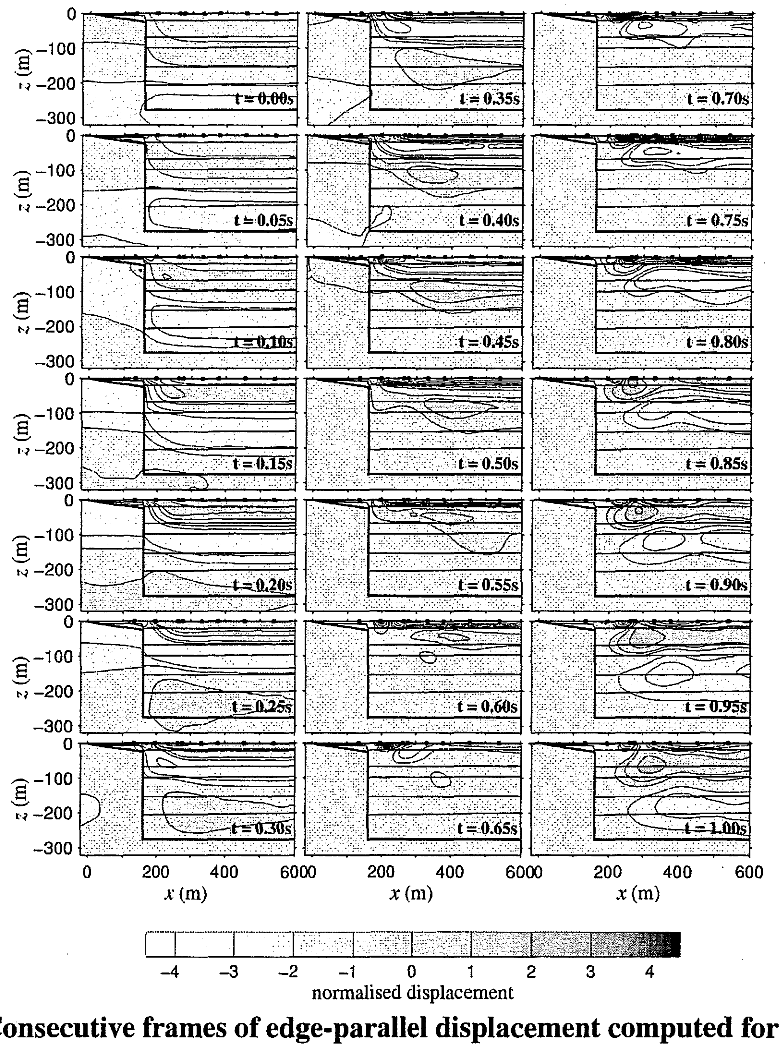

Figure 7. Consecutive frames of edge-parallel displacement computed for the Lower Hutt Valley subject to a vertically incident 2Hz Ricker pulse. Time $t = 0$ occurs when the first peak of the wavelet reaches the surface through the rock on the left hand edge of the model.

Horizontally propagating pulses do not properly form at the shallow edge of the valley ($x = 0$), but rather above the deep vertical edge (at $x = 160$m). The bulk of the Love wave amplitude travels within the top layer and meets the vertical arrival to generate peak displacement at $x = 250$m. This process occurs three times, once for each peak of the Ricker pulse. While the geometry of the problem in this example is significantly more complex than the generic layer edge analysed previously, the same basic mechanism of constructive interference is still apparent.

An array of seismographs was deployed across the fault bounded edge of the Lower Hutt Valley during a six week period from December 1998 to January 1999 (Osborne, 1999). Normalised peak ground motions recorded on the array have been plotted in Figure 8 alongside the results obtained by the numerical FEM analysis. Results from the modelling have been plotted for four different angles of incidence, while peak displacements from each of the 13 recorded events are shown with a lighter colour.

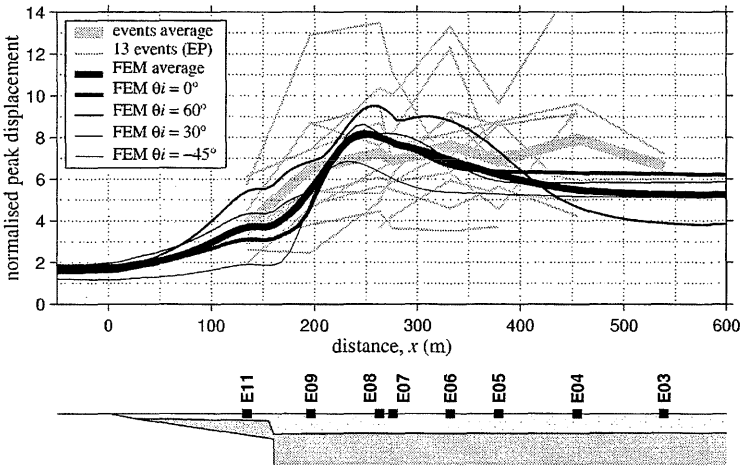

Figure 8. Variation in (edge parallel) peak ground displacement across the array. The locations of 8 recorders (E03-E11) with respect to the valley edge is shown in cross-section on the lower plot.

The general amplitude of average peak displacement is similar, yet the distinct peak in the modelling at x = 250m is not apparent in the recorded motions. Array data also shows a much wider range of peak displacement than does the modelling for different angles of incidence. Both these observations are, however, not a surprising result considering the variety of input motion in the 13 earthquakes.

Discussion

From the results outlined above, it is apparent that the surface response at the edge of a soft layer is governed by several variables, related to either the characteristics of the input signal or those of the basin structure. While the basin-edge effect mechanism is entirely a local phenomenon, created only by the geometry and material properties of the deep basin edge, its characteristics are highly dependent on the angle of incidence, the shape and frequency content of the time-history and the orientation of particle motion or type of wave involved.

The ray path analysis showed that a discrete point of constructive interference may occur between refracted and undispersed wave fields for certain combinations of edge slope and angle of incidence. The position of such interference may be exactly computed given a high-frequency input and simple plane-edge geometry. Finite-element modelling, however, showed that the position and amplitude of constructive interference is often better correlated with the edge-generated (dispersed) Love wave than with the undispersed wave field. In order to accurately predict the position of constructive interference it is thus necessary to understand the propagation characteristics of the edge-generated dispersed wavefields, and the subsequent set-up of a Love wave.

Input Signal Characteristics

Given the multi-pulsed nature of most seismically-induced ground motions it seems reasonable to expect a zone of amplification wider than that generated by a simple Ricker pulse. The maximum extent of amplification would be limited by dispersive deamplification and stretching of the surface wave pulses, and loss of energy in the vertically reflecting wave by material damping and subcritical leakage into the basement. It would thus be expected that the first point of constructive interference would generally be the most significant. That is interference between a pulse in the base-refracted arrival and the matching pulse in the surface wave train, both originating from the same wavefront within the input.

The quality and strength of constructive interference is dependent on the match in not just the timing, but the shape of pulses. An input time-history containing a single prominent monotonic pulse would be expected to create a much more highly amplified and sharp zone of constructive interference than would an input of white noise. The resulting zone of amplification will have a width dependent on the dominant wavelength of the pulse. The more monotonic a pulse is, the less likely it will be distorted by dispersion and thus able to produce the most coherent constructive effect. For a multi-pulsed input signal, the quality of successive constructive interference would necessarily be dependent on a good match between the shapes of successive peaks within the record.

As discussed in the FEM results, the higher the input frequency with respect to the natural frequency of the basin sediments, the sharper and narrower the amplification. High frequency pulses within strong-motion records are, however, generally much less well defined than the lower frequencies and are more susceptible to attenuation within the sediments.

Basin Edge Geometry and Material Properties

Given the same input motion, different sedimentary basins will generate different edge effects. The depth and velocity of soft sediments adjacent to the basin edge control the travel time of vertically propagating shear waves, the fundamental resonant frequency of the layer and the dispersive velocity characteristics of horizontally-propagating Love waves. Deep basins and low-velocity sediments have low fundamental frequencies, and the corresponding ratio between the frequency of input pulses and the basin are higher. This leads to a sharper basin-edge effect as discussed above. Deeper basins and softer sediments also delay the surface arrival of the wave travelling up through the sediments and increase the distance of constructive interference from the edge.

Just as important in defining the position of the basin-edge effect, is the surface-wave dispersive velocity distribution. Dispersion curves for near-surface sediments are a function of the material properties and depths of the sediments. For a given pulse frequency within the input, the sedimentary properties define the nature and velocity of the surface wave propagation, and hence the position of interference. Low frequency input energy will be more likely to travel at higher velocities, while high frequency components travel at velocities closer to that of the near-surface layers.

The ray path analysis and FEM modelling show that the edge-slope has little influence on the velocity of the edge-refracted wavefield and resultant Love wave. Once a Love wave leaves the edge-region, its dispersive velocity characteristics and hence the position of constructive interference depend only on the velocity structure of the sediments.

For very flat edge slopes resembling a wedge shape, constructive interference between the base and edge refracted wave fields is very weak, and spatially-varying amplification occurring above the dipping edge appear to be caused by a different mechanism. Hudson (1963) shows that a Love wave will develop in the wedge when the edge-angle is small (presumably with respect to the critical angle). For larger angles it is likely that there will also be some form of poorly-constrained total internal reflection within the wedge which may show many of the dispersive characteristics of the Love wave. This suggests that amplification is probably the result of some form of Airy-phase phenomenon associated with the post-critically trapped wave reaching the dominant frequency of the input signal. Amplification would then occur between this laterally propagating Love-type wave and the first arrival of the undispersed edge-refraction at the surface.

Conclusions

The seismic response at a basin edge is controlled by edge-generated wave fields, produced by refraction, diffraction and/or total reflection of an incoming seismic wave field at the basin edge. In the anti-plane case, they quickly develop into horizontally propagating Love waves by total internal reflection.

The position of the basin-edge effect is essentially given by the difference in surface arrival times (between waves travelling through the sediments and those travelling through the rock) multiplied by the (dispersive) velocity of the edge-generated Love wave.

For a given input signal, the basin-edge effect amplification will be strongest and most well-defined for very deep basins, and for those with a sharp velocity contrast between the sediments and the basement rock.

The nature of the input motion determines both the width and the quality of constructive interference. A prominent and monotonic pulse within an input signal will generate the strongest amplification. The width of amplification is controlled by the wavelength of the pulse. A multi-pulsed input with a good match in shape between successive pulses will generate a wider zone of amplification.

The frequency of the input signal with respect to the fundamental vertical frequency of the layer has a significant effect on amplification at the edge. An input frequency significantly less than the fundamental will produce little edge amplification. An input frequency close to the fundamental will create an Airy-phase edge effect, provided the velocity contrast is high. Finally, an input frequency significantly higher than the fundamental will generate a sharp basin-edge effect.

Constructive interference has also been shown by a ray path analysis to occur between *undispersed* edge and base refracted wave fields, yet its effect is generally insignificant compared to that which develops between the edge-generated *dispersed* wave field and the base-refraction. The position of constructive interference between undispersed wave fields may, however, be calculated with simple geometrical expressions.

References

Adams (2000) *Basin-edge effects from SH-wave modelling with reference to the Lower Hutt Valley, New Zealand.* PhD Thesis, Department of Civil Engineering, University of Canterbury. 270p.

Alex, C.M. and Olsen, K.B. (1998) Lens-Effect in Santa Monica? *Geophys. Res. Lett.* 25 (18): 3441-3444.

Bao, H.; Bielak, J.; Ghattas, O.; Kallivokas, L.F.; O'Hallaron, D.R.; Shewchuk, J.R. and Xu, J. (1998) Large-Scale Simulation of Elastic Wave Propagation in Heterogeneous Media on Parallel Computers. *Computer Methods in Applied Mechanics and Engineering.* 152: 85-102. Elsevier Science S.A.

Dezfulian, H. and Seed, H.B. (1970) Seismic Response of Soil Deposits Underlain by Sloping Rock Boundaries. *Journal of the Soil Mechanics and Foundations Division, ASCE* SM6: 1893-1916.

Downes, G.; Dowrick, D.; Smith, E. and Berryman, K. (1999) The 1934 Paihiatua Earthquake Sequence: Analysis of Observational and Instrumental Data. *Bull. Natl. Soc. Earthquake Eng.* 32 (4): 221-245.

Graves, R.W.; Pitarka, A. and Somerville, P.G. (1998) Ground Motion Amplification in the Santa Monica Area: Effects of Shallow Basin-Edge Structure. *Bull. Seism. Soc. Am.* 88 (5): 1224-1242.

Haskell, N.A. (1960) Crustal Reflection of Plane SH Waves. *J. Geophs. Res.* 65 (12): 4147-4150.

Higashi, S. (2000) Simulation of Strong Motion During the 1995 Hyogo-Ken Nanbu Earthquake by using the 2D/3D Pseudospectral Method. *Proc 12th World Conf. Earthquake Eng.*, Auckland, New Zealand. Paper No. 1751/4/A.

Hong, T.L. and Helmberger, D.V. (1977) Generalized Ray Theory for Dipping Structure. *Bull. Seism. Soc. Am.* 67 (4): 995-1008.

Hudson, J.A. (1963) SH Waves in a Wedge-shaped Medium. *Geophys. J. Royal Astr. Soc.* 7 (5): 517-546.

Kawase, H. (1996) The cause of the Damage Belt in Kobe: "The Basin-Edge Effect", Constructive Interference of the Direct S-Wave with the Basin Induced Diffracted/Rayleigh Waves. *Seismol. Research Lett.* 67 (5): 25-34.

Kubo, K. and Isoyama, R. (1980) Damage to Buried Utility Pipes in the 1978 Miyagiken-Oki Earthquake. *Proc 7th World Conf. Earthquake Eng.*, Istanbul, Turkey, vol 8, pp 225-232.

Love, A.E.H. (1911) *Some Problems of Geodynamics.* Cambridge University Press.

Moczo, P. and Bard, P.Y. (1993) Wave-Diffraction, Amplification and Differential Motion Near Strong Lateral Discontinuities. *Bull. Seism. Soc. Am.* 83 (1): 85-106.

Motosaka, M. and Nagano, M. (1997) Analysis of Amplification Characteristics of Ground Motion in the Heavily Damaged Belt Zone During the 1995 Hyogo-Ken Nanbu Earthquake. *Earthq. Eng. and Struct. Dyn.* 26: 377-393.

Osborne, N. (1999) The Basin Edge Effect in the Lower Hutt, Wellington using Weak Ground Motions. *BSc Honours Thesis*, School of Earth Sciences, Victoria University of Wellington, New Zealand.

Pitarka, A.; Irikura, K.; Iwata, T. and Sekiguchi, H. (1998) Three-Dimensional Simulation of the Near-Fault Ground Motion for the 1995 Hyogo-ken Nanbu (Kobe), Japan, Earthquake. *Bull. Seism. Soc. Am.* 88 (2): 428-440.

Poceski, A. (1969) The Ground Effect of the Scopie July 26 1963 Earthquake. *Bull. Seism. Soc. Am.* 59 (1): 1-22.

Ricker, N. (1940) The Form and Nature of seismic Wavelets and the Structure of Seismograms. *Geophysics* 5: 348-366.

Sanchez-Sesma, F.J. and Velazquez, S.A. (1987) On the Seismic Response of a Dipping Layer. *Wave Motion* 9: 387-391.

Wojcik, G.L. (1977) Some Effects of a Surface Dipping Layer on Structure and Ground Response in Earthquakes. *Proceedings of the 2nd U.S. National Conference on Earthquake Engineering*, Stanford, 1979. EERI, pp. 1114-1123.

Yuan, Y.; Yang, B. and Huang, S. (1992) Damage Distribution and Estimation of Ground Motion in Shidian (China) Basin. *Proc. Int. Symp. Effects of Surface Geology on Seismic Motion*, 25-27 March, Odawara, Japan. vol 1, pp 281-286.

The assessment of appropriate risk for the design of roading embankments and structures.

James Burr
Tonkin & Taylor Ltd

Bruce Symmans
Tonkin & Taylor Ltd

Alexandra Wilson
Tonkin & Taylor Ltd

Abstract

This paper addressed the issue of the use of appropriate risk in the design of roading embankments and structures. It is based on the stability assessment, design and construction of numerous retaining structures and slopes in Wellington City. The paper presents details of the roles of the Engineer and the Client, the risks and consequences of slope instability and the requirements of the Building Act. Problems experienced in Wellington are presented including a project example. Possible remedial solutions are discussed. The paper concludes that it is not always necessary or appropriate to use a factor of safety of 1.5 for all roading structures and embankments.

Introduction

A significant proportion of the Wellington City Council roading maintenance work involves remediation of slope instability. Tonkin & Taylor have worked closely with the Wellington City Council on many projects concerning the stability of road embankments and retaining structures. In all of these projects, it has been important to consider the following issues:

- What roles are to be assumed by the Engineer and the Client?
- What are the conditions and precursors to the instability?
- What risks are involved?
- What are the consequences of failure?
- What level of risk is the Client prepared to accept?
- What are the relevant requirements of the Building Act?
- What level of remedial work is required to most effectively meet the criteria established above?
- What are the cost implications?

The roles of the Engineer and the Client

Remedial solutions to retain or support the carriageway should be designed with interactive decision making between both the Engineer and the Client.

Engineer's role

The Engineer's role varies from project to project. However in general, the following basic tasks should be undertaken:

- Investigate the site and establish subsurface conditions;
- Interpret the results of the investigation;
- Establish the likely causes of the observed deformation;
- Establish the importance of the structure and the risk of further deformation or failure;

- Assess the potential consequences of ongoing deformation or failure.

The Engineer may then propose remedial solutions. In some instances, the Engineer may propose remedial solutions to the Client that have lesser factors of safety than are typically adopted. Any such remedial solution should be presented to the client with a description of:

- Risks associated with adopting a lesser factor of safety;
- Consequences of further deformation or movement;
- Estimated capital construction cost;
- Ongoing maintenance or repair costs;
- Anticipated design life.

It is the Engineer's role to provide sufficient information to the Client to make informed decisions. The client must make the assessment of what level of risk is acceptable.

Client role

If the Engineer adequately presents remedial options, associated cost, risk and consequence, then the Client is able to make informed decisions as to the solution that best suits their requirements.

With roading networks, the network operator (the Client) is required to make economic decisions based on balancing risk, consequence and cost. The Client's aim is generally to provide the highest degree of security possible to the roading network within the bounds of the available roading budget. This often entails spending a limited budget, thinly over a range of structures and embankments currently in need of upgrading or stabilising. This demands an efficient use of the budget.

Conditions leading to instability

There are a large number of contributing factors to the problem of instability and it is not the intention of the authors to discuss these in this paper. In Wellington City a significant proportion of the instability problems can be traced to a similar cause.

Many of the urban roads in Wellington City were constructed prior to 1960, often on steep marginally stable terrain. Roading design standards of the time were not as rigorous as modern standards. Construction and compaction techniques have also improved over this period. With many structures nearing the end of their design life, it is not surprising to find that the road embankments and retaining walls that were constructed over 40 years ago are now experiencing stability problems.

Many of the embankments were constructed using cut to fill methods, placing fill on steep slopes with little or no foundation preparation, inadequate retention, poor compaction, and poor stormwater control. The resulting marginally stable fill slopes are susceptible to ongoing creep that can be exacerbated by heavy rainfall.

Risk

Risk can be defined as the combined perception of:

1. The likelihood of an event and
2. The gravity of the consequences.

The perception of risk is highly subjective and so is typically described verbally or qualitatively, e.g. high, unacceptable, marginal etc.

Highly probable events with severe consequences are considered high risk. Unlikely events with negligible consequences are considered low risk. In terms of roading structures and embankments perceived risk is often reflected in design by the application of factors of safety (FOS). A high FOS (low risk solution) is generally adopted for high-risk situations.

Acceptable risk vs cost

The management of risk has an associated cost implication. The Client must decide how much risk they are prepared to accept for a structure and at what financial cost.

Generally, low risk solutions have high construction costs. The inverse applies for high risk solutions.

It is possible to repair a damaged or unstable section of wall or embankment to differing standards. For example, remedial work may consist of superficial resealing over tension cracking or it may require the construction of a retaining wall designed to NZS 4203:1992 design loadings. The former option will make the carriageway or footpath trafficable in the short term but is unlikely to provide a significant improvement in slope stability. The ongoing maintenance cost of repeat resealing may be less than the construction cost of the robust structural solution. Provided the consequences of further failure are negligible, the repeat resealing may be a more efficient solution.

If the Engineer presents the Client with enough information, the Client can make better use of the limited budget by managing the risk more efficiently.

Consequences

Consequence can be defined as the result or the importance of an event.

The consequence of failure or ongoing deformation is the single most important aspect to consider in pre-remedial assessment and remedial works design. For roading structures, the consequences that need to be identified by the Engineer and which are relevant to the Client include:

- The extent of deformation or potential failure. Will it affect 1 or 2 lanes? Will it affect the footpath?
- The magnitude of potential failure.
- Any property that the deformation or failure could damage. Will downslope properties be adversely affected?
- Damage to buried services within the road or footpath or to overhead services and poles.
- Any threat to human life.
- The nature of the route. Is the route that the structure is supporting part of an arterial route, a city lifeline or a minor road? The consequences to the Client of a failure on a busy route are far more significant than a minor access road or pedestrian path.
- The condition of the remainder of the route, the design life of the proposed structure and the improvements to the route within that design life. It may not be efficient to design a robust structural solution at high cost for a single section of road if the remainder of the route will be non-operative following a hazardous event.
- Replacement cost and timing. If a structure fails, what are the cost implications of repairing or replacing it and will the time frame be acceptable?
- Potential environmental damage.

Seismic Risk

In Wellington, as with much of New Zealand, seismic hazard is considered significant. A significant proportion of roading structures around Wellington City are unlikely to withstand significant seismic shaking. Wellington City has been built in a seismically active region and on a major fault line. It is not practical with the current resources available to upgrade all of the roading structures to withstand ultimate design earthquakes. As the likelihood of earthquakes is reasonably well defined (based on frequency of past events), the decisions on acceptable seismic risk are dictated largely by the consequences of failure and the cost of replacement.

Building Act Requirements

The Building Act (1991) provides the formal legislation controlling the construction of "Buildings" in New Zealand. A retaining wall is defined as an "Ancillary Building" in the Act. Under Schedule 3 of the Act any wall retaining less than 1.5m without surcharge loading can be considered an exempt building and therefore does not require a building consent. However, the Act also states in Section 7 that "All building work shall comply with the building code to the extent required by this Act, whether or not a building consent is required in respect of that building work". Therefore, essentially the Building Code must be complied with for all retaining walls.

The Building Code is set out in the First Schedule of the Building Regulations. It contains 37 clauses, of which Clause B1 contains the relevant requirements for stability of retaining walls and associated slopes. The Building Code is a performance-based code. It sets out objectives to be achieved rather than prescribing construction methods. The emphasis is on how a building and its components must perform as opposed to how the building must be designed and constructed. The familiar factor of safety requirement of 1.5 for non-seismic design of permanent slopes was part of the previous Verification Method B1/VM4. The latest amendment (December 2000) provides no guidance on acceptable stability and in fact specifically excludes slope stability. We must therefore assume that it is now up to each Territorial Authority to determine what it considers to be an appropriate level of stability. However, it would seem likely that in most situations the Territorial Authority will fall back onto the familiar territory of a minimum FOS of 1.5.

Is a non-seismic FOS of less than 1.5 appropriate for a permanent slope or retaining wall foundation?

Practically speaking, an application for Building Consent that does not achieve a FOS of 1.5 would probably require an assessment of the risks and consequences of failure based on the provisions of the Code. For some walls the risk of failure is considered relatively low and the consequences minor, particularly when compared to the cost of achieving a FOS of 1.5. In these cases there may be a strong case for arguing that alternative solutions are appropriate. This may require significant extra effort during the building consent application process and the outcome may not be guaranteed. Ultimately, the Client must make this decision based on its requirements and the information provided to it by the Engineer and other professionals.

An alternative to this process would be to request a building consent under the provisions of Section 36(2) of the Act (although this Section is currently under review). Given that the roading network referred to in this paper is owned by the Territorial Authority, adopting Section 36(2) will not shift any responsibility from the Authority. There may however be insurance implications to the Territorial Authority.

Residential development

It may not be appropriate to accept higher risk solutions for residential development where there may be many owners of a property over the design life of the structure or slope. Future owners may not be immediately aware of the liability they are accepting in purchasing assets that have been designed with a higher than typically accepted risk. The comments of this paper refer mainly to roading networks where the Client (the Territorial Authority) is likely to be the owner of the structures for the design life.

Remedial Solutions

Repairs & Maintenance

For many Wellington roads where roads are constructed as sidling cut to fills, traversing steep slopes, the fill edges are often prone to creep movement and shallow surface failures. Roads have often been widened and footpaths added post initial construction. The footpaths and outside edges of the road are often formed on loose overspill fill with slopes up to 50°.

Typically, tension cracking and subsidence will be caused by relatively shallow seated creep. In many such instances, while the FOS under normal winter groundwater level is between 1.0 and 1.2, it is cost-effective to simply resurface the edge of road or footpath every 4 to 6 years. The cost of providing any effective retention of the loose overspill fill is high. The consequences of small failures within the road edge or footpath are often minimal and under these circumstances, the cost of retention can acceptably be deferred until complete failure occurs. There are often economic advantages to the Client in deferring capital expenditure until it is absolutely necessary.

Mitigating effects

There are many instances in the steep Wellington terrain where the cost of providing effective retention of slopes is prohibitive, yet the rate of ongoing deformation of the road edge or footpath creates a potential safety hazard and requires remedial work at frequent intervals.

It is possible to mitigate and control the effects of creep so that the rate of resealing becomes acceptable. Such methods will not generally increase the FOS of the slope, or reduce the risk of large failures in the future. Mitigation methods include:

- Fixing batter boards to the downslope edge of the road or footpath to a minimal depth to retain the outside edge to eliminate a majority of the creep movement.
- Placing geogrid reinforcement beneath the road edge or footpath to control cracking within the pavement.
- Providing stormwater run-off control by regularly sealing the cracking in the road and footpath.

Improve stability with lesser than typical FOS

The majority of movement on Wellington's steep roadside slopes occurs within loose overspill fill within the top 1.0 to 2.0m below the level of the footpath. In many cases, the material underlying this fill is a medium dense colluvial material overlying steeply inclined greywacke rock.

While failures within the undisturbed colluvium are uncommon and these deposits have often been in place for hundreds of years, these deposits invariably have a FOS less than 1.5. In some instances, the colluvium may still provide reasonable founding conditions for retaining structures designed to reduce the magnitude and frequency of creep within the overlying loose fill.

The Client can choose a medium cost solution of retaining the loose overspill fill by founding a retaining structure into the colluvium but they must accept an increased risk of damage or failure, particularly under seismic conditions.

Improve stability to provide a FOS of 1.5

A robust, solution would be a wall or a slope designed to verification method B1/VM4. Typically this would require normal limit state requirements (NZS 4203:1992) or a FOS of 1.5 for structures and slopes respectively. This includes design for seismic loading for structures over 4.0m in height. A robust solution should always be adopted where the consequences of failure are considered to be severe.

The medium cost solution may provide a FOS typically in the order of 1.2 to 1.3 for static loading but marginal performance under an ultimate seismic event. However the cost may be only ¼ of the cost of the robust option. The cost difference is dependent on the specific conditions at each site. A lesser FOS should only be adopted on the Client's instruction as it is the Client who must accept the higher risk for the associated cost saving.

Project Example

An example of a roading instability investigation and remedial solution proposed for Wellington City Council is shown in Figures 1 to 4. The project is in Chaytor Street, an arterial road linking the suburb of Karori to Wellington City Centre. Chaytor Street is constructed as a sidling cut to fill, traversing a steep slope standing at 40 to 60°. The slope forms the western side of a valley overlying the Wellington Fault. The fill depth underlying the downslope footpath varies but is in excess of 30m deep at Section 1 (shown on Figure 1) and 17.8m deep at Section 2 (shown on Figures 3 and 4). Significant cracking has been observed in the footpath at both sections and the outside lane of the carriageway at section 2. Downslope creep movement is likely to be the cause of the cracking.

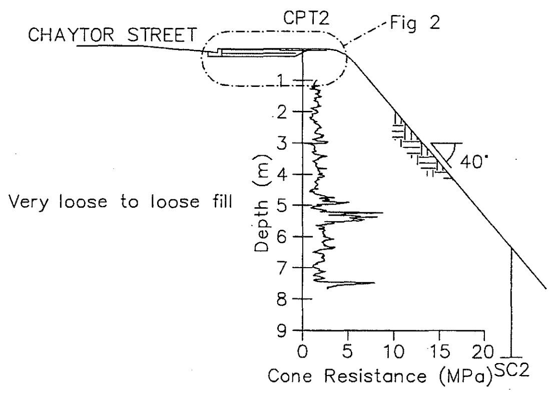

Figure 1: Chaytor Street Section 1 – Sub-surface conditions

Section 1

At Section 1 (Figure 1) the majority of deformation is thought to be surficial occurring in the upper 1 to 2m depth of soil and the analysed FOS for a deep seated failure under seismic loading is likely to be less than unity. The consequence of a large failure under seismic conditions can be mitigated by temporarily diverting the road though a Council park on the upslope side of the carriageway. There is no development or human habitation on the slope below the road. The consequences of a failure are therefore unlikely to warrant the high cost of providing a FOS of 1.5 to the slope. To mitigate the effects of the tension cracking in the footpath and reduce the frequency of future reseals it is proposed to reconstruct the footpath with geogrid tension reinforcement within the basecourse. The geogrid will provide negligible increase in the FOS of the slope but it will mitigate the effects of shallow soil creep. Cracking will preferentially form in the grass berm below the footpath or the joint between the footpath and kerb (where cracking can be easily maintained). This inexpensive measure will defer the high cost of a more secure solution until the remainder of the route is upgraded in the future.

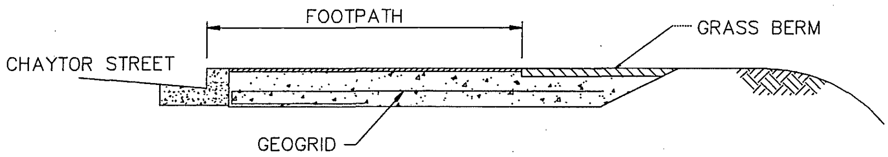

Figure 2: Section 1: Recommended remedial design – geogrid crack mitigation.

Section 2

Section 2 lies 100m to the north of Section 1, but differs in that the observed movement is more deep seated and no alternative route can be provided to traffic if failure of the carriageway were to occur. The section 2 carriageway is constrained on the upslope side by a large cutting and residential development. The consequences of a slope failure at Section 2 include lengthy closure of the arterial route and loss of public services and utilities.

The Client has indicated a preference for a low risk solution for Section 2. Two of several schemes presented to the client are shown in Figures 3 and 4. Shown on Figure 3 is a tied back palisade wall beneath the kerb and channel and a geogrid-reinforced fill supporting the footpath. The conceptual design is designed to support up to 7m of loose fill under an ultimate seismic loading. The geogrid-reinforced fill (and footpath) is likely to undergo significant deformation under this seismic load.

A second conceptual alternative for Section 2 is shown in Figure 4. A tied back retaining structure positioned on the downslope edge of the footpath is designed to provide support to both the carriageway and footpath under ultimate seismic loading. Reducing the risk to the footpath (using the more secure Figure 4 design) is likely to increase the construction cost of remedial works by approximately one third. The client will need to consider if a higher risk for the footpath is acceptable.

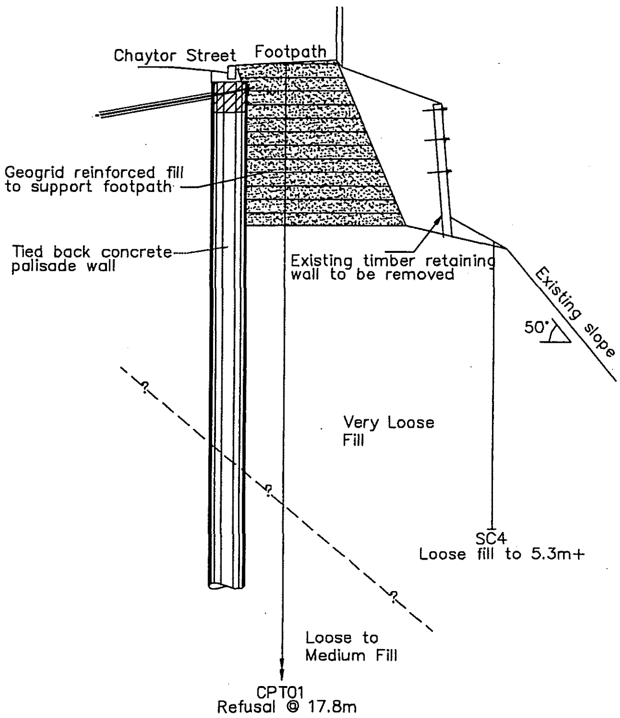

Figure 3: Section 2 Palisade wall and Geogrid reinforcement.

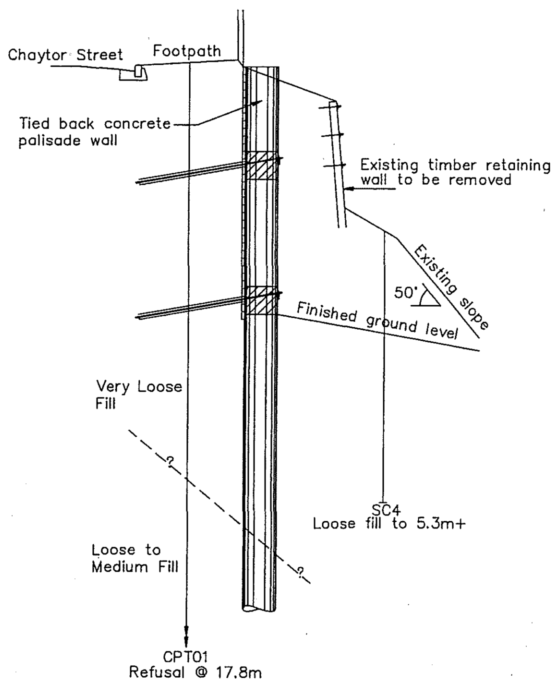

Figure 4: Section 2 Palisade wall only

Conclusion.

This paper attempts to show that it is not necessary and not always appropriate to use a factor of safety of 1.5 for all roading structures and embankments. The Building Code is performance based and does not specify minimum FOS for structures. This provides an avenue to assess each situation carefully and offer alternative options.

The Client has limited resources available and these need to be managed efficiently to provide the best overall result. This may mean accepting higher risk solutions at less cost in some situations. It is the Client who must make the assessment of what risk is acceptable. This decision needs to be based on sound information supplied by the Engineer.

Acknowledgement

The contributions from Peter Sumby and Bruce McLean of Wellington City Council are gratefully acknowledged for assistance in preparing and reviewing this paper.

Reconstruction of landslide affected SH3 at Stockman's Hill

S. Finlan

Montgomery Watson (formerly Opus International Consultants Ltd)

J. Chisnall

CSP Pacific(formerly Opus International Consultants Ltd)

Abstract

July 1998 saw 1:100 years floods in New Zealand's North Island, followed by the wettest October since records began. The intensity and prolonged wet period resulted two separate landslides affecting SH3, one of New Zealand's strategic highway routes.

In July a slip at Stockman's Hill (Stockman's I) resulted in the highway dropping approximately 5m as 320,000 m^3 to 600,000m^3 of material adjacent to, and including, the highway slipped affecting around 8ha of land..

Between July and October a progressive slip occurred some 1.2km from the July event (Stockman's II) resulting in the slip encroaching on the highway.

The landscape of the area is one of rugged high hill slopes of steep rolling country, with limited vegetation cover. Options for the permanent reinstatement needed to take account of the hostile climatic conditions, short construction period and general difficulty in treating local materials for earthworks use. The selected options for the slips included two MSE walls.

This paper considers the geological context of the project, the failure mechanism and remedial options, together with details of the adopted mechanically stabilised (MSE) walls which were completed and opened to traffic after a three month construction period.

Location

Stockman's Hill is located on State Highway 3 (SH3), approximately 12km south-west of Piopio and some 100km north east of New Plymouth (Figure 1). SH3 is part of New Zealand's main transport corridor providing access from the Auckland, Hamilton and the Bay of Plenty to the Taranaki Region in the south-west of the North Island.

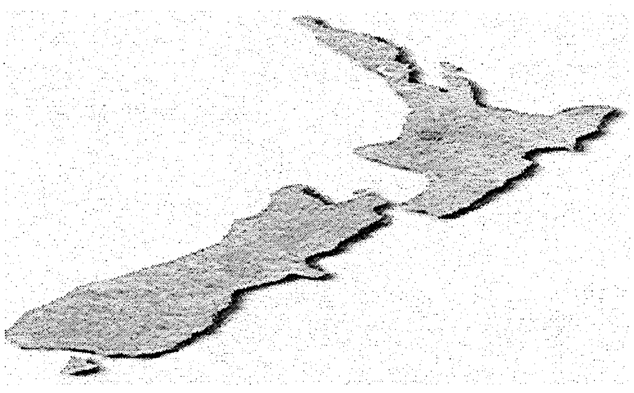

Figure1: Location of Stockman's Hill

The initial slip (Stockman's I) occurred on 8 July 1998 when a 120m-150m section of SH3 dropped 5m (Figure 2) as adjacent land on the eastern side of the road slipped downslope immediately closing the road to traffic. A temporary controlled single lane diversion was constructed around the back of the dropout within six days to enable traffic to cross the site pending remedial works.

Figure 2: Stockman's Hill: 8th July 1998

The second slip (Stockman's II) occurred in October 1998 some 1.2km south of the first which encroached upon the highway. Deformation of the highway was not so severe and the road remained trafficable, although twenty four hour surveillance of the road was maintained due to a continually regression head scarp which continually threatened to intercept the road and sever the highway.

As a major strategic highway in New Zealand, the reopening of the road and its reinstatement were paramount for the state highways roading authority, Transit New Zealand (TNZ) and urgently needed as the Taranaki Region of the North Island was effectively isolated from the north except for a 4hr diversionary route.

Geological Context of the Site

The area is located on the eastern limb of a large syncline which extends between faults running sub-parallel to the west coast (some 20km east of Stockman's) and the Waipa-Aria fault some 10km east of Stockman's. The Triassic marine sandstones and siltstones which form the limb of the syncline dip steeply at around 80° to the west. Overlying the synclinal basin are calcareous marine siltstones, sandstones and limestones of the Mahoenui and Te Kuiti Groups (Tertiary deposits) which have been significantly eroded.

The slip at Stockman's I (Figure 3) is situated in the Mahoenui Mudstone terrain, being of Lower Miocene age and typically slightly calcareous and poorly bedded, locally termed

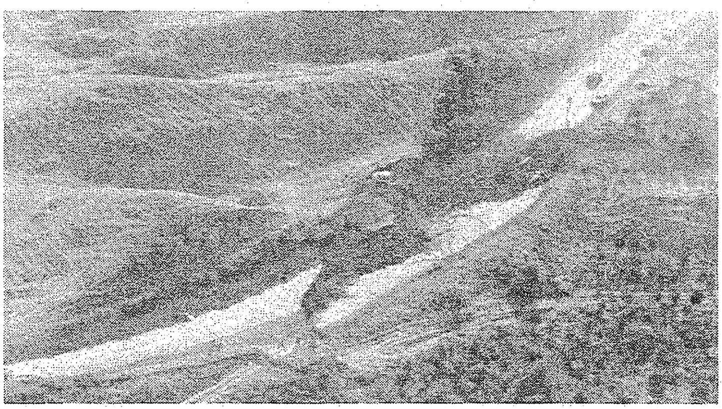

Figure 3: Aerial view of Stockman's I

'papa'. The mudstone contains a high proportion of active, swelling clays which result in slaking degradation of the mudstone and development of blocky regolithic soil cover. An intermediate layer of weathered fractured mudstone generally occurs between the slightly weathered/fresh mudstone and the regolithic soils. This displays open fractures indicating significant dilation of the rock mass.

The slip is located on the southern (eastern) slopes of a narrow divide eroded into the Mahoenui Mudstone where the existing road appears to have been built on fill materials across a saddle between two prominent knolls. The approximate extent of the overall slide (which includes the road) was 150m by 250m. Secondary debris flows generated at the toe of the slide extend several hundreds of metres down the valley. The main body of the slide was extensively deformed, primarily by open tension cracks with an average vertical displacement of 1m and was typical of a retrogressive transitional slide. The average inclination of the slide movement was about 11° to 14°. The depth of the slide block varied between 4m and 10m with a total affected slide area of 8ha and volume of material in the regions of $320{,}000m^3$ to $600{,}000m^3$. Large quantities of water were noted discharging from the toe of the slip.

Stockman's II occurred in a similar geological context to Stockman's I, although the 'papa' appeared shallower than at Stockman's I.

Inferred Failure Mechanism

Examination of aerial photographs between the years 1946 and 1995 show slumping having occurred in the general area, and landowner discussions suggest a fairly widespread occurrence of slips. Given the rugged hilly landscape with limited vegetation cover (the native bush removed in the mid-1900's to develop stock rearing) and highly erodible soils, near surface slips could be expected: the difference at Stockman's was the affected area and volume displaced.

The slide movement at Stockman's I was triggered by extended heavy rainfall that was associated with the resulting 1 in 100 year floods in the lower catchment areas. Groundwater seeps at almost every contact between the intact mudstone and the overlying regoliothic or colluvial soils was evidence of the large permeability contrast between the porous soil/highly weathered dilated mudstone rock and the near impermeable intact mudstone rock beneath. Such sub-surface conditions favour the rapid build up of pore water pressures along the contact inducing slope movement of the regolithic soils along the relatively gentle inclined surface. Infiltration of rain into the slide mass creates saturated conditions which results in the development of debris flows where the mass becomes unrestrained at the crest of the escarpment; in this case a flow which travelled hundreds of metres down into the valley.

An interesting aspect of this slide was the presence of pine trees and some natural bush within the slide. Whilst the pine stand, of around 10 years old, was significantly deformed, the natural bush including some Totara trees (of significant age) were not. Slides in the locality are generally on ground devoid of substantial vegetation, with planting being used to aid stability.

At Stockman's II, the initial slip was triggered by the July rainfall with the slip regressing to around 30m from the road. The subsequent October 1998 rains, which resulted in the highest recorded rainfall for October since records began, resulted in a rejuvenation of the slip and a rapid regression over a number of weeks up to and under the highway verge.

Remedial Options

For Stockman's I, remedial options focused on a local site option after undertaking preliminary costing for major realignment options bypassing the area.

Reinstatement of the highway on the slide mass itself was not considered practicable as any reinstatement would be susceptible to the same potential mechanism of failure as caused the July 1998 slip. Hence options were sought that allowed the reinstated highway to remain unaffected by any future movements of the slide.

Consequently the options considered for reinstatement/repair were:-

- an earthworks solution;
- a half bridge;
- a full bridge;
- a reinforced fill slope;
- piled retaining structure;
- mechanically stabilised earth wall.

The advantages and disadvantages of each of the options was assessed. The earthworks option required removal of up to 600,000m^3 of material which would require disposal and replacement with suitable imported fill; the half bridge would have required a span of in the order of 90m; a full bridge 110m; the reinforced fill slope required similar volumes of material movements as the general earthworks option with uncertainty with regard to founding conditions; the piled retaining structure would require a retained height in the order of 15m; the MSE wall would require excavation down to 'papa' rock of suitable integrity and importation of suitable backfill.

The options report (Opus: 1998) considered that only the MSE wall and bridging options were feasible given the geotechnical, location and weather constraints prevailing at the site. Weather conditions in the area were a significant potential constraint. Located near the west coast of the North Island, the area is commonly subject to late afternoon showers during the summer and prolonged periods of wet and inclement weather from the autumn through to late spring. Such recorded weather conditions, combined with the natural moisture contents of the soils, leads to a very short earthworks construction period combined with the potential for significant weather disruption during the works. These considerations were critical in terms of the solution adopted.

Having selected the reinstatement options, the realignment options were considered more closely ranging from maintaining the existing alignment (vertical and horizontal) to lowering the vertical alignment and easing the horizontal alignment. Ten options were considered in detail in terms of economics, user benefits and alignment improvement.

To ease comparison for the MSE wall, the change in wall cost with wall height was plotted together with that of wall height and earthworks volume. The latter graph was overlaid with the available maximum volume of spoil disposal on-site, based upon discussions with the local and regional councils together with landowners. Disposal over this maximum attracted significant increased rates.

A stability analysis and risk assessment was conducted for the MSE walls for each of the realignment options. This, together with an assessment of constructability issues, including weather, construction earthworks window (November to February), length of contract required to undertake the complete works and the spoil disposal issues were compared in a like manner to the bridge option. The resulting Option selected (Option 5) was developed with an MSE wall based upon economics, improved benefits and the flexibility of the solution to cater for any required increase in length and other 'unknowns'.

For Stockman's II, which developed during the detailed design of Stockman's I, a similar MSE wall option was determined as the most appropriate. This also permitted the works to be included in the Stockman's I tender without introducing any significantly different works.

MSE Wall

From the detailed geotechnical investigations conducted on Option 5, the weathering profile of the dark grey 'papa' siltstone was assessed, from which the maximum depth of excavation required to achieve moderately to slightly weathered 'papa' was determined and then adapted to give a longitudinal excavation profile comprising of a series of excavation benches.

Having assessed the height of the wall, the design proceeded but with an additional depth contingency resulting in a 15m high wall design.

Parameters were determined from the site investigation and previous work done on the properties of 'papa' and general experience and knowledge of the materials held within Opus.

Initial design difficulties were experienced due to seemingly conflicting information and data being supplied by differing geogrid manufacturers. Obtaining reliable comparable parameters proved to be one of the major challenges for the design and for the industry. In addition to the differing test methods, design lives, strains and elogations, 'advice' from manufacturers was also found to be conflicting.

We resolved to adopt an internationally accepted design approach, rather than a manufacturer specific approach, adopting those grids, and hence grid parameters, offering the most demonstrable support in terms of long term testing and quality control available to us in relation to the design method.

The design of the wall was carried out to BS8006:1995, with a commercial software package, together with hand verification checks, using the adopted parameters and a traffic surcharge loading. Factors of safety of 1.5 for sliding, overturning and bearing capacity were adopted for static conditions.

The resulting Stockman's I wall (Figure 4a) was designed for a maximum height of 15m with a 75° front face and overall length of 80m using two grid types and a total of 19 layers of uniaxial geogrids for primary reinforcement, and a biaxial grid for secondary reinforcement.

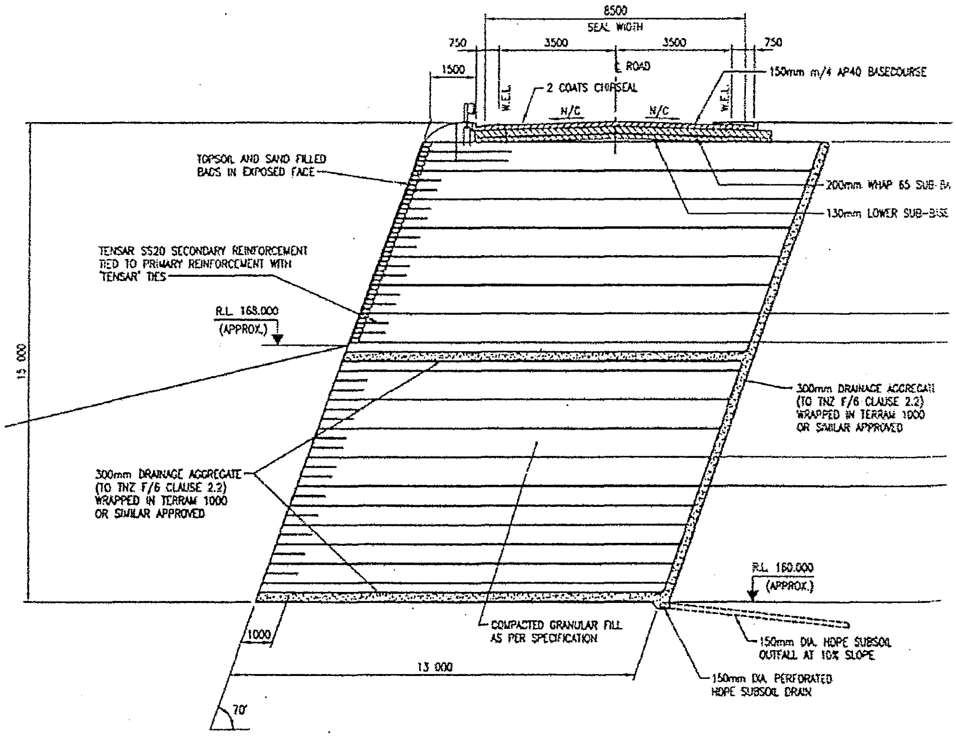

Figure 4a: Stockman's I MSE Wall

Stockman's II (Figure 4b) was designed for a maximum height of 12m with two vertical faces of overall length 160m using three grid types, and a total of 21 layers of primary reinforcement. Both walls were designed to have 'wrap-around' front faces. Hessian bags filled with a mixture of topsoil, sand and grass seed were used to act as formwork for the exposed face and geogrid wrap-around.

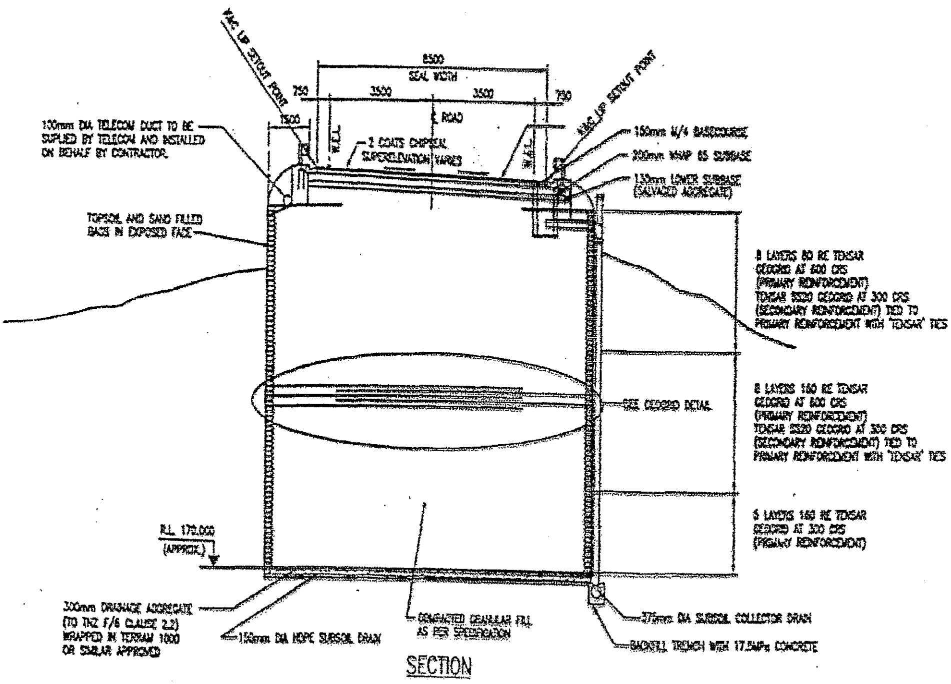

Figure 4a: Stockman's II MSE Wall

Seismic Stability

Mechanically stabilised earth (MSE) structures have been built in seismically active areas for many years. The use of polymer reinforcement to reinforce the soil (such as the geogrids used at Stockman's Hill) results in a composite structure of high ductility. Correctly designed and constructed, such structures are well able to withstand the shaking induced by earthquakes through deformation and absorption of energy, without catastrophic failure.

Recent experiences, most notably at Kobe, Japan in 1995 (Nishimura et al, 1996) have indicated that while many MSE structures have not been designed specifically to withstand earthquake induced loads, the structures perform well with negligible damage.

At Stockman's Hill, while seismic design was not a specific contract requirement, the stability of the proposed MSE wall design under seismic conditions was checked as a matter of routine. The proposed wall was designed to allow limited displacement under seismic conditions. The design methodology was based on Ambraseys and Menu (1988), utilising the critical acceleration ratio to estimate likely displacements. Both wedge and circular failure surfaces were assessed using a commercial program which utilises Modified Janbu and Bishop's Simplified algorithms (respectively) for slip surface analysis, and allows the analysis of seismic loading through he application of pseudo-static loads and short term increase in geogrid strength (by 50% above the LTDS).

Cases for both the likely maximum acceleration (0.33g, based on NZS4203:1992) and to determine the critical acceleration (for a factor of safety = 1) were considered. Under these conditions, the predicted displacements were of the order of between 20 mm and 50 mm, ie less than 100 mm. Such values were considered acceptable for the type of structure under consideration.

Drainage

Detailed attention was paid to drainage aspects. To minimise infiltration into the MSE wall, kerb and channel was specified for the length of the wall discharging into catchpits.

The catchpits also collect drainage from lateral cut-off drains extending up from the 'papa' interface to preclude flow into the reinforced block through the overlying completely weathered materials.

The reinforced soil block itself included a blanket drain at its base and mid-height, discharging into a full height back or chimney drain. These discharged via an outfall into a monitoring catchpit before final discharge into the local waterway away from slip areas.

Construction

To enable rapid construction of the walls the contractor was permitted to stockpile the granular fill required along the lengths of closed highway. This enabled him to essentially resource the walls from site stockpiled materials. Work was also accelerated through working through the night under lighting by working two twelve hour shifts.

The excavations at Stockman's I revealed suitable founding materials at generally higher levels than assessed during the design phase. The criteria for the foundation was the absence of fracture clay infill/lining and no visual evidence of weathering along the fractures. This was achieved by taking the excavation down in a series of benches until the criteria was fulfilled. Thereafter the MSE wall was constructed back up to road pavement level (Figure 5).

Figure 5: Stockman's I under construction

At Stockman's II (Figure 6) the founding levels were generally as assessed during the design phase, although two areas did require deeper excavation to achieve the approval criteria. Whilst this did not affect the wall as designed since allowance for deeper excavation was made, it did cause concern for the quantity of geogrids required. Being sourced from the UK, any major increases in grid quantities would result in long delays or high delivery costs if shipped by air.

However, through designing within the confines of the quantities of each grid type available in the country, and a strong partnering approach with the contractor, it was possible to re-schedule the location of specific grid types without affecting the total quantity of grid needed or the contractors working methods and hence programme.

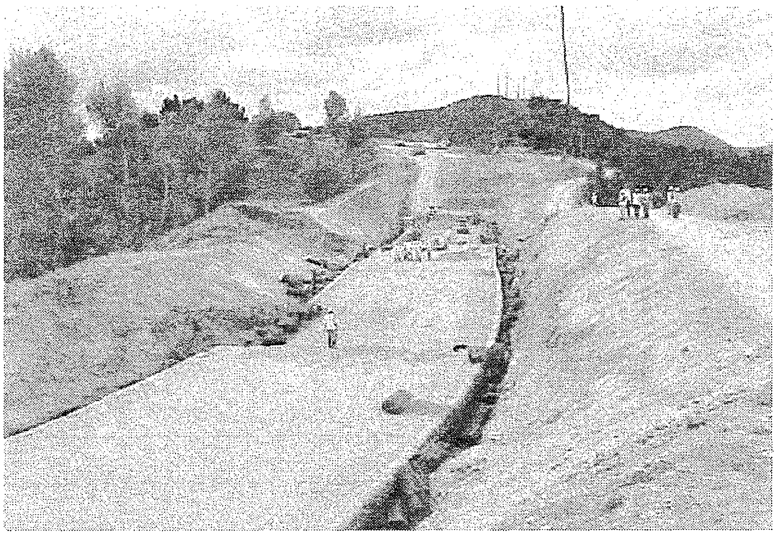

Figure 6: Stockman's II under construction

Following construction of the walls the adjacent weak soils and spoil were placed against the walls such that the full height of the walls is no longer visible (Figure 7). This was not necessary for the stability of the wall, which was designed to be fully free-standing with no lateral support, but was needed to return the land to contours similar to that prior to commencement of the works.

Figure 7: Completed Stockman's I prior to 'backfilling'

Conclusions

The overall concept of using MSE was to provide a fully drained structure capable of construction essentially independent of weather conditions and of being adaptable to ground conditions exposed. These perceived advantages were fully realised.

The ability to work through inclement weather, the relative speed of construction and the ability to work through the night were key attributes to the success of the project, combined with the close co-operation with the contractor and other stakeholders. The perceived advantages of using MSE at Stockman's were therefore realised in achieving one of TNZs most ambitious projects within budget and timeframes.

The design process, itself undertaken within a tight timeframe, highlighted the difficult in obtaining reliable design parameters for geogrids and the differing methods of testing, providing and reporting of quality assurance data which makes selection of grids and design a difficult and arduous task. The industry would do well to establish comparable methods of test, or of reporting characteristics strengths, damage factors and similar design inputs.

The static design undertaken was shown to be acceptable for seismic loading using a displacement type assessment. This concurs with international observations of such structures not designed for, but subjected to, seismic loads.

Acknowledgements

The authors would wish to acknowledge the help and encouragement of David Jennings (Civil Engineer Manager, Opus Hamilton); the support of Ian Cox and the client, Transit New Zealand, in permitting the publication of this paper; Roger High of Opus Auckland and the contractor Fulton Hogan.

References

Ambraseys N.N, and Menu J.M, (1988). "Earthquake-Induced Ground Displacements". *Earthquake Engineering and Structural Dynamics*, Vol. 16, pp 985-1006.

BS8006:1995: "Code of Practice for Strengthened/reinforced soils and other fills" *British Standards Institute*

Nishimura, J. et al (1996). "Earthquake resistance of geogrid reinforced soil walls based on a study conducted following the Southern Hyogo earthquake". *Proc Int Symp on Earth Reinforcement, Fukuoka, Kyushu*, Vol 2, pp105 – 140.

NZS 4203:1992. Code of Practice for General Structural Design & Design Loadings for Buildings". *Standards New Zealand.* Published by Standards New Zealand, Wellington.

Opus (1998). "SH3: RP103/11.5 Stockman's Hill Reinstatement Project Investigation Report". Opus International Consultants, Hamilton.

Remediation in an explosive environment

I. M. Kluckow
Golder Associates Pty. Ltd., Melbourne, Australia

P. N. Thornton
Golder Associates Pty. Ltd., Perth, Australia.

Abstract

The Albion Explosives Factory Remediation Project has involved extensive clean up of soil contamination. Industrial operations associated with explosive chemical manufacturing impacted upon the potential uses of the land with elevated concentrations of a broad range of contaminants including explosive organic compounds remaining in the soil in some areas.

With the close proximity of the community and the risk of exposure to workers to a range of contaminants and physical hazards, a series of risk-based assessments were undertaken to identify, characterise and map the site hazards. Specific design, construction and management procedures were then implemented to mitigate the environmental and health and safety risks posed by these hazards both during the clean-up and for the long term site use following redevelopment.

Background

A major soil contamination remediation project has been undertaken for the Australian Department of Defence at the former Albion Explosives Factory. The site comprises 455 hectares of land on the Western Highway in Deer Park, Victoria, Australia and is now becoming a new suburb in the west of Melbourne. Up to 1986, it was used for almost 50 years for the manufacture of explosives for use in armaments.

The manufacturing processes undertaken have impacted on the land, with elevated concentrations of a broad range of contaminants including explosive organic compounds such as MNT, DNT, TNT and RDX and other contaminants being found in the soil.

The assessment and remediation works undertaken since 1997, focused on 180 hectares of significantly contaminated land in the south east of the site. An integrated development and clean up strategy for the remaining land was developed by the Urban Land Corporation (ULC) and Golder Associates. The development strategy matches the degree of contamination allowed to remain on the site with the sensitivity of the proposed land use. As part of the clean up strategy, it was determined on-site disposal in a high security repository was the only economically viable disposal option. The repository liner and capping system design adopted is one of the most advanced in Australia. The strategy has been successfully implemented with remediation completed in May 2001.

Development of areas for residential, open space and commercial / industrial use began in parallel with remediation and is now well underway. The ULC is undertaking project management of the overall redevelopment for the Australian Department of Defence who funded the remedial works. Golder Associates, has overseen all technical aspects of the remediation of the site from 1997 to its completion in 2001. Thiess Services was the contractor who undertook the remediation works.

This paper briefly outlines the hazard assessment and works implementation strategy aimed at mitigating the risk of health and safety issues such as exposure to contaminants and explosion of residual explosive compounds both during remediation and for the future use of the site.

Identification of site hazards

The site hazards identified for the Albion Remediation Project were both chemical and physical. The basic approach to risk management was to identify materials based on their contaminant concentrations which were a hazard to site workers and eventual site users, map the locations of those hazards and then implement engineering or management controls during site cleanup to mitigate the risks. The following sets out the approaches used for classifying, and managing the identified hazards during the remediation of this large scale facility.

Chemical risk assessment process

Basis for approach to material classification

The site cleanup was undertaken as part of the Victorian EPA Audit System which requires the appointment of an independent environmental specialist as Environmental Auditor. The role of the Auditor is to oversee the remediation process and audit the clean-up so that they may issue a Certificate or Statement of Environmental Audit declaring the site fit for any beneficial land use of if not possible, the intended land use.

Extensive site specific assessment and consultation was undertaken with the Environmental Auditor appointed for the project in order to develop a set of chemical criteria for assessment and auditing purposes. In summary, soil at the site was classified on the basis of contaminant concentrations that in turn determined the fate of the material.

The clean up criteria were developed on the basis that the base-line criteria which represented a very low risk to all site users and the environment be Screening Criteria. Above these Screening Criteria was a zone where acceptable risks were achievable with the implementation of management controls. The upper limit of this zone became the threshold for material that was disposed of to the on-site repository (Acceptance Criteria). The approach is shown diagrammatically in Figure 1.

This approach allowed Material Classes to be defined for the site based on contaminant concentrations and the requirement for management of those materials. The management controls included management of site processes during remediation and in some cases long-term management following site development.

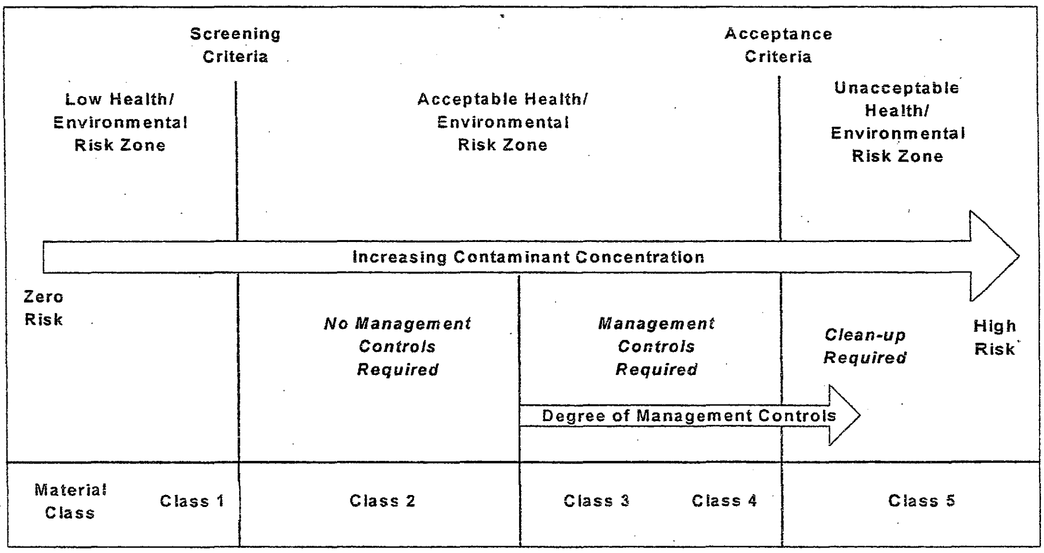

Figure 1. Risk Approach to Contamination Identification and Management

Mapping of chemical material classes

The material classifications were mapped based on existing chemical data for the site. The maps formed the basis for the remediation design identifying the material requiring excavation and the degree of its contamination. Each area was identified with a unique descriptor identifying the area number and material class. A database was used to store the 1000 excavations around the site with information related to the chemicals of concern and their concentration. Once mapped and classified, the removal and disposal of the soil was undertaken in accordance with management and disposal guidelines set down for that material.

Explosive risk assessment process

Risk assessment

Other than the chemical and normal construction physical hazards present on the site, the possibility of an explosive hazard also existed. The need to recognise, identify, locate and manage these hazards lead to the undertaking of an explosive risk assessment for the site. Prior to any excavation of areas on which there had been buildings or drains or remediation excavations where explosives may be encountered, a risk assessment was completed to assess:

- the types of explosives which were likely to be present;
- the practices which occurred within the building which may have led to the creation of an explosive situation;
- the presence of drains within or adjacent to the building which could contain explosive residues that could be the cause of an explosive situation; and
- the remedial activities required to be undertaken.

The risk assessment was undertaken using all available historical and chemical data for each facility including historical drainage plans. The risk evaluation panel comprised representatives from Golder Associates, the remediation contractor and a former manager of the Albion Explosives Factory.

Understanding the types of explosives that may be present was important in completing the review due to the various sensitivities associated with those explosives. Sensitivity for the purposes of the risk assessment was defined as the ease with which an explosion could be caused by the remediation activities due to the presence of residual amounts of these chemicals. The order of sensitivity of these explosives from highest to lowest is shown in Figure 2. The higher sensitivity explosives could be detonated by impact alone while the lower sensitivity explosives were more likely to require a more intense source of ignition.

The review also considered the likely state and quantity in which the chemicals could be remaining on site. For instance, nitroglycerine and nitrocellulose breakdown relatively quickly in the presence of oxygen. Furthermore, due to its fibrous nature, nitrocellulose was unlikely to migrate very far into the clayey soil profile. Hence the highest risk of these materials remaining in such a manner as to cause an explosive risk was likely to be in former pits or pipes from former buildings containing these materials.

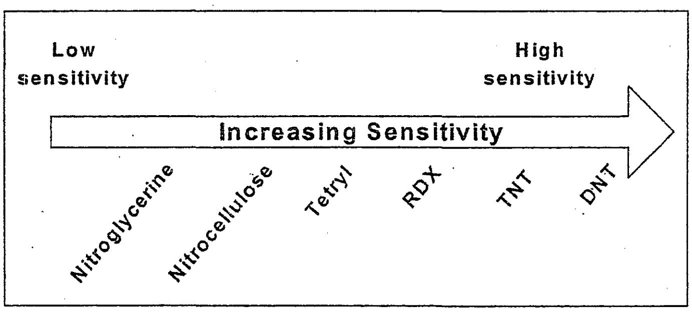

Figure 2. Sensitivity of explosive compounds present on site

The nature of the remedial activity was also of importance. The demolition process was a higher risk activity as it used high impact equipment in areas where explosives buildup was most likely such as concrete pits. Other activities such as the excavation of soil beneath former buildings was considered lower risk due to the lower impact excavation process and lower likelihood of concentrated explosives being present in the soil.

Base on the review of each area undertaken, a low, moderate or high hazard ranking was assigned to each area of the site. The hazard ranking was defined as follows:

Low Hazard	No additional management controls needed to mitigate hazard.
Moderate Hazard	Hazard should be monitored but unlikely to require additional management controls to mitigate hazard.
High Hazard	Management controls and additional procedures required to mitigate hazard.

Using this system, a series of explosive hazard maps were created for the remediation site. An example of the hazard map is shown in Figure 3.

Construction Management

General Procedures

Identification of the hazards, lead to development an implementation of the works procedures needed to be implemented to mitigate the identified risks. A Construction Environmental Management Plan was implemented on the site by the contractor. The aim of the plan was to mitigate the risks associated with the movement and disposal of the identified hazardous soil so that the construction activities do not impact upon the contamination status of the site or neighbouring areas. For site remediation, this was combined with a site specific Occupational Health and Safety plan for construction to limit the potential exposure of site workers to the contaminated soil. Using the hazard Material Class for the soils, specific environmental and health and safety procedures were adopted.

These procedures included the use of exclusion zones, air monitoring and protective respiratory equipment and clothing when dealing with Class 5 material as well as a range of other standard remediation management controls to reduce the potential health and environmental risks associated with the works. There were also some specific work practices that were implemented to mitigate the explosive risk and mitigate the risk of hazardous materials remaining in remediated parts of the site. The on-site repository for long term storage of these materials was also designed, constructed and operated to mitigate the identified risks. Some of these processes are described in the following.

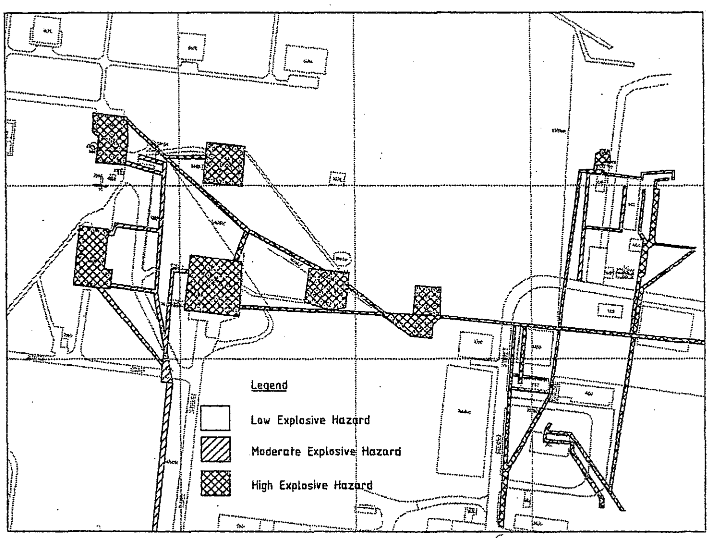

Figure 3. Example of an explosive hazard map

Specific procedures adopted to mitigate explosive risk

Demolition of higher risk buildings

Excavations of concrete slabs associated with buildings assessed to be at a higher risk of an explosive situation were excavated in general accordance with the following:

- All excavators used for this activity were fitted with blast shields;
- The evening prior to excavation, the slab and surrounding soil was soaked with water;
- The following day, the area was soaked with water prior to excavation;
- Demolition of the concrete was then commenced. Where slabs were lifted, the underside of the slab and the subgrade were soaked with water;
- Following removal of the concrete, the area within two metres of the slab was soaked with water and the soil then excavated and disposed in the on-site repository.

Excavation of higher risk pipelines

Pipelines assessed to be higher risk or previously unidentified pipelines were excavated in general accordance with the following:

- All excavators used for this activity were fitted with blast shields;
- The pipe was inspected at its exposed ends prior to excavation starting. The inspection of the pipes was undertaken by a suitably qualified person;
- At least 24 hours prior to the pipe being excavated, the pipe was filled with water by blocking the downstream end with a sand bag or other obstruction;
- Prior to excavation the obstruction was removed and the water allowed to drain into the next section of pipe or into a pit for collection and disposal to the treatment plant;
- The pipe was then excavated in sections (approximately 3 m lengths) from the upstream end. Following the removal of each section, the next section was inspected for explosive chemical residues;
- Pipes with no residues were taken to the on-site repository for disposal;
- If explosive chemical residues were identified, excavation ceased and water was made available. The pipes were then excavated under wet conditions.
- Should cold water not remove the chemical residues, steam or solvents were to be used until the residues had been flushed. The pipe would then be removed.

Material management

A Materials Tracking System was implemented with the aim of tracking every load of material moved around the site. The Materials Tracking System was crucial in providing confidence soil management was achieved during clean-up and that that waste soils and soils for reuse were not incorrectly placed around the site. To this end, all excavations had a sign indicating their number and the contamination class of the soil. The signs were colour coded to match colour coded load dockets. The colour assisted operators in recognising the hazards associated with the materials with which they were dealing.

When moving any load of soil, the source of the soil was recorded on a docket by the truck operator from the sign and the destination was recorded when the soil was placed. The dockets were audited in the field and also recorded in a database system. Approximately 91,000 dockets were used on the site in the completion of the remediation works. Auditing of the system over two years led to approximately three non-conformances of material placement which were able to be rectified without issue.

Material Disposal

An important feature of the remedial design was the construction of the on-site repository for permanent storage of highly contaminated soil. The repository was a feature of the site development and remediation strategy with future house lots to be sold only 200 m away. Hence the technical demonstration of low risk, public perception of low risk and construction management to minimise risk were paramount to the project success.

The repository was 3 ha in area, between 1 and 3 m below surface level, had a maximum height of around 13 m above surface level and a design airspace of around 180,000 m^3. The principle objective in the design of the repository was to protect human health and the environment commensurate with the use of the area as public open space. This objective was met by providing sufficient engineering and management safeguards to reduce the risk of exposure to an acceptable level for workers and the public during construction and for site users in the long term.

The liner and capping system design for the repository provides one of the highest levels of security for a landfill constructed in Australia. The major design features for the repository containment system include the following (Figure 4):

(i) A double liner including a primary geomembrane liner and secondary base composite clay and geomembrane liner;
(ii) A primary and secondary leachate collection/leak detection system;
(iii) A composite clay and geomembrane cap with drainage to minimise infiltration;
(iv) A thick (1.5 m) overlying soil protection layer including topsoil to isolate the material and allow appropriate vegetation to be grown.

The design included a requirement for stringent quality assurance program during construction and a provision for on-going post-closure management including groundwater and leachate monitoring.

The repository has been completed and landscaped and is currently subject to an Environmental Audit to allow on-going use as public open space.

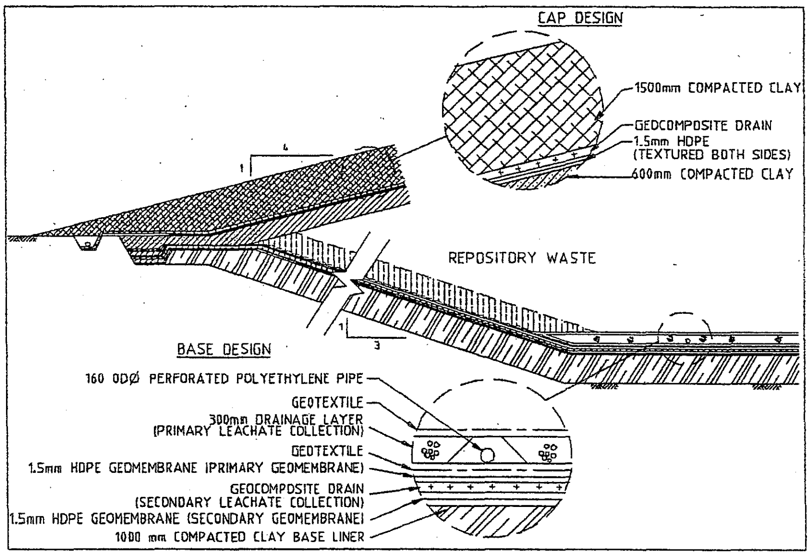

Figure 4. Repository liner and cap design

Conclusion

Identification and management of chemical and physical hazards is an integral part of the successful completion of any remediation project. The Albion Explosives Factory remediation process used risk-based approaches to hazard identification and classification of both chemical and specific physical hazards. Hazard mapping was then undertaken to assist the contractor and site personnel in understanding in which area specific work practices were required for protection of their health. The identification, investigation and removal of these hazards has allowed the site to undergo an Environmental Audit and be declared suitable for on-going use ranging from residential to industrial purposes.

Acknowledgements

We acknowledge the Australian Department of Defence for permission to publish this paper and the Urban Land Corporation for their assistance.

Minimising the Risk with Driven Piles with PDA

A. C. Langbein
Senior Geotechnical Engineering, Tonkin & Taylor

Abstract

This paper presents the findings of dynamic pile testing undertaken on driven steel piles measuring stress during driving and achieved load capacities. The risks associated with driving both steel and concrete piles are presented. Steel piles can be damaged by high compressive stresses at the pile toe when the pile is driven onto strong rock. Concrete piles may be damaged during driving due to tension waves and insufficient longitudinal steel or if the driving hammer overdrives the pile (over-stressed in compression). The ultimate capacity of steel piles driven into the East Coast Bays Formation "bedrock" underlying Auckland has been determined from 98 dynamic load tests. The ultimate capacity has been found to depend upon the driving energy that can be applied to the pile without it being overstressed. A lower bound of the 98 load tests indicates that the pile capacity and section size is related by the following formula – Ru (kN) = 24 × wt (of pile in kg/m). Increases in pile capacity of up to 400% due to "set-up" have been measured on small diameter piles driven into cohesive. Soil "relaxation" may occur when large diameter piles are driven into sands and capacity is reduced with time. Both soil "set-up" and "relaxation" indicate the necessity to undertake all testing of piles at "re-drive" conditions.

Introduction

Driven are used extensively worldwide to support heavily loaded structures. Risks associated with driven piles are the uncertainty of the achievable load capacity and the possibility of damage caused by driving. Dynamic pile testing is widely recognised as a suitable means of measuring both driving stress and deriving load capacities. This paper provides a brief background on dynamic pile testing, provides causes – based upon case histories – of damage caused to driven piles and states the increased confidence in pile capacities by load testing the pile. Specific information, based upon 98 load tests, is presented on the capacity of steel piles driven into the predominant Auckland "bedrock" formation – the East Coast Bays Formation (ECBF). Information on the change in the capacity of the pile with time – attributed to soil "set-up" and "relaxation" is also presented.

Dynamic Pile Testing

Dynamic pile tests have been used to verify the capacity of driven piles in New Zealand for over ten years. The dynamic pile testing involves attaching strain gauges and accelerometers to the sides of the top of the pile prior to driving or immediately prior to final driving. The gauges measure the strain and acceleration of the pile at the top of the pile over the fraction of second from hammer impact. In addition to the impact, wave reflections that occur due to skin friction along the length of the pile and off the pile toe are also recorded.

Based on the pile properties (length, density, modulus of elasticity and cross-sectional area), the Pile Driving Analyser (PDA) can be used to rigorously calculate:

- the mobilised capacity of the pile,
- stress within the pile during driving,
- energy applied to the pile and
- displacement of the pile per hammer blow

for every hammer blow applied to the pile.

Wave reflections occur with each hammer blow at the toe of the pile and where (if any) the pattern of the reflection is affected by changes in the shape and/or stiffness of the pile. If a pile is cracked or poorly welded, the pile section area changes and a wave reflection occurs. The PDA identifies this wave reflection, and by assessing the size of the reflection, provides an indication of the damage at that depth.

Wave matching analysis (e.g. CAPWAP or TNOWAVE) involves a more rigorous analysis of a single hammer blow. Wave matching analyses model the pile as a series of discrete elements, each with value of shaft friction (or toe capacity) soil damping, and quake (soil displacement required to achieve capacity). This form of analysis provides the distribution of resistance along the length of the pile from which a pseudo load-displacement graph for the pile is calculated.

In summary, the PDA measures strain and acceleration at the top of the pile during driving, from which the following can be calculated:

- ultimate pile capacity
- cracks within the pile
- displacement (or set) of the pile
- compressive and tensile stresses within the pile
- energy applied to the pile (from which the efficiency of the piling hammer is calculated).

Pile Damage – Case Histories

The occurrence of structural damage and excessive driving stresses are assessed using the PDA during pile installation. Four case histories are described below indicating how damage can occur to a driven pile.

- Case 'A' Concrete filled steel shell pile. A bottom driven steel shell pile was filled with reinforced concrete and dynamically tested to confirm the ultimate pile capacity. Wave reflections were noted at the depth corresponding to the change of tube thickness and at mid-pile depth. The piling contractor was questioned regarding the possible damage and admitted to overstressing the shell during driving. Additional reinforcing steel had been placed through the damaged section based on the assessment of the project's structural engineer. In this case the PDA was used to independently identify damage to the steel shell of the pile.

- Case 'B' Reinforced Concrete Pile. A lightly reinforced concrete friction pile was driven through stiff to very stiff clays. High tensile stresses were recorded using the PDA. After driving, close inspection of the pile identified fine horizontal cracks near the top of the pile. These cracks were most likely caused by the tension wave reflecting off the pile toe and returning to the unrestrained pile above ground level causing cracking. Insufficient reinforcing had been included in the pile to cope with the tensile stresses induced by this mechanism.

  Experience shows that excessive tensile driving stresses can also occur in a concrete pile as the pile is driven through a hard layer into a softer soil layer. Heavy driving may cause the bottom of the pile to be "blown-off" as it is restrained by the skin friction of the upper hard soil and penetrates into the lower weaker layer where it is unrestrained at the toe. Subsequently, driving can also cause additional cracks coinciding with the interface of the hard and soft soils as the pile penetrates the soft deposit. The completed driven pile may have been driven to achieve its design "set", but is likely to have several horizontal cracks over the length below the interface of the hard and soft layers. The use of a PDA during driving is able to identify the excessive tensile stresses enabling the hammer drop height to be limited or the identification of the cracks and damage to the pile at the end of driving for subsequent repair.

- Case C : Steel Universal Column. A lightweight short steel universal column (200 UC46) was driven onto moderately strong to strong basalt rock. As a pile is driven onto a hard surface, the compression wave reflecting off that surface causes the stress at the toe of the pile to double. Several hammer blows were analysed during final driving, each recording the increase in pile stress as the pile became embedded into the basalt rock. Driving was halted when the measured compressive stress within the pile approached the yield strength of the steel. Hence, by measuring the stress within the pile during driving, limiting set criteria were provided to the contractor that would not cause the pile to be overstressed.

  The PDA is able to identify wave reflections caused by a poorly constructed welded splice.

- Case D : Reinforced Concrete Pile. A 275 mm square precast reinforced concrete pile was driven in an attempt to achieve a required ultimate capacity requested by the projects structural engineer. The compressive driving stresses within the pile were calculated by the PDA as the pile was driven to a smaller and smaller set with subsequent increases in pile capacity. The design set provided to the contractor was based upon maintaining driving stress within permissible levels, but not achieving the required capacity. Additional piles were driven to support the structural loads.

In summary the above cases demonstrate that the PDA can be used to minimises the risk of pile damage and is also able to:

- confirm the integrity of the pile
- provide an indication of depth to and degree of pile damage
- provide a revised "set" criteria so that the pile is not overstressed during driving; i.e. achieving the maximum pile capacity without overstressing the pile during driving.

Pile Capacity

The ultimate capacity of a driven pile has traditionally been estimated using a pile driving formula. The most commonly used formula, and arguably the most accurate, is the Hiley formula. By applying an appropriate Factor of Safety (for working loads) an allowable pile capacity is estimated. A more accurate value of the ultimate capacity can be determined by undertaking a load test on the pile, but this is costly and time consuming. For example a static pile load test may cost up to NZ$100,000. A more rapid and economic test method, albeit slightly less accurate, is to dynamically test the pile using a PDA.

A static pile load test provides the most accurate assessment of the capacity of the pile and a Factor of Safety or strength reduction factor close to unity can be adopted, based on accepted codes of practice. A dynamic load test provides an assessment of pile capacity, the accuracy of which is between that of the Hiley formula and a static load test. The Factor of Safety or strength reduction factor that may be used with dynamic testing reflects this increased confidence, over the driving formulae. The Australian Piling Code (AS 2159, 1995) provides guidelines on appropriate strength reduction factors for various methods of determining pile capacity. These factors are further modified due to the frequency of testing (either dynamic of static) and the uncertainty of the founding conditions. Table 1 presents the guidelines from the Australian Piling Code and Transit New Zealand Bridge Manual (TNZ, 1994) for various pile testing methods.

Table 1. Comparisons of Strength Reduction Factors.

Method of Assessment of Ultimate Geotechnical Capacity	Strength Reduction Factor (ϕ_g) Australian Piling Code[2]	TNZ Bridge Manual
Static Load Test	0.70 – 0.90	0.55 – 0.65
Dynamic Load Test[1]	0.65 – 0.85	-
Dynamic Piling Formula (Hiley)	0.45 – 0.654	0.45 – 0.55

[1]Supported by signal matching (e.g. CAPWAP or TNOWAVE)
[2]Variations depend on the intensity of the site investigation, method of capacity analysis, construction control and testing frequency

Dynamically testing driven piles enables an increased confidence of the ultimate pile load (and lower risk of pile failure), enabling each pile to support an increased design load, or a smaller pile section dynamically able to be used to support a given load. For example, by testing 10% of the driven piles, with subsequent wave matching, the strength reduction factor can be increased from 0.45 to 0.75. Therefore, for a given design load, the required pile section size can be decreased by 60% (= 0.45/0.75). Construction savings in pile materials are evident.

Pile Capacity : Auckland ECBF

Within the Auckland Region over 98 dynamic load tests have been undertaken on driven steel piles founding within the underlying "bedrock". Piles varied in size from 200UC46 to 310UC158. The "bedrock", termed East Coast Bays Formation (ECBF), is a tertiary age, very weak to weak (qu = 1 MPa to 10 MPa), dark grey to grey interbedded sandstone and siltstone. The depth to the ECBF "bedrock" varies, depending upon weathering and erosion, and for the piles tested was between 4 m and 25 m below the surface. Typical embedment lengths range from 1 m to 3 m.

The capacity of steel piles driven into the ECBF "bedrock" has traditionally been taken as 12 to 16 MPa assuming end bearing only. Dynamic pile tests show that the ultimate geotechnical capacity of a pile is dependent not only upon the end area of the pile but also upon the section size of the steel, provided sufficient driving energy is applied to the pile. A larger pile section size enables more energy (larger hammer weight and / or larger drop height) to be applied to the pile without overstressing the pile and hence the pile penetrates further into the "bedrock" developing greater skin friction and densifying the crushed rock around the toe of the pile.

Figure 1 shows the geotechnical ultimate pile capacity for all steel piles dynamically tested by the author and founded in the ECBF "bedrock". For comparison, this graph also shows the ultimate pile capacity if a design end bearing capacity of 16 MPa was used. The results show that for larger pile sections, the pile is able to be embedded further into the ECBF "bedrock" mobilising an increased capacity due to increased length of skin friction and embedment into less weathered rock. The use of an increased pile size also requires an increase in the driving energy - either hammer weight or drop height.

An indication of the applied energy needed for each pile type to achieve the capacity indicated in Figure 1 has been undertaken using a wave equation analysis programme (Goble et al, 1997). The pile model consisted of a 15 m long section, with no cushioning for either the hammer or pile and a hammer efficiency (η) of 60%. Confirmation of the hammer weight, drop height and section size to achieve the required ultimate geotechnical capacity without overstressing the pile during driving will need to be undertaken for each site.

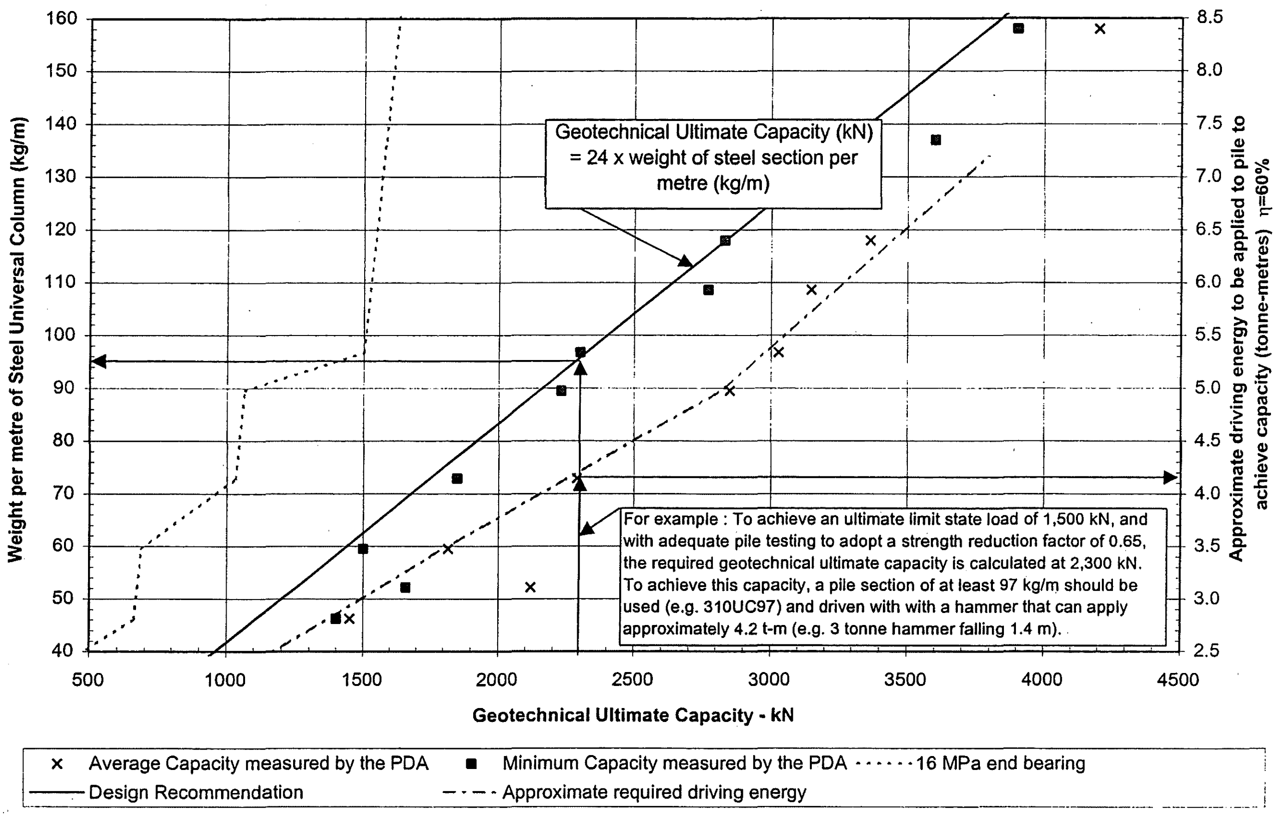

Figure 1 : Capacity of Driven Steel Piles within ECBF "bedrock"

From Figure 1, the following formula (equation 1) provides a lower level of the ultimate capacity of steel piles driven into the ECBF "bedrock".

$$Q_u = 24 \times wt \qquad (1)$$

Where Q_u = Ultimate geotechnical capacity of the pile (kN)
wt = Weight per metre of steel section (kg/m)

From the authors experience the following assumptions and design criteria are applicable for the above formula:

(1) piles embedded within East Coast Bays Formation "bedrock"

(2) yield strength to be at least 250MPa grade steel

(3) set criteria to be verified using PDA to ensure no risk of damage to the pile but with a hammer sufficiently large to prove pile deign capacity

(4) Confirmation of geotechnical ultimate loads undertaken with a pile driving analyser (PDA) or static load test. At least 5% of the piles need to be dynamically tested, with an appropriate strength reduction factor (ϕ_g) to be used based upon the proportion of piles tested and the uncertainty of the ground conditions

Changes in Ultimate Pile Capacity with Time

As a pile is driven into a soil mass, it causes a change in the properties of that soil mass. The magnitude of the change and rate of change is dependent upon the type of soil as well as the size of the pile.

For instance, when large displacement piles are driven into clays or with small displacement driven piles, pore water pressures build up around the pile toe and sides of the pile. These excess pore water pressures lower the effective stress within the soil, making driving of the pile easier. With time, the pore water pressures dissipate increasing the effective stress within the densified ground around the pile. This increase in strength is commonly termed "pile set-up".

Two examples of pile set up occurring with driven steel piles are shown in Figure 2 (founding in ECBF "bedrock") and Figure 3 (founding in alluvial/aerial volcanic deposits). These figures indicate that pile capacity increases significantly with time. For the two piles tested, the pile embedded in the ECBF exhibited a 42% increase in capacity and the pile embedded in the volcanic deposit exhibited a 417% increase in capacity.

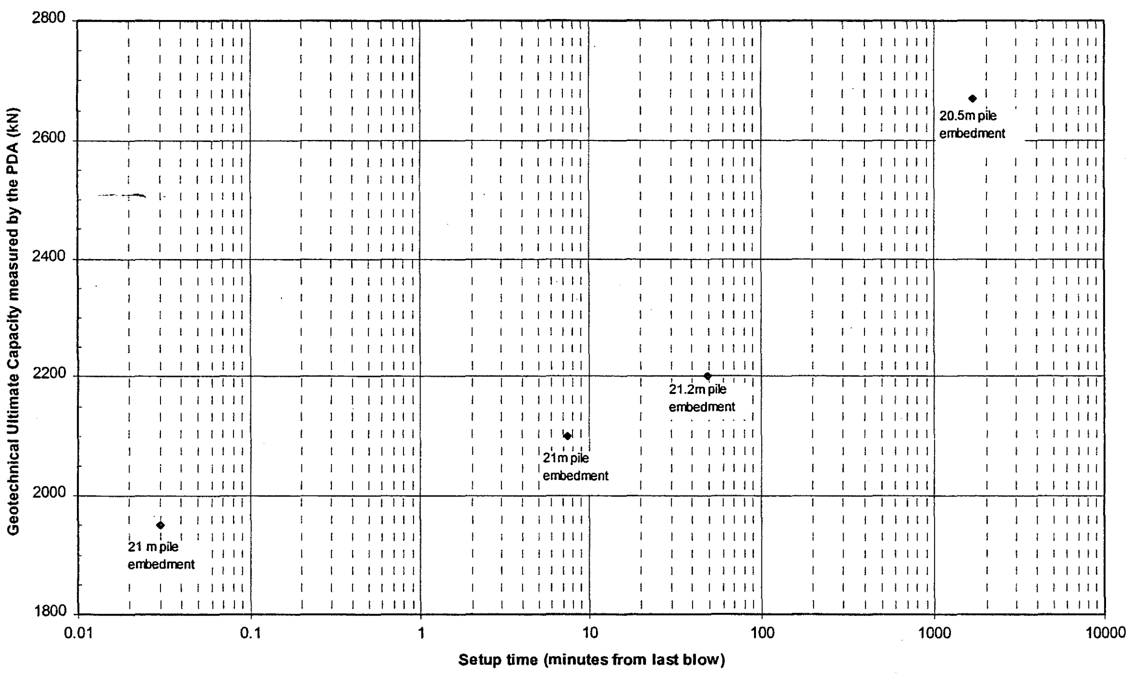

Figure 2 : Pile (310UC97) capacity increase with time within ECBF

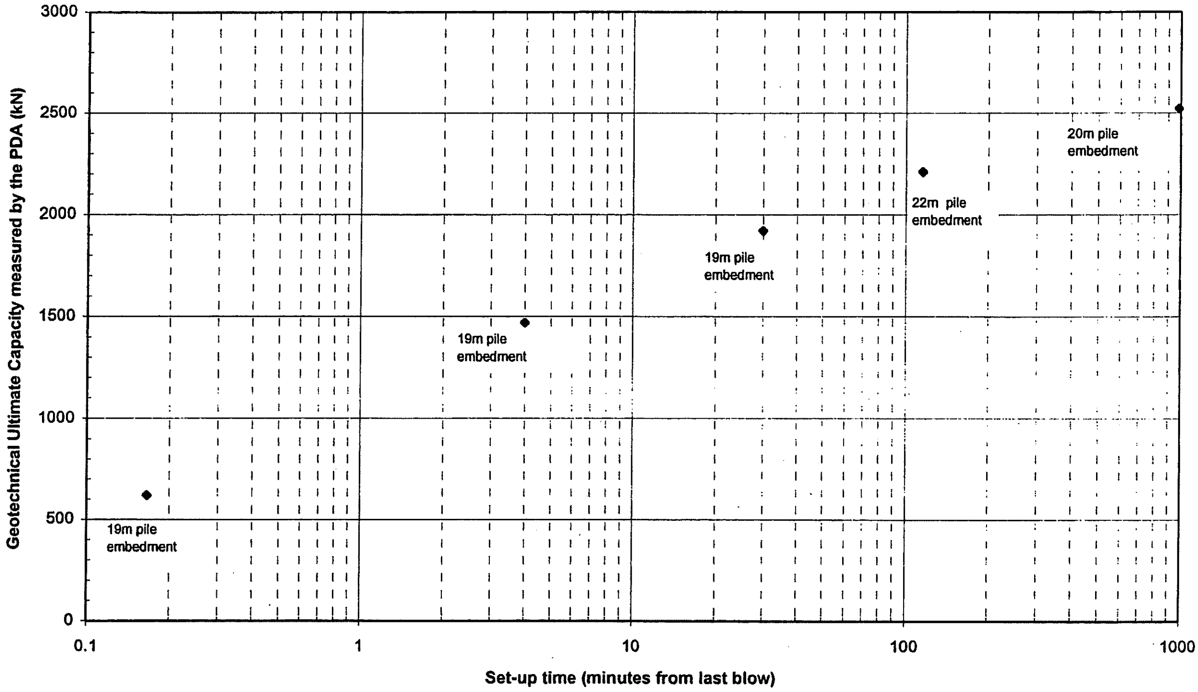

Figure 3 : Pile (310UC97) capacity increase with time within volcanic deposits

When large displacement piles are driven into fine sands and silts the rate of penetration of the pile is often too quick for dissipation of pore water away from the toe of the pile. Continued driving of the pile only results in compression of the water that is dissipating away from the toe of the pile. As the water is effectively "incompressible", large pile rebounds often occur with small permanent sets. With time the water dissipates away from the toe and the pile can be re-driven with larger sets than were measured at the "end-of-drive" conditions. This effect is known as soil "relaxation". Soil "relaxation" has been observed when large displacement piles are driven into medium dense sands of the ECBF.

In this situation an assessment of the pile capacity at the "end of drive" conditions, with the small set and temporary compression, will provide an artificially high indication of pile capacity. By testing the pile at re-drive conditions, when pore pressures have dissipated, a more reliable estimation of pile capacity can be derived.

In summary, it is essential to appreciate site subsurface conditions and test piles at re-drive conditions to enable a more accurate estimation of the long-term capacity of the pile to be determined.

Summary and Conclusions

Dynamic pile testing has been used in New Zealand for over 10 years. It has been used more intensively over the last three years following the availability of PDA equipment on the local market. Extensive testing has been undertaken within the Auckland Region. A number of conclusions are drawn from the pile testing that has been undertaken to date – these include:

(1) Damage to piles during driving may be a result of :

- Insufficient pile shell thickness with bottom driven tubes
- Insufficient longitudinal reinforcing to resist tension stresses in a concrete pile,
- Overdriving a steel pile onto a very hard surface
- Overdriving a concrete pile

(2) The dynamic load testing of driven piles with PDA equipment permits the use of an increased strength reduction factor (ϕ_g) to calculate the capacity of the pile allowing fewer piles, or smaller pile section sizes to be used.

(3) Steel piles driven into the ECBF "bedrock" are able achieve a capacity related to the section size of the steel. The authors proposed approach, based on the test data, is to use the following formula : Ru (kN) = 24 × wt (of pile in kg/m).

(4) Testing of piles should be undertaken at "re-drive" conditions to account for potential soil "set-up" – increase in capacity with time - or "relaxation" – decrease in capacity with time.

Acknowledgements

This study would not have been possible without the assistance of Brian Perry Civil, whom own the PDA equipment and software with which the pile testing was undertaken, and senior staff at Tonkin & Taylor Ltd who reviewed this paper.

References

AS 2159 –1995. Australian Standard. *Piling – Design and installation*

Goble Rausche Likins and Associates, Inc. *GRLWEAP Manual*. April 1997.

Transit New Zealand (May 1994). Bridge Manual

C:\andrew\Pile Talk.chch.doc

Proposed Remediation of Contaminated Sites using Zeolites

P.Lindsay[1*], C. Mowatt[2] and D.Trumm[1]
1. CRL Energy Limited, 77 Clyde Road, Christchurch
2. Resource Refineries, PO Box 175, Matamata

*Present address: Montgomery Watson, 7 Deans Avenue, Christchurch

Abstract

In Europe and North America natural zeolites have been used to treat contaminated mine water and landfill leachate. Preliminary studies using New Zealand zeolites and wastewater flows from local sites were completed to examine the feasibility of duplicating this practice.

Wastewater from three West Coast mine sites and one closed landfill in the Auckland region were treated with zeolites from Ngakuru.

The Ngakuru zeolites are relatively young (250,000 years old) which gives them unique characteristics. The cation exchange capacity and internal surface area range from 40 to 130 meq/100g and 34 to 138 m^2/g respectively, depending on the degree of thermal alteration. The predominant zeolites present at Ngakuru are mordenite (40 to 80%) and clinoptilolite (20 to 60%), with some cristobalite (0 to 10%) also present.

The filtering abilities of zeolites (natural and modified forms) offer a versatile and environmentally friendly option to capture most contaminants found in water systems. Natural zeolites can perform these functions due to their high ion exchange capacity, adsorption-desorption energies and ability to be modified. Zeolites have an open, regular crystalline framework that generates an electric field that interacts, attracts and binds various cations and, after modification, anions.

The results in this paper for New Zealand acid mine drainage and landfill sites indicate that Zeolites can remove ammonium (NH_4^+) and the metal cations Fe, Al and Ni from solutions, with the recovery of ammonium and Fe greater than 97%.

Results indicate zeolite is an effective remediation option at West Coast coal mine AMD sites. Laboratory tests indicate the zeolite would significantly reduce the Fe and Al content entering the streams from acid mine drainage and raise the pH towards natural background levels of approximately 4. It is suggested that a combined wetlands treatment with a downstream zeolite interception trench could be a cost effective method to remediate acid mine drainage sites.

Introduction

Past and current environmental problems such as water pollution have highlighted the effect excessive amounts of nutrients can have on natural waterways. Excessive amounts of iron, ammonium, aluminium, zinc and copper have entered waterways from various industries and landfills. Increased environmental awareness has identified problems and resulted in attempts to find low cost, natural treatment options.

Many European and American studies have reported that the adsorption characteristics of zeolites (natural and modified forms) offer a versatile and environmentally friendly option to capture most soluble contaminants found in water systems.

Zeolites are thermally altered clays that have an open, regular crystalline framework where structural silica and aluminum share a common oxygen thereby generating an electric field or cation exchange capacity (CEC). This characteristic enables zeolites to attract and bind various cations and, after modification, anions. The large cation exchange capacity of zeolites has led to the material being used in the agricultural industry to control odours, to remove ammonia at animal feed lots and as a slow release fertiliser agent (Mumpton, 1984). When the exchange sites are fully occupied by cations the loaded zeolite can be either regenerated for reuse or if the water contaminants are plant nutrients, the loaded zeolite can be used in plant-growing media.

Zeolites deposits are commercially exploited at Ngakuru, Waikato and in Southland, New Zealand. Zeolite from a deposit at Ngakuru has a CEC of about 120meq/100g and has been used for water treatment. In its native state this zeolite contains about 30, 25 and 15 meq of K, Na and Ca respectively and is predominantly mordenite (75%) with potassium feldspar and some cristobalite present. The clinoptilite ($CaAl_2Si_7O_{18}.6H_2O$) and mordenite ($(Na_2,K_2,Ca)(Al_2Si_{10}O_{24}.7H_2O)$) zeolites at Ngakuru are hydrothermally altered tuffaceous lacustrine sediment beds up to 45 metres thick (Mowatt, 2000).

This paper describes the results of research into the potential use of Ngakuru zeolites as a remediation material at contaminated mine and landfill sites in New Zealand.

Use of zeolites to remediate Acid Mine Drainage (AMD)

Water from South Island West Coast coal mine sites contains high levels of iron and aluminium. The most common approach to targeting AMD is lime addition to precipitate metals and neutralise acidity (Atkinson, 1994). This method has the following disadvantages:

1. generates a large volume of sludge which is costly to dispose of and in some cases is classed as hazardous,
2. at around 4°C the precipitation layer undergoes an inversion resulting in mixing of solids and liquids,
3. it may not produce an effluent sufficiently low in metal content, and
4. metal values are lost (Pahlman and Khalafulla, 1988).

On the West Coast of New Zealand, the natural pH of streams draining coal measures are often less than 4.5 (Alarcon-Leon, 1997). Hence, another disadvantage of using lime or alkaline boiler ash for remediation is that the AMD becomes neutralised or even caustic and, therefore, less acidic than natural background stream water (internal report, CRL Energy Ltd. in prep.).

AMD sampled by the authors, at three west coast mines (Castle Point, Sullivans and Stockton) have a pH of between 2.5 and 3.0 and contain various metal cations

(Table1) . It is believed that the main stress factor to ecology in west coast streams affected by AMD, are the precipitates of Fe and Al that coat the sediment substrate and prevent algae growth, thereby removing nutrients for invertebrates. Therefore, to improve AMD on the west coast, we propose that dissolved Fe and Al levels should be reduced and the pH should be raised to background levels of 4 to 5.

If AMD could be run through zeolite, and the cations were removed, then water pH would not be influenced which would reduce associated downstream problems. (PHIL: we say above that we should restore pH to background!)

Methodology

Acid mine drainage samples were collected from Stockton mine, Sullivans mine and Castle Point mine (Table 1). The AMD samples were filtered through zeolite to determine the effective ion exchanging capacity of the zeolite.

Tests were performed using 15 by 3 cm glass columns at ambient temperature. Each column was loosely packed with approximately 35 g of zeolite. The columns were operated under flooded conditions using a reservoir containing 1 litre of loading solution at the top of each column. The bottom outlets of the columns were fitted with control valves to regulate the control of the effluent to 1 ml/min. A separate experiment was conducted with the AMD in which 0.25 litre of AMD was filtered though 35 g of zeolite.

The untreated and treated AMD water was analysed for trace metals using ICPMS and GCS. The unused and used zeoliltes were analysed for trade metals using ICPMS.

Results and Discussion

It appears that the main ion exchange occurring within the zeolite involves K and Na substituting for Fe and to a lesser degree Al (Tables 1 and 2). Previous results suggest that Na is the main element involved in ionic exchange in zeolite filters (Schultze et al., 1994). Previous workers have noted that Ca may compete for substitution sites if the Ca levels are high enough (Schultze, et al, 1994). In the case of the West Coast AMD samples the Ca levels were too low to allow the Ca to dominate competition sites at Fe expense.

Table 1: Chemistry of Acid Mine Drainage and Acid Mine Drainage Filtered through zeolites- Sullivans, Stockton and Castle Point mines, West Coast, New Zealand.

Elements	Sullivans AMD	Sullivans AMD treated with zeolite	Stockton AMD	Stockton AMD Treated with zeolite	Castle Point AMD	Castle Point AMD treated with zeolite
Fe (mg/L)	42.7	0.14	21.6	2.86	15.7	2.1
Mn (mg/L)	0.547	0.805	1.06	1.09	0.95	1.45
Al (mg/L)	15.2	1.25	54.4	20.1	67	22.5
Ni (mg/L)	0.125	0.069	0.266	0.178	0.198	0.154
Zn (mg/L)	0.729	0.44	1.4	0.992	0.647	0.661
Ca (mg/L)	29.4	18.4	16.4	31.1	65.9	73.8
Mg (mg/L)	9.2	40.1	11.3	41.7	37	75.1
Na (mg/L)	3.75	65.1	3.72	52	10.4	78.2
K (mg/L)	3.62	16.8	2.64	13.8	4.09	21.1
PH	2.57	4.34	2.91	3.87	2.53	3.83
Conductivity (mS/m)	795	476	932	892	2010	1346

Table 2: Results of Zeolites Flushed with Mine Drainage from West Coast Mines

		Sullivans AMD				Stockton AMD		Castle Point AMD	
		1.0 litre AMD used		1.25 litre AMD used		1.25 litre AMD used		0.5 litre AMD used	
Element (mg/kg)	Pure Zeolite	Loaded Zeolite	Cations adsorbed	Loaded Zeolite	Cations adsorbed	Loaded Zeolite	Cations adsorbed	Loaded Zeolite	Cations adsorbed
Fe	6600	8700	2100	9400	2800	7600	1000	7000	400
Al	5900	5700	-200	7800	1900	6100	200	6200	300
Ni	0.92	1.4	0.48	1.4	0.48	1.4	0.48	1.5	0.58
Ca	2900	2700	-200	3000	100	3400	500	3000	100
Na	9700	8700	-1000	9600	-100	10000	300	8500	-1200
K	29000	26000	-3000	27000	-2000	33000	4000	25000	-4000
Mg	9.4	8.1	-1.3	14	4.6	7.7	-1.7	8.7	-0.7
Mn	120	180	60	250	130	370	250	160	40
Zn	40	44	4	49	9	49	9	50	10
Co	0.71	1.2	0.49	1.2	0.49	1.5	0.79	1.4	0.69
Cr	2.3	2.5	0.2	2.2	-0.1	2.9	0.6	2.4	0.1

Results in Table 1 indicate that the Ngakuru zeolite adsorbed between 87 and 99% of the Fe in the AMD samples, between 63 and 91% of the Al and between 25 and 50% of the Ni.

Cation selectivity of zeolites has been studied (Schultze et al., 1994) and for zeolites with similar mineralogy and Na, K, Ca and K content, the cation selectivity range is $Pb^{2+}>Zn^{2+}>Ca^{2+}>Cu^{2+}>Fe^{2+}>H^{+}>Mg^{2+}>Al^{3+}$. As expected the Fe was adsorbed to greater degree than the Al. Some competition with Ca in the AMD competing for available sites has happened (Table 2).

Table 3 suggests that the Ngakuru zeolites used in the AMD trials were, as expected, dominated with mordenite. In the USA examples (mainly clinoptilolite) the hector zeolite, with the highest amount of exchangeable Na, was the most efficient contaminant adsorber in AMD trials. Table 2 and Table 3 suggest that K is as important as the Na as an ion exchanger in the mordenite rich Ngakuru zeolite.

Table 3: Chemical Analysis (meq/g) of Ngakuru zeolite and USA zeolites (Schultze, 1994).

	Chemical Analysis (meq/g)			
Zeolite Type	Na	K	C	Mg
Ngakuru, NZ- mix of mordenite/clinoptilolite	0.43	0.74	0.07	0.005
Clinoptilolite, Hector, USA*	1.52	0.23	0.34	0.16
Clinoptilolite, Barstow, USA*	1.17	0.31	0.65	0.34
Clinoptilolite, Buckhorn, USA*	0.52	0.25	1.2	0.91

We assume a cation exchange capacity of 130 cmoles/kg and that the majority of the Fe will be in 2+ form. If the zeolite retains 130 cmoles of Fe charges/kg and Fe is in the bivalent form, then zeolite adsorbs 72.8 x 0.5 = 36.4 g of Fe per kg zeolite. At Sullivans mine the calculated AMD mean flow is approximately 0.05 cumecs (1,576,800 m^3 of AMD per year).

Dissolved Fe levels in the Sullivans AMD are about 40 g per m^3, so for treatment with zeolite, one would need 40g/36.4g = 1.1 kg of zeolite per m^3 of water. Over one year one would need 1,734,480 kg of zeolite to remove all the Fe from solution. Research is being undertaken to determine the critical toxic level that may effect the invertebrates life cycle. With this remediation method, the cost of zeolite could be prohibitive. Instead, it is the authors view that a passive wetlands treatment system with sulphur reducing bacteria may be a viable option to reduce the Fe and Al levels in the AMD, and that a zeolite trench emplaced at the downstream end of the wetlands system may be useful to adsorb the Fe and Al that does not precipitate out in the wetlands. These remediation options will be evaluated further.

Due to the potential for loaded zeolites to release K and Ca to the environment, loaded zeolites can be used as a fertiliser to aid in the regeneration and rehabilitation of vegetation on rock waste dumps and re-contoured mine sites

Closed landfill leachate

In the Auckland area there are a number of landfills that have been closed for many years. Various drainage points at these landfills release small quantities of leachate that contain problematic concentrations of iron and ammonium. There is a clear requirement for development of low cost, simple systems to be installed to ensure leachate contaminate levels complies with local standards.

Natural mordenite has a reported affinity for ammonium and has been used to remove iron from wastewater in a number of instances (Mumpton, 1984) therefore it was decided to test Ngakuru zeolite for ability to remove both contaminants from leachate.

It was also decided that rather than set-up a costly regeneration plant in a high population density area, if possible, the contaminant loaded zeolite could be used as an addition to potting mixes or as an addition to low fertility turf areas.

Landfill Field Trial

A pilot test using 100 kg of zeolite in a pilot plant at a north island landfill site has revealed the following results. Under flow conditions of 2 cumecs ammonia concentrations from the landfill, leachate contaminants were reduced from 280 mg/l to <20 mg/l. The size of zeolite was important in terms of adsorption rates, with the finer fraction (0.5-2.0 mm) adsorbing ammonium at a faster rate. The advantage with the zeolite is that the size of the material can be controlled and an interception trench of zeolite can be prepared with a customised permeability.

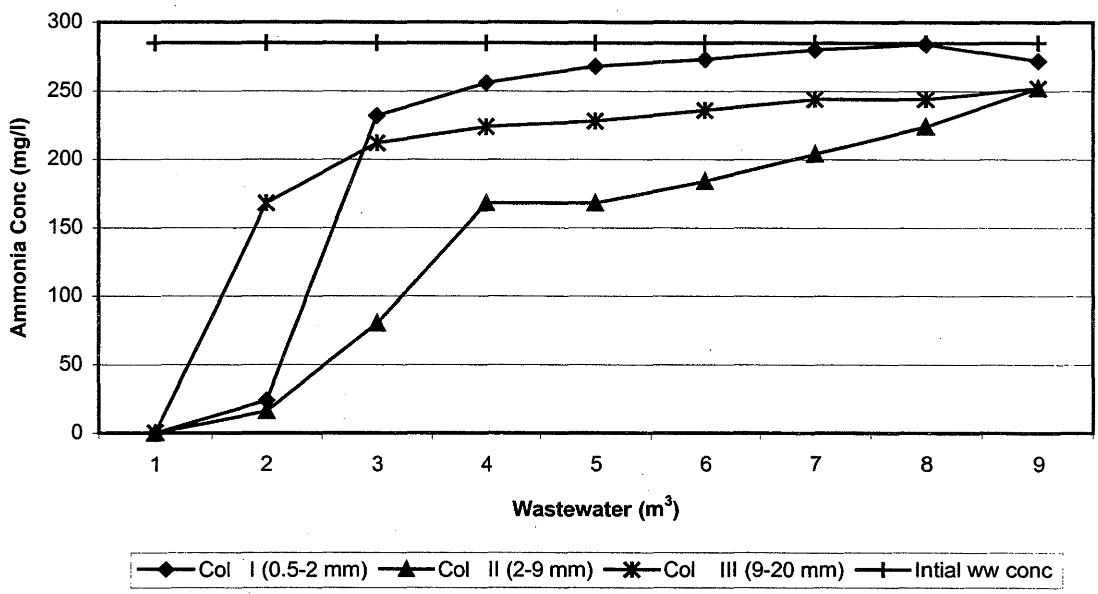

Figure 1: Ammonium absorption by Ngakuru zeolites. Three size fractions are analysed.

Conclusion/Discussion

In a bench-top study, zeolite has proved effective at removing Fe, Al and Ni from AMD from the West Coast of New Zealand. At present the amounts of zeolite needed to treat individual AMD streams is likely to be prohibitive. The authors recommend that a remediation option should be evaluated consisting of a wetlands treatment bed with sulphur reducing bacteria to extract a major proportion of the Fe and Al, with a trench filled with zeolite at the downstream end of the wetlands to adsorb any residual Fe or Al that has not precipitated in the wetlands.

Pre-treatment of zeolite (Carland and Aplan 1994) with HCl could remove the base cations existing in exchange sites and lead to cation exchange capacities of 350 meq/kg. This would reduce the amount of zeolite needed in AMD remediation to 63%.

Future Research

A reusable surfactant-modified zeolite (SMZ) versatile, inexpensive sorbent for removing contaminants from water will be generated using the Ngakuru zeolites. International research followed by commercialization has identified that that SMZ can simultaneously sorb the three major classes of water contaminants: inorganic cations, inorganic anions, and nonpolar organics from wastewater.

SMZ of New Zealand origin will be tested in laboratory and field trials at landfill sites (ammonia, organochloride residues), Taupo and Waikato area water (arsenic), pulp mills (discharge water discolouration) road runoff (a range of contaminants) and mine water discharge.

The objective is to produce sized zeolite, treated with appropriate surfactants to solve specific water contamination problems and that the loaded or exhausted SMZ would be reusable or have an environmentally sustainable end use.

References

Alarcon-Leon, E. (1997) Long Term Mine Site Rehabilitation. M.Sc. thesis, University of Canterbury, Christchurch, New Zealand, 393 p.

Atkinson, K. (1994) The Role of Mineral Processing in Reducing the Environmental Impact of Mining Activity in Cornwall. Minerals Engineering, Vol. 7, No. 8, 967-973.

Carland, R.M. and Aplan, F.F. (1994) Use of Natural Sedimentary Zeolites for the Environmental Remediation of Acid Mine Drainage. Proceedings of the 19th International Mineral Processing Congress. Held: 22-27 October, 1994, San Francisco Littleton, Co, US. Chapter 20, 95-99.

Demchak, J., Skousen, J., Bryant, G. and Ziemkiewicz, P. (2000). Comparison of Water Quality from Fifteen Underground Coal Mines in 1968 and 1999. Proceedings 5th International Conference of Acid Rock Drainage, Denver, 2000, 1045-1052.

Mowatt, C. (2000) Preliminary investigations into the characteristics and potential uses for Ngakuru zeolites. Proceedings of the 2000 New Zealand Minerals and Mining Conference, 29-31st October, 2000, Wellington, 217-219.

Mumpton, F.A. (1984). Development of Uses for Natural Zeolites: A Critical Commentary. In: Natural Zeolites. Eds: D.Kallo and H.S. Sherry, ibid, 333-366.

Pahlman, J., and Khalafalla, S. (1988). Use of lignochemicals and humic acids to remove heavy metals from process waste streams. US Bureau of Mines RI 9200, p. 2.

Schultze, L.E.; Zamzow, M.J. and Bremner, P.R. (1994) AMD Cleanup Using Natural Zeolites. Proceedings of the International Land Reclamation and Mine Drainage Conference. Held: 24-30th April, 1994, Pittsburgh, PA, 341-347.

Treeslides in Doubtful Sound

Tim McMorran
Senior Engineering Geologist, URS New Zealand Limited, Christchurch, New Zealand

Charlie Watts
Senior Engineering Geologist, URS New Zealand Limited, Second Manapouri Tailrace Tunnel Project

Brian Heer
Assistant Project Director, Meridian Energy Limited, Second Manapouri Tailrace Tunnel Project

Abstract

Treeslides are slope failures where the slide mass contains a dominant proportion of vegetation along with minor soil and rock debris. Treeslides are common in steep, high rainfall areas. In Fiordland a large number of such failures occur every year. This paper summarises a study of treeslides in Doubtful Sound.

High grade metamorphic rocks in Doubtful Sound stand in steep slopes typically in excess of 45°. Vegetation grows rapidly owing to annual rainfall in excess of 6 m. Treeslides occur as a result of high intensity rainfall or heavy snowfall. Earthquakes are also a potential trigger. Annually about 315 000 tonnes of treeslide debris directly enters Doubtful Sound.

Introduction

The original tailrace channel connecting the First Manapouri Tailrace Tunnel to the sea is approximately 1km long and was excavated within alluvial and deltaic material in 1969. To construct it a pilot channel was cut and then left to erode to its final profile. The eroded material was flushed out to sea. Such construction practices are no longer acceptable.

The Second Tailrace Tunnel is soon to be completed and a new tailrace channel that connects with the first channel needs to be excavated. This 400 metre long excavation is also within alluvial and deltaic material and construction is expected to result in the discharge of sediment into Doubtful Sound. As part of the assessment of environmental effects for this discharge a comparison has been made with the estimated annual volume of sediment contributed to Doubtful Sound by treeslides. This paper summarises the findings of a study by URS New Zealand Limited (URS) for Meridian Energy Limited (MEL) to estimate the average annual volume of debris from treeslides entering Doubtful Sound.

Methodology

About 20 km of coastline (approximately 10% of the total coastline in Doubtful Sound) was selected as a representative field area (Figure 1). To estimate the average annual volume of treeslides debris entering Doubtful Sound two sets of vertical aerial photographs (SN 4330/9-11 taken in 1970, SN 9066 G13-17, H18-20 taken in 1991) were studied to identify treeslides at each of those dates, and the slides were drawn on a basemap. Field investigations were then made from a boat and helicopter, and the post 1991 slides were added to the basemap.

Identification of treeslides on aerial photographs is relatively difficult owing to the steep topography and the small scale of photographs taken during the period of interest for the study. Shadow resulting from the steep topography obscures much of the detail on the southeast facing slopes.

To establish whether the study area is representative of the whole of Doubtful Sound, Hall Arm was visited by boat and much of the remaining Sound from the heads to Deep Cove was observed by helicopter. The occurrence of treeslides is variable along the coastline. Many large recent treeslides were observed in Hall Arm while some areas of the northern coast of

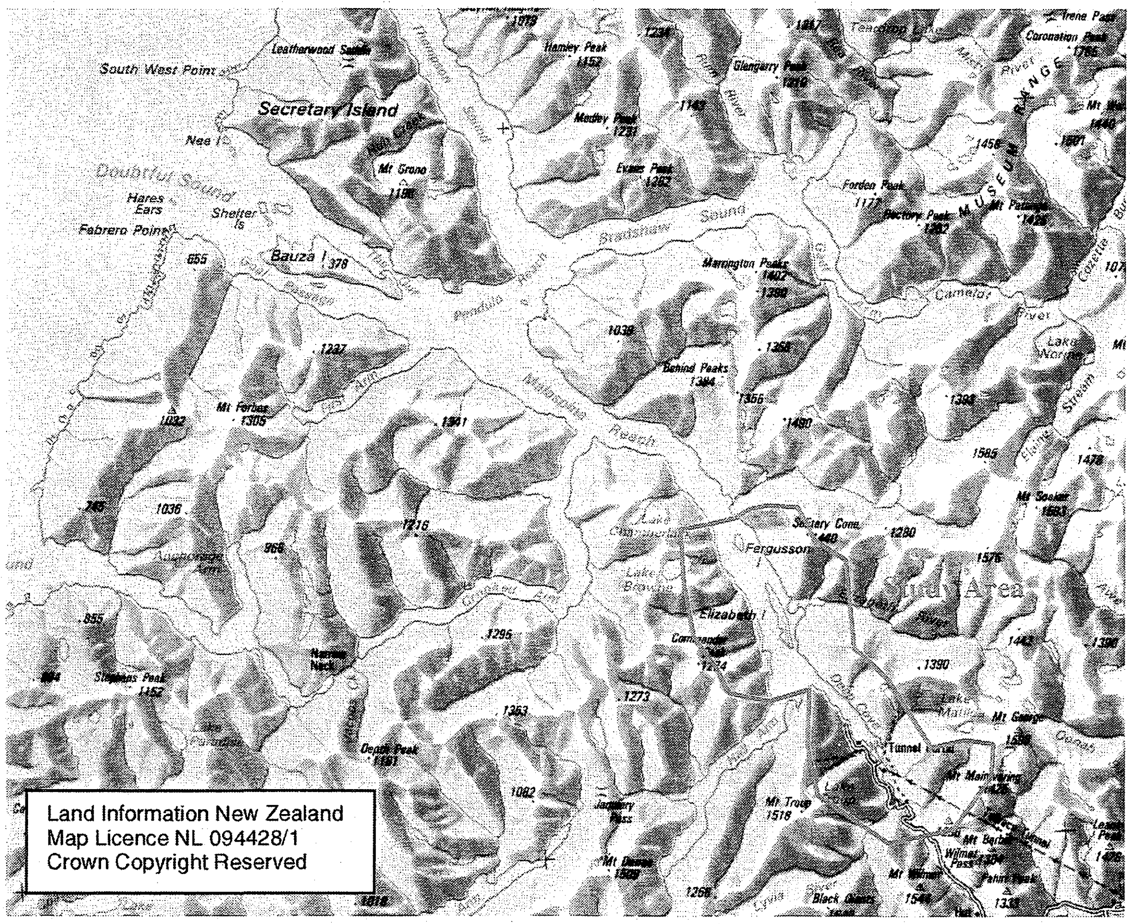

Figure 1 Map of Doubtful Sound showing the location of the Study Area. Scale 1:250 000. The study Area constitutes 20 km of coastline.

Doubtful Sound, particularly the area adjacent to Pendulo Reach, showed few treeslides. We concluded that the study area is generally representative of Doubtful Sound. Therefore an approximate volume of treeslide debris entering the sound can be estimated by multiplying the volume in the study area by ten.

Regional Setting

Doubtful Sound is an area of steep relief and high rainfall. The slopes of the Fiord are greater than 45° and are typically heavily forested. The rocks underlying the slopes are high-grade metamorphic rocks (amphibolite facies), typically varieties of gneiss, including biotite gneiss, hornblende gneiss and calcsilicates gneiss. The rocks are middle Paleozoic (330-370 Ma) in age and of high strength (100 – 150 MPa UCS), and are typically unweathered. These steep fiords were formed during the recent glacial advances (last one approx. 16,000 years before present) where large sheets of ice trimmed and cut the "U" shaped valleys. These valleys were subsequently inundated as the ice melted and the sea level rose.

Treeslides observed during the study are characterised by long narrow strips of bare rock where the vegetation, soil and often some rock has been removed as a rapid landslide (Figure 2). The high rainfall, thick vegetation, competent underlying rock and very steep slopes in Fiordland are conducive to this type of failure.

Mature forest comprises dense cover of mixed beech/podocarp/broadleaf up to about 15 metres in height, with undergrowth of moss, grasses, ferns and broadleaf species. Initial recolonisation of rock slopes bared by treeslides consists of a mat of moss about 10 cm thick, followed by ferns, grasses and broadleaf species.

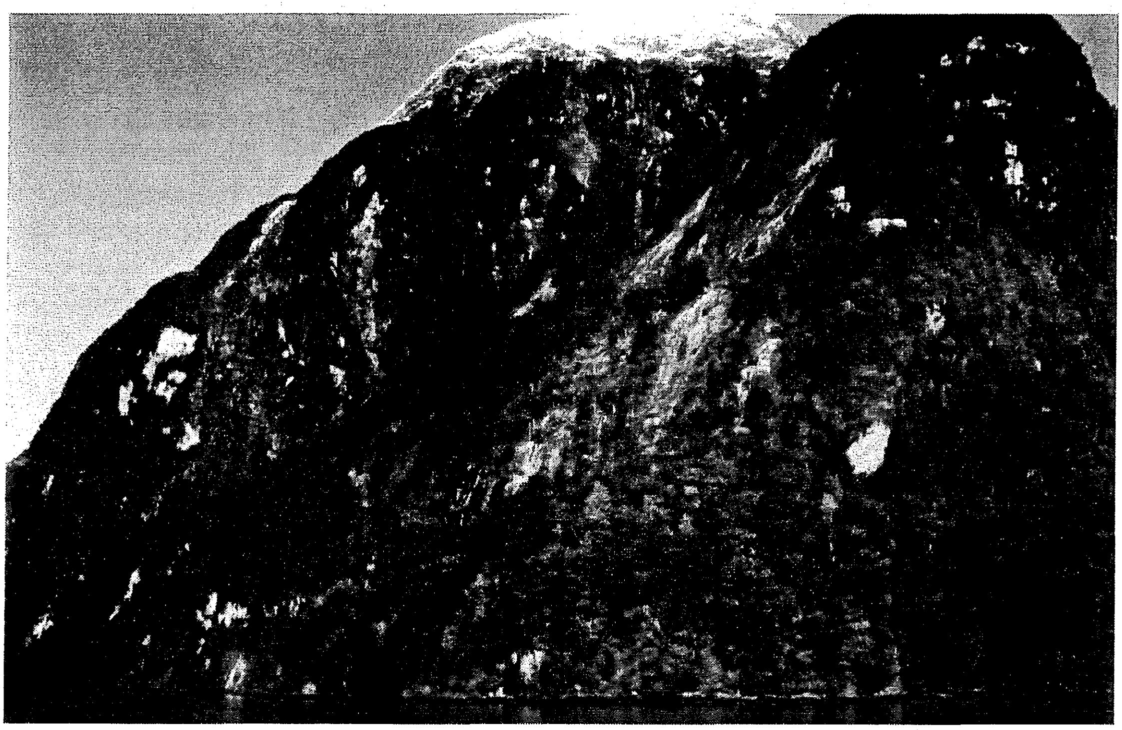

Figure 2 Typical slope in study area (Commander Peak) showing scars resulting from treeslides of different ages.

Typical treeslides are five to twenty metres wide and up to about 500 metres in height. The soil profile typically comprises 0.5 metres of dark brown organic material including leaves, roots, small branches and rock fragments.

Several slides of known age were observed and used to gauge an approximate age for other slides (some examples provided in Table 1). Very recent slides (less than one year old) are easily identified by the lack of vegetation and a brown smear of soil on the exposed rock (Figure 4). Slides of one to about three years age have partial recolonisation by moss and ferns. Slides of three to ten years have general vegetation cover including broadleaf species. Slides older than ten years are heavily vegetated including tree species. In general, older slides are more difficult to date than slides less than about ten years old, and as a result we have used slides that appear to have occurred since the 1991 photos to estimate slide volumes and annual frequency.

Table 1

Recent Treeslides observed in the vicinity of Deep Cove

Slide	Date	Estimated Volume	Comment
Helena Falls (Figure 3)	21 March 1998	25 000 m^3	Sediment observed entering Deep Cove
Marble Creek (Figure 4)	6 February 2000	17 000 m^3	Sediment observed entering Deep Cove via Tailrace
Lyvia	June 2000	6400 m^3	Sediment observed entering Deep Cove via Lydia River

The main trigger mechanism for treeslides is postulated to be heavy rainfall events. Heavy snowfalls and earthquakes may also trigger treeslides. Many slides were noted to have occurred following heavy snowfall during 1996, and treeslides were observed following the 1993 Fiordland earthquake (Van Dissen et al. 1993), though not in numbers significantly greater than would normally occur as a result of heavy rainfall.

Annual Average Treeslide volume

Estimates for the annual mass of treeslides entering Doubtful Sound are presented in Table 2. A conservative annual estimate for the mass of slide debris entering Doubtful Sound can be made by combining data on all slides that have occurred since the 1991 aerial photographs.

Only slides that directly enter the Sound in the study area or enter very steep tributaries were considered in the assessment. This is because not all slide debris in tributary valleys can be assumed to enter the sound. However in the case of the Helena Falls slide of 21 March 1998 (slide volume 25 000 m^3), the slide entered the tributary valley 2 km from Doubtful Sound and considerable debris was observed entering the sound (Figure 3). Similarly Marble Creek slide of 6 February 2000 (volume 17 000 m^3) directed considerable sediment into Doubtful Sound (Figure 4). The Lyvia treeslide occurred in June 2000, with a volume of approximately 6400 m^3 resulting in significant discoloration of the Lyvia River. By excluding the above examples and the considerable number of other treeslides that enter tributaries, the estimate of the annual mass of debris entering Doubtful Sound is conservative.

Estimation Method

The total area of treeslides in the study area was calculated by summing the estimates of slide area for each slide observed. The lengths of the treeslides were estimated from the basemap contours and checked using the helicopter altimeter. The age of the slides was estimated by comparison to slides of known age. The slide areas were calculated based on an average slope angle of 45°.

The total volume of treeslides entering Doubtful Sound was calculated from the total area of treeslides in the study area for each age category and multiplying by 0.5 (average soil depth in metres) and then by ten (the study area represents 10% of the total Doubtful Sound coastline). The total volume was then divided by the number of years in the period.

The annual mass of treeslide debris entering Doubtful Sound was calculated assuming a density of 1.5 tonnes per cubic metre of slide debris. The volume does not include vegetation (trees shrubs etc.).

Figure 3 Plume of dirty water and debris resulting from discharge of floodwater from Helena Falls into Doubtful Sound. The sediment source is the Helena Falls treeslide which occurred in March 1998. *Photograph by Alan Crowther – Meridian Energy Limited*

Figure 4 Marble Creek slid
of 6 February 2000

Table 2

Estimates for annual mass of treeslides entering Doubtful Sound

Age range of Treeslides	Total area of treeslides in study area (m^2)	Total Annual Volume (Doubtful Sound)(m^3)	Total Annual Mass (Doubtful Sound) (tonnes/yr)
Last 3 years	175 000	292 000	438 000
>3 years but post 1991 (6 yr period)	203 000	169 000	254 000
Post 1991 (9 yr period)	378 000	210 000	315 000

Conclusions

The treeslides result from a combination of steep topography, high rainfall and dense vegetation growth. Based on a survey of 10% of the coastline of Doubtful Sound it is estimated that treeslides contribute approximately 315 000 tonnes per year of debris into the sound.

The estimated mass of debris entering the Sound is considered conservative because:

- the average slide thickness used in calculations represents organic rich soils only and an unknown volume of rock material is also contributed by some slides. No allowance has been made for trees and other live vegetation;
- only slides that directly enter the Sound in the study area or enter very steep tributaries were considered in the assessment.

References

Van Dissen, et al. 1994, "The Fiordland earthquake of 10 August,1993." *Bulletin of the New Zealand National Society for Earthquake Engineering* Vol 27, No 2.

Case History: Design of Precast RC Piles by Pile Load Tests in Improved Reclaimed Land, Bangladesh

W. Okada

Geotechnical Engineer, Sinclair Knight Merz

S. Terzaghi

Senior Geotechnical Engineer, Sinclair Knight Merz

Abstract

Piled foundations for a power development near Dhaka, Bangladesh have been designed from a series of Advance Pile Load Tests (APLT's) which comprised on-site static and dynamic load testing of seven true scale test piles. The piled foundations of the Main Power Block were to be constructed on potentially liquefiable reclaimed land. The Main Power Block area was improved by sand compaction piling while the Substation structures were located in a ground partially improved by surcharging with sand stockpiles. The site soils are micaceous loose to medium dense, fine sand and silt. The site comprises 6 m of reclamation fill underlain by inter-layered alluvium. Following extensive site investigations and pilot studies of sand compaction piling, the APLT's were conducted in both improved and partially improved ground. The key objective of the APLT's was to quantitatively evaluate the effect of sand compaction piling on pile load capacity and to establish most economical design of piled foundations in both improved and partially improved ground. It was also necessary to take into account pile capacity reduction due to potential soil liquefaction in the partially improved ground. Overall the pile capacities interpreted from the dynamic and static load testing were consistent. Furthermore, interpretation of the static and dynamic load testing in conjunction with a SPT correlation method allowed optimisation of pile lengths and axial pile capacity. As a result, substantial savings were achieved in material cost and construction duration. This paper describes the site conditions, methodology of APLT's and analytical design of the piled foundations. Moreover, comparison is made to a similar power development design to illustrate the benefits of pile design by APLT's.

Introduction

Numerous pile design methods have been proposed by a number of authors over the last century. Some pile design methods have been developed from consideration of theoretical behaviour of piles based on classical soil mechanics, while others employ an empirical or semi-empirical approach, derived from experimental work, model pile testing and on-site observation of pile driving. These theoretical and empirical (or semi-empirical) approaches provide a useful means of estimating the geotechnical load capacity of piles under given conditions. Nevertheless, due to the complex nature of pile-soil interaction and often varying soil conditions, pile designers often encounter the limitations of the theoretical or empirical (or semi-empirical) approaches under more complex conditions. Pile load tests are particularly useful when piles are constructed in a heavily improved ground where conventional theories of soil mechanics do not apply to the soil stress-state modified by artificial ground improvement.

A 450 MW power development is currently under construction on 28-hectare reclaimed land near Dhaka, Bangladesh. Previous geotechnical studies have identified a potential for liquefaction to occur at the site during strong ground motion. The Main Power Block area has been improved with sand compaction piling to mitigate the liquefaction potential. The Substation will be constructed in ground partially improved by inadvertent stockpiling of sand. The production piles in both areas have been designed based on a series of Advance Load Pile Tests (APLT's). The APLT's comprise both static load testing and dynamic testing of seven true scale test piles. As will be shown later, the sand compaction piling has completely modified the stress state in the improved ground from the initial at rest stress state. The APLT's have demonstrated that theoretical and empirical pile design approaches predict rather inaccurate pile capacities in such ground conditions.

The design of the foundation piles in the improved and partially improved ground based on the APLT's is presented in this paper. The pile design is compared to the foundation piles at a nearby power development of similar scale in similar reclamation. Three static load tests were undertaken at this site with a pile driving hammer different from the hammer that was used for production piling. The capacity of the pile and its behaviour under loading depends on the equipment used for driving. So, the results of these three pile tests are not directly applicable to the design of the production piles. The comparison of the pile design at these two power developments demonstrates that the APLT's allow economical pile design by optimisation of the number of piles and pile length.

Site Conditions

The development site comprises a 6 m reclamation fill layer overlying interlayered fine sand and silt. The top of the reclamation fill is at +7.8 m PWD (Public Works Datum). The site soils are characterised by their high mica content, ranging from 2 – 10%. A series of Cone Penetration Tests (CPT's) have been undertaken at the site to assess the potential for liquefaction during strong ground motion, in accordance with the method recommended by a panel of leading experts (Youd and Idriss, 1997). It was found that the factor of safety evaluated by this method was lower than the required factor of safety of 1.3 in the Quaternary loose alluvium layers that occur between PWD +1.0 m and –7.0 m. The in-situ soil density increases significantly from loose to medium dense at –7.0 m PWD, and continues to densify with increasing depth. No significant potential for liquefaction has been identified in the denser alluvium layers that occur below –7.0 m PWD.

The power development is located next to a river. The average river level recorded during the site investigations was +5.3 m PWD. All of the foundation piles are designed for a ground water level of +6.5 m, which corresponds to the highest groundwater level that would result from the extreme flood event.

A summary of the site conditions is presented in Table 1 below

Table 1. Ground Conditions

Geological Unit		USCS	Depth m ± PWD	Description[1]
Reclamation Fill	RF	SP/SM	+7.8 to +6.5	Medium dense, fine to medium poorly graded sand, minor silt
			+6.5 to +2.0[2]	Becomes very loose to loose
Top Soil?/ Alluvium	Qal_1	ML/SM	+2.0 to 0.0	Soft silt, occasional loose silty sand, trace organic material
Alluvium	Qal_2	SM	0.0 to –7.0	Loose to medium dense silty sand
			-7.0 to –20.0	Becomes medium dense
Older Alluvium?	$Qalo_1$	SP/SM	-20.0 to –29.0	Medium dense to dense silty sand
	$Qalo_2$	MH	-29.0 to –32.0	Firm to stiff, clayey silt

1) A characteristic of the site soils is the presence of mica. Haskoning (2000) reported mica contents ranging from two to ten percent in the soils at the site.
2) Layer not continuous across the site.

Advance Pile Load Test Methodology

Test Piles

Advance Pile Load Tests were conducted using 400 mm x 400 mm square precast concrete test piles. The test piles were constructed using 12 m spliced segments, which were cut off as necessary to the required test pile length. The characteristic compressive strength of the concrete was 45 MPa, and the reinforcement arrangement and structural detailing of the test piles was identical to that of production piles. The locations and penetration depths of the test piles are shown in the following table.

Table 2. Summary of APLT Test Piles

	Location	Ground Improvement	Penetration Depth (m)	Remarks
APLT01	Substation	Surcharging	22.3	Sleeve to PWD –3 m
APLT02	Substation	Surcharging	22	
APLT03	Main Power Block	Nil	26	
APLT04	Main Power Block	SCP @ 1.5 m spacings	21	
APLT05	Main Power Block	SCP @ 2.0 m spacings	21	
APLT06	Main Power Block	SCP @ 2.0 m spacings	12	
APLT07	Substation	Surcharging	12	

APLT01 and APLT02 are located in the Substation area, which has been improved to some extent by surcharging by sand stockpiles. The soil in this area has densified to some extent as a result of the surcharging. Nevertheless, the soil may still be subject to liquefaction during strong ground motion since no sand compaction piling was planned for this area. ALPT 01 was sleeved to a depth of –3 m PWD, simulating the partial loss of skin friction during soil liquefaction.

APLT03 was constructed in unimproved ground in the Main Power Block area. This test pile was used as a reference pile to assess the effect of surcharging and sand compaction piling.

APLT04, APLT05 and APLT06 were constructed in Sand Compaction Piling Pilot Study areas where trial sand compaction piling of various spacing and arrangement had been constructed. APLT04 was tested in Pilot Study Area A, where sand compaction piles had been constructed at 1.5 m intervals on a triangular arrangement. APLT05 and APLT06 were both located in Pilot Study Area B, where the sand compaction piled were spaced at 2 m intervals on a triangular arrangement. As shown in the above table, APLT05 and APLT06 vary in length.

APLT07 is an additional 12 m test pile that was constructed in the Substation area at a later date following the inspection of the results of APLT01-06. The Substation piles were initially designed as 18 m long two-segment piles with a required geotechnical axial capacity of 1700 kN. However, it was decided later that the design axial capacity of the Substation piles could be reduced to 1300 kN so that single 12 m segment piles could be used, thus saving material cost and construction time.

Theoretical Axial Capacity of Test Piles

The theoretical axial capacities of the test piles were calculated using a static method and an SPT correlation method. The static method is based on the classical formula for calculating the resistance of piles in cohesionless soils (Tomlinson, 1994) shown below:

$$Q_p = N_q \sigma'_{vo} A_b + \frac{1}{2} K_s \sigma'_{vo} \tan \delta A_s \tag{1}$$

The above formula is a generalised equation applicable only to a uniform cohesionless soil. The development site, however, consists of layered soils so the second term of equation (1), which is the skin friction of the pile, must be modified to account for the multi layered soil. The term ½ σ'_{vo}, which is the mean effective stress over the pile length in a uniform soil, has been replaced by σ'_{vm}, the mean effective stress in each soil layer. The skin friction has been calculated for each layer using this modified form of equation (1), and the total skin friction has been obtained by summing the skin friction of each layer.

The axial capacity of the test piles has also been calculated using Meyerhof's SPT correlation method referenced by Bowles (1996). The axial pile capacity is expressed in terms of SPT N value as follows:

$$Q_p = A_b \cdot 40N \cdot \left(\frac{L_b}{B}\right) + 2NA_s \qquad (2)$$

where

$$40N \cdot \left(\frac{L_b}{B}\right) \leq 400$$

Using the geotechnical parameters and SPT N-values obtained from site investigations, the theoretical capacities of all the test piles were calculated from the static and SPT methods. The calculated axial capacity of the test piles is summarised in Table 3.

Table 3. The theoretical capacities of test piles

	Theoretical Axial Capacity (kN)	
	Static	SPT
APLT01	2240	1350
APLT02	2650	1790
APLT03	4290	2650
APLT04	2790	2250
APLT05	2820	2430
APLT06	1260	2330
APLT07	940	1210

The axial capacities calculated from the two different methods vary by up to 65%. This clearly demonstrates that the calculated theoretical pile capacities depend largely on the method of calculation, and could contain a large margin of error. The difference in the pile capacities predicted from the static and SPT method may be attributable to the fact that the static method assumes at rest stress state in a normally consolidated soil whereas the in-situ stress state has been heavily modified through the reclamation and ground improvement works. The effects of the modified stress state should have been reflected in the SPT N-values to some extent, but there is bound to be some inherent error associated with the empirical SPT method.

Sequence of Testing

For all of the seven test piles, dynamic testing was conducted first, and followed by static testing. The methodology of the dynamic and static testing is as follows:

Dynamic Testing

Dynamic records of acceleration and strain in the test piles were recorded and analysed with a Pile Driving Analyser (PDA). From the acceleration and strain data, the PDA evaluates the axial force in the pile, particle velocity of the waves travelling through the pile, and pile set per blow (Coduto, 1994). The PDA also generates a plot of the Case method pile capacity versus depth. The Case method capacity is the static pile capacity determined from the analysis of wave trace data. The pile capacity was also calculated from the more rigorous CAPWAP analysis, which combines the Case analysis with the wave equation analysis.

The test piles were re-struck five days after the initial driving to allow the soil to tighten around the piles, and excess pore pressure generated during the initial driving to dissipate. During the re-striking, the CAPWAP analysis of the PDA data was performed with a range of hammer stroke heights to evaluate the effect of hammer stroke height on the pile capacity.

Static Testing

Static load tests were performed with a hydraulic jack and a kentledge reaction system. Precast concrete blocks were used to provide the reaction force to the hydraulic jack.

The loading sequence comprised a two stage Maintained Load Test (MLT) followed by a Extended Load Test (ELT) as recommended in the Institution of Civil Engineers (ICE) guidelines (ICE, 1996). The procedure of the MLT and ELT was modified slightly from the ICE guidelines to suit the site constraint and testing program. In the first and second stages of the MLT, the test piles were loaded to the design verification load (DVL) and DVL plus 50% of the design working load (DWL) respectively, and then unloaded. The ELT maintains a rate of pile settlement. The table below summaries the loading sequence of the static testing.

Table 4. Static Test Loading Sequence

Loading Cycle	Applied Load	Minimum Holding Time (see note 1)
1st Stage/MLT	25% of DVL	30 min
	50% of DVL	30 min
	75% of DVL	30 min
	100% of DVL	6hr
	75% of DVL	10 min
	50% of DVL	10 min
	25% of DVL	10 min
	0% of DVL	1 hr
2nd Stage/MLT	100% of DVL	1hr
	100% of DVL + 25% of DWL	1 hr
	100% of DVL + 50% of DWL	6 hr
	100% of DVL + 25% of DWL	10 min
	100% of DVL	10 min
	75% of DVL	10 min
	50% of DVL	10 min
	25% of DVL	10 min
	0% of DVL	1 hr
3rd Stage/ELT (see notes 2 and 3)	100% of DVL	1 hr
	100% of DVL + 25% of DWL	1 hr
	Test loads shall then be applied in increments 25% of the Design Working Load up to 100% of DWL. Increments of load shall not be applied until the rate of settlement of the pile is less than 0.1 mm in 20 minutes.	

1) Increments of load shall not be applied until the rate of settlement of the pile is less than 0.1 mm in 20 minutes.
2) Stage 3 is for APLT03 and APLT04 only.
3) Stage 3 may be deleted, or terminated if the total movement of the pile head is equal to 15% of the base diameter.

The DVL and DWL were established from the theoretical capacities of the test piles. The DVL and DWL were 1500 kN and 600 kN for APLT01, 06 and 07, and 2000 kN and 800 kN for all the other APLT's. Failure of the test piles was observed in all of the APLT's with the exception of APLT03. In APLT03, the loading was terminated prior to the failure of the test pile because the applied load reached the maximum load that could be applied with the available kentledge.

Interpretation of Advance Pile Load Tests

Geotechnical design of production piles in the Main Power Block and Substation was carried out based on the findings and interpretation of the dynamic and static tests. The axial pile capacity, settlement, founding levels, and set per blow required to obtain the desired axial capacity were interpreted from the results of the APLT's.

Axial Capacity

The axial capacities of the test piles have been evaluated from both the static and dynamic tests. The results of the static load test were taken as the axial capacities of the test piles. These were then compared to the capacity derived from the Case and CAPWAP analysis. In most cases, the results showed good agreement between the static and dynamic testing, as shown in Table 5.

The axial pile capacity was interpreted from the load displacement relationship using five different methods, namely British Standard 10% method, Davison, Chin, DeBeer and Brinch Hansen. Some of these methods are described in Canadian Foundation Engineering Manual (Canadian Geotechnical Society, 1992). In all cases, the load capacities of the test piles are interpreted graphically from the load-displacement relationship. There is no particular method that is more applicable to the site conditions than others, so the mean of the capacities calculated from the above methods was adapted as the ultimate capacity of each test pile. The axial capacities of the test piles interpreted from the static and dynamic tests are summarised in the table below.

Table 5. Axial Capacities of Test Piles (Units: kN)

		APLT01	APLT02	APLT03	APLT04	APLT05	APLT06	APLT07
Theoretical Capacity	Static	2240	2650	4290	2790	2820	1260	940
	SPT	1350	1790	2650	2530	2430	2330	1210
Static Test	10%	1450	1850	2400	2250	1830	1860	1000
	Davisson	1100	1650	2550	2000	1550	1620	1000
	Chin	1720	2040	3730	2440	2170	2000	1300
	DeBeer	1100	1600	2200	2000	1700	1600	1000
	Brinch Hansen	1570	1880	-	2470	2230	1880	1400
	Mean	**1388**	**1804**	**2720**	**2232**	**1896**	**1792**	**1140**
Dynamic Test	CAPWAP Initial Driving	-	-	-	-	2274	1882	1330
	CAPWAP Re-strike	1665	2000	1986	1864	1864	1874	-
	Case	1570	2560	2020	2590	2310	1690	-

The scatter of the static test pile capacities determined from the various interpretation methods is not significant. It is noteworthy that the 10% method is generally in good agreement with the mean pile capacity. The mean pile capacity is also consistent with the CAPWAP analysis within 20% margin of error in all of the APLT's with the exception of

APLT03. The fact that APLT03 did not fail under the maximum load applied during the static load test suggests that the dynamic testing results may be grossly conservative.

Founding Level

The PDA generates a plot of the Case method pile capacity versus depth. One can identify favourable soil layers that provide a good end bearing capacity by observation of this Case method pile capacity plot. It was decided that a 12 m test pile would provide a sufficient capacity following inspection of the Case capacity plot for APLT01-05. To demonstrate this point, the Case pile capacity plot for APLT01 is shown below.

Figure 1. Case resistance versus depth – APLT01

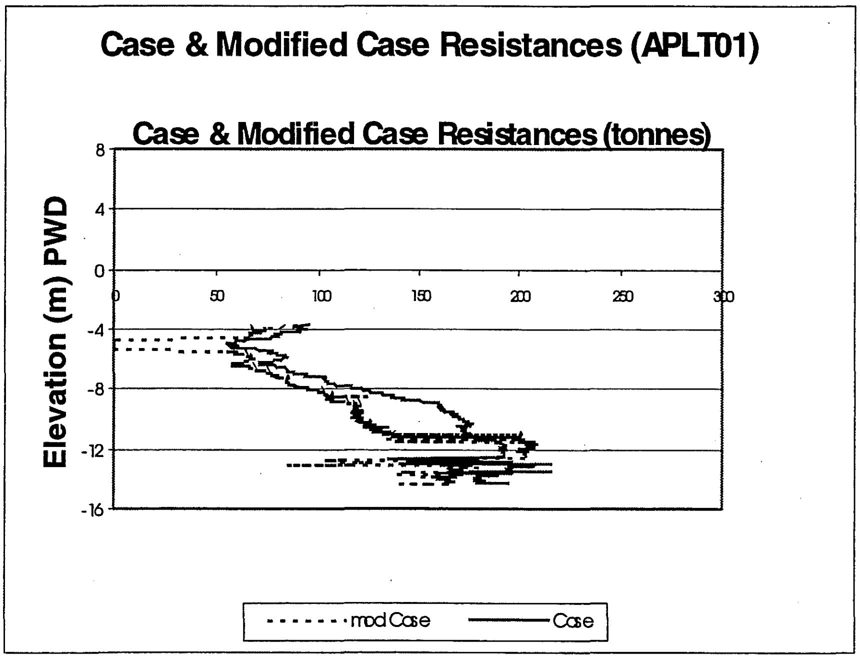

The modified Case resistance is a modified version of the original Case method. In the figure above, local maximums of the Case and the modified Case resistance occur at PWD –4 m, –6 m, and –12 m, indicating that there is a favourable founding layer that provide a high bearing capacity at these levels. Similar trends were observed in the other APLT's as well. A 12m pile driven from the ground level of PWD +8 m would be founded at PWD –4 m, which is a favourable founding level. The above figure indicates that the 12 m pile founded at PWD –4 m would have approximately the same capacity as a 15 m pile founded at PWD –7 m.

Settlement

The load-displacement curve from the static load tests can be used to estimate the settlement of a production pile under the design working load. For example, consider the load-displacement curve for APLT06 shown below.

By inspection of the above figure, the estimated settlement of a 12 m pile in the improved ground carrying a design working load of 800 kN is 2-3 mm. Similarly, the settlement of a Substation pile under the design working load was estimated from the load-displacement curve of APLT02 (Fig. 3). It was found that the expected settlement of the Substation pile was also less than 5 mm. Settlement of less than 10 mm is generally considered acceptable.

Figure 2. Load-displacement curve for APLT06 (Main Power Block)

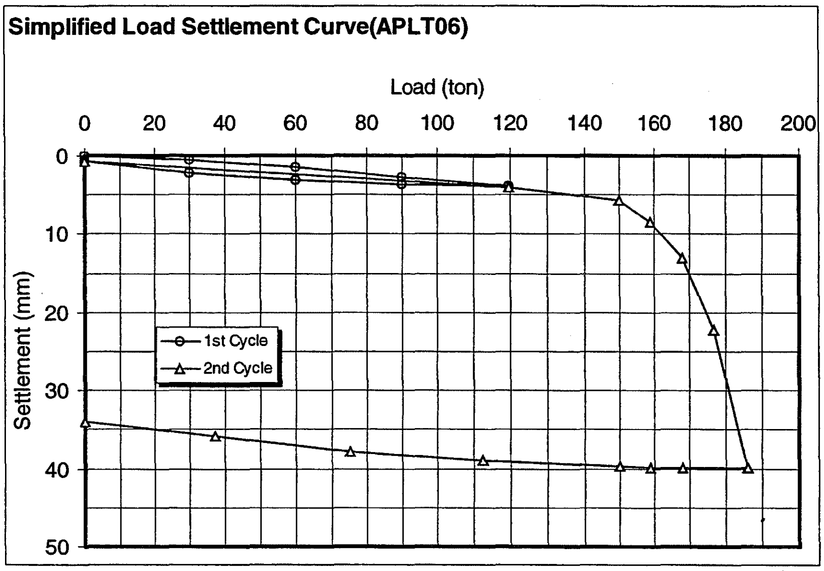

Figure 3. Load-displacement curve for APLT02 (Substation)

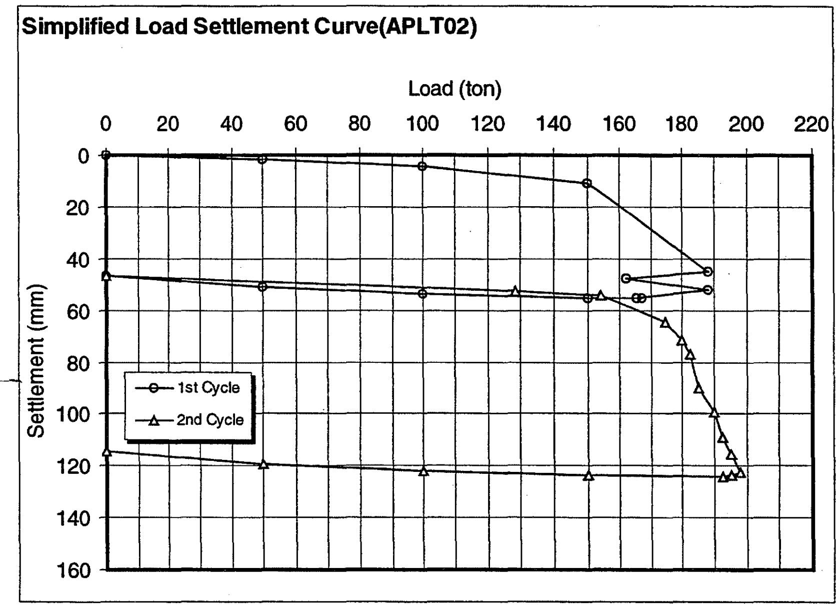

Pile Set

The CAPWAP analysis of the dynamic piling records gives an estimate of the pile set per blow that would be observed when the full pile capacity is mobilised. This information provides a useful acceptance criteria to determine whether a pile has achieved the required capacity during the installation of production piles.

Design of Production Piles

Pile Length

It was decided following the completion of the APLT's that both the Main Power Block and Substation piles would be designed as 12 m single segment piles. Comparison of APLT05 and APLT06 shows that the difference between the pile capacities of 18 m and 12 m piles in the improved ground is rather small. Use of 12 m piles would bring about substantial savings in the construction duration and pile material which would outweigh the small additional pile capacity that the 18m would provide. For the same reason, the Substation piles were also designed as 12 m single segment piles.

It is noted that, unlike the test piles, the top 2 m of the production piles will be cut back to expose the pile rebars and tie them to the pile cap so that the piles are structurally connected to the pile caps. The pile caps are typically 2 m below ground level, so the production piles are effectively 10 m piles founded at 12 m below the ground level. In other words, the production piles will have the capacity of a 12 m test pile with the top 2 m of skin friction deducted.

Effect of Production Ground Improvement

The APLT's 04-06 were conducted in the ground improved with sand compaction piling spaced at 1.5 m and 2.0 m centres. Following the sand compaction piling pilot study, the liquefaction analysis of the CPT results in the improved ground indicated that production sand compaction piling of 2.2 m centres would sufficiently densify the liquefiable layer to prevent liquefaction during the design earthquake. It was therefore necessary to consider the effect of altering the ground improvement arrangement to 2.2 m centres by extrapolation from APLT04 and APLT05.

Ultimate Pile Capacity and Design Working Load

The ultimate capacities of the production piles were estimated from the results of the APLT's with manipulation of the SPT correlation method to account for the 2m cut off and the change in ground improvement arrangement. As discussed earlier, the SPT correlation method provides more accurate estimates of the axial capacities of the test piles. So the SPT correlation method was adopted as the pile design method.

The spreadsheet calculations of the ultimate capacities of the Main Power Block production piles and Substation piles are appended to this paper.

The N values of the reclamation fill and liquefiable alluvium layers were back calculated so that the pile capacities predicted by the SPT correlation method actually match the pile capacities of the test piles determined from APLT's (Calculation 2, Appendix). The axial capacity of a Main Power Block production pile was then calculated based on the back calculated N-values allowing for the loss of skin friction over the top 2m and the increased spacings of 2.2 m for the production ground improvement (Calculation 3, Appendix).

The ultimate axial capacity of a pile in the Main Power Block was found to be 1600 kN. Applying a factor of safety of 2, the design working load (DWL) was 800 kN.

The ultimate axial capacity and DWL of an 18 m Substation pile was determined in a similar way. However, it was decided later that 12 m piles would be adopted as production piles in the Substation area despite consequent reduction in the pile capacity. The ultimate axial capacity of a 12 m Substation pile was simply obtained from the static load test capacity based on Chin's method, and the PDA analysis of APLT07. The ultimate capacity of 1300 kN, was divided by a factor of safety of 2 to obtain the DWL of 650 kN. Although this approach appears to be simplistic and less conservative than the Main Power Block pile, it is justifiable given the secondary priority of the Substation.

Discussion

This case study has illustrated applicability of various design methods for piles in improved and partially improved ground. Consistent pile capacities were calculated from the static and dynamic testing, indicating the validity of the APLT's. The conventional static method proved to be very inaccurate, overestimating or underestimating the pile capacity by as much as 60% in most tests. The SPT correlation method provided much more accurate estimates of the test pile capacities for APLT01–03 which were located in surcharged and unimproved ground, but did not accurately estimate the pile capacities of APLT04-06, which were constructed in the ground improved with sand compaction piling. This suggests that neither the conventional static methods nor empirical methods are applicable to piles in improved ground where the stress state has been heavily modified from the initial at rest state. Therefore pile load tests provide a very useful design method for piles in such ground conditions.

The APLT's provide some other useful information such as the Case method pile capacity and load-displacement curves. It was the inspection of the plot of the Case method pile capacity versus depth that lead to the testing and subsequent adoption of 12 m single segment piles as production piles. The Case method pile capacity plot revealed that a 12 m pile would have almost the same capacity as a 18 m pile. The load displacement curves from the static load tests provide estimates of pile settlement under the DWL and ultimate load capacity.

Comparative Study

In order to illustrate that the pile design based on the APLT's is indeed optimum, comparison is made with another power development of slightly smaller scale (365 MW power plant), also near Dhaka, Bangladesh. This 365 MW plant has also been constructed on reclaimed land adjacent to a natural river. The reclamation platform was improved by 1.5 m of surcharge with wick drains. The soil conditions are very similar at these two development sites. The pile design at the two power plants is compared in terms of the number of piles per unit area, pile length, design working load. The table below summarises the pile design at these plants.

Table 6 Pile design at two similar power developments in Bangladesh

		450MW Plant (Study Project)	365MW Plant
Approximate plant area[1]	m^2	46,000	36,000
Total no. of piles	No.	1,199	1,184
Total driven length	m	≈14,400	≈28,400

[1]Total area that the plant structures and facilities actually occupy. Not the total area of reclamation platform.

The 450 MW Plant is supported on approximately the same number of piles that were used for the smaller 365 MW Plant, indicating the efficiency of the pile design. The total metre length of the piles has been reduced to almost half of that of the 365 MW. The design working load of the Substation piles has decreased, but the overall cost efficiency of the pile design is substantial.

Conclusion

The geotechnical design of production piles at a power development in Bangladesh has been developed based on a series of Advance Pile Load Tests (APLT's) that comprise dynamic and static testing of test piles. The preliminary calculation of the theoretical pile capacities was carried out using the conventional static method and SPT correlation method. The preliminary calculation indicated that 18 m piles would be required for both the Main Power Block and Substation areas to achieve the ultimate single pile capacity of 1600 kN (DWL 800 kN). However, following careful consideration of the results of the APLT's, it was found that 12 m piles could be adopted as production piles with a very small reduction of pile capacity compared to 18 m piles. Use of 12 m piles resulted in substantial savings in pile material and construction duration.

The APLT's have also demonstrated that the conventional static method and SPT correlation method were not a desirable design approach if piles are constructed in improved ground. The conventional static method and SPT correlation provided rather inaccurate estimates of the capacities of the test piles, particularly in the ground improved with sand compaction piling. The APLT's, on the other hand, provided consistent results from both static and dynamic tests, suggesting that the design of the production piles are neither overly conservative nor under designed. On-site observations of production piling at a later date also confirmed that the design was optimised.

Acknowledgements

The authors wish to thank our Hyundai Engineering and Construction Co. (HDEC) for their permission to publish this paper. We also acknowledge and appreciate AES, the plant developer. Special thanks go to Mr. K.Y. Jeong (Project Control Manager), Mr. D.H. Kim (Project Manager), Mr. D.S. Choi (Civil Manager) and Mr. O.D. Kwon (Assistant Civil Manager) of HDEC, and Peter Fox (Construction Manager) of AES for their continual support and kindness on and off site.

References

Bowles, J.E. (1996). *Foundation Analysis and Design*, 5th Edition, McGraw-Hill Companies Inc.,1175 p.

Canadian Geotechnical Society (1992). *Canadian Foundation Engineering Manual*, 3rd Edition, pp. 356-359

Coduto, D.P. (1994). *Foundation Design Principles and Practices*, Prentice Hall Inc., New Jersey, pp. 412-416.

Haskoning (2000). *Final Report, Meghnaghat Site Inspection*, Unpublished report prepared for AES Meghnaghat Limited.

Gadre, A. and Dobry, R. (1998). "Lateral cyclic loading centrifuge tests on square embedded footing," *Journal of Geotechnical and Geoenvironmental Engineering,* ASCE, New York, Vol. 124, pp. 1128-1138.

The Institute of Civil Engineers (1996). *Specifications for Piling and Embedded Retaining Walls*, Thomas Telford, London, pp. 55-62.

Tomlinson, M.J. (1994). *Pile Design and Construction Practice*, 4th Edition, E & FN Spon, London, pp. 114-119.

Youd, T.L. and Idriss, I.M. (1997). *Proceedings of the NCEER Workshop on Evaluation of Liquefaction Resistance of Soils*, Technical Report NCEER-97-0022, National Centre for Earthquake Engineering Research

Appendix – Calculations

CALCULATION 1

PRELIMINARY PILE CAPACITY ASSESSMENT - UNIMPROVED GROUND
Pile Lengths as-built

Require 1000kN at SF=2.5

Layer	c'	ϕ'	N_q	δ	K_s	N	Unit Wt. γ / γ
RF	0	34		24	0.88	16	20
RF'	0	34		24	0.88	16	10
Qal_1	0	28		20	1.06	7	9
Qal_2	0	30	20	21	1.00	11	9
Qal_2'	0	32	30	22	0.94	16	9
$Qalo_1$	5	36	50	25	0.82	48	9

$K_s/K0$ 2
δ/ϕ' 0.7

	AP 1 -substation (BH5)			Static		SPT	
Layer	Thickness	σ'_{vm}	σ'_{v0}	Skin (kPa)	End (kPa)	Skin (kPa)	End (kPa)
RF	1.3	13	26	5		32	
RF'	4.7	50	73	19		32	
Qal_1	1	78	82	29		14	
Qal_2	4	100	118	38	2360	22	3300
Qal_2'	11.3	169	220	65	6591	32	4800
$Qalo_1$	0	220	220	85	11575	96	8000
	22.3			1183	1055	579	768
With liquefaction			Total		2237		1347
(sleeved to top of Qalo1)				1183	1055	579	768
Driving			Total		2237		1347

	AP 2 -substation (BH1)			Static		SPT	
Layer	Thickness	σ'_{vm}	σ'_{v0}	Skin (kPa)	End (kPa)	Skin (kPa)	End (kPa)
RF	1.3	13	26	5		32	
RF'	5.7	55	83	21		32	
Qal_1	1	88	92	33		14	
Qal_2	5	115	137	44	2740	22	3300
Qal_2'	9	178	218	69	6540	32	4800
$Qalo_1$	0	218	218	85	11490	96	8000
	22			990	1046	461	768
With liquefaction			Total		2037		1229
				1599	1046	1018	768
Driving			Total		2645		1786

Require 2000kN at SF=2.5

	AP 3 -main power block (BH21)			Static		SPT	
Layer	Thickness	σ'_{vm}	σ'_{v0}	Skin (kPa)	End (kPa)	Skin (kPa)	End (kPa)
RF	1.3	13	26	5		32	
RF'	4.7	50	73	19		32	
Qal_1	1	78	82	29		14	
Qal_2	2	91	100	35	2000	22	3300
Qal_2'	16	172	244	67	7320	32	4800
$Qalo_1$	1	249	253	96	13240	96	8000
	26			1860	2118	973	1280
With liquefaction			Total		3979		2253
				2175	2118	1373	1280
Driving			Total		4293		2653

PRELIMINARY PILE CAPACITY ASSESSMENT - PILOT STUDY A

$K_s/K0$ 2.5
δ/ϕ' 0.7

Layer	c'	ϕ'		δ	K_s	N	Unit Wt. γ / γ
RF	0	40		28	0.89	22	20
RF'	0	40		28	0.89	22	10
Qal_1	0	38		27	0.96	35	9
Qal_2	0	38		27	0.96	32	9
Qal_2'	0	35		25	1.07	16	9
$Qalo_1$	5	36		25	1.03	48	9

	AP 6 -main power block			Static		SPT	
Layer	Thickness	σ'_{vm}	σ'_{v0}	Skin (kPa)	End (kPa)	Skin (kPa)	End (kPa)
RF	1.3	13	26	6		44	
RF'	4.7	50	73	24		44	
Qal_1	1	78	82	38		70	
Qal_2	5	105	127	50	3810	64	8000
Qal_2'	0	127	127	62	3810	32	4800
$Qalo_1$	0	127	127	62	6940	96	8000
	12			652	610	1046	1280
With Ground Improvement			**Total**		1262		2326

Layer	c'	ϕ'		δ	K_s	N	Unit Wt. γ / γ
RF	0	40		28	0.89	22	20
RF'	0	40		28	0.89	22	10
Qal_1	0	38		27	0.96	35	9
Qal_2	0	38		27	0.96	32	9
Qal_2'	0	35		25	1.07	16	9

	AP 5 -main power block			Static		SPT	
Layer	Thickness	σ'_{vm}	σ'_{v0}	Skin (kPa)	End (kPa)	Skin (kPa)	End (kPa)
RF	1.3	13	26	6		44	
RF'	4.7	50	73	24		44	
Qal_1	1	78	82	38		70	
Qal_2	8	118	154	57		64	
Qal_2'	6	181	208	88	6240	32	4800

CALCULATION 2

AS-BUILT PILE CAPACITY ASSESSMENT - SURCHARGED GROUND (SUBSTATION)
Pile Lengths as-built

Require 1000kN at SF=2.5

Layer	c'	φ'	N_q	δ	K_s	N	Unit Wt. γ'/γ
RF	0	34		24	0.88	16	20
RF'	0	34		24	0.88	16	10
Qal_1	0	28		20	1.06	7	9
Qal_2	0	30	20	21	1.00	11	9
Qal_2'	0	32	30	22	0.94	16	9
$Qalo_1$	5	36	50	25	0.82	48	9

$K_s/K0$ 2
δ/φ' 0.7

	AP 1 -substation (BH5)			Static		SPT	
Layer	Thickness	σ'_{vm}	σ'_{vo}	Skin (kPa)	End (kPa)	Skin (kPa)	End (kPa)
RF	1.3	13	26	5		32	
RF'	4.7	50	73	19		32	
Qal_1	1	78	82	29		14	
Qal_2	4	100	118	38	2360	22	3300
Qal_2'	11.3	169	220	65	6591	32	4800
$Qalo_1$	0	220	220	85	11575	96	8000
	22.3			1183	1055	579	768
With liquefaction			Total		2237		1347
(sleeved to top of Qalo1)				1183	1055	579	768
Driving			Total		2237		1347

	AP 2 -substation (BH1)			Static		SPT	
Layer	Thickness	σ'_{vm}	σ'_{vo}	Skin (kPa)	End (kPa)	Skin (kPa)	End (kPa)
RF	1.3	13	26	5		32	
RF'	5.7	55	83	21		32	
Qal_1	1	88	92	33		14	
Qal_2	5	115	137	44	2740	22	3300
Qal_2'	9	178	218	69	6540	32	4800
$Qalo_1$	0	218	218	85	11490	96	8000
	22			990	1046	461	768
With liquefaction			Total		2037		1229
				1599	1046	1018	768
Driving			Total		2645		1786

	AP 3 -main power block (BH21)			Static		SPT	
Layer	Thickness	σ'_{vm}	σ'_{vo}	Skin (kPa)	End (kPa)	Skin (kPa)	End (kPa)
RF	1.3	13	26	5		32	
RF'	4.7	50	73	19		32	
Qal_1	1	78	82	29		14	
Qal_2	2	91	100	35	2000	22	3300
Qal_2'	16	172	244	67	7320	32	4800
$Qalo_1$	1	249	253	96	13240	96	8000
	26			1860	2118	973	1280
With liquefaction			Total		3979		2253
				2175	2118	1373	1280
Driving			Total		4293		2653

AS-BUILT PILE CAPACITY ASSESSMENT - PILOT STUDY A

$K_s/K0$ 2.5
δ/φ' 0.7

Layer	c'	φ'		δ	K_s	N	Unit Wt. γ'/γ
RF	0	40		28	0.89	16	20
RF'	0	40		28	0.89	16	10
Qal_1	0	38		27	0.96	22	9
Qal_2	0	38		27	0.96	22	9
Qal_2'	0	35		25	1.07	16	9
$Qalo_1$	5	36		25	1.03	48	9

	AP 6 -main power block			Static		SPT	
Layer	Thickness	σ'_{vm}	σ'_{vo}	Skin (kPa)	End (kPa)	Skin (kPa)	End (kPa)
RF	1.3	13	26	6		32	
RF'	4.7	50	73	24		32	
Qal_1	1	78	82	38		44	
Qal_2	5	105	127	50	3810	44	6600
Qal_2'	0	127	127	62	3810	32	4800
$Qalo_1$	0	127	127	62	6940	96	8000
	12			652	610	730	1056
With Ground Improvement			**Total**		1262		1786

Layer	c'	φ'		δ	K_s	N	Unit Wt. γ'/γ
RF	0	40		28	0.89	16	20
RF'	0	40		28	0.89	16	10
Qal_1	0	38		27	0.96	18	9
Qal_2	0	38		27	0.96	18	9
Qal_2'	0	35		25	1.07	16	9

	AP 5 -main power block			Static		SPT	
Layer	Thickness	σ'_{vm}	σ'_{vo}	Skin (kPa)	End (kPa)	Skin (kPa)	End (kPa)
RF	1.3	13	26	6		32	
RF'	4.7	50	73	24		32	
Qal_1	1	78	82	38		36	
Qal_2	8	118	154	57		36	
Qal_2'	6	181	208	88	6240	32	4800

CALCULATION 3

PILE CAPACITY ASSESSMENT - SURCHARGED GROUND (SUBSTATION)

$K_s/K0$ 1
δ/ϕ' 0.7

							Unit Wt.					Static		SPT	
Layer	c'	ϕ'	N_q	δ	K_s	N	γ' / γ	Layer	Thickness	σ'_{vm}	σ'_{vo}	Skin (kPa)	End (kPa)	Skin (kPa)	End (kPa)
RF	0	39		27	0.37	16	20	RF	2	20	40				
RF'	0	39		27	0.37	16	10	RF'	5	65	90	12		32	
Qal_1	0	36		25	0.41	7	9	Qal_1	1	95	99	18		14	
Qal_2	0	36	20	25	0.41	11	9	Qal_2	4	117	135	23	2700	22	
Qal_2'	0	32	30	22	0.47	16	9	Qal_2'	6	162	189	31	5670	32	
$Qalo_1$	5	36	50	25	0.41	48	9	$Qalo_1$	0	189	189	37	10040	96	
									18			301	907	307	768
								With liquefaction			Total		1209		1075
												576	907	726	768
								Driving			Total		1483		1494

Note: Skin friction has not been included for the top 2m (pile cut-off)

PILE CAPACITY ASSESSMENT - GROUND IMPROVED TO 2.2m SQUARE SPACING PRODUCTION SCP

$K_s/K0$ 2.5
δ/ϕ' 0.7

							Unit Wt.					Static		SPT	
Layer	c'	ϕ'		δ	K_s	N	γ' / γ	Layer	Thickness	σ'_{vm}	σ'_{vo}	Skin (kPa)	End (kPa)	Skin (kPa)	End (kPa)
RF	0	40		28	0.89	16	20	RF	2	20	40				
RF'	0	40		28	0.89	16	10	RF'	4	60	80	28		32	
Qal_1	0	38		27	0.96	21	9	Qal_1	1	85	89	41		42	
Qal_2	0	36		25	1.03	21	9	Qal_2	5	112	134	54		42	
Qal_2'	0	35		25	1.07	16	9	Qal_2'	0	134	134	65	4020	32	
$Qalo_1$	5	36		25	1.03	48	9	$Qalo_1$	0	134	134	65	7290	96	
									12			680	643	608	1056
								With Ground Improvement			**Total**		1324		1664

Note: Skin friction has not been included for the top 2m (pile cut-off)

Assessment of Fibre Reinforced, Lime-Stabilised Soil for Erosion Control

Mohsen Rahimi

NSW, Department of Public Works and Services

Abstract

This paper presents results of an investigation carried out on the evaporation basin for salt production in Australia. The problem is erosion of the earthen banks constructed with compacted local soil without any protection measures. The erosion is caused by the natural elements wind and rain, or from wave action. Due to the high incidence of wind in the area, wind erosion and wave erosion of the banks are major problems. Bank-protection trials have been undertaken by others, using granite spalls, redgum timber, grout matt and shotcreting. Long-term performance of these trials was not satisfactory.

The prime objective of this investigation is to provide an economical solution to the erosion problems, and to assess long-term performance of the adopted solution. Soil stabilised with different percentages of lime and reinforced with straw fibres was selected for this purpose.

Mineralogical, chemical and geotechnical tests were carried out on the soil samples. Specimens were made of local soils and lime-stabilised soils, with and without reinforcement. The specimens were subjected to wet and dry cycles, fully and partially immersed in water. The performance and durability of the specimens was evaluated. The findings show that erosion of lime-stabilised soil depends on the rate of lime application. It is also shown that erosion of stabilised soil depends on physical soil conditions and environmental conditions. It is linear for uncracked soil, and non-linear for cracked soil. The erosion of stabilised soil with 8% lime is linear. Furthermore it is shown that the erosion of lime-stabilised soil reinforced with randomly distributed straw fibre is less than 25% of the lime-stabilised soil without fibre.

Review of Literature

Soil Erosion and Soil Durability

Soil erosion is the most important form of soil degradation. Resistance to erosion may be termed durability. Poor durability can be a problem both for natural and stabilised soils. Durability is one of the most difficult material evaluation problems. The amount of erosion (weight loss) within a selected period is defined as a difference between weight of sample at initial and end of a period. The erosion rate is defined as the slope of the line relating weight loss versus time.

Erosion rate of saturated soil using a rotating cylindrical apparatus, for a short duration, was discussed by Arulanandan, K., et al (1975). Erosion rate of compacted sodium-montmorillonite clays with different percentage of clay content, under a range of tractive stresses from surface flows in a flume test, for a short duration, was discussed by Shaikh et al, (1988). The results of their study show that the erosion rate increases when clay content decreases. The relationship between surface erosion rate and tractive stress is linear. Their results show that identifying a soil as dispersive does not necessarily mean it will exhibit high rates of surfacial erosion. They use the phenomenon of slaking to explain their results and suggest that the calcium-montmorillonite, identified as nondispersive, slaked when immersed in water, while the sodium-montmorillonite identified as dispersive, did not slake. They conclude, therefore, that the phenomenon of slaking has a greater influence on surface erosion of an unsaturated clay than does dispersivity. It should be noted that "dispersion" is described as the tendency for the clay fraction of a soil to go into colloidal suspension in water, and "slaking" is the break up of soil particles when immersed in water. Dispersive soils are also erodible, but not all erodible soils are necessary dispersive. However, erosion of saturated soil at steady state (soil under water), and long-term durability of soil, to our knowledge, has not been investigated in the past.

Dispersive Soil

Dispersive clays occur throughout the world. Their detrimental effect on the performance of hydraulic structures has been well documented in the literature (Ralling, 1966, Khan, 1983, Bell, et al. 1994). Experience shows that the considerable number of dispersive clay failures investigated have almost all been through homogeneous dams (Elges, 1991). The first research results relating to the behaviour of dispersive clays, mainly in homogeneous earth dams, were published in mid-1960's in Australia (Aitchison and Wood, 1965; Ingles and Wood, 1964; Rallings, 1966). These led to research in the USA published in the early 1970's (Sherard et al, 1976a).

Dispersive clay soils usually are difficult to recognise and cannot be identified by routine classification or index tests normally performed in geotechnical laboratories. Melvill et al (1980) carried out the percent dispersion, Emerson Crumb, Pinhole and chemical tests for pore water salts at Elandsjagt Dam, and showed that the percent dispersion test is one of the more consistent indicators of dispersive characteristics. Sherard, et al (1976a), have noted that for certain soils, small differences in compaction can have important influence on the pinhole test results and their susceptibility to erosion.

Another property which has been shown to govern the susceptibility of clay soils to dispersion is the total content of dissolved salts in the pore water (Sherard et al., 1976b). The lower this is, the greater the susceptibility of sodium saturated clays to dispersion (Bell et al., 1994). It is also reported that dispersive soils contain a higher content of dissolved sodium (up to 12 percent) in their pore water than ordinary soils, and their pH value generally ranges between 6 and 8. Dispersion is usually a problem when the eroding water has an electrical conductivity lower than of the pore water in the soil.

The sodium absorption ratio (SAR) and exchangeable sodium percentage (ESP) are used to quantify the role of sodium where free salts are present in the pore water. Aitchison and Wood (1965) regarded soils as dispersive, when the SAR is greater than 2. Physical tests are unable to identify dispersive soils when free salts are present. The effect of salt concentration in the eroding fluid was studied by Arulanandan, et al. (1975) using the same SAR, total salt concentration and moisture content. The test results indicate that the erodibility of a soil depends also on the salt concentration of the eroding fluid, decreasing with an increasing salt concentration. The ESP and SAR measures are affected by the presence of lime, gypsum, organics and pH. The reasons for this are complex and reader is referred to more specialist literature.

Internal erosion and piping are discussed elsewhere (Khilar, et al. 1985). Although a number of dispersion tests have been developed, no single test can be relied on completely. Watermeyer (1991) reported that it is unwise to place too much reliance on either a chemical or physical type test in isolation to assess the dispersion potential of the soils. He found there was a poor agreement in the chemical and physical test results.

Lime Stabilisation

Lime has been used in soil stabilisation of civil engineering structures for durability Bell (1988 and 1989), Rogers (1988), McElroy (1985), Mateous, (1964), Ingles et al. (1972). Lime was used in the construction of the Shensi Pyramid in Tibet and some of the Roman roads. At several points along the Great Wall in China, a calcium-hydrate reinforced earth wall in sandwiched between the two 1m brick walls. Lime stabilised soil had also been used for construction purposes in China. Its re-introduction started around 1930 after the development of soil mechanics tests, and high-level mechanisation has given further resurgence to this technique (Kezdi, 1979). Lime has been used to reduce the plasticity and to improve the workability of a soil and, increase its strength and resistance to deflocculation and erosion. One present deficiency of stabilisation practice is the lack of useful tests by which to assess the durability of soil and stabilised soil.

Soil Reinforcement

Early civilisations commonly used sun-dried soil bricks as a building material. Somewhere in their experience it became accepted practice to mix the soil with straw or other fibre available to them to improve its properties (e.g., Exodus 5:6-7). The practice seems to have been developed independently in various locations (Freitag, 1986).

Since ancient times, straw fibres have been used in Iran, Egypt and Mexico to reinforce clay. Mud bricks reinforced with straw fibres have been used in Australia during last century. The best example was the Warren house at Oura, NSW in 1911, goldminer's wattle and daub cottage at Hill End, NSW in 1875, and many building at Montsalvat, Victoria, during 1800s (Archer, 1985).

Reinforcing of slope surface by grass is a common solution and usually the cheapest method of slope stabilisation in stable soil especially in sand. Marram in coastal sandy conditions, Ray in dry conditions and Kikuyu, Couch or Weeping Love Grass in wet conditions performs well (Ingles, et al. 1972). Tests of silty clay loam and clay loam soils in which plant roots have grown show that the roots increased the shear resistance of the soil by factors as great as 290% for alfalfa, although other plant roots yielded increases on the order of 10 to 30% (Waldron, 1977). Grass roots acting as soil reinforcement bind the soil in a sufficient depth providing slope protection against erosion.

Randomly distributed fibres in a compacted fine-grained soil can result in greater strength and toughness. The amount of strength gain is about 25% (Freitag, 1986). Fibres are known to act as crack arresters and are used in a portion of the thickness of the structure to be reinforced for strength or durability. There is a similarity with fibre reinforced concrete; flexural strength tests of the concrete show that the fibres can increase the strength by 28% (Rahimi and Kesler 1979). Experimental results reported by various investigators (Gray, et al. 1986, Maher, et al. 1990, Lawton, et al. 1993, and Ranjan, et al. 1996) have shown that fibre reinforcement causes significant improvement in strength and stiffness of soil.

Combined Stabilised and Reinforced Soil

From the above discussion of existing practice and investigation to develop it, it appears that durability and long-tem performance of dispersive soil stabilised with lime should be enhanced by strengthening with fibres. To our knowledge no information is available on the durability and long-term performance of a stabilised soil, or fibre reinforced soil, which is the main objective of this investigation.

Experimental Investigation

Soil Properties

The physical and chemical properties of two soil samples of embankment fill tested are summarised in Tables 1 to 4.

Table 1 Summary of geotechnical test results

Sample	Field Permeability (cm/sec)	Field density (t/m^3)	Liquid limits (%)	Plasticity index (%)	Linear shrinkage (%)	Gravel (%)	Sand (%)	Silt (%)	Clay (%)
3196	3.47×10^{-6}	1.64	58	43	15.5	0	30	22	48
3198	1.44×10^{-4}	1.67	46	29	13	4	27	37	32

Table 2 Summary of dispersive test results

	Emerson Crumb (LW)	% dispersion in (DW)	% dispersion, in (LW)	Pinhole in (DW)	Pinhole in (LW)	pH
3196	2	4 (ND)	7 (ND)	PD2 (PD)	ND1 (ND)	6.4
3198	1	10 (ND)	4 (ND)	ND1 (ND)	ND1 (ND)	8.2

-DW= Distilled water -LW= Local water -ND= Non dispersive -PD= Possible dispersive

Table 3 Summary of test results on clay mineralogy by X-ray diffractometry

Sample	Kaolinite (%)	Illite (%)	Smectite (%) (Montmorillonite)
3196	13	41	46
3198	14	42	44

Table 4 Summary of chemical analysis by X-ray fluorescence spectometry (wt%)

Sample	SiO2	TiO2	Al2O3	Fe2O3	MgO	K2O	Na2O	CaO	SO3	Loss in ignition (LOI)
3196	69.6	0.57	12.09	3.99	0.92	2.18	1.64	0.49	0.19	9.33
3198	69.1	0.72	13.75	4.53	1.01	2.81	1.58	0.46	0.1	6.35

Erosion tests of compacted and stabilised soil samples were carried out in 2 stages:

Stage 1, Soil Samples Fully Immersed in Sydney Water and Local Water

Initially, both samples were subjected to standard compaction tests to determine maximum dry densities and optimum moisture contents. Two series of soil specimens were stabilised with 0%, 4%, 6% and 8% hydrated lime and remoulded to 98% standard compaction in cylindrical specimens, 50mm diameter and 100mm long. The specimens were positioned vertically in prefabricated frames for safe handling. Both series of specimens were cured at room temperature under plastic cover, for a period of 24 hours before being fully immersed in Sydney tap water (SW) and in local water (LW) respectively (refer to Figure 1). To simulate dry and wet site conditions, the specimens were kept in water at a temperature of 15°C ± 2°C for a duration of 3 days. Then they were removed from the water, cleaned of any eroded soil particles at the base plate of the frame, weighed and their physical conditions recorded. The specimens were left at room temperature for 6 hours before transferring them to an oven. The specimens were kept in the oven at a temperature of 43°C ± 5°C for a duration of 3 days. Selection of the oven temperature was based on expected maximum temperature in the evaporation pond area. The specimens were then removed from the oven and weighed after cooling, and their physical conditions recorded. This was repeated for seven wet and dry cycles with duration of 2-4 days in each cycle. The total duration of testing was 23 days.

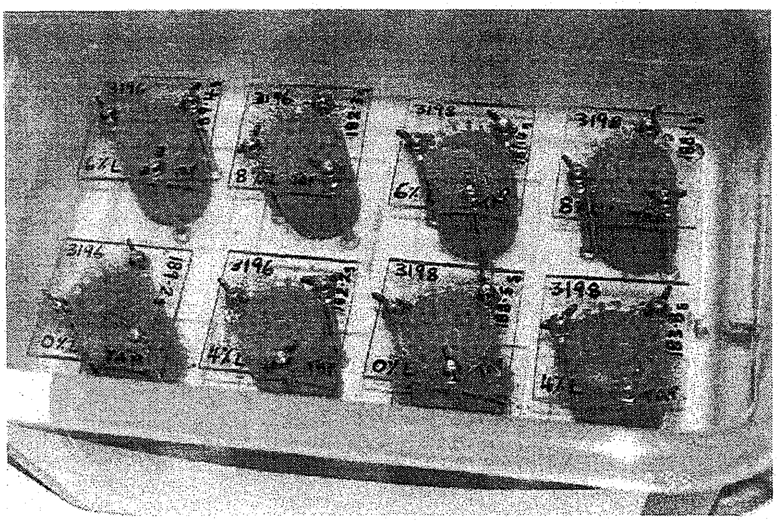

Figure 1 Specimens immersed in water

Apart from the bottom of the specimens, erosion occurred from the top and circumference of the cylinderical specimens. Considering that any error in water content measurement causes error in estimating the initial dry weight of the specimen, which in turn causes error in weight loss, saturated weight of specimen were used in the interpretation of test data. Based on the initial void ratio, dry and saturated densities of the specimens, and saturated weights at the end of each wet cycles, an equivalent cylinder height and surface area for each specimen was calculated. The initial saturated weight of the specimen is calculated by measuring the initial water content, wet weight, void ratio and degree of saturation of the specimen. The amount of erosion (weight loss) was defined as the difference between the saturated weights of the specimens after each wet cycle. The weight loss per unit surface area for both samples plotted versus erosion time is presented in Figures 2 and 3. Please note that both specimens with 0% hydrated lime collapsed within few hours during first wet cycle and are therefore not shown in the figures. In the figures, SW and LW denoted for Sydney water and local water, and numbers 4, 6, and 8 denoted for specimens stabilised with 4%, 6% and 8% hydrated lime respectively.

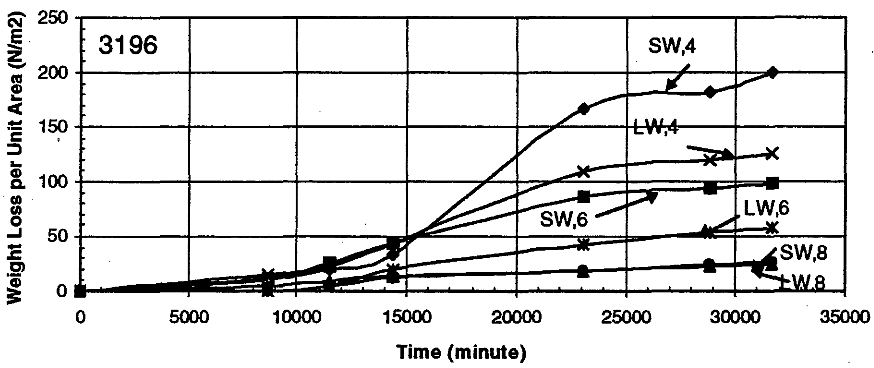

Figure 2 Weight loss per unit area for specimen 3196.

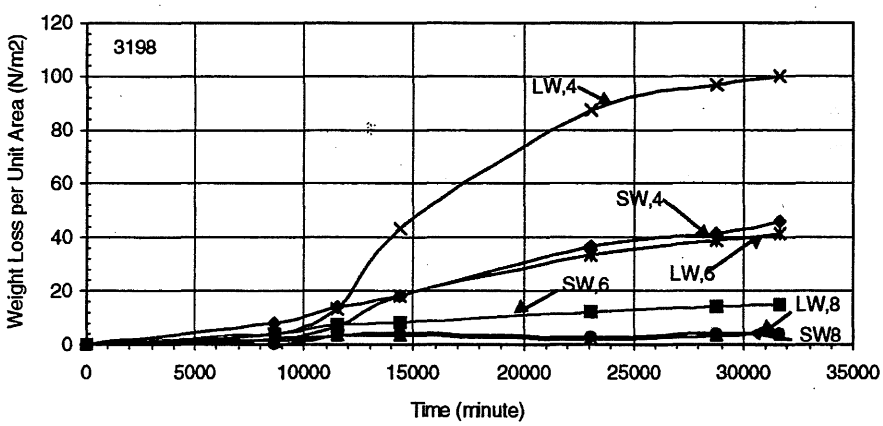

Figure 3 Weight loss per unit area for specimen 3198.

Stage 2, Soil Samples Partially Immersed in Local Water

It appears that the most critical section of the batter slope in the evaporation pond is within the water fluctuating zone. This section is continuously in wet and dry conditions, and vulnerable to cracking due to shrink – swell and tension strains. Knowing that fibres will act as crack arresters (Rahimi, et al 1979 and Lawrence, et al 1990), straw fibres were selected for this purpose, which were cheap and abundant on site.

Based on Stage 1 test results a minimum of 8% hydrated lime was selected for soil stabilisation. Two series of specimens were made, denoted with NF and WF for no fibre and with fibre respectively. Straw fibres selected for reinforcement were approximately 2.8% by weight, with aspect ratio of 15-20 (ratio of length to diameter). The straw fibres were soaked in Sydney tap water for 3 days, before preparation of the specimen. The soil samples were mixed thoroughly with 8% hydrated lime and 2.8% straw fibres and formed into a brick specimen of approximately 205mm x 85mm x 63mm. The densities achieved were 98% standard compaction. The specimens, were cured at room temperature under a plastic cover for 24 hours before partially immersing in LW at temperatures of 17°C ± 2°C for a duration of 6 days. A pump operating at 400-600 l/h was selected to circulate water and simulate wave action. The specimen was partly immersed, and partly water sprayed, and was considered to be saturated within 2-3 days (refer to figure 4). The procedures adopted are identical to those described in Stage 1. Six wet and dry cycles with varying duration of wet and dry cycles were repeated for a total duration of 74 days.

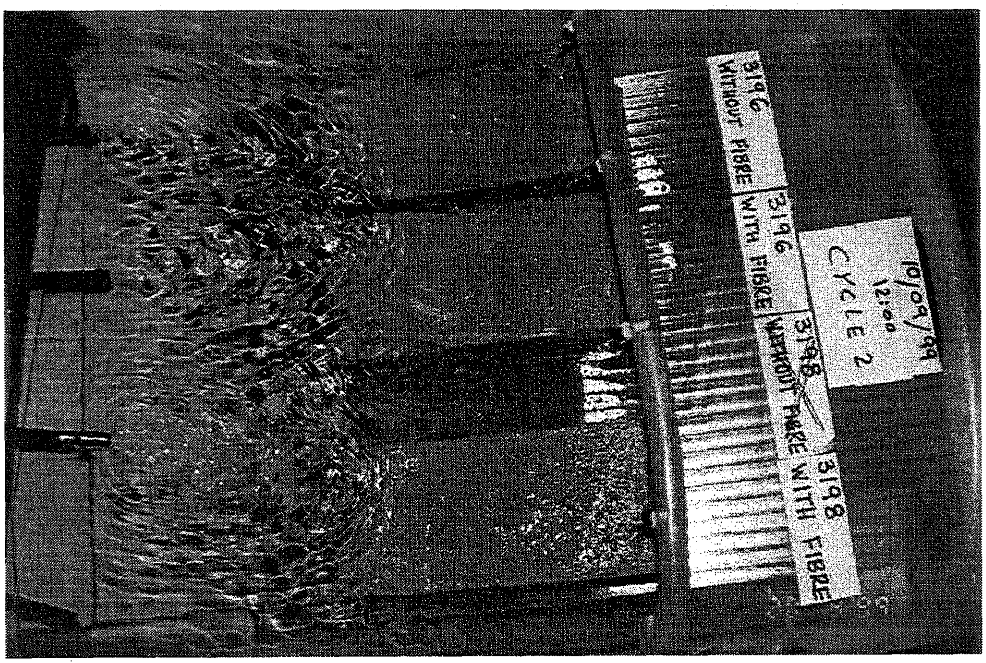

Figure 4 Specimens partially immersed

The weight loss of the specimen per unit surface area was plotted versus erosion time, and is presented in Figure 5. Please note that the specimen 3198NF failed during handling after the first wet cycle and is not shown in the figure. Specimen 3198WF failed after 6 wet and dry cycles (74 days).

After completion of testing, specimens with 8% hydrated lime, with and without fibre were crushed by a rubber mallet, and geotechnical properties of soil samples were determined. A summary of the test results is given in Table 5.

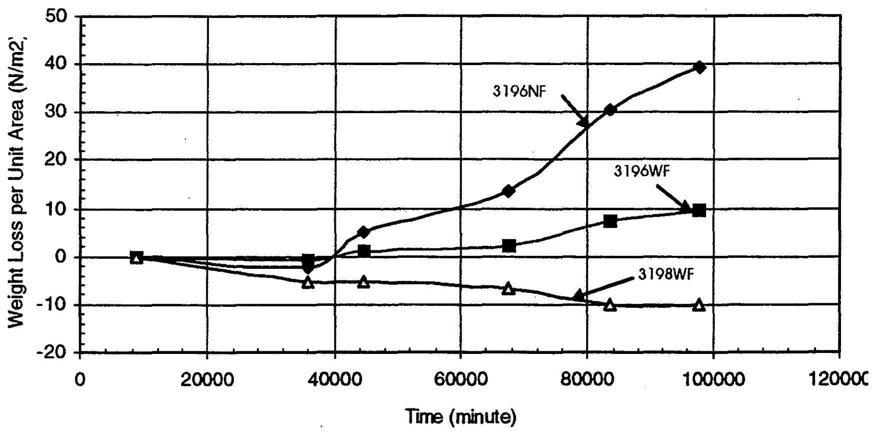

Figure 5 Weight loss per unit area for specimens partially saturated.

Table 5 Summary of laboratory test results before and after completion of testing

Samples	3196				3198			
	Non - Stabilised	8% Lime Stabilised after completion of test			Non - Stabilised	8% Lime Stabilised after completion of test		
		NF	WF	Ave.		NF	WF	Ave.
Liquid limit	58	41	46	44	46	43	41	42
Plasticity Index	43	10	22	16	29	18	13	16
Linear shrinkage	15.5	9	12	11	13	10	7.5	9
% Dispersion	4	5	12	9	10	4	6	5
<425μm	95	74	83	78	84	78	76	77
<75μm	72	44	51	48	71	60	56	58
<1μm	45	7	12	10	29	9	5	7

Interpretation of Test Data and Discussions

Non Stabilised Soil Samples

Mineralogical and chemical analysis of the soil samples revealed that both samples are very similar. Therefore, it appears that, both samples are from the same origin. Sample 3196 is somewhat darker in colour, relative to 3198. Together with the slightly higher loss on ignition (LOI), for the same sample, this probably reflects inclusion of organic matter. Sample 3196 also appears to contain a trace of gypsum ($CaSO4.2H2O$), and was subject to flocculation in the early stages of the oriented-aggregate preparation process. Although sulphur (as $SO3$) is slightly higher in this sample, the overall proportion of CaO is nevertheless very little different in either soil sample.

The total fine contents (silt and clay) for both samples are almost the same (70% and 69%). These samples are classified as silty clay with sand and clayey silt with sand respectively. The fines are of high plasticity with liquid limits of 58% and 46%, corresponding plasticity indices of 43% and 29%, which classify the materials as CH and CI respectively.

Field tests revealed that the in-situ dry densities of the soil samples are 1.64t/m3 and 1.67 t/m3 corresponding to a degree of compaction of 95.5% and 93% respectively. Field permeability tests at locations 3196 and 3198 revealed that the in-situ permeability of the material is $3.47x10^{-6}$ cm/sec and $1.44x10^{-4}$ cm/sec respectively. The soil samples are classified as very low and low permeability respectively to Terzaghi and Peck (1967) classifications.

The Emerson crumb tests on the samples 3196 and 3198 in LW resulted in Class 2 (some dispersion) and Class 1 (complete dispersion) respectively. It should be noted that dispersion was initiated by slaking after the samples were immersed in water for around 2 hours. The percent dispersion tests on both samples yielded 4% and 10% using distilled water and 7% and 4% using local water respectively. Both samples have "Non Dispersive" characteristics in both water types.

Pinhole tests indicated "Non-Dispersive" ND1 category for all specimens apart from sample 3196 in Sydney tap water which yield a "Possible Dispersive" PD2 category. The above results indicate that both samples are non-dispersive. It should be noted that physical tests are unable to identify dispersive soils when free salts are present (refer to Section Dispersive Soil). However, laboratory test results on the compacted soil samples immersed in water indicated that non stabilised soil specimens were eroded and completely failed within first wet cycle in SW and LW. Therefore, both samples should be considered as dispersive and erodible. It should be noted that, highly dispersive soils are also highly erodible. The erodibility of a soil depends also on the salt concentration of the eroding fluid, decreasing with an increasing salt concentration. It is expected that dispersion/erosion due to rain should be higher than erosion due saline water. In the investigation of the evaporation pond, stormwater runoff has formed very deep erosion channels along the embankment crest and down the batter slope. This has resulted in internal erosion of the batter and crest at many locations (refer to Figure 6).

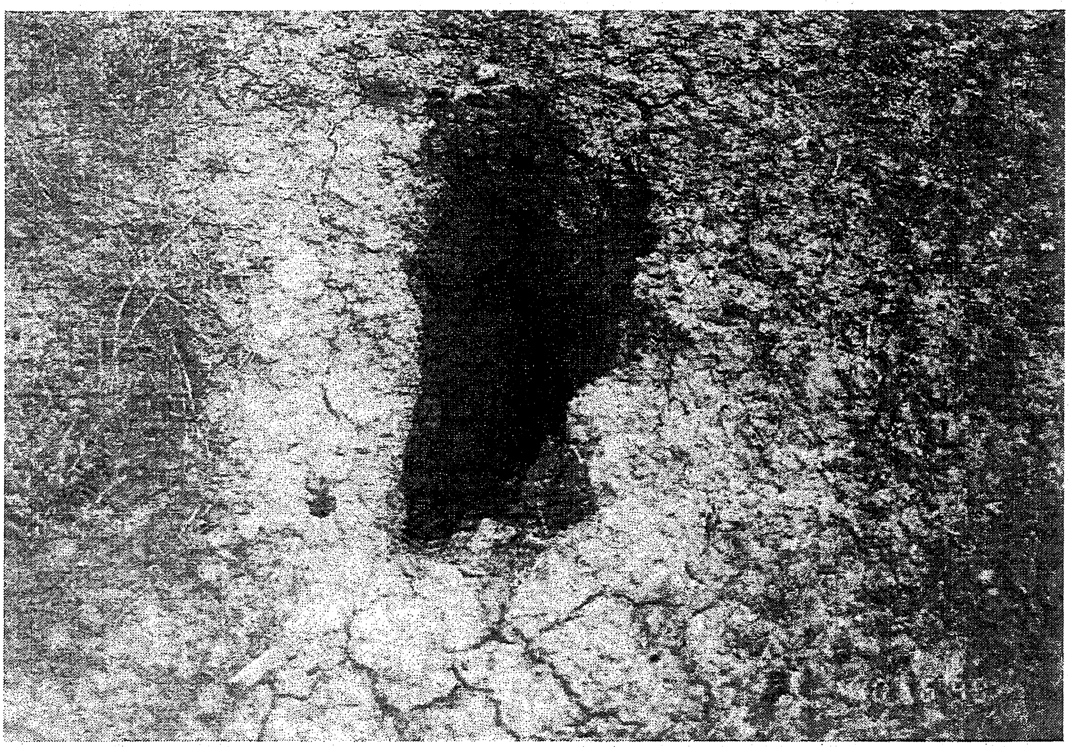

Figure 6 Internal erosion

Stabilised Soil Samples, Fully Immersed

From the test results and visual evaluation of specimen conditions it is revealed that:

The specimens with 0% hydrated lime collapsed during first wet cycle within few hours after immersion in both SW and LW. Both samples 3196 and 3198 are considered to be highly dispersive and erosive.

Salt residue in a form of jelly (white film) appeared around specimens in LW during the first wet cycle. The concentration of salt was higher around specimens 3198 with a high percentage of lime. The jelly turned into solid crystal salt deposit at the specimens' surface and peeled off during successive cycles. This is related to chemical action between lime and salts in eroding water.

Erosion for specimens 3196 stabilised with 4% and 6% hydrated lime in SW is higher than the specimens stabilised with the same rate of lime in LW. This could be related to lower electric conductivity of eroding water (SW) than pore water (LW) (Arulanandan, et al. 1975, and 1983).

Erosion for specimens 3198 stabilised with 4% and 6% hydrated lime in LW is higher than the specimens stabilised with the same rate of lime in SW. This could be related to higher hydraulic conductivity and lower shear strength of specimens. Salt content is increasing in pore structures causing expansion, cracking and removing soil particles.

Erosion for both specimens stabilised with 4% and 6% hydrated lime is linear within short-term (within first cycle) and non-linear within long-term. The reason for non-linearity can be explained by analysing specimen conditions during wet and dry cycles. It was observed that horizontal and vertical micro cracks were apparent during first dry cycle at the top edge of the specimens. These cracks were spreading and deepening during successive cycles, until vertical and horizontal cracks joined together to form rectangular blocks. These blocks collapsed in a form of soil lumps and removed during the next cycle. This condition is similar to that observed on site (refer to Figure 7).

Erosion for both specimens 3196 and 3198 stabilised with 8% hydrated lime in SW and LW is generally similar and of the same order. Apparently, no cracking was observed during testing. The erosion is linear with a constant erosion rate of 7E-4 N/m2/min.

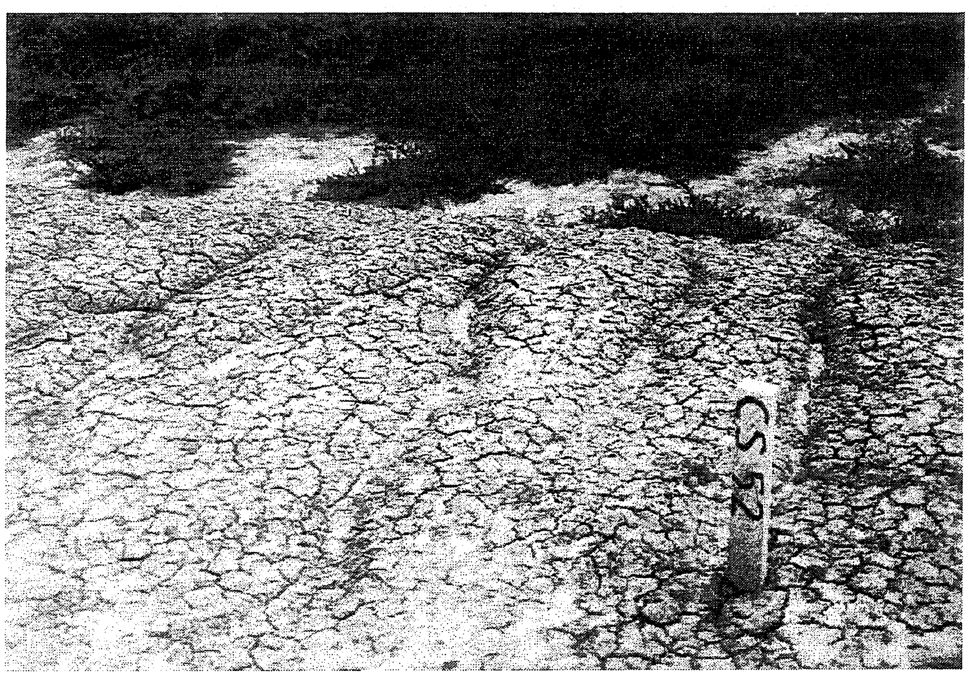

Figure 7 Surface erosion

Stabilised Soil Samples, Partially Immersed

From the test results and visual evaluation of specimen conditions it is revealed that:

As for fully saturated samples, salt residue in form of jelly appeared around the areas of the specimen partially immersed in the water. The concentration of salt was very high in specimen 3198NF.

The specimen 3198NF was highly cracked during first wet and dry cycle, and failed on handling during the second wet cycle. This could be related to its higher hydraulic conductivity and lower shear strength properties. Salt content is increasing in pore structures causing expansion and cracking.

Erosion for the specimen 3198WF is negative and linear. The negative erosion is due to increase in salt deposits. The specimen became highly cracked during the sixth dry cycle and failed on handling, when removing saturated specimen from water.

The specimen 3196NF gradually eroded along the edges without apparent cracking. The minor weight increase (negative erosion) of specimen during first cycle is due to the formation of salt deposit. Ignoring the first section of the erosion curve, it appears that erosion of the specimen is linear with erosion rate of 6.6E-4N/m2/min. The erosion rate is almost the same as for specimen fully immersed.

The specimen 3196WF is the most resistant to erosion with minor erosion occurred around the edges. The erosion is linear with a constant erosion rate of 1.6N/m2/min.

Conclusions

Based on the limited laboratory testing carried out during this investigation, the results and interpretation of test data should be regarded as preliminary only. To better understand the mechanism of erosion and durability of stabilised soil it is recommended that additional testing should be carried out including chemical, geotechnical, with more fibre reinforced specimens and different fibre type (synthetic, and natural) with higher aspect ratios. Based on the limited test results, the following conclusions can be made.

There is a poor agreement in the dispersion test results using different test methods. It is found that the Emerson Crumb Test is a more consistent indicator of dispersive/erosion characteristic of soil, subject to considering a longer testing time than a routine testing time.

Erosion of lime-stabilised soil depends on the rate of lime application.

Erosion of stabilised soil depends on physical soil conditions and environment conditions; it is linear for uncracked soil, and non-linear for cracked soil.

Erosion of lime-stabilised soil with 8% lime is linear.

Erosion of lime-stabilised soil reinforced with randomly distributed fibre is less than 25% of the lime-stabilised soil without fibre.

The study undertaken indicates that reinforced, lime-stabilised soil is a promising and economic solution for stabilising embankment soil against erosion. However, for a better understanding of the mechanism of erosion and durability of stabilised soil additional testing would need to be carried out.

Acknowledgment

The author thanks the Murray Irrigation Limited for permission to use the investigation data in the preparation of this paper and to the Department of Public Works and Services for permission to publish this paper.

References

Aitchison, G.D., Wood, C.C., (1965). "Some interactions of compaction, permeability and post-construction deflocculation affecting the probability of piping failure in small earth dams," *Proc. Sixth International Conf. on Soil Mech. Found. Eng.*, Montreal, Vol. II.

Anonymous, (1990). "Dispersive soils in earth dams," Review*: International Commission on Large Dams*, Paris, France, P53.

Archer, J. & G. (1985). "Dirt Cheap, The Mud Brick Book," *Compendium Second Back Row Press.*

Arulanandan, K., Loganathan, P. and Krone, R.B., (1975). "Pore and eroding fluid influences on surface erosion of soil," *Journal of Geotechnical Engineering,* ASCE, Vol. 101, No. 1, pp51-65.

Arulanandan, K. and Perry, E.B., (1983). "Erosion in relation to filter design criteria in earth dams," *Journal of Geotechnical Engineering*, ASCE, Vol. 109, No. 5, pp682-698.

Bell, F. G. and Maud, R. R., (1994). "Dispersive soils and earth dams with some experiences from South Afric," *Bulletin of the Association of Engineering Geologist* Vol. XXXI, No. 4, pp.433-446.

Bell, F. G. (1988), "Stabilisation and treatment of clay soils with lime," *Ground Engineering,* Volume 21, Number 2, pp10-15 and pp22-30.

Bell, F. G. (1989), "Lime Stabilisation of Clay Soils," *Bulletin of the International Association of Engineering Geology,* No. 39, Paris.

Elges, H.F.W.K., (1991). "Dispersive soils in South Africa-State of the art," *Proc. Ninth Regional Conference for Africa on Soil Mech. And Found. Eng.,* Akinmusuru, Malomo & Meshida (eds), Balkema, pp905-916.

Freitag, D.R., (1986). "Soil randomly reinforced with fibres," *Journal of Geotechnical Engineering,* ASCE, Vol. 112, No. 8, pp823-826.

Gray, D.H. and Al-Refeai, T., (1986). "Behavior of fabric-versus fiber-reinforced sand," *Journal of Geotechnical Engineering,* ASCE, Vol. 112, No. 8, pp804-820.

Ingles, O.G. and Metcalf, J. B., (1972). "Soil Stabilisation, Principles and Practice," *Butterworths*, pp127-143.

Ingles, O. G., Wood, C. C., (1964). "The recognition of failure in earth dams by aerial survey," *Australian Journal of Science,* Vol.26, No.11.

Kezdi, A., (1979). "Stabilized earth roads," *Elsevier*, pp.163-174.

Khan, I.H., 1983. "Failure of an earth dam: a case study, " *Journal of Geotechnical Engineering,* ASCE, Vol. 109, No. 2, pp244-259.

Khilar, K.C., Fogler, H.S. and Gray, D.H., (1985). "Model for piping-plugging in earthen structures," *Journal of Geotechnical Engineering,* ASCE, Vol. 111, No. 7, pp833-846.

Lawrence, S.J. and Rahimi, M.M., (1990). "Fibre reinforced render for repair of damaged masonry," CSIRO, Division of Building, Construction and Engineering, DOC, 90/05(S).

Lawton, E.C., Khire, M.V. and Fox, N.S., (1993). "Reinforcement of soils by multioriented geosynthetic inclusions," *Journal of Geotechnical Engineering,* ASCE, Vol. 119, No. 2, pp257-275.

Maher, M.H. and Gray, D.H., (1990). "Static response of sands reinforced with randomly distributed fibers," *Journal of Geotechnical Engineering,* ASCE, Vol. 116, No. 11, pp1661-1677.

Mateous, M. (1964). "Soil-lime research at Iowa State University," *Journal of Soil Mech. Found..* ASCE Div., 90, SM2, pp127-153.

McElroy, C. H. (1985). "Using Hydrated Lime to Control Erosion of Dispersive Clays," *ASTM, Lime for Environmental Uses, ASTM Committee C-7 on Lime*, Los Angeles, CA, 25 June 1985, ASTM Special Technical Publication 931.

Melvill, A. L. and Mackellar, D. C. R., (1980). "The identification and use of dispersive soils at Elandsjagt Dam South Africa," *Proc. Seventh Regional Conf. for Africa on Soil Mech. And Found. Eng.,* Accra, June, pp449-456.

Ralling, R. A., (1966). "An investigation into the causes of failure of farm dams in the Brigalow Belt of Central Queensland," *Water Research Foundation of Australia*, Bulletin No. 10.

Rahimi, M.M., and Kesler, C.E., (1979). "Partially steel-fibre reinforced mortar," *Journal of the Structural Division,* ASCE, Vol. 105, No. ST1, pp101-109.

Rahimi, M.M., and Cao, H.T. (1989). "Properties of sandwich beams with thin layer of steel fiber reinforced mortar," American Concrete Institute, Convention, SP124-14, pp265-278.

Ranjan, G., Vasan, R.M. and Charan, H.D., (1996). "Probabilistic analysis of randomly distributed fiber-reinforced soil," *Journal of Geotechnical Engineering,* ASCE, Vol. 122, No. 6, pp419-426.

Rogers, D. F. (1988), "Lime Stabilisation 88," *Ground Engineering*, Volume 22, Number 3, pp7-10.

Sherard, J. L., Dunnigan, L. P., Decker, R. S., Steele, E. F., (1976a). "Pinhole test for identifying dispersive soils," *Journal of Geotechnical Engineering,* ASCE, Vol. 102, No. GT1, pp69-75.

Sherard, J. L., Dunnigan, L. P., Decker, R. S., (1976b). "Identification and nature of dispersive soils," *Journal Geotechnical Engineering,* ASCE, Vol. 102, No. GT4, pp287-301.

Terzaghi, K. and Peck, R.B., (1967). "Soil mechanics in Engineering practice," *2nd ed. John Wiley and Sons*, New York.

Waldron, L.J., (1977). "The shear resistance of root-permeated homogeneous and stratified soil," *Soil Sci. Soc. Am. J.,* 41 (5), Sept., pp.843-849.

Watermeyer, C.F. and Botha, G.R., (1991). "Countering potential piping at an earth dam on dispersive soils," *Proc. Of the tenth Regional Conf. for Africa on Soil Mech. And Found. Eng. And the third International Conf. on Tropical and Residual Soils*, Maseru, 23-27 September, Blight et al. (eds), Balkema, pp321-328.

Case History: Sand Compaction Piling to Reduce Liquefaction Potential, Bangladesh

Jon Sickling

Formerly Geotechnical Engineer, Sinclair Knight Merz (NZ) Ltd.

Rob Stroop

Formerly Senior Geotechnical Engineer, Sinclair Knight Merz (NZ) Ltd.

Abstract

Sand compaction piles were the chosen method of ground improvement for a power development on reclaimed land near Dhaka, Bangladesh. Ground improvement was required to decrease the potential for liquefaction to an acceptable factor of safety under the design earthquake. The site soils are micaceous loose to medium dense fine sand and silt, and comprise 7m of reclamation fill underlain by inter-layered alluvium. An extensive site investigation of drillholes and cone penetration testing were used as input for analyses to quantify the susceptibility and extent of possible liquefaction. It was found that the effects of liquefaction could include up to 200mm of settlement, in addition to flow sliding and lateral spreading impacting the margins of the reclamation platform. Pilot studies were undertaken to determine the optimum design of sand compaction piles, with the relative effectiveness of each pilot study assessed by pre and post site investigations. Production ground improvement was installed with a target replacement ratio of 8 percent, and a target CPT tip resistance (q_c) of 7.3 MPa for clean sands. Over 7000 sand compaction piles were installed to depths of 15m below ground surface, with a total length of 105,000 linear metres. This paper describes the site conditions, observational and analytical methods of design, acceptance testing requirements and observations made during production ground improvement.

Introduction

This paper presents a case history of the ground improvement works undertaken to mitigate the effects of potential soil liquefaction beneath a 450MW combined cycle power plant near Dhaka, Bangladesh. The site is a two year old reclaimed platform, with the source material being silty micaceous sands dredged from the adjacent Meghna River. Ground beneath critical infrastructure was required to resist liquefaction or severe cyclic degradation, to ensure serviceability requirements of the power plant were met following a M6 earthquake event.

Regional Seismicity

Bangladesh is located in a region of moderate to strong tectonic activity, as the Indian Plate under-thrusts the Asian Plate resulting in upheaval of the Himalayan Mountain Range. Seismic source zones in Bangladesh are located in the northern and eastern portion of the country. The Dauki fault is located about 175km north of the site. A tectonic zone of weakness occurs about 75km north-east of the site, although earthquakes have not been associated with this structural feature. Significant historical earthquakes of Magnitude 6 (Richter) or more have been located more than 100km from the project site.

Between 1833 and 1971 the country experienced over 200 earthquake magnitudes between 5.0-8.5 on the Richter scale (Mollah, 1995). Liquefaction was initiated over wide areas of Bangladesh by many of these earthquakes, with sand vents and fissures observed in numerous locations. Mollah (1995) identifies an event in 1988, where two tremors induced the liquefaction of 4-5ha of Railway Land on the banks of the Meghna River (approximately

100km north of the Meghnaghat site). The magnitude and epicentral distance of the 1988 tremors was unfortunately not detailed in the referenced paper.

Our client specified the seismological parameters listed below as input to the Meghnaghat liquefaction analyses, based on the Bangladesh National Building Code, 1993.

Design Basis Earthquake (Richter Magnitude)	6.0
Peak Horizontal Ground Acceleration (PGA)	0.15g

Geographical Setting

Bangladesh is situated below the south-east foothills of the eastern Himalayas, where a number of major rivers (Ganges/Padma, Jamuna/Bhramaputra, Meghna) drain northern India, Nepal and Bhutan. During the monsoon season (June-October), the majority of Bangladesh is subjected to floods considered extreme by the standards of most other countries (Mollah, 1995). During this period, huge volumes of sediment are eroded from the Himalayas and foothills, before being deposited in the lower energy alluvial environment of the Bangladesh lowlands. As a consequence, much of south-eastern Bangladesh (including the project site) may be regarded as a giant river delta.

Geological Summary

The geology of Bangladesh consists primarily of Pleistocene to Holocene aged deltaic alluvial sediments, of thickness ~ 180m in the north-west and thickening to the south-east where the project site is located (Mollah, 1995). In eastern Bangladesh, the basement rocks are estimated to lie more than 3km below mean sea level (Ali, date unknown). The sediments consist of an alternating sequence of sands and silts, the recent sediments being predominantly flat bedded. Much of the sediments contain abundant quartz grains and a minor to moderate component of mica. The minerals owe their origin to the predominantly schistose and quartzose rocks of the Himalayas. The upper sediments tend to be loose and normally consolidated, and together with the common occurrence of high groundwater level present a potential for liquefaction during earthquake shaking. Large liquefaction events have occurred in the region in the recent past.

Subsurface Conditions

Assessment of the ground conditions was based on a baseline site investigation programme, and existing site information. Existing information from previous site investigations in 1999 included logs of 21 Drillholes, 9 Static Cone Penetration Tests (CPT), and the results of a reasonably comprehensive laboratory testing programme. Baseline site investigations consisted of 33 Piezocone Cone Penetration Tests (CPTU) located on a 30m grid spacing across the site.

The typical soil stratigraphy within the depth and potential influence of piled foundations is presented in Table 1 below. Interpretation of the site investigations suggested consistent layering, with occasional pockets or lenses of looser/denser material in the natural soils beneath the reclamation fill.

Table 1. Summarised Ground Conditions

Geological Unit		USCS Class.	Elevation m ± PWD[3]	Description[1]
Reclamation Fill	RF	SP/SM	+7.8 to +6.5	Medium dense, fine to medium poorly graded sand, minor silt
			+6.5 to +2.0[2]	Becomes very loose to loose
Top Soil/ Alluvium	Qal_1	ML/SM	+2.0 to 0.0	Soft silt, occasional loose silty sand, trace organic material
Alluvium	Qal_2	SM	0.0 to –7.0	Loose to medium dense silty sand
			-7.0 to –20.0	Becomes medium dense
Older Alluvium	$Qalo_1$	SP/SM	-20.0 to –29.0	Medium dense to dense silty sand
	$Qalo_2$	MH	-29.0 to –32.0	Firm to stiff, clayey silt

[1] A characteristic of the site soils is the presence of mica. Previous studies reported mica contents ranging from two to ten percent in the soils at the site.

[2] Layer not continuous across the site.

[3] PWD is Public Works Datum.

Reclamation Fill (Rf)

Reclamation fill comprises the upper soils at the site. The fill consists of silty sand, with sand grain sizes ranging from fine to coarse. It is likely that the source material for this fill was dredging of alluvium (Qal_1 and Qal_2, see below) from the adjacent Meghnaghat River bed. Although the fill soil constituents are fairly homogeneous, there are local variations in relative density, ranging from very loose to medium dense. The fines content was on average 11%.

Quaternary Alluvium Upper Layer (Qal_1)

This layer is interpreted to be the original floodplain/river bed, which is continuous with the upper soil layers outside the reclamation platform. The layer occurs across most of the site, with a thickness ranging between 1m and 2m. The soil is predominantly non-plastic silt, with occasional fine sand or lenses of cleaner sand and lenses of organic materials. Qal_1 is interpreted to be the top layer of a sequence of normally consolidated alluvial sediments, and consequently typical penetration resistances in this layer are much lower than soils above and below. This layer is also interpreted to locally comprise remnant topsoil. The in-situ density correlated from the various penetration tests (SPT and CPT) is mostly loose and occasionally soft where fine-grained materials occur. The fines content was on average 54%.

Quaternary Alluvium Lower Layer (Qal_2)

This layer is variably up to 20m thick, comprising inter-layered non-plastic silt/sand and thicker units of silty sand. The inter-layering within this unit is complex, possibly from the migration of braided river channels. The in-situ density interpreted from the various penetration tests indicates a marked increase in density from loose to medium dense at –7m PWD (varies slightly across the site). This indicates partial pre-consolidation due to erosion of past overburden. The fines content was on average 44%.

Groundwater Conditions

The design ground water level for the assessment of liquefaction was specified by the client as +6.5m PWD. Relatively large (5m) seasonal fluctuations from changes in the river level and flooding can be expected annually.

Potential for Liquefaction

Liquefaction is a phenomenon where saturated granular soils lose their strength as a result of strong ground motion. A rapid increase in groundwater pressures (excess soil pore water pressures) is the mechanism that causes the loss of soil strength. Liquefaction typically occurs in granular soils, such as sands, silty sands and to lesser extent clayey sands that are loose and located below groundwater. Liquefaction usually does not occur at depths greater than 20m due to the effect of overburden pressure. The major factors known to influence the potential for liquefaction comprise the following:

- Soil type: fine to medium sand sized materials are most susceptible.
- Soil gradation: poorly-graded materials are more susceptible.
- Relative density: loose materials are more susceptible.
- Groundwater level and degree of saturation: water level near the surface, 100% saturation.
- Clay content and plasticity: less than 20% clay and low to non-plastic fines.
- Intensity and duration of strong ground shaking.

The influence of soil fabric and structure and in particular the presence of mica on the resistance of liquefaction is not well understood at this time. Mica exists in the soils at the project site. Some workers (Kramer, 1996) report that the occurrence of flaky or platelike particles (such as mica) can create sufficient cohesion to inhibit liquefaction. Recent work in Bangladesh (Hight, 1999) reports that the structure of the mica bearing soils will have significant influence on the behaviour of the soil. Certain structures that develop in the soils due to their depositional environment will be highly prone to collapse (such as liquefaction), whereas other structures are very dilatant and resistant to liquefaction. It should also be noted that the pore pressure generation of fine-grained soils with very low plasticity, such as non-plastic silts, is similar to that for sands (Guo and Prakash, 1999) and should be considered fully susceptible to liquefaction (Ishihara,1993).

The potential for liquefaction was assessed at each drillhole and CPT location within the Main Power Block and Substation and at some of the test locations that were near to this infrastructure. The calculations were performed on all soil layers. The factor of safety against liquefaction (FoS_{liq}) is defined as the ratio of the cyclic stress ratio required to generate liquefaction, CRR, divided by the cyclic stress ratio generated by the design-basis earthquake, CSR, (Seed and Idriss, 1982 and Youd et al., 1997). A potential for liquefaction was assumed where the $FoS_{liq} \leq 1.3$. This safety factor was specified by the client, and is marginally higher than the safety factor 1.25 recommended in Eurocode 8.

The calculations use SPT (N) values and CPT parameters: tip resistance (q_c), local friction (f_s) and pore pressure (u) as input. The primary reason for using CPT-based methods of liquefaction assessment was to consider the continuous and more repeatable soil profile data available from this method of testing. Considering these factors, greater emphasis has been placed on the liquefaction analyses using the CPT data. However, SPT-based methods of liquefaction are still widely considered the standard of practice within the geotechnical community.

The semi-empirical method (by Seed et al., 1985) was used to calculate FoS_{liq} when using SPT N as input. The calculations adopted revisions proposed by the NCEER - National Center for Earthquake Engineering Research (Youd et al., 1997). Analyses using CPT data were also based on the NCEER recommendations.

The results indicate that liquefiable soils consistently range from approximately +4.0m to –7.0m PWD (from 4m to 15m below ground level). For SPT-based methods, the average cumulative thickness of soil with FoS_{liq}<1.3 is 4m, while the average cumulative thickness of soil with FoS_{liq}<1.0 is about 1m. For CPT-based methods, the average cumulative thickness of soil with FoS_{liq}<1.3 is 8m, while the average cumulative thickness of soil with FoS_{liq}<1.0 is 0.2m (3% of FoS_{liq}<1.3). The CPT-based assessment also shows that a FoS_{liq} near unity is commonly calculated from about -1m PWD to –4m PWD.

The differences noted above can be attributed to following factors:

- The discontinuous data obtained using drillholes with SPT sampling versus the continuous data obtained from CPT's.
- The actual fines content measured in the laboratory from SPT samples versus the fines content correlated from CPT tip resistance (q_c) and friction ratio (f_r).

Of particular importance to the interpretation of the potential for liquefaction are the much thinner zones of soils identified in the CPT-based analyses where the FoS_{liq}<1.0. The data illustrates the benefits of such continuous and reliably repeatable in-situ testing where there are inter-layered soils, such as the alluvium at the Meghnaghat site.

Effects of Liquefaction

The detrimental effects of liquefaction relevant to the project include settlement, lateral spreading, and flow sliding. Loss of bearing capacity due to liquefaction was not specifically investigated, as it had already been specified by our client (due to contractual reasons) that ground improvement would be used beneath all important structures and plant, many of which would also be piled. Piles were to be driven precast concrete piles, of dimensions 400mm by 400mm. Installation of these piles also has a significant densifying effect on the soils, which was not taken into account when assessing the liquefaction potential.

Settlement

Liquefaction-induced total settlement was assessed at each drillhole for every soil layer considered susceptible to liquefaction. The Tokimatsu empirical method (Tokimatsu and Seed, 1987) was used to calculate settlement. This method was developed from the observations of settlement that occurred during previous liquefaction events at sites underlain by *clean* sands. The second approach used a less widely known method proposed for silty sands (Soydemir, 1998). Soydemir extended the Tokimatsu method by correcting SPT data for fines content for specific use in liquefaction-induced settlement calculations. An adjustments for fines was made to the Tokimatsu method by reducing the calculated settlement by one-half for every soil layer where the fines content was 15% or more. This approach is based on observations made following the 1989 Loma Prieta Earthquake in San Francisco, California, (O'Rourke et al., 1991), where it was reported that the Tokimatsu method overestimated settlement by nearly 100% for soils with 15% fines content, based on observations. Using these methods, the magnitude of total settlement was estimated to average about 80mm, with an upper bound of 170mm.

Engineering judgement is required to assess the magnitude of localised differential settlement since a reliable and consistent methodology to evaluate differential settlement does not exist at this time. Local differential settlement from liquefaction is often assessed to be approximately two thirds of the estimated total settlement (DMG, 1997).

The presence of a 3-4m thick stiffer crust near the reclamation surface will probably significantly reduce the effects of liquefaction for lightly loaded structures on shallow footings.

Lateral Spreading

Lateral spreading is the deformation that may occur near unconfined free faces during strong ground motion. The potential for lateral spreading is greatest where there is insufficient natural and/or artificial lateral restraint to contain soils subject to liquefaction, such as the formed slopes at the edge of the reclamation platform. Lateral spreading typically manifests at the ground surface as blocks of displaced soil separated by fissures.

The effects of lateral spreading were estimated using the following methods:

- Hamada et al. (1986) (Kramer, 1996):
- Bartlett and Youd (1992) (Kramer, 1996)

Note: Hamada's database contains earthquakes that are much larger than the design basis earthquake for this project.

The following results were obtained using the above methods:

Hamada:	Displacement = 3.2m (assumes M • 7.1 earthquake)
Bartlett & Youd:	Displacement = 1.3m for an earthquake epicentral distance within a 10km radius.

The methods discussed above for estimating permanent displacement from lateral spreading calculate deformations interpreted to be on the order of 1m for the design magnitude earthquake. The accuracy of these methods can be considered to be 0.5m (CDMG, 1997). It should be noted that the deformations are lower when calculated using epicentral distances within the potential seismic source zones (refer to the Seismicity section of this paper). Observations of previous lateral spreading events report that the permanent ground deformations mostly occur within distances of less than 200m from the unconfined free-face (Bartlett and Youd, 1992). This assessment has adopted 100m, considering that the reclamation platform surface is flat with engineered slope faces that are inclined at a relatively shallow angle.

Flow Sliding

The stability of the formed slopes along the southern perimeter (south embankment) of the reclamation platform immediately following a design-basis earthquake has been evaluated using the residual strength that may remain in the liquefiable soil layers. The slope analysed is approximately 10m high and formed at an angle of 18°. Table 2 presents the results of the slope stability analyses. A factor of safety greater than 1.1~1.2 is generally considered to be acceptable for flow slide failures.

Table 2. Flow Slide Slope Stability Analyses

Condition	Water Level	Factor of Safety
Post-Earthquake Flow Slides	+3.0m PWD	1.1 (Bishop) Sr = 10kPa 0.8 (Bishop) Sr = 5kPa 1.1 (Morgenstern-Price), Sr = 10kPa

The conventional method of limit-equilibrium analysis has been carried out to evaluate the factor of safety against deep-seated rotational and/or translational slope failure.

The following assumptions were used in the analyses:

1. An undrained residual strength (Sr) was used where there were soil layers with a $FoS_{liq}<1.3$. The undrained residual strength was estimated to be 8kPa. The correlation developed by Seed and Harder (1990, as referred to in Kramer, 1996) using Standard

Penetration Tests $(N_1)_{60}$ corrected for fines content $(N_1)_{60cs}$ was used to estimate residual strength. The calculations assumed 5kPa and 10kPa.

2. Soil layers not susceptible to liquefaction or with a $FoS_{liq}>1.3$ were assumed to be resistant to the generation of cyclic (excess) pore pressures and a consequent reduction in shear strength. Constant volume shear strengths (ϕ_{cv}') were adopted considering that some deformation would develop in the non-liquefiable layers during strong ground motions.

The potential for very large displacements from flow sliding is considered to be moderate to high since the factor of safety against this mode of slope instability is less than 1.1~1.2, using the mean residual shear strength for soils that could liquefy. The effect of the mica is likely to exacerbate the potential and effect of flow sliding.

Ground Improvement

To mitigate the effects of liquefaction beneath and surrounding sensitive structures and plant, it was decided to undertake a programme of ground improvement. The chosen method of ground improvement was Sand Compaction Piles (SCP), following a review of the literature, available contractors, and client experience. SCP is a widely used method in south-east Asia, but is uncommon in Europe, USA, and Australasia where stone columns or vibroflotation are usually used.

The SCP installation involved sinking a 400mm diameter casing, with a hinged reinforced shoe at the tip to assist soil displacement. Compressed air jetting was used to aid penetration. After vibrating the casing to the target depth (in this case 15m below ground level), the casing was filled with clean coarse sand and slowly extracted. During extraction, the casing vibrates and compresses the introduced sand into the surrounding ground creating a column of sand. Completed sand columns are approximately 700mm diameter. The plant used for SCP installation is shown in Figure 1.

Sand Compaction Piles are installed to increase the relative density of sandy soils, which decreases the potential for liquefaction. SCP places and compacts sand into the ground by vibration. The initial installation of the sand column and subsequent placement and compaction of additional sand in the column by vibration decreases the Void Ratio (e) of the surrounding in-situ soils. The decrease in Void Ratio increases the Relative Density and the resistance of the in-situ soils to liquefaction.

Due to the silty nature of the sand at the site, it is expected that there is a significant time-aging effect. Installation of the SCP's will generate excess pore water pressures, which may take some time to dissipate. Thus soils will not reach maximum density until some time after installation.

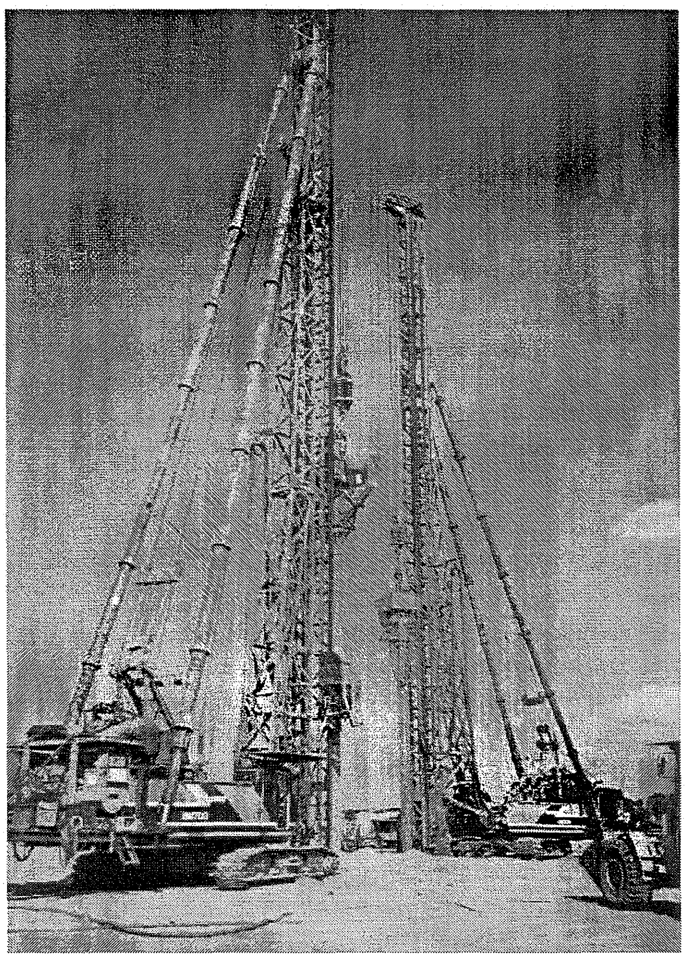

Figure 1. Sand Compaction Piling Rigs

Pilot Studies

Due to the magnitude of the project, and the uncertainty of the effect of the mica constituent on liquefaction, it was decided that the best design approach was to implement a series of pilot studies. The liquefaction potential was evaluated by CPTU and SPT before and after ground improvement for a variety of trial spacings on both triangular and square arrangements.

Initial design of pilot study SCP spacing was estimated using simple soil mechanics density-volume (phase) relationships provided by the Japanese Port and Harbour Research Institute (PHRI, 1997) with estimated in-situ and target Void Ratios.

The first two pilot studies were constructed at 1.5m and 2m spacings on a triangular arrangement, with replacement ratios of 20% and 11% respectively. It was observed during verification CPTU testing that a far greater level of densification had occurred than was expected. Virtually all CPTU's had difficulty in penetrating the upper soils, and were terminated early. Attempts at pre-boring to different depths for the CPTU tests also resulted in early refusal.

Two additional pilot studies with trial spacings of 2.5m and 3m on a square arrangement were installed, with replacement ratios of 6% and 3% respectively. CPTU penetration was slightly easier in these wider spaced pilot studies.

Ground Improvement Design

Upon reviewing the verification testing of the four pilot studies, it was decided to implement a production SCP design spacing of 2.2m on a square arrangement corresponding to a replacement ratio of 8%. It was interpolated from liquefaction analyses on the pilot study verification tests that this spacing would correspond best to the required FoS_{liq}• 1.3. The level of improvement corresponds to a target CPT tip resistance $(q_{T1N})_{cs}$ of 7.3 Mpa. $(q_{T1N})_{cs}$ is the CPT tip resistance value corrected for pore pressure, overburden stress and fines to an equivalent clean sand value (Youd et al., 1997).

The lateral extent of ground improvement outside the footprints of the various infrastructure was assessed using methods outlined in the Japanese Port and Harbour Research Institute (PHRI, 1997). Depending on the type and location of structure, the horizontal width ranged up to 11m outside the structure footprint. These widths were designed to ensure a buffer zone with sufficient lateral support, assuming ground outside the improved areas has liquefied. All ground beneath critical infrastructure footprints was improved. Sheet piled walls and anchors were also improved, to ensure continuing function during and after strong ground motions. Improvement was undertaken along the margins of the reclamation platform, where there was interpreted to be a hazard from lateral spreading or flow sliding. The requirement for improvement to mitigate the hazard from lateral spreading was relaxed in an area where a sheet piled jetty (see Figure 2) had been formed, with well compacted backfill and deadman anchors restraining the facing sheet piles with tierods.

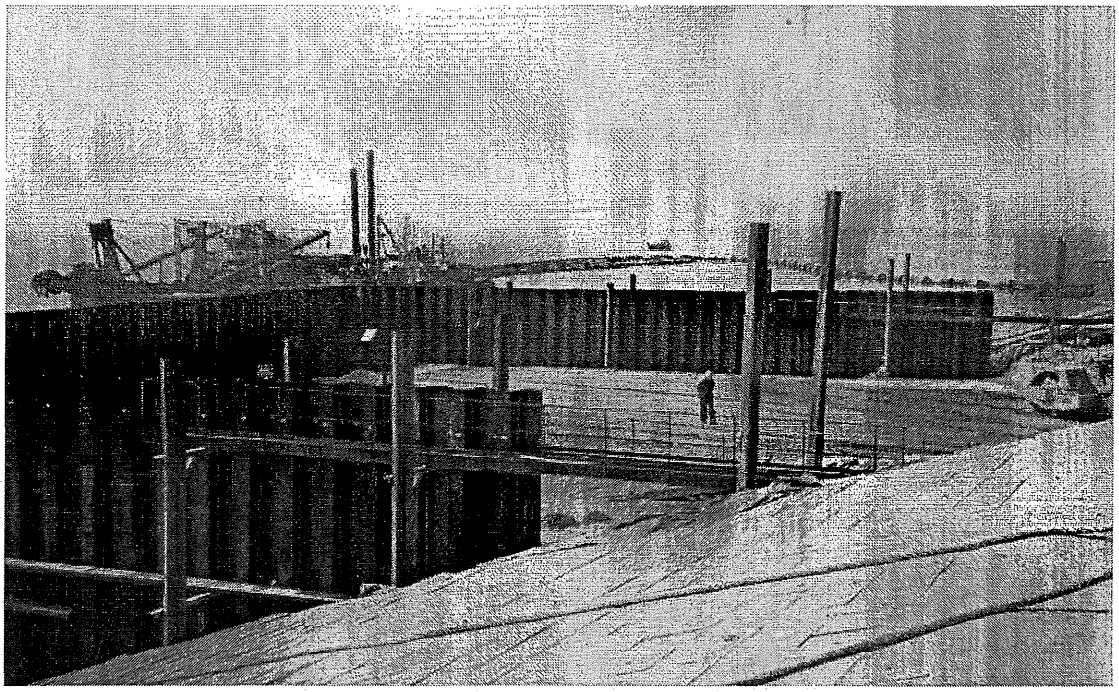

Figure 2. Unrestrained armoured slope face and sheet-piled jetty.

Production Ground Improvement

In total, over 7000 sand compaction piles were installed to depths of 15m below ground surface, with a total length of nearly 105,000 linear metres. Installation took three and a half months using two rigs, with each rig installing up to 80 SCP's per day.

It was observed during excavation that the exterior of each sand compaction pile was surrounded by a halo up to 100mm thick of 'baked' soil with a highly disturbed fabric (see Figures 3 and 4). The 'baked' soil is likely to have formed by interaction between heat (from soil/casing friction during installation) and moisture. It is likely that this halo has a decreased permeability relative to the horizontal permeability of the surrounding soil, and drainage is likely to be retarded. It is therefore suggested that it may be inappropriate to include drainage of excess porewater pressure via the sand pile as a component of liquefaction mitigation, when considering air jetted columns in silty sands.

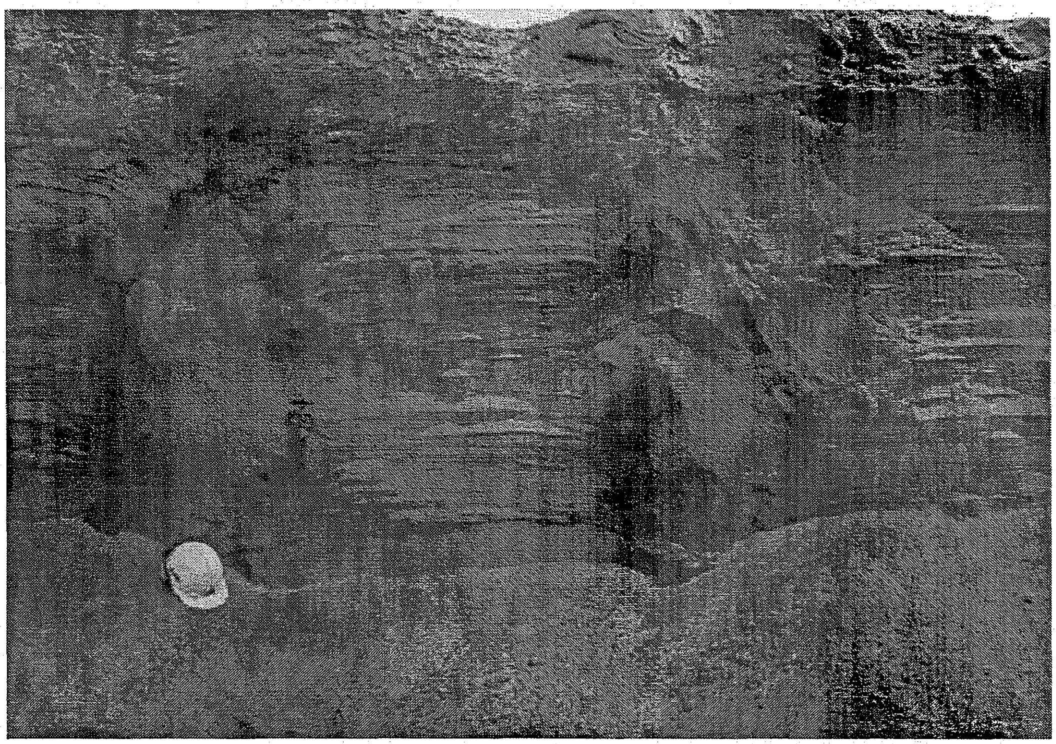

Figure 3. Exposed Sand Compaction Piles

Figure 4. Close-up of exposed Sand Compaction Pile (on right side of photograph)

The CPTU investigations had indicated a layer between 0.5m to 1.0m thick of harder or denser material at a depth of about 3m, prevalent across the site. As this layer was within the reclamation soils, it is assumed that this may be attributed to desiccation or some form of compaction (or a combination of these) during reclamation construction. This layer presented some difficulties to penetration of the SCP casing, and in some areas it was necessary to remove this layer of material by excavation. By chance, the area of the site where this problem layer was thickest was adjacent to a large excavation for the cooling water intake structure, and it was relatively easy to extend the excavations to facilitate removal.

In several locations, the sequence of SCP installation resulted in premature tightening of the ground.

Ground Improvement Verification

Verification testing during production ground improvement consisted of over 35 CPTU tests undertaken on a 30m grid spacing, positioned as close as possible to the baseline test positions. CPTU's were conservatively undertaken mid way between SCP's, to assess conditions in the zone of least compactive influence. Four drillholes with SPT's were undertaken during the verification testing to provide an additional assessment of soil conditions, with two drillholes located in the centre of SCP's to assess the quality of the replaced ground. SPT 'N' values within the sand columns were typically over 30.

Acceptance testing indicated that approximately 80% of the production ground improvement had achieved or exceeded the required factor of safety against liquefaction. The non-compliance of the remaining ground can be attributed to either: poor installation by contractor, locally variable ground conditions, or insufficient delay between installation and testing. The consequences of non-compliant ground are generally small, as these were isolated locations with no potential for lateral spreading or flow sliding. Most of the structures with a remaining (but greatly reduced) potential for settlement are piled structures, end bearing below the base level of liquefaction.

Residual Risk of Liquefaction

A probablistic assessment of the risk of liquefaction before and after ground improvement is undertaken using the procedure outline by Juang (Juang et al., 2000). This procedure is based upon artificial neural network training on a database comprising 243 liquefaction performance cases. The result is the construction of a liquefaction limit state function, defining the liquefaction/no liquefaction boundary. The inherent conservatism built into the Seed et al. (1985) method (and in the 1997 NCEER version) can be removed, and the factor of safety calculated using a particular method can be related to the probability of liquefaction occurring for a given design earthquake event. The probability is a more meaningful measure for use with risk assessment than factor of safety.

The factor of safety against liquefaction (F_S) is related to the probability of liquefaction (P_L) by the expression:

$$P_L = \frac{1}{1+\left(\frac{F_S}{A}\right)^B}$$

The coefficients A and B are given as 0.80 and 3.5 respectively for the Seed et al. (1985) method, as presented in the 1997 NCEER version. The average F_S before improvement is approximately $F_S = 1$, and $F_S = 1.3$ after improvement. Therefore:

- Prior to improvement, $P_L = 0.31$
- After improvement, $P_L = 0.16$

Thus the probability of liquefaction occurring during the design earthquake has been halved by the ground improvement. In specific locations where ground improvement did not achieve design targets, the probability of liquefaction will lie between these values. For most test locations where $F_S > 1.3$, the probability of liquefaction will be less than 0.16.

Conclusions

The potential for liquefaction has been assessed for the site using the method of Seed et al. (1985) method, as updated in the 1997 NCEER version. This has been undertaken for both Standard Penetration Tests (CPTU), and Piezocone Penetration Tests (CPTU). The CPTU is considered to be more repeatable and reliable than SPT, for the layered fine sands and silts at the project site.

Various commonly accepted methods were used to assess the effects of liquefaction. Of great use to the practicing engineer would be the development of a model for predicting liquefaction-induced settlement based directly on CPT tests, without correlation to SPT.

Sand compaction piling as a method is probably at the limit of its' range of effectiveness in the soils at Meghnaghat. The reclamation soils showed consistent high levels of improvement, while improvement by densification of the underlying layers was possibly retarded by the higher fines contents. The effect of mica on the liquefaction potential was not resolved by the work at Meghnaghat, but this can probably only be quantitatively assessed by comprehensive cyclic triaxial and centrifuge testing on a range of reconstituted samples. Despite the variable fines content and mica constituent the soils proved to be densifiable, as evidenced by extensive in-situ testing.

The method was largely effective in achieving the design targets, but in several localised areas was found to be deficient. This is attributed to installation scheduling problems, equipment incapacity to penetrate a hard layer, variation in soil conditions (eg. locally high fines content), and lack of time between installation and verification testing.

It is our opinion that drainage (as a means of reducing excess pore water pressures) should not be relied upon as contributing to the effect of improvement. This applies to air jetted sand compaction piles in soils with over 20% fines and 10% mica.

Ground improvement has been used to reduce the potential for liquefaction to an acceptable level of risk, with a probability of liquefaction occurring during the design earthquake generally less than $P_L = 0.16$.

Acknowledgements

The work outlined in this paper was undertaken by Sinclair Knight Merz Limited (SKM) for Hyundai Engineering and Construction Company limited. The input of all the engineers and staff at both firms who contributed to this work is gratefully acknowledged. The second author of this paper was the design and project manager for this work, while at SKM. The ground improvement works were completed by EunSung Construction Co. Ltd. of Korea, and the Piezocone Cone Penetration Testing was undertaken by Han Mac Geotechnical Institute, also of Korea. Thanks to Tony O'Brien for comments received on this paper.

References

Ali, H., (date unknown – post 1995), Earthquake Hazard and Seismic Zoning of Bangladesh, *publication unknown.*

Bartlett, S.F. and Youd, T.L. (1992). "Empirical Analysis of Horizontal Ground Displacement Generated by Liquefaction-induced Lateral Spreads", *Technical Report NCEER-92-0021, Multidisciplinary Center for Earthquake Engineering Research.*

Division of Mines and Geology, (1997). *Special Publication 117, Guidelines for Evaluating and Mitigating Seismic Hazards in California*, California Department of Conservation, DMG website.

Eurocode 8 (1994). *Design provisions for earthquake resistance of structures,* European Committee for Standardization.

Guo, T. and Prakash, S. (1999). "Liquefaction of Silts and Silt-Clay Mixtures", *Journal of Geotechnical Engineering*, ASCE, New York, Vol. 125, No. 8, p. 707-710.

Hight, D.W. (2000). *Anisotropy in Soils – Its Measurement and Practical Implications*, 2nd Annual GRC Lecture, New Zealand Geotechnical Society.

Juang, C.H., Chen, C.J., Jiang, T., Andrus, R.D. (2000). "Risk-based liquefaction potential evaluation using standard penetration tests", *Canadian Geotechnical Journal, Vol. 37*, December 2000, p. 1195-1208.

Kramer, S.L. (1996). *Geotechnical Earthquake Engineering*, Prentice-Hall International Series in Civil Engineering and Engineering Mechanics, 653p.

Mollah, M.A. (1995). "Liquefaction of the Alluvial Soils of Bangladesh (Paper No. 3.38)", *Proceedings: Third International Conference on Recent Advances in Geotechnical Earthquake Engineering and Soil Dynamics*, April 2-7, 1995, Volume 1, St. Louis, Missouri.

O'Rourke et al. (1991). "Lifeline Performance and Ground Deformation in the Marine during the 1989 Loma Prieta Earthquake", *Proceedings, Third Japan - US Workshop on Earthquake Resistant Design of Lifeline Facilities and Countermeasures for Soil Liquefaction*, Technical Report NCEER-91-0001, pp 129-146.

O'Rourke, M.J. and Liu, X. (1999). "Response of Buried Pipelines to Earthquake Effects", *Monograph No. 3*, Multi-disciplinary Center for Earthquake Engineering Research, 249p.

PHRI. (1997). "Handbook on Liquefaction Remediation of Reclaimed Land", Port and Harbour Research Institute, Balkema, Rotterdam, 312 p.

Seed, H.B. and Idriss, I.M. (1982). "Ground Motions and Soil Liquefaction During Earthquakes", *Earthquake Engineering Research Institute, Monograph*, 134p.

Seed, H.B., Tokimatsu, K., Harder, L.F., and Chung, R.M. (1985). "Influence of SPT Procedures in Soil Liquefaction Resistance Evaluations", *Journal of Geotechnical Engineering*, ASCE, New York, Vol. 111, No. 12, pp. 1425-1445.

Soydemir, C. (1994). "Earthquake Induced Settlements in Silty Sands for New England Seismicity", *Ground Failures under Seismic Conditions: Proceedings*, New York: ASCE, 1994, p. 77-91.

Tokimatsu, K. and Seed, H.B. (1987). "Evaluation of Settlements in Sands due to Earthquake Shaking", *Journal of Geotechnical Engineering*, ASCE, New York, Vol. 113, No. 8, p. 861-878.

Youd, T.L. and Idriss, I.M. (1997). *Proceedings of the NCEER Workshop on Evaluation of Liquefaction Resistance of Soils*, Technical Report NCEER-97-0022, National Centre for Earthquake Engineering Research.

Development on an Actively Gassing Landfill Site

W. Starke

Geo-Environmental Engineer, Sinclair Knight Merz Limited

Abstract

Since 1995 Sinclair Knight Merz have been involved in the investigations and planning for the development of a residential retirement village on a 9 ha site of an old abandoned landfill in central Auckland, New Zealand. Early geotechnical investigations showed that the site contained enough organic material to consider landfill gas as a significant hazard that required further investigation prior to submitting a resource consent for re-development.

Subsequent detailed landfill gas investigations indicated high methane concentrations, but emission flow rates were very low. As the risk of landfill gas to development is defined as the combination of concentration and flow rate (as opposed to concentration alone), it is shown that the site can be safely developed with appropriate landfill gas protection and mitigation measures.

1. Introduction

Development on, or near, a landfill site has always been a contentious issue, both from a geotechnical and geo-environmental perspective. Important questions for the developer to answer in order to obtain consents are:

a) Can it be done in a safe manner?

b) What are the hazards?

c) How do we quantify these hazards and minimise the risk to future occupants of the site

Some of the principle hazards are ground settlement, soil and groundwater contamination, and landfill gas (LFG) emissions. The latter is the focus of this paper.

Throughout the period 1995 to 2001 Sinclair Knight Merz, formerly known as Kingston Morrison Limited, has been involved in the LFG investigations at the site.

This paper describes:

- LFG Hazards (section 2)
- The Site and Site History (section 3)
- Ground Conditions (section 4)
- Proposed Development (section 5)
- LFG Concentration and Flow Rate Testing (section 6)
- LFG Generation Model (section 7)
- Comparison of LFG Generation Model and Field Tests (section 8)
- Guidelines: LFG Building Protection Measures (section 9)
- Conclusions (section 10)

2. LFG Hazard

LFG is a mixture of gasses that vary from landfill to landfill, but commonly contains approximately equal amounts of methane and carbon dioxide by volume. Other gasses found as trace constituents in LFG are hydrogen sulphide (H_2S) and Volatile Organic Compounds (VOCs). This paper addresses the major constituents of LFG, CH_4 and CO_2, but it is noted that H_2S and VOCs were also investigated as part of the resource consent application.

3. The Site and Site History (KML, 1995)

The 9 ha site is currently a nine hole golf course and driving range located between high value residential development to the east, an 18 hole golf course to the north and long established industrial land to the east and south of the site.

The site was operated as a basalt quarry from the 1920s to 1965, initially by J.J. Craig and later by Winstone Aggregates Ltd (Winstone). A 1964 site plan from Winstone shows that the main quarry pit was located in the central part of the site and comprised an area of approximately 3 ha and depth of around 20m. Ground levels outside the quarry pit had also been lowered to a degree.

In 1965 Winstone was granted a permit by then Mount Wellington Borough Council to fill the old quarry pit with inorganic materials. The filling operations commenced around 1965 and were completed in 1975. Exact records of the type of fill material were not kept. No liner was placed on the quarry floor prior to filling operations and clay or hardfill were used as a daily cover over the waste materials.

Minor amounts of clean filling occurred in the period 1975 to 1992, as indicated by various site plans. After filling ceased a final cover was placed over the landfill. The final cover comprised clay and reject material (hard waste) from the council compost plant.

In 1992 the site was contoured for the nine-hole golf course, driving range and club house facilities. Clean fill was imported from nearby excavations and included small amounts of demolition rubble. The clubhouse, workshop and other site buildings are constructed with a ground bearing concrete slab with no LFG protection measures. No LFG problems were experienced during this period.

4. Ground Conditions

Seven separate ground investigations were carried out in the period 1985-2000 as indicated in Table 1.

Table 1. Ground Conditions

Year	*No. Of Bhs*	*Depth Range (m)*	*Geotech Vs LFG*	*Location of boreholes*	*Consultant, borehole locations, see site plan*
1985	17	1.8-17	Geotech	All outside former quarry pit except two, to natural ground	(TSE, 1985)
1990	1	47	Geotech	Inside former pit, through basalt to Waitematas	(PDP, 1990)
1995	10	5-22	Geotech	Inside & outside former pit, to basalt and Waitematas	(KML, 1995)
1995-1996	20	3-7	LFG (temp wells)	Outside former pit, to basalt and Waitematas, ALSO, 3 test pits to 4-5m depth and a spiking survey	(KML, 1996)
1998	5	6-22	Geotech	Inside & outside former pit, to basalt and Waitematas	(KML, 1998)
1999	5	9-12	LFG (perm wells)	Inside former pit, to Basalt, wells located immediately inside former quarry pit	(SWE/SKM, 2000)
2000	4	6-11	LFG (perm wells)	Outside former pit, to basalt and Waitematas, wells located around site perimeter	(SWE/SKM, 2000)
	TOTAL: 62 boreholes and 3 test pits				

The organic component of the investigated ground has been estimated at around 15%, as opposed to <5% that would normally be expected for an inert fill site. An organic fill content of 15% is sufficiently high to generate some LFG. For comparison it is noted that municipal solid waste landfills typically contain up to 60% organic matter.

The fieldwork also showed that organic fill material extended north and west of the former quarry pit, suggesting that the volume of fill material was greater than the originally estimated 600,000 m^3. This is an important factor in estimating the site's LFG generation potential/model.

The ground conditions underlying the fill material site are basalt except for the central-western part of the site where weathered Waitemata Group silty clays were encountered. The near surface ground conditions generally comprised a firm to stiff scoria-gravelly clay with occasional fragments of concrete and plastic.

The near surface soils cannot be regarded as an impermeable barrier that would prevent escape of LFG to the atmosphere. Further, anecdotal information suggests that the site's capping layer is semi-permeable is found during heavy rain. Surface water soaks into the ground relatively easily and the golf course is nearly always the last to close in the Auckland region.

The groundwater table is located on average approximately 7m below ground level and does not vary with time. The majority of the fill is therefore below the water table. This is important in interpreting the field LFG concentrations measurements and selecting the appropriate LFG generation model parameters.

5. Proposed Development (SWE & SKM, 2000)

The proposed development can be summarised as a comprehensive retirement village comprising single storey villas, 5 storey apartments, a hospital facility and recreational areas.

The development layout plans were designed so that the larger structures and recreational areas are positioned over the old quarry pit and the villas outside the former pit. The reason for this is that fewer and larger diameter piled foundations are generally economical for large structures and that recreational areas are less sensitive to future settlement than the single storey villas.

The development concept also incorporated minimal excavation work at the site, thus reducing the risk of exposing buried waste materials.

6. LFG Concentration and Flow Rate Testing

The 1995-1996 investigation comprised:

a) A ground surface spiking survey at 35 locations.

b) Installing ten 'shallow' wells (<1.5m depth,) at those locations where the spiking survey recorded elevated methane concentrations.

c) Installing ten 'deep' wells (4-10m depth, nos. K-T, see site plan) where the shallow wells recorded elevated methane concentrations

d) Excavating three large test pits (nos. 1, 2, 4) were excavated to 4-5m depth to make a visual assessment of the organic content of the near surface material.

The 1995-1996 'deep' wells investigation recorded methane concentrations up to 92%. Although several measurement were carried out over a period of four months the test result were interpreted with some degree of caution. The reasons for this were that:

a) methane concentrations measured at different test dates sometimes varied significantly at one sample location, and

b) occasionally the sum of all the gasses measured, methane, carbon-dioxide and oxygen, exceeded 100-105%.

The 92% methane reading is significantly higher than that normally produced in a municipal solid waste (MSW) landfill (around 55%). However, as a significant portion of the fill material is located below the groundwater table, the elevated methane concentration is considered to be a consequence of the dissolution of carbon-dioxide in water.

Flow rate testing was carried out on both the 'shallow' and 'deep' wells using a hot-wire anemometer. The accuracy of the instrument and it's inability to measure lower flow rates was identified as a significant limitation in this investigation. All test results recorded borehole/well flow velocities less than 0.25 m/s or around 700 L/hr (for a 32mm diameter well). These are very low flow rates when compared to that reported in actively gassing MSW landfills where flows of 2000-3000 L/hr are common (CIRIA, 1995a).

The 1999 investigation consisted of installing five wells G1-G5 (see site plan) around the perimeter and immediately inside the former quarry pit. The well locations were strategically selected to deliberately target the locations where the maximum LFG emissions were expected. LFG migration pathways inside the former quarry pit are expected to be more horizontal than vertical due to the daily cover placed each day. Therefore LFG is expected to preferentially migrate in a horizontal direction until the quarry walls where the preferential migration path would be vertical because of the relatively low permeability of the adjacent country rock.

The 2000 investigation comprised the installation of an additional four wells (G6-G9) around the perimeter of the site to investigate the potential for LFG migration off-site.

The range of methane concentrations and carbon-dioxide concentrations are shown in Table 2. The G1-G5 methane test results confirmed the elevated concentrations recorded in the 1995-1996 investigation.

Flow rate testing was carried out using a GF-60D. This precision mass flow transducer is specifically designed to detect the low flow of gas into or out of ground boreholes. It is pre-programmed to calculate standard volumetric flow rates and total standard volumes for any given mixture of methane, carbon dioxide and air. Total and methane borehole gas flow rates are presented in Table 2. For comparison the total gas flow rate of an actively gassing landfill has been included.

Table 2. Methane and Carbon Dioxide Concentrations, Flow Rate Test Results

Well No.	*Min CH_4 (%)*	*Max CH_4 (%)*	*Min CO_2 (%)*	*Max CO_2 (%)*	*Min CH_4 (L/hr)*	*Max CH_4 (L/hr)*	*Min Total LFG (L/hr)*	*Max Total LFG (L/hr)*
G1	53	86	10	18	1.5	14	2.5	18
G2	55	74	12	33	2.5	10	3	13
G3	0	39	12	2	0	1.5	0	4.5
G4	65	82	15	19	4	14	6	18
G5	70	79	21	28	3	17	4	21
G6	0	0.3	6	10.1	0	0	0	+8 / -0.25
G7	0	1.3	0	7.6	0	0	0	+7 / -2
G8	0	0.1	0	4.8	0	0	0	+7 / -3
G9	0	0.1	0	0.9	0	0	0	+4 / -8
Municipal Solid Waste actively gassing landfill, typical upper maximum (CIRIA, 1995a)								2000-3000

Note: +8 / -0.25 indicates a +8 L/hr flow from the borehole and -0.25 L/hr flow into the borehole at the same time of measurement (within a 5 minute test period).

7. LFG Generation Model (United States Environmental Protection Agency, 1995)

LFG generation modelling has been conducted for two principal reasons:

- check the model output with actual field measurements, and

- demonstrate that LFG generation is decreasing with time.

It is commonly assumed that the LFG generated in a landfill can be calculated using a first order decay equation such as that used by presented in the USEPA Landfill Gas Emissions Estimation Model:

$$Q=Lo \cdot R \cdot (e^{-kc} - e^{-kt}) \tag{1}$$

where:

Q= methane generated in current year (m^3/yr),

Lo= methane generation potential (m^3/Mg of refuse),

R= average annual waste acceptance rate (Mg/yr),

k= methane generation rate constant (L/yr),

c= time since/to landfill closure (yr), and

t= time since landfill opened (yr).

Three simulations of the model were performed using the following values:

a) USEPA Clean Air Act defaults values (Lo=170, k=0.05),

b) USEPA AP-42 values (Lo=100, k=0.04), and

c) New Zealand k-value of 0.15 because of the generally saturated nature of the fill material, and selecting a conservative value of Lo=170.

The LFG generation model output from the three simulations is presented in the attached graph. The model assumes that methane is 50% of the total LFG production, therefore the results must be doubled to estimate the total LFG production.

For each model the LFG generation is a maximum in 1975 when the filling operations stopped and an exponential decline from 1975 onwards. In the year 2001 the estimated LFG production ranges from 10 to 50 m^3/hr. This range can be compared to the actual field test results.

8. Comparison of LFG Generation Model and Field Tests

Reasonably good agreement can be obtained between the LFG generation model and the actual field test results. To achieve this we have to consider ground surface LFG emission rates (L/hr/m^2).

The LFG generation model predicted flow rates of 10-50 m^3/hr for the whole site. It is assumed that the total LFG is emitted over a 5 ha area. This is based on the 3 ha quarry pit area and an additional 2 ha buffer zone surrounding the former pit as indicated by the organic content in the boreholes outside the former pit. Therefore the total LFG ground surface emission rate ranges from 0.17-1.0 L/hr/m^2.

The actual field test results show that the maximum total LFG borehole flow rate ranges from 4.5-21 L/hr, with an average of 14.7 L/hr. The cylindrical zone of influence from a 50mm diameter well has conservatively been assumed to be 1.78m, providing a ground surface area of 10m^2 (Pecksen, 1985). Therefore the total LFG ground surface mission rate is calculated as 1.5 L/hr/m^2.

9. Guidelines: LFG Building Protection Measures

Guidance on LFG building protection and mitigation measures are provided in CIRIA report 149 (CIRIA, 1995b) and by Wilson and Card, 1999, Tables 5 and 6. Both guidelines require classification of the site as a Characteristic Situation and provide guidance on gas protection measures.

Table 3 shows that Wilson & Card would classify the site under investigation as Characteristic Situation 4 if we ignore the maximum methane flow rate at well G4 of 17 L/hr for the following reasons:

a) the average maximum methane flow rate at well G5 was 10 L/hr,
b) a total of 17 methane flow rate tests were carried out, and
c) only 1 out of 17 tests recorded a flow rate >15L/hr.

Table 3. Comparison of Characteristic Situation: CIRIA Report 149 vs Wilson & Card

Report 149 (CIRIA, 1995b)			***(Wilson & Card, 1999)***	***Characteristic Situation*** *(both CIRIA and Wilson & Card)*
CH_4 (%)	*CO_2 (%)*	*Total LFG Emission Rate (m/s)*	*Limiting Borehole Gas flow of CH_4 And CO_2 (L/hr)*	
>5 – 20	<20	<0.01	<15	4
>20	>20	>0.01 – 0.05	<70	5

CIRIA report 149 would classify the site as Characteristic Situation 5 since the footnote of Table 28 in CIRIA states that the "highest measured parameter should be used as the determining factor" and this is the methane concentration of >20%. Since Table 2 shows that the maximum total LFG flow rate is 21 L/hr and the fact that the high methane concentrations are elevated due to the solution of carbon dioxide in the groundwater, it is considered more appropriate that the CIRIA report 149 Characteristic Situation 4 is selected.

For residential development a comparison of the typical scope of LFG protection measures as recommended by CIRIA report 149 and Wilson & Card has been provided in Table 4. CIRIA report 149 provides gas control systems for both new development and existing development and both have been included in Table 4.

It is interesting to note the difference in recommended LFG protection measures for new and existing development. Active in-ground venting is not recommended by Wilson & Card and it is therefore considered it is not an essential required for Characteristic Situation 4.

Table 4. Comparison of LFG Protection Measures: CIRIA Report 149 vs. Wilson & Card

Characteristic Situation	***Report 149 (CIRIA, 1995b)***		***(Wilson & Card, 1999)***
	New Development	*Existing Development*	
4	a, b, c, d, f, g, & possibly k	a, k, e, f & possibly i	b, c, d, e, f, i & possibly g

Notes:
a= ventilation of confined spaces within building,
b= well-constructed ground slab,
c= low-permeability gas membrane,
d= minimum penetration of ground slab by services,
e= in-ground barrier,
f= passive in-ground venting,
g= active in-ground venting,
i= passive venting to building, granular filled void, and
k= gas monitoring of installed measures with alarms

10. Conclusion

The case study described in this paper has shown that an old abandoned landfill can be safely redeveloped for residential use. Measured landfill gas flow rates from boreholes were low, around 10 L/hr, though methane concentrations of over 90% were tested. Both the flow rate and concentration were required to characterise the site and design suitable foundation gas protection measures.

Further confidence in the safe redevelopment of the site was gained when the modelled landfill gas ground surface emission rate was in good agreement with that calculated from borehole flow rate tests.

The resource consent submitted for the redevelopment of the site used a conservative approach with respect to building foundation landfill gas protection and mitigation measures which can be summarised as follows:

- Concrete slab on grade construction with minimal penetration of the ground slab by services.
- Incorporate a low permeable membrane in the ground slab.
- Providing a 200mm thick layer of no-fines aggregate below the ground slab with 100mm diameter perforated uPVC terminated above the roof line of the building.
- Methane alarm detection units in the majority of the buildings on the site.
- Use piled foundations to natural ground except where the thickness of fill material is relatively thin (<3m) and it becomes more cost-effective to excavate and replace the existing fill.
- Install an active venting system comprising extraction wells located throughout the former quarry pit and surrounding area.
- Install additional perimeter wells for monitoring immediately prior, during and post site development.
- Implement a comprehensive LFG long term monitoring programme in all buildings and underground services.
- Ensure that the site will be managed by a corporate structure controlling all future operations or modifications on the site to minimise the risk of causing harm to the integrity of the LFG protection systems.

Acknowledgments

The authors wish to thank Ryman Healthcare Limited for their permission to publish this paper. We also acknowledge and appreciate the help received from SCS Wetherill Environmental during the investigations.

References

CIRIA, 1995a, Report 149, G.B. Card, *Protecting Development from Methane*, Construction Industry Research and Information Association.

CIRIA, 1995b, Report 151, C.R. Harries, P.J. Witherington, J.M. McEntee, *Interpreting Measurements of Gas from the Ground.*

Kingston Morrison Limited (now SKM), August 1995, *Geotechnical Investigation, Abbotts Way Village, for Abbotts Way Holdings Ltd*, ref. no. P1707.02.

Kingston Morrison Ltd (now SKM), April 1996, *Landfill Gas Survey, Abbotts Way Village, for Abbotts Way Holdings Ltd*, ref. no. P1707.12.

Kingston Morrison Ltd (now SKM), December 1998, *Geotechnical and Geo-Environmental Work, Abbotts Way Development, for Abbotts Way Holdings* Ltd, revision A, ref. no. P1707.13.

Pattle Delamore Partners Ltd, May 1990, *Investigation of Leachate Contamination at Craig's Quarry Landfill, Mount Wellington*, report A131/2.

Pecksen, G.N. 1985, *Methane and the Development of Derelict Land*, London Environmental Supplement No. 13, Summer 1985.

TSE Group Ltd, September 1985, *Craig's Quarry, for Winstone Property Management Services*, ref. no. 4077/12/100.

SCS Wetherill Environmental in association with Sinclair Knight Merz, April 2000, *Landfill Gas Management Plan, for Ryman Abbotts Way Limited*, file no. 14199016.01.

United States Environmental Protection Agency, February 1998, *User's Manual, Landfill Gas Emissions Model*, Version 2.0.

Wilson and Card, February 1999, *Reliability and Risk in Gas Protection Design*, Ground Engineering, The Magazine of the British Geotechnical Society.

LANDFILL GAS FLOW TESTING: 11 NOVEMBER 1999
Client: Ryman Abbotts Way Limited

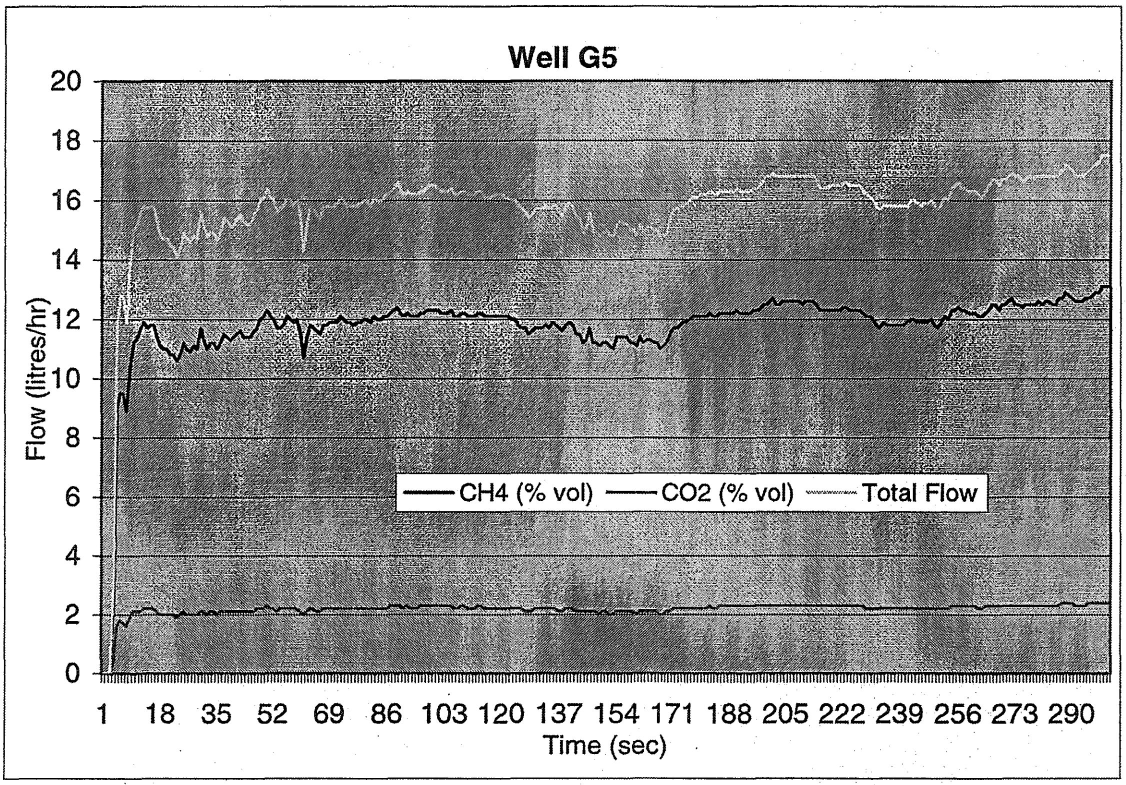

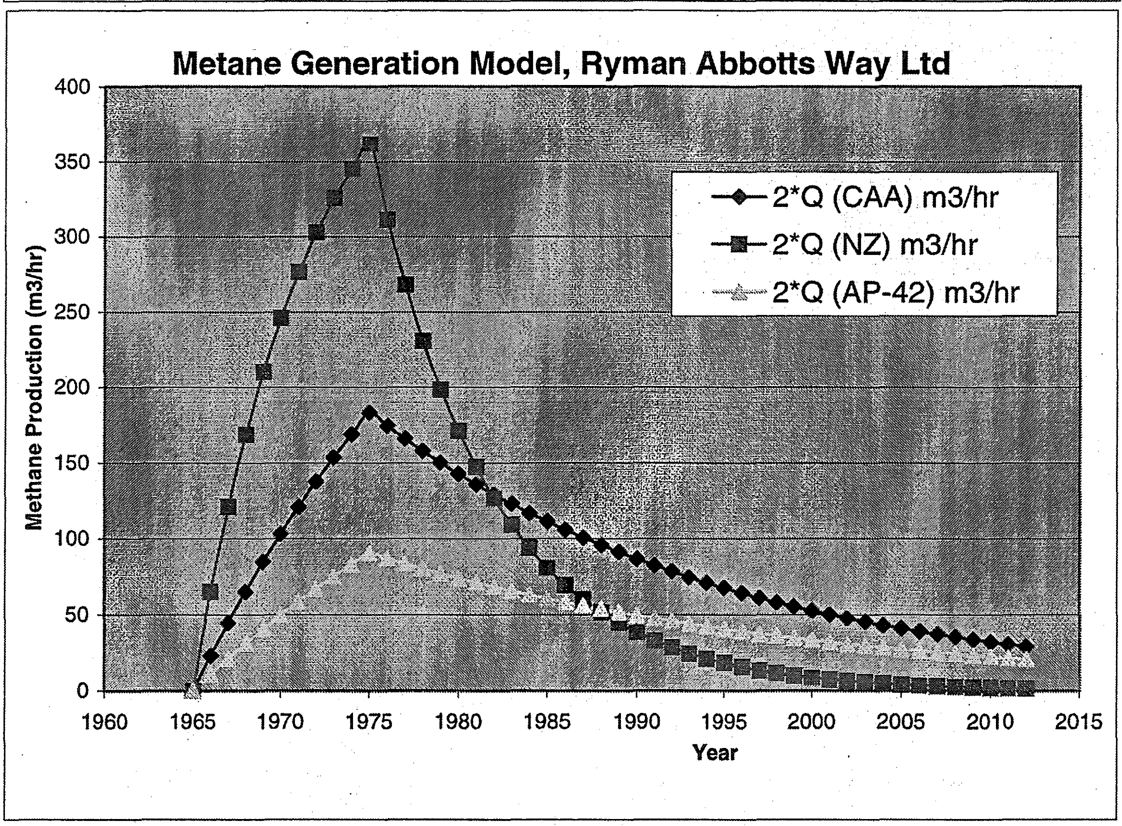

Verify all dimensions prior to construction - Do not scale

LEGEND

Symbol	Description
BH A-J	BOREHOLES FROM KINGSTON MORRISON INVESTIGATION MAY 1995
BH K-T	BOREHOLES FROM KINGSTON MORRISON INVESTIGATION FEBRUARY 1996
BH U-Y	BOREHOLES FROM KINGSTON MORRISON INVESTIGATION NOVEMBER 1998
4	TEST/EXCAVATION PIT FROM KINGSTON MORRISON INVESTIGATION, FEBRUARY 1996
BH 1-16	BOREHOLES FROM TSE GROUP INVESTIGATION SEPTEMBER 1985
PD 10	GROUNDWATER INVESTIGATION BOREHOLE, BY PATTLE DELAMORE, DECEMBER 1989, JANUARY, MARCH 1990
WWC-1	GROUND WATER INVESTIGATION BOREHOLE, WOODWARD CLYDE, JULY 1991
G1-G5	LAND FILL GAS MONITORING WELLS, FROM SINCLAIR KNIGHT MERZ INVESTIGATION OCTOBER 1999
G6-G9	LAND FILL GAS MONITORING WELLS, FROM SINCLAIR KNIGHT MERZ INVESTIGATION JANUARY 2000
	EXISTING PONDS
T2	EXISTING TEE'S
G2	EXISTING GREENS
	LIMIT OF SITE
----37----	EXISTING GROUND LEVELS COUNTOURS, (RELATIVE LEVELS), MAY 1995
	APPROXIMATE OUTLINE OF FORMER QUARRY PIT BOUNDARY

NOTES

1. LEVELS TO DOSLI DATUM.

Rev	Reason	By	Chk	Appr.	Date
A	RESOURCE CONSENT ISSUE	OD	WS	JGM	17/04/00

Scales 1 : 2000 (A3) Drawn RAG Designed WS
Date 3/8/95 (17:05 26/06/01) Ref 21194--AC012 Checked JGM

RYMAN HEALTHCARE LTD

RYMAN ABBOTTS WAY LTD

RETIREMENT VILLAGE
APPLICATION FOR RESOURCE CONSENT
LAND FILL GAS MONITORING
LOCATION PLAN

Job	Drawing	Revision
21194.03	G-101	A

ATTACHED XREF FILES
21194--ACM02.DWG
21194--ACM03.DWG
21194--ACM06.DWG

SINCLAIR KNIGHT MERZ

SINCLAIR KNIGHT MERZ Limited Auckland ph +64 9 9138900 fax 9138901 Wellington ph +64 4 4734265 fax 4733369 Christchurch ph +64 3 3790135 fax 3772209 Invercargill ph +64 3 2187102 fax 2144843 Queenstown ph +64 3 4424300 fax 4424244

202

Land Development Zones for Structure Plans

S. C. Tilsley
Beca Carter Hollings and Ferner Ltd

A. L. Williams
Beca Carter Hollings and Ferner Ltd

D. V. Toan
Beca Carter Hollings and Ferner Ltd

Abstract

Structure Plans establish guidelines for development, balancing land capability constraints and environmental and amenity values with economic feasibility and development objectives. The plans identify zones suitable for different levels of development intensity and appropriate services and infrastructure strategies, recognising community needs and the character of the land.

In the Auckland Region, where structure plans have been widely utilised, land stability assessment is a pivotal input to delineation of development zones, particularly as urbanisation spreads into more marginal areas.

Engineering geological field mapping in conjunction with a detailed study of aerial photographs is integral to land stability assessment. Historic slope movements identified in field mapping and stereoscopic studies of aerial photographs can be integrated with slope contouring from digital terrain models and published geologic data using a GIS-based mapping tool. Land capability and land development zones are derived from the superposition of these inputs.

A careful description of engineering constraints and stabilisation guidelines must accompany each zone to ensure that zones are both robust and sufficiently flexible to allow acceptable future land use and development.

Introduction

Structure Plans evaluate constraints to development such as geotechnical, landscape, ecological, hydrological, cultural and community values. The plans generate residential development density zones based primarily on land capability. Many of the Territorial Authorities (TA) have recognised that slope movements are the most frequently occurring natural hazard in the region, and geotechnical assessment of land stability has become a key input to Structure Plans.

This paper presents a methodology for slope stability hazard investigation as an input to Structure Plan development, within the Auckland Region. A qualitative risk assessment approach, based on both direct and indirect mapping techniques, has been found to be effective for the scale and requirements of Structure Plans. Each 'layer' of inputs (past instability, slope grade, engineering soil/rock type) is superposed visually or using geographic information systems (GIS) to establish land capability zones.

Some of the pitfalls of zoning land in terms of urban density distribution and the conflicts of commonly used stabilising measures with current resource management practices are also discussed. The current residential development approach in the Auckland Region consists of free-standing one to two storey housing. This approach is challenged.

The paper raises issues for consideration in development of a New Zealand Slope Stability Guideline to aid the practitioner, their clients and the regulatory authorities in planning and design.

Methodology

The qualitative approach described below is considered appropriate for the level of detail required for structure planning. Probabilistic risk assessment approaches are not considered appropriate at this early stage of land use planning.

Preliminary: Hazard Identification

The Auckland Regional Council (ARC) has commissioned regional studies of natural hazards as part of the Auckland Engineering Lifelines Project (AELP) with outputs including reconnaissance scale (1:100,000 and 1:250,000) slope instability hazard maps (Williams 1996; AELP 1997). It is recommended that a review of these hazard maps be undertaken at the outset of the project to identify in a preliminary way, the likely susceptibility of the land area to slope instability and flooding. In addition to slope instability, the following ground hazards should be considered:

- Active soils, soils susceptible to shrinkage or swelling with changes in groundwater conditions;
- Erodible soils, soils prone to piping and/or tunnel gully erosion;
- Collapsible soils, sensitive soils;
- Compressible soils, soils prone to settlement;
- Potential for rock dissolution or subsidence from underground cavities (natural or man-made).

In addition, potential susceptibility to the following hazards (also mapped as part of the AELP) should be assessed:

- Fault Rupture (AELP 1997, 2000) – The present understanding of fault activity in the Auckland area is limited, in part due to slope movement debris and volcanic deposits masking fault traces, and a short historic record. Active faults are known in the southern part of the Auckland Region.
- Liquefaction (AELP 1997, 2000) – Areas underlain by some soil types may be susceptible to liquefaction in the event of ground shaking associated with earthquake, for example sites located on reclaimed ground and low-lying sites underlain by sensitive silts and sands.
- Inundation – Susceptibility to flooding is generally assessed as part of a hydrological study and is not discussed further in this paper.

Because the site of a future eruption from within the Auckland Volcanic Field cannot presently be predicted, although it is unlikely to occur at the location of existing vents, volcanic hazard is not addressed in structure planning.

Other natural hazards such as tsunami have not been mapped for Auckland due to their relatively low risk, but may need to be considered elsewhere in New Zealand.

Slope Stability Assessment

Stability assessment at the urban planning (structure plan) stage, should comprise a reconnaissance survey, including a field walk-over and desk based study. In some cases shallow sub-surface investigation and soil/rock testing may be necessary to confirm principal lithologic distribution and engineering geologic properties, where these are not known.

Desk Based Study

The desk based study should include a review of regional hazard maps, published geologic maps and land inventory maps, the TA hazard register and additional information such as previous geotechnical investigation reports, records of remedial works undertaken on public land, and the Auckland Regional Council (ARC) water bore database.

Stereoscopic evaluation of aerial photographs has a key role in focussing the field walkover part of the study and aerial photographs should be examined both prior to and following the field walkover. The initial review identifies geomorphic features for "on-the-ground" inspection. The subsequent study allows confirmation of field interpretations and more accurate mapping of the extent of features. Air photo mapping may also identify lithologic boundaries, fault traces, and defect lineaments. Comparison of a series of historical sets of aerial photos allows changes over time to be observed, and it may be possible to estimate frequency of events or rates of erosion, particularly in the coastal domain.

Field Walkover

Both direct (field) and indirect (back-analysis) mapping techniques are recommended.

Direct mapping techniques are used to record observed information such as slope movement (historic, recent and ongoing), ground movement (eg cracking in buildings, and published, previously investigated or reported movement noted in TA hazard registers), and surface and ground water characteristics such as areas of seepage and saturated ground.

The type of slope movement should be identified as far as possible (eg Varnes 1984) and grouped with other features that have similar triggering mechanisms (for example, small scale rotational slides and creep movement commonly triggered by saturation of the soil mantle).

There are advantages in undertaking the field mapping part of the study with a colleague or in taking video footage, as this facilitates discussion and peer review. Photography may not distinguish the subtle aspects of some geomorphic features (eg larger scale historic slides).

Indirect Mapping

It is important to consider that most natural slopes have been modified by erosion or slope movement and have marginal stability, ie the factor of safety against sliding is low, in the order of 1.0 to 1.2. Indirect mapping is used to evaluate the "risk" of movement by "back-analysis" of slopes of different height, slope angle, soil/rock mass composition and groundwater level, identifying the relative importance of each factor to slope stability. Indirect mapping allows field observation (geomorphology, surface hydrology, previous hydrogeologic and geotechnical investigation) to be correlated with the desk based data (published lithologic data, air photo interpretation, topography) to delineate areas of potential slope movement.

Indirect mapping has become quicker and more accurate with the aid of recent CAD and GIS packages. Slope grades derived from Digital Terrain Models (DTM) can be grouped into zones, and risk of slope failure identified in terms of inferred groundwater conditions and engineering properties for given soil and rock types. For example rotational slides in saturated Waitemata Group residual soils tend to occur on slopes steeper than 14°; failure can be expected on slopes of 26° and steeper within the typical range of groundwater conditions.

The map of slope grades is superposed on the maps of engineering geologic units and the direct mapping of past and ongoing instability to delineate slope instability zones (Figure 1).

Land Capability Zonation

It is considered appropriate to distinguish three land capability zones using the investigation and stability assessment techniques described above. These zones are:

- Zone A: Suitable for Development (*Very Low Risk*)
- Zone B: Probably Suitable For Development (*Low to Medium Risk*)
- Zone C: Probably Unsuitable for Development (*High to Very High Risk*).

The equivalent risk descriptions proposed for New Zealand and Australian draft guidelines by Walker et al (1985) and Crawford and Millar (1998) are shown in brackets.

In areas of wide spread instability, the use of additional sub-categories may assist in providing some relative raking of land areas but is not recommended.

A classification system for land capability zoning in terms of slope instability hazard assessment is proposed in Table 1. The system considers the findings of field and desk based work and implications for development in terms of current legislation.

A

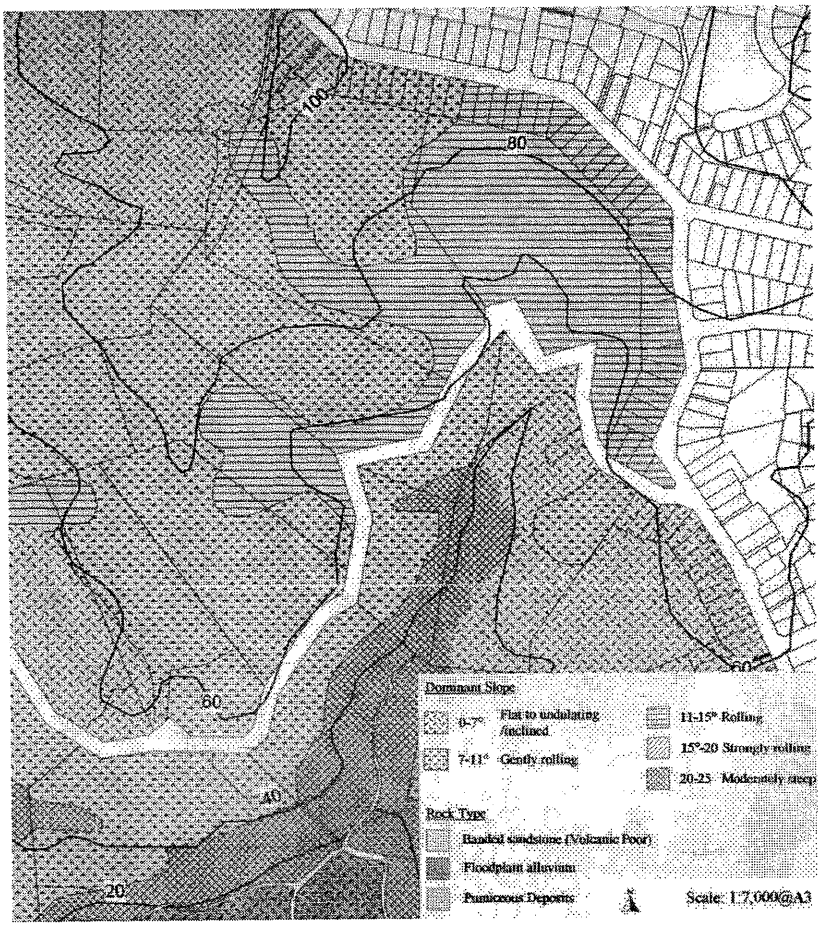

B

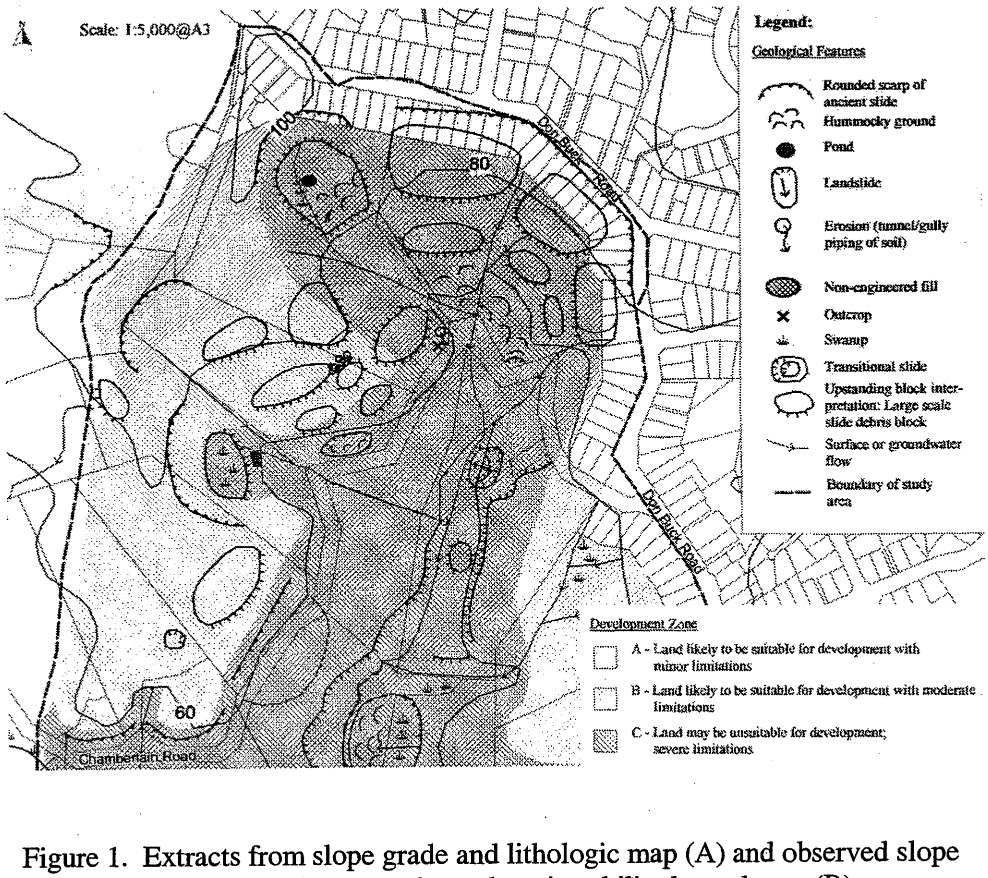

Figure 1. Extracts from slope grade and lithologic map (A) and observed slope movements overlain on resultant slope instability hazard map (B).

Table 1. Suggested Classification of Land Capability Zones

Zone	Risk of Instability	Explanation and Investigation	Description - results of mapping investigation	Development Implications
A	Low	Assessed to remain "stable" as defined by the Building Code for the design life required by the Building Act. Further investigation likely at sub-division stage to verify sub-surface assumptions, assess foundation and groundwater conditions.	• No signs of historic or recent instability; • No signs of saturation (eg swampy ground or associated vegetation); • Underlying geology has previously been investigated and assessed to have a factor of safety of greater than 1.5 for the typical and overall slope gradient and typical groundwater levels.	**Suitable** • Suitable for high density residential development; • Very low risk of instability during the design life of the structure due to natural hazards at specified design levels (eg 100 yr storm), excluding failure of man-made structures (eg drainage).
B	Medium	Likely to be stable or can be stabilised by minor engineering works. A sub-surface investigation and assessment is required to determine stability criteria specified in the NZ Building Code.	• Land adjacent to or slopes above an area of past instability; • Historic shallow instability or creep; • Low lying portions of historic deeper slides that may now be stable (require investigation to prove this criteria or stabilisation by minor engineering works such as drainage); • Elevated groundwater conditions (eg swampy or wet ground, creep).	**Probably Suitable** • Typical urban development can be designed so that it will not adversely affect land stability; • Sub-soil drainage and stormwater/sewage reticulation likely to be required; • A stable building platform and stable access as defined by the NZ Building Code for each Lot. Stable sites could be created on medium or low density development lot sizes; • High density development possible on investigation and minor to some engineering improvement works. Impacts from these works can be mitigated as specified in the RMA.
C	High	Unstable or high risk of instability as defined by the NZ Building Code. An extensive sub-surface investigation and assessment is required to determine stability criteria specified in the NZ Building Code.	• Areas of historic deep seated instability or recent instability; • Areas adjacent to, below and along water courses and coastal margins; • Areas underlain by uncontrolled fill; • Steep slopes and other slopes where the underlying geology has previously been found to be unstable under typical groundwater fluctuations.	**Probably Unsuitable** • Low density development; if stable house sites can be established by investigation or as specified in Section 36/2 of the Building Act, the remainder of the land is nevertheless likely to be subject to future slope movement. • High density development would generally require significant earthworks or costly retention solutions. • Earthworks stabilising measures will require Resource Consents and mitigation measures are likely to be significant.

Development Density Issues

Structure Plans equate the land capability zones derived from geotechnical and other inputs directly or indirectly with development density zones (that is high density residential or low density 'life-style' development). This is principally to allow Councils to assess the viability of subdivision based on the likely number of residents, infrastructural requirements and revenue. Increasingly, this type of correlation has been found to be restrictive or unacceptable to landowners seeking to subdivide, whose land is zoned B or C. This is particularly so in rural areas adjacent to sites where higher density development and significant land modification have been permitted in the past.

Land capability zones identify areas with different levels of risk of future slope movement, and those areas that require further sub-surface investigation and assessment to identify risks. The zoning provides a preliminary guide to the types of stabilisation techniques that may be required. The zones do not classify density of development, except that Zone A (very low risk) is likely to be suitable for development without significant land modification or engineering works (using good engineering practice). All land capability zones could be developed at various densities depending on the level of investment of the developer (in geotechnical investigation, land modification, stabilising works and foundation design) provided this meets the intent of the RMA and Structure Plan.

Once a Structure Plan is accepted by the Regional Council alteration of zone boundaries and definitions is difficult. In this regard, a suggested scenario of density zoning based on the land capability zones is as follows:

- Zone A – Suitable for development. High density development permitted.
- Zone B – Possibly suitable for development. High density residential development may be possible. Developers required to prove engineering feasibility of proposal in accordance with the current legislation (RMA 1991, Building Act 1991). Green and service (access) areas could be planned in these areas.
- Zone C – Probably not suitable for development. May be suitable for certain styles of low density residential development, "high value" development or green zones. At specific locations planners should consider the potential for "high value" development (such as high-rise buildings with communal outdoor living spaces) depending on factors such as site location (eg proximity to coastal areas, where significant stabilisation works may prove cost effective). Planners should therefore consult with landowners and developers to consider community concepts for development prior to implementation of structure plans. As for Zone B, developers would be required to prove the suitability and engineering feasibility of the development proposal in accordance with current legislation.

Authorities may need to consider amendments to District Plans to allow flexibility in terms of density zonation.

Implications of Legislation

The Land Capability Zones must comply with the stability requirements stated in the Building Act 1991 and the standards specified by the New Zealand Building Code 1992 (stability section modified in 2000) as well as conditions specified in the Resource Management Act 1991 (RMA). The implementation of this legislation in Regional and District Plans has had a significant impact on development over the last few years.

The latest amendment (Amendment 4) of the Building Code requires that overall ground stability is verified before foundations are designed. No methodology or criteria is provided on how the stability is proven. Previous versions of the Code (as well as some existing regulations such as Manukau City Council's) require that permanent slopes should have a factor of safety greater than 1.5 against movement. This means that ground movement should have a very low risk of occurrence in response to naturally occurring events except where they are extreme. The problem with this approach is that most slopes created by natural processes (eg stream, river or ocean erosion) do not naturally have a factor of safety of 1.5, and this is generally true for the more marginal areas now being considered for development in the Auckland Region. The old code meant that geotechnical investigation and some engineered improvement of ground conditions would generally be required as part of land development. Now there is no code of practice for land stability and it appears that each TA will have to determine its own criteria, as documented in the RMA legislation.

The implications of Section 36, Part 1 and 2 of the Building Act on development were reviewed by an NZGS Working Party (NZGS Working Party on Section 36 2001). The review noted that the Act does not cover all natural hazards and that there are inconsistencies between the Act and other legislation. The review recommended that Part 1 be amended and Part 2 modified or removed. If modified, it was suggested that Part 2 include qualifying statements relating to the area of land that it should be applied to, the type of hazard, a time period for which the hazards were to be considered and the level of uncertainty accepted in the assessment. These qualifying statements could become the framework for Guidelines for slope stability hazard assessment (as discussed below).

The RMA requires Regional or District Councils to assess natural hazards for:

- Contingency planning (Section 30);
- Avoidance or mitigation of hazards in urban development planning (Section 31); and
- Protection against ground movement for subdivisions (Section 220).

A significant impact of the RMA on land development has been to require common stabilising techniques such as cut and fill earthworks and buttress fills in valleys to be designed so that they protect river or stream beds (excluding ephemeral streams) and sediment yield is mitigated. We have found that the Resource Consent mitigation and protection criteria are so demanding as to make some development uneconomic (eg cut to fill terracing) and some stabilising techniques non-complying (eg earth toe buttresses). This has a particular impact on the economic viability of stabilising most Zone C land.

Other stabilising techniques such as drainage measures are cost effective, but first must be proven to be effective, and must be maintained if they are to operate over their design life. Generally drainage is not a desirable option for TAs, unless the developer produces a reliable and sustainable maintenance program.

Stability Assessment Guidelines

A draft stability assessment checklist was produced by Crawford and Millar (1998) for New Zealand conditions and called for the publication of New Zealand Slope Stability Guidelines. Such guidelines have been developed in Hong Kong and Australia, and together with classification systems published by others (eg Aloetti and Chowdhury, 1999) would assist in the review of Section 36 of the Building Act and provide a framework for hazard assessment in urban planning.

South African geotechnical groups have also recently published guidelines for urban engineering geological investigations (SAIEG and SAICE, 1997; van Rooy and Stiff, 2001). The tabulated approach of the South African guidelines is considered particularly useful. Tables address:

- Levels of investigation required for all types of urban planning and residential design;
- Hazards (including ground movement) and classify them into three risk levels;
- Foundation conditions and foundation design procedures for particular problem soil types (eg expansive, collapsible and compressible soils).

Together with the definitions provided here, these established guidelines could form a sound basis for development of urban planning hazard investigation practice in New Zealand.

Conclusions

Reconnaissance scale studies comprising a field walk-over and desk based study, coupled with indirect mapping, are considered appropriate for development of geotechnical inputs to Structure Plans. Air-photo interpretation is an integral part of the desk based study.

It is recommended that three zones of land capability or "risk" are defined in urban planning:

- Land that is suitable for residential development, without engineering improvements;
- Land that may be suitable for residential development but requires sub-surface investigation and is likely to require some stabilisation or land modification works (in compliance with the RMA);
- Land that is probably unsuitable for dense residential development without significant earthworks and/or stabilisation measures.

The allocation of Land Capability Zones does not define the density of development but rather allows Councils to zone areas that require a specific level of investigation, design and stabilising works to be carried out prior to approval of development. The cost of engineering works and/or cost of compliance with the RMA to stabilise Zone C land may render a higher density development uneconomic or non-complying. Multi-storied developments with communal outdoor living may allow higher density development on unstable land.

Urban planning and land development is currently defined by legislation that is considered inconsistent and inadequate. Development of a Slope Instability Hazard Assessment Guideline for Urban Development may assist in resolving some of the present confusion in this area.

References

Aloetti, P. and Chowdhury, R. (1999). "Landslide hazard assessment: summary review and new perspectives," *Bulletin of Engineering Geology and the Environment,* Vol. 58 (1), pp. 21–44.

Auckland Engineering Lifelines Project (1997). Stage One Report July 1997.

Crawford, S.A. and Millar, P.J. (1998). "The design of permanent slopes for residential building development." Project 95/183 for the EQC Research Foundation. *NZ Geomechanics News* No. 55, pp. 62-85.

NZGS Working Party on Section 36 (2001). "Discussion document on the review of the Building Act 1991, legislative submission" In *New Zealand Geomechanics News Issue 61,*pp. 25-33, Newsletter of the New Zealand Geotechnical Society Inc.

South African Institute of Engineering Geologists and South African Institute of Civil Engineering (1997). "Guidelines for urban engineering investigations," *Boutek, CSIR,* Pretoria.

Van Rooy, J.L. and Stiff, J.S. (2001). "Guidelines for urban engineering geological investigations in South Africa," *Bulletin of Engineering Geology and the Environment,* Vol. 59 (4), pp. 285–295.

Varnes, D.J., IAEG Commission on Landslides (1984). "Landslide hazard zonation. A review of principles and practice", *UNESCO,* Paris, 63pp.

Walker, B., Dale, M., Fell, R., Jeffery, R, Leventhal, A., McMahon, M., Mostyn, G. and Philips, A. (1985). "Geotechnical Risk Associated with Hillside Development," *Australian Geomechanics News* No. 10.

Williams, A.L., (1996). "Slope instability hazards in the Auckland Region: a preliminary assessment. *Auckland Regional Council Technical Publication* No.71.

The Fairfield Motorway: Management of risks associated with subsidence of underlying mines.

Ian Walsh

Opus International Consultants, Dunedin

Colin MacKay

Transit New Zealand

Abstract

Construction of the Fairfield Motorway is occurring over an area of abandoned underground coal mine workings near Dunedin in New Zealand that has experienced trough subsidence and crown hole collapse mechanisms in the past. This paper describes the risk management processes that are being applied to ensure that project safety and performance objectives are satisfied.

Introduction

The Fairfield Motorway project is located south of Dunedin in New Zealand and forms part of the Southern Motorway system on State Highway 1.

In the South Island, S.H.1 is the key strategic route for freight and this needs to be maintained and upgraded to provide the appropriate level of service and function as a reliable link for the economic benefit of the region.

The project involves the construction of 4.8 km section of 4 lane, median divided highway between Abbotsford to the East and Saddle Hill to the West (see Figure 1) and will replace an existing section of S.H.1, which carries 20,000 vehicles per day and passes through the residential area of Fairfield.

The National Roads Board identified the need for an improved alignment in the 1950's and an initial corridor designation was placed in 1960.

Very little further work was done until the early 1990's when Transit New Zealand continued the development of the motorway proposals. The 5 year period between 1995 and 1999 was required to develop the detailed design of the project and a physical works construction contract was let in January 2000.

The motorway is currently under construction and due for completion in April 2002. The construction budget is approximately $NZ 20 Million.

The project team is:

Client-	- Transit New Zealand, Dunedin Regional Office
Designer -	- Duffill Watts & King Ltd, Consulting Engineers
Contractor	- Fulton Hogan Ltd
Risk Review Engineer-	- Opus International Consultants

Background

The topography surrounding Dunedin restricts the choice of routes for the State highway network. There are only 2 possible routes into Dunedin – along the existing State Highway 1 and the Three Mile Hill route. In 1960 the National Roads Board rejected this latter route as being too mountainous and subject to frequent snow/ice closures. A decision was therefore made to develop an improved alignment following the low level route between Abbotsford and Saddle Hill and an initial designation was placed to protect the new motorway corridor.

This new motorway corridor provided an improved and more direct alignment than the existing State highway and was positioned well away from all residential areas when it was first designated in 1960.

However, by the time the detailed design had been fully developed in 1997, a significant new residential area had developed - known as the Walton Park area - in the vicinity of the Old Brighton Road Bridge, and Transit considered it necessary to lodge a new Designation application so that construction could proceed.

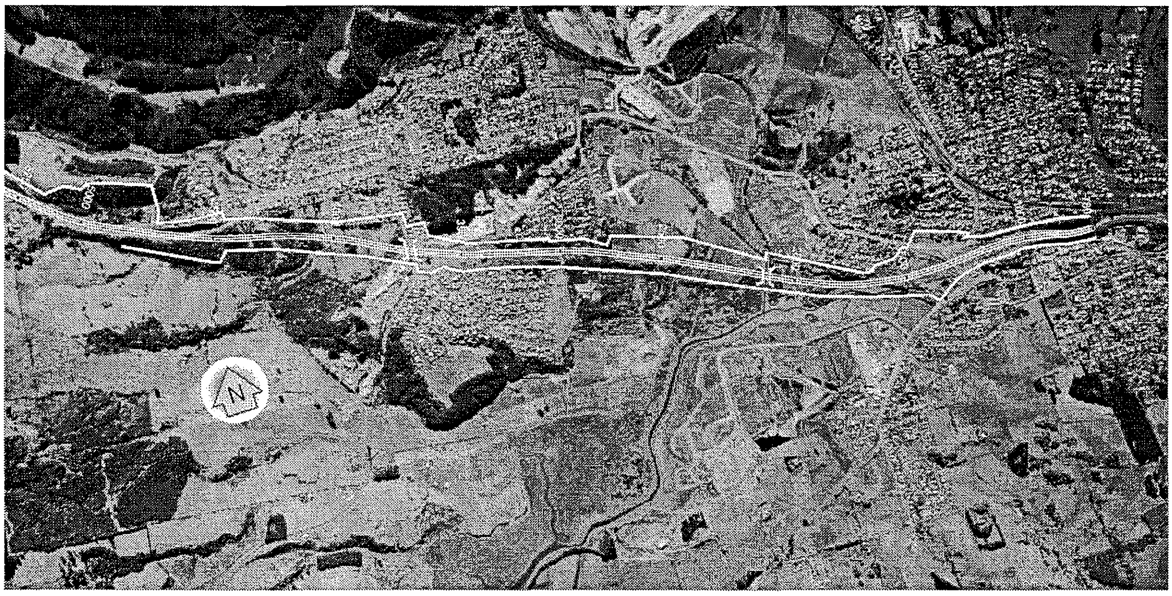

Figure 1 : Site Layout Plan

The Main Concern

In the 1960's when the National Roads Board initially confirmed that this motorway route was to be developed, it was well known that a section of the proposed route passed over an area that had previously be extensively mined between 1870 and 1955.

The extent of the underground coal mines (Stewart & Glassey 1998) was shown to result in the new motorway alignment passing directly over these mines over a length of approximately 890 m.

The mines are relatively deep towards the east (Stewart & Glassey 1998) but rise significantly in the west, being very shallow in the Old Brighton Road area (near 3600m in figure 1 above) with the original portals expected to daylight within the motorway formation at this location.

Ideally of course in selecting the route for a motorway development, such areas of significant underground disturbance would normally be avoided. In this case there was little option but to pass directly over the mines due to the limited route options available and the extensive nature of the mines themselves.

Transit identified the need to carefully assess the potential effect of these mines and the hazards they presented when it commenced the detailed design phase of the project in 1995. This was clearly a risk that needed the most careful study and consideration if sound engineering proposals were to be developed. Additional to this however, was the fact that in 1998 Transit was required to demonstrate the integrity of its proposals in the environment court due to an appeal by a group of residents in the area. This in itself required Transit to be able to credibly present its assessment of the likely hazards on the motorway due to the existence of the mines but also its assessment of the potential effect of the operation of a motorway on the mines themselves. The residents who appealed Transit's proposals had real concerns that construction activities and operational traffic vibration could trigger collapse of the old mine workings. There were clearly a number of safety issues that needed serious consideration before Transit could confirm that it was going to proceed with construction.

These included:

- Safety of the Contractors work force during construction
- Safety of the adjacent residents during and after construction
- Safety of road users during operation of the motorway

The Risk Management Strategy

In developing the detailed design of this project, Transit addressed the mine risk potential in the following way:

- The 1995 Design Brief - this required the designers to carefully consider the existence of underground features and their potential effect in developing a robust design, to ensure adequate safety to all parties affected.
- Mine Subsidence Hazard Assessment - the Institute of Geological and Nuclear Sciences was commissioned in 1995 to prepare an assessment of the hazards and risks of ground subsidence involving an extensive literature study and an assessment of the results of an extensive drilling programme.
- Review of Mine Hazard Mitigation Proposals - John St George – an expert independent Civil Engineer with Mining Engineering expertise was commissioned to review the mine hazard mitigation proposals developed by the designers.
- Appointment of a Risk Review Engineer - in 1999 Opus International Consultants (represented by Ian Walsh) were appointed to provide risk management advice in terms of the principles outlined in AS/NZS 4360; including:
  - independent risk assessment of the hazards associated with subsidence of the underlying mines and to assess the adequacy of the design proposals that had been developed.
  - Development of a mine hazard monitoring strategy for implementation both during and after completion of construction
  - review of the monitoring results during and after construction and reassessment as necessary of the adequacy of the design proposals throughout the construction phase and to advise on changes considered appropriate.

The Risk Management Process

The understanding of risk, and the identification of techniques to avoid or mitigate undesirable outcomes have advanced rapidly in recent years. Generalised risk management processes are now presented in documents such as the Australian/New Zealand Standard AS/NZS 4360:1999. In broad terms, the risk management process can be usefully broken down into four primary elements as follows:

1. **Incident Identification (or, what is the situation that we wish to avoid?)**
2. **Risk Analysis (or, what is the degree of risk?)**
3. **Risk Evaluation (or, is the degree of risk acceptable?)**
4. **Risk Treatment Strategy (or, what can be done to avoid, minimise, or mitigate the effects of unacceptable risks?)**

There is a further element, which is usefully applied across the whole process as shown in the figure below. Consultation and feedback are necessary if an integrated approach is to be taken, and the most useful outcome obtained.

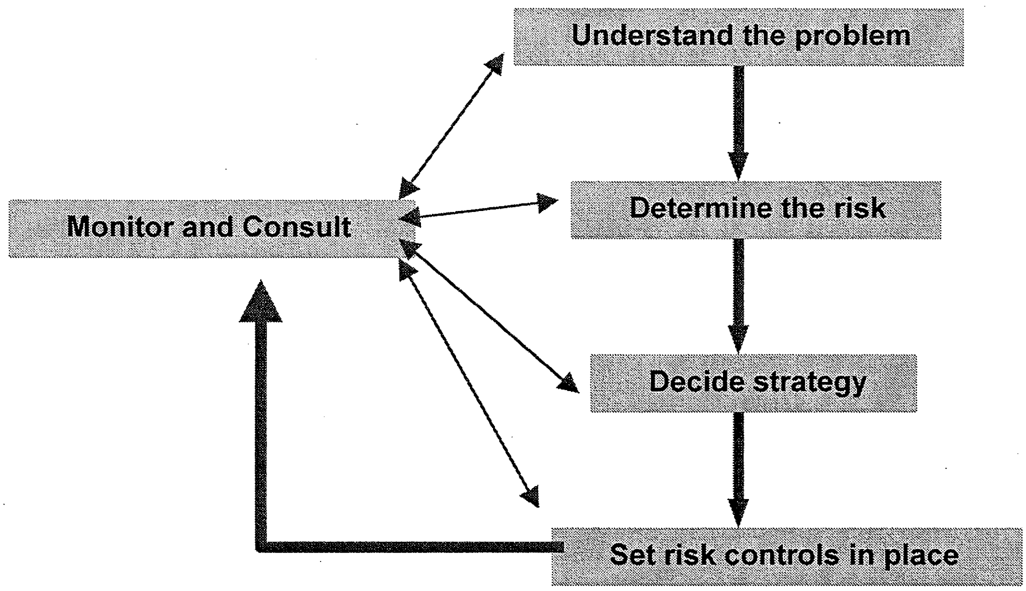

Risk Analysis is widely understood to be a quantitative exercise with a rigorous statistical approach to probability. However, in many instances there is not adequate information from previous cases to apply this scientific method and reliance needs to be placed on expert subjective opinion and qualitative methods if progress is to be made. In geotechnical engineering, given the infrequent nature of geotechnical failures in a given site with regular material properties and loading conditions, it is usually not possible to rely simply on statistical examination of past events (ie, Frequentist Approach) to predict the future outcome. Rather, a high degree of experience and judgement is needed to weigh up the influence of any uncertain variables and to arrive at an opinion on the probability of failure (i.e. Subjectivist Approach). Given this need to rely on subjectively derived probability estimates, any quantitative probability analysis should not be given the authority of a mathematically derived proof. Rather, the quantitative calculation of probability should be seen as complementary to the qualitative work that is done in arriving at an overall risk management strategy. The real value of the process is generally in the development of the most appropriate risk management strategies, rather than in the numerical calculations. For infrastructure development projects of this type, a cautious approach to the subjective determination of probability is generally appropriate. Returns to the developer and/or the community are usually moderate in scale, and there is little incentive to take on high risk exposure. Hence, in the absence of specific scientifically derived information, a set of conservative and simplifying assumptions were made when quantifying probability. This approach can lead to conclusions being challenged by those with opinions or judgements that differ from those adopted in the study. It is therefore necessary to transparently present all the assumptions used to reach the conclusions

There is no universal basis upon which the acceptability of a given risk can be evaluated. The context within which the risk is experienced will be important, as will degree to which the risk exposure is voluntarily or involuntarily imposed. The degree to which notice of impending exposure can be given such that avoidance action can be taken will also be an important consideration. In the context of infrastructural engineering development, risks generally fall into the following categories for evaluation during both the development and operational phases of the project.

(a) Health and safety of employees and contractors

(b) Health and safety of users of the facility and the public

(c) Environmental protection

(d) Development Cost exposure

(e) Benefit Shortfall, (Delayed commissioning, operational performance, operational costs etc)

In evaluating the acceptability of risk, compliance with legislation requirements and with accepted standards and codes of practice will provide the first point of reference. Performance expectations of the developer, users and affected members of the public will also need to be known.

Geotechnical Context

The motorway passes over mines between stn 2800 in the east and stn 3690 in the west – a total distance of 890 m. The geology comprises Otago Schist, overlain by Taratu Formation coal measures, the upper part of which comprises the uncemented Fernhill Sand. Overlying the Fernhill Sand is the Abbotsford Formation (weak marine sandstone, mudstone and greensand). The superficial deposits comprise loess, clay and/or bouldery slope deposits and stream/estuarine deposits. The strata generally dip to the southeast at an angle of 4° to 7° from the horizontal. Mine workings extend under the proposed motorway route between 2850m and 3700m. The mine workings were generally excavated by room and pillar methods between 1870 and 1955, with the unworked pillars initially being left to support the overburden. After initial extraction, more coal was taken from pillar and room workings by partially or totally "robbing" the pillars. A single lignite grade coal seam was worked, with extracted room height in the range 1.8 to 3m. The coal seam workings are shallowest (5-10 m), at Old Brighton Road at 3700m to the west, and deepen towards the east (up to 60 m deep) at 2850m. Access to the mines was gained through shafts and adits, many of which still exist. The mine cavities are drained in the higher western portion, and undrained in the eastern portion that extends below sea level.

The study area is approximately 850 m long (2850m-3700) and extends approximately 150m either side of the proposed motorway centreline. Crown hole collapse features and zones of trough subsidence have been mapped within the study area, specifically in the area underlain by old mine working. A crown hole is a surface depression or cavity created by the collapse of overburden soil into a mine working. The size of the 23 crown hole features identified within the study area range from 3 m to 46m diameter, and these have occurred over the last 100 years. The date of each crown hole development is not certain, but crown holes have been appearing on a regular basis. The known cavities are graphed on Figure 2 according to cavity size.

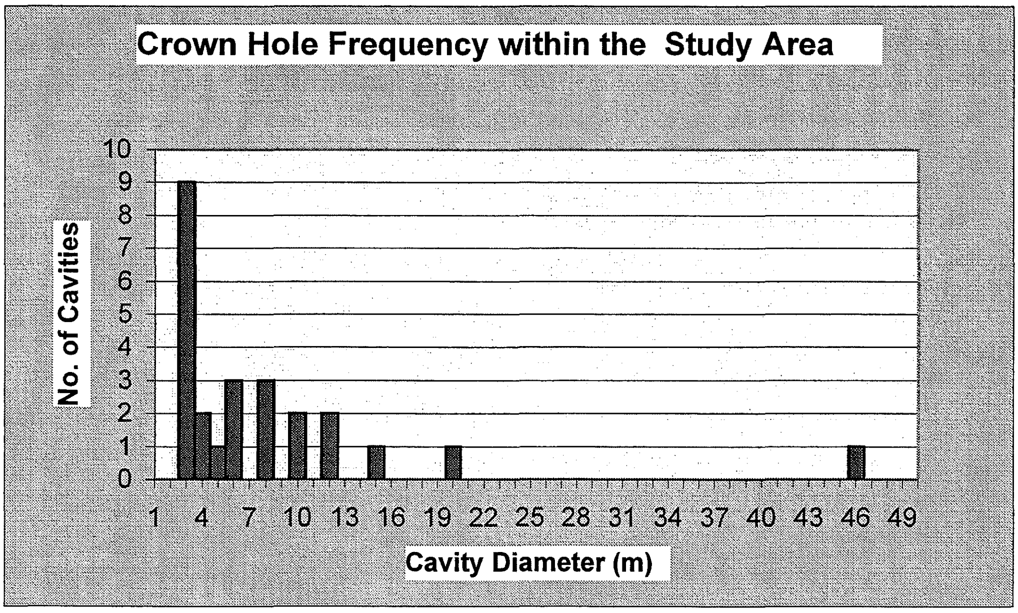

Figure 2 Distribution of Crown Hole Diameters within the Study Area.

The crown holes appear to be randomly distributed over the study area, although the larger cavities (20 m+) appear to predominate towards the centre of the area, and the smaller holes predominate to the west of the study area. Overburden (rock and superficial materials) thickness above the worked coal seam does not appear to affect crown hole development. In fact the largest crown holes occur where the overburden thickness is greatest. For these larger holes (eg Bremner St, and on motorway shoulder at 3200m), the ratio of mine workings height to overburden rock thickness (i.e. excluding superficial materials) is 1:19. It is likely that the presence of the uncemented sand layer some distance above the workings may disrupt the usual bulking mechanism. The larger crown holes dominate the study area. To illustrate the dominance of the large crown holes, Figures 3a and 3b show a comparison between the number of holes of various sizes and the area they affect. If a cavity exists it is likely to affect an area around the cavity as well, and the affected area has therefore been taken as two cavity diameters.

The summary graphs in Figure 3 show the area directly affected by crown holes covers some four percent of the study area. While the smaller diameter crown holes occur more frequently than the larger diameter holes, the larger holes affect a far greater area of land.

Further to considerations related to mine overburden instability, there are also potential hazards associated with phosphorus thought to be dumped in the abandoned workings, and with mine gases and fire risks.

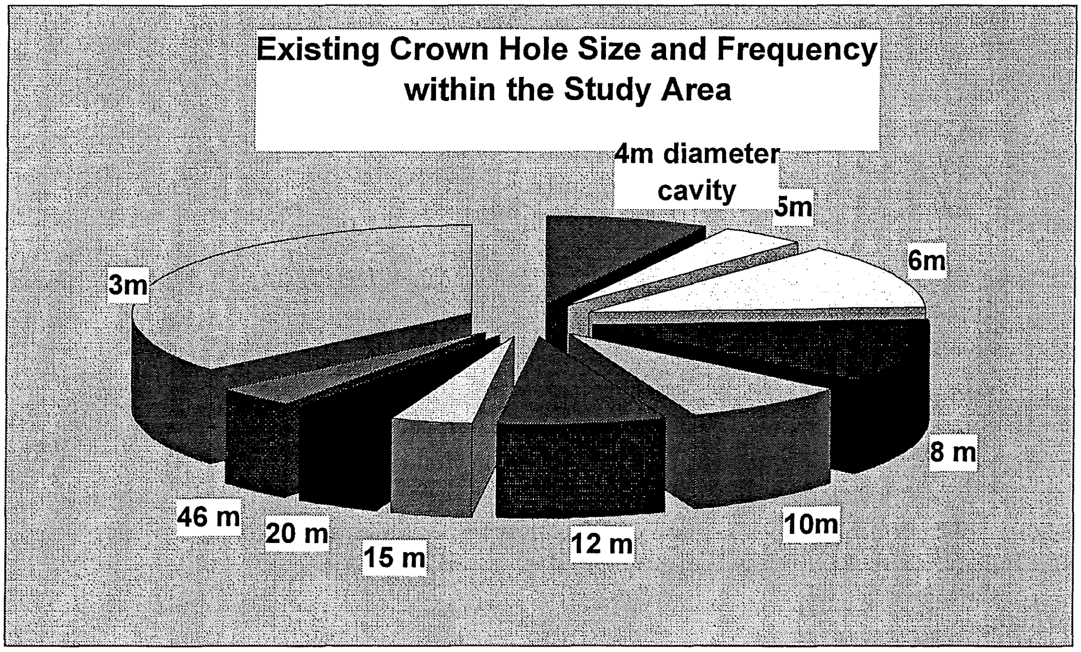

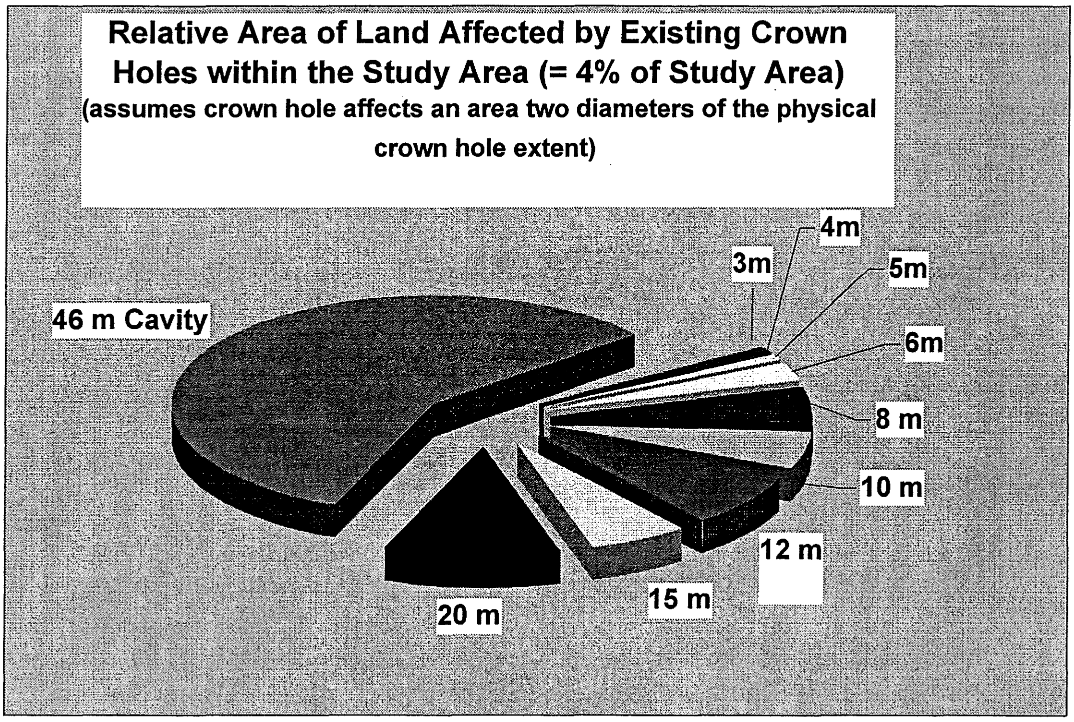

Figures 3a and 3b Size and Effect of Crown Holes within the Study Area

Hazard Identification

In risk management terms, the following hazards associated with the mine workings were identified.

- Reactivation/Development of crown hole collapse mechanisms
- Future trough subsidence
- Mine gasses (methane, CO_2 etc)
- Mine fire

- Exposure/disturbance of phosphorous dumps
- Slope instability of undercutting in vicinity of mine portal

Risk Assessment

Trough Subsidence

Given the period of time since mining has ceased, further trough subsidence is not expected. However, the effect of existing trough subsidence on pavement performance and ongoing settlement will be a need to be carefully assessed as the affected areas are exposed and testing is able to be carried out.

Slope Instability

The slopes immediately west of the mine portal area are thought to contain old landslide features, and very low residual material strength (c'=3kPa, _'=11 deg) has been revealed by laboratory testing. Significant risk of instability was assessed to be associated with excavation in the northern batter cuts and undercutting in this area. In risk management terms, there is no margin for further on site slope reduction within the available property boundaries, so contingency measures in this area are limited to adjusting the scope of supporting and/or drainage measures

Crown Hole Mechanisms

In the absence of specific historical failure dates, we have not been able to establish the rate at which crown hole development has occurred since the mines were abandoned. For risk assessment purposes, we have adopted a conservative assumption to ensure that adequate contingency planning is undertaken and appropriate resources allocated to respond effectively to any reasonably foreseeable incident. An estimate can be made of the assumed probability of a crown hole occurring at any site within the study area as follows:

P(crown hole formation) = Ai / T.Ac

Where P = probability, T = time period, Ai = area affected by incidents, and Ac = area of mine workings (equivalent to study area).

Based on this conservative approach, and observing that a total crown hole area of around 2880 m2 has occurred over the last approximately 100 years, the background probability of a particular point being affected (ie. within twice the diameter of a crown hole) in any one year is calculated as follows:

(2880 m2 x 4) / (100 years x Area of Study (266000m2)) = 0.00043.

For example, the proposed motorway formation (ie carriageway area) has an area of 18,700m2 over the mine workings, and the expected cavity size to develop during one year then becomes 18,700 x 0.00043 x 1 = 8 m2 (ie a 3m diameter affected area or a 1.5 m diameter crown hole per year, or a single 3m crown hole over a 4 year period, or a single 5 m crown hole over a ten year period). Similar predictions of the background risk of crown hole formation can be obtained for any given section of land within the study area. These calculated background figures are obviously higher than what is currently being experienced, but they do at least give an indicative basis for project risk management decision making. It is likely that the actual background frequency is well below 0.0001 per annum or < 1% per 100 years.

To gauge the likely effect of crown holes developing following construction disturbance, a weighting factor has been applied which decreases exponentially away from the road formation to reflect the decreasing influence of static stress changes and vibration with increasing distance. The land for 150m on either side of the motorway centreline has been divided into the motorway formation plus three zones parallel to the motorway at increasing distance, and a weighting has been applied to each zone. A construction damage weighting of 30, 10, 3 and 1, and an operation damage weighting of 5, 3, 2 and 1 has been applied to the formation; 2 formation widths, a 2 further formation widths and 2.5 formations widths on either side of the motorway formation respectively. These zones equate to the formation, the shoulder, immediately adjacent properties, and background properties outside the influence of motorway construction activities. The damage weighting value has been arbitrarily assigned based on an exponential series, which is intended to reflect the attenuation characteristics of any disturbance. We stress that this model is highly subjective and open to technical debate. However, in taking a conservative approach, and applying the technique as a management tool rather than as a scientifically rigorous model, it is argued that useful risk management strategies will result.

The predicted affected areas obtained from this method are intended to be a conservative assessment for risk planning purposes and should not be viewed as the expected outcome. Summary figures showing the model development steps, and the subsequent expected surface area affected by crown hole development during construction and during operation are presented in Figures 4 to 6 below.

These graphs indicate approximately 700m2 or 3.9% of the formation corridor may possibly be affected by crown hole features during construction (e.g. four 7.5 m diameter crown holes). The areas arrived at above are not the expected values, but rather they reflect a conservative possibility that it would be prudent to plan for. That is, the subjectively derived 90-95%ile outcome. The most likely outcome could well be an order magnitude lower than these figures.

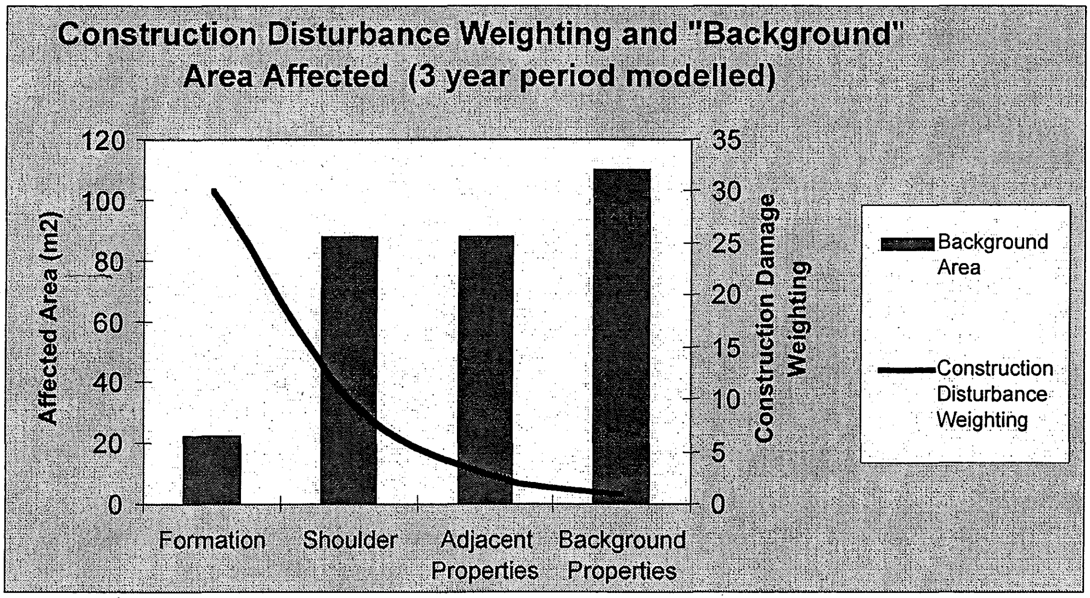

Figure 4. Methodology for weighting areas potentially affected by Crown Hole formation during construction

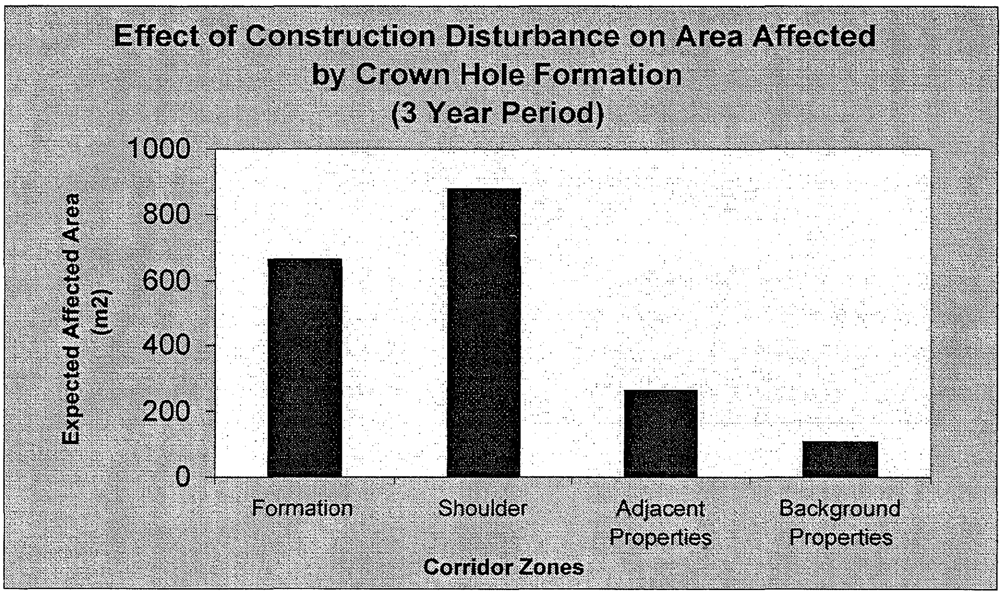

Figure 5 Effect of Construction Disturbance on Area affected by Crown Hole Formation

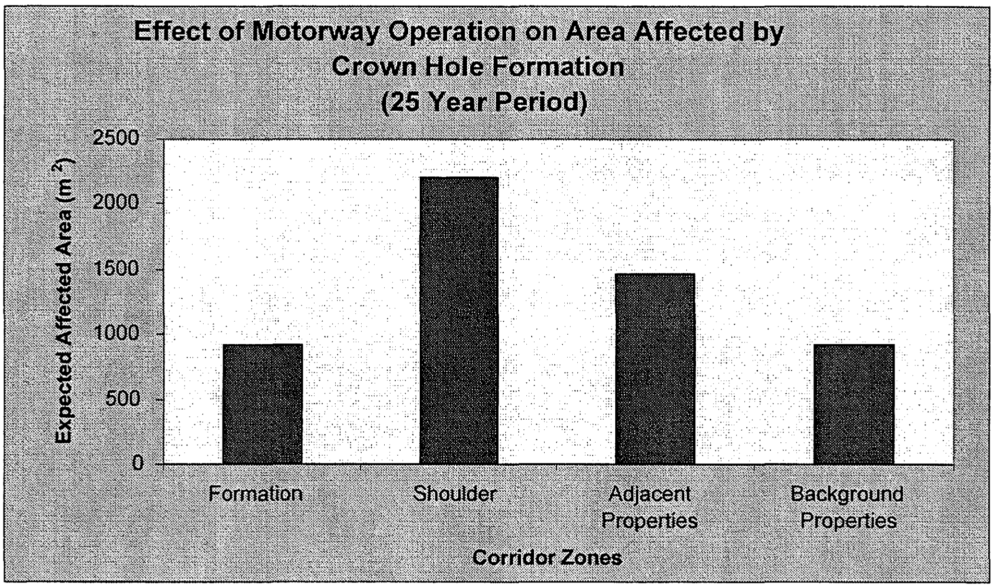

Figure 6 Effect of Operational Disturbance on Area affected by Crown Hole Formation

Risk Evaluation

The hazard identification and risk assessment exercises undertaken revealed that a systematic risk treatment plan needed to be put in place for the final design, construction, and operational phases of the project.

Risk Treatment

A risk treatment plan has been formulated noting that the risks could not be avoided by rerouting the motorway, but that the risks could be minimised by putting appropriate additional management steps into the project. The treatment plan covers the following areas:

Risk Minimisation

- Further investigations
- More conservative or developed design
- Development of contingency plans
- Re-assessment of design proposals during construction
- Development of monitoring strategy
- Careful review of monitoring results
- Risk Financing/contingency assessment

Further Investigations

Additional drilling and testing was undertaken prior to calling tenders, and provision has been made for ongoing investigations as access becomes available during the construction process. Personnel entry into the mines was not considered to be an option, and the use of a remotely operated mine rescue vehicle was also not practical due to access dimensional limitations. Down hole video inspection has proven to be a valuable tool in the drained section of the mine workings, particularly where large diameter bored pile excavations have enabled lighting equipment to be lowered into the cavities. Use of down hole geophysical techniques to assess actual mine crown conditions in the undrained section is currently being pursued.

Design Development

The design has been further developed or modified to increase confidence in the performance of the constructed works.

Pavement over Mine Workings: The mine features that are considered to present a subsidence hazard are the existing known crown holes and shafts and any unknown shafts or developing crown holes yet to progress to the ground surface. Trough subsidence is not thought to present a significant hazard. There are geological hazard sub-zones within the 2850-3700m section of motorway related primarily to the overburden depth and historical behaviour. These zones are prefixed with a G to avoid confusion with the property monitoring zones. Up to station 3280m in hazard zone G3 there are large crown holes present which may relate to specific mining activity and which are not likely to reoccur. Hazard zone G2 from station 3280m to 3420m has not experienced historical crown hole collapse. Hazard zone G1 from station 3420m to Old Brighton Road contains many smaller crown holes. A structural concrete pavement design is proposed for zones G1 & G2. No specific construction treatment is proposed for zone G3 where the deeper workings are situated, and the shallow mine workings west of Old Brighton Road have been undercut and backfilled. The structural concrete pavement originally intended to be constructed between 3280m and 3630m has been extended by some 30m to station 3660m to replace the deeper portion of the mine access drive undercutting. The pavement is designed to remain operational while experiencing a loss of direct support up to 6m diameter, and to deform but not rupture with a loss of support up to 12m diameter. This design replaces the preliminary high strength geosynthetic reinforced pavement concept, which was thought to have significant risk of poor performance when used in a thin granular pavement. The pavement is designed to carry normal highway loading but not abnormal overloads which would require permission to use the route. The added section of pavement west of Old Brighton Road (3630m) will be in close proximity to the mine workings, and there will be increased probability of collapse features being experienced in this area. Provisional has been made for bored piled support to the pavement in this area, with the piles extending to below the mine workings in a similar manner to the bridge structure foundations.

Drainage: The originally proposed groundwater recharge drains within the cutting over the mine workings has been deleted to prevent surface drainage water from discharging into the

Fernhill Sand layer where concentrated pressure gradients could activate flow failures into the mine workings.

Risk Allocation: Although the construction contract was structured around maximising the number of items which could be converted from measure and value payment terms to lump sums, the mine hazard mitigation and treatment items were retained as measure and value. Apportionment of the risk remained with the developer, as the contractor did not have the ability to control these risks.

Risk financing

While it is not within the scope of this document to present financial project details, the ability to access contingency funds is an important element in the management of construction risk. A comprehensive risk based financial model has been prepared for this project to enable the developer to make adequate provision for provisional contingency items and for appropriate professional review of the work during construction.

Risk Monitoring Strategy

Land areas both within and adjacent to the motorway corridor have been zoned for monitoring purposes to focus effort onto the perceived higher risk areas. A total of seven zones have been adopted.

Crown Holes & Shafts: Existing crown hole and shaft depressions have been located by survey from existing maps, plans and photographs when construction commenced. A progressive photographic record of their condition is being kept. The surface profiles of depressions in close proximity to the motorway works, and near developed properties, are being monitored by precise levelling surveys of installed marks. Ground penetrating radar (GPR) was initially chosen as the preferred geophysical tool to identify the presence of unknown cavities or lower density disturbed material beneath the construction corridor. In order to assess the effectiveness of this method in the specific conditions encountered at this site, a trial involving various combinations of buried 600mm plastic barrels was undertaken. GSSI SIR System 2 ground penetrating radar was used with a 200MHz antenna (an alternative 400MHz antenna was not trailed as the depth of penetration with this antenna is less than with the 200MHz unit). The GPR could not identify an effective cavity size of 1.2m at a depth of 3m, but two barrels at a depth of 1.1m, and a single barrel at a depth of 0.5m could be detected. Following further trials it was concluded that the GPR method did not have adequate range in these materials to detect incipient crown holes that may have presented a construction hazard. An alternative electromagnetic (EM) survey technique was then tested using Geonics EM31 equipment to indirectly measure the electrical conductivity in the soil to a depth of 6m. This equipment does not provide high resolution imaging, but by surveying a series of parallel scan lines, a contour plan of conductivity can be generated. Capped shafts and changes in material type were readily identified with this technique, and it has been adopted for regular monitoring over fixed lines along the formation between 2850m and 3700m. It is hoped that registration of scan lines and data processing should enable results between surveys to be compared and to thereby identify changing subsurface conditions between surveys. These surveys are intended to continue into the operational phase of the project. The potential to utilise other geophysical remote sensing methods is also being assessed. Deformation under proof loading with a pushed or towed 80 tonne load on the formation at 3.5m lateral spacing is also included as part of the monitoring programme.

Groundwater: Stability of the existing mine workings is dependent upon consistent groundwater conditions being maintained in the mine cavities and in the overlying Fernhill Sand layer. Standpipe piezometers are installed in both the workings and the overlying sand at stations 3254 and 3272, with automatic logging in place using vibrating wire transducers installed in the standpipes. Natural water level within the crown hole near 3200m is also be monitored by visual observation of a staff gauge.

Vibration: Peak ground vibration induced by construction operations is being measured at ground level for a range of distances up to 50m to confirm that vibration levels are within design expectations for the area over mine workings. Measurements are being taken at locations representing both shallow and deep overburden conditions.

Mine Gases: Gas sampling tubes have been installed in boreholes to facilitate regular monitoring of conditions within the drained portion of the mine workings.

Residential Property Condition: Properties in the vicinity of the motorway over the mine workings have been zoned into several broadly based risk categories. Preconstruction property condition surveys have been undertaken to identify any existing defects, and survey precise levelling is being undertaken on selected kerb lines in residential areas to provide an early indication of any deformation.

Monitoring Frequency: Measurement frequency ranges from near continuous logging through to a single reading at the appropriate construction point. In general, readings are being taken on a monthly basis to suit the project reporting cycle, with more intensive readings being programmed when major construction activity is taking place in a given area or near a specific feature. All monitoring activity is subject to ongoing review and adaptation throughout the construction phase of the project, and monitoring activity is planned to extend into at least the first three years of the operational life of the motorway.

Monitoring Results During Construction

Mine stability encountered so far in the construction phase of the project (eighteen months into the twenty seven month programme), has proven to be considerable more favourable than the conservative assessment made for risk management contingency planning purposes. Although the GPR technique was shown to be unsuitable for the detection of incipient crown holes, no unmapped features of this type have been encountered during the construction of cuttings over the mine workings. This finding suggests that the time scale associated with progressive crown hole development in this environment is considerably shorter than our assumed period of likely activity. Limited video inspections also suggest that the mine crown is generally in better condition than was anticipated. The need for the structural concrete pavement in the G2 zone (3280 m to 3420m) has been reviewed and a reduced area has been constructed.

Settlements in the order of 100mm have been recorded within the existing crown hole depression in the motorway shoulder at 3200m. The detailed relationship of this deformation mechanism to the motorway works (if any) is not clear, as an adequate period of initial data gathering was not undertaken to establish background trends. Recent investigation drilling in the vicinity of this feature has not revealed the presence of cavities likely to adversely affect the motorway formation, but further assessment of the mechanism is required.

Some alteration of the groundwater patterns following stripping of the motorway corridor has been suggested by observed behaviour of springs within a nearby property. As the groundwater monitoring plan targeted changes within the mine workings area and at local cut slopes, it has not been possible to confidently establish from the monitoring if changes of a more general nature have occurred.

Conclusions

On balance, the formal risk management approach adopted for this project has significantly improved confidence in the performance and in the adequacy of funding provision for the works. Several design changes were made to reduce risks associated with the presence of mine cavities, and in the absence of some detailed knowledge on the abandoned mine workings and their associated instability mechanisms, conservative assumptions were adopted for contingency planning purposes. The risk treatment plans developed have so far proven to be adequate to deal with the issues that have arisen, and the ongoing review process is has enabled some savings to be made as the degree of conservatism has been adjusted to suit the additional knowledge gained during the construction phase of the project. A major benefit of the risk management approach is the integration of decision making process throughout all phases of the development.

Acknowledgments

The authors wish to thank Transit New Zealand and Opus International Consultants for the opportunity to publish this paper, and to acknowledge the investigation and design work undertaken for this project by Duffill Watts and King and their various specialist subconsultants.

References

Stewart D L and Glassey P J, 1998: "Mine Subsidence Hazard Assessment for Fairfield Bypass SH1", *Proceedings of Roading Geotechnics "98*, NZ Geotechnical Soc. Symp., Auckland, July 1998.

The use of expanded polystyrene as lightweight geotechnical fill for a mountain access road Po-Cheon City, South Korea

W. H. Yoo
BASF South Korea

Abstract

Providing roads in mountainous areas is often an engineering "challenge", both from a design and from a construction perspective. Roading infrastructure in South Korea, where seventy percent of the land area is mountains, is a prime example of such issues. In a roading project that was completed in 1995 at Po-Cheon City (near Seoul, South Korea), expanded polystyrene was successfully used as a lightweight geotechnical fill material. In one particular section of the project, there was a need to construct the road on the steep side of a mountain. The initial option was to make a significant cut into the mountainside to create the necessary roading platform. This would have required a substantial retaining wall structure to stabilize the upper part of the slope above the road. Instead, the project design team decided to use expanded polystyrene to essentially build a level platform on the mountainside, on which the road itself could then be formed. This option did not require the normal retaining wall structure and considerably less earthworks. Not only did the use of expanded polystyrene save the client money, but this section of the work was completed in two weeks, compared to an estimated 3 months for the conventional construction method. This paper presents a case study of the use of expanded polystyrene in hazardous terrain, focusing not only the geotechnical engineering aspects of the project, but also looking at the wider benefits to the project.

Introduction

The work which is the subject of this paper was part of a larger project involving the construction of an access road into a golf course. The project as a whole was constructed through a steep, mountainous area. The design for the project had made extensive use of cut-and-fill methods. In one particular section of the access road, the rapidly approaching completion deadline meant that alternative methods needed to be urgently considered by the project managers. A study was commissioned to look at other viable options. The original design concept, as well as two alternatives were considered. Using Expanded Polystyrene as lightweight geotechnical fill (the EPS Method) was chosen as the best option.

The EPS Method option consisted of cutting the first part of the road platform into the mountainside, with the balance being formed with EPS blocks, as shown in Figure 1.

Site and Ground Conditions

The ground conditions in the area were ideal for road construction, with an underlying solid stratum. The major consideration in selecting the EPS Method however was speed of construction. With a slope of 45 ~ 60 degrees, extensive earthworks would have been required for conventional construction methods, as well as a substantial retaining wall to stabilise the mountainside above the road platform.

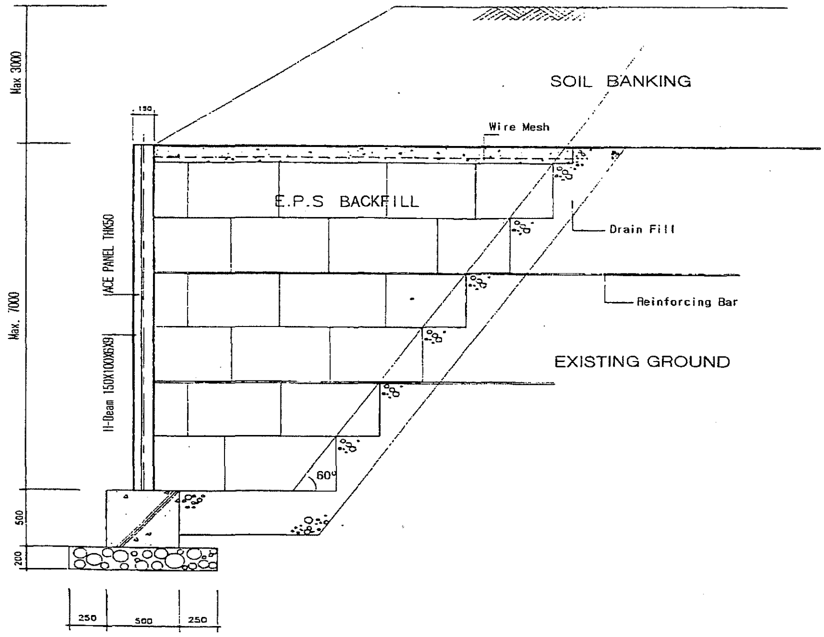

Figure 2. Part section of embankment showing EPS.

Analysis

The major area of concern in using the EPS Method was to ensure that unacceptable levels of differential settlement did not occur between the existing ground and the EPS blocks. FDM (Finite Difference Method) analysis was used to check this important issue.

Properties of EPS

With reference to compressive stress/strain properties, EPS can be characterised as an elasto-plastic material, exhibiting elastic behaviour at low levels of strain, progressing through a transition region into permanent deformation.

Experimental Behaviour

Figure 2 shows various densities of EPS ranging from D-12 (12kg/m^3) to D-30 (30kg/m^3), as well as a comparison with 29kg/m^3 Extruded Polystyrene, denoted as XPS DX-29. By way of clarification, XPS is a generically different form of polystyrene to EPS.

In the range 0 ~ 2% strain, the EPS graphs are linear (i.e. elastic). Above a strain threshold of ~ 2%, plastic deformation of the EPS commences with further increases in the applied compressive load. It can also be noted that as density increases, the deformation modulus (the gradient of the graph) increases. The rate of load application also influences this value, albeit marginally. Another factor affecting the deformation modulus is the level of applied confining pressure.

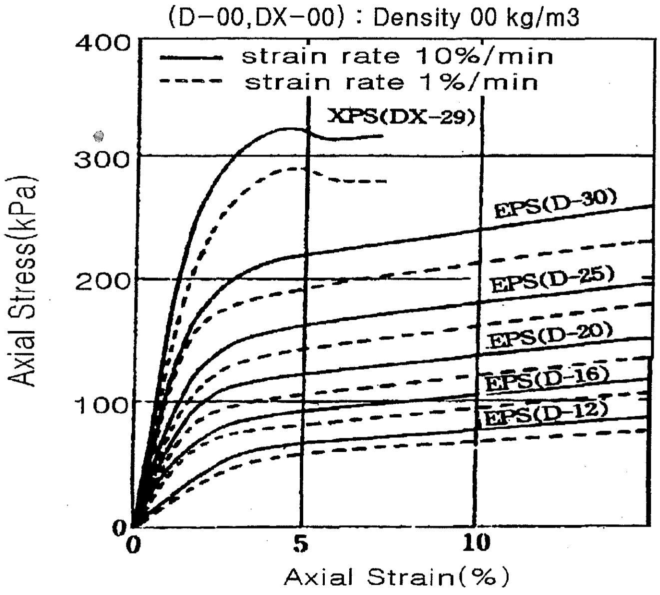

Figure 2. Typical stress-strain curve of EPS (from EPS C.M.D.O., 1993)

Numerical Modelling

To input the material properties into the computer analysis package, it was necessary to derive representative equations which incorporated both the EPS density and confining stress (Chun et al., 1996). The EPS behaviour was modelled as being non-linear elastic.

Under this regime, the axial stress can be represented by the following equation:

$$\sigma_1 = \frac{a \cdot \varepsilon_1^b}{c + \varepsilon_1^b} \tag{1}$$

where

$\sigma_1 =$ axial stress

$\varepsilon_1 =$ axial strain

$a, b, c =$ coefficients which are a function of EPS density and confining stress

$a = -60.995 + 9843.4 \cdot d + 0.339 \cdot \sigma_3$

$b = 1.135 + 41.97 \cdot d - 0.008 \cdot \sigma_3$

$c = -0.437 + 101.906 \cdot d - 2007.1 \cdot d^2 + 0.011 \cdot \sigma_3 - 0.389 \cdot d \cdot \sigma_3$

$d =$ EPS density

$\sigma_3 =$ confining pressure

Differentiating the axial stress with respect to the axial strain to get the tangent modulus (i.e. the gradient of the curve) results in the following equation:

$$E_t = \frac{a \cdot b \cdot c \cdot \varepsilon_1^{b-1}}{\varepsilon_1^{2b} + 2 \cdot c \cdot \varepsilon_1^b + c^2} \tag{2}$$

where

$E_t =$ tangent modulus

Poisson's ratio for the EPS was also required, and is represented by:

$$\upsilon = 0.0967 + 3.0863 \cdot d - 0.0023 \cdot \sigma_3 \qquad (3)$$

where

$\upsilon =$ Poisson's ratio of EPS

Computer Modelling

The FLAC (Fast Lagrangian Analysis of Continua) computer package was used to analyse the proposed embankment. This package is a two-dimensional explicit FDM programme which solves differential equations using known boundary condition values. The programme utilised equation (2) and (3) at various levels of axial stress to calculate axial strain and confining stress.

The input data to the programme for the existing soil was determined from values of cohesion and internal friction angle resulting from tri-axial compression tests and consolidation tests.

Table 1 summarises the input data used by the programme.

Table 1. Input data for FLAC programme

Classification	Unit weight	Internal friction angle	Cohesion	Elastic Modulus	Poisson's ratio	Bulk modulus	Shear modulus
Natural ground and the upper part of embankment ground	1.90	30	1.5	1.96×10^4	0.30	1.63×10^4	7.5×10^3
Non-linear elastic EPS model	0.02	-	-	Eq. (2)	Eq. (3)	-	-

The most important part of the design of the EPS fill was to reliably estimate the settlement that would occur at the interface between the existing ground and the EPS blocks. The complicated geometry involved meant that conventional design methods would not have given meaningful results.

As well as incorporating the non-linear elastic behaviour of the EPS into the analysis, the Mohr-Coulomb method was used for the section that consisted of soil. Figure 3 shows the geometry used in the computer analysis.

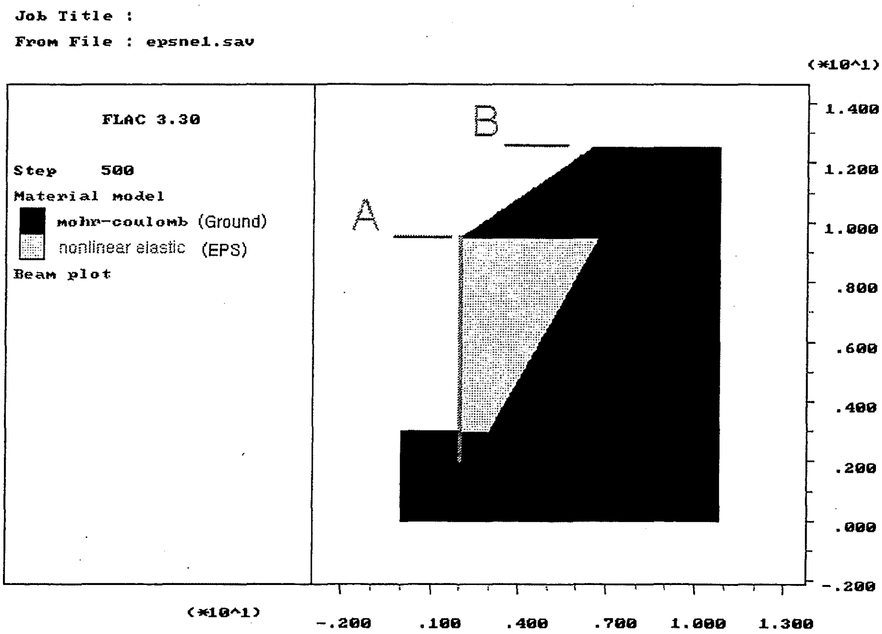

Figure 3. Geometry of model

Results of Simulation

The FLAC programme provided a prediction of the settlement and stress distributions, as illustrated in figures 4. to 7.

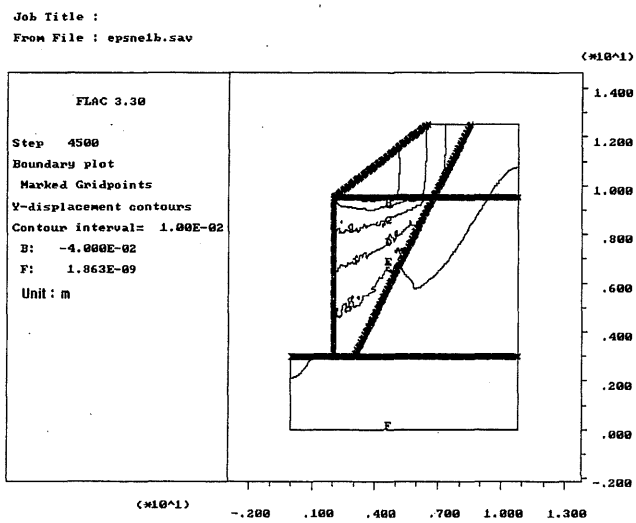

Figure 4. Vertical settlement distribution

The resulting settlement of the ground surface at points A and B is shown in Figure 8. Based on the analysis, a maximum vertical settlement of 3.6cm was expected to occur at the boundary between the embankment and the original ground (point A). At the proposed new ground surface (point B), which resulted from soil fill on top of the embankment, vertical settlement of 1.8cm was predicted by the analysis. On the basis of these results, it was judged that differential settlement between the two different materials would not be significant. In addition, it was clear that there would be minimal differential settlement in the area adjacent to the embankment.

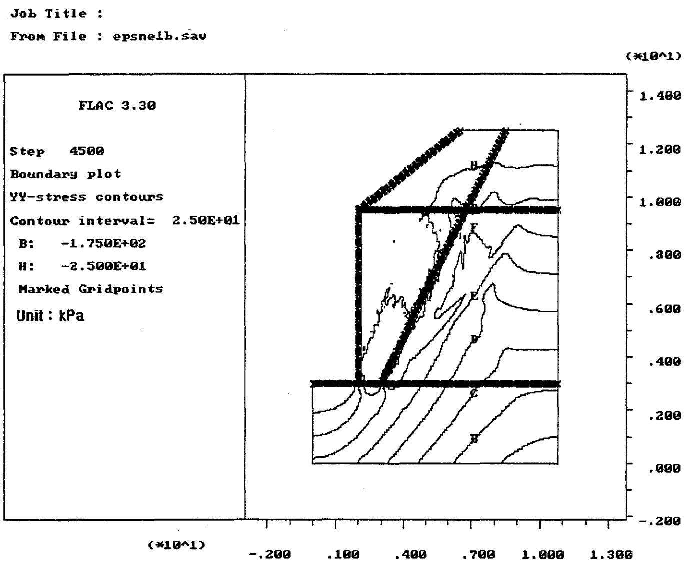

Figure 5. Vertical stress distribution

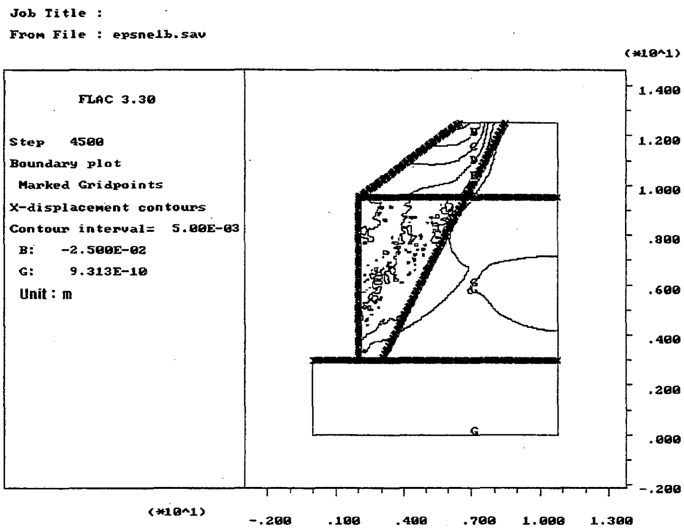

Figure 6. Horizontal settlement distribution

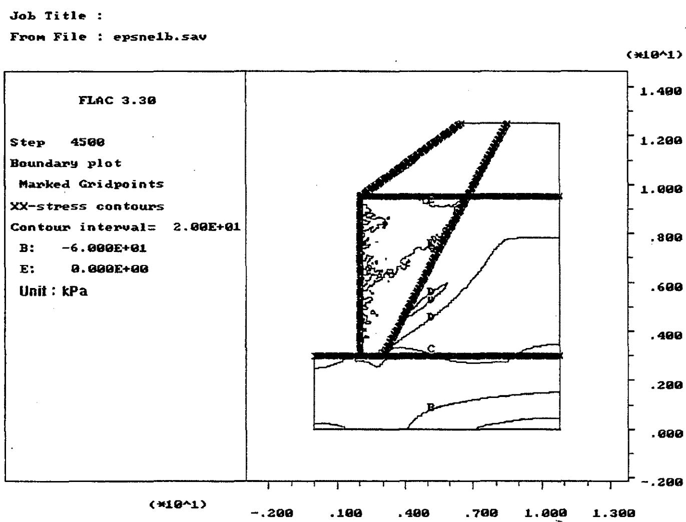

Figure 7. Horizontal stress distribution

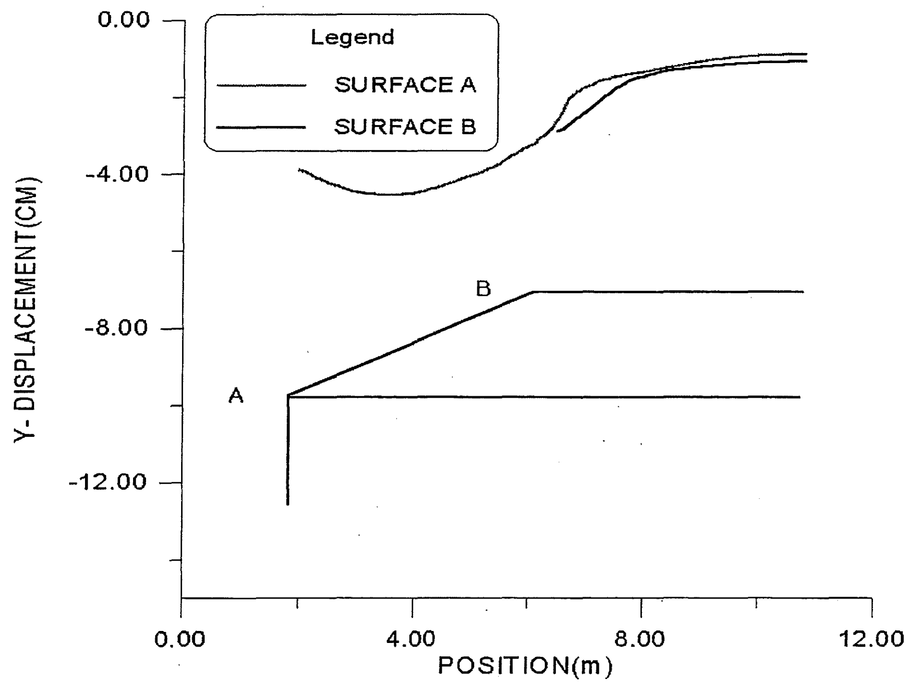

Figure 8. Vertical settlement relative to horizontal

The stress distributions generated by the programme indicated that using the EPS Method resulted in significant reductions in comparison to conventional fill material. This had the flow-on effect of a traditional retaining wall not being required and very low pressure on the existing ground.

Construction

Construction Details

The details on the EPS used for the work as summarised as follows:

- Length 31m
- Height 1.5 - 7m
- EPS density 20kg/m^3
- Volume of EPS 480m^3

Figure 9 shows a long-section through the part of the embankment that contained EPS.

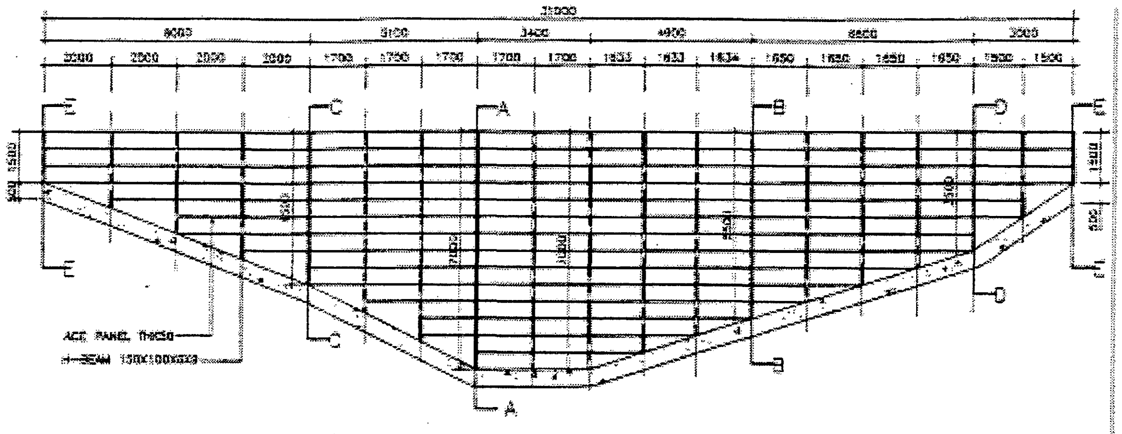

Figure 9. Long-section of EPS fill

A lightweight wall was constructed to protect the EPS blocks from environmental exposure. The wall consisted of a reinforced concrete footing, steel posts bolted into the footing and lightweight concrete infill panels between the posts, as shown in Figure 10. The steel posts were anchored back into the existing mountainside to provide stability under lateral load.

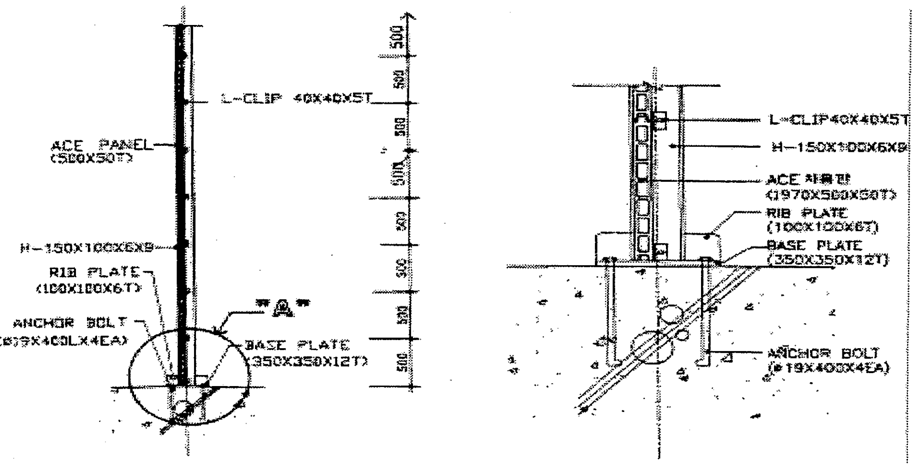

Figure 10. Cross-section of EPS retaining wall

Installation of EPS

In the area where the EPS was placed, loose soil and organic material was removed back to solid bearing prior to placement of blocks. A drainage layer was also provided at the sloping interface between the existing ground and the stepping EPS blocks (refer Figure 1.). Figures 11 and 12 show the EPS being installed.

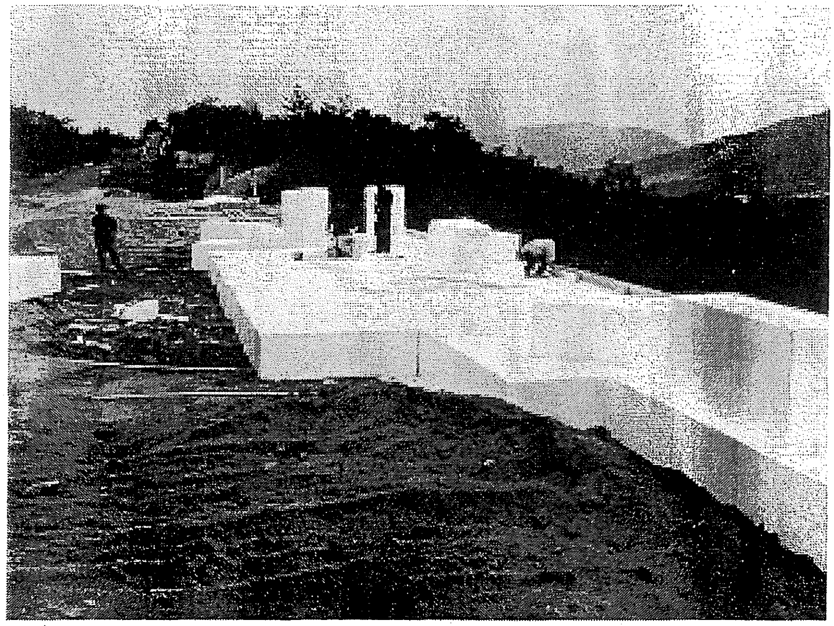

Figure 11. EPS block being placed

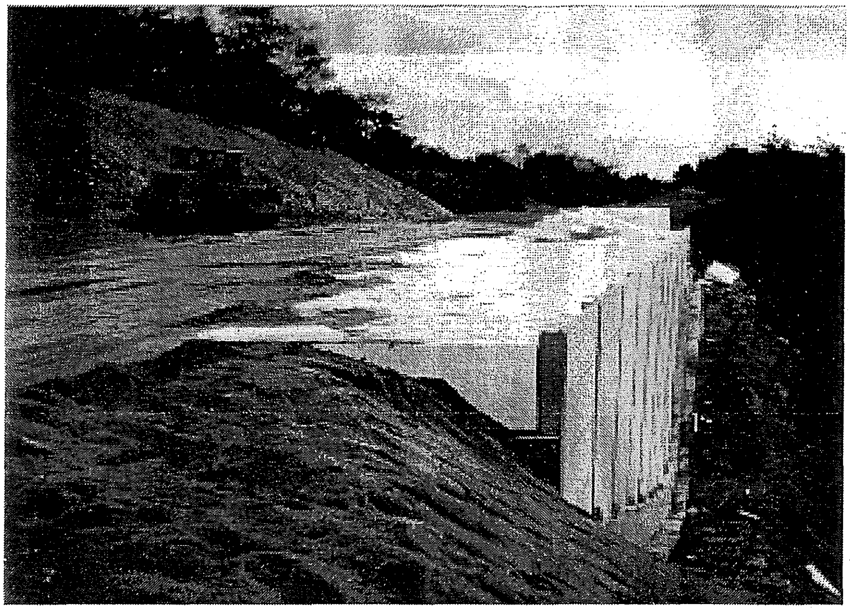

Figure 12. EPS blocks after placement

Performance In Service

Since the embankment was constructed in 1995, there have been no observed problems of settlement or the like. A thorough visual inspection in early 2001 showed that this section of the access road was performing very well and that the lightweight EPS fill was standing up to all in service loads satisfactorily. Figure 13 shows the embankment six years after it was built.

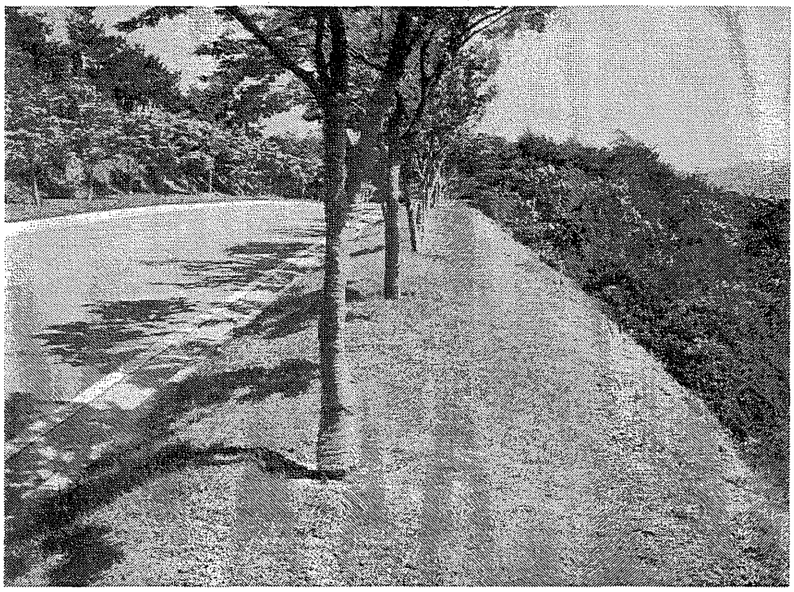

Figure 13. Embankment and access road , 2001

Discussion

The EPS Method was ideally suited to this project. The biggest factor in favour of this alternative method was the significant time savings that could be made. If traditional methods had been employed, it is estimated that it would have taken approximately 12 weeks to complete this section of the project, whereas with the use of EPS fill, the work only took a fortnight. Reductions to the construction period were made in three main areas. Firstly, the extent of the earthworks was reduced significantly. Secondly, a substantial retaining wall structure was replaced by a lightweight wall which acted as protection to the EPS blocks. And thirdly, the actual placement of the EPS blocks was much quicker than placing and compacting conventional fill.

Yet another advantage of using the EPS Method related to the question of safety during construction. The EPS Method eliminates a number of the risks associated with traditional roading construction.

Overall, the EPS Method was a very successful alternative for this project and after six years in service continues to perform up to expectation. Based on the success of the job, the method has been used on a number of other similar projects in Korea.

Conclusions

The use of the EPS Method in this project proved to be a successful alternative to more conventional embankment construction methods for the following reasons:

1. Significant construction time was saved with resultant cost savings
2. The required level of long-term stability has been provided
3. The very low EPS density significantly reduced the overburden pressure on the existing ground
4. Potentially unacceptable differential settlement was reduced to acceptable levels
5. The need for a traditional retaining wall was eliminated and the extent of earthworks was significantly reduced

References

"Code of Practice Using Expanded Polystyrene for the Construction of Road Embankments – Edition 1995," *Roadbuilding on Soils of Low Bearing Capacity Working Committee,* German Institute for Road and Transport Research, Cologne, pp. 7-9.

EPS Construction Methods Development Organisation (1993). "EPS Construction Methods," Tokyo, pp. 1-58.

Chun, B. S., Yoo, H. K., Lim, H. S. (1996). "A Study on the Application of Numerical Model to Predict Behaviour of EPS," *Journal of the Korean Geotechnical Society,* South Korea, Vol. 12, No. 6, pp. 185-195.

Cho, Y. (1992). "Behaviour of Retainign Wall with EPS Block Backfill," *Thesis for Masters Course,* University of South Dakota, pp. 1-29.

Yoo, W. H. (2000) "A case Study on the Application of Expanded Polystyrene as Reduction Materials of Load above Box Culvert," *Thesis for Masters Course,* Hanyany University, South Korea, pp. 1-30.

Slope Failures II

Geotechnical Aspects – Candy's Bend Road Widening, Arthur's Pass

G. J. Saul
Opus International Consultants, Wellington

Abstract

Widening of a 850 m long section of State Highway 73, in the mountainous terrain of the Otira Gorge near Arthur's Pass is currently nearing completion. This section of highway included two single lane sections of highway, which were cut into bedrock on steep hillside slopes that extend up to 1000 m above the highway.

This paper describes the geotechnical aspects of the project including investigations, risk assessment and development of measures to mitigate extreme rockfall risks. The integration of engineering solutions with landscape and environmental aspects of the project, provided an optimal solution for widening to two lanes. This involved some unusual structures including two overhead rockfall protection structures to mitigate sections of extreme rockfall risk, and half bridging (one propped, one cantilevered).

Geotechnical analysis included stereographic evaluation of rock defects, stability analysis of potential rock wedge and planar failures and assessment of rockfall energy. A range of cut batter stabilisation measures were designed for steep cuts of up to 35 m in height. These were specified on a provisional basis, and were optimised during construction using an observational approach.

Introduction

A 850 m long section of State Highway 73 in the Southern Alps of New Zealand was upgraded by Transit New Zealand to reduce the risk of instability to the road and to provide a two lane carriageway throughout. This enabled a 13 m vehicle length restriction to be removed. The highway was cut into steep hillside slopes, with almost precipitous slopes below the existing road. It crosses an area of previous instability within rock avalanche and debris flow materials. This section of highway has a history of rockfall and debris flow hazards.

This paper describes the geotechnical aspects of the project including investigations, risk assessment and development of measures to mitigate extreme rockfall risks. Some unusual structures, including two overhead rockfall protection structures were adopted to mitigate sections of extreme rockfall risk, and half bridging structures (one propped, one cantilevered). The observational approach to cut batter and foundation stabilisation was employed and is outlined.

Topography

The highway is located 30 to 50 m above the Otira River with steep slopes and near vertical rock bluffs below the road, which form one side of the Otira Gorge. The highway is flanked by rugged mountains, which rise up to 1000 m above the highway. The hillside slopes above the road are inclined at more than 45 degrees and have been disected by a number of small streams to form gullies. There are areas of colluvium on the hillside between the gullies.

The highway was originally formed by cuts up to 30m high into bedrock and was only one lane wide at two locations, requiring opposing traffic to stop at wider areas such as the Passing Bay.

The highway crosses an area of rock avalanche and debris flow material between Candy's Bend and Candy's Creek. Slope instability had previously been caused by river erosion at the toe of the slope in this area. Massive concrete gravity walls were installed to provide river erosion protection below the road, and support for potential slope failure above the road.

Candy's Creek is the most prominent stream which crosses the highway. The stream bed is inclined at about 35 degrees and is formed within rock avalanche, alluvium and debris flow materials. The stream at Reid's Falls issues from a 3 m wide gorge cut into bedrock and falls 20 m onto the road berm. In high flows water carries bed load materials and impacts on the road carriageway. Smaller permanent and intermittently flowing streams occur at a number of other locations.

Climatic Conditions

The site experiences extreme weather conditions, resulting from an average annual rainfall of 4 to 5 m, plus snow and ice during winter.

Seismicity

Arthur's Pass lies in one of the most active seismic regions of New Zealand. It is within 3 km of the active Kakapo Fault and within 20 km of the Active Alpine and Hope Faults. The Australian-Pacific plate subduction zone is causing 6 – 10 mm per year of uplift to the Southern Alps, in which the site is located. A number of large earthquakes have caused damage in the region in the recent past including the M7.1 Arthur's Pass earthquake of June 1994 and the M5.5 earthquake of May 1995, both centred within 20 km of Arthur's Pass. A massive wedge failure occurred at the Passing Bay in the 1994 earthquake as evidenced by the fan of debris remaining in the gorge below (Photo 5).

Recent investigation of paleoseismicity (Yetton et al, 1998) indicates that the nearby central region of the Alpine Fault may cause a magnitude M8 earthquake and there is a 65% probability of an earthquake occurring on this section of the fault in the next 50 years. This could result in high seismic shaking intensities of about MMIX at the site. An equivalent static acceleration of 0.7 g was evaluated from site specific seismic studies from the nearby Otira Viaduct project, as being appropriate for design of the structures for Candy's Bend.

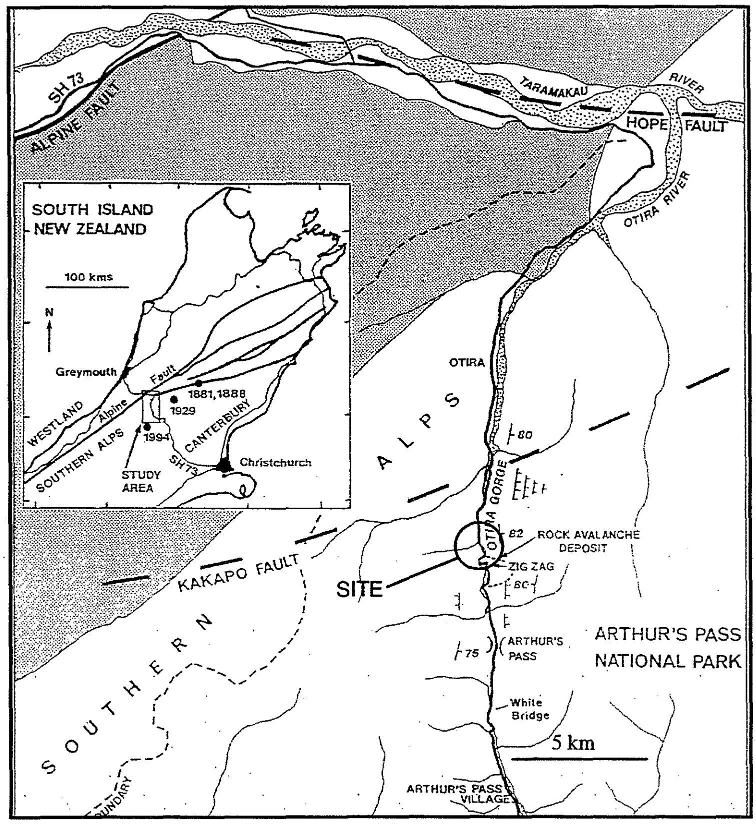

Figure 1: Locality plan (after Paterson and Coates)

Geology

The bedrock is strong to very strong, pale grey greywacke sandstone and minor black fissile mudstone (argillite) of Late Triassic age (Torlesse Terrane).

Bedding is the most predominant defect set and varies in spacing from 0.5 m near the Passing Bay to more than 10 m elsewhere. Bedding generally strikes north to north east, slightly oblique to the Otira valley, and dips steeply towards the east or west. The rock mass has several joint sets which vary from closely to widely spaced, and are open near the surface due to stress relief. Most joint sets dip steeply although there are some which dip out of the slope at around 40 to 50 degrees, such as a persistent set in the area between the Passing Bay and Starvation Point.

There are some shear and crush zones within the rock mass. These are often within mudstone and are oriented parallel to bedding. Several prominent intersecting shear zones formed the basal failure planes for the rock wedge failure in the 1994 earthquake. A number of near vertical shear zones, 1 to 2m thick, are located in the rock mass at Starvation Point. The adjacent rock is tectonically disturbed and more weathered than elsewhere at the site.

Rock avalanche deposits partially block the Otira valley upstream of Candy's Bend. Candy's Creek bed is formed in alluvial gravel and boulders of up to 2 m or more in size, and is derived from rock avalanche deposits. Deposits of colluvium, comprising boulders in a matrix of sandy gravel, cover portions of the hillsides above the highway between Candy's Creek and Starvation Point.

Investigations

Site investigations were carried out in two stages in 1998 and 1999, and included:

- Examination of aerial photographs.
- Geological rock defect mapping along the highway and up to 25 m above and below road level by Paterson and Coates, and Opus, using crane and abseil access.
- Logging of five trial pits of up to 5 m in depth.
- Logging of nine drill holes of up to 25 m depth in the road bench.
- Monitoring of a piezometer installed in a borehole at Candy's Bridge.
- Laboratory unconfined compression testing on selected samples of intact rock.

Instability Hazards and Risk Assessment

The slope instability hazards along this section of SH 73 include :

- Debris flows, down Candy's Creek at about 5 to 10 year intervals, and potential for renewal of debris flows from a gully just south of Starvation Point
- Debris flows and isolated water borne rocks at Reid's Falls.
- Rockfall, at the Passing Bay Wedge failure, and from cut batters and hillside slopes throughout the project.
- Instability of cut batters, existing slopes, and particularly of colluvium at the head of cuts.
- Large scale landslides triggered by river erosion and/or earthquakes.

A qualitative assessment of the risks associated with slope instability throughout the project was carried out in accordance with the risk management standard (AS/NZS 4360:1995). Risk was evaluated as a combination of the consequence and likelihood of failure based on :

- Evidence of slope instability obtained during the investigations
- Observation of aerial photographs
- review of the historical records of rockfall in the area

The risks were mapped throughout the project and the implications for risk management were considered. Mitigation of risks was justified economically for a number of critical sites.

Two sections of the highway at the Passing Bay and Reid's Falls, were assessed to have an 'extreme' risk from rockfall, and were mitigated by constructing a rockfall protection shelter and a chute over the road to give an assured level of protection. The alternative of using rockfall netting was also considered, but was not appropriate at either site because of the slope geometry, high energy of rockfall, need for multiple nets, lack of a catch bench at road level and on going maintenance requirements. Two sections of 'great' risk from rockfall and instability in rock and colluvium were identified at Starvation Point and between Candy's Bridge and Reid's Falls. The risks associated with additional cuts in these sections were to be mitigated with anchored Geobrugg cable netting and wire mesh. Rock bolt stabilisation was designed for a short section of cut batter immediately south of the Passing Bay rockfall protection structure. Also, stabilisation of all cuttings and scaling of loose rock blocks and wedges above cuttings was proposed.

Economic risk analyses were carried out to evaluate appropriate risk mitigation options for two sites. The risk to Candy's Bridge from debris flows which had previously occurred at 5 to 10 yearly intervals was analysed. A bridge structure with a robust deck, located down stream of the original bridge was indicated to be the most cost effective solution. The potential for renewed rockfall activity from a colluvium filled gully, just to the south of Starvation Point, was also considered. This suggested that it was more cost effective to defer mitigation, providing that the roading works would not prevent future mitigation should the rockfall become active.

The residual risk profile is greatly improved from the original profile as a consequence of this project. However, not all risks could be cost effectively mitigated at this site due to the nature of the topography. For example, mitigation of all risks of rockfall would require either continuous rockfall protection structures, or the road to be constructed in a tunnel. Such schemes would not be economically viable on current roading benefit/cost criteria, given the relatively low traffic volume of about 1000 vehicles/day.

Geotechnical Input to Route Optimisation

Geotechnical aspects of a number route options were assessed and integrated with other aspects of the design to evaluate the optimal route. Small shifts in alignment had major impacts on the height of cuts and extent of half bridging required. Cuts of up to 80 m in height were contemplated to minimise bridging, but the final option involved cuts of up to 35 m in height. The scope and cost of potential cut slope stabilisation measures was evaluated for cost comparison of the options.

Geotechnical Design

Geotechnical input and design was undertaken during the design phase of the project, as follows:

Rockfall Characterisation

Rockfall characterisation was required throughout the project but in particular for design of the Passing Bay rockfall protection structure. The extent of the rockfall hazard was assessed and the minimum length and location of the structure was defined. The typical and maximum size of individual rocks and volume of rockfall were evaluated by inspection of colluvial materials and historical records of rockfall. A design rockfall of 1 m diameter was adopted and an maximum impact energy of 810 kJ was evaluated from analysis using the Colorado Rockfall Simulation Programme (CRSP).

Cut Slope Stabilisation

A cut slope profile of 0.25H:1V (76°) was adopted for most cuts after examination of the existing cut batters and rock defects. The potential scope of cut batter stabilisation measures was developed for the proposed cuts and essential measures were included in the earthworks design. This included pattern rock dowels with an ultimate tensile strength (UTS) of up to 440 kN in the head of all cuts above 8 m in height. Anchored cable netting and wire mesh stabilisation was designed for Starvation Point rock cut, and for stabilisation of colluvium at the head of two other cuts.

Details were specified for provisional stabilisation measures including passive and tension spot bolting of various capacities, draped rockfall netting, HRC mesh and horizontal drainholes. Shotcrete was specifically avoided because it was not considered aesthetically acceptable. Most of these measures were used during construction, and some shotcrete stabilisation was accepted and implemented. The specified stabilisation represented 30% of the earthworks cost and the provisional stabilisation measures amounted to 20% of the earthworks cost.

Structure Foundations and Anchorage

Geotechnical input was required for the design of foundations and anchorage for various structures. The conceptual form of the structures is shown in Figures 2 to 5.

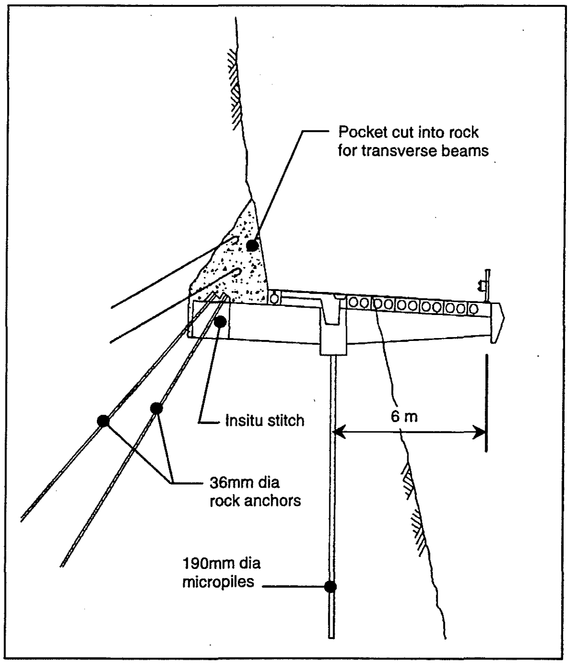

Figure 2: Cantilever Half Bridge

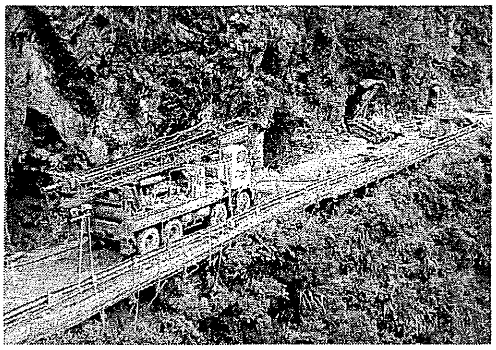

Photo 1: Pockets for Cross Beams and Piling Rig

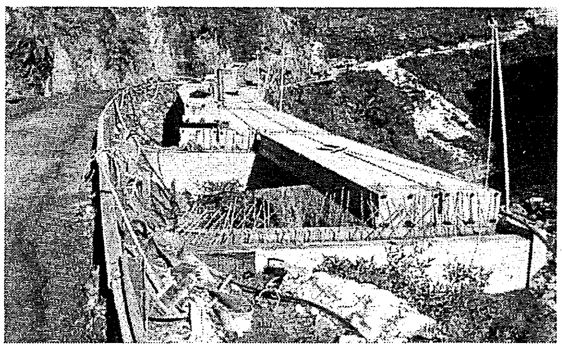

Photo 2: Cantilever Half Beams

Cantilevered Half bridging

Cantilevered half bridging with pre-cast double hollow core deck units on cross beams (12 spans), was adopted for a 94 m long section of highway between Reid's Falls and the Passing Bay (Photo's 1 and 2).

The cross beams were tied down with anchors and encased in rock pockets excavated within the rock on the uphill side of the road (Photo 1). The pockets provided adequate lever arm for the beams and added security to uplift. Two, 36 mm diameter, 1250 kN UTS anchors were installed at each cross beam. The anchors were double corrosion protected with plastic encapsulation and were pre-stressed to 65% of the bar UTS. The anchors were tested and installed to BS8081:1989 with three proving and suitability tests, and acceptance load testing on each anchor. The load test results indicated a rock to grout bond strength of greater than the 900 kPa, used in design.

Support for the downhill side of the cross beams was provided by a longitudinal pile cap on four, 190 mm diameter micro-piles per cross beam. The piles were required to carry the concentrated loading that would be applied to the generally poorer rock near the surface of the road bench. Multiple micro-piles, fewer 400 mm diameter piles, or a single 750 mm diameter pile, were considered. It was decided to adopt the micro-piles, because smaller and more manoeuvrable equipment could be utilised, which would be less constrained by the narrow road width and relatively steep vertical road gradient. The micro-piles also provided effective spread of loads into the rock mass below the road bench. The piles were up to 15 m in length. Permanent steel casing was installed in the top 3 m of the piles to ensure that the load was not transferred to the poorer rock at the ground surface. Potential failure mechanisms were assessed for the rock mass below the road bench and stability analyses, using Swedge and other slope stability software, were carried out to determine the minimum length of the piles.

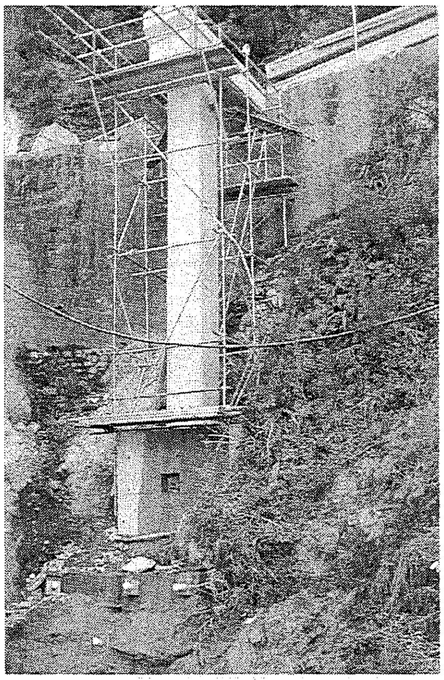
Photo 4: Propped Half bridge

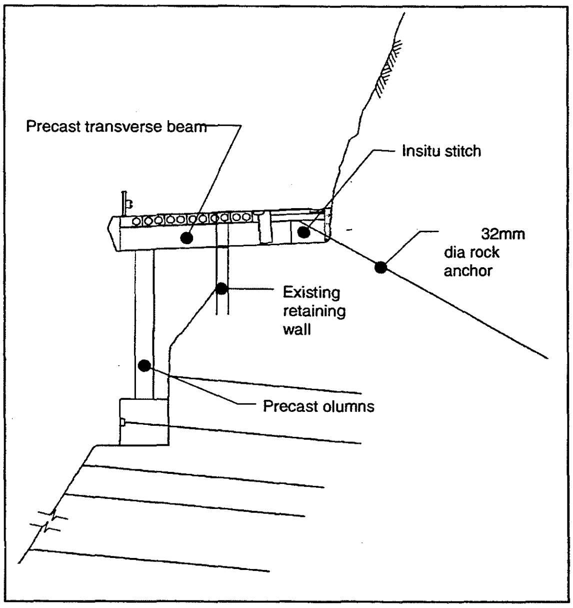

Figure 3: Propped Half Bridge

Propped Half Bridge

The 48 m long section of half bridging between the Passing Bay and Starvation Point (5 spans) was able to be supported on the outside by columns with pad foundations because the slope below the road reduced to about 50°. However a predominant joint set dips parallel to the slope and required anchorage of the column bases and additional anchors for stabilisation of the rock below. Also poorer rock was encountered at the northern most column foundation during construction, which required additional anchorage and a load beam between anchors immediately downslope from the column. Structural rock anchors were provided on the uphill side of each cross beam for lateral load resistance. The vertical load resistance was less critical than for the cantilever beams.

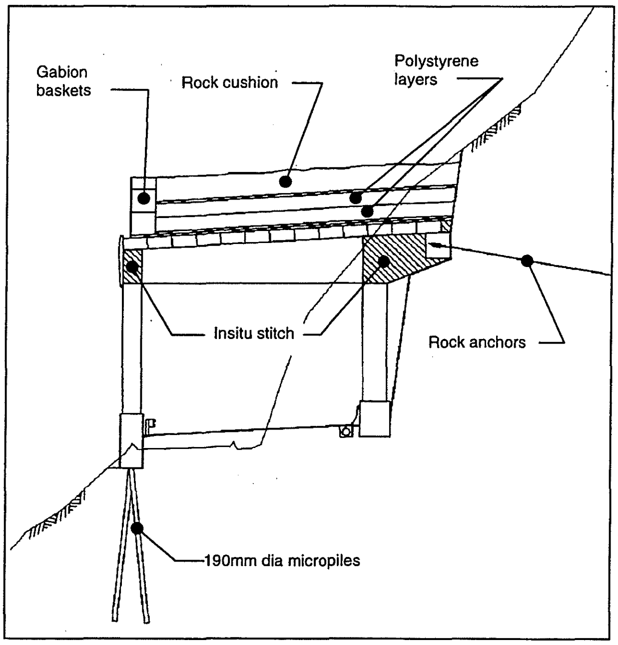

Figure 4: Passing Bay Rockfall Protection Shelter

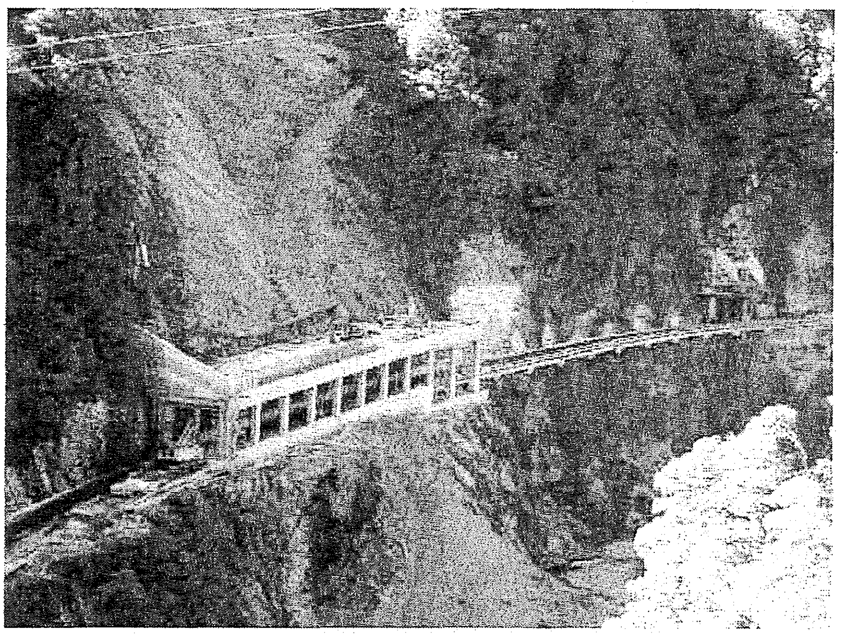
Photo 5: Passing Bay Rockfall Protection Shelter

Passing Bay Rockfall Protection Shelter

A 60 m long section of rockfall protection structure (Photo 5) was required at the Passing Bay (10 bays). A steep, self cleaning, rockfall protection structure was considered, but would have continued too far upslope and would have been vulnerable to impact damage. Instead a relatively flat roof framed structure was adopted (Figure 3). A cushioning layer of gravel, overlying polystyrene blocks, was included to absorb the energy and spread the impact load of the design rockfall. Design loading utilised South African and Japanese research, but judgement was required as no standards provide guidance on design for rockfall impact. The highway was widened by cutting 5 m into the uphill side of the road, and this allowed the uphill column of each frame to be founded on a continuous foundation beam. Micro-piles and a pile cap provide support for outer columns. Structural rock anchors tie the roof beam to the slope above the road and provide lateral seismic load resistance for the frames. The roof beams carry the vertical loading from rockfall debris, and no vertical support is required where the roof beam meets the rock slope.

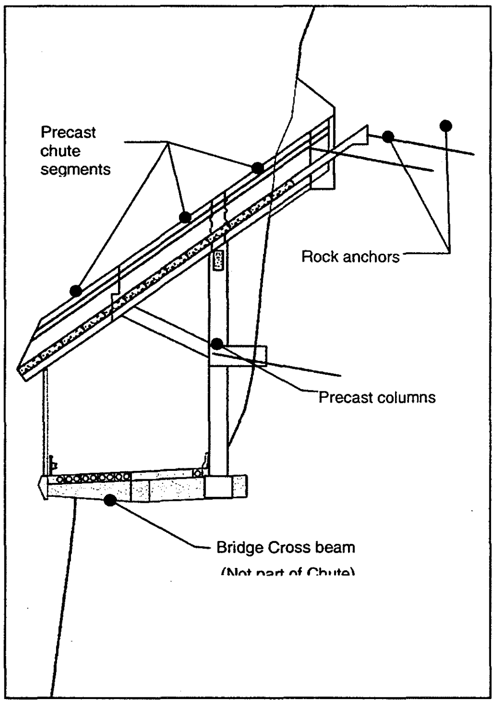

Figure 5: Reid's Falls Chute

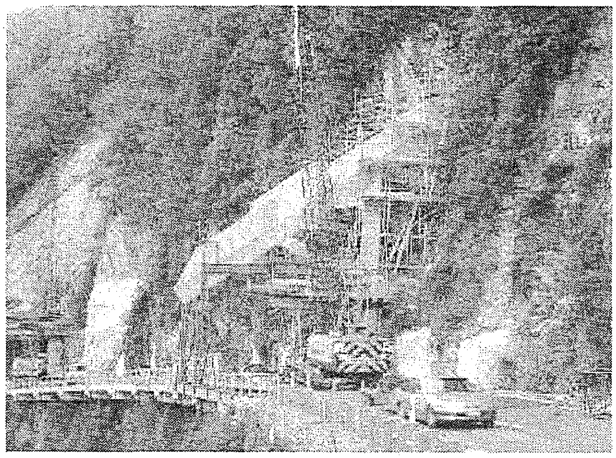

Photo 6: Reid's Falls Chute

Reid's Falls Chute

The water flow and debris loading of the stream at Reid's Falls is carried in a 20 m high, steep and narrow, U shaped chute over the highway (Figure 5 and Photo 6). The chute is supported by a diagonal prop from the uphill columns to avoid additional vertical loading to the outside of the cantilever half bridge at this location. The column is founded on a shallow pad foundation. Lateral support is provided by, structural anchors at two levels. A facia wall prevents wind from blowing water back onto the road.

Candy's Creek Bridge

A 40 m long bridge comprising four, 10m long spans, was designed at Candy's Creek (Figure 6). The original bridge abutments were reused and the bridge was widened in the downstream direction. The bridge was extended with three land spans. The bridge extensions were founded on 400 mm diameter, 12 m deep piles in gravel and boulders of Candy's creek bed. The piles have permanent casing to provide additional resistance to deformation.

The stability of the slope below the bridge is marginal, particularly under seismic conditions, and erosion may occur during flooding. Therefore, lateral and longitudinal resistance for the bridge was provided by structural anchors. These anchors are within gravel and boulders. Proof load testing proved that the skin friction and anchor capacity was greater than the required overall design skin friction for gravel of 300 kPa.

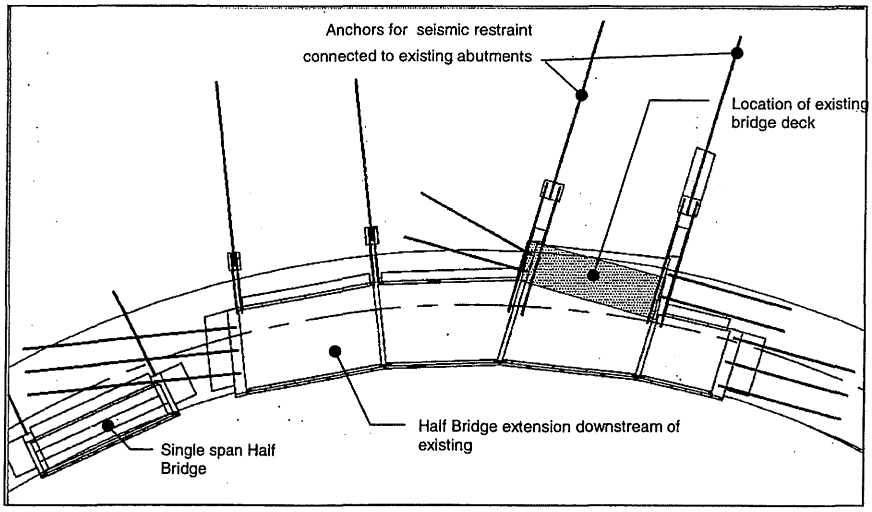

Figure 6: Candy's Creek Bridge Plan

Geotechnical Input During Construction

The contract was let to Fulton Hogan Ltd and work commenced in December 1998. Allowance was made in the contract for 60 days of full road closure, with a bonus for reduction in closure days. Public consultation indicated that the local community and interest groups preferred, a continuous 5 week closure in April/May between the summer and winter seasons, and two full day closures per week for the remaining 25 days. The contractor carried out sufficient critical work, before and during the 5 week closure and with 5 two day closures, to complete the rest of the project under intermittent road closures of not more than 20 minutes. The project was formally opened in June 2001, at total cost of $11.0 million.

Safety measures were adopted for workmen and the travelling public. These included rockfall netting above the Passing Bay rockfall shelter, fencing and barriers on the road side below cuts, and safety observation for rockfalls while workers or the public were in critical areas. A fatality occurred to a workman on site, due to impact from a boulder in the Passing Bay shelter area, before the roof was completed.

Hand work from safety ropes was required to clear vegetation from the head and face of cut batters and to commence excavation. A large box cut in bedrock at Candy's Bend was accessible by tracked equipment and was excavated by drilling and blasting with pre-split blasting of the cut face. The other cuts were relatively thin trims of less than 5 m into the hillside and these were excavated by hydraulic breaker on a small excavator on a crane supported platform.

An observational method was adopted for the assessment of cut batter stabilisation measures. Opus International Consultants' site engineer was on site throughout the project. He provided regular digital photographs by e-mail as excavation proceeded and carried out initial appraisals of potential instability. This maximised the effectiveness of assessment and site visits by the geotechnical engineer. Sections of cut requiring stabilisation were inspected and rock defects were mapped, to assist with design of appropriate stabilisation measures. Measures were designed for critical areas and the scope of stabilisation was marked up on digital photographs to assist location in the field.

A planar rock failure of about 10 m^3 in volume occurred on adversely orientated joints dipping steeply out of a cut face immediately south of the Passing Bay rockfall protection shelter. The failure occurred before planned rock bolting was installed and was exacerbated by the presence of a rock pocket for one of the cantilevered cross beams. This was subsequently stabilised with steel strapping, rock bolts, and shotcrete.

A localised area of colluvium at the head of a 10 m high cut, between Candy's Bridge and Reid's falls, failed just as the lowest row of anchors and bottom cable of the anchored and cable netting was about to be installed. The failure required a greater area of colluvium to be stabilised. An economic risk analysis indicated that on the balance of probabilities shotcrete would be the most costs effective solution, but the life of the treatment could not be guaranteed. This was accepted and a sprayed shotcrete surfacing was applied which linked into the previously installed anchors.

Photo 7: Passing Bay Rockfall Protection Shelter and Reid's Falls Chute

Conclusions

The steep mountainous topography, narrow road bench, severe climatic conditions and potential for rockfall and instability, made this a difficult and potentially hazardous project. Detailed geological mapping and identification of geological hazards along the route, provided the basis for developing appropriate models for stability analysis, and the inputs to risk assessment. The subjective risk assessment process allowed rationalisation of a wide range of diverse risks and highlighted which risks would require mitigation.

Rockfall characterisation by size and volume based on site observation, historical records and impact energy modelling, provided the basic inputs for design of the Passing Bay rockfall protection structure and Reid's Falls Chute. The unusual structures which were adopted enabled a cost effective and acceptable solution to be implemented. Details, such as utilising rock pockets and structural anchorage of the Cantilever Half Bridge cross beams, reduced design loading to acceptable levels while providing a measure of redundancy. Micro-piles provided a robust solution for the support of the outside of the cantilevered cross beams, where load was concentrated near the bluffs below the road bench.

Careful consideration of the potential construction process and build-ability of the project at the design stage, combined with the contractors endeavours, contributed to the success of the project. The observational approach to cut batter stabilisation enabled cost effective and appropriate measures to be implemented and maximised the value of geotechnical input during construction.

The project has provided a two lane highway throughout this section of state highway 73 and has significantly reduced the risk profile for the travelling public and Transit New Zealand, the roading authority. The level of risk to road users is now consistent with other parts of the state highway through the Otira Gorge.

References

Maylin, M (2000) "Design Aspects – Candy's Bend Road Widening Arthur's Pass" *Proceeedings NZ Concrete Association Annual Conference 2000*, Wairakei.

Yetton, M.D., Wells, A. and Traylen, N. (1998) "*The Probability and Consequences of the Next Alpine Fault Earthquake*" EQC Research Report 95/193, March 1998.

Acknowledgements

I wish to thank Transit New Zealand for permission to publish this paper.

My main acknowledgement goes to Consulting Engineering Geologist, Brian Paterson who provided valuable input to the early stages of the project and who's sudden death, due to ill health, meant that he did not get to complete this project in one of his favourite geological play grounds.

I also acknowledge the various members of the Opus design team, Deane McNulty the site engineer, and Fulton Hogan who combined to make this a successful project.

Roading in Northland Allochthon Terrain – Auckland and Northland

Glyn RW East
Opus International Consultants Ltd

Aaron K George
Opus International Consultants Ltd

Abstract

Roading in the Northland Allochthon terrain is problematic. The Northland Allochthon forms more than two thirds of the rocks in the Northland region and extends south as far as Auckland. Although typically undulating with gentle slopes, the Northland Allochthon is known for slope instability problems that pose particular hazards to roading development.

This Paper addresses what the Northland Allochthon is, its geological history, the rock and soil units present and particular hydrogeological features. The paper will outline hazards the Northland Allochthon geological terrain can pose to roading development, with particular examples drawn from major roading developments including the ALPURT Sector A2 (Redvale to Silverdale) motorway, the Kamo Bypass, and slips throughout the State Highway Network in Northland including Whirinaki Hill.

Roading design in Northland Allochthon Terrain to date has successfully been undertaken with an emphasis on a terrain evaluation approach, rather than an analytical approach, when addressing the design of cut slopes. There is an economic risk in construction, which if arbitrarily adopted could preclude roading projects from being funded.

Introduction

Geological Setting

The rocks that form more than two thirds of Northland originally accumulated on the floor of the deep ocean several hundred kilometres northeast of present day Northland between 80 to 25 million years ago, as fine-grained sand, mud, limy shells and planktonic ooze. Over time these sediments consolidated and hardened into sandstone, mudstone and muddy limestone. Further east large volumes of basaltic lava were erupted onto the ocean floor forming oceanic crust.

Approximately 25 million years ago, the boundary between the Pacific and Indian-Australian tectonic plates became active through the New Zealand area. The leading edge of the south-west moving Pacific plate was pushed down beneath ancestral Northland, carrying the ocean-floor sandstones, mudstones, muddy limestones and lava flows along on top of it. As these rock layers collided with Northland, they were scraped off the down-going plate and pushed upwards out of the sea in a layered stack. With further pushing from behind, huge slabs of these rocks (as much as 2km thick and up to hundreds of square kilometres in area) were peeled off and thrust on to Northland from the northeast. The top or youngest layers of rocks were scraped off and thrust in first, followed later by successively deeper and older rocks and lastly by the ocean-floor basalt flows that had accumulated further to the east.

As the slabs were thrust on to Northland from the northeast, about 25 to 22 million years ago, ancestral Northland subsided and was flooded by the sea to depths of several thousand metres. Consequently not only were these giant, uplifted slabs of displaced rocks thrust on to Northland, but many of them continued to slide westwards and south westwards under the pull of gravity into the deepening sea areas. As these slabs continued to thrust further on to Northland, many broke up into smaller blocks and more mixed, sheared and chaotic layers developed between the more cohesive blocks of harder rocks (Hayward et al., 1989).

The slabs of lava flows, sandstones and limestones were harder and stayed more intact and today commonly form quite large areas of Northland. Slabs of ocean-floor lava flows now form many of the more rugged mountain areas, such as the Mangamuka, Herekino, Warawara, Mangakahia, and Tangihua ranges. The muddy limestone is quarried on farms in many parts of Northland and is also the main raw material for Wilson's cement works at Portland, near Whangarei.

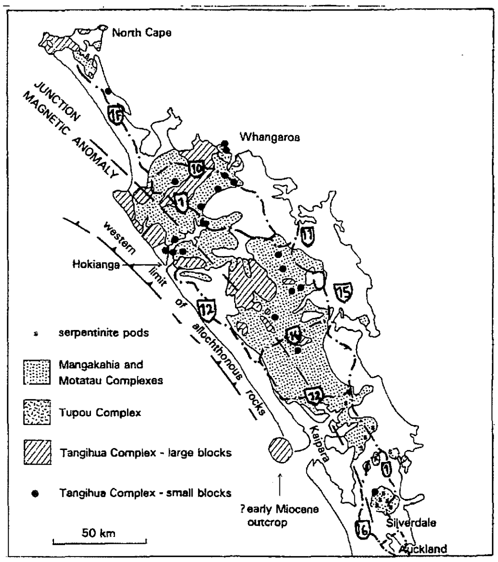

Fig.1 Outcrop distribution of Allochthonous rocks in Northland. Transit New Zealand State Highway network has been overlaid. (After Hayward et al. 1989)

The deep-water mudstones on the other hand, are rich in clays and when mixed with water readily flowed and helped lubricate the movement of the huge blocks of rocks as they were displaced up to 200 or 300km west and south across Northland. These slide blocks reached as far south as Redvale and Dairy Flat, just north of Auckland as sheared blocks incorporated into the Waitemata Group.

Many parts of Northland today are notorious for their instability and are highly prone to slumping failures. These are mostly underlain by the clay-rich mudstones or chaotic mixed units with their sheared mudstone matrix. As time has gone by the more resistant slabs of displaced lava flows remain standing as the highest ground, while the softer mudstones and sandstones have eroded and undergone slope movement to form gently rolling hills.

Dominant Units Associated with the Northland Allochthon

The Northland Allochthon is comprised of four main geological units that include the Tangihua Complex, the Tupou Complex, the Mangakahia Complex, and the Motatau Complex. All these units can pose difficulties related to shearing and degradation associated with their emplacement. Of primary concern however, to roading development, are the sheared mudstone units comprising the Mangakahia Complex. Figure 1 above shows the widespread extent of these units across the Northland Region.

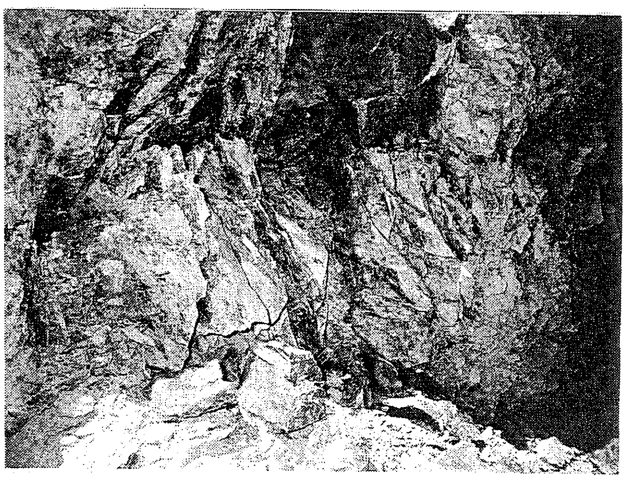

Photograph 1: Typical sheared Onerahi Chaos mudstone with highly polished fractures. The rock had undergone stress release dilation and fell apart on handling.

In the past the units of the Mangakahia Complex and Motatau Complex units have been assigned the terms Onerahi Formation, the Onerahi Chaos Breccia, or more typically the Onerahi Chaos. Although current geological terminology has abandoned this term with respect to stratigraphic and structural implications, Engineers still use the term to describe the material type. Hence the Onerahi Chaos term is commonly accepted and used as an Engineering Lithological Unit (IAEG, 1988) of the sheared mudstone varieties, which are typically unstable in the Northland and Auckland regions, and as such is useful to use.

The Onerahi Chaos consists of grey sometimes black and chocolate brown very fractured and sheared weak mudstone/muddy limestone with slickensided and polished surfaces, some with clay matrix. Smectite content (measured by Clay Index) decreases with increased limestone. Correspondingly relative frictional strength along the fractures decreases with a decrease in limestone content (Toan, 1981).

Typical Engineering Conditions

Slope Engineering Conditions

The Northland Allochthon is known for slope instability problems that pose particular hazards to roading development. Roading in Northland Allochthon geological terrain is most problematic primarily with respect to natural slope and cut slope stability.

Natural slope failures develop as an apparent intermittent viscous fluid creep type failure, where toe bulging can occur downslope without necessarily any ground breaking occurring. Graben type terracettes often occur below the head scarp area with typical drop heights ranging from 0.5m to 1.0m. In general such failures commence on the lower flanks of ridges and regressed to the ridge divide and can be considered a phase of ongoing "slope flattening". The size of natural slopes vary from 0.25ha to some 10ha depending on the topography.

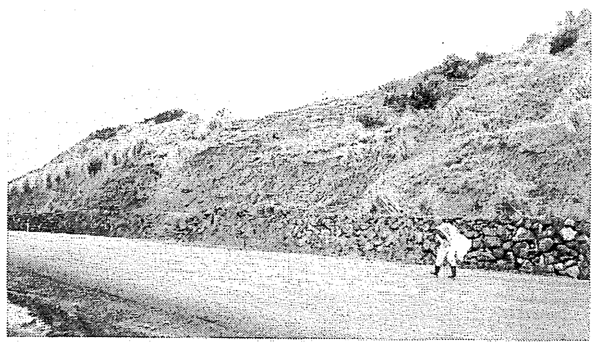

Photograph 2: Whirinaki Hill. Overslip in a cut batter with limited toe support.

Cut slope failures initiate with toe dilation followed by progressive displacement and wetting and drying that softens the material to then regress rapidly upslope and extend laterally across slope. As the slip develops the toe is often thrust out from the toe of the original cut batter slope. The head scarp areas are similar to natural slope failures.

Other Engineering conditions

With the construction of fill embankments in Northland Allochthon terrain note should be made of where proposed fills cross natural slope failures. A common instability feature in roading involves shallow embankment fills constructed over an apparent dormant gully head scarps as part of a geometric shape corrections which leads to ongoing underslip problems. In recent new road construction the remnant slip is undercut and the fill keyed into a more stable foundation.

With other engineering conditions such as bearing capacity (piles), and recompaction properties for bulk fill and subgrade fill Northland Allochthon materials pose no particular problems for designers.

Hazards To Roading Development

- Natural failures are nearly always underslips that cause problems ranging from poor ride and high roughness to vertical Graben drops in the pavement up to 1m at a time.
- Cut slope failures are generally overslips that can cause Highway blockages and damage to upslope property. Without remediation these slips continue to fail rapidly regressing upslope and extending laterally across slope.

The consequences of these types of failures are high roughness, a reduction in road width and higher maintenance costs. This results in a corresponding reduction in road safety and an increase in user costs.

Engineering Properties

Engineering Bore logs in Onerahi Chaos (Northland Allochthon)

A bore log for engineering purposes requires the log to include properties that have some engineering significance and may perhaps be indexed to insitu tests carried out in the borehole. Of significance in the Onerahi Chaos material of the Northland Allochthon is the presence and amount of clay/silt matrix within the fractures, as an indication of whether the material acts as a soil or fractured rock. Opus has used a grading (Table 1) similar to the rock-weathering grade to differentiate the sheared Onerahi Chaos mudstone material. Of particular note is that slope instability generally lies within the grade II to III materials.

Northland Allochthon (Onerahi Chaos) Physical Degradation Description		
Grade	**Generalised Structure**	**SPT N blows/ 300mm**
Completely weathered Onerahi Chaos soil (V-VI)	Firm to stiff silty clay.	3 - 5
Highly degraded Onerahi Chaos "rock/soil" (IV)	Firm/stiff slightly structural clay. Firm plastic clay with claystone / siltstone / muddy limestone clasts.	1 - 20
Moderately degraded Onerahi Chaos "rock" (III)	Very fractured slickensided and polished very weak grey black and chocolate brown claystone / siltstone / muddy limestone in a clay / silt matrix.	20 -60
Onerahi Chaos "rock" (II)*	Very fractured slickensided and polished weak grey claystone / siltstone / muddy limestone with some clay matrix.	60+

Table 1

* Because of the deposition process Onerahi Chaos Grade II can be expected to contain occasional crushed weak zones within the more competent fractured rock.

Another useful logging tool is the use of a crushing/shearing index on the logs to augment the description of the material. This index applies a numerical value of 0-10 to the degree of physical shearing and degradation of the unweathered rock/soil mass. The following index (after Gage and Black 1979) developed for similar rock terrain on the east cape of the North Island, uses an overall scale from 0-10:

0 = massive, virtually free from joints, shearing and crushing.

1 = significant jointing, no crushing or shearing, no displacement between joint separated fragments.

2 = discernable crushing; slight dislocation of joint fragments, and/or shearing (traces of slickenside polish, but little loss of overall strength).

(and so on to -)

10 = totally crushed and sheared to large and small fragments with slickenside polish, embedded in pug; overall strength very low.

Some Typical Properties of the Onerahi Chaos (Northland Allochthon) Mudstone

The fractured structure of the mudstone is such that the index and engineering properties are confined to disturbed samples or insitu testing. The following are typical values of the various properties for the mudstone although values outside these ranges are not uncommon (see Table 2).

Water Content	15 to 20
Calcite Content	0* to 25%
Clay Index	7* to 25
Standard Penetration Test SPT	20 to 60 blows/300mm
CPT Cone Resistance	6 to 20 MPa
Pressuremeter Limit Pressure**	0.5 to 3 MPa
Permeability (Rising Head)	10^{-7} to 10^{-11} m/s

Table 2

* Low range boundaries as reported by (Toan 1981).

** The insitu pressuremeter is the only practical direct test to confirm the undrained strength of the fractured mudstone for foundation design. Relationships have been developed between pressuremeter results and the more common SPT or CPT testing, from comparison testing such that the latter test results can be used as a guide to the undrained strength.

Effective Stress Properties

The slope mass effective stress strength parameter of the Onerahi Chaos (Northland Allochthon) mudstone within the overall slope controls the stability conditions. In this material this is dependent on both the internal friction of the fractures and/or matrix and the dominant direction of the fractures. Experience has indicated that the direction of the fractures relative to the slope direction appears to dominate the gross effective stress strength. For this reason the results of triaxial and shear box testing are likely to be misleading and terrain evaluation of existing or constructed cuts is likely to yield more appropriate values.

To obtain the true value of the slope mass effective stress strength of a slope, rather than the angle of repose, from terrain evaluation, some knowledge of the piezometric conditions are required for a back analysis. This generally would require the installation of piezometers within the slope although an assumption can be made that the piezometric level is at the ground surface. Using this approach, and assuming that in the overall slope, the material is solely frictional, a slope mass angle of friction (ϕ') of some 20^{o} has been found to be a lower bound for most slopes that fail in Northland Allochthon geology.

Theoretically, the angle of repose for a slope with a slope mass angle of friction (ϕ') of 20^{o}, with a Piezometric level at the ground surface, is some 10^{o} or 5.5V:1H. Higher slope mass angles of friction typically exist depending on the dominant direction of the fractures relative to the slope direction. The trial cut slopes at the Alpurt Motorway indicates a slope mass angle of friction of some 26^{o} to 29^{o}.

Factors That Influence Slope Stability

Hydrogeological Conditions

Piezometric head typically increases with increasing depth and is commonly "artesian" at a depth of 10 to 20 metres. The piezometric head does not appear to be related to local infiltration or influences of local topography. It is not unusual to find artesian groundwater levels at the top of ridges during periods of dry weather.

High piezometric heads are more likely related to confined water bearing fractures, (some with high flows) within the rock mass material and the low permeability of the rock mass. Typical rates of permeability for the Onerahi Chaos rock mass are range from 10^{-7} m/s to 10^{-11} m/s.

Macro Structure

Shear surfaces in Onerahi Chaos rock on a macroscopic scale can have a dominant direction in local areas. Consequently the orientation of cut slopes in Onerahi Chaos rock with respect to a dominant shear direction can result in stable cuts being steeper or shallower in a similar way to bedding orientation in other lithologies. This macro structure appears to dominate the slope mass angle of friction.

Subsequent to the emplacement of many of the units in the Northland Allochthon, particularly the widespread sheared mudstone, ongoing "slope flattening" due to past slope movements has resulted in mélange zones where the macrostructure of the sheared mudstone rock has degraded and softened. These mélange zones consist of sheared mudstone clasts suspended in a matrix of soft to firm clay. They can contribute significantly to natural slope instability, resulting in slope failures in Onerahi Chaos occurring on slopes as little as 6H:1V.

In some situations both the above conditions can exist where shallow failures overlie potentially deeper failures. This would necessitate the remedial design to take into account both failure mechanisms.

Insitu Stress Conditions

It is postulated that insitu stress conditions are such that K_0 is near or greater than unity. This condition can initiate slope instability after excavation commencing with dilation of the fractured rock mass at the toe, which on displacement and wetting and drying softens to then begin regressing upslope into a larger feature.

Natural Topographic Relief

Generally results in moderate to low relief slopes in the order of 20 degree or less. Where the limestone contents increase or fracturing is less dominant the slope can range to up to 45 degrees. This is the primary tool for terrain evaluation.

High Risk Scenarios

Two situations exist where conditions could be described as a "high risk" scenario:

Natural slopes: Soil slopes softened by past slope movement combined with a high Piezometric head from hydrologically confined fractures. Slopes with the above conditions have an angle of repose of as low as 10 degree (6H:1V) but the more typical repose angle is 20 degree.

Cut Slopes: Highly fractured mudstone, downslope dominant shears, and high Piezometric head from hydrologically confined fractures.

Methods Of Evaluation For Cut Slope Design

Standard geotechnical investigations including borehole drilling, test pitting, and posthole work, will identify most soil and rock units, however they will not necessarily identify key factors that may cause a problem.

Because of this the following methods of evaluation in addition to a standard geotechnical investigations are necessary:

Terrain evaluation (Dominant Method): Due to the difficulties in determining meaningful effective stress strength (c', ϕ') properties in sheared mudstone materials, cut batter design will often rely on terrain evaluation in the first instance. This will involve assessing natural slope inclinations for identified soil and rock units, i.e. which slope inclinations are stable and which are not for given material types. In addition it will highlight areas where localised steepening and flattening of cut slope batters may be required. It may also identify areas where additional geotechnical testing may help to resolve design difficulties.

Trial cut: If a project is large enough and sufficient time is available, it is desirable to undertake a trial cut scenario in materials that are typical to the project. Different cut batter designs are constructed and then monitored to assess each performance, with the use of visual monitoring, inclinometers, and piezometers. The types of failures that occur and the typical mechanisms and conditions of failure can be assessed to determine appropriate remedial solutions prior to the main phase of construction. This is invaluable in determining contingency cost for earthworks in a large-scale project.

Note 1: When using both terrain evaluation and trial cuts to determine cut batter design it must be accepted that a traditional equilibrium factor of safety of 1.5 cannot be guaranteed. All that is known is that natural slopes (and the trial cuts) that are not failing have a safety factor in excess of unity. For slopes that have a high consequence of failure, slope flattening and deep drainage is undertaken (bored drains) to increase the factor of safety over the slope evaluated by the terrain evaluation.

Note 2: The use of trial cuts over one section of a project to determine cut batter design does not guarantee that the design can be transported over the whole project. As mentioned previously, the stability is highly dependant on the dominant shear direction, which is highly variable. Combining the trail cut with terrain evaluation will minimise the risk of an inappropriate cut batter design but the risk remains high.

Note 3: Probabilistic techniques may offer a more qualitative approach but the number or variables are significantly greater than slopes in more homogeneous autochthonous terrain. More significantly some of the factors, notably the slope mass angle of friction that results from the dominant shear direction, and the piezometric conditions, would be difficult to statistically quantify over any length of highway. Probabilistic techniques require a reasonable evaluation of the mean and standard deviation of the various factors that influence the slope stability.

Methods Of Slope Stability Remediation

- To drain the confined water bearing fractures and reduce the piezometric head deep sub-surface drainage, generally utilising deep bored horizontal drains, is undertaken.

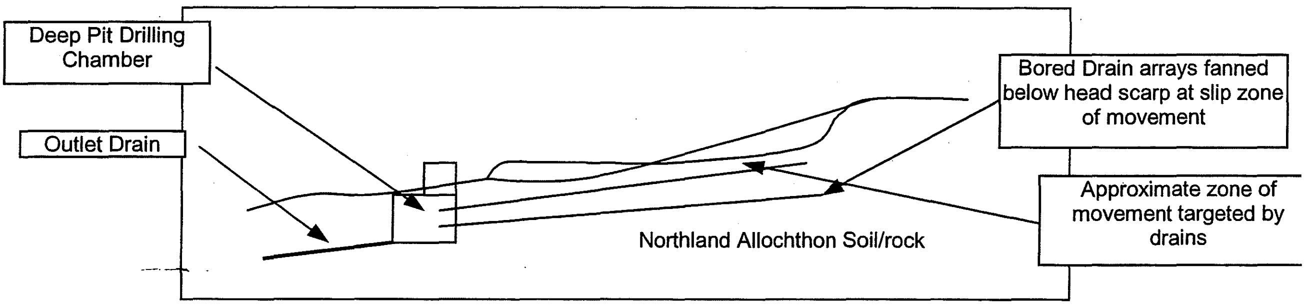

- Toe support using Gabion or rock buttresses is also utilised to alleviate the initiation of dilation and regressive type failures in cut slopes.

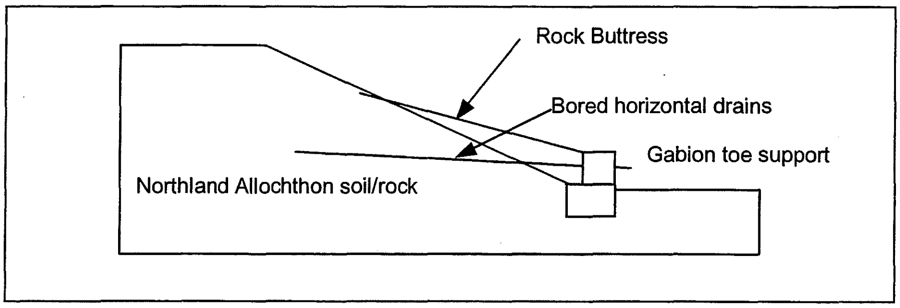

- Another cut slope remedial measure involves capping a batter with compacted soil to alleviate dilation resulting from stress release perhaps in combination with bored drainage to drain the confined water bearing fractures (see next page).

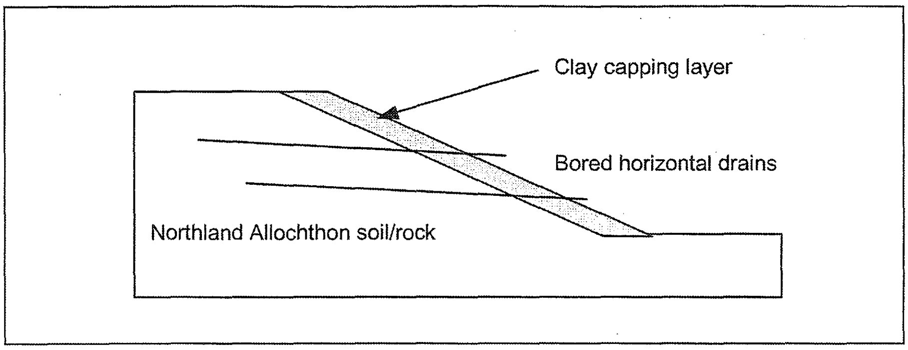

- Pile pinning walls, typically used in more competent geology, are not recommended unless it is known for certain the position of the failure plane. Inclinometer evidence from slope movements in Northland Allochthon terrain have shown failure planes that are kinematically unusual or unlikely compared to what would be expected elsewhere.

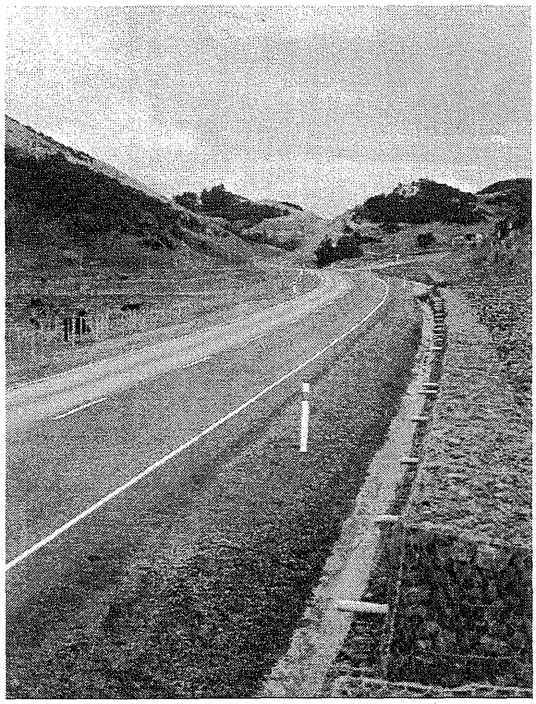

Photograph 3: Whirinaki Hill. Toe buttress support in the foreground, box cut in the background (see Photograph 2).

Photograph 4: Prides Slip SH16 – Construction of deep pit drilling chamber. Horizontal drains are drilled through E-Sections.

Case Histories

ALPURT Sector A

The ALPURT Sector A project was a 16km long "Greenfields" extension of Auckland's Northern motorway. The northern half was constructed in Northland Allochthon Terrain from the Okura River to Silverdale. The alignment required a number of cut slopes up to 15 metres in height. A terrain evaluation approach was utilised to determine the stable slope angle of existing cut batters based on cuts along local roads and the nearby Redvale Quarry. This was followed by a trial cut undertaken during the enabling phase of the construction. This was cut in an area that was to have a large cut built during the main construction phase of the project. The trial cut consisted of three cut batters cut at 2H:1V, 3H:1V and 4H:1V. Inclinometers were installed above each cut along with sealed piezometers. Following 6 months of monitoring over the winter and before the main phase of construction was set to begin. The 2H:1V batter had failed, and the 3H:1V batter had shown signs of cracking that would lead to failure with time. The 4H:1V batter showed no signs of failure.

A 4H:1V cut batter design was adopted for the project, which encountered mostly Onerahi Chaos rock. A 1m thick clay-capping layer was incorporated to stop dilation failures and bored drains were spaced at 5m intervals across the batter. Provision was allowed in the contract for the construction of Gabion toe and rock buttresses if failures were to occur during construction. A simplistic frictional back analysis of this condition (ru=0.4) results in a theoretical safety factor of some 1.2 to 1.4 based on the slope mass angle of friction obtained from trail cut(s) performance. A probability of failure as high as 1 in 1000 can be assessed using a probabilistic approach largely because the standard deviation of the slope mass angle of friction can be qualified from the trail embankment to a moderately low value.

Localised areas immediately north of Okura River had cut batters of 3H:1V where terrain evaluation indicated this would be possible.

This approach in the end was largely successful, with only two minor slumps occurring in two of the larger cut batters some 3 years after construction.

Whirinaki Realignment

This project was a 2km realignment of SH12 south of the Hokianga Harbour in Northland. The realignment required a number of box cuts some 15m high in Northland Allochthon terrain during the late 1980's. Terrain evaluation was undertaken however a traditional design approach was subsequently used where benched batters were constructed without toe support, clay capping or deep bored drainage. A large proportion (some 25%) failed within the first year after construction and continues to fail. Some portions of cuts have been remediated with toe support and deep bored drains with various success.

Happy Valley Slip Repair

This project involved a typical natural slope slip repair in Northland Allochthon terrain. The 100m long section is typical of slope movement for some 30km of State Highway 1 north of Okaihau in Northland. The highway corner had been built as sidling fill across the head scarp of an historic slip some 120m wide and 300m long. The slip is in very subdued topography and consists of sheared clay and mudstone mélange overlying sheared and fractured mudstone rock. The slip had intermittently moved over many years resulting in cracking and undulation in the pavement and a bulging toe. The slip had required ongoing maintenance and a considerable thickness of asphalt lay in the slumping head scarp. Deep pit drainage is the method used for slope remediation.

Orewa Bridge Replacement

This project involved replacing the then SH1 Bridge over the Orewa River north of Auckland. Associated with this was a realignment of the southern approach to the bridge that required moving the road some 20m further east into an unstable cut in Northland Allochthon terrain. Following a terrain evaluation, a standard geotechnical investigation augmented with inclinometers and sealed piezometers was undertaken, which successfully identified the depth of shallow slope movements that had occurred at some 5m to 6m in a mélange zone near the soil rock interface. Following this a large reinforced concrete bored pile wall was utilised to support the slope with success. The design of the retaining wall as well as addressing the shallow movement encountered in the inclinometers was also designed for potential movements deeper down in the rock some 9m below ground surface. The reason for this was the high risk posed to properties upslope behind the wall and to the State Highway by any unidentified failure zone in the rock.

Kamo By Pass

This project was a 3km realignment of SH1 by passing Kamo town ship north of Whangarei in Northland. The road was to be constructed in non-Allochthonous geological units west of a Northland Allochthon slopes. During construction the excavation of more recent basalt materials uncovered a localised remnant of Northland Allochthon materials that had penetrated into the underlying geological units severely weakening the structure of the material. This was not identified during a standard geotechnical investigation including a terrain evaluation. Before remedial measures could be undertaken the batter failed during a period of unseasonable rainfall putting at risk a railway line upslope and threatening to delay completion of the project on time. Subsequent remedial measures, including associated costs, were well in excess of the earthworks contingencies for the project.

A New Northland Roading Project

A current scheme assessment for a 3km "Greenfields" road proposed within Northland Allochthon terrain. Current evaluation using photogrammetry has indicated severe risks to the cost assessment and the viability (B/C) of the project.

Geotechnical Hazard And Project Risk

All geotechnical assessments and design involve an element of risk even after extensive site investigation and testing. The higher risks generally result from an unknown geological or geotechnical hazard where the consequence is deemed to be severe to the project and the risk is rated as high. This risk broadly belongs to the commonly referred to "Unforeseen Ground Conditions". The geotechnical specialist is required to qualify the likelihood of the hazard and quantify this risk prior to construction, with a mitigation cost to be included in the project contingencies. With Transit New Zealand projects it is now mandatory to undertake a project study to identify and rank all risks (TNZ Z/10).

In Northland Allochthon terrain, instability is a known significant geotechnical hazard in roading even with relatively conservative geotechnical design. In this case the hazard is that the magnitude of the instability conditions cannot be meaningfully quantified prior to construction. Unlike less hazardous terrain it could never be economic to mitigate totally the known risk as part of the construction. The geotechnical specialist can only make some judgement as to likelihood of the magnitude of the actual and potential instability hazard, the likely factors present that may influence the stability, and then assess the risk. From this judgement generic stabilisation methods can be designed for use where required and a corresponding remediation cost estimate generated to be included in the project contingencies. With new roads and major realignment construction such a contingency estimate could be significant, relative to the project's construction estimate.

The contingency budget needed for a project within Northland Allochthon terrain may, for new road construction or realignments decrease the Benefit Cost Ratio (B/C) to an extent that the project is at risk of not being funded.

The relative contingency estimate is likely to be higher for new construction than for the upgrading of existing roads. The extent of instability is largely known on existing roads and while the factors that influence the stability are not completely known until construction is under way a stabilisation method(s) has been chosen that can generally be made to work. Hence the costs associated with upgrading existing roads can be better quantified.

Mitigation Of The Geotechnical Hazard And Project Risk

It is difficult to mitigate the geotechnical hazard and the corresponding risk due to the difficulties in identifying factors influencing the instability conditions, and quantifying the magnitude of the instability condition.

There is little value gained doing more geotechnical investigation than is carried out less hazardous terrain during the design stage. While geotechnical investigation may recognise the potential for instability, it will not necessarily quantify the risk.

The client and project manager need to take account of the geotechnical risks in developing the contingency estimate. For the same level of risk, construction in Northland Allochthon geological terrain, and similar, will be significantly higher than construction in less hazardous terrain.

The contingency estimate may decrease the Benefit Cost Ratio (B/C) for new construction and realignments in Northland Allochthon terrain to a degree that the project may not satisfy the criteria for funding. This may result in it being more appropriate to consider upgrading the existing highway where the risks can be better quantified ("do minimum") despite the strategic advantage of a new road with higher safety and economic benefits. Probabilistic techniques for estimating geotechnical contingencies has some promise and may be appropriate for a single slope failure. At this stage the variables, notably the slope mass angle of friction that results from the dominant shear direction, and the piezometric conditions, would be difficult to statistically quantify over any length of highway.

In view of the above, the following initiatives, could be considered by Transfund or Transit New Zealand:

(i) The client could make some decisions as to the rating of the consequences and the risk when constructing in Northland Allochthon terrain. As an alternative to funding the potential instability within the project the client could, where practical, leave some, if not all, of the instability that results from the construction to be repaired as part of later maintenance or a "flood damage" project. This is very unsatisfactory both a technical and publicity reasons. From a technical point of views instability in Northland Allochthon will regress and extend rapidly making any stabilisation measures significant more difficult and costly.

(ii) Stabilisation costs due to instability could be separated off, and set against projected maintenance budgets. If the failure had occurred subsequent to construction this is where the costs would lie.

(iii) To designate special areas in NZ where projects can proceed without the strict Benefit Cost Ratio guidelines applied elsewhere in less hazardous terrain.

(iv) To specifically designate the road as strategically necessary.

(v) To review the use of the contingency estimated as part of the project construction cost and Benefit Cost Ratio. There may be a case for the contingencies of all projects put forward for funding to be placed in a separate national funding pool and separated from the calculation of the Benefit Cost Ratio. The risk management procedures could be used as a means of documenting the cost contingencies for each project.

Summary

- In any new road construction the Allochthonous nature of the material is such that the potential or magnitude of instability cannot be predicted with any certainty. Mitigation measures can be put in place but it is not generally cost effective to treat the full length of any road construction for instability. As a general rule it is better to have in place methods to treat those areas that do fail during construction. This results in very uncertain cost contingencies for new works and a possible relatively large increase from that estimated at design. There need to be a full understanding between Transit New Zealand, Transfund, and the design consultant of this situation prior to the commencement of the project.
- While geotechnical investigations are necessary to identify the potential for instability in new road construction they are unlikely to predict if, or where, instability will occur or the extent of instability. Little value would result from increasing the quantity of investigation testing.
- Terrain evaluation using photogrammetry and detailed inspection, appear the best tool to evaluate the potential of instability of existing highways and new road construction. New road construction may require the use of trial cut excavations as part of the investigation.
- Further displacement and the magnitude such displacement on an unstable section of an existing highways cannot be predicted with any certainty.

- Apart from minor slip repairs ("Flood Damage") projects are required to satisfy a Benefit Cost Ratio to obtain funding from Transfund (currently 3.5). The use of Benefit Cost Ratio to satisfy funding criteria when constructing in Northland Allochthon, or similar geology, cannot be accurate when the geotechnical contingency is added to the construction estimate. The potential for instability is such that whatever contingency estimate is applied to the overall construction cost to generate the Benefit Cost Ratio it would be, at the best, an educated guess. Probabilistic techniques for estimating the geotechnical contingencies have some promise but more research is needed into statistically quantifying the variables.
- This points to a requirement for different criteria of funding for road construction or major slip repair in such geology. The use of a true Benefit: Cost criteria would likely mean that no road construction would be funded in this type of geology. Perhaps the mitigation measures necessary in new construction should be set against projected future maintenance costs. Alternatively special areas could be zoned in New Zealand where, for strategic reasons, the ranking of Benefit Cost Ratio is set aside. More controversially some consideration could be given to funding all contingencies in road construction nationally and separating the contingency estimate from the calculation of the Benefit Cost Ratio.

References

Gage, M.; Black R.D., 1979: Slope Instability and Geological Investigations at Mangatu State Forest. *New Zealand Forest Service Technical Paper No. 66 O.D.C. 114:116 – 014.1*

Hayward, B.W.; Brook, F.J.; and Isaac, M.J., 1989; Cretaceous to Middle Tertiary stratigraphy, paleogeography and tectonic history of Northland, New Zealand. Geology of Northland: accretion, allochthons and arcs at the edge of the New Zealand micro-continent / editors, Bernhard Spörli, David Kear. Wellington, N.Z.: *The Royal Society of New Zealand Bulletin 26, pg 47-64.*

I.A.E.G. 1981: Rock and soil description and classification for engineering geological mapping, Commission on engineering geological mapping. *Bulletin of the International Association of Engineering Geology 24: 235-274.*

Toan, D.V., 1980: Report on Onerahi Chaos Breccia for Rodney District Council. *Beca Carter Hollings and Ferner Ltd*

Transit New Zealand: Minimum Standard - Assessment of Risk Z/10.

Rock fall remediation along the Torrens River Valley, Adelaide.

A. G. Meyers
Mining Engineering, University of South Australia

R. A. Herraman
Transport SA.

J. R. Blyth
Transport SA.

Abstract

In 1999 and 2000 several large rockfalls and wedge failures blocked Gorge Road, which follows about 20km of the Torrens River Valley in the Adelaide foothills. Subsequent investigation of the high, steep slopes along the road indicated that many of them were in poor condition due to weathering. The safety issues resulting from rockfalls are compounded by much of the road being narrow, having poor sight distance and having little or no clear-fall zone at the toe of the slopes to catch the rocks. The road provides the only convenient access through the valley and increasing numbers of vehicles are using it to access new housing developments and industry throughout the hills. This paper discusses the remediation program immediately embarked upon to secure the unstable slopes and the development and implementation of a classification system for identifying and prioritising those slopes prone to rock fall. It also discusses the procedures employed to manage risk during remediation as a result of the necessity to maintain traffic flow while the work was being carried out

Introduction

The mouth of the 20km long Torrens River Valley, shown in Figure 1, is located about 15km east of the centre of Adelaide on the western edge of the Mount Lofty Ranges. This deeply entrenched east-west trending river system dissects northerly trending ridges and branches which contribute to a rugged topography with distant valley walls rising up to 250m above the river below.

Gorge Road was originally excavated in the floor of the valley in the mid 1800s. It provided one of only few access roads across the northeastern section of the ranges for bullock teams travelling to the small townships beyond. Even though the road was, and still is, only 4.5m wide with no clear-fall zone or shoulder verges and poor site distances, it was adequate for the original purpose. No rock support or reinforcement was installed in the slopes at the time even though, by the standards of today, the rock structure warranted it.

In 1969 the Kangaroo Creek dam was constructed 8.5km up the valley. Part of this project involved constructing a 5.6km diversion road adjacent to the reservoir up to 75m above the valley floor. This road has a 6.5m carriageway, an average 1.5m wide clear-fall zone and 0.3m wide shoulder verges. Like the original section of road it replaced, the condition of the slopes and their height warranted the use of support or reinforcement however virtually none was installed at the time.

Most of the slopes adjacent to the new and original sections of road were constructed with a single batter with heights ranging up to 50m. Batter angles range from 50° to 90° and some faces on the older sections overhang the road.

The road now handles an average of 800 light and heavy vehicles per day that use it to service the light industry and housing developments that have sprung up throughout the Ranges.

Geology

Figure 1 shows the regional geology around Gorge Road. The overall structure is largely a result of faulting and folding of the Adelaide Geosyncline sediments during the Cambro-Ordovician Delamerian Orogeny, 510m years ago.

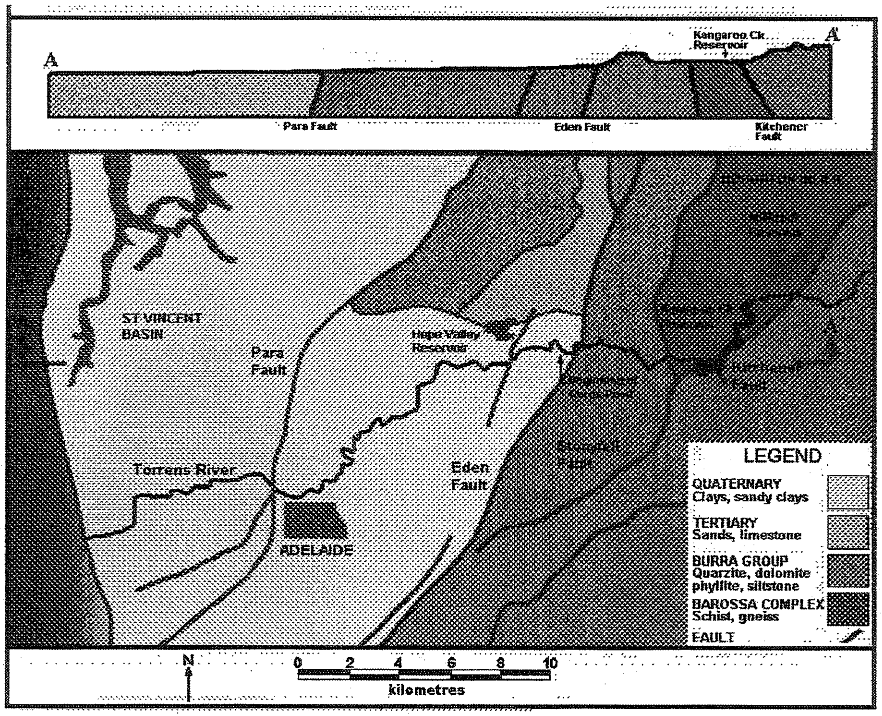

Figure 1 Geology of the region around Gorge Road

The older Palaeoproterozoic Barossa Complex metamorphics occur in the Houghton Inlier. These rocks are considered to be the basement rocks of the Mount Lofty ranges and have been affected by steep up-thrusting during the Delamerian causing retrograde metamorphism and shearing (Preiss, 1993). The Inlier is bounded to the east by the Kitchener Fault and to the west by a continuation of the Stonyfell fault. Spry (1951) describes the rocks as augen gneisses, schists and granulites. Talbot (1963) found them to have variable chemical and mineralogical composition but grouped them into feldspar rich rocks with minor amphibole and diopside and quartz-feldspar-mica schists and gneisses. According to Preiss (1993) the distribution of the rock types within the Barossa Complex is subject to considerable uncertainty and their structural relationships are poorly understood.

The faults separate the older Houghton Inlier from the overlying Neoproterozoic Adelaidean metasediments of the Burra Group. These rocks consist of phyllites, dolomites and quartzites. The Castambul Dolomite uncomformably overlies the Barossa Complex at a faulted contact. The Dolomite is approximately 120m thick, white to pale pink containing up to 20% quartz grains. These rocks are overlain by the Unnamed Phyllites, which have a thickness of approximately 200m. The unit comprises phyllites and siltstones up to 50m thick interbedded with fine to medium grained arkosic quartzite bands up to 5m thick (Trudinger, 1973). The phyllites tend to be highly jointed. Conformably overlying this unit is a 250-300m thick band of massive Montacute Dolomite. These rocks are actually a blue-grey siltstone containing dolomite lenses and minor quartzite (Spry, 1998) and are used as construction and road building materials around Adelaide. The Lower Phyllite unit conformably overlies the Dolomite and is about 200-350m thick. Its lithology is predominantly that of a siltstone, however, it contains sandy and calcareous bands and shows a prominent cleavage. The overlying Stonyfell Quartzite is arkosic, medium grained and interbedded with siltstone. It too is used in construction and road building around Adelaide. The Quartzite is greater than 300m thick and is bounded to the west by the Eden Fault. Zoitas (1995) found it to be separated from the underlying Phyllites by a faulted contact. Sedimentary structures including ripple marks and cross bedding are common within this unit.

Geotechnical Conditions

Near horizontal and steeply dipping joints within the Burra group rocks have produced near orthogonal blocks along much of the older section of road. Significant toppling instability in these blocks occurs at approximately 30 locations along the road. Slope faces of highly variable orientation, and the moderately to highly weathered nature of much of the rock, have also allowed wedge failures to occur at many locations particularly on northeast facing slopes.

The strongly foliated schists of the Barossa complex in the newer section of road tend to be more susceptible to weathering than the quartzo-feldspathic gneisses, allowing differential weathering to occur. The structure in these rocks tends to produce daylighting wedges involving intersecting joint planes or shear zones and daylighting sheet joints. The rocks close to the carriageway tend to be less weathered than those higher up on the faces.

Much of the rock on the older section of road has now been exposed for more than 150 years and is extremely weathered and unstable particularly in the higher sections of each slope. The problem of instability was exacerbated at many sites by the presence of roots from large eucalypts and casuarinas that were growing on many of the faces.

Figure 2 Large wedge failure on Gorge Road

In recent years large deep-seated instabilities have occurred on average every few months during or immediately after rainfall exceeding 15-20mm in a day. Whenever intensive short-term downpours have occurred, individual rocks of up to 1000cc have fallen however rocks of up to $1m^3$ have also fallen (Figure 2). In all cases, the thin or non-existent clear-fall zones have been unable to prevent the rocks from landing on to the carriageway and the thin pavement widths have made negotiating around the rocks difficult or impossible. Last winter, 2000, was particularly wet with much of the rain coming from the north, which is unusual for this region. Several large rockfalls, involving up to $50m^3$ of rock, occurred from faces not usually exposed to direct rainfall. These falls damaged several vehicles.

A subsequent visual inspection of the slopes indicated that the rock in most sections had deteriorated to such an extent that immediate remediation work was necessary to limit the number of additional falls that could occur.

Rockslope Remediation

Two actions were initiated in view of the severity of the rockfall problem. One action was to develop a method for managing rockfall hazard in a systematic manner. This aspect of the work is discussed later in this paper. The other measure was to embark on a program to scale those slopes highlighted as being most hazardous. Due to the urgency of the work there was no time to design for or to organise reinforcement or support measures such as rock bolting, shotcreting or rockfall netting.

One of the authors, Dr Meyers, was engaged by Transport SA to inspect all cuttings along the road and rate them according to the likelihood for rockfall. Engineers from Transport SA then prioritised sections of the road for further work depending on hazard to traffic on the basis of the probability for rockfall, clear fall zone width, sight distance and outside shoulder width.

It was realised at an early stage that scaling of the high priority slopes would have to be carefully planned and managed to avoid harm to traffic and the contractor's employees from the large volumes of rock that would have to be removed during the operation. It would also have to avoid causing excessive delays to traffic. A suitable contractor was sought to undertake the work. Fortunately one of Transport SA's maintenance contractors was experienced in scaling and had appropriate equipment. In view of the difficult nature of this work the contractor engaged an experienced engineer full-time to run the gang for the 4 months required to complete the work. In the opinion of the authors, experienced supervision was critical to the success of this project.

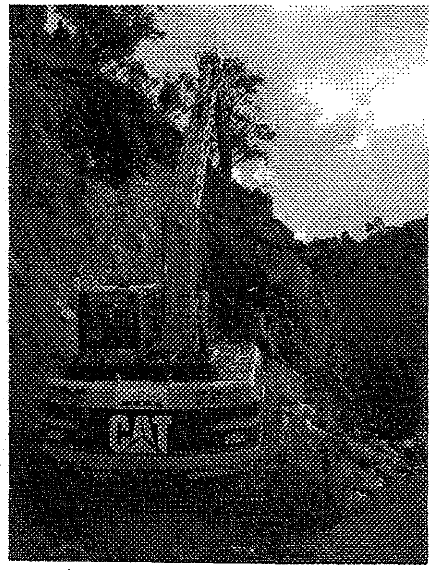

Figure 3. Scaling face

In general, the work involved scaling the loose blocks with a long-boom excavator with a 15m reach fitted with a pick (Figure 3). Additional height was obtained by standing the excavator on a 2m high bench constructed on the road out of scaled rock. When the zone of soil and extremely weathered rock at the top of a batter could be reached, it was trimmed back to reduce the batter angle to approximately 35 degrees. To dislodge boulders out of reach of the excavator, workers operating from an elevating platform used an inflatable mat placed in the crack at the back of the boulder. By inflating the mat with compressed air even large boulders could be removed.

Hazard ranking theory

The slopes to be remediated were ranked using a rating system that aimed to quantify the potential for rock falls to occur from a slope. This system is currently being extended so that it will quantify the risk associated with these rockfalls causing damage to vehicles. This risk is defined on the basis of the definition of AGS (2000), which broadly defines risk as hazard multiplied by consequence. More specifically, for damage to a vehicle, the risk is calculated from:

$$\text{Risk} = P_h \times P_{s(v:h)} \times V_{(v:h)} \times E \qquad (1)$$

where

- P_h is the annual probability of a rockfall occurring from a particular slope. It is assumed that this fall will affect the traffic in the lane closest to the toe of the batter.
- $P_{s(v)}$ is the probability that a vehicle is below the rockfall. This parameter depends on the number of vehicles per day on that section of road, the length of the vehicles and the velocity of the vehicles. $P_{s(h)}$ is the probability that a vehicle impacts the rockfall. This parameter depends on the number of vehicles per day on that section of road, the velocity and stopping distance of the vehicles, the carriageway and shoulder widths and the decision site distance.
- $V_{(v:h)}$ is the vulnerability of the vehicle to the impact. V_v depends on the height from which the rockfalls can occur and the volume of rock that falls. V_h depends only on the volume of rock that falls.
- E is the value of the vehicle at risk.

AGS (2000) also define the risk of personal injury resulting from rockfalls however the current system does not consider this risk, as damage to vehicles rather than personal injury has predominated from falls. It is, however, intended that personal risk will be considered at a later stage.

To date, the rating system has concentrated on determining the P_h parameter in Equation 1. The other parameters are currently being incorporated into the system even though data for them has always been collected during field logging.

The P_h parameter is based on the rockfall hazard rating (RHR) for a slope. Table 1 lists the individual rock mass and discontinuity characteristics considered when determining this rating. The rating is based on work by Romana (1985), Bieniawski (1989), Pierson et.al. (1990) and Meyers (1993). An indication as to typical ranges of values is also indicated in the table however, for several of the ratings, the system actually uses a progressive rather than the "bin" type allocations shown. The characteristics assessed in the system and the relative values assigned to them were found to be appropriate to the conditions throughout the Adelaide Hills and may or may not be appropriate to other locations.

For rockfalls occurring due to planar and toppling type mechanisms, the parameters F_1, F_2 and F_3 consider the relative orientations of each discontinuity set (α_w, β_w) and the orientation of the face of the batter (α_s, β_s). For wedge type mechanism the parameters consider the relative orientations of the line of intersection of two sets (α_i, β_i) and the face of the batter.

The value for the RHR ranges up to a maximum of 140 and is determined as:

$$RHR = R_1 + R_2 + R_3 + R_4 + R_5 + R_6 + R_7 + R_8 + R_9 + R_{10} + R_{11} + (F_1 \times F_2 \times F_3) \qquad (2)$$

The RHR is defined in terms of a probability by considering the rainfall statistics. For example, rocks fall from those slopes for which the RHR is greater than 100 whenever rainfall exceeds 100mm in a day. The probability associated with this RHR is therefore assumed to be the same as the probability that rainfall will exceed this amount.

Table 1 The Rockfall Hazard Rating System

Strength of intact rock (Grade)	R6	R5	R4	R3	R2	R1	R0
Score, R_1	0	1	2	4	7	12	15
Weathering	FR	SW	DW	EW			
Score, R_2	0	5	10	15			
Angle above slope	< 25	25 - 35	35 - 45	> 45			
Score, R_3	0	2	4	5			
Previous failures	No	Yes					
Score, R_4	0	5					
Adverse features (Rock)	None	Few	Some	Many			
Cumulative Score, R_5	0	3	6	10			
Adverse features (Soil)	None	Few	Some	Many			
Cumulative Score, R_6	0	6	12	20			
Water source	No	Yes					
Score, R_7	0	5					
Visible seepage	None	Slight	Mod	High	V.High		
Score, R_8	0	4	6	8	10		
Slope Height (Soil Only)	< 5m	5–10 m	10–20 m	20–30 m	> 30 m		
(x % of soil) Score, R_9	0	14	19	26	30		
Effective Support	None	Shotcrete	Barriers	Rockbolts	Netting	Dowels	
Cumulative Score, R_{10}	0	-10	-10	-10	-10	-10	
Discontinuity frequency (/m)	<0.5	0.5–1.6	1.6-5	5-17	>17		
Score, R_{11}	0	5	10	15	20		
Planar/Wedge $\lvert \alpha_{w/i} - \alpha_s \rvert$ Toppling $\lvert \alpha_{w/i} - \alpha_s \rvert - 180^\circ$	$>30^\circ$ $<-25^\circ, >25^\circ$	20°-30° $<-15^\circ, >15^\circ$	10°-20° $<-5^\circ, >5^\circ$	5°-10° $<-2^\circ, >2^\circ$	$<5^\circ$ $>-2^\circ, <2^\circ$		
Score, F_1	0.15	0.40	0.70	0.85	1.00		
Planar/Wedge $\beta_{w/i} - 30^\circ$ Toppling	$< (-15^\circ)$ 1.0	-6°–(-15°) 1.0	(-5°)–(-1°) 1.0	0°-10° 1.0	$> 10^\circ$ 1.0		
Score, F_2	0.15	0.40	0.70	0.85	1.00		
Planar/Wedge $\beta_{w/i} - \beta_s$ Toppling $\beta_{w/i} + \beta_s$	$>10^\circ$ $<110^\circ$	10°–0° 110°-120°	0° $>120^\circ$	0°–(-10°)	$< -10^\circ$		
Score, F_3	0	4	18	37	45		

Developing the database

The benefit of using an electronic database is that it allowed the data collected from all sites to be easily stored, manipulated and retrieved as required. The database used in this project was Microsoft Access due to its transportability and relative ease of use. After completing an intermediate course in using this software, most engineers with reasonable programming skills can develop the skills necessary to create a database that will carry out the necessary computations and produce ranked output. A background in slope classification was found to be a useful attribute for this engineer to have. It was also found useful for the engineer to be closely involved with the field aspects of the project as the development and testing of the database tends to be a fairly "fluid" process with many updates and refinements being needed along the way.

The database has been set up with two primary keys, the slope identification number and the inspection date. These keys are set up in such a way that there can only be one distinct slope identification number yet multiple inspection dates. Each section of the inventory system has been separated into its own group. The description and location of a slope has its own table and query and the discontinuities have their own table and query and so on. The query for each section has been set up to update its own table with its rating so that all information collected from a slope and the hazard rating calculated from that information remain together. A simple query is used that links together all tables and sums up the individual ratings to obtain an overall hazard rating for a slope.

One of the main reasons for creating a database is its ability to produce all manner of output. In this database, the slopes can be ranked in order of a decreasing rockfall hazard rating (Figure 4). Doing so enables slopes to be prioritised for remediation. Field data sheets can also be generated which contain records of all data that was logged in the field. The ability to do so should enable assessors in future years to produce a report that can be used as a reference when a slope is re-inspected. All output data can also be exported to Microsoft Excel, which greatly simplifies the task of data ranking.

One problem found while creating the database, was Microsoft Access's inability to easily compute large equations. An example of such equations are those used for determining the discontinuity ratings as these equations require large block IF statements. With equations such as these the software tends to crash once a change has been made to the database due to limitations in memory handling within the software. To solve this problem, the equations had to be broken down into separate parts. Doing so reduced the size of the individual computation that had to be carried out at any one time. Update queries were then used to compute each part of the equation and to store the result from the computation into a table. Once all parts of an equation had been computed and stored, the results could then be combined in a more simple equation. The only drawback of using these queries is that several of them are necessary for calculating one equation and that they have to be activated using a separate button on a form.

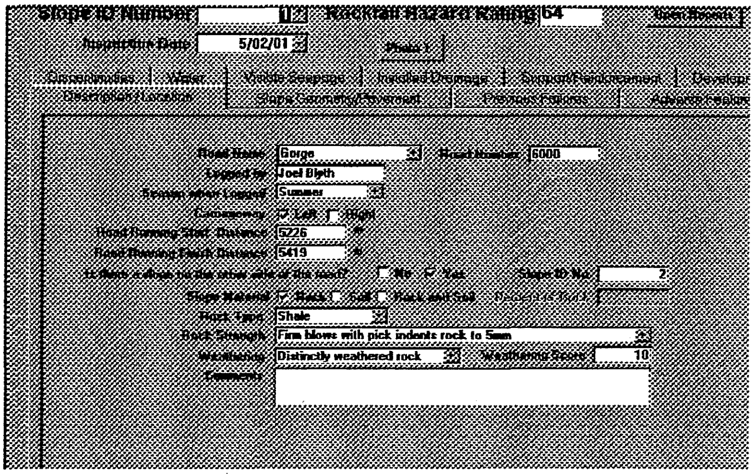

Figure 4 Data entry into database.

Field Logging

All slopes along this road and along other roads in the Adelaide Hills are currently being logged using the new rating system. To date over 270 slopes have been logged. As working on these roads poses a hazard to both traffic and workers, a requirement of the field logging is that it be conducted by a minimum of two staff at all times and that at least one of these staff is accredited in work-zone traffic management. Appropriate signage is used to warn motorist that workers were on the road and to reduce speed in the work-zone down to 25km/h.

Logging the input data, particularly that pertaining to the characteristics of the discontinuities, requires significant expertise. To date the only staff permitted to log this data have been a rock mechanics engineer experienced in engineering geology and several geotechnical engineers trained by him. Approximately 10% of slopes logged by the trainee engineers are logged again by the experienced engineer as a check on the quality of the data. Any discrepancies in the data are altered in the database although these discrepancies are generally found to be minor. Fewer changes became necessary as the trainees gained more experience.

Several methods of recording the data were trialed in the field to reduce as much as possible the necessity to double handle the data back in the office.

Several methods of recording the data were trialed in the field to reduce as much as possible the necessity to double handle the data back in the office.

(a) A handheld data logger. The data entry method on this device was found to be too inflexible to be practical and too time consuming to input the data in the manner required by the device. The device also had limited capacity to store data from the numerous slopes that could be logged in a day.

(b) A palmtop computer. This device could only run a small spreadsheet and not Microsoft Access, the software around which the database was built. In addition, data entry was found to be cumbersome and it was difficult to see the screen in the bright daylight

(c) A notepad computer. This device appeared to be an attractive option because it could run Microsoft Access. However, in the field the monitor proved to be far too difficult to see in the bright daylight. The device also had limited operating time on batteries and it was relative fragile.

In view of these problems the decision was made to write data down on a pro-forma. The time to re-enter the data into the database back in the office has not proved to be a problem. The same pro-forma can be used for slopes of rock, soil or combinations of the two.

Conclusions

The problems associated with rockfalls along the 20km long Gorge Road will be ongoing due to the highly weathered nature of the rock within the cuttings. However, the immediate problems created by the harsh weather conditions in 2000 enabled Transport SA to develop a two-pronged approach to the problem. An efficient, safe and effective system for scaling was developed, as was a database for prioritising the slopes on the basis of rockfall potential. The work on the database is continuing as will scaling if conditions in 2001 warrant it to be necessary.

References

Bieniawski, Z.T. (1972) Engineering Classification of Jointed Rock Masses Trans. S. Afr Inst. Civ. Eng. **15** pp 335-344.

Meyers, A.G. (1993) The Determination of Rock mass Strength for Engineering Design, PhD Thesis, University of Adelaide.

Pierson, L.A., Davis, S.A. and VanVickle, R. (1990) The Rockfall Hazard Rating System: Implementation Manual. Technical Report FHWA-OR-EG-90-)! FHWA, U.S. Dept. of Transportation.

Preiss, W.V. (1993) Palaeoproterozoic, *The Geology of South Australia, Vol. 1, The Precambrian*, Chap. 4, State Print, South Australia, pp. 102-104.

Romana, M (1985) New Adjustment Rating for Application of the Bieniawski Classification to Slopes. Proc. Int Symp. Rock Mech Min. Civ. Works ISRM Zacatecas, Mexico, pp 59-63.

Spry, A.H. (1951) The Archaean Complex at Houghton, South Australia. *Trans. Royal Soc. S. Aust.*, 74(1), pp. 115-134.

Spry, L. (1998) *Slope Stability Along Gorge Road.* Honors Thesis, University of South Australia, 155 pages.

Talbot, J.L. (1963) Retrograde metamorphism of the Houghton Complex, South Australia. *Trans. Royal Soc. S. Aust.*, 87, pp. 185-197.

Trudinger, J.P. (1973) Engineering Geology of the Kangaroo Creek Dam, *Dept. of Mines, Geological Survey of South Australia, Bulletin 44*, Adelaide.

Zoitas (1995) A Geotechnical Study of Slope Stability along Gorge Road from Black hill conservation Park to Kangaroo Creek Reservoir. Masters Thesis, University of South Australia.

Residential Development on Landslide Terrain

Mark Foley, BSc (Geol)
Tonkin & Taylor Ltd, Nelson

Gary Smith, BSc (Geol) MSc (Eng Geol)
Tonkin & Taylor Ltd, Wellington

Chris Hansen, BRP (Hons)
Tonkin & Taylor Ltd, Wellington

Abstract

As the area of available undeveloped land in Nelson reduces, developers are looking at marginally stable land. Under the Resource Management Act, a consenting authority is required to ensure the effects of hazards are avoided, remedied or mitigated.

This paper presents a case study of residential development in Nelson where the geotechnical consultant has worked with the developer to enable subdivision of landslide terrain. The complex engineering geological environment necessitated investigations utilising the observation approach and development of a robust engineering geological model. This model formed the basis for a risk management process. Landslip hazards were assessed by a combination of judgement, relative stability analysis and, less often, absolute factor of safety analysis. Risks were evaluated in terms of satisfying the requirements of the existing legislation and unacceptable risks were either remedied, mitigated or avoided. An aspect of risk mitigation has been the recommendation of building development conditions and periodic monitoring and maintenance of the subsurface drainage system.

Introduction

Nelson City has a complex geological setting and a high level of landslide risk compared to other cities in New Zealand. The city's development is constrained by steep topography and there is widespread instability on the hillsides. With limited flat land available for growth, much of Nelson's recent residential development has been on hillslopes. Many of these hillslopes are on landslide terrain and Nelson has a history of landslips affecting residential land.

In the late 1970's Nelson City Council introduced a requirement that, as part of subdivision development, a geotechnical professional must certify that a stable building site exists on each lot of a subdivision. In addition, since 1991 landslip hazards have been addressed by Nelson City Council under the Resource Management Act, (NZ Government, 1991). Despite this, many landslips have occurred on land which has been subdivided and/or developed in the last 20 years, and the trend is not improving. Nelson City Council's landslip register, set up in 1983, lists 225 landslips of which 120 have been recorded in the last 10 years.

This paper presents a case study from the recently completed Stage 3B Malvern Hills Subdivision in Nelson. This development has proceeded with the developer and geotechnical consultant working together in the investigation, design and construction phases to identify and assess hazards and manage geotechnical risks associated with land development on landslide terrain.

Malvern Hills is located in Atawhai, a suburb occupying steep hillside slopes 3km north of Nelson City, (Figure 1). Stage 3B occupies the upper slopes of the Malvern Hills Subdivision and is the final phase of a staged development. It covers 6.5 hectares of moderate to steep undulating terrain, and comprises 15 residential lots numbered Lots 31 to 45.

Background

The Resource Management Act 1991 (RMA) is the principal Act by which subdivision and land uses are assessed and controlled. The purpose of the RMA is to promote the sustainable management of New Zealand's natural and physical resources. The Act has a fundamental philosophy that states that a land use activity can occur, unless a rule in a plan prevents it. The RMA requires any adverse effects of activities on the environment to be avoided, remedied or mitigated.

Subdivision is essentially a legal act where a new title is issued by the District Land Registrar for the creation of a new lot or lots. While subdivision has no adverse environmental effects, it often leads to changes in land use and it is these land uses that can have adverse environmental effects. Subdivision that contravenes Section 11 of the RMA requires a resource consent in terms of Section 88 of the Act.

Where a subdivision occurs on land that is subject to a hazard such as erosion, subsidence, slippage, or inundation, consenting authorities are restricted by Section 106 and Section 220D which require certain conditions to be imposed on any consent. The consenting authority is required to ensure the *effects* and identified hazards are avoided, remedied or mitigated. *Effects* are defined in the RMA in Section 3 and include:

- any positive or adverse effect; and
- any temporary and permanent effect; and
- any past, present or future effect; and
- any cumulative effect which arises over time or in combination with other effects – regardless of the scale, intensity, duration, or frequency of the effect, and also includes –
- any potential effect of high probability; and
- any potential effect of low probability which has a high potential impact.

The RMA provides a context for subdivision and the engineering and geotechnical input into the approval of subdivisions endeavours to minimise the risk or *effects* associated with land that has the potential for hazards that is to be used for residential development.

Geological Setting

The general geological conditions on the site are shown on Figure 1 and Figure 2. Bedrock consists of an indurated tuff, mapped as Botanical Hill Formation, on the northeastern (upper) half of the subdivision, and a clay bound gravel, mapped as Port Hills Gravel Formation, on the, western, lower half of the subdivision. Marybank Formation, an indurated dark grey siltstone, is locally exposed at the foot of the steeper slopes in the south east corner of the subdivision and has been mapped (Johnston, 1981) to the north of the subdivision.

A broad crushed zone (fault) transverses the middle of the site from northwest to southeast and this fault separates the Port Hills Gravel Formation downslope from the Marybank and Botanical Hill Formations upslope. This fault, referred to here as the Ledbury Fault is a reverse fault which dips steeply to the southeast. It is inferred to be part of the Waimea - Flaxmore Fault System. Johnston et al (1993) consider the Waimea – Flaxmore Fault System to be active, as movement has occurred on individual faults within the system within the last 10,000 years.

The majority of the subdivision is covered by mass movement deposits. These deposits are up to 20m thick and have accumulated over tens of thousands of years as a result of numerous episodes of landslippage. Two major landslide deposits were distinguished, the Seawatch Slide and the Ledbury Slide.

Away from the areas of mass movement deposits the bedrock is overlain by a veneer, up to four metres thick, of residual soil and colluvium.

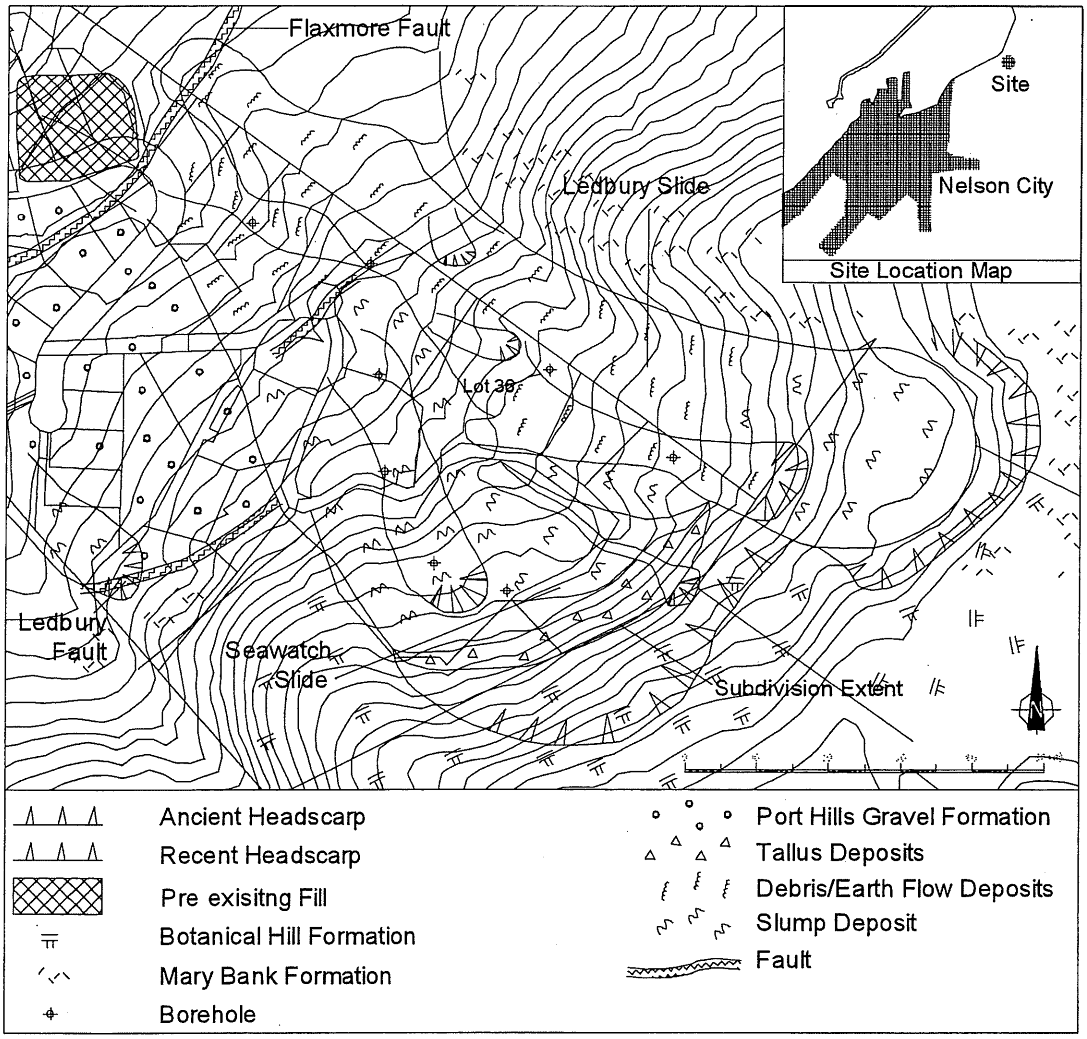

Figure1: Location and Geology

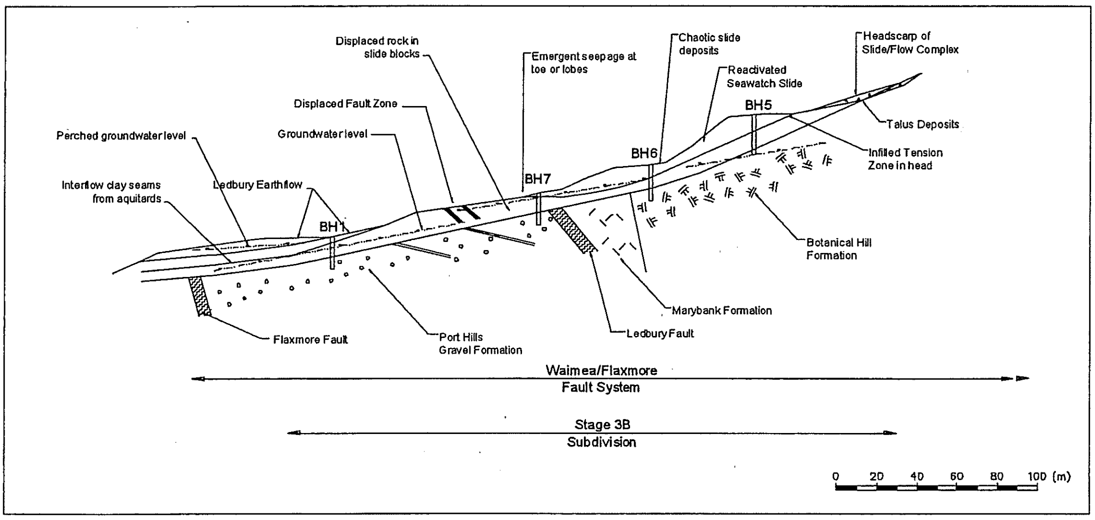

Figure 2: Simplified Engineering Geological Model

Investigations

Field investigations were carried out in three phases. Phase 1 was carried out in 1997 in conjunction with the planning and design of the general subdivision layout. This involved aerial photographic interpretation, mapping, test pitting and the drilling of four boreholes. Groundwater monitoring in four standpipe piezometers installed in the boreholes commenced at that time and a ground deformation survey network was set up.

The preliminary engineering geological model indicated a complex assemblage of bedrock and mass movement deposits and the decision was made to proceed with detailed design and construction using the observation method.

Phase 2 commenced in February 2000, prior to construction and continued throughout the construction phase. This involved regular site visits and documentation of ground conditions during the main construction works. Three additional investigation boreholes were drilled and groundwater monitoring standpipes were installed on further five sites.

Phase 3 involved post construction testing to confirm suitability of building sites prior to certification.

Investigations of the site were constrained by property boundaries, limited access to the steeper slopes and the very dense vegetation covering much of the site.

Rock and Soil Characteristics

Botanical Hill Formation is a typically moderately weathered and strong in shallow excavations and grades into slightly weathered very strong rock at depth. Rock joints are moderately widely to widely spaced. The rock appears to have a high secondary permeability, but widely spaced crushed zones impede groundwater flow. The rock is locally altered and weak in the vicinity of crushed zones.

Marybank Formation is a typically moderately weathered and weak to moderately strong siltstone in shallow excavations, and grades into strong rock at depth. Joints are closely spaced with a preferred orientation sub parallel to bedding which dips east into the slope at 50 to 70 degrees. There are numerous thin sheared zones within the rock mass. This rock generally has a low secondary permeability.

Port Hills Gravel is a extremely weak to very weak rock. It weathers to dense silty to sandy gravel in shallow excavations. The Port Hills Gravel is sub massive with occasional sandstone beds which dip to the east, into the slope, at 30 to 40 degrees. Permeability is very low, however confined groundwater flows are often associated with the sandstone beds.

Slide deposits were characterised by moderately to slightly weathered, closely jointed to shattered, dilated rock. On the upper slopes, little of the parent structure is preserved and the debris is chaotic in appearance. In the mid slope portion, where in excess of 50m translational displacement is inferred, the rock mass is dilated but retains the original structure. The slide deposits are generally well drained except where relic sheared and crushed zones (displaced tectonic faults) are preserved as aquitards.

Flow deposits are characterised by a complex mixture of firm to hard, low to high plasticity silty clays and loose to very dense, silty gravel. Identifying different flow deposits was difficult, and although low strength sheared and slickensided clay seams were present at inter-flow boundaries (Figure 3), these were often thin and could only be confirmed by visual examination in exposure.

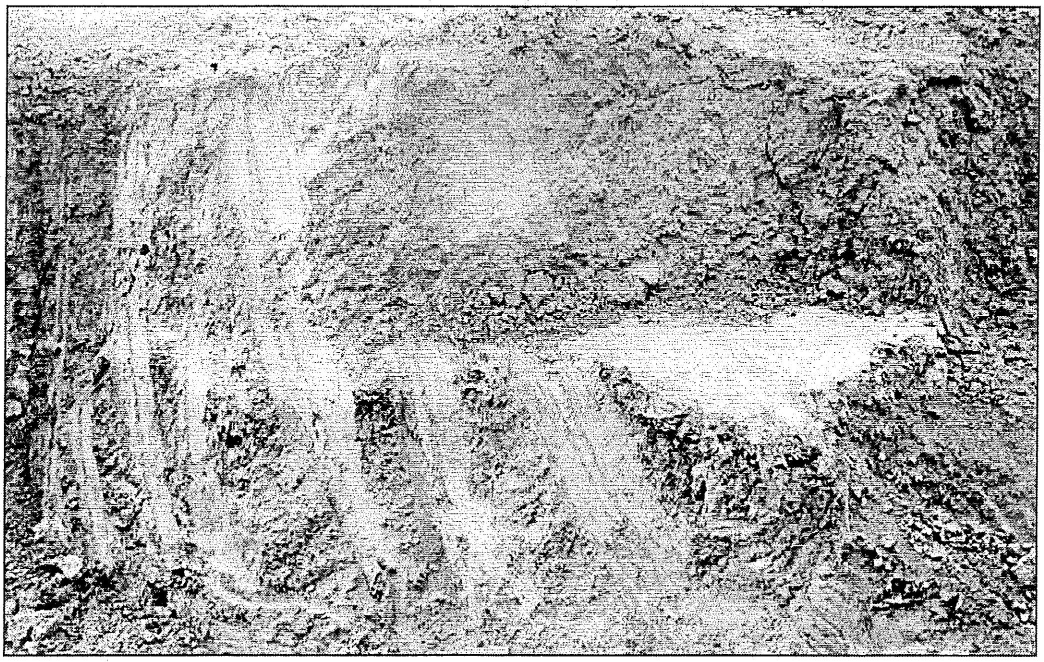

Figure 3. Inter-flow sheared clay seam

A characteristic of the younger earthflow deposits was a layer of loose silty gravel or gravelly silt immediately above a slickensided basal clay seam. The basal clay seam is inferred to be a remnant topsoil layer, although no organic matter is now present. Slickensides on this surface indicate shearing, while flow movement is indicated within the deposit immediately above the clay surface.

The older earthflow and slide deposits were mantled with colluvium and a well developed topsoil/subsoil profile has developed. The younger flow deposits associated with the Ledbury Slide do not have a well developed "B" soil horizon and following a 1998 fire, broom was the predominant re-colonising plant species. This vegetation contrast was a useful mapping tool.

Slope Instability

The majority of the mass movement deposits are considered to be very old (several thousand, to ten's of thousands of years old) but there is evidence of repeated episodes of landslippage. Using the terminology of Cruden and Varnes (1996) the landslides are complex, composite slides and flows, which include relict, dormant, reactivated and active portions.

The oldest mass movement is the Seawatch Slide, Figure 1. The Seawatch Slide includes an upper portion, with characteristics of rotational slide movement. The central portion shows characteristics of translational sliding, and the downslope portion shows characteristics of both sliding and flowing. Consolidated colluvium mantles the slide debris and the deposit has locally been incised by stream erosion and then undergone partial reactivation.

The Seawatch Slide is overlain on the northern half of the subdivision by the Ledbury Slide, (Figure 4). The Ledbury Slide consists of an upper portion upslope of the subdivision where rotational slide movement in rock is inferred. Within the subdivision it is a complex composite of earth flow and earth slide lobes. The Ledbury Slide is approximately 3.6km long (from the crown to the toe). The youngest lobe mantles the older landform and extends 2km downslope.

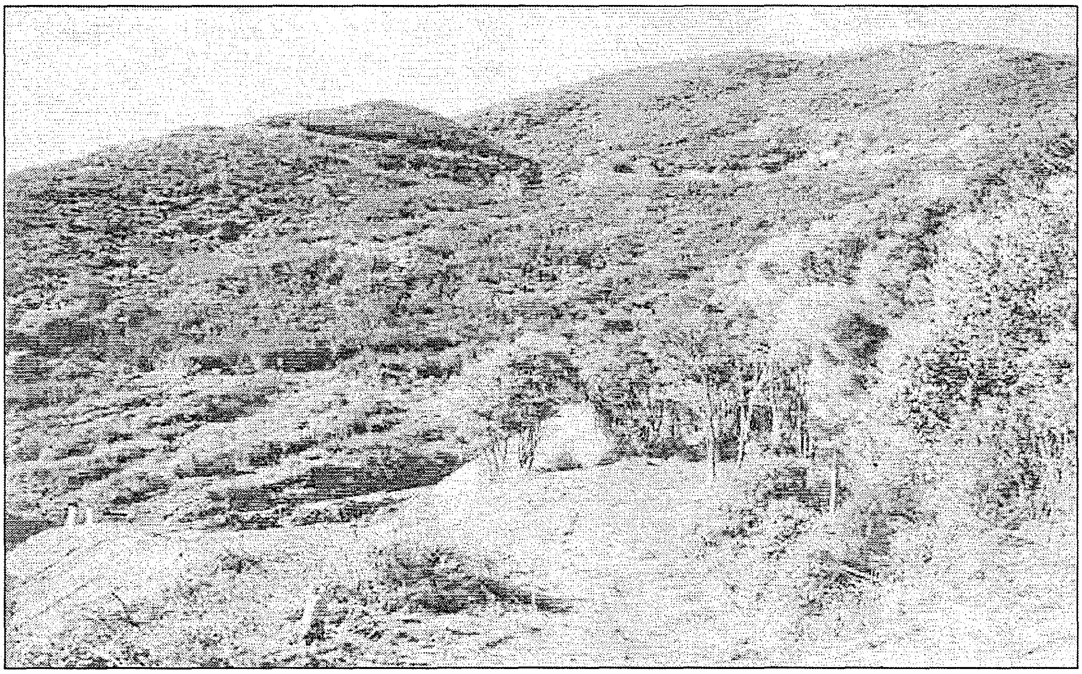

Figure 4. View across headscarp of reactivated portion of Seawatch Slide towards Ledbury Slide.

Recent instability on the Subdivision has involved local reactivation of the younger, less consolidated, Ledbury Slide deposits, and shallow earth flows originating on the partially degraded Seawatch Slide headscarp. The most recent recorded landslide on the subdivision occurred in July 1998 and involved a debris slide-flow failure of $200m^3$ of soil and weathered rock on the Seawatch Slide headscarp and developed into an earthflow extended 120m downslope.

Groundwater

A simplified groundwater model is shown on Figure 2. Groundwater monitoring indicates a regional groundwater table that is low within the bedrock beneath upslope and to the southeast of the Seawatch Slide. The regional groundwater table approaches the ground surface in two areas: locally at the toe of the degraded headscarp of the northern part of Seawatch Slide, and beneath the mid slope portion of the subdivision. Within bedrock, groundwater is probably compartmentalised with the Ledbury Fault and other crushed zones acting as aquitards. The Ledbury Fault forms a step in the hydraulic gradient and is associated with spring lines. Displaced crushed zones within the slide mass also impede groundwater flow and give rise to locally elevated groundwater levels. Groundwater levels within bedrock and the upper slide mass show a seasonal fluctuation of 1 to 3 metres.

The flow deposits are characterised by perched ground water levels, associated with inter-flow boundaries. Groundwater monitoring indicates that perched groundwater levels on the lower slopes can fluctuate by up to seven metres in response to daily rainstorm events. This gives rise to spring lines where the younger Ledbury slide lobes blanket the lower slopes northwest of the subdivision.

Landslide Hazard Assessment and Risk Management

Risk assessment is being increasingly used as a management tool in a wide range of applications. In AS/NZS 44360:1999 (Australian Standards Association, 1999) guidelines for the implementation of the risk management process are set out. In the case of the Stage 3B of the Malvern Hills Subdivision, and on other subdivisions in Nelson, Tonkin and Taylor are applying risk management strategies to optimise development potential and to ensure that the geotechnical risks associated with the development are acceptable. Within this process the requirements of the Resource Management Act, 1991 (as discussed in the background to this paper) and Nelson City Council's certification requirements are addressed. That is, the likelihood and effects of landslip hazards are assessed, and when it is considered appropriate, adverse effects and likely hazards identified are avoided, remedied or mitigated.

The risk management process, as adapted from AS/NZS 44360:1999 is summarised in Figure 5. Using risk management terminology, consequence is the outcome, or effect, of a hazard, and risk is the chance of something happening that will have an impact on objectives. Risk is measured in terms of consequences and likelihood.

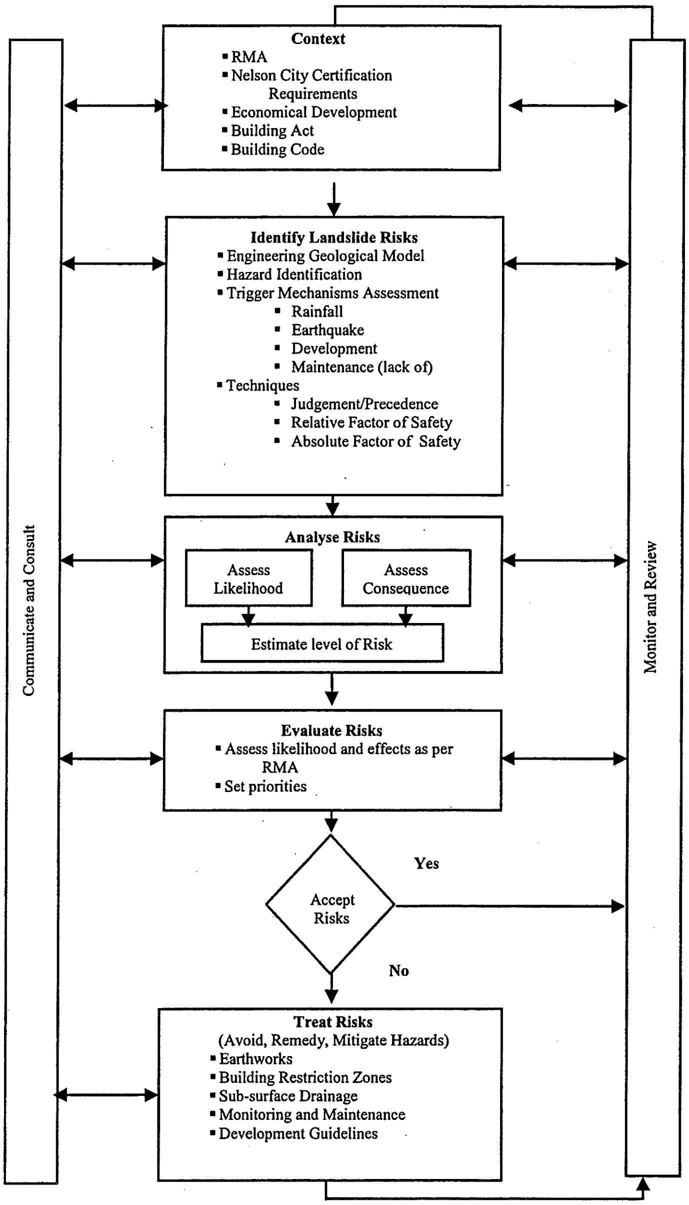

Figure 5: Landslide Risk Management Process

The engineering geological model forms the basis of the risk management process when applied to landslide risks. At Malvern Hills, the preliminary engineering geological model highlighted the extent and approximate depth of mass movement deposits. Based on preliminary risk assessment, potential building sites were identified and the scope of earthworks and drainage were defined. As investigations progressed, the engineering geological model was developed further to reflect the complexity of the landslides and the groundwater. In addition, specific engineering geological models were prepared for each proposed building site and further risk assessment was carried out. Through interaction with the developer, designer and contractor, physical works were detailed or amended as required, depending on the assessed level of risk.

Subdivision Scale Risk Management

Overall slope stability was addressed and subdivision layout was planned using a combination of engineering judgement based on precedent, and numerical analysis based on relative stability modelling. Absolute factor of safety analysis was not used in assessing the large scale landslides risks. This is because the complex nature of the landslides and groundwater levels are difficult to accurately quantify. In addressing the global stability issues, the objective in designing remedial or mitigation works was to ensure that the relative stability of the large landslides would be improved by the subdivision construction. This has involved:

- siting cuts and fill berms to enhance overall slope stability; approximately 40,000m^3 of earth works were carried out;
- installing 390 linear metres of inclined bored drains;
- installing 1100 linear metres of deep (up to 7m) subsoil drains in areas of high and perched groundwater levels zones of recharge;
- constructing 120 linear metres of debris deflection bunds and channels to prevent inundation from upslope failures;
- surface water interception and diversion.

Building Site Risk Management

Analysis of the ground model for each building site addressed both global stability and site specific stability issues. Specific hazards were in some cases easier to define on the building site scale and, where appropriate, absolute factor of safety design was incorporated with judgement and relative stability modelling.

In addition to the range of remedial and mitigation measures outlined above, risk management for individual building sites included ground improvement by sub excavating weak soil layers and construction of gravity buttresses and "shear key" fills. Risk management also included measures to avoid risks, such as specifying building restriction zones and as part of the required certification, conditions have been placed on future development within the lots to minimise adverse effects on stability.

Table 1 is an example of the risk management approach used for a proposed building site, Lot 36.

Monitoring and Maintenance of the Drainage System

The extensive network of subsoil and inclined drains installed as part of the subdivision works is to ensure the existing stability is maintained. One of the conditions of building site certification is the regular monitoring and periodic maintenance of the sub surface drainage system (comprising subsoil and bored drains), such as with other subdivision services such as stormwater, sewerage and road pavements, to ensure the continued operation of the system.

A monitoring schedule for the initial twelve months following completion of subdivision construction has been prepared and at the end of the first 12 months, a monitoring report will be prepared. The report will include a template for the key features to be observed and recorded, a photographic record of the site, specification of alert levels and a contingency plan detailing required actions.

Maintenance inspections of surface stormwater systems, subsoil drain and horizontal drain outlets will be carried out periodically and will involve periodical probing and cleaning of drains and repair or replacing of damaged drains. Property owners are encouraged to report any sudden variations to water levels or discharges, repeated maintenance requirements and observed damage to the drainage system. The preliminary maintenance schedule is shown in Table 2. This will be reviewed after the first twelve months.

Table 1: Landslide Hazard Risk Assessment Process –Lot 36

Preliminary Risk Assessment*				Hazard Analysis and Mitigation Design techniques			Mitigation Options			Revised risk assessment*		
Landslide Hazard	Likelihood	Consequence	Risk	Judgement/ Precedent	Relative F.O.S.	Absolute F.O.S.	Physical Works	Building Development Conditions	Mitigation Constraints	Likelihood	Consequence	Risk
Shallow Earthflow/ slide	D	2	H	✓		✓	Drainage Shear key Fill	Limit cuts	-	E	1	L
Deep-seated Earthflow/ slide	C	1	L	✓	✓		Drainage	Monitoring and maintenance of drainage system	Size of feature	E	1	L
Downslope Surficial slumping	B	3	H	✓	✓			Building Restriction Zone, Limit fills Drainage system maintenance	Size	E	1	L
Debris Flow Inundation	D	2	H	✓	✓		Deflection Bund	Building Set Back	Landslide source off site	E	1	L

Notes:

- Risk Classification adapted from AS/NZS 4360:1999
- Likelihood categories; - A (almost certain) < B (likely) < C (unlikely) < D (possible) < E (rare)
- Consequence categories are; insignificant < 1 (minor) < 2 (moderate) < 3 (major) < 4 (catastrophic)
- Risk categories are; L (low) < M (medium) < H (high) < E (extreme)
- Assessment by experienced engineering geologist familiar with area terrain/geology

Table 2. Maintenance Schedule

Feature	Scope	Frequency
Bored Drains	Probe and flush to full depth	Every 10 years (2011) or as review of monitoring information requires.
	Inspection	Annually
Stormwater Drains	Dye test and probe and flush	Every 10 years (2011) or as review of monitoring information requires.
	Inspection	Annually
Monitoring Wells	Purge and carry out recovery test	Every 5 years, or as review of monitoring information requires.
	Inspection	Annually
Subsoil Drains	Inspect outlets, clear of obstructions	After year 1, then every 5 years.

Conclusions

The geology on the Malvern Hills site is complex, necessitating a combination of judgement and relative stability analysis modelling in assessing overall slope stability and in identifying instability mitigation measures. On the building site scale, this approach has been supplemented with absolute factor of safety analysis based design of specific remedial works.

A Landslide Risk Management process has been successfully followed for subdivision planning and design. The basis for the Landslide Risk Management process has been a robust engineering geological model that has been updated throughout the phases of the project. Landslide Risk Management has assisted in optimisation of the subdivision development potential of landslide terrain while ensuring compliance with the requirements of the Resource Management Act.

In addition to identifying the scope of physical works to remedy or mitigate the effects of hazards, risk management incorporated measures to avoid risks, such as specifying building restriction zones. As part of the risk management process the need for ongoing monitoring and maintenance has been identified.

This project has demonstrated that landslide terrain can be developed for residential use, but this requires detailed geotechnical investigations governed by the observational approach, structured risk management analysis, and an ongoing commitment to manage the landslide risks.

Acknowledgement

The authors wish to thank Mr K and Mrs P Neal, the developers, and Mr R Grant, the developer's representative for their co-operation and assistance in preparing this paper.

References

Cruden, D.M., and Varnes D.J. (1996). "Landslide Types and Processes," In *Landslides: Investigation and Mitigation*, Ed: Turner, A.K. Schuster, R.L. Special report/Transportation Research Board, National Research Council;247.

NZ Government (1991). "*The Resource Management Act 1993*", Crown Publication, Wellington.

Standards Association of Australia (1999). "*AS/NZS 43600:1999 Risk Management*", Strathfield, NSW, Australia.

Johnston, M.R., Hull, A.G., and Downes, G.L (1993). "Earthquake, Landslide and Coastal Hazards in Nelson City," *IGNS Report prepared for Nelson City Council.*

Johnston, M.R. (1981) "Part Sheet O27 – Dun Mountain 1st Ed." *Geological Map of New Zealand 1:50,000. With notes.* Wellington, New Zealand DSIR.

Volcanic Hazards / Other Issues

Assessment and mitigation of dam-break lahar hazards from Mt Ruapehu Crater Lake following the 1995-96 eruptions

G. T. Hancox

Institute of Geological and Nuclear Sciences, Lower Hutt

H. (J. R.) Keys

Department of Conservation, Turangi

M. G. Webby

Opus International Consultants, Wellington.

Abstract

The 1995-96 eruptions of Mt Ruapehu caused significant changes to the crater area, which have important implications for the hazard from future lahars when the lake refills. A ~7 m thick layer of tephra (weak ash and scoria) now covers the lake outlet area, creating a situation similar to that after the 1945 eruptions, which led to the 1953 Tangiwai lahar disaster after collapse of a tephra barrier retaining the lake. Simulation flow modelling has shown that a future tephra barrier collapse (dam-break) lahar from Crater Lake will in the worst case be 54-72% larger in the Whangaehu River at the Tangiwai rail bridge. The flow is expected to be greater than the 1953 lahar because glacial recession has removed the Crater Basin Glacier and ice tunnel, which for that event restricted outflow from the breach at the lake outlet. Some of the future lahar (~7%) is expected to overflow into the Waikato Stream, Tongariro River, and Lake Taupo. Overall, the lahar could cause greater damage to bridges, roads, and power lines than has occurred in the past, and significant environmental damage in affected catchments and Lake Taupo. After public consultation and consideration of a range of options to mitigate hazards from a future dam-break lahar from Ruapehu, an acoustic warning system to prevent loss of life, and a bund to prevent overflow into Waikato Stream and Lake Taupo was recommended by the Department of Conservation. There was only limited support for a trench at the Crater Lake outlet (a pristine area of Tongariro National Park), although that option would prevent damage to infrastructure sites along the Whangaehu River, as well as prevent loss of life. The Minister of Conservation has recently approved installation of an Eastern Ruapehu Lahar Alarm System (ERLAS), and construction of a bund to prevent overflow into Waikato Stream. These measures will reduce risk to lives and environmental contamination from lahars on the east side of Ruapehu, including those generated by future eruptions and dam breaks, but they will not prevent possible damage to infrastructure.

1. Introduction

1.1 Setting and geology of Mt Ruapehu

Mt Ruapehu is a large active andesite stratovolcano located within Tongariro National Park, about 40 km southwest of Lake Taupo near the southern end of the Taupo Volcanic Zone (Figure 1). Ruapehu is the largest of the central North Island volcanoes, and its 2797 m summit is the highest peak in the North Island of New Zealand. This large composite volcano has been built by a long series of eruptions dating back at least 250,000 years. Its formation has occurred in short bursts of intense activity separated by long periods of relative quiet (Hackett and Houghton, 1989). Three summit craters have been active in the last 10,000 years, including South Crater, which contains the currently active vent, and is usually occupied by the Crater Lake.

Over the past 10,000 years volcanic activity at Ruapehu has been characterised by relatively frequent, but small to moderate-scale eruptions of lava, ash, pyroclastic flows, (Donoghue *et al.*, 1995), and occasional debris avalanches caused by partial collapse of the edifice (Palmer and Neall, 1989). Activity has also been accompanied by *lahars* formed either by phreatic (hydrothermal) and gas eruptions through Crater Lake, or collapse of the crater rim, resulting in significant hazard in watercourses draining the mountain (Paterson, 1980; Palmer, 1991; Palmer *et al.*, 1993, Otway *et al.*, 1995), including entering the headwaters of tributaries to the Tongariro River and Lake Taupo (Hancox *et al.*, 1995, 1997, see Figure 1).

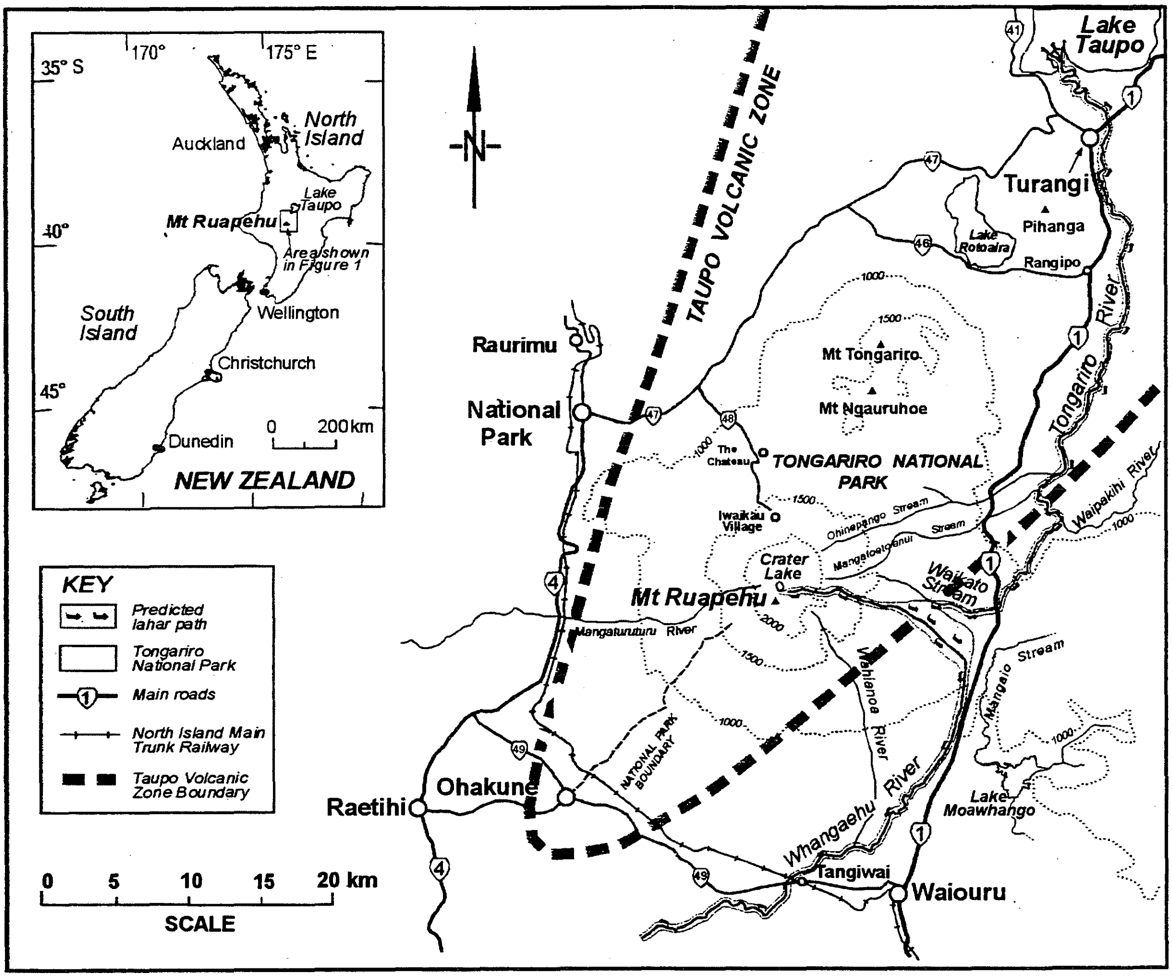

Figure 1. Locality map of Mt Ruapehu and surrounding area, showing the Taupo Volcanic Zone boundary, Tongariro National Park, main rivers, lakes, towns, roads, and potential flow paths of a future dam-break lahar in the Whangaehu and Tongariro rivers.

1.2 Lahars on Mt Ruapehu

There have been many eruptions and lahars from the summit area of Mt Ruapehu over the past 10,000 years. *Lahars* (or volcanic mudflows) are rapidly flowing mixtures of rock debris (volcanic ash to boulder-size material) and water. The material moves down slope as a gravity-driven debris flow in the form of a slurry rather like wet concrete, and flows with laminar (rather than turbulent) motion. The fluid bulk densities of lahars typically range from 1.8 to 2.3 g/cm^3, with about 50-75% sediment by volume. They are 10^4 to 10^5 times more viscous than water, achieve velocities about twice as fast as water (>70 km/hr), and travel distances of more than 100 km (Pierson, 1995).

The major hazard from Ruapehu eruptions in historical times has been destructive lahars caused by ejection of Crater Lake water onto the outer slope of the mountain and into the major catchments such as the Whangaehu, Mangaturuturu, Whakapapaiti and Whakapapanui rivers (Figure 2). However, non-explosive lahars caused by collapse of the crater rim, as occurred in 1953, or displacement of the Crater Lake by inflowing lava as occurred in 1968 generally affect only the Whangaehu River (Otway *et al.*, 1995). All significant explosive eruptions in Crater Lake send lahars down the Whangaehu River, but only relatively large (10^6 m^3 or greater) events eject water into other catchments. Return periods calculated for lahars from Ruapehu are: 20-50 years for 10^6 m^3, 220-270 years for 10^7 m^3, and 10,000 to 100,000 years for 10^8 m^3 (Houghton *et al.*, 1987). In the last 150 years, about 20 lahars have affected the Whangaehu River, with the largest (~6 million m^3) occurring in 1861. In the Whangaehu valley lahars with volumes between 10^6 m^3 and 10^7 m^3 occur on average once every 29 years, or ~3 % annual probability (Hodgson, 1993).

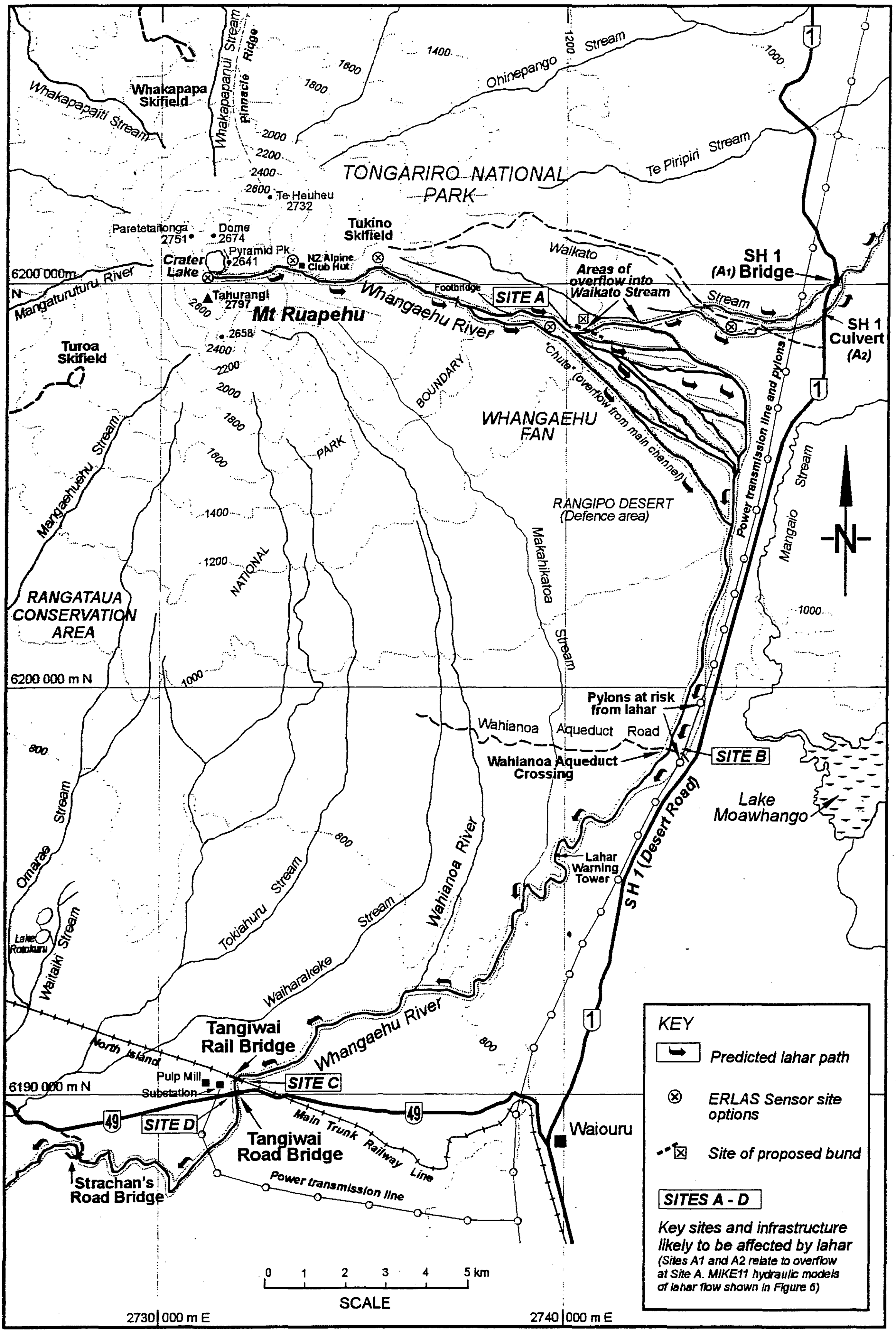

Figure 2. Map of the Mt Ruapehu area showing the predicted flow path of a potential lahar formed by collapse of the 1995-96 tephra barrier at the Crater Lake outlet. Key sites and infrastructure likely to be affected, and proposed hazard mitigation options are also shown.

The most significant lahars on Mt Ruapehu in the last 100 years, and their known cause and effects (after Otway *et al.*, 1995, and Houghton *et al.*, 1996) are as follows:

▪ Jan 1925, ~100,000 m^3 (phreatic eruption)	*- Destroyed farm bridge in Whangaehu valley.*
▪ Feb 1925, ~100,000 m^3 (phreatic eruption)	*- Undercut rail bridge piles at Tangiwai.*
Dec 1953 ~1,650,000 m^3 (Failure of tephra barrier at Crater Lake outlet)	*- Destroyed rail and road bridges at Tangiwai, 151 lives lost when train plunged into torrent.*
▪ Feb 1968, ~730,000 m^3 (lava extrusion into lake)	*- Minor affects in Whangaehu valley.*
▪ June 1969, ~200,000 m^3 (large phreatic eruption)	*- Lahars in several valleys draining Mt Ruapehu, minor damage on Whakapapa ski field.*
▪ May 1971, ~130,000 m^3 (phreatic eruptions)	*- Significant flows in Whangaehu valley, no damage.*
▪ April 1975, ~3,000,000 m^3 (large phreatic eruption)	*- Lahars in several valleys draining from Mt Ruapehu. Minor damage at Whakapapa ski field and Wahianoa aqueduct.*
▪ Nov 1977, ~130,000 m^3 (phreatic eruption)	*- Minor affects in Whangaehu valley.*
▪ 23 Sep 1995 – (Large phreatic eruption)	*- Large lahars in 3 valleys draining Mt Ruapehu.*
▪ 25 Sep –12 Oct 1995 - Continuing eruptions	*- Series of ash eruptions and smaller lahars. Crater Lake emptied by 12 October 1995.*
▪ 28 October –1Nov 1995	*- Rainfall-induced lahars destroyed footbridges in Whangaehu, Mangatoetoenui, Ohinepango stms.*
▪ June-August 1996 - Eruptions resumed	*- Further ash eruptions and smaller lahars. Crater Lake was again emptied by 17 June 1996. 36 lahars in the Whangaehu valley alone over period Sep 1995 –July 1996.*
▪ Sep 1996	*- Eruptions and ash emissions decline.*

Although most significant lahars from Mt Ruapehu have been caused by volcanic eruptions, by far the most damaging was the 24 December 1953 lahar, which resulted in the destruction of rail and road bridges at Tangiwai, and the loss of 151 lives when the northbound Wellington-Auckland Train plunged into the torrent. Several other bridges across the Whangaehu River were destroyed by the lahar (47, 55, 57, and 75 km downstream of Crater Lake), but no other rivers or streams were affected. The 1953 lahar resulted from collapse of a barrier of *tephra* (unconsolidated, ash, scoria and lava blocks) and possibly some lava at the former lake outlet. This material had been deposited over the outlet area during the 1945/46 Ruapehu eruptions, allowing the Crater Lake to refill (by March 1953) to a level ~7-8 m higher that it was prior to 1945 (Healy, 1954). Overflow into the Whangaehu River was via a ~600 m long tunnel under ice of the Crater Basin Glacier, which at that time formed a significant barrier about 120 m thick south of Crater Lake (Beetham, 1982; Hancox *et al.*, 1997). Although historical eruptions may have ejected greater volumes of water from Crater Lake (e.g., 1975), this was distributed by lahars in several valleys on Ruapehu, resulting in much smaller peak flows in the Whangaehu valley than those produced in 1953.

1.3 Effects of the 1995-96 eruptions of Mt Ruapehu

The numerous explosive eruptions of Mt Ruapehu in September-October 1995, and June-August 1996 produced many lahars, emptied the Crater Lake (see above), and modified the summit area. The crater rim and upper Whangaehu valley were noticeably changed by erosion and deposition of a thick tephra layer (ash, scoria, and lava blocks) over the crater area. Parts of the southeastern crater rim - between Pyramid Peak and the outlet, the spur west of the outlet, and the ridge between Pyramid and (monitoring station) J Peak (Figure 3) were all eroded by cascading lake water and explosions during the 1995 eruptions (Keys and Williams, 1996). The crater was also enlarged (by ~40%) and the crater walls south of Pyramid thinned and parts of the crater rim lowered.

Changes to the Ruapehu crater area by the 1995-96 eruptions have potential implications for the stability of the crater rim, and the size and paths of future lahars generated from the Crater Lake. Immediately following the eruptions the former lake outlet was known to be covered by at least 5 m of tephra, which was deposited over the resistant grey lava "sill" that had controlled the Crater Lake overflow level since the 1953 Tangiwai Lahar, and probably before the 1945 eruptions. Therefore, when the Crater Lake refills to the new overflow level, the potential exists for the weak tephra barrier *("dam")* to fail suddenly, releasing the lake water into the Whangaehu River. It was recognised that such an event could create a lahar of proportions similar to the 1953 Tangiwai lahar, possibly resulting in substantial damage to transport and power systems, riverside areas and the riparian ecology downstream (Keys and Williams, 1996).

The 1995 lahars also modified the northern parts of the Whangaehu Fan and caused aggradation near the boundary of Tongariro National Park so that some lahars spilled over into the northernmost channel of the fan (at Site A in Figure 2). Because of these changes the possibility exists for future lahars to break out of the Whangaehu Valley and flow into the Waikato Stream, and then into Tongariro River and Lake Taupo (Hancox *et al.* 1995, see Figure 1). On an annual basis the potential for this to occur has been low (2%, or once in 50 years) compared to the frequency of lahars down the Mangatoetoenui directly into the Tongariro River (5%, or once in 20 years). Because of aggradation, however, the Whangaehu River channel capacity is now less than before the 1995-96 eruptions, so the annual overflow probability may now be as high as 5%. In addition, when the Crater Lake refills to the top of the tephra *dam*, the lahar hazard from collapse of this barrier will be potentially much higher in the Tongariro River system than it is normally.

1.4 Previous studies and background to this paper

After the 1995 eruptions a Debriefing Workshop was held in April 1996, at which changes to the Ruapehu crater area were discussed, and a work programme was developed to investigate and address them (Keys and Williams, 1996). It was recognised that a barrier collapse lahar would not be an imminent problem until the Crater Lake refills to its former overflow level (2530 m) and nears overflow, but it was uncertain how long this would take. After the 1945 eruption the lake took ~7½ years to reach its maximum level prior to the 1953 Tangiwai Lahar (~7 m higher than the pre-1995 eruption overflow level of 2530 m). It was thought that the lake could refill in about 4-6 years after the eruptions had ceased, but it could take longer. This would depend on many factors including future snowfalls, melting, rainfall, evaporation, and volcanic activity. To help evaluate the changes, new aerial photography was obtained and a detailed map made of the crater area.

In response to concerns about future lahar and stability hazards from the Crater Lake after it refills, the Department of Conservation (DOC) organised meetings of potential "stakeholders", including ECNZ, Trans Rail, Trans Power, Transit NZ, NZ Army, Winstones Pulp International, Manawatu-Wanganui Regional Council, Environment Waikato, Ruapehu District Council, Taupo District Council, and the Institute of Geological Nuclear Sciences (GNS). At these meetings an investigation programme was developed, and funding provided by interested parties (listed above) to carry it out. The main work planned included: lake level monitoring, oblique aerial photography, further mapping of the crater area; and an engineering geological investigation of the stability of the eastern rim to the outlet area.

1997 and 1998 studies

The crater rim stability studies were led by GNS, with funding coordinated by DOC. The 1997 study included: (a) ground surveying and (b) geological/geomorphic mapping of the crater area, (c) oblique aerial photography, (d) review of relevant historical and geological data, (e) sampling and testing of tephra deposits at the outlet area, (f) stability analysis of the southeastern crater rim, and (g) hydraulic lahar flow modelling of past lahars (1953, 1975) and a possible future lahar formed by a tephra barrier collapse when the lake refills. This first stage (Phase 1) of the investigation was carried out between February-May 1997, and reported on in June 1997 (Hancox, *et al.,* 1997).

Following review and comment on the results of the 1997 study, Phase 2 of the investigations was undertaken and reported on in 1998 (Hancox *et al.*, 1998). This later study included: (a) ground surveys of channel cross sections and gradients at 13 key sites in the Whangaehu River and Waikato Stream, (b) refinement of hydraulic flow modelling of a potential tephra barrier collapse lahar in the Whangaehu River and Waikato Stream, (c) estimation of peak lahar flow depths at surveyed channel sites, (d) assessment of hazard and possible damage to infrastructure (bridges, power pylons) sites, (e), estimation of lahar paths and inundation zones in the Whangaehu River and Waikato stream, and (f) assessment of possible environmental damage (erosion, aggradation) and contamination in rivers and streams and lakes. The National Institute of Water and Atmosphere Research (NIWA) were commissioned to report on potential effects of the lahar in the Tongariro River and Lake Taupo.

More recent studies

The 1997 and 1998 hazard assessments led to a range of engineering options being considered to mitigate future dam-break hazards from the Mt Ruapehu Crater Lake. This information was subsequently used to prepare an Assessment of Environmental Effects (AEE) aimed at identifying appropriate mitigation measures (Keys, 1999). Following consideration of this report the Minister of Conservation approved its main recommendation, which was to design and install a public lahar alarm system on Mt Ruapehu. A scoping report was then prepared for an alarm and warning system in the Whangaehu and Tongariro catchments by the Department of Conservation (Keys, 2001). This included planning and consultation with a number of interested organisations, including: Genesis Power Ltd, the Police, Transit NZ, Trans Rail, local authorities (Horizons Manawatu, Environment Waikato, Ruapehu and Taupo district councils), the Institute of Geological and Nuclear Sciences, the National Institute of Water and Atmosphere (NIWA), the United States Geological Survey (USGS), and others.

1.5 Purpose and scope of paper

The main objectives of this paper are to: (a) provide a summary of the crater rim stability and lahar flow modelling studies carried out during 1997 and 1998 (Hancox *et al.*, 1997; Hancox *et al.*, 1998), (b) present the findings of the AEE Report prepared by the Department of Conservation (Keys, 1999), and (c) outline the strategy that has been recommended by DOC, and approved by the Minister of Conservation, to mitigate the hazard from a future Ruapehu tephra barrier collapse lahar *(hereafter referred to as a dam-break lahar)* and eruption generated lahars in the Whangaehu and Tongariro rivers. The main study findings are discussed, and the proposed strategy for lahar hazard mitigation, potential infrastructure damage and social issues are examined.

2. Crater rim and lahar hazard assessments

2.1 Changes to Crater Lake area

The 1995-96 eruptions of Mt Ruapehu emptied the Crater Lake and caused significant changes to the crater area, which have important implications for the hazard from future lahars when the lake refills. Figure 3 shows the topography and important geomorphic features in the Crater Lake area as it was in April 2001. Most of the important features seen following the 1996-96 eruptions (Hancox *et al.*, 1997) are still present, but over the past four years there has been substantial gullying and erosion on the inside walls of the crater. Slumping into the rising Crater Lake has led to extensive cliff formation in the tephra deposits around the lakeshore. These features are also illustrated by cross sections (Figure 4), and photos taken in 1997 and 2001 (Figure 5). The main conclusions resulting from the 1997 study (Hancox *et al.*, 1997) are summarised below. Noteworthy changes seen at the crater in April 2001 are also described.

(a) The 1995 and 1996 eruptions covered most of the crater and lake outlet channel area with about 5 to 15+m of *tephra* (weak bedded ash and blocky scoria) with intercalated layers of snow and ice. At the lake outlet, about 6-7 m of this material was deposited on the grey lava sill, which previously controlled the lake overflow level (Figure 4, Section A). On the inside of the crater, erosion and slumping has produced a steep cliff around the lake edge (Figure 4, Cross Section (B), and Figure 5c).

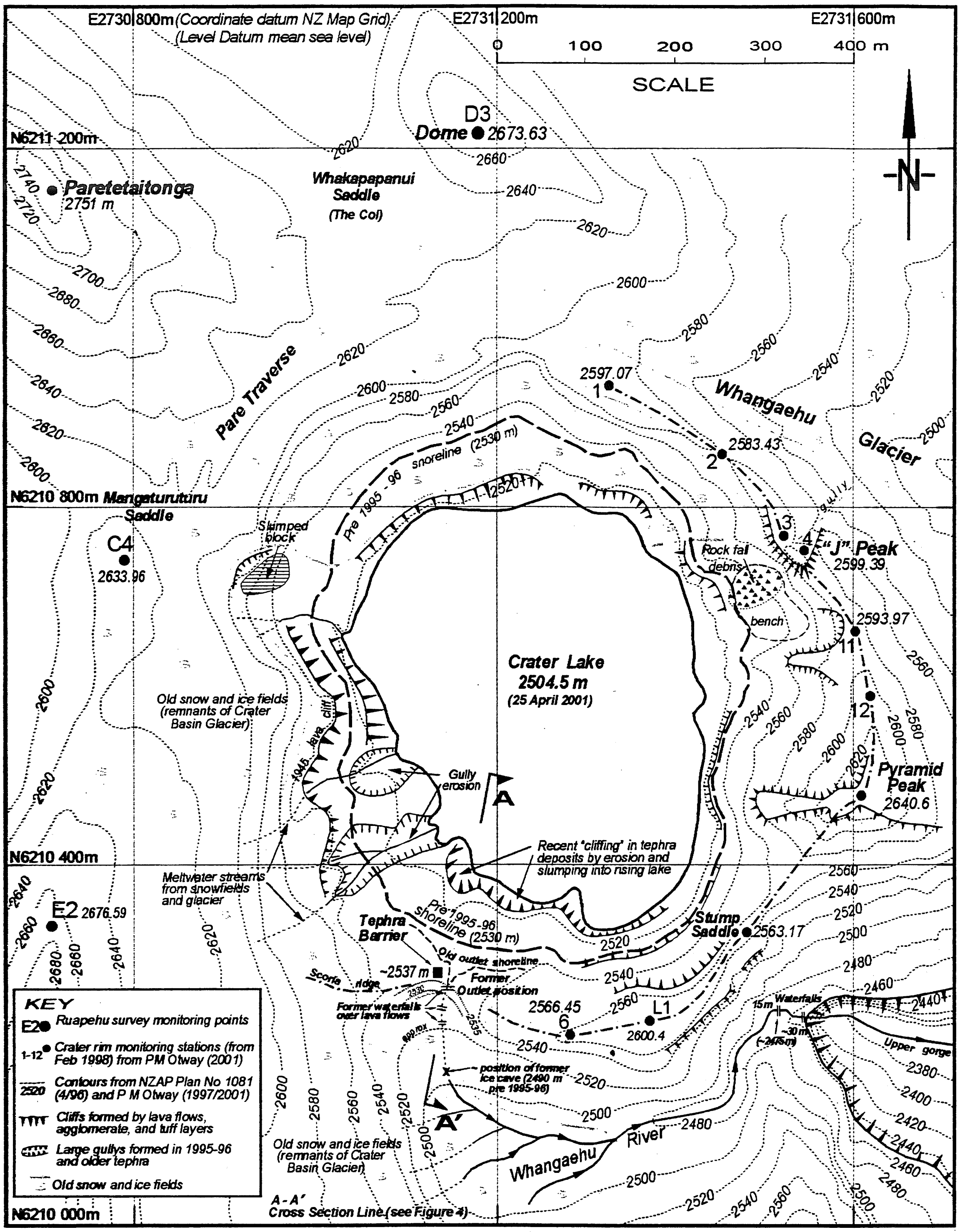

Figure 3. Map of the Mt Ruapehu crater area showing the topography and main geomorphic features developed after the 1995-1996 eruptions. Recent erosion and lake filing effects (as at 25 April 2001) and some crater rim survey stations and monitoring pegs are also shown.

(b) The most significant changes occurred on the southeastern side of the crater rim where it is thinnest, with at least 20 m lost off *Stump Saddle*, and ~50 m of erosion and steepening on the inside of the crater. In this area, crater rim thickness was reduced by 20% at the 2450 m level, but there was only about a 7% reduction at the former lake overflow level of 2530 m, with rim width reduced from 114 m to 104 m. Despite these changes, the broad cross section of the crater rim suggests there has been little overall reduction in its strength or ability to retain a crater lake once it has refilled. Stability analysis indicates that deep-seated failure is unlikely under normal (non eruptive) conditions, even with strong (MM8) earthquake shaking.

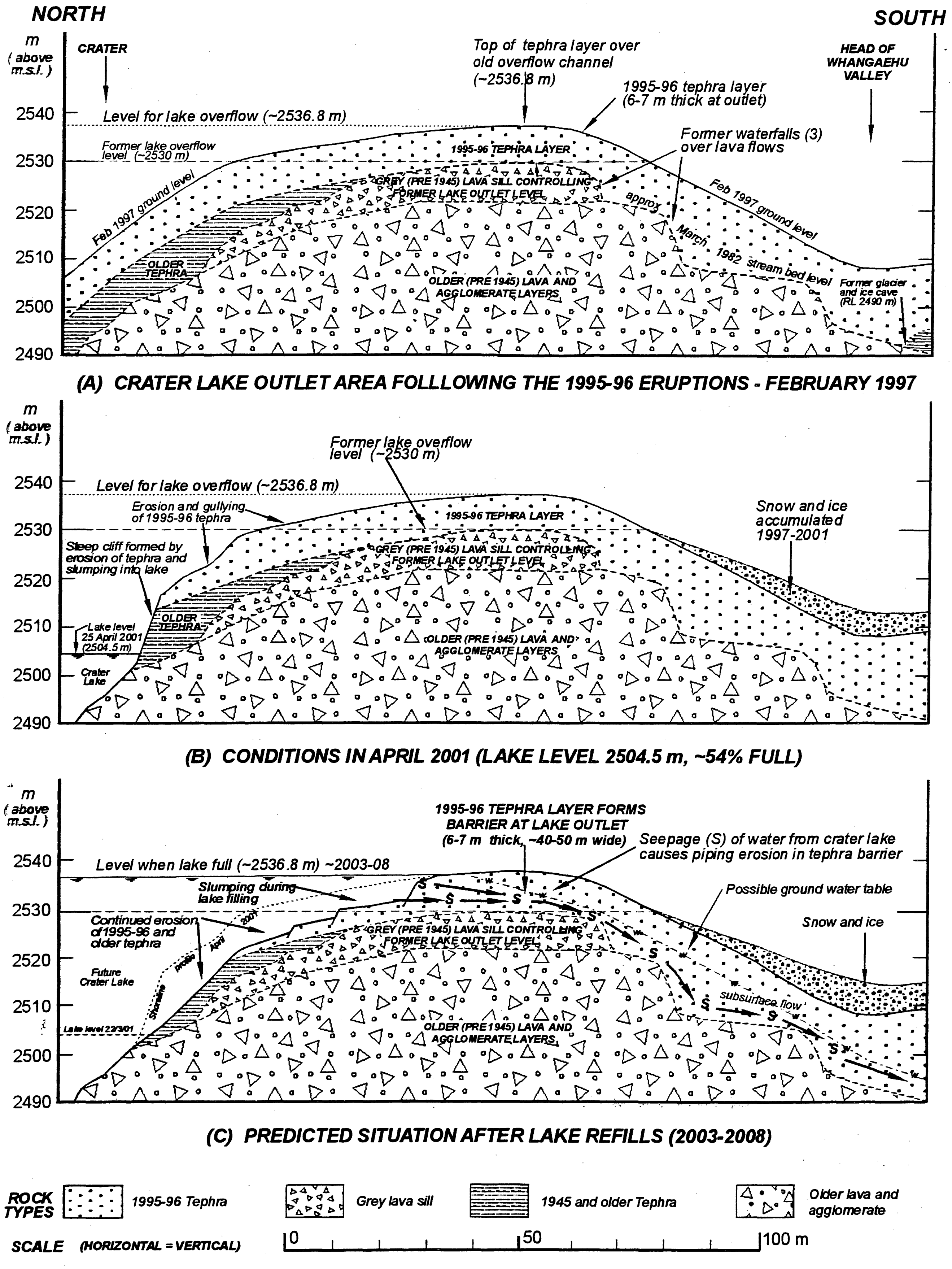

Figure 4. Cross section of the Ruapehu Crater Lake outlet area (Section A-A' in Figure 3) showing the tephra layer deposited by the 1995-96 eruptions (A), conditions as at 25 April 2001 (B), and the predicted situation when the lake refills in 2003-2008 (C).

(c) The strength of the crater wall was not significantly affected by small collapses and superficial landslides on the eastern crater rim from Pyramid Peak to the north of J Peak, where the rim is much wider. The most significant recent (post 1997) changes in this part of the crater rim have been rock falls and crack development on *J Peak* (warm and streaming ground present nearby up to 1999, and rock fall debris shown in Figure 3). However, these slope movements are considered to be local, and are unlikely to extend to the former lake shoreline (2530 m) or the future maximum lake overflow level of ~2537 m. Based on present evidence and conditions, any future crater rim failure at *J Peak* is unlikely to extend below the ~2570 m level and would not lead to a release of Crater Lake water (Hancox, 2001).

(d) The 1995-96 eruptions and lahars greatly reduced the size of the former Crater Basin Glacier to the south of the former lake outlet, with only thin remnants now remaining (see Figure 3). The upper Whangaehu River channel is now very broad and open (see Figures 5a and 5c), compared to conditions that existed from 1953-1982, when the lake outflow stream had to flow through a ~600 m long ice tunnel before reaching the open Whangaehu River channel. Figure 5 (d) shows the thick Crater Basin Glacier and ice cave in February 1954, two months after the 1953 Tangiwai lahar. These changes are thought to be very significant, because in the event of a breach of the tephra barrier at the lake outlet when the lake refills, there is no glacier or ice tunnel to restrict peak outflow from the lake into the Whangaehu River.

2.2 Lake filling and effects on crater area

The Crater Lake is now refilling, and by 25 April 2001 lake level was at ~2504.5 m, or approximately 54% full, and still ~25 m below the former overflow level of 2530 m (see Figures 3 and 5). The lake is not expected to reach the 2530 m level until late 2002 to 2005 (or later if the fast filling rate seen during the 2000/01 summer is not repeated). The top of the tephra layer in the former outlet area (~2537 m) would be reached several months to a year or more after that, depending on snowfall, rainfall, lake temperature, and melting (and assuming there are no eruptions, significant heating events, changes at or beneath the lake floor or slumps into the lake). Continued rising of the lake is expected to result in ongoing cliff formation, with further collapses of undercut material. This process may eventually thin the tephra barrier at the outlet, from ~80 m wide to possibly ~40-50 m wide (Figure 4 c). When the lake has refilled, the tephra layer overlying the outlet area will create a weak "dam" of unconsolidated but relatively dense, gravelly-sand ~ 6-7 m high, and retaining ~1.45 million m^3 of water (~13% of lake). However, evidence from the 1953 Tangiwai lahar suggests that the tephra barrier will not last long after the lake refills.

2.3 Expected manner of tephra barrier collapse

The December 1953 lahar has been attributed to collapse of a barrier of 1945 ash and scoria at the lake outlet, after being weakened for several months by piping or internal seepage erosion, and loss of support from the glacier due to melting of ice (Hancox *et al.*, 1997). The tephra layer deposited over the former lake outlet during the 1995-1996 eruptions is thought to be essentially the same type of material that was present after the 1945 eruption. It is likely therefore, that over a period of several weeks or months, as the lake rises to the present level required for overflow (~2536.8 m), internal seepage flow will occur through the permeable tephra (Figure 4c). This is expected to result in internal piping erosion within the tephra layer, weakening it, and eventually leading to a rapid (~15-45 minutes, or in an extreme worst case, possibly less) breach and discharge of lake water into the head of the Whangaehu valley. This flow of lake water would rapidly incorporate river alluvium and transform into a lahar similar to that of 1953. However, because the flow can now discharge directly into an open channel (rather than travelling through a ~600 m long ice tunnel), the potential peak discharge and lahar produced by a future tephra collapse is likely to be considerably larger than that of 1953, as discussed later. Because of the high porosity and ice within the tephra deposits, it is less likely that the barrier will be overtopped, causing channel development and slower lowering of lake level. It is possible that wave action erosion and slumping back into the crater may remove some of the tephra barrier (Figure 4c), but based on the 1953 precedent, slow erosion of the entire barrier and controlled release of lake water is unlikely.

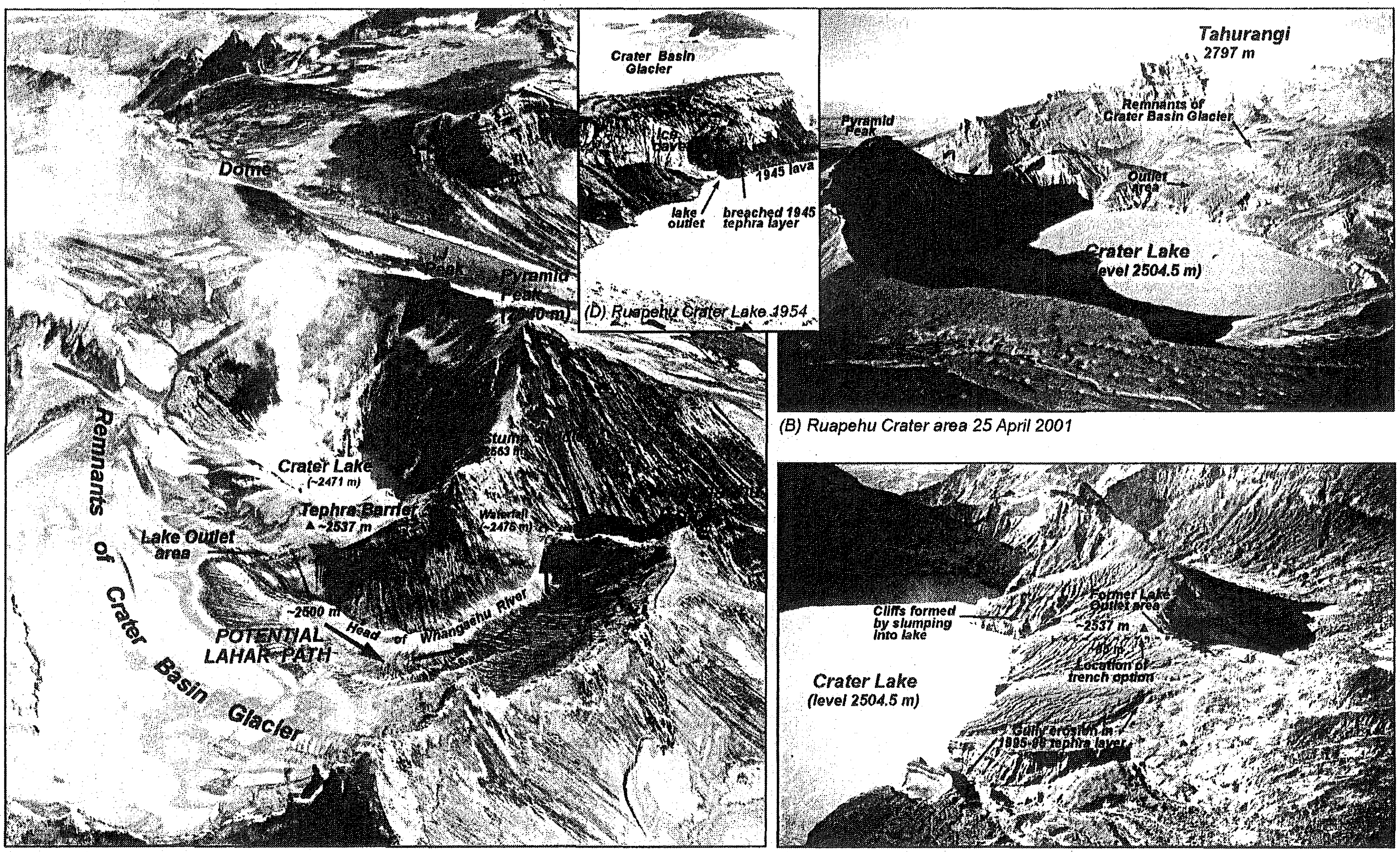

(D) Ruapehu Crater Lake 1954

(B) Ruapehu Crater area 25 April 2001

(A) Ruapehu Crater Lake and outlet area February 1997.

(C) Lake outlet area 25 April 2001

Figure 5. Photos showing the Ruapehu Crater area shortly after the 1995-1996 eruptions (A), and the refilling Crater Lake as it was in April 2001 (B and C). Photo (D) shows the lake in Feb 1954, after the 1953 Lahar. Note the ice cave and thick Crater Basin Glacier south of the lake outlet.

3. Hydraulic simulation flow modelling of lahars

3.1 Methods and assumptions

During the 1997 and 1998 studies (Hancox *et al.*, 1997 and 1998) simulation of lahar floods in the Whangaehu River was carried out using the computer-based hydraulic model to estimate flow characteristics of the 1953 and 1975 lahars, and a hypothetical *dam-break lahar* generated by collapse of the tephra barrier at the lake outlet when the lake is full. This involved use of one-dimensional hydraulic modelling software MIKE11, produced by the Danish Hydraulic Institute. Although the MIKE11 software is designed for simulating the passage of water flood events, the model used assumes turbulent fluid flow behaviour to simulate historical and future dam-break lahars in the Whangaehu River. Although this model has limitations due to the assumption of turbulent fluid flow behaviour, the authors are confident that the approach provides a reliable qualitative prediction of the hazard posed by a future dam-break lahar from Ruapehu Crater Lake.

Preliminary lahar simulation flow modelling results were presented in the 1997 Report (Hancox *et al.*, 1997). These were based on a MIKE11 model of the Whangaehu River, using simplified river channel geometry for different reaches (i.e. gorge, boulder fan, river parallel to SH1), approximated by a constant width channel, and slope data from the 1:50,000 topographic map. The 1997 results confirmed speculation (based on geomorphic changes at the lake outlet since 1953) that a future dam-break lahar from Ruapehu is likely to be considerably larger than the 1953 lahar, and provided a basis for more detailed and refined flow modelling at key sites during 1998.

The 1998 studies extended previous (Hancox *et al.,* 1997) simulation modelling of the 1953 and 1975 lahars in the Whangaehu River and a hypothetical dam-break lahar. The current Mt Ruapehu Crater lake outlet barrier situation mirrors the pre-1953 situation so that the 1953 event was used as an analogue for a future barrier collapse lahar. Estimates of peak flood discharge and flows for the 1953 lahar were obtained to enable the potential flood hazard at the Tangiwai rail and road bridges and other key infrastructure sites to be determined.

A review of the Hancox *et al.* (1997) report by Dr Shane Cronin and Professor Vince Neall of Massey University gave particular scrutiny to the hydraulic model simulations of different lahar events, with the beneficial knowledge of recent field data obtained from lahar events, which occurred during the course of the 1995-1996 Mt Ruapehu eruption sequence. That review arrived at different conclusions regarding the flood hazard at the Tangiwai Bridge posed by a lahar event resulting from a future Crater Lake outlet barrier collapse. However, the reasons for these differences were subsequently identified and resolved at a technical review meeting, at which it was agreed to undertake additional hydraulic modelling of lahar events using the knowledge gained from the field data obtained from the 1995-1996 lahar events.

Specific objectives of simulation flow modelling undertaken in 1998 included: (a) revising the simulations of the 1953 lahar and a future dam-break lahar; (b) estimating the most credible peak discharge flows at the lower end of the Whangaehu Gorge and at the Tangiwai rail bridge; (c) defining an upper bound estimate of peak discharge flow and the range of uncertainty; and (d) estimating the maximum credible peak discharge depths at a number of critical points and key infrastructure sites down the Whangaehu River and Waikato Stream. The latter required ground surveying of channel cross sections at key sites.

Many aspects of the lahar flow simulations were uncertain. For example, for the 1953 lahar model there was uncertainty about the size of the ice tunnel. Although the breach development time is generally important for dam-break events, it was not significant for the 1953 lahar because an ice tunnel restricted outflow. The size of the tunnel is therefore very important in modelling the 1953 event, as outflow from the lake would be controlled mainly by its narrowest diameter. Although a large ice cave (~46m wide and 30 m high) was formed in the glacier at the lake outlet by warm water after the breach, the cave tapered down to a narrow tunnel extending under the glacier (see Figure 5d). Estimates of tunnel diameter (4-5 m) used in the modelling are based on observations from photographs of the tunnel outlet after the 1953 event. The 1953 lahar model was calibrated by adjusting the size of ice tunnel, so that the travel time and discharge at Tangiwai matched the field observations (Harris, 1954). Other areas of uncertainty, and their relevance to the modelling are summarised in Table 1. Assumptions and values used in the lahar flow simulations are listed in Table 2 (after Hancox *et al.*, 1998).

Table 1. Main areas of uncertainty in lahar simulation modelling

Area of uncertainty	Significance and input to model
(a) Tephra barrier breach time	Not significant for 1953 event if ice tunnel acted as a throttle. Very significant for hypothetical future lahar event. Assumed range of breach development time (0.25 to 0.75 hrs) based on data from failures of man-made earthfill embankment dams (Froehlich, 1997; Singh and Scarlatos, 1988). In an extreme worst-case scenario the breach time may be less than 0.25 hrs.
(b) Ice tunnel diameter	Not relevant for future lahar event. Very significant for 1953 event - lake outflow controlled by narrowest diameter along tunnel length. Estimates of tunnel diameter (4-5 m) are based on visual observations from photographs of the tunnel outlet after the 1953 event. Model for 1953 event calibrated by adjusted size of ice tunnel so that discharge and travel time to Tangiwai matched field observations. Tunnel diameter would have increased in size during the course of the 1953 event due to effect of warm lake water melting the ice walls.
(c) Transformation of water flow into lahar flow/transformation of lahar flow back into hyper-concentrated water flow	Very poor understanding of processes at present. No theoretical model available. Simplified approach is most practical one available in view of limited understanding of transformation processes and unavailability of an adequate theoretical model.
(d) Spatial and temporal variation of sediment concentration by volume of lahar event	Sediment concentration values of 0.38 and 0.85 obtained for 2 reconstituted sediment deposit samples from the 1953 lahar. Field data from 1995 lahar events is best available guide for hypothetical future lahar events.
(e) Fluid mechanics behaviour of lahar event	Turbulent flow model requires use of channel roughness/friction parameter as energy dissipation parameter.
(f) Channel roughness (energy dissipation) parameter for lahar event	Values based on experience with water flows are best available guide. Estimated *Manning's n values* (Hicks and Mason, 1991) used in models.
(g) Channel geometry	Surveyed cross-sections for specific sites and reaches of the Whangaehu River provide reasonable estimate of dimensions and steepness of channel slopes. Overall channel slope determined from 1:50,000 topographic maps.

Table 2. Summary of assumed values used in MIKE11 lahar simulation modelling

Parameter	1953 Lahar	Future dam-break lahar
(a) Volume of water released (m^3)	1.82×10^6 *(8 m high dam)*	1.45×10^6 *(6.5 m high dam)*
(b) Foundation level (m, asl)	2530	2530
(c) Maximum breach depth (m)	8	6.5
(d) Maximum breach width (m)	60	60 *(* see note[1] below)*
(e) Breach development time (hrs)	0.25 to 0.75	0.25 to 0.75 *(* lesser and greater values possible[1], but not modelled for a worst case scenario event)*
(f) Ice tunnel dimensions (m)	Length 500 m; width 4-5 m	NA
(g) Peak outflow modelled from Crater Lake	~250 m^3/s from ice tunnel exit into Whangaehu gorge	480-850 m^3/s at lake outlet into open Whangaehu channel.
(h) Sediment concentrations (%)	*% by volume and Bulking Factor (assumed for both models)*	
▪ *End of Whangaehu Gorge*	70 3.3	
▪ *End of outwash fan*	55-60 2.2 - 2.5	
▪ *Tangiwai rail bridge*	45 ±5 1.8 ±0.2	
(i) Peak flow depths at specific sites	The MIKE11 models used surveyed cross section data, supplemented by 1:50,000 topographic data for overall channel gradients. Field observations during the 1953 and 1975 lahars were used to calibrate the models.	
(j) Channel roughness parameters *(energy dissipation)*	Manning's roughness (n) values assumed for various reaches. (Whangaehu gorge 0.150, fan 0.100, SH 1 –Tangiwai 0.035-0.040)	

3.2 Results of simulation flow modelling

The main results of simulation flow modelling of the 1953 Tangiwai lahar and a possible future lahar generated by collapse of the tephra barrier at the Crater Lake are summarised in Figure 6 (modified from Hancox *et al.*, 1998). This shows the predicted discharge (flows) and travel times to sites down the Whangaehu River for simulated tephra dam-break lahars. MIKE11 hydraulic models show the estimated peak flow depth of a maximum credible future lahar at key locations on the Whangaehu River (Sites A-D). Figure 2 shows the locations of these sites, along with the predicted flow path of a potential dam-break lahar from Ruapehu. The main conclusions drawn from the lahar flow modelling illustrated by Figure 2 and Figure 6 are as follows:

(1) The ice tunnel under the Whangaehu Glacier, through which the 1953 flood exited into the Whangaehu River, had a significant throttling effect on the initial peak discharge. The tunnel is thought to have been enlarged due to the erosion of the ice walls by the flow of warm water. The best estimate of ice tunnel average diameter is 4.7 m, giving a peak outflow *(water only, from the tunnel exit into the upper Whangaehu gorge)* of about 250 m^3/s (Figure 6).

(2) Bulking of the water flow (by entrainment of sediment) released in the 1953 event down the steep Whangaehu Gorge would have increased the peak discharge at the end of the gorge to about 800 m^3/s (lower curve in Figure 6).

(3) Attenuation of the 1953 lahar down the multi-channel fan below the Whangaehu Gorge, and then down the wide bed of the Whangaehu River (Figure 2), would have occurred due to the redeposition of sediment (and hence the reduction in sediment concentration by volume) and the effects of channel friction. Peak discharge at Tangiwai Bridge is calculated to have been ~590 m^3/s, which matches fairly well the estimated discharge based on a reanalysis of some slope/area measurements made by Harris (1954) following the 1953 event (see Figure 6). The effects and damage resulting from the lahar at Tangiwai are shown in Figure 8 (a).

(4) The flood resulting from a future dam-break at the Crater Lake outlet will not be constrained by an ice tunnel (as in the 1953 lahar) due to shrinking of the Crater Basin Glacier below the outlet (see Figures 2 and 5). The outflow will be controlled by the rate of the dam-break. Breach development times in the range 0.25-0.75 hours are expected, based on evidence from failures of earthfill embankment dams (Froehlich, 1997; Singh and Scarlatos, 1988). This range of breach development time gives maximum credible peak outflows (water only) of 480-850 m^3/s at the lake outlet, which are 2-3 times greater than the 1953 outflow into the upper gorge (Figure 6). This outflow range represents a realistic worst case scenario.

(5) For the future dam-break lahar, bulking of the water flow (by entrainment of sediment) released down the steep Whangaehu Gorge will increase the peak discharge at the end of the gorge to about 1540-2340 m^3/s. Overflows of the order of 50-290 m^3/s into the southern "Chute" channel of the Whangaehu, and 20-160 m^3/s into the Waikato Stream–Tongariro River system at Site A are predicted to occur (Figure 2 and Figure 6).

(6) Attenuation of the future dam-break lahar will occur down the outwash fan below the gorge and down the Whangaehu River for the same reasons as for the historic 1953 event (that is, redeposition of sediment, see (3) above).

(7) Peak discharge at Tangiwai for the future dam-break lahar is estimated to be 910 ±105 m3/s giving an upper bound credible discharge of 1015 m^3/s. This flow is *54-72% larger* than the 1953 lahar at Tangiwai. *Self similarity* or convergence of the future dam-break discharge curves is achieved at about Tangiwai, and of all three curves by the Tirorangi Marae bridge, about 52 km from the Crater Lake (Figure 6). *Self similarity* describes the behaviour of a flood wave travelling downstream whereby, for the same initial volume released from an upstream reservoir, the peak discharge and travel times become independent of the rate of volume release or breach development time. An assumption of *self similarity* was used in previous modelling of lahars from Ruapehu (Weir, 1982; Vignaux and Weir, 1990).

(8) Because of the greater discharge predicted for the dam-break lahar, it would also travel faster downstream than the 1953 lahar. A travel time to the Tangiwai rail bridge is predicted to be 1.8-2.1 hours for the future event, compared to about 2.3 hours for the 1953 event (Figure 6).

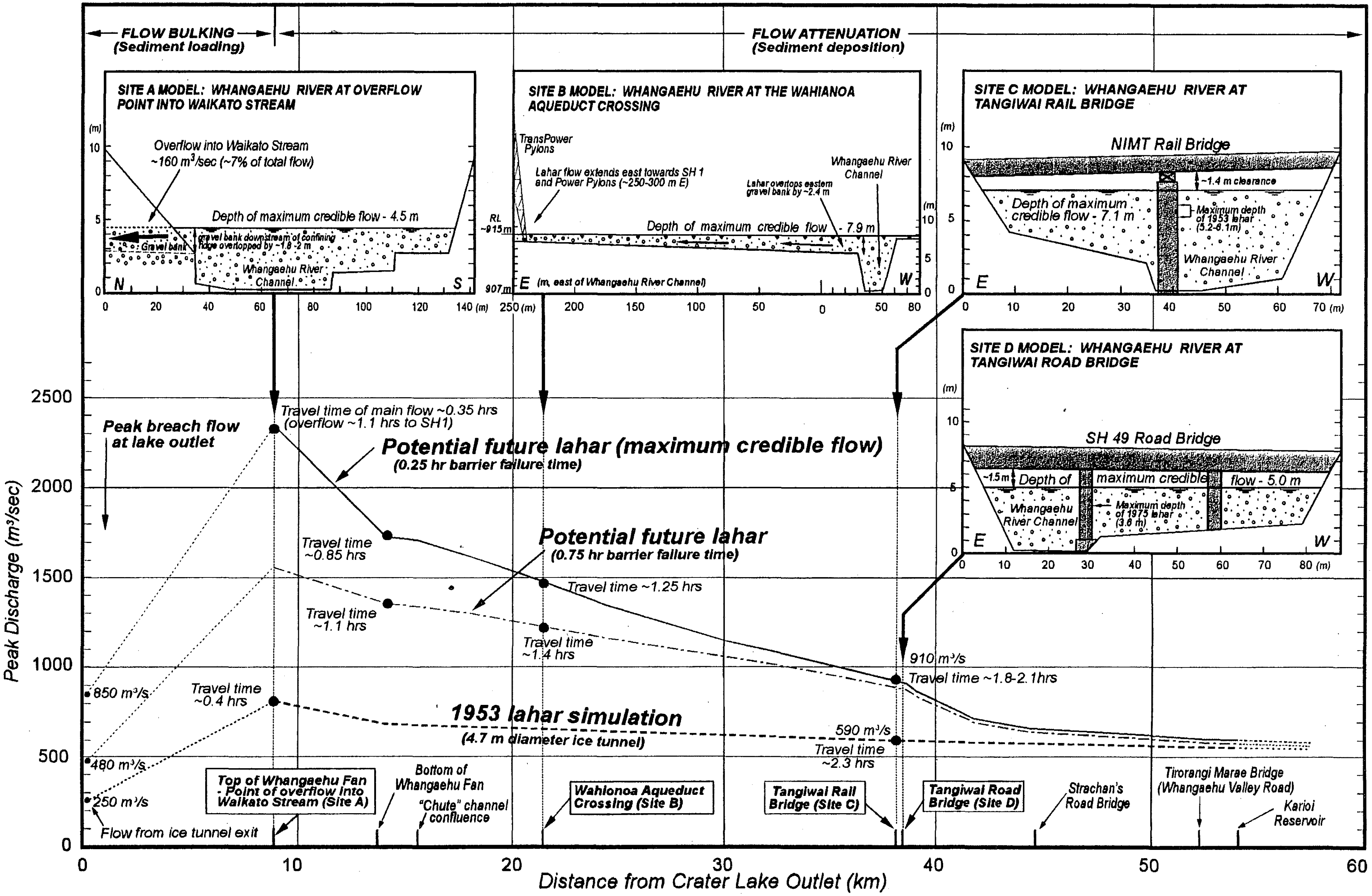

Figure 6. Predicted peak discharge and travel times for simulated tephra dam-break lahars on Mt Ruapehu. MIKE11 hydraulic models (Sites A-D) show the estimated peak flow depths of a maximum credible future lahar at key locations down the Whangaehu River.

Peak flow depths at specific sites

Peak flow depths of a future dam-break lahar were estimated along the Whangaehu River and Waikato Stream at 13 selected sites. This required construction of local MIKE11 hydraulic models of each site, using the surveyed cross-sections, 1:50,000 topographic data, and construction data from the Tongariro Power Scheme (Wahianoa Aqueduct, Site B Figure 6). Input hydrographs for the models were obtained from results of the lahar simulations, and the coarse MIKE11 model of the whole Whangaehu River from the Crater Lake to the Karioi hydrological recording station.

It is believed that the 13 surveyed cross sections and models (Hancox *et al.*, 1998) gave a reasonable estimate of possible flows and depths of a future dam-break lahar down the Whangaehu River and Waikato Stream, particularly at key infrastructure sites.

The four models shown in Figure 6 have been annotated to show maximum credible discharge depths in relation to nearby bridges, roads, and power pylons. Models for the Tangiwai rail bridge and SH 49 road bridge (Sites C and D, Figure 6), were calibrated and verified against estimated flow depth data from the 1953 and 1975 historic lahar events. The potential peak lahar flows and depths predicted at key sites in the Whangaehu River and Waikato Stream are summarised in Table 3, and important features at the sites are illustrated in Figures 7 and 8.

Table 3. Peak discharge and depths of a future dam-break lahar at key sites in the Whangaehu River and Waikato Stream based on simulation flow modelling.

Model Site	Average Peak Discharge (m^3/s)	Maximum Credible Discharge (m^3/s)	Depth for Average and Maximum Credible Discharge (m)
Whangaehu River at point of overflow into Waikato Stream *(Site A, Figure 6)*	1940 (±400)	2340	4.0 - 4.5
Whangaehu River at Wahianoa Aqueduct crossing *(Site B, Figure 6)*	1305 (±230)	1535	7.7 – 7.9
Whangaehu River at Tangiwai Rail Bridge *(Site C, Figure 6)*	910 (±105)	1015	5.8 - 7.1*
1953 lahar at Tangiwai rail bridge	*590 (±110)*		*5.2 - 6.1**
Whangaehu River at Tangiwai Road Bridge *(Site D, Figure 6)*	910 (±105)	1015	4.0 - 5.0*
SH Bridge over Waikato Stream *(Site A1, Figure 2)*		160**	2.7**
SH crossing of Waikato Stream *(Site A2, Figure 2)*		160**	1.2**

* *Allows for "observational uncertainty" and "bow wave effect", as seen during 1953 and 1975 lahar*

** *Overflow from Whangaehu River at Site A (Figure 2). Assumes all flow travels down the north (Site A1) or south (Site A2) branch of Waikato Stream.*

The maximum credible discharge values (Table 3 and Figure 6) indicate reasonable worst case scenario flows for a future dam break lahar at various points down the Whangaehu River. These estimates are particularly sensitive to the peak outflow at the Crater Lake outlet, and hence the method, time, and dimensions of the tephra barrier breach. Some breach development models (e.g., slow piping and breach erosion) result in outflows 50-60% lower than the modelled worst case scenario range (480-850 m^3/s). On the other hand, some failure models involving multiple piping failures and "flow sliding" may result in more rapid collapse (~5-15 minutes) and a wider (~90 m) breach, giving much higher initial outflow (~1000-1200 m^3/s). Although such an extreme outflow for a future dam-break lahar is possible, the modelled outflow range of 480-850 m^3/s is considered to be realistic and appropriately conservative for estimating flows downstream, and for hazard and risk assessment. *Lahar flow bulking* within the river channel is another debatable parameter, with bulking factors as high 5 (with proportionately higher peak flows) observed in lahars on some overseas volcanoes (Pierson, 1998, 2001). However, evidence from historical Ruapehu lahars suggests that such extreme flow bulking (beyond the modelled range of 1.8-3.3, Table 2) is unlikely in the Whangaehu River channel during the future dam break lahar.

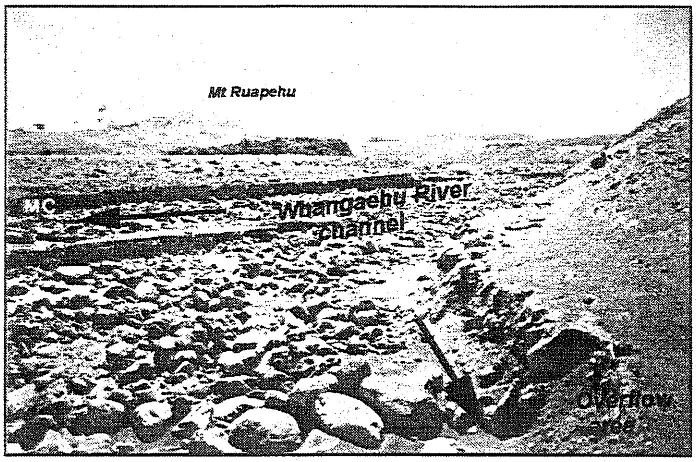

(A) Whangaehu River channel at the point of potential lahar overflow towards Waikato Stream, and from there to the Tongariro River and Lake Taupo (see Figure 1). (Site A, on Figures 2 and 6).

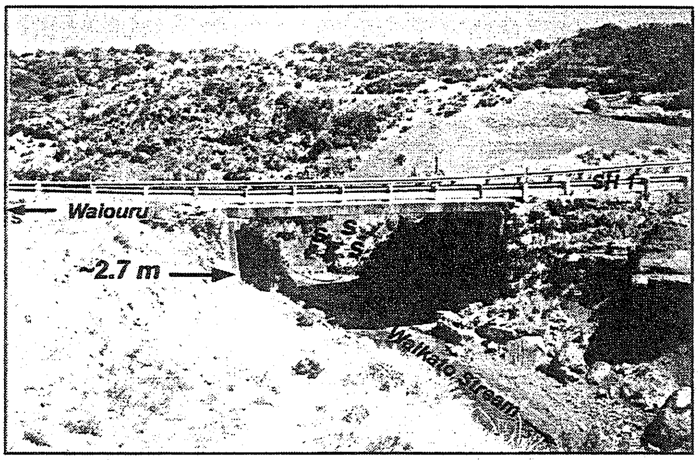

(B) SH 1 Bridge across Waikato Stream showing the depth of a possible lahar, due to overflow from the Whangaehu River. The lahar flow could cause scouring of the north abutment (s), and possibly damage the bridge.

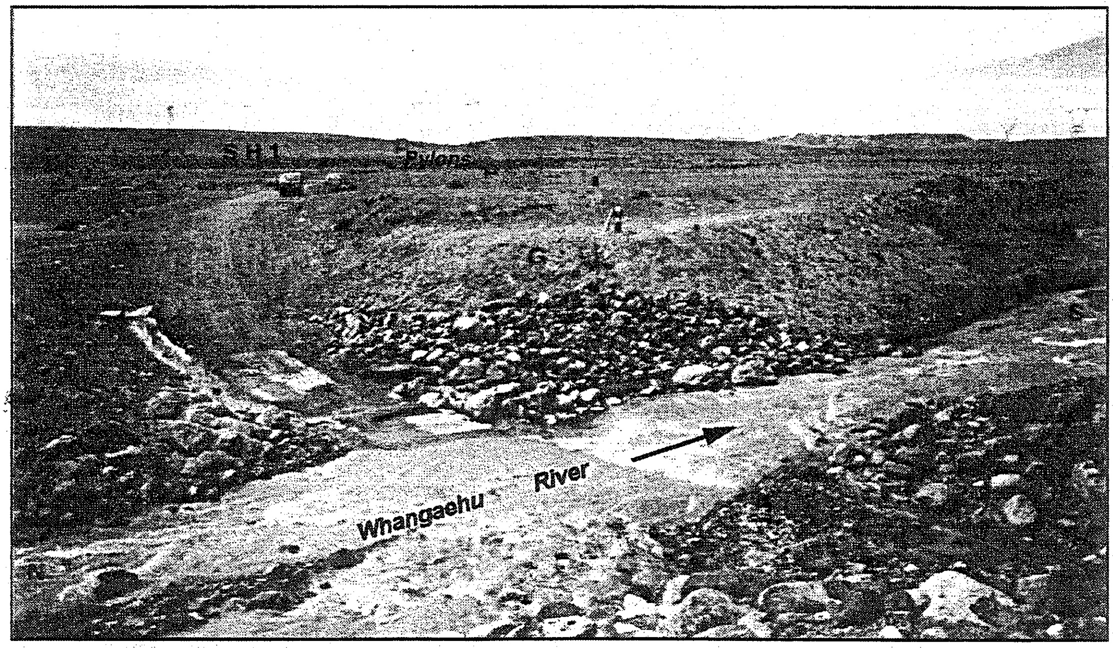

(C) Whangaehu River at the Wahianoa Aqueduct crossing. SH 1 and power pylons at risk from a potential tephra barrier collapse lahar are shown in the distance (Site B in Figure 6).

Figure 7. Photos of sites along the flow path of a possible future lahar on the Whangaehu River, formed by collapse of the tephra barrier at the lake outlet (Sites A & B, see Figure 6). The SH 1 Road Bridge across Waikato Stream, which is at risk from a lahar overflow from the Whangaehu River at Site A is also shown (Photo B above).

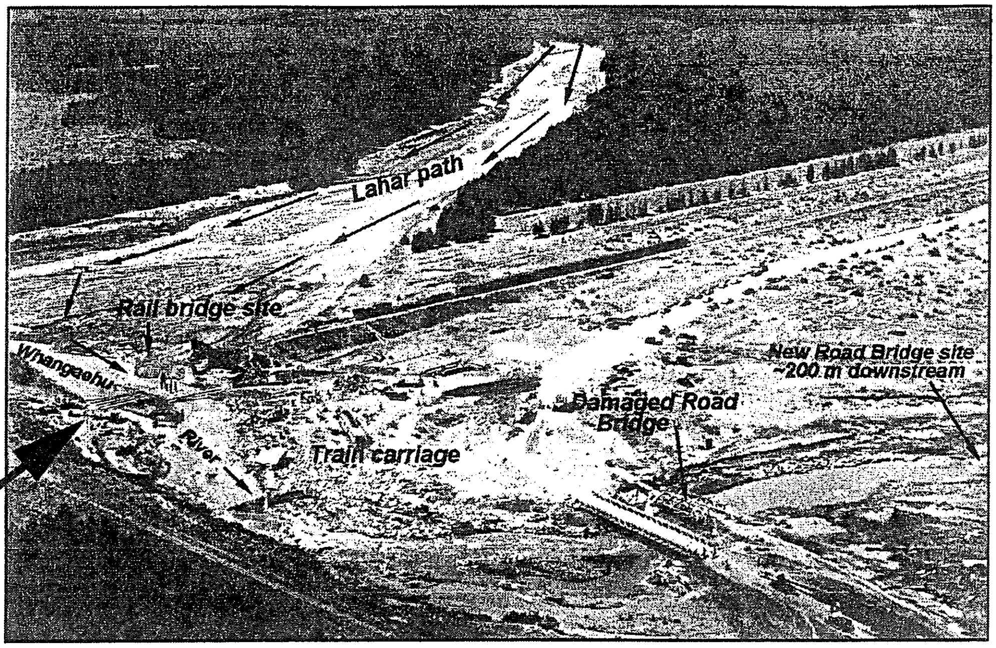

(A) Scene of the 1953 Tangiwai Lahar Disaster, showing the destroyed rail and road bridges, and remains of the train.

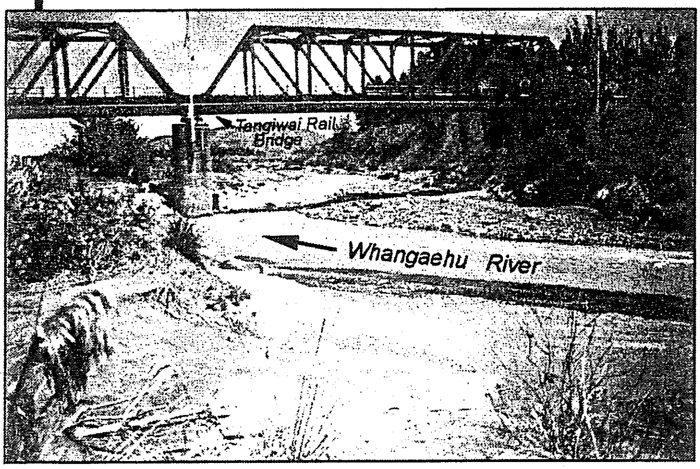

(B) Existing Rail Bridge at Tangiwai (Site C, Figure 6).

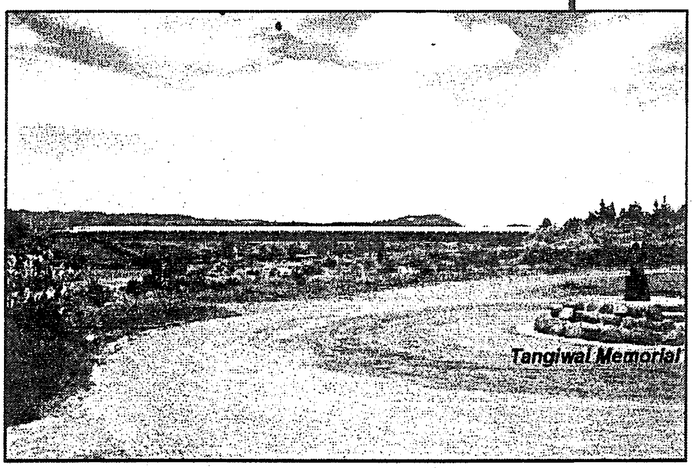

(C) New SH 49 Road Bridge at Tangiwai (Site D, Figure 6).

Figure 8. Photos of the 1953 lahar disaster site on the Whangaehu River at Tangiwai. The existing rail and road bridges are at risk from a potential future lahar formed by collapse of the tephra barrier at the lake outlet. That lahar is predicted to be 54-72% larger at Tangiwai than the 1953 lahar. Figure 5 shows the likely peak flow depths at the bridge sites (Sites C and D).

4. Possible effects of dam-break lahar

Flow simulation modelling allowed Hancox *et al.* (1998) to predict the potential flow path of a future tephra dam-break lahar (see Figure 2), and assess the hazard and possible damage to key infrastructure sites (roads, railway lines, bridges, power pylons) in the Whangaehu River and Waikato stream. These assessments were based on the maximum credible *(worst case scenario)* discharge flows and depths (Table 3), which were considered to be realistic and appropriate for hazard assessment purposes. The lahar flow path shown in Figure 2 provides a generalised best estimate of the predicted event, using (as a guide) aerial photos taken of the Whangaehu Fan, and the Tangiwai disaster site (Figure 8a) shortly after the 1953 lahar.

In discussing the possible effects of the lahar, Hancox *et al.* (1998) noted that damage to a particular structure will depend on: (a) the depth and velocity of the high density flow (which may have a sediment bulking factor of 1.8 to 2.5, Table 2), and (b) the capability of the structure's design and construction to withstand the power and erosiveness of a debris flow containing boulders up to 1 m or more in diameter. Given the maximum credible (worst case) flow depths of a future barrier collapse lahar it was concluded that there was significant hazard and potential for damage to structures in the Whangaehu River and Waikato Stream. Possible effects of the lahar could include the following:

- The SH 1 road bridge across the north branch of Waikato Stream (Figure 7b) may be affected by abutment scouring and possibly damaged or destroyed *(hazard moderate to high).*
- The SH 1 crossing of Waikato Stream south branch (Figure 2) may be washed out over 30-40 m *(hazard moderate to high),* but power pylons nearby are unlikely to be affected *(hazard low).*
- Power pylons near the Wahianoa aqueduct crossing (Figure 7c) are at significant risk from footing inundation and leg damage *(hazard high to very high).*
- The Tangiwai rail and road bridges (Figure 8)are at risk from pier damage, displacement, and possible collapse, even for the average peak flow. The road bridge approach embankments are likely to be overtopped and washed out *(hazard very high).*
- The TranzRail lahar warning gauge sited ~12 km upstream of the Tangiwai bridges (Figure 2) is not expected to be overtopped by the lahar, but its "bow wave" may damage or destroy communication equipment on top of the tower.
- The Strachans Road bridge is likely to be overtopped and destroyed *(hazard very high)*, but the Tirorangi Marae bridge (~8 km downstream) is unlikely to be affected *(hazard low-moderate).*
- The "Round-the-Mountain" walking track bridge in the Whangaehu Gorge will be destroyed by the lahar, unless it is removed first *(hazard very high).*

Significance of potential lahar and hazard mitigation

The overall conclusion reached during the 1997 and 1998 studies was that a future lahar caused by collapse of the 1995-96 tephra barrier will result in higher peak flows in the Whangaehu River than have occurred in any previous historical lahar since 1861. At the Tangiwai Rail Bridge the lahar could be ~72% larger than the 1953 lahar. Upstream the peak discharge could be more than twice as large. The possible damage outlined above reflects the significance and potential hazard from such an event in the Whangaehu valley. Engineering design assessments were recommended for structures that could be affected by the lahar (especially the rail and road bridges at Tangiwai, and power pylons near the Wahianoa Aqueduct) to allow costs and benefits of hazard mitigation options to be evaluated with greater confidence.

However, as already mentioned it is not only the Whangaehu River that could be affected. Some of the lahar (up to ~160 m^3/s, or 7% of the total flow) is expected to overflow into the Waikato Stream (at Site A, Figure 7a) and then travel down the Tongariro River and into Lake Taupo *(hazard high).* The sediment-laden flow of acidic water could cause significant riparian contamination and damage to the Rangipo Power Station (as occurred during the1995-96 lahars), unless the intake gates were closed. Construction of a bund at the overflow point (Figure 2) was recommended (Hancox *et al.*, 1995; 1998) to prevent the overflow of future lahars into the Tongariro River and Lake Taupo.

Hancox *et al.* (1997) discussed mitigation measures to eliminate hazard and effects of a dam-break lahar when the Crater Lake refills in 2003-2005, and recommended that a trench should be excavated in the tephra barrier at the outlet channel area. In order to reach the grey lava "sill", the trench would have to be ~6-7 m deep, 80-100 m long, and 10-30 m wide (see Figures 4 and 5c). Such an excavation could easily be accomplished with a large (D10) bulldozer, which could be walked to the site on snow in early spring. Another possible action discussed was a deeper trench extending 10-30 m into the lava (below the former overflow level). This would decrease the future lake volume (by ~20-40%) and lead to more rapid emptying of the Crater Lake during future eruption sequences. However, such a measure could cause an earlier transition to ash eruptions and an increased frequency of small eruptions depositing ash on the skifields. Nevertheless, it would probably reduce the size and effects of lahars during future volcanic eruptions, possibly with significant benefits to Mt Ruapehu skifields and rivers draining from the mountain.

5. AEE Report and hazard mitigation options

Information provided by the Hancox *et al.* (1997, 1998) studies of crater rim stability and a future tephra barrier collapse lahars from Ruapehu was used by the Department of Conservation to prepare an Assessment of Environmental Effects (AEE) Report for the Minister of Conservation (Keys, 1999). That report discussed the potential hazard and effects of a tephra dam-break lahar (as outlined above), and outlined a wide range (25) of possible mitigation options. The main types of options presented for consideration included:

- *Option 1* No engineering intervention. Instead, this would involve land use planning, an acoustic warning system, and response and contingency planning.
- *Option 2* Intervention only in lahar run-out zones, involving construction of gravel (or gabion) bunds, earth dams, asset protection works, and lahar containment basins. This option includes the bund at the point of overflow into Waikato Stream.
- *Option 3* Harden (grout, bio hardening, weir construction) or perforate the tephra barrier with a culvert or tunnels.
- *Option 4* Excavate trench through 1995-96 tephra layer using small or large bulldozers, excavators, pumping and sluicing, high explosives, or manual digging.
- *Option 5* Excavate trench into underlying lava at outlet (light or heavy plant and explosives, aerial delivery of high explosives).
- *Option 6* Other possible options (siphoning of lake water, and a barrier truss).

After public release of the draft AEE in 1998, the consultation process continued between DOC and affected stakeholders (owners of assets that could be affected such as TranzRail, TransPower, Transit NZ, Genesis, Winstones, Regional and District Councils etc), and more widely with the general public. This process showed that there was most support for *Option 1 (alarm system, with no engineering intervention)*, and limited support for *Option 1* in conjunction with *Option 2 (containment dams)*, or *Option 4 (trench at lake outlet excavated with bulldozers flown to site)*. The Ruapehu District Council and Taupo District Council supported *Option 4*, in addition to *Option 1*. Both regional councils (Environment Waikato, Manawatu Wanganui Regional Council) supported *Option 1,* although the latter decided not to comment on the other options in order not to compromise a subsequent resource consent process that would be needed for those options. The Taupo District Council subsequently supported *Options 1 and* 2, *rather than 4*.

The Department of Conservation have therefore promoted the adoption of *Option 1* for mitigation of a tephra dam-break lahar, and recommended installation of: a reliable real-time lahar alarm system high on the eastern side of Mt Ruapehu. It suggested that an acoustic-based system and practical alternatives should be investigated. Other recommendations included the need for drawing up contingency plans for warning and response actions by responsible agencies (Police, District and Regional Councils, asset managers, DOC).

In making its recommendation to the Minister of Conservation the Department of Conservation took the following key factors into account:

- The chosen option had to reduce risks to public safety to very low levels.
- Installation of an alarm system and responses to it would reduce the risks to the public to very low levels.
- Risk assessments carried out by agencies such as the Army, ECNZ/Genesis, TransPower and TranzRail that concluded the risks to their infrastructure were not so large as to require engineering work at the crater.
- The alarm system would have long-term benefits, as opposed to the short-term benefits of a trench at the crater outlet, which could be filled in by an eruption before the lahar occurred.
- There are other ways a hazardous lahar could be generated, apart from the collapse of the outlet dam, including future volcanic eruptions and possibly collapse of other parts of the crater rim.
- There was significant opposition to engineering works at the crater from a wide variety of iwi, recreation, and conservation groups, who favoured protection of the unique Crater Lake area which has natural, cultural and scientific values of national and international importance.
- Engineering at the Crater Lake in a National Park World Heritage Area raises concerns about precedents being set.

The Minister of Conservation has approved all recommendations contained in the AEE, but has not ruled out engineering options. Following this approval, DOC has recently prepared a scoping report (Keys, 2001) defining the objectives and technical options for an Eastern Ruapehu Lahar Alarm System (ERLAS). The main objectives identified for the ERLAS system are to:

(1) Install equipment in the upper Whangaehu and Tongariro catchments (proposed ERLAS sensor sites shown in Figure 2) that will detect the passage of lahars to a high level of reliability and certainty, at least 1 hour before they reach the Desert Road (the approximate travel time for a lahar to reach SH1), electricity transmission lines, and the rail and road bridges at Tangiwai (travel time ~2 hours).

(2) Develop a system to respond to this alarm system that will warn responsible authorities, transport and utility agencies, so that risks to the public are averted and avoided.

The scoping report (Keys, 2001) also discussed the possible integration of the lahar detection system with the GNS-run Geohazards Network, and mechanisms to enable lahars to be studied and documented for research purposes, but these issues are of lower priority. As a part of the process of reviewing the draft scoping report, staff of GNS critically examined monitoring strategies that could be adopted to mitigate a future dam-break lahar from Ruapehu (Gledhill and Scott, 2001).

6. Discussion

The AEE Report was reviewed for the Minister of Conservation by Professor Vince Neall (Neall, 2000). That review supported DOC's recommendation of an acoustic-based and telemetered lahar warning system in the Whangaehu River *(Option 1)*, noting that such a system would reduce risk to human life from a dam-break lahar. The review also urged the Minister to approve construction of a bund (armoured earth dam) in the Whangaehu valley at the point of overflow to Waikato Stream (Figures 2 and 7a), which was included in *Option* 2. The main benefits of this were seen to be reduced risk to lives, assets, endangered wildlife, and economic activity in the Waikato Stream–Tongariro River catchment and Lake Taupo. The Minister has recently approved the *bund option,* and design work is now underway with construction planned for November 2001.

Of the alternative options discussed in the AEE, engineering works at the lake outlet (such as a trench) would prevent a dam-break lahar from occurring. However, such intervention was opposed by many submissions in the public consultation process, and although it would remove the current (short-term) dam-break lahar problem, future eruptions could recreate the situation. Neall (2000) therefore concluded that Options 1 and 2 would have longer-term benefits, reducing the risk from future dam-break and eruption generated lahars on the eastern side of Ruapehu.

Adoption of an alarm system to respond to the hazard from a tephra barrier collapse lahar from Ruapehu Crater Lake, suggests that the event should be treated as a typical dam-break event. As discussed by Scott and Gledhill (2001), an appropriate response to this situation should also include observational monitoring methods aimed at assessing performance of the "dam" as the lake is filling, especially after it has reached the lava sill level (2530 m). Regular visual inspections, lake level measurements, seepage and dam deformation monitoring would provide valuable data indicating the dam's condition. While seepage may be difficult to quantify in the partially snow and ice-covered terrain below the crater outlet, this information could allow the time of dam failure to be more closely estimated, possibly days or weeks before the event. The main benefits of such an observational approach, in addition to the acoustic alarm system would be to: (a) provide more definite warning of the impending lahar, and (b) give responsible authorities, transport and utility agencies more time to plan and initiate an appropriate response. It would also allow risks to the public to be averted and avoided, possibly with greater reliability and less disruption than might be expected with just an alarm that is triggered only after the lahar has begun.

Installation of an automatic lake level recorder (possibly a gas purge or pressure sensor based system) was seen as being very valuable and was recommended, especially if an alarm system can be triggered by a sudden drop in lake level (Gledhill and Scott, 2001). Inclusion of a robust and reliable automated lake level monitoring system will add to the reliability of a warning system based on only acoustic flow monitors. The GNS report also recommended establishment of a panel of specialists to help DOC manage the Crater Lake issue. DOC have recently supported this concept and recommended that a *Science Panel* should be set up to independently advise the Minister of Conservation on: (a) the stability of the outlet dam as the lake rises, (b) the likely dam failure mode and duration, (c) any modifications to the predicted worst case dam-break lahar hazard (pers. comm. Paul Green).

The problem with and alarm and monitoring approach is that, *Options 1 and 2* (discussed above) alone will not prevent the possible damage to bridges, roads, and power pylons. A trench at the outlet *(Option 4)* offers a relatively cheap (~$100-280k) solution to prevent damage to important infrastructure sites from a future dam-break lahar. This can be compared with a recent estimate of ~$300k for the alarm system, plus the cost of repairing any damage to structures. On this basis it may seem that there is a good case for a trench at the lake outlet. The trouble is that, while we do not know exactly what damage will occur if no action is taken, we do know that engineering works at the lake outlet would directly impact on National Park and World Heritage values, and possibly create an undesirable precedent for Tongariro National Park and elsewhere.

Structures are tangible objects that can be repaired. Damage to environmental and cultural values are more intangible and not so easily repaired. People not associated with environmental protection or close to Mt Ruapehu do not necessarily place much value on the need for, or benefits of national park management and sustainable development. However, if significant damage does result from a future dam-break lahar, when it could have been prevented, it will ultimately be for society to judge, with the benefit of hindsight, whether the correct decisions were made.

7. Summary and conclusions

(1) The 1995-96 eruptions of Mt Ruapehu emptied the Crater Lake and caused significant changes to the crater area, which have important implications for the hazard from future lahars when the lake refills. A ~7 m thick layer of tephra (weak ash and scoria) now covers the crater and lake outlet area, creating a situation similar to that after the 1945 eruptions, which led to the 1953 Tangiwai lahar disaster after collapse of a tephra barrier retaining the lake.

(2) The Crater Lake is now refilling, and by April 2001 lake level was at ~2505 m (~54% full) and about 25 m below the former overflow level of 2530 m. The lake is not expected to reach the new overflow level at the top of the tephra layer (~2537 m) until late 2002-2005, depending on snowfall, rainfall, melting, lake temperature, and volcanic activity. . When the lake has refilled, the tephra layer overlying the outlet area will create a weak, permeable barrier retaining ~1.45 million m^3 of water (~13% of its total volume).

(3) Evidence from the 1953 Tangiwai lahar suggests that the tephra barrier will not last long after the lake refills. Rapid collapse of the barrier is likely as a result of internal piping erosion, leading to a lahar in the Whangaehu River similar to that of 1953. Erosion and slumping into the rising lake may thin the tephra layer, but based on the 1953 precedent overtopping of the barrier, channel erosion, and slow lowering of the lake is unlikely.

(4) Simulation flow modelling of the 1953 lahar, and a possible worse case future tephra barrier collapse (dam-break) from Crater Lake has shown that, compared to the 1953 lahar, the peak discharge at Crater Lake will be 2-3 times higher (480-850 m^3/s). The maximum credible (worst case) flow at Tangiwai rail bridge will be 54-72% larger (910 ±105 m^3/s), and the travel time to bridge will be faster (~1.8-2.1 hours, compared to ~2.3 hours in 1953). Considerably higher peak flows are predicted for a future barrier collapse lahar because there is now no ice tunnel at the lake outlet to restrict discharge into the Whangaehu River.

(5) In the worst case scenario the present Crater Lake situation presents a greater lahar hazard than in the historical past, with higher peak flows in the Whangaehu River than have occurred in any previous lahar since 1861. Some of the lahar (up to ~7%) is expected to overflow into the Waikato-Stream -Tongariro River system and enter Lake Taupo. Overall, the lahar would probably cause greater damage to bridges, roads, and possibly power lines and the Rangipo Power Station than has occurred in the past. There would also be significant environmental damage in the Whangaehu and Tongariro river catchments and Lake Taupo.

(6) The main structures that could be damaged by a worst case lahar flow are: (a) the SH 1 bridge across Waikato Stream *(*abutment *scouring)*; (b) power pylons at the Wahianoa Aqueduct crossing *(footing and leg damage)*; (c) the Tangiwai rail and road bridges *(pier damage, erosion of abutments and approaches, possible collapse),* and the (d) Strachans road bridge *(likely to be overtopped and destroyed).* In addition, communication equipment on the TranzRail lahar warning gauge (~12 km upstream of Tangiwai) could be damaged, and the footbridge in the Whangaehu Gorge would almost certainly be destroyed if not removed first.

(7) A number of engineering options were considered by DOC to mitigate future dam-break hazards from the Mt Ruapehu Crater Lake. After extensive public consultation, these options were presented by DOC in an Assessment of Environmental Effects (AEE) Report for the Minister of Conservation. This process showed most support for an acoustic alarm system and planned response to the lahar event, in conjunction with a bund to prevent overflow into Waikato Stream and Lake Taupo. There was only limited support for an engineering solution involving a trench at the Crater Lake outlet excavated by light bulldozers flown to site. Although that option would prevent damage to key infrastructure and loss of life, there was a belief by most of the agencies involved that engineering was not necessary. There was also considerable opposition from iwi, recreation and conservation groups to intervention at the Crater Lake, the most special part of Tongariro National Park World Heritage Area.

(8) The Minister of Conservation has recently approved installation of an Eastern Ruapehu Lahar Alarm Warning System (ERLAS), and construction of a bund to prevent overflow into Waikato Stream. These options will avoid undesirable impacts within Tongariro National Park, and offer longer-term benefits of detecting and reducing the risk of loss of life from future dam-break and eruption-generated lahars on the east side of Ruapehu, but they will not prevent possible damage to infrastructure.

8. Acknowledgements

The authors wish to thank the Department of Conservation and Institute of Geological and Nuclear Sciences for their support in preparing this paper, and to acknowledge the valuable contributions of our colleagues, particularly Peter Otway and Ian Nairn. We also wish to thank Brad Scott, Vern Manville, and Phil Glassey (GNS), Horace Freestone and Peter Foster (Opus International Consultants), and Paul Green (Tongariro Taupo Conservator, Department of Conservation) for helpful discussions and review comments.

9. References

Beetham, R.D. (1982). Mount Ruapehu Crater Lake and Rim Stability Study. *N Z Geological Survey Engineering Geology Immediate Report EGI 82/023.*

Donoghue, S.L., Neall, V.E., and Palmer, A.S.(1995). Stratigraphy and chronology of late Quaternary andesitic tephra deposits, Tongariro Volcanic Centre, *New Zealand. Journal of the royal society of New Zealand 25: 115-206.*

Froehlich, D.C. (1987). Embankment - Dam Breach Parameters. *Proceedings 1987 ASCE National Conference on Hydraulic Engineering, Williamsburg, Virginia, Aug. 1987, 570-575.*

Gledhill, K. and Scott, B.J. (compilers) (2001). Monitoring strategies that could be developed to deal with a Crater Lake dam-failure at Ruapehu volcano. *Institute of Geological and Nuclear Sciences science report 2001/6. 22p.*

Hackett, W.R. and Houghton, B.F. (1989). A facies model for a Quaternary andesitic composite volcano: Ruapehu, New Zealand. *Bulletin of Volcanology 51: 51-68.*

Hancox, G.T., Hodgson, K.A. and Nairn, I.A. (1995). Reassessment of lahar hazard in the upper Tongariro River. *Institute of Geological and Nuclear Sciences Limited client report 43605B.*

Hancox, G.T., Nairn, I.A., Otway, P.M., Webby, G., Perrin, N.D. and Keys, J.R. (1997). Stability assessment of Mt Ruapehu Crater Rim following the 1995-96 eruptions. *GNS Client Report 43605B (Open File report prepared for DOC Turangi, June 1997).*

Hancox, G.T., Otway, P.M. and Webby, M.G. (1998). Possible effects of a lahar caused by future collapse of the tephra barrier formed at the Mt Ruapehu Crater Lake outlet by the 1995-96 eruptions. *GNS Client Report 43711B (Open File report for DOC Turangi, September 1998).*

Hancox, G.T. (2001). Stability assessment of "J" Peak area of Mt Ruapehu Crater Rim. *GNS File Report (Job 43009B.10), 10 pp. (unpublished report for Department of Conservation June 2001.*

Harris, R. W. (1954). A Report on Flood - Whangaehu River, 24 December 1953. *Report to Rangitikei Catchment Board dated 25 January 1954, included in Report of Proceedings of Board of Inquiry Regarding the Derailment of No. 626 Train between Tangiwai and Karioi Railway Stations on 24 December 1953.*

Healy, J. (1954). Statement of geological evidence presented to Board of Inquiry Regarding the Derailment of No. 626 Train between Tangiwai and Karioi Railway Stations on 24 December 1953. *Included in Report of Proceedings of Board of Inquiry Regarding the Derailment of No. 626 Train between Tangiwai and Karioi Railway Stations on 24 December 1953.*

Hicks, D.M. and Mason, P.D. (1991). Roughness Characteristics of New Zealand Rivers. *Water Resources Survey, DSIR Marine and Freshwater, Wellington, New Zealand.*

Hodgson, K.A. (1993). Late Quaternary lahars from Mt Ruapehu in the Whangaehu River Valley, North Island, New Zealand. *Unpublished PhD Dissertation, Massey University N Z.*

Houghton, B.H., Neall, V.E. and Johnston, D. J. (1996). Eruption: Mount Ruapehu Awakes. *Penguin Books (N Z) Limited, Auckland, New Zealand.*

Keys, H. (J.R.) (1999). Environmental and risk assessment for the mitigation of the hazard from Ruapehu Crater Lake. *Assessment of Environmental Effects Report, Department of Conservation, Turangi, April 1999.*

Keys, H. (J.R.) (2001). Scoping the alarm and warning system for Mt Ruapehu lahars in Whangaehu and Tongariro catchments. *Planning Report, Department of Conservation, Turangi, 31 March 2001.*

Keys, J.R. and Williams, K. (Editors) (1996). Eruption Debriefing: A workshop to discuss the management of the 1995 eruptions of Mt Ruapehu in Tongariro National Park. *Report prepared by Department of Conservation Tongariro/Taupo Conservancy, September 1996.*

Neall, V.E. (2000). Independent Scientific Review of Department of Conservation's Assessment of Environmental Effects Report. *Unpublished report for Minister of Conservation, June 2000.*

Otway, P.M., Hodgson, K.A. and Nairn, I.A. (1995). Whakapapa skifields lahar study. *Institute of Geological and Nuclear Sciences science report 95/39.*

Otway, P.M. (2001). Report on Ruapehu Crater Rim Monitoring Survey of 22 March 2001. *Unpublished report for the Department of Conservation, 6p.*

Otway, P.M. (2001). Report on installation and survey of additional control points to monitor Ruapehu Crater Rim, 25 April 2001. *Unpublished report for the Department of Conservation, 4p.*

Palmer, B.A. (1991). Holocene lahar deposits in the Whakapapa catchment, northwestern ring plain, Ruapehu volcano (North Island, New Zealand). *New Zealand journal of geology and geophysics 34: 177-190.*

Palmer, A.S., Purves, A. and Donoghue, S.L. (1993). Controls on accumulation of a volcaniclastic fan, Ruapehu composite volcano, New Zealand. *Bulletin of volcanology 55: 176-189.*

Palmer, B.A. and Neall, V.E. (1989). The Murimoto Formation B 9500 year old deposits of a debris avalanche and associated lahars, Mt Ruapehu, North Island, New Zealand. *New Zealand journal of geology and geophysics 32: 477-486.*

Paterson, B.R. (1980). The hazard of lahars to the Tongariro Power Development, New Zealand. *Third Aust-NZ Geomechanics Conference 1980. N Z I E Proceedings 6/1:(2)7-14.*

Pierson, T.C. (1995). Flow characteristics of large eruption-triggered debris flows at snow-clad volcanoes: constraints for debris flow models. *Journal of Volcanology and Geothermal Research, 66: 283-294.*

Pierson, T.C. (1998). An empirical method for estimating travel times for wet volcanic mass flows. *Bulletin of Volcanology, 60:98-109.*

Pierson, T.C. (2001). Summary report of site visits to Mt Ruapehu 19-20 February 2001. *Unpublished report to DOC 21 June 2001*

Singh, V.P. and Scarlatos, P.D. (1988). Analysis of Gradual Earth Dam Failure. *Journal of Hydraulic Engineering, 114 (1), 21-42.*

Vignaux, M. and Weir, G.J. (1990). A General Model for Mt Ruapehu Lahars. *Bulletin of Volcanology, 52, 381-390.*

Weir, G.J. (1982). Kinematic Wave Theory for Ruapehu Lahars. *New Zealand Journal of Science, 25, 197-203*

Aoraki - Mt Cook Village
Flood / Debris Flow Hazard Mitigation

Ian McCahon
Geotech Consulting Ltd, formerly with Montgomery Watson Ltd

Andrew Hurley
Montgomery Watson Ltd

Nigel Skermer
EBA Engineering Consultants, Vancouver

Abstract

Aoraki/Mt Cook Village is built in a geologically very active environment on alluvial fans at the base of steep mountains. Although elevated, the site is subject to aggradation and flooding hazards from the Kitchener and Black Birch Streams as well as a debris flow hazard from the Glencoe Stream. These hazards were evaluated by IGNS in 1995 and EBA in 1997 and mitigation works subsequently built in 1999. Quantification of events for the design of the works was difficult because of the sparse data available. Standard flood prediction models did not fit the extreme topographical and weather conditions of Mt Cook. In addition, flooding of the steep mountain streams is frequently associated with large and rapid bed aggradation as the streams disgorge onto the fans. Sediment supply is affected by the nature and location of landslide and erosion events within the catchment. Because of these uncertainties, secondary banks and flowpaths beyond the primary stopbanks provide some control for a super-design event. No major difficulties were encountered during construction, but methods were tempered by the availability of rock of sufficient size and constraints imposed from working within a National Park.

Introduction

Aoraki/Mt Cook Village is built in a geologically active, steep mountain environment. The village site was selected because of its elevation on a glacial moraine terrace some 20m above the Hooker Valley floor, giving both views of Mt Cook and security from an earlier risk of flooding from the Mueller Glacier. Unfortunately, the elevation is provided in part by the actively aggrading fans of two small but very steep streams. The streams present flood and debris flow hazards to the village. It is ironic that the original Hermitage site, abandoned in 1913 because of flooding, is now a much safer area than the current site on the Glencoe fan, due to the retreat of the Mueller Glacier. Development of the village extended onto the Black Birch fan in 1969 with the building of the oxidation ponds and the first river training works to the Black Birch Stream. Housing development followed.

Floods in the Black Birch stream caused evacuations of part of the village in 1979 and 1994 and subsequently led to the MacKenzie District Council declining building consents. The perception that the Black Birch stream flood protection was unsafe, led to a review of the natural hazards to the village. That Natural Hazard Assessment for the village, by the Institute of Geological and Nuclear Sciences in 1995, showed not only that there were deficiencies in the Black Birch stream protection works but also identified a previously unidentified debris flow hazard in Glencoe Stream. Mitigation measures for the Glencoe Stream and the Black Birch Stream were considered in separate studies following the IGNS report. The Glencoe Stream catchment, where the hazard is dominated by debris flows, was addressed by EBA Engineering Consultants Ltd from Vancouver who have experience with similar issues in Canada. The

Black Birch Stream is a more typical, flood flow plus aggradation, hazard and was studied by Montgomery Watson. The mitigation work consisted mainly of constructing and strengthening stopbanks, but also involved a debris training wall, a debris storage area, secondary flow routes and the relocation of some services. The village and main mitigation structures are shown in Figure 1. The construction work was completed in late 1999 at a cost of $1.3million.

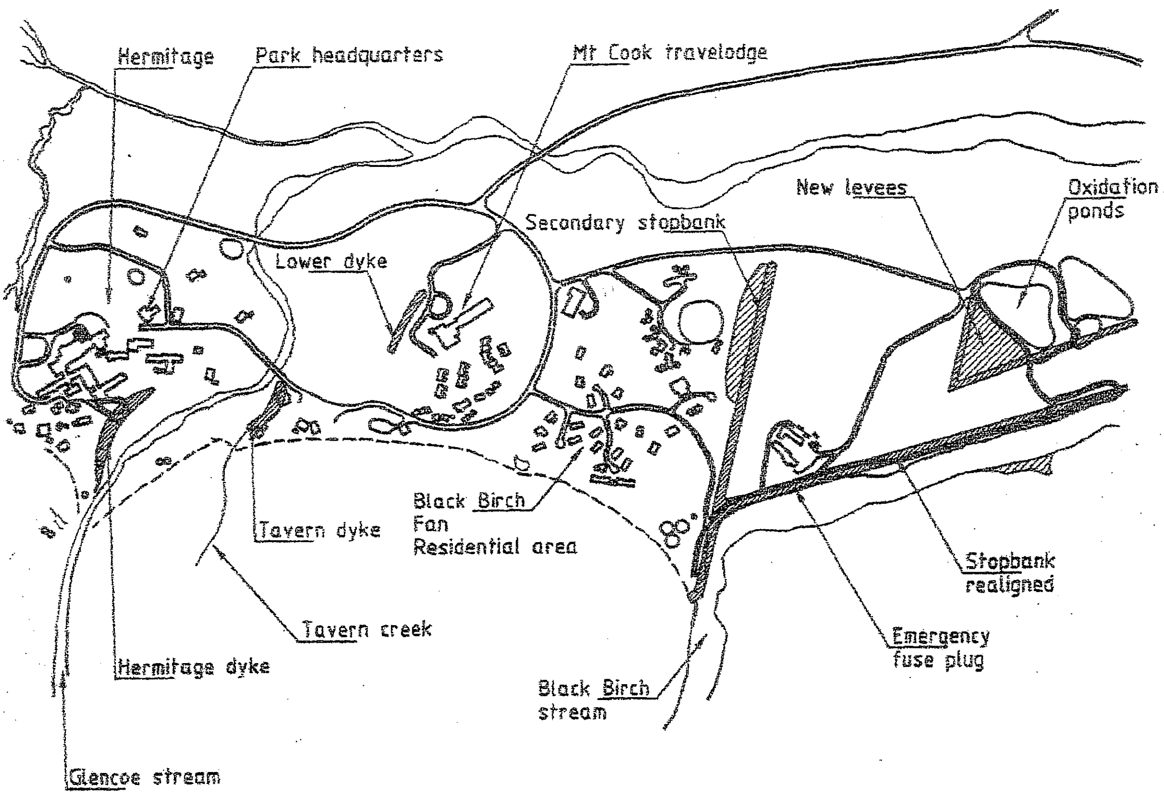

FIGURE 1 : Plan of Mt Cook Village Proposed Flood Protection Works

Scale 1:10,000

Glencoe Stream Debris Flow Hazard

The Glencoe catchment is 0.23 km^2 in area, 1 km long and rises from 800 m elevation at the fan head to over 1400 m. Tavern Creek contributes a further 0.15 km^2 area. Although the catchment is small, it is steep with an average stream gradient of 28 degrees and side slopes of between 30 and 50 degrees with some much steeper rock faces. A high percentage of exposed weak and shattered greywacke and argillite rock provides a large sediment source. The flood size is relatively small and easily contained within the natural banks, but the potential occurrence of large debris flows is of real danger to the Hermitage Hotel. The hotel lies below and in line with the Glencoe stream where it exits from a gorge onto the glacial moraine and fan.

Historically, there is evidence from aerial photographs from the 1954 – 1986 period, that debris flows and water floods have occurred at intervals. A 24 hour rainfall of 491mm in December 1957 caused flooding and significant aggradation of the stream and lower fan, with an estimated 70,000m^3 of material carried out of the catchment.

The EBA report assessing the long-term probability of a debris flow event, observed that there is clear evidence of past events which suggest that large debris flows can occur at relatively short return intervals (10 - 20 years). The volume of debris currently available to be mobilised as a debris flow has been estimated to be 30,000 to 40,000 m^3. Not all this is likely to be mobilised in any one single event and events of a higher frequency could mobilise smaller volumes of material of perhaps 10,000 to 20,000m3. Debris is being produced on a continual basis (1,000 to 2,000m^3/year) and depending on the frequency of flushing by minor events, significantly more debris could build up over future years. A long period of quiescence might lead to a debris flow as large as 100,000m^3. They also perceived a potential for slope failures to temporarily block the stream channel and cause a discharge of water and debris far in excess of statistically determined flood flows

Glencoe Stream Protection Measures

As the catchment is too steep and rugged for any stabilisation or instream check dams, the preferred option was to enhance the natural channel storage in the upper fan, where the steep confined channel flattens and widens leading to deposition of the largest boulders. The Glencoe works are sized for a design debris flow of 100,000 m^3 volume with a peak instantaneous debris flow discharge of 280 m^3/. This has been estimated as having an expected frequency of between 1 in 50 (2% probability of occurrence in any one year) and 1 in 200 years (0.5% probability in any year). The 200 year return period peak flood flow for the combined Glencoe Stream and Tavern Creek at the Bowen Drive bridge is 25 m^3/s, which could increase to about 50 m^3/s when bulked with entrained debris.

The mitigation measures for the Glencoe Stream are intended to deflect and confine debris flows to within a defined "debris basin" following the present stream channel. At the end of the gorge, a large earthfill embankment, known as the Hermitage Dyke, is tied into a rock spur at the upper extremity of the fan with a 32m long and 8m high concrete training wall, and deflects flows around the bend in the stream to protect the Hermitage. The dyke, 180m long, is up to 5.5m high, but the location along the top of a terrace riser increases its effective height to 9m. Just above the Bowen Drive bridge a second 4m high 110m long embankment, known as Tavern Dyke, stops any tendency for floodwaters or debris to avulse from the current bed down the former fan surface between Bowen Knoll and Governor's Bush through the Glencoe Lodge area. A third stopbank is sited at the head of the lower fan to protect the Glencoe Lodge from flooding over the lower fan from below the Bowen Drive bridge. The stream zone between the first two dykes forms a storage area for debris with a designed capacity of 100,000 m^3. This will need to be cleared after any significant aggradation to maintain the capacity for subsequent debris flow events.

All these structures were designed to the concepts by EBA, who also reviewed the final design and the completed works. The Hermitage & Tavern Dykes were built with steep 1.33:1 stream batters to minimise the potential for a debris flow to ride up and overtop them. They are faced with grouted rock. The training wall had to be designed for large impact forces and was anchored to the rock at its upstream end where rock was at an accessible depth.

Two water supply reservoirs and associated pipework had to be replaced with a new steel tank to make room for the training wall and embankment. Room for the second embankment could only be gained by the removal of the Tavern – now relocated as the DOC office. An 11kV power cable was relocated within the debris storage area, and a footpath and footbridge removed to dissuade the public from lingering in the stream area.

Black Birch Stream Flood Hazard

The Black Birch catchment is 4.8 km^2 in area and rises about 1,300m in its 3 km length. The river flows out of a small gorge onto a low gradient alluvial fan. Development on the fan in 1969 was followed by the construction of stopbanks to protect the oxidation ponds and subsequently the first housing, and infrastructure. The stopbanks hold the stream through a right angle bend at the very head of the fan to keep it to its pre-1969 course against the true right edge of the fan.

The December 1957 storm occurred before any development on the fan, but photographs show that most of the fan surface was flooded and covered with sediment. In December 1979 a

24 hour rainfall of 537mm caused a large flood in the Black Birch Stream. It also triggered the erosion of a gully in the side of Mt Sebastopol. The erosion was of a vegetated moraine slope not obviously at risk and deposited an estimated 93,000m^3 of sediment into the Black Birch Stream just above the head of the fan, within a few hours. This enormous volume of material resulted in a 7m aggradation of the bed at the head of the fan and the main flow being forced against the stopbank. The houses on the fan were evacuated, but the stopbank was not quite breached.

Evacuation also occurred in January 1994 when a smaller cone of gravel was formed at the 1979 site, the bed aggraded 3 to 4m at the fan head and sections of the stopbank were scoured out.

The Black Birch gorge and fan are not steep enough to carry debris flows, but it is clear that the combination of flood flows and abundant gravel close to the fan head can lead to very rapid and unpredictable changes to the stream regime. The design of the mitigation works required that this combination of events had to be modelled. A 100 year return period (1% probability of occurrence in any one year) flood flow of 150 m^3/s, together with a previously aggraded bed and an assumed concurrent 100,000 m^3 of sediment aggradation was taken as the design event

Black Birch Stream Flood Modelling

The flood flow (150m^3/s) was assessed by the TM61 method using 30 minute rainfall intensity derived from NIWA research on rainfall distribution across the Southern Alps, which correlates rainfall data for similar sized catchments at a similar distance from the Alpine Fault. Other methods were trialled but gave either unreasonably low flows (45m^3/s Regional Flood Estimation) or unrealistically high flows (300+ m^3/s TM61 and modified rational methods using rainfall data from Mt Cook Village), similar to the mean annual flood for the much larger Hooker River.

The aggradation event was based on the December 1979 event, which was the largest observed in 70 years and has been assessed as having a return period of approximately 50 years.

As well as the considerable uncertainty in determining the flood and sediment supply figures, there is similar uncertainty in modelling the flood and sediment flows through the area of the protection works. With a lack of useable data from past events it was assumed that the bed aggraded in a uniform pattern from zero at the downstream end of the stopbank to a maximum aggradation 1km upstream, at the sediment input location. Flow patterns had to be assumed with a uniform flow from bank to bank with a level aggraded bed across the 40-60m wide channel, to give computed flow depths of 0.9 - 1.2m and velocities of about 3m/s. Clearly these are crude simplifications of reality, as the stream will undoubtedly form one or more deeper and narrower channels with potentially higher velocities, and aggradation will not be uniform.

Because of the simplifications necessary for the computational model, and the severe curvature imposed on the upper channel by the existing developments, a physical model was tested at Lincoln University. The stream was modelled from the location of the 1979 debris cone to downstream of the training works and included a sediment supply at the upstream end. The model confirmed the general assumptions, but showed that aggradation and overtopping of the banks tends to occur below the bend where the gradient reduces and the channel becomes slightly wider. The model also showed that the geometry of the stream channel upstream tended to push the main flow channel across the bed to impact on the stopbank bend with resultant scour and high velocities against the armouring. It demonstrated that the greatest potential for failure of the stopbank system and resulting avulsion of the stream is at the head of the fan.

Black Birch Stream Mitigation Measures

Since 1969, the Black Birch Stream has been controlled with a stopbank to keep the stream close to the south side of its fan. A secondary levee ran directly down the fan as an additional protection to the housing area on the north side of the fan. The uncertainties inherent in the modelling and the results of the physical model suggested the retention and upgrading of this existing very basic spillway and secondary flow path close to the head of the fan. This is to allow release from the main channel, in a controlled location, in the event of a larger than design event, or aggradation or flow patterns that are markedly different from those assumed.

The mitigation work included an upgrade of rock armouring on the primary and secondary stopbanks, raising the stopbank at the fan head, realigning the upper part of the secondary levee, constructing an emergency spillway in the stopbank to release floods in extreme (larger than design) events, and realigning sections of the lower stopbank. A new stopbank was also built as secondary protection to the oxidation ponds. Construction was conventional gravel stopbanking with armouring rock on the stream batter. The spillway is armoured on the stream side only. If it is overtopped, the downstream batter will scour, undermine the armouring and lower the crest level in a fuse plug manner.

As the aggradation event has the major impact on stopbank levels required, regular monitoring of the bed level is necessary with periodic clearance of aggraded material to maintain storage for the design aggradation event. To facilitate this process, bed level monitoring markers were positioned at three cross sections. If the bed aggrades above pre-determined levels, either gradually or through a single event, the excess material will be excavated.

Construction

There was no shortage of good granular fill material for embankment construction. Both streams appear to produce an almost limitless supply of well graded "AP65" subangular gravels which was readily handled and compacted up to about 2.3 t/m3. Aggregate for the 300m3 of 25MPa concrete used in the Training Wall and approximately 600m3 of 17.5MPa grout for rock armour in Glencoe Basin was obtained from nearby Sawyer Stream.

Rock Armour

Obtaining suitable sized stone for the rock armour was seen as a difficulty from early in the design process. Only small quantities were obtainable from the immediate streams. A source within the National Park was required for ecological reasons including visual appearance and to avoid importation of unwanted plant species. The Hooker River and Hoophorn Stream were both considered as sources, with Hoophorn Stream preferred, primarily because of its relative invisibility from the public eye, but also as it allowed the use of an off-road haul route.

In all, about 15,000 m3 of rock was extracted from Hoophorn stream, but finding sufficient suitably sized stones was difficult. The nominated borrow area was quickly picked over and the easily obtained stones removed. It was then necessary to sift through the fan in a mining operation with surprisingly low yields except in occasional productive seams. The borrow area was extended further upstream where the fan narrowed into a gorge, although this area too was quickly emptied. There was initial concern about depletion of the rock resource but floods in the following spring quickly restored the stream to a natural appearance and exposed the next layer of good sized boulders for future use.

Training Wall Foundations

A trial pit investigation for ther Glencoe training wall was not carried out because of high mobilisation costs for an excavator and the amount of highly visible destruction that would occur well ahead of the main construction programme.

The inferred bedrock profile and the apparent solidity of an old concrete water tank gave every indication that rock would be present at the proposed foundation level. In the event it was discovered that the old Tank was founded on a scree slope with a remarkably high topsoil component and that reasonable foundation conditions (still not rock) were 2.5m below where expected.

The founding level was raised by 1 m, with roller compacted concrete, utilising stream gravels and cement mixed with a digger bucket and the main wall redesigned for the remaining extra height required. Construction was carried out cautiously because of the potentially unstable ground and rockfall hazard from the slopes above.

Flood Event

On 1 November 1999 a flood event of 1 in 7-8 yr magnitude occurred, causing small but significant erosion to the completed main stopbank armour within the Black Birch stream. This flood was not accompanied by aggradation and some general scour occurred as the stream regraded to fill a construction borrow area downstream of the stopbank. Localised scour occurred against the bank where the meandering flood flow impinged on the stopbanks with high velocity water.

Following this event the lower basin was regraded and channelised to keep low flows away from the stopbank. Larger boulders from the river were pushed against the toe of the stopbank during this work as additional scour protection and the new alignment has held in place through another spring and summer of floods since then.

Effect of Mitigation Measures on the Hazard

Following the preliminary design of the protection works, the Canterbury Regional Council commissioned Montgomery Watson to assess the flood and debris flow hazard to the village both with and without the works in place. There are significant uncertainties and assumptions involved in zoning flood hazard in a steep mountain environment such as at Mt Cook. Except in a few low lying areas where ponding may occur, the hazard is from relatively shallow flows carrying and depositing debris.

Flooding could occur into one part of the village early in a flood event but, with sediment and debris deposition, the flow path could rapidly change and flooding move to another area during the flood event. Rapid aggradation with debris flows can thus change the vulnerability of a site during an event. Different areas in the village, although having the same hazard rating, are unlikely to be all flooded in a single event.

The hazard zoning indicates that the proposed works significantly reduce the flood/debris flow hazard in the area to the rear of the Hermitage, the area on Bowen Drive between Alpine Guides and the Public Shelter, the southern side of the Black Birch residential area, and the oxidation ponds. There will be some reduction for the front wing of the Hermitage, the area around the Park Headquarters and The Chalets, the Glencoe Travelodge and motels, and most of the Black Birch residential area.

Overall the proposed works have appreciably enhanced the security of the village to a level where building consents can again be issued within the terms of the Building Act, but in the longer term the village can expect inundation and damage from large debris flows and floods. Because of this residual risk, land use zoning has also been implemented. The zoning gauges the residual risk and the consequences and allows only developments which are relatively insensitive to the risk due to their use, levels of occupation, or method of construction.

In this respect a major earthquake on the Alpine Fault can be expected to have a serious effect on the village. A M8 earthquake on the fault, which has a surface trace 25km to the west but dips east under the Mt Cook region, is likely to generate large amounts of debris and sediment in both catchments. This in turn can be expected to bring about aggradation in both streams that could fill and possibly overwhelm the protection works.

Acknowledgments

The mitigation works were carried out for Aoraki/Mount Cook Developments Ltd and the Department of Conservation with the flood hazard assessment being commissioned by the Canterbury Regional Council. There have been many contributors to the work summarised here, including The Institute of Geological and Nuclear Sciences, Department of Natural Resources Engineering Lincoln University, Lincoln Ventures Ltd. The construction was by Works Infrastructure, South Canterbury.

References

McSaveney, M.J., Davies, T.R.H. and Gough, J.D. (1995). *"Natural Hazard Assessment for Mount Cook/Aoraki Village & Environs"* Unpublished Report 49500D.11 for Department of Conservation by Institute of Geological & Nuclear Sciences Ltd.

EBA Engineering Consultants Ltd, (1997). *Geotechnical Report No 1, Mount Cook/Aoraki Village*. Unpublished Report for Department of Conservation

Royds Consulting Ltd (1996). *Geotechnical Report No 2, Mount Cook/Aoraki Village*. Unpublished Report for Department of Conservation

Montgomery Watson Ltd (1998). *Mt Cook Village Flood and Debris Flow Hazard Assessment for the Establishment of a Differential Rating Sysytem*. Unpublished report for Canterbury Regional Council, CRC Publication no. U98/11

McSaveney, M.J., Davies, T.R.H. (1998) *"A Hazard Assessment for Aoraki/Mt Cook Village"* Proceedings of the Natural Hazards Management Workshop, Christchurch, November 1998, Institute of Geological and Nuclear Sciences Information Series 45.

Natural Hazards to Auckland Engineering Lifelines

T. J. Larkin

Department of Civil and Environmental Engineering, University of Auckland

A. L. Williams

Beca Carter Hollings and Ferner, Auckland

Abstract

This paper presents some of the results of the Auckland Engineering Lifelines Project (AELP). The AELP took place over a period of 3 years and was performed by a number of voluntary task groups and consultants. The aim was to investigate the risks posed by selected natural hazards to the critical utility networks in the Auckland region. The work has been published as ARC Technical Publication 112 in December 1999.

The hazards addressed here are volcano, earthquake (ground shaking, liquefaction and slope instability) and rain induced slope instability. The critical lifelines facilities considered at risk are communication networks (land and cellular), energy supply (petrol, gas, electricity), transport (road, air, port and rail) and civil facilities (water supply and treatment, wastewater collection and treatment and stormwater drainage).

The study concluded that the effects of a major natural hazard event on some of Auckland's lifeline utilities are potentially severe and identified land transport and energy supply as significant points of vulnerability. While return periods are difficult to estimate it appears the most significant risk is from volcanic eruption.

Introduction

The Auckland Engineering Lifelines Project (AELP) was initiated in 1996 by the Auckland Regional Council and involves some 40 organisations comprising local government, utility service providers and interest groups. The Civil Defence Emergency Management Bill now requires that utilities are able to function to the fullest possible extent (even if at a reduced level) during and after an emergency. The passing of this bill is likely to add considerable exposure to the work achieved in the AELP.

The Auckland Engineering Lifeline Project follows similar successful ventures in Wellington and Canterbury. Auckland has a large urban community comprising approximately 30% of New Zealand's population. The region is a gateway to much of New Zealand and its long, narrow shape, constrained by coastlines, has resulted in largely North-South movement of people, goods and services.

Following a significant natural hazard event the potential for "lock up" of the region's roading network is very high. Energy, communication and infrastructure lines are also tightly constrained in a narrow corridor and 95 % of the electricity demand of the region is satisfied by the national grid, which brings power from the south.

A major part of the study was the development of credible scenarios that would provide a reasonable level of exposure of the region to the hazard and would test the region's lifelines. The objective was to assess the vulnerability, response and recovery of the infrastructure. Natural hazards considered were those with the potential to inflict damage on more than one lifeline at the same time. The exceedance probabilities for specific scenarios for each hazard are summarised in Table 1.

The concept of a recovery profile was developed to assess how quickly the facility recovered after the event. The recovery profile provides answers to the questions:

(i) Day 1: What percentage of service is available immediately after the event?

(ii) Week 1: What percentage of service is available one week after the event?

(iii) Time to full recovery: How many days, weeks or months are required to recover back to full service. This includes temporary fixes to restore 100% service.

This paper addresses those hazards that have the greatest potential to cause geotechnical risk to structures, namely volcanic eruption, earthquake and tropical cyclone.

Table 1. Exceedance Probabilities for Hazards Considered

Hazard	Return Period (years)	Probability of Exceedance (%)		
		1 year	50 years	100 years
Earthquake:				
Ground Shaking (Peak Ground Accelerations)	2000 (≤ 0.3g)	0.05	2.5	4.9
	500 (≤ 0.2g)	0.2	9.5	18
Liquefaction	2000	0.05	2.5	4.9
Seismic Slope Instability	2000	0.05	2.5	4.9
Volcanic Eruption:				
Distant andesitic	50 - 300	0.33 – 2.0	15 – 63	28 – 86
Distant rhyolitic	1000 - 2000	0.05 – 0.1	2.5-4.9	4.9-9.5
Local basaltic	1000	0.1	4.9	9.5
Tropical Cyclone:				
Rain Induced Slope Instability	100	1.0	39	63

Volcanic Hazard

Auckland is situated in a volcanic field that contains 50 identified vents in an area of 360km^2. Activity from these vents has occurred over the past 140,000 years. The field is a monogenetic one, thus the vent erupts in a single episode and then becomes blocked. Further activity is from new pathways to the surface and involves new and unpredictable vent locations. At present calculation of meaningful probabilities of occurrence are not possible, however for this project the return period has been taken as 1000 years.

A scenario eruption on the downtown waterfront was chosen to assess the impact on the infrastructure of the region. This event will produce both explosive and effusive styles of eruption (ie wet and dry activity) and test the CBD, rail, port and residential areas. The characteristics of the scenario were developed from the geologic record of the Auckland volcanic field and data from similar fields overseas. Such an event will involve lava flows, ballistic block impacts, pyroclastic surges, lightning strikes from ash clouds and severe ground shaking, all of which constitute a high risk to life and would destroy near vent facilities. Figure 1 shows the location of the scenario vent and the areas impacted by ash fall. The scenario eruption was expected to totally destroy above ground services within a 3km radius of the vent and below ground services for a distance of 1km from the vent.

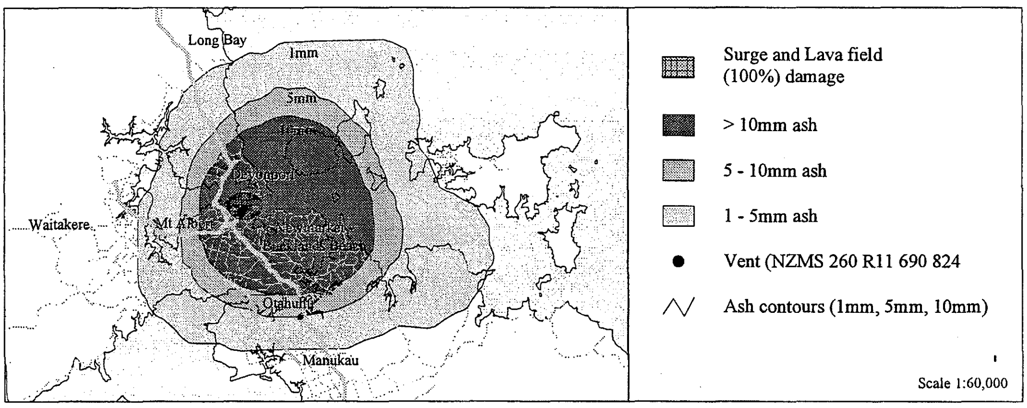

Figure 1. 1000-year Volcanic Eruption Scenario: total eruptive mass of 0.01km^3, column height of 6km, 3 wind shifts over 5 days (Refer ARC Technical Publication 79, 1998)

The main hazard to more distant parts of the Auckland region is from ash fall. Experience overseas shows that the deposition of only a few millimetres of ash is sufficient to disrupt transport, electricity, sewerage, water and stormwater systems. A fall of 50mm or less will require a few days to weeks to restore full service.

Auckland is also at risk from more distant events. This study considered two possible distant eruptions. These were the andesitic cone of Mt Taranaki and the rhyolitic caldera complex of Okataina. Return periods for Mt Taranaki and Okataina are taken as 300 years and 2000 years respectively. Such events will impact uniformly across the Auckland region, which contrasts with the local event scenario just described. Ash is the major hazard from distant eruptions. These events are different with respect to size of eruption and volume (and hence depth) of ash fall. The Mt Taranaki event could deposit 1mm of ash over greater Auckland while the Okataina event could produce 100mm.

Parts of the country south of Auckland will experience greater depths of ash fall from these events. This will hinder the recovery in Auckland since resources will also be required in these areas for clean-up and it is likely that requests will come for heavy equipment to be transferred from Auckland.

The Auckland Engineering Lifeline Group has recently published a report detailing the impacts on lifelines of ash fall and collection/disposal issues. This is available as ARC Technical Publication Number 144.

The specific effects on the infrastructure will depend on the quantity of ash, weather conditions at the time and the manner in which a clean up operation is performed. The potential quantities of ash requiring collection and disposal are estimated to range from 131,000m^3 to 6,000,000m^3. It is estimated that the total cost of transport and disposal could be between $2,400,000 and $108,000,000. Detailed disposal options have yet to be investigated.

Earthquake Hazard

A seismic hazard assessment for the Auckland region was undertaken to provide a basis for assessment of the secondary hazards: ground shaking, liquefaction and earthquake induced slope instability. This was achieved by using historical seismicity data in conjunction with developing an understanding of the seismo-tectonic setting of the region. The results of this study were applied to the ground shaking, liquefaction and slope stability projects.

While New Zealand is considered seismically active, the Auckland region is not part of the most active domain of the country. The region is approximately 300km from the major north-east/south-west orientated fault zone of the plate boundary. The nearest large fault was considered to be the Kerepehi fault observed onshore near Thames and inferred to pass to the north of Waiheke. There was considered to be a lack of knowledge of local faults which reduces the level of understanding of the potential for damaging events. This uncertainty, together with consideration of the large population of the region, suggests that the hazard should not be underestimated.

The objective of the hazard study was to provide a basis for the development of ground shaking, liquefaction and slope studies at a level of seismic exposure slightly in excess of that suggested by the current loadings code. The code is based on a return period of 450 years and the Auckland study used a return period of 2000 years.

The hazard study included the effects of the Kerepehi fault on expected ground motion in Auckland. The fault has the potential to create an event of about Richter magnitude 7, with a return period of approximately 5000 years. The fault is segmented, and this event would require rupture of the entire fault system, which would produce peak ground surface accelerations of approximately 0.15g in Auckland. Given that the fault is some distance (43 km) from Auckland city (allowing significant attenuation), and the relatively long return period of the event, consideration was given to smaller more frequent events that could occur within the region.

A uniform hazard study was undertaken utilising the seismicity of the Auckland and Coromandel areas, as well as the Kerepehi fault. It was found that the level of ground shaking predicted by this analysis, for return periods of 2000 years, was more severe than that arising solely from the Kerepehi fault. The hazard study established levels of peak ground acceleration of 0.17g for a return period of 500 years to 0.28g for a return period of 2000 years. These figures include a contribution from the Kerepehi fault, however neglecting the Kerepehi fault would have reduced the figures by less than 10%.

The figures given above refer to peak ground surface acceleration (PGA) on a site of "standard soils". These sites comprise of a soil profile greater than 3m in depth of firm to stiff sediment, or in some cases coastal deposits, of Pleistocene or Holocene age. It is well known that site geology may significantly alter the ground surface acceleration from that incident at the site. To account for this, modification factors were used for other ground conditions. These are based on studies carried out in the United States.

Ground Shaking

The ground conditions in the Auckland region were generalised into four site categories. These are shown in Table 2. The categories were chosen to generally conform to the classification published by Borcherdt (1996) and NEHRP (Crouse and McGuire 1996). Borcherdt used site response factors that are a function of the mean shear wave velocity to a depth of 30m, V_{30}. In recognition that this parameter is often not available, Borcherdt used an extensive correlation between geotechnical description of sites and measured V_{30} values to develop descriptive site classes where the shear wave velocity is unknown. These correlations have been considered in the shear wave values given in Table 2.

The amplification factors used in the study for adjusting the PGA were specified by Borcherdt (1994) as being applicable to the short period range 0.1 to 0.5 seconds. This is not strictly the same as the PGA, which is a zero period spectral ordinate, however for the purposes of this study the short period amplification factors have been accepted for use as the PGA amplification factor. The amplification factor varies between 0.9 (Hazard zone 4, 0.4g) to 1.6 (hazard zone 2, 0.1g).

The lifeline facilities of the region are spread over a considerable distance. In the event of an earthquake, there is likely to be considerable variation in intensity of motion between different ends of the region, especially considering its elongate nature. To simulate this variation in response, a scenario earthquake was developed that would produce about the same PGA for the CBD of Auckland as the uniform hazard study predicts.

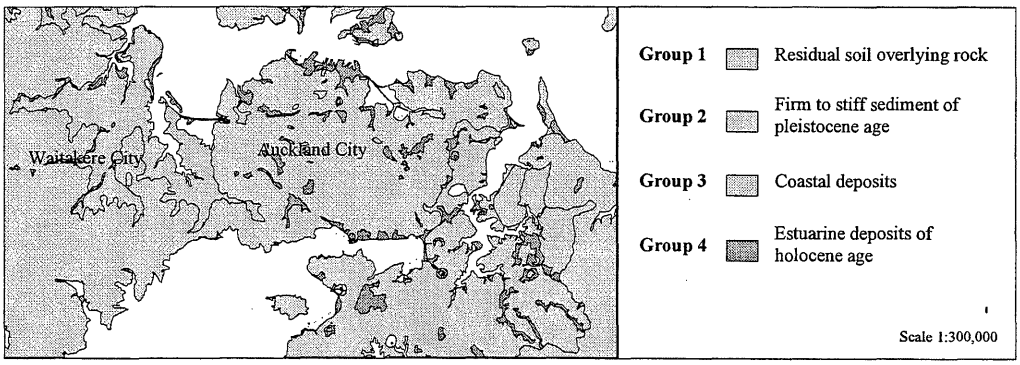

Figure 2. Extract from ground shaking hazard map showing the distribution of soil/rock mass categories defined in Table 2

The earthquake scenario chosen was a magnitude 6 event 20 km due east of Auckland with a focal depth of 10km. The ground shaking hazard is shown in Figure 2. This map has been constructed by overlaying the attenuation grid with the soil class grid and calculating the appropriate PGA from the amplification factor based on site type. Companion studies using Modified Mercalli intensities were also carried out. The map indicates that much of Auckland

City lies within the zone of least shaking amplification, while Manukau city and a large part of Waitakere City contain a significant area of moderate ground shaking amplification. Significantly higher ground shaking amplification may occur in reclaimed land surrounding Auckland's ports, northern CBD, airport and wastewater treatment facilities.

Liquefaction

Repeated shaking of saturated cohesionless soils during earthquakes may result in liquefaction-induced slope movement, lateral spreading and subsidence. Soils within the Auckland Region likely to be most susceptible to liquefaction include some Pleistocene-aged sediments, in particular soft to firm (to loose to medium dense) sensitive pumiceous deposits up to several metres thick; Holocene age deposits comprising both sandy coastal deposits and soft silty estuarine deposits; and man-made fills overlying these materials (Groups 2, 3 and 4, Table 2). The less dense saturated Holocene sands and man-made ground (including reclamations constructed from sandy hydraulic fill) are most likely to liquefy.

Liquefaction susceptibility was assessed both in terms of the uniform hazard model and the scenario event described. Parameters used to assess response to earthquake shaking include the density and grading of soils, depth and thickness of sand layers, likelihood of saturation, and duration and strength of ground shaking.

At PGA's of 0.1 – 0.15g, the risk of liquefaction was considered to be low. At PGA's of 0.2g or more, the risk becomes high, with some 30-90% of all potentially liquefiable soils expected to exhibit liquefaction behaviour. The 2000-year return period earthquake scenario is expected to generate PGA's in excess of 0.2g within 20km of the epicentre, equating to a high risk of liquefaction in this zone (that is, in the order of 30 – 90% of potentially liquefiable soils might liquefy). The selected scenario event suggests that on average, 0.5 – 10% of such soils in the northernmost part of the region will also liquefy (Figure 3).

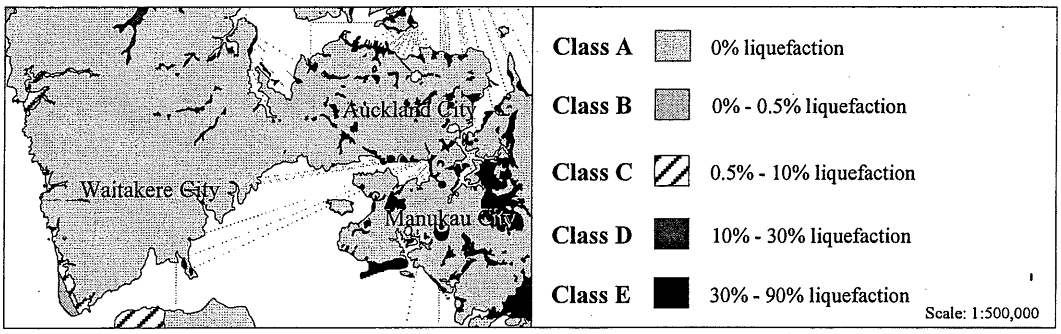

Figure 3. Extract from Liquefaction Hazard map: scenario earthquake with epicentre 2.5km east of the northeastern corner of map

Essential lifelines services particularly vulnerable to liquefaction include Auckland International Airport sited on both in-situ Pleistocene sands and reclaimed ground, and Auckland's port and rail facilities located on reclamations comprising a range of hydraulic and other fill materials.

The consequences of liquefaction include loss of vertical support, large lateral movements (including lateral spreading and liquefaction-induced slope failure) which would damage structures founded at a shallow depth, failure and/or severe damage to coastal reclamation structures, and rupture of pavements and infrastructure such as pipelines constructed over or founded within these soils.

Table 2: Soil and Rock Groups: Physical Properties and Response to Earthquakes

Soil / rock mass group	Soil foundation condition	Soil category	Engineering description of soils/rock	SPT blows/ 300mm (N)	Shear wave velocity (m/s)*	Typical ground failures resulting from earthquakes
1	Residual Soil Overlying Rock	Residual and colluvial soils, ash and weathered tuff:-up to 30m, over greywacke; up to 20m over interbedded sandstone and mudstone; conglomerate and basalt	CW:-** sand/silt/clay; HW:- gravel in a silty sand /clay matrix; MW:- very weak rock; SW-UW:- weak to moderately strong rock	5 - 25+ 15 - 50+ 30 - 100+ 50 - 200+	100 - 300 200 - 500 300 - 1000 500 - 2000	Generally minor to nil damage to gentle slopes; Movements on critically steep slopes, and on gentle slopes in sandstone and mudstone with clay seams, undercut by streams and coastal erosion.
2	Firm to Stiff Sediment of Pleistocene age	Alluvium; and basalt, ash and tuff overlying alluvium	Soft to very stiff alluvium; Sensitive pumiceous silt; silt, peat, clay; Loose to dense sand, breccia; Ash, tuff and basalt overlying these deposits	5 - 25***	100 - 300	Widespread failure of coastal cliffs and river banks; Movement on moderate to steep slopes; Localised liquefaction of saturated loose sand lenses in severe**** shaking
3	Coastal Deposits	Beach and dune sands; Man-made fills overlying zone 1 or 2 deposits	Medium dense fine sand and shell, saturated; Loose fine sand, unsaturated	5 - 40	100 - 500	Localised liquefaction of saturated loose sand pockets
4	Estuarine Deposits of Holocene age	Stream alluvium and swamp deposits; Man-made fills overlying zone 3 or 4 deposits	Very soft to stiff mud, silt, peat, pumiceous clay; typically saturated	0 - 10	50 - 200	Widespread sliding failures of moderate slopes; Widespread liquefaction of saturated sand deposits in moderate shaking

* Values of shear wave velocity are assessed

** Rock Weathering Grades: - CW completely weathered; HW highly weathered (soil); MW moderately weathered (very weak rock); SW slightly weathered; UW unweathered (rock)

*** Where basalt rock overlies deep alluvium, the rock stiffness does not significantly influence site behaviour

**** Shaking levels: - Severe ≥ 0.40g ≥ Strong 0.20g ≥ Moderate 0.15g ≥ Moderate to Low 0.1g ≥ Low 0.05g

Earthquake –Induced Slope Instability

The stability of a series of slopes of different height, angle, soil/rock mass composition and groundwater level were back-analysed for differing levels of earthquake acceleration. This provided an assessment of conditions under which the margin of stability is reduced during earthquake, and indicated the relative importance of each factor to maintaining stability.

These data were presented as factor maps, superposed using GIS systems to produce hazard maps for the region for both the uniform and scenario earthquakes. The hazard maps identify zones of low, moderate, moderately high and high hazard as described in Table 3 (Figure 4).

The assessment shows that ground shaking associated with a 2000-year earthquake in the Auckland region is likely to cause widespread failure of slopes within 20km of the earthquake epicentre and beyond. A number of Auckland's key lifelines could be temporarily shut down in such an event.

Table 3. Interpretation of Hazard Score

Hazard Class	Factor of Safety*	Interpretation	Factor Score
A	≥ 1.5	Low Hazard: 0.5% of slopes fail	> 0.2
B	≥ 1.2 - 1.5	Moderate Hazard: 0.5% to 5% of slopes fail	> 0.10 - 0.20
C	≥ 1.1 - 1.2	Moderately High Hazard: 5% to 20% of slopes fail	≥ 0.05 - 0.10
D	1.0 - 1.1	High Hazard: 20% or more of slopes fail	≤ 0.05

* During or immediately following earthquake or cyclone as appropriate.

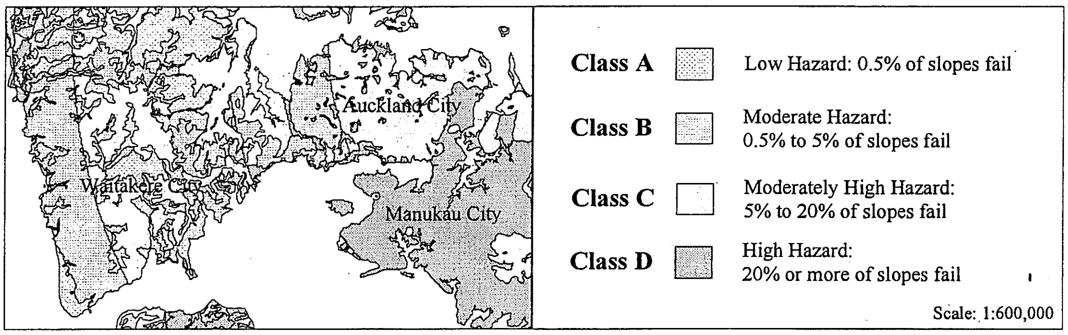

Figure 4. Extracts from earthquake induced slope instability hazard maps: scenario earthquake; epicentre 2.5km east of northeastern corner of map

Rain Induced Slope Instability

Records identify 5 tropical cyclones passing within 220km of Auckland city since 1970, suggesting a return period in the order of one in 6 or 7 years. Cyclones affecting Auckland generally develop over the south Pacific Ocean and migrate south, changing from tropical cyclones with a core of warm air to extra-tropical cyclones with a core of cold air. These extra-tropical cyclones can potentially produce some of the most damaging weather experienced in mid-latitude countries such as New Zealand. A 100-year cyclone scenario was modelled from data on the characteristics of events documented since 1970 (ARC Technical Publication No.76). This scenario comprises an accumulated rainfall of 230mm to 415mm distributed over the Auckland Region in 4 days. Scenario rainfalls are given in Table 4.

Table 4. 100 Year Cyclone Scenario

Average 24 hour Rainfall (mm) [Range of 24hr Rainfall in Different Parts of the Region]				Accumulated Rainfall (mm)
Day 1	Day 2	Day 3	Day 4	
74 [30-115]	124 [65-185]	93 [55-120]	24 [10-50]	325 [230-415]

As for earthquake-induced slope stability assessment, a series of slopes of different height, angle and soil/rock mass composition were back-analysed to provide an assessment of conditions under which the margin of stability is affected by varying groundwater conditions. The sensitivity of slopes to short-term (24 hours) high rainfall events was simulated by modelling a water-filled tension crack, and the sensitivity to longer term high rainfall (more than 3 days) was modelled by raising the groundwater level by different amounts for the different slopes analysed.

Contributing factors were adjusted, in a similar way to that described for earthquake induced slope instability, to produce rain-induced slope instability hazard maps. The hazard maps designate areas of low to high hazard corresponding to expected percentages of all slopes within each hazard zone likely to fail as a result of the proposed 100 year cyclone scenario (Table 3). Within the medium to high population and services density part of the region, the scenario would result in only low or moderate rain-induced slope instability hazard (ie in the order of 0.5% to 5% of slopes in the region might fail). However, in areas where higher rainfall is predicted and steeper slopes occur, for example in the Whitford and Hunua areas in the southeast, the Waitakere Ranges in the West, and coastal cliffs, failure of 5 – 20% of slopes is anticipated.

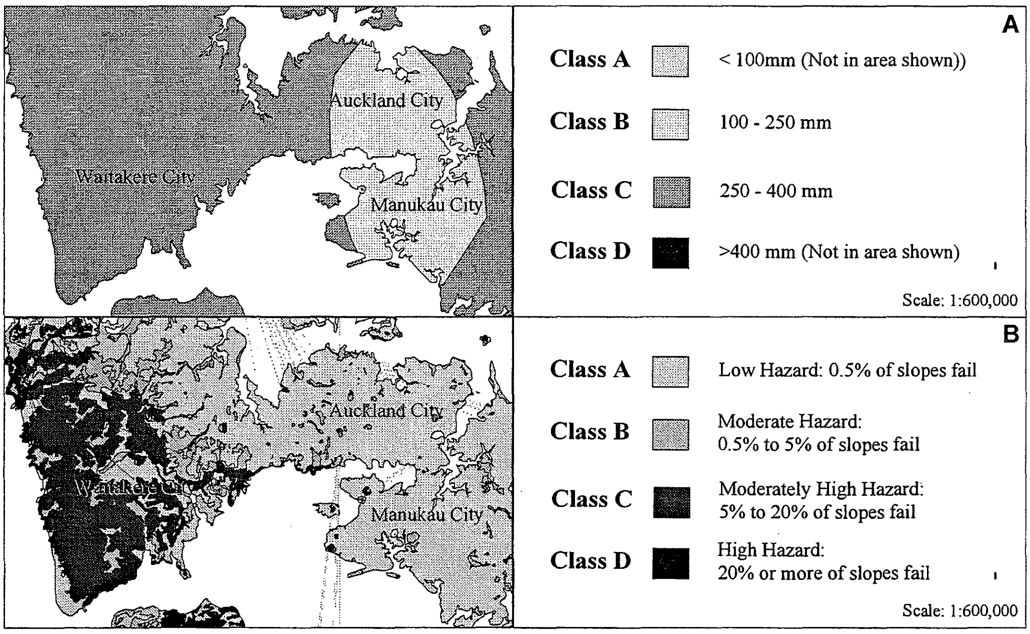

Figure 5. A. 100-year cyclone scenario; B. Extract from rain induced slope instability hazard map

Impact of Hazards on Lifelines

The AELP has examined the effects of hazards on the communications, transport, energy and water lifelines through development of scenario events for which utility inter-dependencies were considered and recovery profiles developed. Significant disruption to most services was anticipated only for the earthquake and volcanic eruption scenarios. For both hazards, the level of associated risk to infrastructure is dependent on event location which cannot be readily predicted: volcanic eruption will occur at a new vent site and future seismicity may not be associated with activity on the Kerepehi Fault. Estimated recovery profiles for these events are compared in Table 5.

The profiles suggest that in terms of duration of service loss, the volcanic eruption scenarios are likely to have a longer term and more severe impact on most utilities, and a local eruption would have devastating impacts on the area within 1km to 3km of the vent. A local eruption could continue for a period of a few to several months or more, resulting in prolonged or repeated exposure to hazard and requiring repeated clean-up and repair effort.

The interdependence of utilities differs for each scenario, however telecommunications, fuel and road access were prioritised for all hazards and utilities, along with other needs such as fuel for emergency generators and water supply for clean-up.

Table 5. Simplified Recovery Profiles Following 2000-year Earthquake and 1000-year Volcanic Eruption

Lifeline	Earthquake		Volcano	
	Day 1	Full Recovery	Day 1	Full Recovery
Communications:				
Land lines	Severe loss	1 – 7 days	0 – 100%	2 – 7 days
Cellular networks	Moderate loss	1 – 2 days	0 – 100%	2 – 7 days
Transport:				
Road	0 - 10% capacity of some key roads	1 month (roads) to 6 months (bridges)	30 – 100% capacity**	A few days to several weeks
Rail	0% capacity	6 months	0 – 80% capacity immediately following eruption*	4 – 7 days*
Ports	10% capacity	3 months	0% capacity at Waitemata port – destroyed; temporary disruption Onehunga	No recovery at Waitemata; 1 week Onehunga*
Airports	10% capacity	1 – 2 days	<50% capacity until ash settles	1 week*
Energy:				
Electricity	Some outages and shortages	7 days (longer for CBD)	0% capacity at affected services; disruption to adjoining services	Several weeks
Petroleum	Key service area and pipeline unlikely to be damaged; possible loss of Avgas fuels	24hrs or longer	0% capacity at affected services; disruption to adjoining services	Depends on extent of loss of services
Gas	Possible loss of main gas spare parts store	24hrs or longer	Total loss for duration of ashfall*	Several weeks
Water:				
Water supply	Identify problem areas and isolate burst mains	3 months	0% capacity at affected sites; commence co-ordination of portable supply	4 months minimum assuming unlimited resources
Wastewater	Divert sewer overflows	3 months	Localised complete destruction of network with widespread leaks and breaks; sewer overflows	4 months minimum assuming unlimited resources
Stormwater	Most serious problems identified	3 months	Local disruption of network	More than 4 months: higher priority of resources for water and wastewater

* Depending on the duration of ashfall

** Depending on the volume of ash and direction of prevailing winds

Bridges were identified as key points of vulnerability to earthquake hazard. Mitigation by way of seismic retrofitting of significant bridges could be undertaken to reduce this vulnerability and future development of a level of redundancy in principal networks could be considered.

Few mitigation options are available for many of the volcanic hazards, however the likely performance of key structures (for example, hospitals, civil defence co-ordination centres) under ash loading should be reviewed and upgraded where required. Identification and preparation of sites for ash disposal, and identification of methods and protocols for clean-up can be prepared well in advance of eruption.

Conclusions

Hazard scenarios have been effectively used in the Auckland Engineering Lifelines Project to identify the hazards and risks that are likely to be associated with earthquake, volcanic eruption and cyclone. Scenarios have also been used to investigate the potential effects on Auckland's key infrastructure. The effects of a major hazard on the lifelines of the region are potentially severe, with recovery times of several months or more anticipated.

Lifeline utilities rely on telecommunications, energy and transport (road access) in particular to facilitate recovery and maintain operation. Volcanic eruption (return period of 1000 years) is considered to be the most likely hazard. In terms of recovery time, it is also likely to have the most severe impact on the Auckland region. While the location of the next eruption site within the Auckland Volcanic Field and the epicentre of a future magnitude 6 earthquake are not known, the AELP has enabled utilities operators to assess the risk to the lifelines for which they are responsible and to work towards reducing the level of damage and recovery time prior to the event.

Acknowledgements

A large number of willing volunteers participated in the work of the Auckland Engineering Lifelines Project. Work was undertaken by consultants, regional councils and managed by Carson group. This paper contains work of a geotechnical nature taken from the various reports produced as part of the study.

References

Auckland Regional Council Technical Publication No 76, "Meteorological Hazards in the Auckland Region: A Preliminary Assessment", November 1996.

Auckland Regional Council Technical Report No.112, "Auckland Engineering Lifelines Project, Final Report – Stage One", November 1999.

Auckland Regional Council Technical Publication No 116, "Auckland Engineering Lifelines Project Stage One Report", July 1997.

Auckland Regional Council Technical Publication No 144, "Volcanic Ash Review – Part 1, Impacts on Lifelines Services and Collection /Disposal Issues.

Borcherdt, R.D. (1994). "Estimates of site-dependent response for design", *Earthquake Spectra,* Vol 10, pp 617-653.

Borcherdt ,R.D. (1996)."Preliminary amplification estimates inferred from strong ground motion recordings of the Northridge earthquake of January 17, 1994", *Proceedings of the International Workshop on site response subjected to strong earthquake motions*, Yokosuka, Japan, January 16-17,1996, Vol 2, pp 22-46.

Crouse C.B. and McGuire,J.W. "Site response studies for purpose of revising NEHRP seismic provisions", *Earthquake Spectra*, Vol 12, pp 407-439.

National Institute of Water and Atmospheric Research Ltd 1997: Tropical Cyclones in Auckland: A 100-year Extreme Event Scenario. Report prepared for the Auckland Regional Council, February 1997.

Engineering geology of an embankment dam on a hazardous karst foundation.

F. J. Baynes

Consulting engineering geologist, Western Australia

Abstract

The investigation, design, construction and performance of a 20 m high embankment saddle dam built on karst foundations is presented as a case history of engineering geology in hazardous terrain. The ground conditions included cavernous limestone partially infilled with glacial gravels and erodible silts and there was potential for subsidence, collapse, piping failure and gross leakage. The presence of a "natural cut-off" was postulated based on examination of pre-impoundment ground water levels and this advantageous feature was used in optimising the location of the dam. The investigation and design philosophy and the practicalities of the dam layout, construction and operation are discussed and related to the engineering geology of the site.

Introduction

This paper follows the convention of describing the *hazard* as a condition with the potential for causing an undesirable consequence and the *risk* as being the product of the probability of the hazard occurring and the resulting consequences.

A geohazard is a geological condition with the potential for causing an undesirable consequence. The term karst describes a suite of solution landforms characterised by closed depressions, sinkholes, caves and underground drainage. Karst limestone typically contains open fissures or even large caverns which can provide extremely permeable pathways through the bedrock and can cause subsidence collapse at the surface. As such, karst is an important class of geohazards requiring careful consideration in dam and reservoir engineering.

Engineering for geohazards involves understanding the geological and geomorphological conditions and processes, and transforming that knowledge for use in engineering decision-making. In the last decade there has been an increasing use of quantitative risk assessment as a technique for dealing with the uncertainties that are implicit in knowledge of geohazards. However this project is an example of non-quantitative risk engineering and thus provides an opportunity to consider some alternative approaches.

The Project

The Darwin Dam is located at the southern end of Lake Burbury, which is an impoundment constructed for the King River Power Development on the west coast of Tasmania, Australia. The scheme was investigated, designed, constructed and operated by the Hydro Electric Commission of Tasmania and consists of an 80 m high concrete faced rockfill dam with an "over the face spillway" (Crotty dam) built on the King River, a 47 km^2 storage (Lake Burbury), a 7 km long power tunnel, and a single machine of 140 MW installed capacity in a surface power station at the downstream confluence of the King and Queen Rivers.

The Darwin Dam functions as a saddle dam across a low divide on the reservoir rim and consists of a gravel filled embankment about 400 m long with a maximum height of about 20 m. The Divide is underlain in part by gravels and sandstones and in part by gravels and silts overlying cavernous limestone. The gravels also infill a deep buried channel between the Divide and the Andrew River (Figure 1).

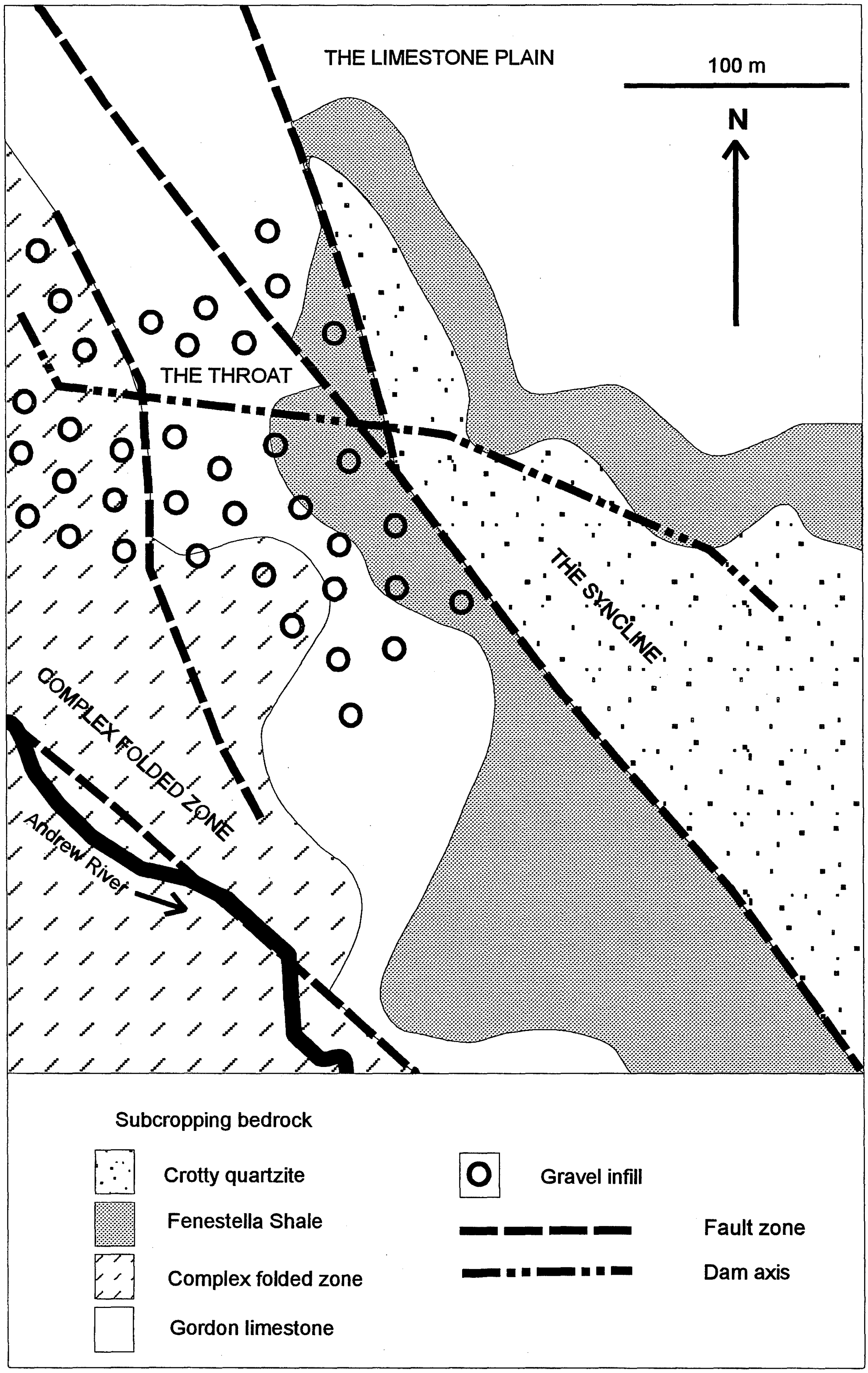

Figure 1 - Geology and features of the Darwin damsite

Hazards

At an early stage in the investigation of the damsite it was apparent that the association of silts, gravels and cavernous limestone in the dam foundation could lead to the following problems:

- Subsidence collapse of the dam foundation where underlain by cavernous limestone, leading to loss of freeboard, overtopping and breaching, with the alternative possibility that more localised subsidence collapse could produce a permeable zone running beneath the dam.
- Internal erosion of the silt at the permeable silt/limestone interface, leading to leakage, internal erosion, piping and subsidence of the embankment.
- Gross leakage through cavernous limestone.

These hazards are depicted in Figure 2. The potential for these hazards to adversely impact on the project led to a very detailed series of investigations.

The Investigations

The possibility of leakage through the Andrew Divide was cited by Blainey (1954) as one of the reasons for the abandonment of the original 1920's scheme for the development of the power potential of the King River. Investigations of the Divide undertaken in the 1950's involving 16 boreholes and geological mapping also concluded that leakage could occur. In 1980 11 seismic lines and 5 boreholes were used to further the investigations and it was again concluded that there were significant problems associated with the karst conditions at the site.

In 1983 the King River Power Development commenced after the cessation of work on the Gordon River Power Development Stage 2 (the Gordon-below-Franklin scheme), following intervention by the Australian Commonwealth Government. The decision to proceed with the King River Power Development involved both political and engineering considerations. In order to be able to build the power development it was necessary to engineer a solution to the karst problems at the Andrew Divide.

Accordingly, a programme of investigation was undertaken at the Divide involving 24 boreholes, 68 test bits, 5 large test trenches, 7 probe holes, 3120m of seismic refraction survey, the collection of ground water data and a limited laboratory testing program. On the basis of this investigation a dam axis was chosen in 1985 that was located where the minimum depth of limestone would be encountered, in anticipation of minimising the cost of a positive cut-off taken down to the top of the limestone.

On review of this design in April 1987, questions were raised as to the integrity of the design due to concerns relating to the potential for gross leakage, internal erosion and subsidence, and the difficulty of constructing a positive cut-off on an extremely irregular karst bedrock which in places was close to the surface, but which contained "holes" where the bedrock was overlain by up to 25 m of gravels and silts. It was decided to carry out investigations of alternative dam arrangements.

Further investigations in 1987 and 1988 included regional mapping, air-photo interpretation, 116 boreholes, 35 piezometers installed with an Odex rig, 570 probe holes, 1700 m of seismic refraction surveys, 73 test pits, mineralogical and chemical analyses of soil and water samples, an extensive laboratory testing programme and grouting trials. During the final stages of these exhaustive investigations the findings were subject to external review by a consulting engineering geologist.

To complete the process, all of the information pertaining to the site was compiled into a consolidated report with three levels of text (an overview, a synthesis and a detailed account), appended volumes of supplementary information including all of the drill logs, tabulated test results, photographs of the site, and 47 A0 figures depicting the geological and hydrogeological conditions in plan and cross section. The drawings were carefully designed to illustrate and document the nature and location of the geohazards at the site.

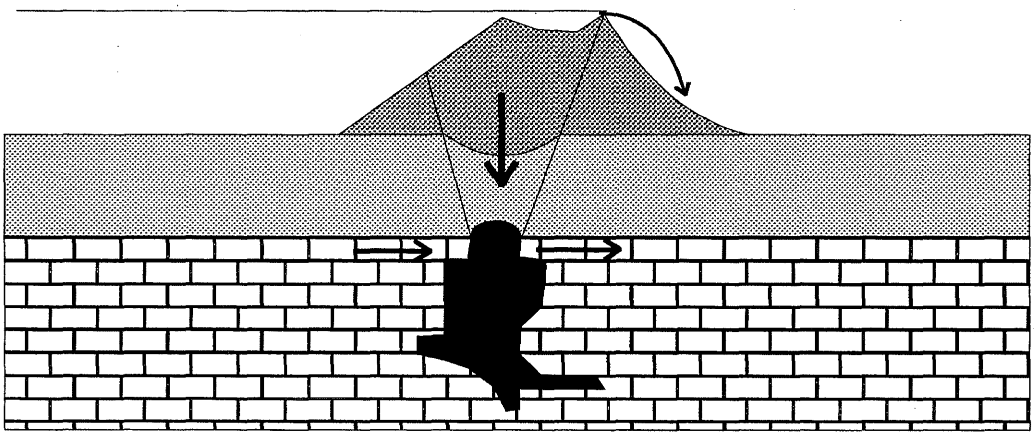

Local subsidence or collapse into an existing cavity leads to loss of freeboard and breaching of embankment and/or permeable leakage paths

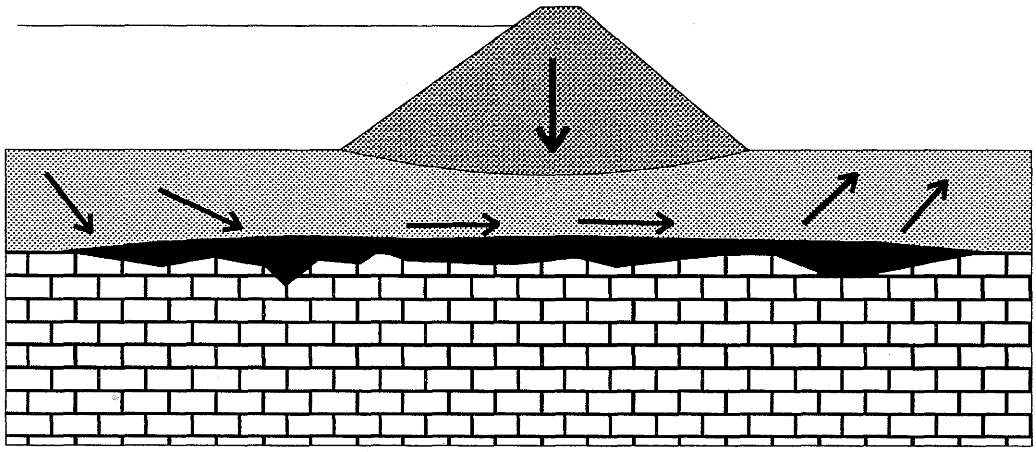

Groundwater flow along permeable zones at the superficial/bedrock interface leads to internal erosion of silts, increasing leakage and the possibility of piping failure and/or subsidence leading to loss of freeboard

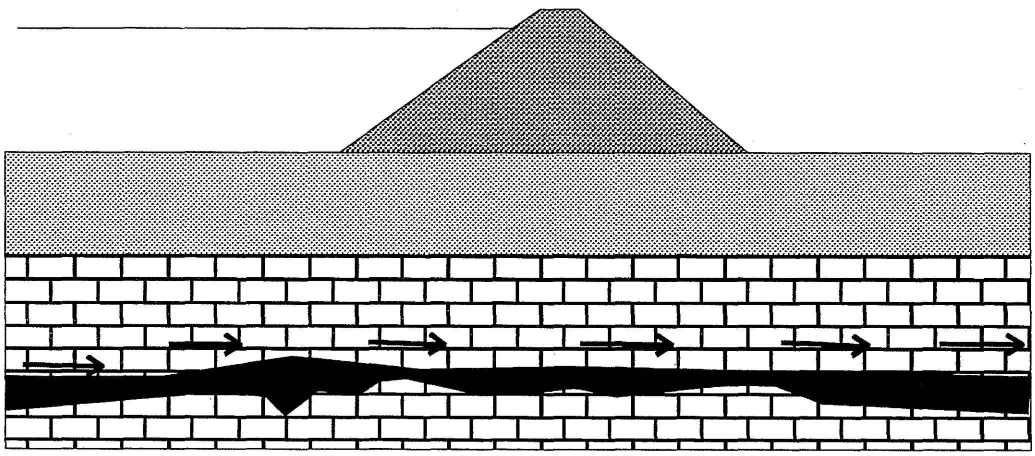

Groundwater flow along permeable fissures and cavernous ground leads to gross leakage and loss of stored water

Figure 2 - Karst geohazards to dam engineering

Engineering Geology

The geological conditions are summarised in Figure 1 and Figure 3.

The damsite is at the topographical divide between the impoundment that forms Lake Burbury to the north, and the valley of the Andrew River, which flows south-east. The Divide has an elevation of about 230 m and forms a saddle between the foothills of the West Coast Range and the low rolling hills to the east. Button grass plains occupy the low lying flatter parts of the Divide and light scrub covers the surrounding hills.

Rock and soil types

For engineering purposes the strata at the damsite may be considered to consist of the following:

Glacial Gravels - These generally form a thin veneer between 1.5 and 5 m thick north of the Divide and infill a buried channel up to 60 m deep, south of the Divide. The gravels are mostly compact, have a high proportion of strong clasts and have a high shear strength. At the surface the gravels are weathered, have a high fines content and are well graded, and generally have measured permeabilities in the range 10^{-6} to 10^{-9} m/s. However, within the deep infill, gravels with measured permeabilities up to 10^{-4} m/s exist. Open-work gravels with high permeabilities were observed at the surface. These open-work gravels were probably developed in close proximity to an ice front and are likely to be in the form of irregular lenses of limited lateral extent.

The Crotty Quartzite - Locally this is a sandstone formation with some siltstones, which has an aggregate thickness in the area of about 500 m. Over much of the site this formation has been removed by erosion, but the remainder forms the higher ground on the west abutment and the ridges to the east of the Divide. The sandstones are generally highly to moderately weathered, weak to strong, and form fine sands when completely weathered. Joint spacings are generally in the range 20-200 mm. Limited testing suggests that the formation has permeabilities in the range 10^{-5} to 10^{-7} m/s.

The "Fenestella Shale." - This is a siltstone formation which occurs stratigraphically between the Crotty Quartzite and the underlying Gordon Limestone and is between 10 and 30 m thick. The "Fenestella Shale" is generally highly to completely weathered, weak, and the joint spacings are less than 100 mm. Low permeabilities of around 10^{-8} m/s were estimated for this formation.

The Gordon Limestone - This formation forms the lowermost unit at the Divide. It includes some siltstones and has a thickness in excess of 500m. The limestone underlies the reservoir north of the damsite beneath the superficial deposits and extends to the west of, and beneath, the ridge of Crotty Quartzite to connect with limestone south of the Divide. The Gordon Limestone is generally very strong with joint spacings varying between 20 and 2000 mm. In-situ solution of the limestone was encountered during drilling as deep as RL156 and caverns, some silt filled but others open, occur within the limestone. The Gordon Limestone was regarded as having the potential for extremely high permeability.

Weathering Products - The limestone and siltstone weathering products are difficult to distinguish but fall into two main categories:

- Clayey silt weathering products of limestone which are the insoluble residue remaining after solution of the calcium carbonate which forms the bulk of the limestone. The residue forms a mantle on the irregular limestone surface and contains pyrite, which oxidises producing aggressive acidic groundwater. At the interface between silt and limestone the silt is frequently loose and sloppy and the interface is generally locally permeable and possibly cavernous.
- Clayey silt and sandy silt weathering products of the "Fenestella Shale" and of siltstones within the limestone. They are generally structured and of higher strength than the silts derived from the weathering of limestone.

For engineering purposes the silts derived by weathering from these two different sources may be regarded as being one material having a range of engineering properties. The material

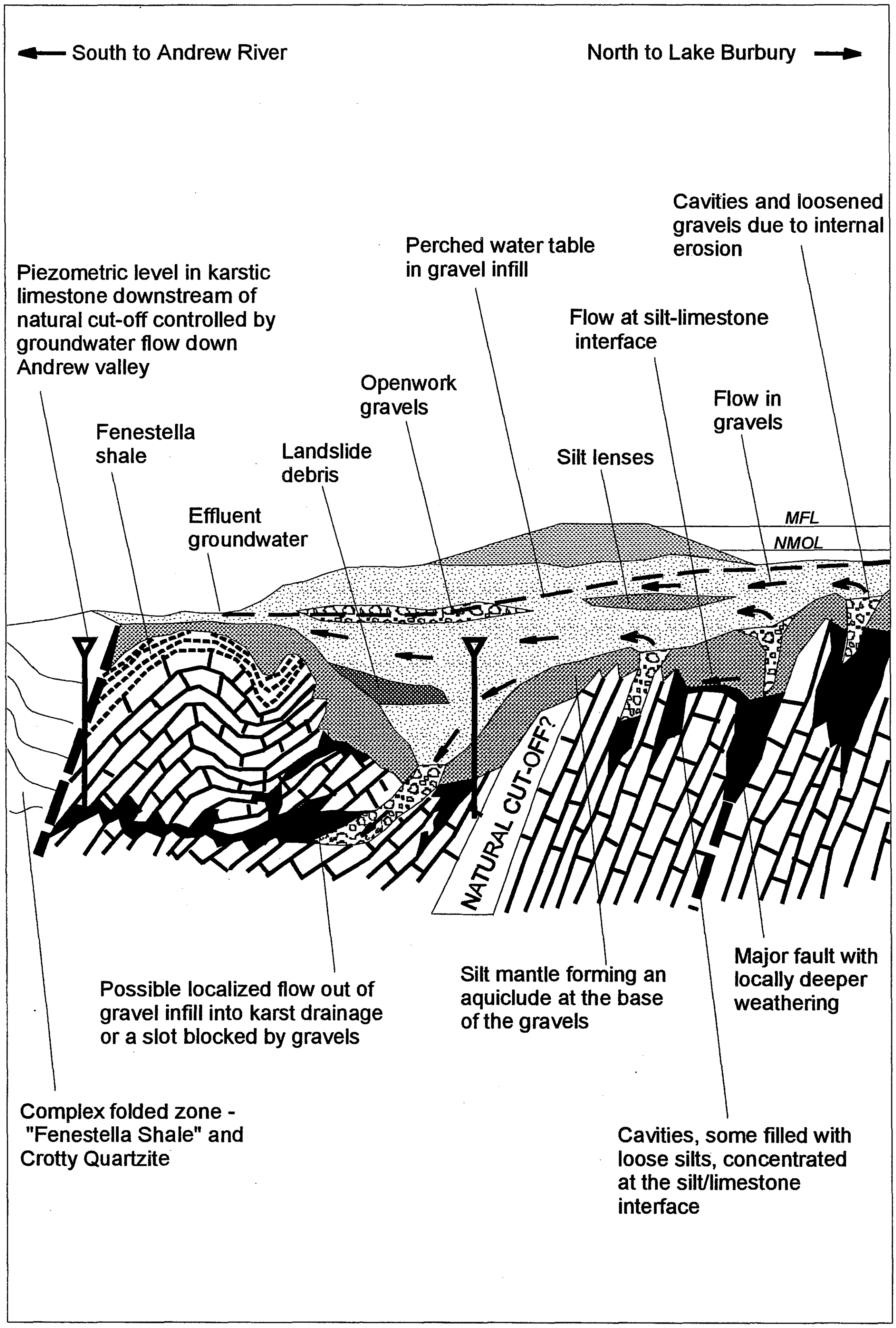

Figure 3 - Schematic section along the Throat illustrating the geological model

consists predominantly of silt sized mineral grains of quartz with mica, some kaolinite and minor montmorillonite. The clayey silts generally classify as "non dispersive", but occasional samples classify as "potentially dispersive". Where the materials are compact permeabilities of 10^{-6} to 10^{-9} m/s were measured. Where loose and sloppy, high permeabilities are associated with the presence of cavernous limestone nearby and a tendency to internal erosion was anticipated. The silts contain numerous but discontinuous slickensided surfaces and have measured shear strengths in the range:

- Peak values $c' = 0\text{-}39$ kPa, $\Phi' = 27\text{-}41°$, Residual values $c' = 0\text{-}30$ kPa, $\Phi' = 21\text{-}33°$

The lack of continuity of shear surfaces in the in-situ materials suggests that peak behaviour is the dominant shear strength characteristic. A complication existed in that the silts may consist in part of aggregated particles and the proportion of these particles may exert some control over in-situ and measured shear strengths. Aggregated particles may or may not occur in zones, dependent upon the genesis of the silts. In view of the uncertainties regarding the choice of material properties and the small difference between peak and residual shear strengths, a conservative approach was adopted with a lower bound value of $c' = 0$, $\Phi' = 29°$ for effective stress analysis.

Where the silts were loose and sloppy they exhibited little or no shear strength. However loose silts could only exist between high strength limestone pinnacles where arching of overburden stress prevents consolidation. Extensive continuous areas of loose silts could not exist, thus the loose silts did not present any threat to embankment stability.

Where the silts were derived from decalcification of impure limestone, potentially metastable materials with high void ratios could result. However any tendency to liquefaction is minimal as extensive reworking is required before metastable behaviour could be demonstrated. Therefore it was considered unlikely that the levels of seismic shaking that the dam might experience would be sufficient to induce liquefaction. Similarly, dam construction, impoundment and operation were unlikely to produce any liquefaction problems, with the exception of repeated trafficking of silt directly beneath pavements, and care was taken during construction to avoid such situations.

Features of the site

The principal geological features of the site are summarised in Figure 1. The site may be considered as consisting of the following distinctive areas:

The Limestone Plain - This is a broad area to the north of the Divide, but includes the western part of the Divide itself, which is underlain by limestone at relatively shallow depth. The irregular karstic surface of the limestone is mantled with silt weathering products which are overlain in turn by a veneer of fluvio-glacial gravels. In the more elevated parts of this area irregular troughs and hollows have developed at the surface due to subsidence consequent upon local solution of the limestone. The lower parts of this area are infilled with swamp deposits.

The Syncline - The most conspicuous feature of the site is the sandstone ridge which forms the eastern abutment. The ridge consists of an eastward plunging Syncline of Crotty Quartzite and "Fenestella Shale" and forms part of the "natural cut-off" extending from the eastern abutment part way across the damsite. The Syncline is developed adjacent to a major thrust fault, the Carey Fault, and splay faults running from the Carey Fault partially break up the Syncline. The Gordon Limestone is presumed to extend beneath the Syncline at considerable depth, ie beyond the limits drilled. The Crotty Quartzite and "Fenestella Shale" rocks forming the Syncline are generally deeply weathered to silty fine sand and sandy clayey silts respectively.

The Complex Folded Zone - This is an area between the Divide and the Andrew River underlain by deeply weathered and tightly folded Crotty Quartzite and "Fenestella Shale", which in turn are underlain in part by relatively shallow Gordon Limestone. There are occasional outcrops of siltstone in this area, but it is generally covered by glacial gravels.

The Throat - This is an area where weathered limestone occurs directly beneath gravels and extends south from the Limestone Plain to form a strip between the Syncline and the Complex Folded Zone. The continuity of the subcrop of limestone is interpreted as being broken by a thin bed of siltstone, which forms part of the "natural cut-off". Any leakage, internal erosion and/or subsidence that might affect the embankment is most likely to occur where the embankment crosses the Throat and this area was of critical concern with regard to the effectiveness of the dam design.

The Gravel Infill - A deep buried channel incised 40 m below the current level of the Andrew River occupies the south-western corner of the Divide. The course of the channel probably reflects an early Pleistocene drainage system and the channel has since been infilled by glacial gravels. The channel appears to originate from the Andrew River upstream of the Divide area but the exit was not located. The channel may have terminated in a doline (a funnel shaped cavity which leads to an underground drainage system) in karstic limestone or may have discharged through a narrow slot, neither of which were located.

The Bedrock Groundwater Regime

In the Limestone Plain groundwater gradients were sub-parallel to and generally within a few metres of the ground surface. The existence of a groundwater gradient of around 1 vertical to 20 horizontal indicates that the limestone is not highly permeable over very large areas.

South of the Divide, in a part of the Throat area and in those parts of the Complex Folded Zone underlain by shallow limestone, the piezometric surface in the limestone was gently sloping and at or about the level of the Andrew River. This suggests that in these areas the limestone is more permeable and draining towards the valley of the Andrew River.

Between the two distinct piezometric levels in the limestone there was a relatively impermeable barrier across which the gradient in the piezometric surface steepened to 1 vertical to 6 horizontal and, in places, to 1 vertical to 1 horizontal. The existence of a "natural cut-off" was postulated even thought its nature was not determined. It was considered to be most probably due to a zone of impermeable bedrock, probably siltstone, which extends from the Syncline across to the Complex Folded zone.

The Gravel Infill Groundwater Regime

Above the Throat the piezometric level in the Gravel Infill was higher than in the underlying cavernous limestone. The perched water table above the Throat was recharged from the north west where groundwater from the Limestone Plain flowed into the Gravel Infill down the bank of the buried channel, and appeared to drain south-east to an area where the groundwater was effluent and formed a series of springs. In the deepest part of the Gravel Infill the perched water table was almost horizontal. This may indicate gravels of higher permeability or may be due to localised underdrainage into a doline or slot at the base of the buried channel. Irregularities in the piezometric contours in the recharge boundary and steeper gradients in the Gravel Infill to the west may reflect the presence of less permeable zones within the Gravel Infill.

Other considerations

Other aspects of the site that required consideration were:

- The potential for instability of the slope downstream of the embankment and above the Andrew River.
- The possibility of differential settlement of the embankment induced by variations in the depth of compressible silts in the foundation.
- Increased rates of solution of the limestone induced by acidic groundwater consequent upon increased flow rates.
- Leakage through the gravels beneath the dam.

Design

Despite the extensive investigations many details of the site still remained unclear when the dam was finally designed eg. the existence of the natural cut-off was postulated but its nature was unknown, and the presence of a buried doline was possible but the precise location of the feature had not been established. However, the investigations had reached the stage where the additional information being collected was not contributing significantly to the further development of the geological model, thus it was necessary to make some pragmatic engineering decisions on the basis of the available information.

The original design involved a dam axis that was located where the minimum depth to the limestone would be encountered. The final design involved locating the dam further south for three reasons:

- The depth of silts and gravels over the limestone increased to the south, and the design could take advantage of the capacity of the silts and gravels to control and minimise seepage.
- The depth to the permeable silt limestone interface increased to the south, and the design minimised the relative increases in water pressure at that interface that would result from reservoir operation.
- A favourable condition existed in the form of a "natural cut-off" which runs across the Divide and impedes ground water flow. The precise nature of the cut-off was never determined, but it is likely to be a steeply dipping siltstone layer within the bedrock sequence. By shifting south the Dam could be located over the natural cut-off as indicated by the ground water contours.

The philosophy of the design was that it was better to make use of the positive geological features at the site, even if they were imperfectly understood, rather than attempt to disturb the existing relatively impervious foundations with an imperfectly executed cut-off (Giudici, 1999).

Further mitigating measures to counter the perceived risks were incorporated into the design, including:

- A conservative embankment section with a crest width of 20 m and relatively flat upstream and downstream slopes (1 vertical to 3 horizontal).
- A stockpile of gravels incorporated into the embankment for filling sinkholes should they develop.
- A 0.5 m crest camber to allow for settlement
- An upstream blanket consisting of a uniform engineered surface of compacted gravels which would assist in choking any leakages that developed in the reservoir floor and also indicate the presence of subsidence, by virtue of the deformation of the smooth engineered surface.
- A contingency plan for controlled filling, the capacity for de-watering using a jet valve installed in the diversion tunnel, and a plan for emergency grouting using "tube-a-manchete" systems.
- An extensive monitoring system to measure settlement, piezometric pressures and leakage both from the dam and through the karst system.

Performance

Crest settlement of about 30 mm has occurred with about half of the total settlement in the first year. Downstream and transverse crest deflections are 10 and 12 mm respectively. All deformation rates are well within expectations and are decreasing. There have been no depressions which may be associated with sinkholes developed in the upstream engineered surface.

Piezometric levels within the embankment and foundations have been measured continuously, except for a period when there was damage to the installations due to lightning strike. There has been little change in piezometric levels. There are changes in the piezometric levels in response to reservoir levels but those change are more subdued the further downstream of the centre line that the measurements are made. A remarkably low piezometric level has been measured in the dam foundation which may reflect a connection to a deep karstic path that flows to an exit point on the Andrew River.

Leakage is measured both from collecting weirs around the dam site and along the Andrew River that flows close to the toe of the dam site, and those measurements show that there has been no measurable increase in leakage and no measurable change in the flow of the river.

It is concluded that the dam has established some form of equilibrium with the ground conditions and this is regarded as a successful outcome of the investigation, design and construction of the structure. However, with these complex karst limestone foundations monitoring and surveillance will continue for the life of the structure, as it is possible that the system could deteriorate at any time (ibid).

Discussion

Engineering geology contributed to the successful engineering of this dam on a hazardous karst foundation due to the following factors:

- There were no unrealistic time or budget constraints on the investigation and consequently sufficient investigation were carried out to develop and confirm the geological model and to be able to present that model in some detail to the dam designers. In fact, at the end of the investigations, which took place within an area of less than one km^2, there was some concern that the numerous boreholes could themselves lead to leakage, and they were therefore located and sealed with grout.
- The investigations were carried out by a team of engineering geologists with wide-ranging skills in investigation, design, construction, engineering geology, hydrogeology and geophysics, and those different skills were brought together and synthesized to develop a sound understanding of the site conditions. There were excellent interpersonal relationships between the geologists and the engineers within the Hydro Electric Commission, which facilitated the communication of that understanding.
- A well conceived and well presented geological model was developed for the site and clearly communicated to the dam designers who themselves were responsive to the concerns regarding the potential geohazards of the site and very knowledgable of the site conditions. Consequently a design was developed that addressed all of the geohazards realistically. The investigation and design was subject to external expert review, which is the most effective way of verifying the findings of a complex investigation and design process (Stapledon, 1983).
- The vast engineering expertise of the Hydro Electric Commission supported pragmatic decision making based on avoiding geological problems, particularly problems of constructability. This approach involved carrying out thorough investigations to identify, understand and locate geohazards and then modifying general arrangements to avoid them wherever possible. Where geohazards could not be entirely avoided the approach involved taking advantage of what little the ground had to offer and then building several levels of contingency into the design to cater for the remaining uncertainty.

In view of the geohazards that had to be catered for in this project a quantitative risk engineering approach might have been adopted. In the period when the investigations and design were carried out such approaches were advocated by Whitman (1984) and the details of a quantitative risk analysis of dam design in karst was published (Vick and Bromwell, 1989). In the last decade quantitative risk assessment techniques have become increasingly used in the investigation and mitigation of geohazards (Australian Geomechanics, 2000).

Quantitative risk assessment techniques are extremely valuable in that they provide transparency to the decision making process ie. the systematic formulation of an analysis aids greatly in understanding the major sources of risk. However, sometimes the pursuit of quantification seems to dull the awareness of practitioners to the imprecision attached to the very numbers that are being generated. Estimates of very low probabilities typically associated with some geohazards can be so imprecise that the resultant risk assessment cannot be meaningfully compared with acceptance criteria.

This project is a case where attempts at quantification of the geohazard and resultant risk would not have contributed a great deal to the design process, because the basic geological understanding was far from perfect when the design was formulated. Any attempts at quantification of the hazards and risks would have involved judgements based on such an imperfect understanding as to render them meaningless. Instead, and because of overall project imperatives, a pragmatic design that was sensitive to the ground conditions and based on a reasonable level of geological understanding, and a design that had plenty of different kinds and levels of contingency, was successfully used to build the Darwin Dam.

Acknowledgements

This paper is published with the permission of Hydro Tasmania. I would like to acknowledge the assistance, encouragement, thoughtful advice and friendship provided by all of my colleagues in the Hydro Electric Commission both during this period of my career and during the preparation of this paper. The opinions expressed in this paper are my own.

References

Australian Geomechanics Society sub-committee on landslide risk management (2000). "Landslide risk management concepts and guidelines", *Australian Geomechanics*, Vol. 35 (1), pp 49 – 92.

Blainey G. (1954) The Peaks of Lyell, University Press, Melbourne

Giudici, S. (1999). "Darwin dam, design and behaviour of an embankment on karstic foundations", *Dam foundation problems and solutions*, 67th Annual Meeting of ICOLD, Antalia, Turkey pp 619 – 636.

Stapledon D.H. (1983). "Towards successful waterworks", *Proceedings of the Symposium on Engineering for Dams and Canals*, Institution of Professional Engineers, New Zealand, pp 1.3 – 1.15.

Vick S. G. and Bromwell L.G. (1989). "Risk analysis for dam design in karst", *Journal of Geotechnical Engineering*, ASCE 115 (6), pp 819 –835.

Whitman, R. V. (1984) "Evaluating calculated risk in geotechnical engineeering", *Journal of Geotechnical Engineering*, ASCE 110 (2), pp 145 –188.

Landslide Risk from the Hipaua Geothermal Area Near Waihi Village at the Southern End of Lake Taupo

B.D. Hegan
Tonkin & Taylor Ltd

J.D. Johnson
Tonkin & Taylor Ltd

Charlotte Severne
NIWA

Abstract

Tonkin & Taylor Limited have undertaken an assessment of Hipaua Geothermal Area to assess the potential for future large-scale slope instability and the risk of slide debris flowing into Lake Taupo. Devastating landslides originating from the Hipaua Thermal Area in 1846 and 1910 were responsible for a large loss of life.

There has been much speculation over the trigger mechanisms for the 1846 and 1910 events with little definite conclusions. Aerial photograph interpretation and geological mapping shows that geothermal activity at Hipaua appears to be shifting north along the Waihi fault. We consider it likely that cooling of the southern edge of thermal area has allowed the re-establishment of groundwater within the highly altered rock mass that was previously kept dry by superheated steam. The resulting increase in pore pressure from this new groundwater profile initiated the large-scale slope failures noted above within the hydrothermally altered rock mass. The debris forming landslide dams that once breached resulted in flow avalanches down the stream valley.

Two areas are identified that could produce similar landslide events and debris flow in the future. Estimates of landslide volumes and run-out distances have been made along with a risk assessment to determine the probability of such an event due to both thermal cooling and seismic triggering.

Thermal heat flow monitoring of the Hipaua Thermal Area by infra red imaging is now carried out on a regular basis to identify cooling areas.

Introduction

In 1846 and 1910 landslide debris originating from the Hipaua geothermal area flowed out from the steep escarpment out to the southern shores of Lake Taupo (Figure 1). The 1864 failure resulted in the loss of 64 lives and one life was lost in 1910. Concerns over the potential for the occurrence of further failures has lead to the Taupo District Council co-ordinating a study of the stability and risk of future failures.

This paper presents a summary of geological and slope stability models developed for the failures together with an assessment of run out potential and an assessment of probability and expected return periods.

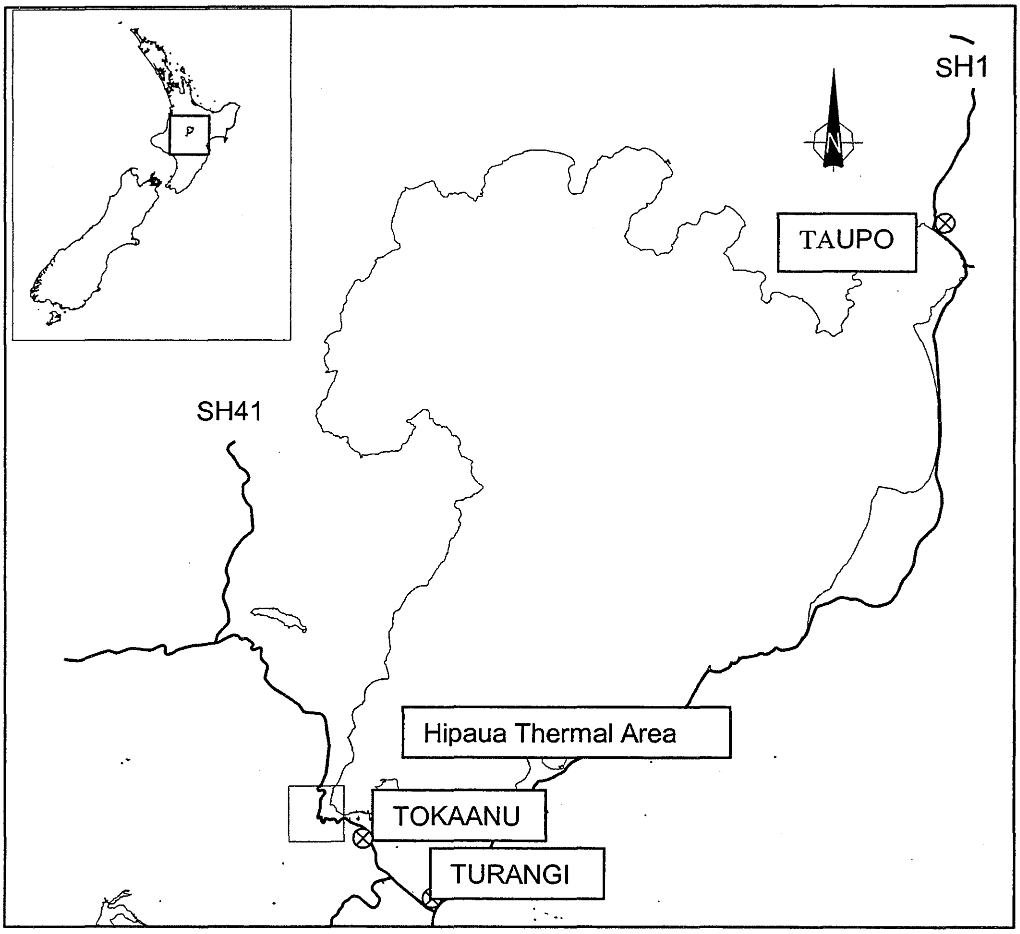

FIGURE 1 – Location Plan

Geologic Setting

The Hipaua thermal area is part of the Tokaanu –Waihi geothermal area near the Kakaramea-Tihia massif which forms part of the Tongariro Volcanic Centre (TVC) and is located on the western side of the Taupo Volcanic Zone (TVZ)

(Healy:1970, Severne:1995). The area is characterised by a zone of complex geology and very active faulting and volcanism.

The Hipaua thermal area straddles the Waihi Fault, which forms an east facing major escarpment along the western side of Lake Taupo. The fault forms part of the western boundary to the Taupo Volcanic Zone and in the study area comprises a number of splinter faults. The Waihi Fault also provides a pathway for high temperature geothermal fluids to rise to the surface.

The rock mass exposed on the Waihi Fault escarpment consists of hard platey andesite lava with bands of autobrecciated lava. Crude flow banding within the rock mass indicates that the lava was most likely to have been emplaced from west to east, dipping at a shallow angle to the east. The rock mass within the thermal area has been altered.

Geothermal Activity

The Hipaua thermal area is presently the most active part of the Tokaanu-Waihi geothermal area (Severne: 1995). The thermal area covers 116,000 m^2 and is characterised by bare, and covered, steaming ground, hot (not steaming) ground, fumeroles and steam vents and minor mud and acid pools. These features occur within a 900 m long, up to 200 m wide, segment of the eroded Waihi fault scarp.

Comparison of aerial photographs taken in 1941 and 1977 and recent field mapping has noted that over the last 50 years there has been an increase in area of Class I (>70^0C at 0.2m depth) thermal ground. The increase is from about 3000 m^2 in 1941 to approximately 10,000 m^2 at present. The thermal ground has extended to the north over the past 20 years at a rate of approximately 8 m/year.

Hydrothermal alteration of the rock mass is extensive due to H_2S in the steam oxidising and mixing with meteoric water and steam condensates. Hydrothermal alteration clay minerals identified consist of kaolinite, halloysite, and smectite (Severne:1995).

The extent of the thermal ground is shown on Figure 2. Three areas of thermally altered ground are shown. The main thermal area follows the escarpment south of the SH41 lookout area terminating abruptly in the Waimatai Stream. A second smaller thermal area is developed behind the escarpment terminating against a small-unnamed stream to the west. A third thermal area exists immediately above SH41 where it crosses the Waimatai Stream.

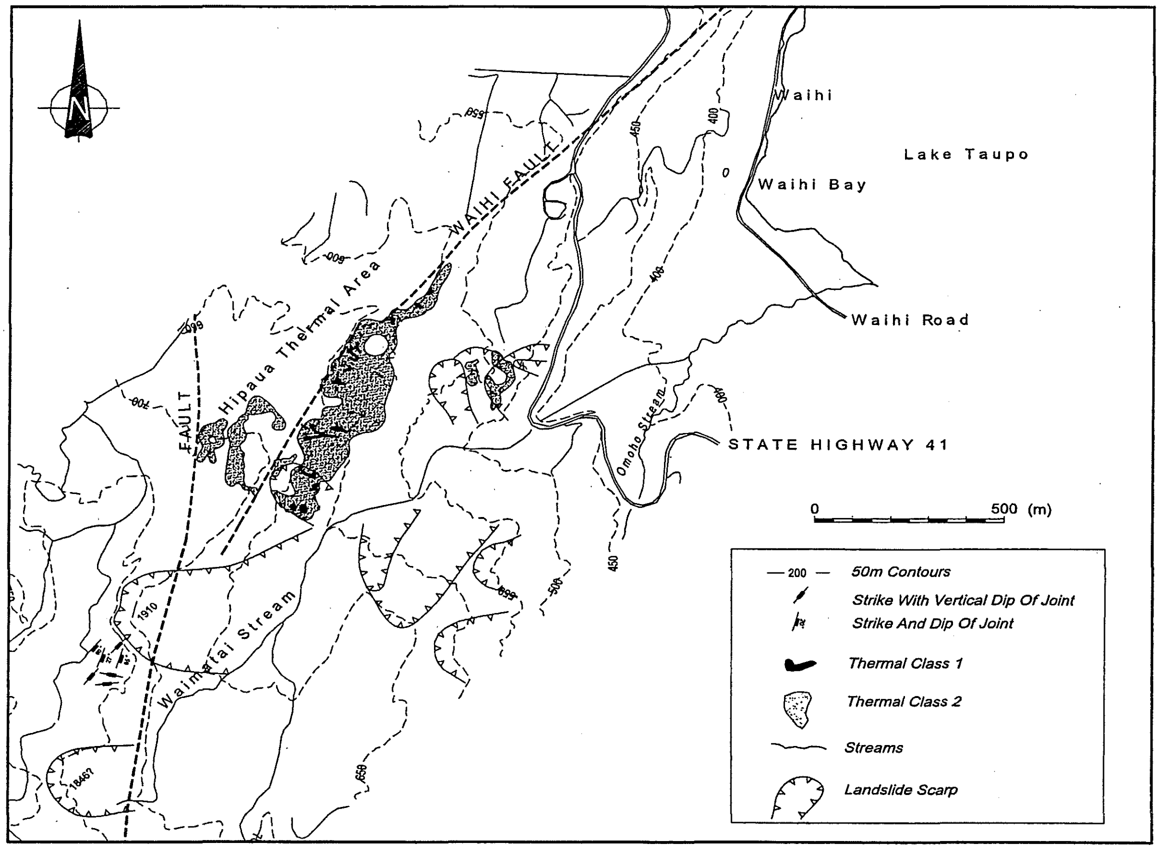

FIGURE 2 - Hipaua Thermal Area

Topography

The main topographic feature of the study area is the sharp, steep escarpment along the western edge of Lake Taupo which extends south forming the western side of the Waimatai Stream. Two large embayments (vacated landslides) occur in the escarpment immediately south of the thermal area. The northern most embayment is known to be the headscarp of the 1910 landslide. The southern embayment is likely to have been the source of debris for the 1846 event.

The flat land in Waihi Bay is formed by deltas from both the Waimatai and Omoho Streams prograding out into the lake. The smaller protrusion into the bay immediately north of the present mouth of the Waimatai Stream is the debris lobe from the 1910 landslide.

A number of other landslide scarps along the Waihi Fault and there is other historical evidence (unwritten) indicating that the Waihi fault zone has been the source of other earlier landslides.

Description of the 1846 Event

On May 7 1846 a large landslide originated from the Hipaua geothermal area with an associated rapid debris flow reaching the shores of Lake Taupo resulted in the loss of 64 lives. Details on the 1846 event are limited. Based on the contemporary evidence the 1846 landslide had two distinct stages with an unknown time period between. The first stage consisted of a failure that blocked the Waimatai Stream forming a natural dam. Taylor (1855) places this initial failure at approximately 2000 ft above Lake Level and states that the dam was breached three days later resulting in the debris avalanche. However, Cowan (1910) states that it was some years before the great 1846 landslip that the Waimatai Stream was dammed by landslips. He goes on to state that a new slip came down in 1846 and raised the level of the lake and the failure occurred later that year when the dam was overtopped during heavy rainfall.

The initial slide that dammed the stream is considered to have originated from embayment in the fault escarpment immediately south and upstream of the 1910 source area. It is noted that there is no thermal activity in this area now.

Description of the 1910 Event

On the morning of 20 March 1910 a large landslide originating from the Hipaua geothermal area produced a large debris flow which reached the shores of Lake Taupo resulting in the loss of one life. The volume of the 1910 landslide has been estimated to be approximately 2.8 Mm^3. The failure may have occurred as a two stage event with the thermally altered ground yielding initially followed by a later failure of now oversteepened slopes in the unaltered andesite lava. It is reported that a loud noise was heard in Waihi Village at 9 a.m. on the 20 March 1910 but the debris flow was not reported until later in the morning. A detailed eye witness account by Mr J Hanlon was reported in the March 31 1910 edition of the *Weekly News* which described a terrific roar, a large column of dust, and a great crack in the hillside at 11.30 a.m. This chronology supports a two stage event.

Our reconstruction of the pre-failure slope (Figure 3) shows a lower toe area of the original slope consisting of thermally altered ground backed by unaltered lava with a platey jointing dipping at approximately 30^0E (down slope) behind the Waihi fault. This geometry is similar to that existing at the present time immediately to the north.

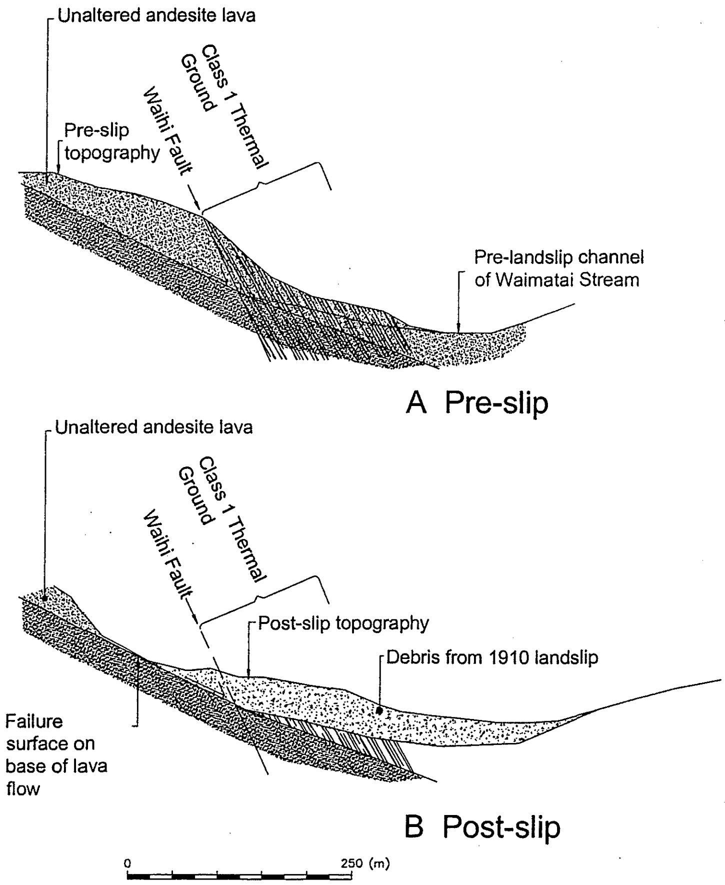

FIGURE 3 - 1910 Landslip Geometry

The debris avalanche had an estimated average velocity of 8 m/sec based on the report that it took 3 minutes from the time a loud noise was heard to when the debris arrived at the lake edge. The H/L ratio is measured at 0.2 based on a height of 320 m and a travel length of 1500 m from the landslide centroid to the exit point from the confining channel. The run-out distance was approximately 700 m reaching a width of 450 m with a thickness of between 3 m to 10 m.

Failure Trigger Mechanisms

Others, notably Healy (1970), have speculated on the trigger for the landslide event. Although heavy rain was reported immediately prior to the breach of the landslide dam in 1846, a trigger for the initial slide has not been clearly established. In 1910 there is no mention of significant rain before the event and March 1910 was reported as not being a wet month. Furthermore, there were no reported or recorded earthquake events on or immediately before these events. The possibility that initial failures were a result of a phreatic (steam) explosion has been discountered as the overburden pressures based on reconstructed site morphology were too great.

A possible explanation for the failures is related to the migration of the geothermal area northwards. Alteration of rocks suggests that, prior to failure, an active thermal profile existed in each of the failure areas similar to that seen in the present Hipaua thermal area. This system has a boiling interface at a considerable depth with a steam phase immediately above which degrades to a wet condensate layer near the ground surface. In the steam phase we postulate that there is no free water and pore pressures in the ground are taken as the steam pressure. The pressure gradient and heat supplied by the steam phase essentially keeps the soil profile unsaturated to considerable depth and prevents the ingress of any downwards percolating meteoric waters. The steam pressure is estimated at 13 bars (1300 kPa) at boiling interface by Severne (1995) and is expected to approximately decrease linearly to the ground surface. This steam pressure is approximately half the pressure that would exist throughout the soil profile if a water table developed with an soil/rock profile near the ground surface.

While the above conditions remain in place the slope profile remains stable with possible failures limited to within a few metres of the ground surface (i.e. similar to that seen in the steeper parts of the Hipaua thermal area today). However, on cooling we expect that pore pressures within the slope would rise significantly and the potential for instability increase as the heat flow in the steam phase declines.

Potential for Future Failures

Two areas of possible future instability have been identified by this study. The first area is approximately 700 metres to the north of the 1910 landslide. Here the slope is almost identical in geometry with the inferred 1910 pre slip geometry with the exception that it extends further west and involves a larger area of thermally altered ground behind the Waihi fault. This area is currently thermally active and is considered stable but is identified as the next area expected to cool as the thermal field migrates northwards.

A second area of future instability is identified immediately above SH41 near the Waimatai Stream crossing. This is in an area of thermal activity away from the main fault. While this appears to be increasing in heat flow with the development of bare steaming ground (Severne, 1995), the slope is extremely steep and our assessment indicates that the ground alteration alone could be sufficient to lead to slope failure.

Potential Scale of Future Landslide Events

Estimates of the volumes of each of the possible landslides have been made based on the assumed geometry of the landslide mass. Using these volumes the run-out distance of each has then been calculated using the approximate relationship that the width is half the length of the run-out distance. The potential landslides source and run out distances are listed below and illustrated on Table 1 and on Figure 4.

- Event A - 700 m north of the 1910 event extending but back behind the fault
- Event B - 700 m north of the 1910 event with material from the thermal alteration zone only
- Event C - Immediately above SH41

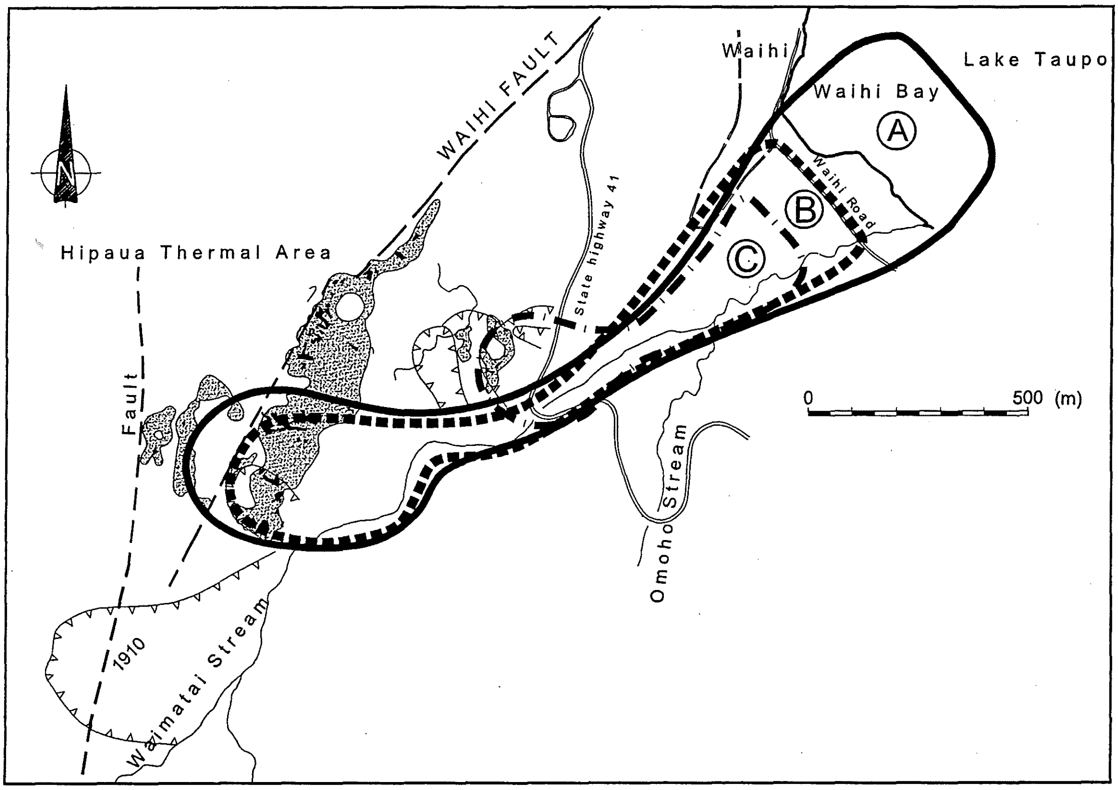

FIGURE 4 - Runout Areas for Potential Landslides A, B, & C.

Table 1. Potential Landslide Dimensions

Landslide	Volume (m^3)	L (m)	H (m)	H/L	D (m)
1910	2,800,000	1500	320	0.21	700
A	4,875,000	1000	250	0.25	1100
B	1,500,000	900	200	0.22	600
C	750,000	400	100	0.25	430

Where L is horizontal travel distance
H is height of landslide centre above exit point
D is the run-out distance.

Approach to Risk Analysis

A probabilistic analysis was performed to assess the risks associated with the possible development of future slope failures from the Hipaua thermal area. These analyses were developed using the approximate relationships described previously but, instead of using set values for each variable, a range of potential values is established and the calculations carried out many times with random selection of combinations of values within these ranges. This is achieved with the computer programme @RISK and enables simulation of randomly selected values.

For this risk assessment, there are two probabilities that need to be calculated, namely:

1. Probability of a landslide event occurring (P_1) – includes both a thermal cooling event and an earthquake triggered event.
2. Probability of the debris flow causing damage, given that an event has occurred (P_2) – for the purposes of this paper P_2 depends on the travel distance from the channel exit

point. It is noted that a detailed discussion of downstream effects and risks to lives and property is beyond the scope of this paper.

The assessment of probability of slope failure due to cooling effects has been made based on the frequency of historic failures combined with estimates of rates of thermal field migration. Consideration of earthquake induced failures indicates critical accelerations of about 0.2g for the existing slope correspond with a return period of 75 years based on Matuschka et. al. (1985) and Dowrick (1995). The probability of combined effects of cooling and the yield acceleration being exceeded within a given time from present is then determined assuming a Poisson model.

The probability of consequences of a landslide (P_2) depends on the volume of the slip, the energy, and the various empirical relationships between these and debris spread width at run-out distance (Corominas 1996, Finlay et.al (1999) and Hunger et. al. 1998). This has been assessed in terms of probability of exceedence for run-out distance measured from the "channel" exit point (Figure 4) and in particular the probability of debris reaching the lakefront and generating a wave within the lake.

The greatest hazard is clearly an Event A failure. The expected run-out distance for probable landslide Event A is of the order of 1100 metres which will place the distal end in Waihi Bay. The wave height calculated for such an event is between 4m to 5.5 m high assuming that:

- the depth of Waihi Bay reaches 3 m at a distance of 200 m from the shore and that beyond this point the lake deepens rapidly
- the debris velocity will be approximately 5 metres/sec when it enters the water

Results of risk assessment

The assessed probability of future significant landslide events over the next 10 to 50 years from the Hipaua is summarised on Table 2 below. The results clearly illustrate that the risks of future significant slope failure within the next 10 years are high (>10%) but the risks of a slope failure reaching the lake and affecting the shore at Waihi Village is comparably low.

However, the risks are shown to increase proportionally with time. Over the next 50 years the risk of a potential futures reaching the lakes edge is very high and the probability of wave being generated by a debris avalanche at the lake edge of 5 m of greater also increases. Correspondingly the risk that a wave may propagate away from the entry point of a debris avalanche resulting in waves of >2m on the shore edge at Waihi Village increases with time to a high level.

Table 2. Summary of Risk Assessment

Hazard	Probability of an Event in the next 10 Years	Probability of an Event in the next 50 Years
Large Scale Slope Failure	13%	65%
Failure Debris Reaching the Lake	2%	43%
Generation of wave >2m on the lake shore at Wahi Village	<1%	13%

Future Monitoring

It is clear from the above discussion that the risks associated with slope failure from the Hipaua Thermal area are significant and will increase with time as the southern end of the thermal area cools. Recommendations for monitoring of the thermal field activity have been put in place and Taupo District Council is now monitoring the heat flow over the Hipaua Thermal Area. Installation of a real time slope monitoring network will be considered if cooling of the currently active areas is monitored. In addition a local Civil Defence plan has been developed by Taupo District Council to ensure all residents know where to move to in the event of either severe earthquake shaking or reported slope movements (including sounds of slope failure initiation) from the Hipaua Thermal area.

Summary

The key points to come from this study of the Hipaua thermal area are as follows.

- Landslides originating from the Hipaua Thermal Area in 1846 and 1910 have followed the Waimatai Stream valley down to the shores of Lake Taupo.

- The historical accounts of both the 1846 and 1910 landslide events suggest that both occurred in two stages probably damming of the Waimatai Stream prior to the main flow event.

- Geothermal activity at Hipaua appears to be shifting north along the Waihi Fault at a rate of approximately 8 m/year.

- We consider it highly likely that the earlier landslides were initiated as a result of the cooling of that part of the thermal area. This cooling allows the groundwater table to re-establish itself from the ground surface down and the increase in pore pressure within the thermally altered rock mass initiates a slope failure where the slope is steep.

- Two areas are identified that could produce a landslide in the future. They are immediately above SH41 and 700 m north of the 1910 vacated landslide. These areas are currently stable but stability is expected to reduce with time as the thermal activity reduces at these two sites.

- A risk assessment has been made to determine the probability of future landslide events from combined geothermal cooling and seismic triggering. The risks of slope failure are shown to be high and increase significantly with time.

- Monitoring of Hipaua Thermal Area is now being carried out as part of the overall risk management of the area and includes accurate monitoring of the thermal area. A specific Civil Defence plan has also been prepared for the area.

Acknowledgements

The authors would like to thank Taupo District Council for granting permission to publish the results of our study. The authors would also like to thank Tonkin & Taylor Limited for support in the preparation of this paper.

References

Corominas, J., (1996): *The Angle of Reach as a Mobility Index for Small and Large Landslides*. Canadian Geotechnical Journal, Vol. 33, pp 260-271.

Cowan, James, (1910): *Lake Taupo and the Volcanoes.* Auckland

Dowrick, D.J., Gibson, G., McCue, K. (1995): *Seismic Hazard in Australia and New Zealand*, Bulletin of New Zealand National Society for Earthquake Engineering, Vol. 28, No. 4.

Finlay, P.J., Mostyn, G.R., Fell, R., (1999): *Landslides: Prediction of Travel Distance and Guidelines for Vulnerability of Persons.* Proceedings 8th Australia New Zealand Conference on Geomechanics, Hobart.

Healy, J., (1970): *Waihi Landslides:* Unpublished New Zealand Geological Survey Report.

Hungr O., Yau H.W., Tse L.F., Cheng A.D., (1998). *Natural Slope Hazard and Risk Framework.* Proceedings of the International Conference on Urban Engineering, Hong Kong.

Lowe, H.J. (1910): *Report on Landslip at Waihi, Tokaanu*, Report of Lands Department, 1910, C-1, Appendix V, p.43.

Matuschka, T., Berryman, K.R., O'Leary, A.J., McVerry, G.H., Mulholland, W.M., Skinner, R.I. (1985): *Bulletin of the New Zealand National Society for Earthquake Engineering*, Vol. 18, No. 4.

Severne, C. (1995): *Hipaua Geothermal Area, Tokaanu-Waihi Geothermal System, Taupo Volcanic Zone, New Zealand*, MSc thesis lodged with the Auckland University.

Taylor, R., (1855): *Te Ika a Maui.* Published by Wertheim and Macintosh, London, pp 320-321.

J:\1680\6jdj220601.GCPAPER.doc
16 July 2001